EURO
CVD&ALD

EUROCVD & ALD 24

2nd June-5th June 2025

Book of Abstract

Monastery of San Nicolo L'Arena, Catania, Italia

Uni ct SCIENZE CHIMICHE

INSTM

EUROCVD & ALD 24

List of Invited Speakers

Angel Barranco
Spanish National Research Council, Materials Science Institute of Seville (ICMS-CSIC-US), *Spain*

Davide Barreca
ICMATE-CNR and INSTM c/o Department of Chemical Sciences, Padova University, Padova, *Italy*

Ausrine Bartasyte
FEMTO-ST Institute, Université Marie et Louis Pasteur Institut Universitaire de France (IUF) C2N, CNRS, Université Paris Saclay, *France*

Mariadriana Creatore
Eindhoven University of Technology, *Netherlands*

Maarit Karppinen
School of Chemical Engineering, Aalto University, *Finland*

Caroline E. Knapp
University College London, *United Kingdom*

Alessio Lamperti
CNR-IMM, Unit of Agrate Brianza, *Italy*

Maria Losurdo
Consiglio Nazionale della Ricerche, Istituto di Chimica della Materia Condensata e di Tecnologie per l'Energia (CNR-ICMATE), *Italy*

David Muñoz-Rojas
Université Grenoble Alpes, CNRS, Grenoble INP, LMGP, *France*

Henrik Pedersen
Linköping University, *Sweden*

Gloria Tabacchi
Department of Science and High Technology and INSTM, Insubria University, Como, *Italy*

EURO
CVD&ALD

EUROCVD & ALD 24

Conference Program

2
MON

AM

h8:45-9:15 **Welcome**

AM_1.1 h.9.15 -10.30
INVITED: **Maarit Karppinen**
Innovative Processes I

h.10.30-11.00

AM_2.1 h.11.00-12.30
INVITED: **Caroline E. Knapp**
Precursor Design I

h.12.30-14.00 Lunch

PM

h. 14.00-14.30
INVITED: **Ausrine Bartasyte**

Parallel Sessions

PM_1.1
h14.30-15.30
Piezoelectrics

PM_1.2
h14.30-15.30
Semiconductor I

h.15.30-16.00

h.16.00- 16.30
KEYNOTE: **Patrik Hoffmann**

Parallel Sessions

PM_1.3
h16.30-17.30
Semiconductor II

PM_1.4
h16.30-17.30
Ferroelectrics & Multiferroics

h.18.00 **Poster Session**
h.20.00
Guided Tour to the Monastery

3
TUE

h8:45-9:15 **Welcome of the Rector**

h. 8.45-9.15 INVITED: **Maria Losurdo**

Parallel Sessions

AM_2.1
h.9.15 -10.45
Functional Materials I

AM_2.2
h.9.15 -10.45
Precursor Design II

h.10.45-11.15

h.11.15-11.45
INVITED: **Alessio Lamperti**

Parallel Sessions

AM_2.3
h.11.45-12.45
High-k dielectrics

AM_2.4
h.11.45-12.45
Materials for Energy: Photocatalysis

h.12.30-14.00 Lunch

h. 14.00-14.30
INVITED: **Davide Barreca**

Parallel Sessions

PM_2.1
h14.30-15.30
Materials for Energy: Water Splitting

PM_2.2
h14.30-15.30
Dielectics

h. 15.30-16.00

h.16.00- 16.30
INVITED: **Mariadriana Creatore**

Parallel Sessions

PM_2.3
h16.30-17.30
Materials for Energy: Photovoltaics

PM_2.4
h16.30-17.30
Innovative Plasma Assisted Processes

h.19.00 **Gala Dinner**
Palazzo Biscari

EURO
CVD&ALD

EUROCVD & ALD 24
Conference Program

AM

PM

4
WED

h. 8.30-9.00
INVITED: **David Muñoz-Rojas**

Parallel Sessions

AM_3.1
h.9.00 -10.30
Innovative Processes: SALD and Area-Selective Deposition

AM_3.2
h.9.30 -10.30
Innovative Processes II

h.10.30-11.00 ☕

h.11.00-11.30
INVITED: **Gloria Tabacchi**

Parallel Sessions

AM_3.3
h.11.30-12.30
Modeling

AM_3.4
h.11.30-12.30
Functional Materials II

h.12.30-14.00 Lunch 🍴

h. 15.00
Mount Etna Excursion

5
THU

AM_4.1 h.8.30-10.30
INVITED: **Henrik Pedersen**

C/N based materials

h.10.30-11.00 ☕

AM_4.2 .h.11.00-12.15
INVITED: **Angel Barranco**
Materials for Energy: Photonics

h12.15-12.45 Greetings & Closing Remarks

h.12.45-14.00 Lunch 🍴

Session AM_1.1 INNOVATIVE PROCESS I

Chair: **Graziella Malandrino** | Main Hall “Santo Mazzarino”

Invited: **Maarit Karppinen** | 9.15-9.45
Organic-component-engineering of novel inorganic-organic ALD/MLD thin film structures for next-generation applications

K. Ashurbekova, I. Saric Jankovic, **Mato Knez** | 9.45-10.00
Biomimetic Metallosaccharides: A Novel Approach to Multifunctional Coatings for Biomedical and Food Safety Applications

Ivo Utke, P. Swiderek, K. Höflich, J. Jurczyk, K. Madajska, P. Martinović, I.B. Szymańska | 10.00 - 10.15
Non-thermal gas-assisted focused electron beam induced deposition of metals and insight gained from thermal ALD and CVD mechanisms

J.R. van Ommen, A.Y. Rwei, A.G. Denkova, V. van Steijn | 10.15-10.30
ALD for medical applications

Session AM_1.2 PRECURSORS DESIGN I

Chair: **Elisabeth Blanquet** | Main Hall “Santo Mazzarino”

Invited: **Caroline E. Knapp** | 11.00-11.30
The First Non-Pyrophoric Precursor for the Low Temperature Deposition of Metallic Aluminium

Ioana Nuta, S. Fadloun, T. Mourrier, A. Mantoux, E. Blanquet | 11.30-11.45
Understanding the decomposition mechanisms of the bis(2- dimethylamino propoxy) copper (II) precursor: total vapour pressure measurement using Knudsen effusion method

Andrew Johnson | 11.45-12.00
Development of Precursors for Atomic Layer Deposition of p-Type Oxides

J. Obenlüneschloß, N. Huster, D. Zanders, H. Parala, M. Gock, M. Unkrig-Bau, **Anjana Devi** | 12.00-12.15
Ru metal CVD: The role of the precursor

Ruben Blomme, A. Chalishazar, L. Henderick, F. Munnik, J. Meersschaut, M. Minjauw, C. Detavernier, J. Dendooven | 12.15-12.30
Tris(dimethylamino)phosphine as Phosphorous Precursor for Metal Phosphate ALD

Session PM_1.1 PIEZOELECTRICS
Chair: **Sven Van Elshocht** | Main Hall “Santo Mazzarino”

Invited: **Ausrine Bartasyte** | 14.00-14.30
Advances and challenges in growth of LiNbO$_3$ thin films for acoustic and photonic devices

Léo Lapeyre, A. Sharma, A. Müller, L. Pethö, P. Raynaud, J. Michler, I. Utke |14.30-14.45
Exploring Early-Stage ALD Growth Dynamics of LiNbO$_3$ on NMC 811 Cathodes: An In Situ QCM Study for Artificial CEI Applications

Ian Povey | S. Hussain, L. Keeney | 14.45-15.00
Strain Modulation and Piezoelectric Response in Chemical Vapor Deposition Grown MoS$_2$ Monolayers

Nelly Scheibel, V. Astie, L. La Spina, G. Larger, E.Crevon, P. Boulet, S. Margueron, J.-.Manuel Decams, A. Bartasyte | 15.00-15.15
Epitaxial LiNbO$_3$ thin films with controlled stoichiometry

Session PM_1.2 SEMICONDUCTORS I
Chair: **Gloria Tabacchi** | Room “Coro di Notte”

Pawan Kumar, N. Trainor, B. Groven, H. Medina, D. Vranckx, J. M. Redwing, A. Delabie, C.J. Lockhart, G.S. Kar, P. Morin | 14.30-14.45
Cl$_2$ etching selectivity for defects in two-dimensional transition metal dichalcogenides (TMDs)

Venkat S.K. Channam, I. Belov, P. Dhakras, S. Tasneem, R. Chukka, A. Jourdain, A. Sepulveda | 14.45-15.00
Advances and challenges in gapfill oxides

Kousumi Mukherjee, T. Staps, C. van Helvoirt, C. H. L. Weijtens, M. Verheijen, M. Creatore | 15.00-15.15
Exploring the Impact of Atomic Layer Deposition Processing on NiO Chemistry and Opto-electrical Properties

Iryna Kandybka, P. Kumar, H. Medina Silva, B. Groven, A. Nalin Mehta, Y. Shi, S. Banerjee, P. Morin, A. Delabie | 15.15-15.30
Unraveling mechanisms to achieve singlecrystalline MoS$_2$ monolayer by metal organic chemical vapor deposition

Session PM_1.3 SEMICONDUCTORS II

Chair: **Henrik Pedersen** | Main Hall “Santo Mazzarino”

Keynote: **Patrik Hoffmann** | 16.00-16.30
How to help the planet – Parallel processing of free design complex object

Houyem Hafdi, A. Carlson, H. Pedersen | 16.30-16.45
Life cycle assessment of CVD and ALD of GaN

L. Demelius, **A. M. Coclite,** M. Losego | 16.45-17.00
ZnO vapor phase infiltration into photo-patternable polyacrylate network

Daniel Hiller, S. Nagarajan, I. Ratschinski, S. Shams, S. Shah, S. Schmult, S. Wirth, T. Mikolajick, D. König, J. Trommer | 17.00-17.15
ALD Metal Oxide Monolayers on Si/SiO$_2$ Core-Shells Nanowires Enable High p-type Doping Without Mobility Deterioration

B. Peek, M. Werner, **Paul R. Chalker** | 17.15-17.30
Growth of p-type SnO by ALD and pulsed CVD using a diamidostannylene precursor

Session PM_1.4 FERROELECTRICS & MULTIFERROICS

Chair: **Ausrine Bartasyte** | Room “Coro di Notte”

Topias Jussila, L. Saltarelli, N. Dix, M. Gich, M. Karppinen | 16.30-16.45
Epitaxial ALD of ε-Fe$_2$O$_3$ thin films to unlock scalable production of multiferroic thin films for next-generation spintronics

Hyun-Cheol Kim, M. I. Popovici, G. De, D. S. Kwon, A. Pavel, G. Kim, H. Dekkers, L. Nyns, A. Delabie, J. Van Houdt | 16.45-17.00
Capping layers engineering for oxygen supply in solid and nanolaminate Hf$_x$Zr$_{1-x}$O$_2$ for sub 10nm ferroelectric memory applications

Gourab De, M. I. Popovici, P. K. Parida, D.S. Kwon, S. Mukherjee, H. Kim, G. Kim, O. Richard, P. Favia, A. Delabie, J. Van Houdt | 17.00-17.15
Atomic layer deposition of preferentially c-axis oriented ferroelectric hafnium zirconium oxide thin films for enhanced ferroelectric response

Gwon Kim, D. S. Kwon, G. De, H. Kim, L. Nyns, M. I. Popovici | 17.15-17.30
Optimized Annealing and Seed Layer Processing of Zr-Doped HfO$_2$ Thin Films for Ferroelectric Applications

Session AM_2.1 FUNCTIONAL MATERIALS I
Chair: **Mato Knez** | Main Hall “Santo Mazzarino”

Invited: **Maria Losurdo** | 8.45-9.15
Chemical Vapour Deposition as the Key to Unlock Tailoring of Van der Waals Phase Change Materials

Mari Heikkinen, M. A. Francis, K. Meinander, G. C. Tewari, M. Nisula, M. Karppinen | 9.15-9.30
Atomic/molecular layer deposition of copper ethenetetrathiolate thin films for thermoelectric applications

Raul Zazpe, J. Rodriguez-Pereira, J. Charvot, M. Klikar, F. Bures, J. M. Macak | 9.30-9.45
ALD Synthesis of Transition Metal Phosphides

P. Liu, A. Baby, B. Dietzek-Ivanšič, V. Klimkevičius, **Vladimir Sivakov** | 9.45-10.00
Emission peculiarities in MOCVD deposited undoped SnO_2 *layers*

S. Azpeitia, M. Knez | 10.00-10.15
Synthesis of Lanthanum-based Perovskite Thin Films by Atomic Layer Deposition

Marielena Velasco Enriquez, I. Gelard, C. Jimenez, H. Roussel, S. Ortega, L. Rapenne, P. Ferrandis, E. Sarigiannidou, V. Consonni | 10.15-10.30
Pulsed-Liquid Injection MOCVD of epitaxial Ga_2O_3 *thin films*

Brent Van Neste, M. M. Minjauw, A. Chalishazar, C. Detavernier, J. Dendooven | 10.30-10.45
ALD of Zinc Ruthenate using RuO_4 *as a Multiconstituent Reactant*

Session AM_2.2 PRECURSORS DESIGN II
Chair: **Anjana Devi** |Room “Coro di Notte”

Anthony Tacnet, A. Bartasyte, J.M. Decams, V. Astie, S. Daniele | 9.15-9.30
Innovative Fluorinated Aminoalkoxide Precursors for DLI-CVD Growth of High-Quality $LiNbO_3$ *and* $KNbO_3$ *Thin Films*

Premrudee Promdet, P. Niiranen, P. Bagherzadeh, D. Lundin, H. Pedersen | 9.30-9.45
Deposition of copper from copper triazenide precursor and plasma electrons

Joshua Buckingham, F. De Leeuw, A. L. Johnson | 9.45-10.00
Single-Source Precursors for the Aerosol Assisted Chemical Vapour Deposition of Tantalum Oxides and Tantalum Oxynitrides

Marcel Schmickler, H. Parala, A. Devi | 10.00-10.15
Molecularly engineered yttrium precursors for deposition of yttrium(III) oxide thin films

Shreya Mrig, C.E. Knapp | 10.15-10.30
Unraveling the Steric Link to Copper Precursor Decomposition: A Multi-Faceted Study for the Printing of Flexible Electronics

Anish Philip, M. Madadi, E. Haimi, and M. Karppinen | 10.30-10.45
The role of lithium precursors in tuning Lithium-terephthalate thin film properties.

Session AM_2.3 HIGH-K DIELECTRICS
Chair: **Patrik Hoffmann** | Main Hall “Santo Mazzarino”

Invited: **Alessio Lamperti** | 11.15-11.45
HfO_2 thin layers by low temperature thermal ALD processes for neuromorphic and spintronics applications: challenges and opportunities

Raffaella Lo Nigro, B. Galizia, E. Schilirò, S. Peters, J. Zessin, F. Roccaforte | 11.45-12.00
Comparison between ALD and PE-ALD growth of Al_2O_3/AlN dielectric stacks on silicon carbide by In-Situ Spectroscopic Ellipsometry

Seonyeong Park, J. Yoo, J. Park, P. Yun, D. Ha, H. Kim | 12.00-12.15
Optimization of High-k Gate Insulators for Amorphous IGZO channel-based 3D DRAM: Materials and Process Development

Emanuela Schilirò, G. Greco, P. Fiorenza, S. E. Panasci, S. Di Franco, R. Lo Nigro, F. Giannazzo, F. Roccaforte | 12.15-12.30
Atomic Layer Deposition of Al_2O_3 as gate insulator in GaN-on-GaN capacitors and effect of annealing treatments on the film quality

Julie Chaussard, C. Guérin, A. Lefèvre, P. Gonon, V. Jousseaume | 12.30-12.45
Exploring low-k/high-k multilayers for improved dielectric performances in MIM capacitors

Session AM_2.4 MATERIALS FOR ENERGY: PHOTOCATALYSIS
Chair: **Angel Barranco** | Room “Coro di Notte”

Mario Ziegler, V. Ripka, A. Drewitz, M. Diegel, M. Kühnel, U. Hübner | 11.45-12.00
Self-assembled silver-decorated titania and zinc oxide nanowires by MS-ALD for photocatalytic dye degradation

S. Lotitoa, D. Cignolo, J. Gubitosa, G. Barucca, P. Mengucci, M. Striccoli, F. Palumbo, P. Cosma, P. Fini, S. Murgolo, V. Rizzi , A. Milell, **Alberto Perrotta** | 12.00-12.15
Nanoengineering Of Chitosan Sponges Via Atomic Layer Deposition Of ZnO For Water Remediation Technologies

Carmen Jiménez, L. Deblock, L. Fellah, O. C. Poggi, C. Hellio, M. Weidenhaupt, F. Faÿ | 12.15-12.130
The photocatalytic properties of microstructured TiO_2 coatings grown by MOCVD as ecofriendly antibiofouling solutions

Chiara Laferrera, M. Zimbone, G. Sfuncia, G. Nicotra, L. Vitiello, S. C. Carroccio, G. Impellizzeri | 12.30-12.45
ZnO deposited on hemp shives by ALD for a sustainable wastewater remediation

Session PM_2.1 MATERIALS FOR ENERGY: WATER SPLITTING

Chair: **Mariadriana Creatore** | Main Hall “Santo Mazzarino”

Invited: **Davide Barreca** | 14.00-14.30
Nanoarchitectonics of multi-functional metal oxide systems: a multi-purpose toolbox for human/environmental protection and sustainable energy production

Muhammad Awais Khan, D. Martinez Martinez, N. Boscher | 14.30-14.45
Atomic Layer Deposition of Heterostructure of Tantalum Oxide and Tantalum Nitride on CNTs for Photoelectrochemical Water Splitting

Charlie Brown, Q.Y. Tey, M. K. Surman, F. Marken, A. L. Johnson | 14.45-15.00
Aerosol-Assisted Chemical Vapour Deposition of α-Fe_2O_3 *and* $BiFeO_3$ *as effective Photoanodes for Photoelectrochemical Water Splitting*

Katherine Encalada Flores, J.R. van Ommen, R. Kortlever | 15.00-15.15
Ultrathin Overlayers for Anode Protection in Offshore Green Hydrogen Production via Saline Water Electrolysis

Juliette Delbreuve, R. Chanson, D. Coutancier, F. Miserque, L. Artaud, I. Nuta, F. Rouillard, N. Schneider | -15.15-15.30
Innovative protective coatings prepared by Atomic Layer Deposition (ALD) and Direct Liquid Injection MOCVD (DLI-MOCVD) for Solid Oxide Electrolyzer Cells (SOEC) interconnects

Session PM_2.2 DIELECTRICS

Chair: **Alessio Lamperti** | Room “Coro di Notte”

Robert K. Grubbs, T. van Pelt, S. Nemeth, D. Cott, B. Groven, P. Morin, C Lockhart de la Rosa, G. Sankar Kar, J. Swerts | 14.30-14.45
Nucleation of ALD Grown Gate Dielectrics on WS_2 *using Low Temperature Oxygen Plasma Pretreatment*

Toomas Daniel Viskus, J. Merisalu, M. Otsus, J. Aarik, A. Kasikov, H. Mändar, L. Aarik, K. Kukli | 14.45-15.00
Resistive switching in hafnium-titanium-oxide thin films grown by atomic layer deposition

P. Dubreuil, U. Legallois, O. Gauthier-Lafaye, **Stephane Calvez** | 15.15-15.30
In-situ-monitored Chemical Vapor Deposition of silicon oxynitride layers

Jorden De Bolle, M. Granata, J. Steinlechner, J. Dendooven, C. Detavernier | 15.15-15.30
Deposition and Characterization of ALD Ta_2O_5 *Coatings for Gravitational Wave Detectors*

Session PM_2.3 MATERIALS FOR ENERGY: PHOTOVOLTAICS

Chair: **David Muñoz-Rojas** | Main Hall “Santo Mazzarino”

Invited: **Mariadriana Creatore** | 16.00-16.30
ALD layers and interfaces in metal halide perovskite-based photovoltaics

Maria Chiara Spadaro, H. Rabelo-Freitas, F. Salutari, A. Urbonavicius, T. Hagger, R. Lemerle, S. Escobar Steinvall, A. Fontcuberta i Morral, A. Dick K., J. Arbiol | 16.30-16.45
Detailed investigation of earth abundant nanostructures for PV

Francesca Lo Presti, A. L. Pellegrino, E. Milan, E. Radicchi, A. Speghini, G. Malandrino | 16.45-17.00
Structural and Luminescent Characterization of Eu-Doped BaF_2 Thin Films Deposited via MOCVD

Amr Ghazy, D. Spee | 17.00-17.15
Hight throughput solution towards roll-to-roll S-ALD coatings for packaging , batteries and flexible PV applications

Aubin Parmentier, D. Coutancier, S. Cros, T. Bejat, M. Fivel, J. Alvarez, J-P Kleider, D. Muñoz-Rojas, N. Schneider | 17.15-17.30
Study of gas diffusion mechanisms within ALD and SALD (Spatial ALD) thin films for the encapsulation of perovskite-based photovoltaic cells.

Session PM_2.4 INNOVATIVE PLASMA ASSISTED PROCESSES

Chair: **Maria Losurdo** | Room “Coro di Notte”

A. Dhara, A. Werbrouck, J. Li , **Tippi Verhelle**, M. Minjauw, J. Meersschaut, L. Henderick, J. Dendooven, C. Detavernier | 16.30-16.45
Strategy to produce boron-containing ALD thin films using a combined plasma approach

Chiara Maccato, E. Scattolin, D. Barreca, A. Gasparotto, L. Signorin, N. El Habra, A. Šuligo, U. Lavrenčič Štangar, G. A. Rizzi | 16.45-17.00
Controlled growth of nanostructured NiO by plasma assisted-chemical vapor deposition

Arthur de Jong, S.A. Peeters, W.M.M. Kessels, A.J.M. Mackus | 17.00-17.15
Tailored waveform biasing for precise ion-energy control during plasma-enhanced ALD of AlN

Maria Del Mar Rodriguez Robles, A. Crisci, M. Fivel, D.Muñoz-Rojas, A. Mantoux, M. Bonvalot, D. Bellet, E. Blanquet | 17.15-17.30
Protection of Transparent Electrodes based on metallic nanowires by nitrides deposited by Plasma-Enhanced ALD

Session AM_3.1 INNOVATIVE PROCESSES: SALD AND AREA-SELECTIVE DEPOSITION

Chair: **Maarit Karppinen**| Main Hall “Santo Mazzarino”

Invited: **David Muñoz-Rojas** | 8.30-9.00
New processes for the Spatial Atomic Layer Deposition (SALD) of functional materials

Mira Baraket | M. Plakhotnyuk, A. C. Varga, I. Kundrata, J.Bachmann | 9.00-9.15
Recent Advances for Spatial Atomic Layer Deposition Process: Microreactor Direct Atomic Layer Processing (μDALP™)

Hindrik de Vries, I. Aretz, J. Bolding, F. Souren | 9.15-9.30
Towards Low Temperature Spatial Atomic Layer Deposition of Moisture Barriers using a Synergystic Co-reactant Dosing Approach

Camilla Minzoni, C. Hain, K. Mackosz, Al. Figura-Jagoda, A. Szkudlarek, S. Klejna, M. Sikora, E. Kokkonen, P. Hoffmann, I. Utke | 9.30-9.45
Inherent Area-Selective Atomic Layer Deposition of Copper on Metal-Patterned Silicon Substrates

Benjamin Cossou, C. Descamps | 9.45-10.00
Evaluation of the Infiltration Capability Improvement for a Very Low-Pressure SiC CVI Process

A. Tsarapkin, K. Maćkosz, C.S. Jurredy, I. Utke, **Katja Höflich** | 10.00-10.15
Area Selective Chemical Vapor Deposition of Gold by Electron Beam Seeding

Silvia Mirallas García, G. Botta, A. Álvarez Yenes, M. Borraz Casanova, S. Azpeitia Coscarón, M. Knez | 10.15-10.30
Area Selective Infiltration of polymers with inorganics

Session AM_3.2 INNOVATIVE PROCESSESS II

Chair: **Anna Maria Coclite** | Room “Coro di Notte”

J. Lin, J. Connolly, **Ian M. Povey** | 9.00-9.15
Incorporation of Dopants into CVD and ALD grown MoS_2

A. M. V. L. Nayakom Mini, G. Botta, S. De la Rosa-García, S. Gómez-Cornelio, M. Knez, **Aranzazu Sierra-Fernández** | 9.15-9.30
Innovative Approaches to Coating Systems for Stone Heritage Conservation

Stefan Cwik, M. J. Aviles, S. M. Clarke, C. J. Hamel, A. V. Lyashenko, M. A. Popecki, J. W. Elam, T. Curtis, A. Tremsin, O. H. Siegmund, M. J. Minot | 9.30-9.45
Next generation ALD functionalization of lead-free high-gain microchannel plates for photomultiplier tubes

Jorge Luis Vazquez Arce, A. Bahrami, S. Lehmann, K. Nielsch | 9.45-10.00
Low Temperature Atomic Layer Deposition of (00l)-Oriented Elemental Bismuth

Pamburayi Mpofu, P. Promdet, H. Hafdi, J. Lauridsen, O. Alm, T. Larsson, E. Kokkonen, J. Schnadt, H. Pedersen | 10.00-10.15
Surface chemistry in the early growth stages of TiN ALD using operando APXPS

Hugo Patureau, T. Encinas, A. Crisci, F. Mercier, E. Gicquel, A. Mantoux, E. Blanquet | 10.15-10.30
Influence of different oxidants in the growth of Al_2O_3 *elaborated by atomic layer deposition on cellulose*

Session AM_3.3 MODELING
Chair: **Davide Barreca** | Main Hall “Santo Mazzarino”

Invited: **Gloria Tabacchi** | 11.00-11.30
An atomistic viewpoint on Chemical Vapour Deposition precursors, processes and applications

Wojciech Szmyt, L. Lapeyre, I. Utke | 11.30-11.45
Analytical Model for 3D Island Growth Mode in ALD

Wednesday, 04th June 2025

Cristiano Invernizzi, G. Tabacchi, R. Seraglia, M. Benedet, M. Roverso, C. Maccato, S. Bogialli, D. Barreca, E. Fois | 11.45-12.00
On the fragmentation of Ni(II) β-diketonate-diamine complexes as molecular precursors for NiO films: a theoretical and experimental investigation

Rosemary Jones, E. Kokkonen, J. Schnadt | 12.00-12.15
Advancing the operando study of ALD chemistry with time-resolved ambient pressure x-ray photoelectron spectroscopy

Michal Pecz, A. Seifertová, B. Hudec | 12.15-12.30
Experimental verification of kinetic growth model of ALD TiO_2 *using Titanium isopropoxide and water*

Session AM_3.4 FUNCTIONAL MATERIALS II
Chair: **Caroline E. Knapp** | Room “Coro di Notte”

Renee van Limpt, C.A.A. van Helvoirt, M. Lao, M. Creatore, M.N. Tsampas, M.A. Verheijen | 11.30-11.45
On the epitaxial growth in ALD Co_3O_4*- and NiO-based bilayers*

Juha Linjala, Y. Singh, G. C. Tewari, T. Tripathi, M. Karppinen | 11.45-12.00
Atomic layer deposition of crystalline NiS thin films from elemental sulphur

Andy Séguret, I. Jellal, M. Weber, H. Roussel, I. Gélard, H. Okuno, L. Rapenne, E. Sarigiannidou, E. Monroy, V. Consonni | 12.00-12.15
ALD of epitaxial Ga_2O_3 *thin films on c-plane sapphire*

Mahtab Salari Mehr, L. Aarik, T. Jõgiaas, A. Kasikov, H. Mändar | 12.15-12.30
Atomic Layer Deposition of Hard Epitaxial $(Cr_{1-x}Al_x)_2O_3$ *Thin Films on Sapphire.*

Jussi Kinnunen, A. Philip, F. Gao, J. Karttunen, M. Utriainen | 12.30-12.45
Bottleneck-Effect on High Aspect Ratio ALD Thin-Film Conformality

Session AM_4.1 C/N-BASED MATERIALS

Chair: **Ivo Utke** | Main Hall “Santo Mazzarino”

Invited: **Henrik Pedersen** | 8.30-9.00
Conformal CVD of boron carbide onto carbon nanotubes

Catherine Marichy, T. Souvignet, B. Toury, C. Journet | 9.00-9.15
Investigation of the Chemical Vapor Deposition of Boron Nitride using borazine

Ana Álvarez-Yenes, V. O. Koroteev, M. Knez | 9.15-9.30
Low-Temperature Atomic Layer Deposition of Boron Nitride using the In-Situ Decomposition of Ammonium Carbamate

Laurent Souqui, S. Baserga, A. Hellgren, L. von Fieandt, P. Eklund | 9.30-9.45
Investigation of CVD-deposited $Ti_xW_{1-x}(C, N)$ *hard coatings for cutting tool applications*

Athina Tzavara-Roussi, V. van Steijn, J. R. van Ommen | 9.45-10.00
Boosting PEM electrolyser performance with niobium (oxy)nitride coating using Plasma-Enhanced ALD

Z. Ahaliabadeh, **Sanaz Zarabi**, Z. Wang, P. Liljeroth, O. Laitinen | 10.00-10.15
Process Optimization of ALD TiN Thin Films for Superconducting Applications Using TFS-200 Reactor

Silke A. Peeters , A. A. de Jong , G. F. K. Krieger , R. Bărbuceanu , W. M. M. Kessels , H. C. M. Knoops | 10.15-10.30
Mitigating blistering in TaC_xN_{1-x} *prepared by plasma-enhanced ALD for quantum technologies*

Session AM_4.2 MATERIALS FOR ENERGY: PHOTONICS

Chair: **Graziella Malandrino** | Main Hall “Santo Mazzarino”

Invited: **Angel Barranco** | 11.00-11.30
Remote Plasma Assisted Vacuum Deposition (RPAVD) of Multifunctional coatings for Photonic and Energy Applications

Kaat Lambrecht, B. Tam, Z. Lin, A. Kafizas | 11.30-11.45
Plasmonic Pd-TiO_2 *Coatings via Aerosol Assisted Chemical Vapour Deposition for Enhanced Photocatalytic NOx Remediation*

Dan M. Mason, A. L. Johnson | 11.45-12.00
Lithium Sulfide (Li_2S_x*) Deposition through Aerosol-Assisted Chemical Vapour Deposition for Battery Materials*

Boris Hudec, M. Pecz, A. Seifertová, P. P. Sahoo, M. Precnerová, K. Fröhlich | 12.00-12.15
Analysing growth behaviour of low temperature ALD ZnO films on meso-porous Si/Gr battery anodes for improved performance

EUROCVD & ALD 24

Poster Session - Monday, 2nd June 2025

P01 | P. Liu, A. Makarova, S. Turishchev, **Vladimir Sivakov**; *Nanoengineering of tin-based coatings using nanostructured silicon matrix*

P02 | P. Liu, A. Makarova, S. Lippmann, , K. Freiberg, D. C. Grinter, P. Ferrer, S. Turishchev, **Vladimir Sivakov**; *Volcano-like effect at the nanoscale: efficient oxygen exchange at the Si/SnO$_2$ interface*

P03 | Kalani Ostermeijer, E. A. Pidko, J. R. van Ommen; *Copper's Cozy Blanket – Even Metals Need Comfort*

P04 | Aditya Chalishazar, A. Dhara, M. M. Minjauw, E. Solano, F. Munnik, C. Detavernier, J. Dendooven ; *ALD of Zinc Phosphate films with Tuneable Structure and Stoichiometry*

P05 | Vanessa Spanò, M. Barcellona, G. Gautier, T. Defforge, B. Le Borgne, and M.E. Fragalà; *Characterization of TiO$_2$ layer ALD deposited onto porous 4H-SiC fabricated by Electrochemical Etching*

P06 | Y. Aviziotis, E. D. Koronaki, A. G. Boudouvis, Z. Georgiopoulou, M. Vasilopoulou, **Dimitris Davazoglou**; *Chemical Vapour Deposition of Silicon Films on Tungsten filaments*

P07 | Naida El Habra, F. Visentin, F. Russo, A. Galenda, A. Famengo, M. Rancan, M. Losurdo, L. Armelao; *Supported MOCVD TiO$_2$ Thin Films Grown on Modified Stainless-Steel Mesh for Sensing Applications*

P08 | Weihua Wu, R. van de Kruijs, A. Y. Kovalgin; *Film thickness non-uniformity and crucial role of water dosage for atomic layer deposition of yttrium oxide from cyclopentadienyl yttrium precursor*

P09 | Helle-Mai Piirsoo, P. Krížik, Š. Nagy, B. Hudec; *Functionalization of Metal Powders with Atomic Layer Deposition in Fluidized Bed Reactor for Nanocomposites Fabrication*

P10 | Blagoy Blagoev, B. Georgieva, K. Starbova, N. Starbov, I. Avramova, K. Buchkov, P. Tzvetkov , V. Mehandzhiev; *Characterization of Submicron Ni-, Co-, and Fe-Doped ZnO Fibers Fabricated by Electrospinning and Atomic Layer Deposition*

P11 | A. Figura-Jagoda, **Mateusz Marzec**, S. Klejna, C. Minzoni, K. Mackosz, C. Hain, A. Szkudlarek, I. Utke, E. Kokkonen, M. Sikora; *In situ AP-XPS study of Cu ALD from copper (II) hexafluoroacetylactonate*

P12 | Vincent Sallet, A. Perez, B. Mundet, B. Ballesteros, J. Santiso, C. Sartel, E. Chikoidze, Z. Chi, J.M. Chauveau, Y. Zheng; *Transmission Electron Microscopy Analysis of Ga$_2$O$_3$ Thin Films Homoepitaxially Grown on (010), (-201) and (001) Substrates*

P13 | F. Lo Presti, A. L. Pellegrino, **Luca Pulvirenti**, G. G. Condorelli, D. Muñoz-Rojas, G. Malandrino; *Combine SALD/MLD Synthesis and XPS Characterization of ZnO-Europium Complex Bilayers for Enhanced Photovoltaic Applications*

P14 | Dominik Hartmann, P. Dreher, J. Pilz, J. Patscheider; *A Novel Microwave ECR Plasma System for DamageFree PEALD*

P15 | Sara Baserga, L. Von Fieandt, P. Eklund; *On the properties of tungsten carbonitride as a function of the composition*

P16 | Harish Parala, J.-L. Wree, S. Beer, A. Devi; *Metalorganic chemical vapor deposition of ferromagnetic metal sulfides*

EUROCVD & ALD 24

Poster Session - Monday, 2nd June 2025

P17 | **Alessandro Cataldo**, A. Li Bassi, A. Lamperti; *Study of chemical-physical properties of* HfO_2 *thin layers from TEMAHf and* H_2O *in thermal ALD at low temperature down to 100 °C*

P18 | C. Miersch, S. Seidel, J. Heitmann, **Franziska C. Beyer**; *Influence of different ALE process sequences on the electrical performance of gate recessed AlGaN/GaN HEMTs*

P19 | **Gamze Kökbudak Baldan**, S. Lancaster, U. Schroeder, T. Mikolajick, R. Alcala; Advances in a PEALD TiN Deposition Process at Temperatures below 300°C for Ferroelectric Hafnium Zirconium Oxide Integration

P20 | **Beatriz De Morais Batista**, D. Samélor, J. Esvan, C. Charvillat, H. Vergnes, B. Caussat, A. Sekkat; *Exploring the Role of Process Parameters in oCVD-PEDOT: Toward Tailored Material and Functional Properties*

P21| **Jan Leithäuser**, M. Becker, P. Klement, S. Chatterjee; *Enhancing Thermochromic Smart Windows via Low-Temperature ALD of Rutile Titanium Dioxide*

P22 | **Daniel Hiller**, S. Shams, S. Shah, S. Schneider, I. Ratschinski, M. Venzke, P. Hönicke; *Atomic Layer Deposition of Metal Oxide Monolayers on Thermal Oxide for SiO2-Modulation Acceptor Doping*

P23 | **Pentti Niiranen**, D. Lundin, H. Pedersen ; *Pulsed e-CVD of iron*

P24 |**Galaad Arnould Dallet**, L. Imhoff, G. Combe, P. Buirey, B. Huynh, I. Pochard, M. C. Marco de Lucas; *Pulsed heating atomic layer deposition of* TiO_2 *thin films on soft substrates*

P25 | **Bhavesh Chavan**, R. Kortlever, J. R. van Ommen; Advanced Functional *Coatings via Atomic Layer Deposition for High-Performance Proton Exchange Membrane Water Electrolysis*

P26 | **Federica Scardaci**, F. Lo Presti, R. Valiente, G. Malandrino; *MOCVD as a Versatile Tool for Luminescent Europium-Doped* GdF_3 *and GdOF Thin Films*

P27 | **Anna Lucia Pellegrino**, F. Lo Presti, G. Malandrino; *From engineering of heterobimetallic Na-Y precursor to MOCVD synthesis of* $NaYF_4$ *thin films*

P28 | **Laura Salamone**, F. Lo Presti, M. Bombaci, G. Malandrino; *MOCVD of ferrite materials: a novel approach to promising photoelectrodes for water splitting*

P29 | **Chiara Maccato**, M. Benedet, D. Barreca, A. Gasparotto, G. A. Rizzi, G. Pagot, V. Di Noto, L. Zeng, E. Olsson; Cu_xO*-gCN-*TiO_2*-Au (x=1,2) nanosystems as efficient platforms for photoactivated hydrogen evolution*

P30 | S. Panisset, K. Kreka, D. Jauffres, **Carmen Jiménez**, A. Tarancón, M. Burriel; $LaPrNiO_4^{+\delta}$ *films grown by MOCVD as oxygen electrode thin films*

P31 | **Ji Liu**, M. Nolan, H. H. Sønsteby; *DFT Simulations on the Precursor Ligand Exchange Mechanism for Depositing* $BaTiO_3$

P32 | **Ettore Fois**, C. Maccato, D. Barreca, C. Invernizzi, G. Tabacchi; *Modelling Surface -OH Defects on NiO (100) thin films fabricated via CVD Routes*

P33 | I.G. Aviziotis, **Giorgios Gakis**, E.D. Koronaki, D. Davazoglou, A.G. Boudouvis; *A hybrid computational model for the design of CVD processes. The case of silicon deposition on filaments*

EUROCVD & ALD 24

Poster Session - Monday, 2nd June 2025

P35 | Takahiro Takahashi, A. Morishita, T. Ozawa; *Automated modeling of reaction mechanisms for batch CVD processes based on multi-objective optimization algorithms*

P36 | Hervè Rouch, D. Longo; *MOCVD modelling for large scale deposition oh wide HTS tapes*

P37 | Joe Goodall, A. L. Johnson; *Development of a New Class of Precursors for Atomic Layer Deposition of Tin(II) Oxide (SnO)*

P38 | Oliver W. S. Clark, A. L. Johnson; *Development of Novel Precursors for Atomic Layer Deposition of Tin(II) Oxide (SnO)*

P39 | Macsen Laming, A. L. Johnson; *Bismuth Precursors for the Atomic Layer Deposition of p-Type* Bi_2O

P40 | Jaroslav Charvot, R. Zazpe, J. Rodriguez Pereira, J. Macák, F. Bureš; *Phosphorus Precursors for ALD of Metal Phosphides*

P41 | Laurianne Ornella Matchim-Fondjo, A. Tacnet, S. Daniele; *Design of new fluorinated aminoalkoxide ligands for MOCVD alkali niobate precursors: Synthesis, characterizations, and thermal validation*

P42 | Claudia Barbagallo, F. Lo Presti, A. L. Pellegrino, G. Malandrino; *Novel heterobimetallic precursors for fluoride-based functional materials*

P43| Stijn Engelaar, F. Lo Presti, A. L. Pellegrino, G. Malandrino; *Innovative β-diketonate Alkali Metal Precursors for Lead Free Piezoelectric Crystals*

P44 | Mari Napari, A. Y. Bykov, H. Cossey, A. V. Zayats; *Atomic layer deposition of subwavelength epsilon-near-zero indium tin oxide thin films for nonlinear photonics*

P45 | Kham Niang, X. Chen, B. Peek, O. Clark, J. Goodall, P. Chalker, A. Johnson, A. Flewitt; *Atomic Layer Deposited P-type Tin Monoxide Thin Film Transistors for low power CMOS Applications*

P46 | Kim Jaehyeok, H. Yoon, I. Sohn, T. Nakazawa, Y. Ohshima, H. Sato, J. Yoo, S. Eom, S. Chung, H. Kim; *Bandgap Tunable* $RuS_{2x}Se_{2-2x}$ *Thin Films for Near-Infrared Photodetector by Chemical Vapor Deposition and Post-Sulfurization Process*

P47 | Johnny Azzi, H. Roussel, S. Ortega, F. Ducroquet, J. L. Deschanvres; *Advancing Transparent Conductive Oxides:* $SrNbO_3$ *Thin Films by Pulsed Liquid Injection MOCVD*

P48 | Catarina Matos, I. Santos, M. Cortinhal, J. Deuermeier, P. Barquinha; *Atomic Layer Deposition of Aluminium-doped Zinc Oxide Thin-Films for Electrodes in Transparent TFTs*

P49 | Mikhail Mirushchenko, I. Labbaveettil, L. Basyrova, S. Margueron, F. Lo Presti, G. Malandrino, V. Astié, J.M. Decams, A. Bartasyte; *Growth Optimisation of* $KNbO_3$, $KTaO_3$ *and* $KTa_{1-x}Nb_xO_3$ *thin Films by DLI-CVD*

P50 | Zoé Viéron-Lepoutre, G. Larger, S. Margueron, V. Astié, J.M. Decams, N. Findling, L. Largeau, A. Bartasyte; *Challenges and Advances in Ultra-Thin* $LiNbO_3$ *Film Deposition by DLI-CVD for Beyond-5G Acoustic Resonator Integration*

***P51 | Sylwia Klejna**, A. Figura-Jagoda, C. Minzoni, K. Mackosz, C. Hain, M. Marzec, A. Szkudlarek, M. Sikora, E. Kokkonen, I. Utke; Surface chemistry of copper (II) hexafluoroacetylactonate studied by DFT and APXPS for copper ALD*

Session AM_1.1 INNOVATIVE PROCESS I

Monday 2nd June 2025 | 9.15-10.30

Chair: **Graziella Malandrino** | Main Hall “Santo Mazzarino”

Organic-component-engineering of novel inorganic-organic ALD/MLD thin film structures for next-generation applications

Maarit Karppinen

Department of Chemistry and Materials Science, Aalto University, FI-00076 Aalto, Finland
e-mail: maarit.karppinen@aalto.fi

The combined ALD/MLD (atomic/molecular layer deposition) technique involving both inorganic and organic precursors allows us to fabricate novel functional hybrid materials not readily accessible through any other fabrication route.[1] In particular, by innovatively choosing the organic precursor, novel hybrid materials can be developed.

From the fabrication point of view, the most critical requirements for the organic precursor are its sufficient volatility and reactivity towards the inorganic precursor under the deposition conditions used. Then, in the resultant hybrid thin-film material, the fundamental role of the organic component is to act as a structural linker between the metal species. By smart design of the backbone and its reactive groups, the organic precursor may be used as a structure-directing agent even towards the in-situ growth of porous metal-organic framework (MOF) crystal structures.[2]

To widen the horizon further, we have been enthusiastic to look for much more active roles for the organic component. By on-demand tailoring the chemistry of the organic precursor, the organic backbone can be chosen to contribute to, *e.g.*, electrical conductivity, light absorption, or bioactivity of the metal-organic hybrid, or inorganic-organic multilayer structures built by combining the ALD/MLD cycles with additional ALD cycles.[3] Most excitingly, the organic moiety could act as a stimuli-active switcher (*e.g.* UV-active azobenzene) if properly embedded within the inorganic matrix to respond to changes in the chemical or physical environment.

In this presentation, I will discuss the recent efforts of my research group and our collaborators to develop novel metal-organic thin-film materials and inorganic:organic multilayer structures through organic-component engineering towards (i) redox-active Li-organic materials for potential microbattery application,[4,5] (ii) photoluminescence coatings relevant to bioimaging or solar cell applications,[6,7] (iii) inorganic:organic superlattice thin films for tailored electrical and thermal transport properties relevant to thermoelectrics,[8] and (iv) flexible magnetic multilayer structures with UV-Vis switchable organic layers for future spintronics applications.[9]

References

1. J. Multia & M. Karppinen, Atomic/molecular layer deposition for designer's functional metal-organic materials, *Adv. Mater. Interfaces* **9**, 202200210 (2022).
2. J. Multia, D.E. Kravchenko, V. Rubio-Giménez, A. Philip, R. Ameloot & M. Karppinen, Nanoporous metal-organic framework thin films prepared directly from gaseous precursors by atomic and molecular layer deposition: implications for microelectronics, *ACS Appl. Nano Mater.* **6**, 827 (2023).
3. M. Heikkinen, R. Ghiyasi & M. Karppinen, Layer-engineered functional multilayer thin-film structures and interfaces through atomic and molecular layer deposition, *Adv. Mater. Interfaces* **2024**, 2400262 (2024).

4. J. Multia, J. Heiska, A. Khayyami & M. Karppinen, Electrochemically active in-situ crystalline lithium-organic thin films by ALD/MLD, *ACS Appl. Mater. Interfaces* **12**, 41557 (2020).
5. J. Heiska, M. Nisula, E.-L. Rautama, A.J. Karttunen & M. Karppinen, Atomic/molecular layer deposition and electrochemical performance of dilithium 2-aminoterephthalate, *Dalton Transact.* **49**, 1591 (2020).
6. A. Ghazy, M. Lastusaari & M. Karppinen, Excitation wavelength engineering through organic linker choice in luminescent atomic/molecular layer deposited lanthanide-organic thin films, *Chem. Mater.* **35**, 5988 (2023).
7. Ghazy, J. Ylönen, N. Subramaniyam & M. Karppinen, Atomic/molecular layer deposition of europium-organic thin films on nanoplasmonic structures towards FRET-based applications, *Nanoscale* **15**, 15865 (2023).
8. R. Ghiyasi, M. Milich, J. Tomko, P.E. Hopkins & M. Karppinen, Organic-component dependent thermal conductivity reduction in ALD/MLD grown ZnO:organic superlattice thin films, *Appl. Phys. Lett.* **118**, 211903 (2021).
9. A. Philip, Y. Zhou, G.C. Tewari, S. van Dijken & M. Karppinen, Optically controlled large-coercivity room-temperature thin-film magnets, *J. Mater. Chem. C* **10**, 294 (2022).

Biomimetic Metallosaccharides: A Novel Approach to Multifunctional Coatings for Biomedical and Food Safety Applications

K. Ashurbekova[1], I. Saric Jankovic[2], M. Knez[1,3,*]

[1] CIC nanoGUNE BRTA, San Sebastian, Spain
[2] University of Rijeka, Faculty of Physics, Croatia
[3] Ikerbasque, Basque Foundation for Science, Spain
e-mail: m.knez@nanogune.eu

In nature, the intricate interplay between organic and inorganic components often results in materials with exceptional properties. One such example is the cuticle of arthropods, where chitin, a polysaccharide, combines with proteins and minerals to form a robust, multifunctional exoskeleton. Inspired by these natural structures, we developed an approach to creating artificial cuticles with enhanced bioactivity.

We have successfully developed and optimized a new strategy for growing coatings of artificial cuticles consisting of organic chitinoid and hybrid chitin-based films from the vapor phase using Molecular Layer Deposition (MLD). This innovative approach has led to the introduction of a new family of materials: metallochitins. These novel materials synergistically combine the properties of organic chitinoid polymers and inorganic metal oxides, exploiting a biomimetic approach to achieve unique functionalities.

The synthesis of these metallochitins was accomplished through a solvent-free vapor-phase MLD process, coupling sugar-type monomers with metalorganics. This method allows for precise control over the composition and structure of the resulting hybrid films, enabling tailored properties for specific applications.

We focused on two metallochitins: alumochitin and titanochitin. In vitro assessments of these materials against S. aureus and E. coli bacteria revealed strong antimicrobial properties, partly selective, ion dependence on the metal involved. The selectivity allows for designing specialized antimicrobial surfaces by optimizing various metal-saccharide combinations.

Beyond their antimicrobial properties, we extensively investigated the biocompatibility of our metallochitins using human embryonic kidney (HEK293T) cells and human fibroblasts. Both alumochitin and titanochitin demonstrated excellent biocompatibility, promoting greater cell proliferation than reference coverslips. Notably, titanochitin outperformed pure titania in promoting HEK293T cell growth, suggesting a synergistic effect between the chitin and titanium components within the hybrid film. Conversely, fibroblasts showed a preference for aluminum-based surfaces. These findings highlight the potential to selectively regulate cell proliferation by manipulating surface charge and metal composition, underscoring the versatility of metallochitins as biomaterials.

The dual functionality of our metallosaccharides - deterring bacterial adhesion while facilitating controlled cell growth - positions them as highly valuable materials for a wide range of applications. In the field of tissue engineering, these coatings could promote the growth of desirable cell types while preventing bacterial contamination, potentially revolutionizing the development of scaffolds and implants. For medical device fabrication, our metallochitins offer a promising solution to the persistent challenge of device-associated infections, potentially reducing the need for systemic antibiotics and improving patient outcomes. For food safety, these coatings could be applied to food processing equipment or packaging materials to inhibit bacterial growth and extend shelf life without compromising food quality.

Non-thermal gas-assisted focused electron beam induced deposition of metals and insight gained from thermal ALD and CVD mechanisms

I. Utke[1,*] , P. Swiderek[2,*], K. Höflich[3,4,*], J. Jurczyk[1,5], K. Madajska[6], P. Martinović[2], I.B. Szymańska[6,*]
[1] Empa - Swiss Federal Laboratories for Materials Science and Technology, 3602 Thun, Switzerland
[2] Institute for Applied and Physical Chemistry (IAPC), University of Bremen, 28359 Bremen, Germany
[3] Ferdinand-Braun-Institut gGmbH, Leibniz-Institut für Höchstfrequenztechnik, 12489 Berlin, Germany
[4] Helmholtz-Zentrum Berlin für Materialien und Energie, 14109 Berlin, Germany
[5] AGH University of Science and Technology Kraków, 30-059 Kraków, Poland
[6] Nicolaus Copernicus University in Torun, Faculty of Chemistry, 87-100 Toruń, Poland
* ivo.utke@empa.ch, swiderek@uni-bremen.de, katja.hoeflich@fbh-berlin.de, pola@umk.pl

Non-thermal gas-assisted focused electron beam induced deposition (FEBID) is the only direct-write technique that can fabricate nanostructures with arbitrary shape and dimensions down to the sub-10 nm regime, see fig 1. It is by concept spatially selective (only proceeds where the finely focused electrons impinge on the sample covered with physisorbed molecules being continuously supplied) and thus is minimally invasive, maskless, one-step, and shape flexible. Mechanistically, the non-thermal electron-induced adsorbate dissociation processes of the frequently used metalorganic precursors molecules is complemented by thermally activated surface kinetics (adsorption, desorption, surface diffusion of the intact molecules and their fragments). The complex interplay of them is still relatively poorly understood and thus far from being optimized with respect of deposited material composition, see fig. 1. Yet, impressive demonstrators of 2D and 3D FEBID nanoprinted structures have been already achieved in the fields of nanophotonics, nanomagnetics, and functional scanning probe tips [1].

Here, we review in a comparative manner the performance and the underlying chemical reactions of surface deposition processes, namely, chemical vapour deposition (CVD), atomic layer deposition (ALD), and FEBID itself [2]. The knowledge gained in CVD and ALD as related surface deposition techniques will help us to understand the spatially selective chemistry occurring in FEBID. Fundamental surface and gas-phase studies provide insight to electron-induced chemistry and desorption of precursor fragments. Specific emphasis is put on the type of the ligands and their different behaviour under thermal, surface-related, and electron-induced processes.

The comprehensive overview includes reactive environments and purification approaches as these may provide valuable information on the design of novel precursors. The evaluation of the precursor and process performance comprises group 10 elements (Ni, Pd, Pt), group 11 elements (Cu, Ag, Au), W, Co, Fe, Ru, Rh, and Ir to represent a general guide towards future developments in FEBID, see Fig. 2. These may not only rely on the design novel compounds but also on optimized FEBID deposition strategies inspired by ALD and CVD.

[1] V. Reisecker, R. Winkler, H. Plank, A Review on Direct-Write Nanoprinting of Functional 3D Structures with Focused Electron Beams. Adv. Funct. Mater. 2024, 34 (46), 2407567. https://doi.org/10.1002/adfm.202407567.
[2] I. Utke, P. Swiderek, K. Höflich, J. Jurczyk, K. Madajska, P. Martinović, I.B. Szymańska, Coordination and organometallic precursors of group 10 and 11: FEBID of metals and insight gained from chemical vapour deposition, atomic layer deposition, and fundamental surface and gas phase studies; Coord. Chem. Reviews 445 (2021), 213851. https://doi.org/10.1016/j.ccr.2021.213851.
[3] H. Plank, R. Winkler, C.H. Schwalb, J. Hütner, J.D. Fowlkes, P.D. Rack, I. Utke, M. Huth, Focused Electron Beam Based 3D Nanoprinting for Scanning Probe Microscopy: A Review, Micromachines 2020, 11, 48; doi:10.3390/mi11010048

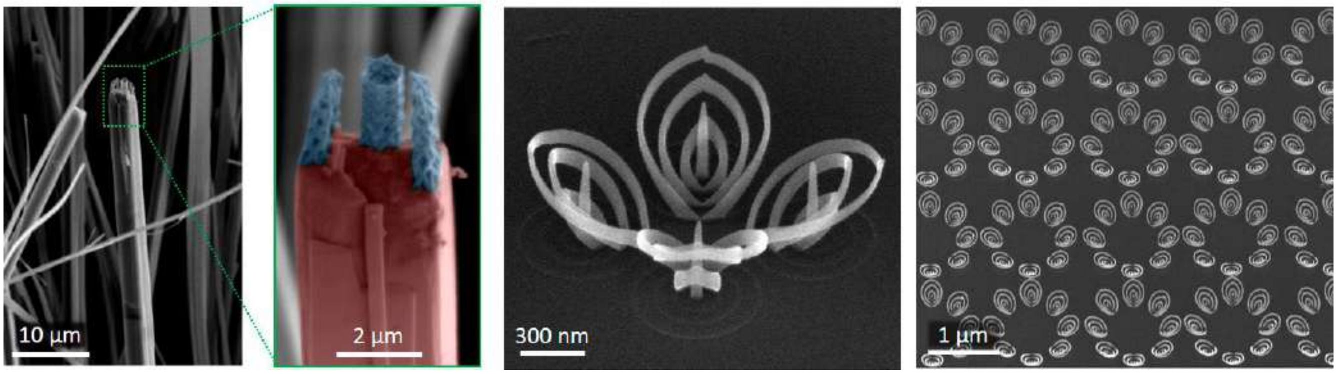

Fig. 1: Demonstration of FEBID's minimally invasive nature and spatial resolution (blue: FEB deposit on red: mineral whisker). Images with flower demonstrate 3D FEBID nanoprint potential and scalability [3].

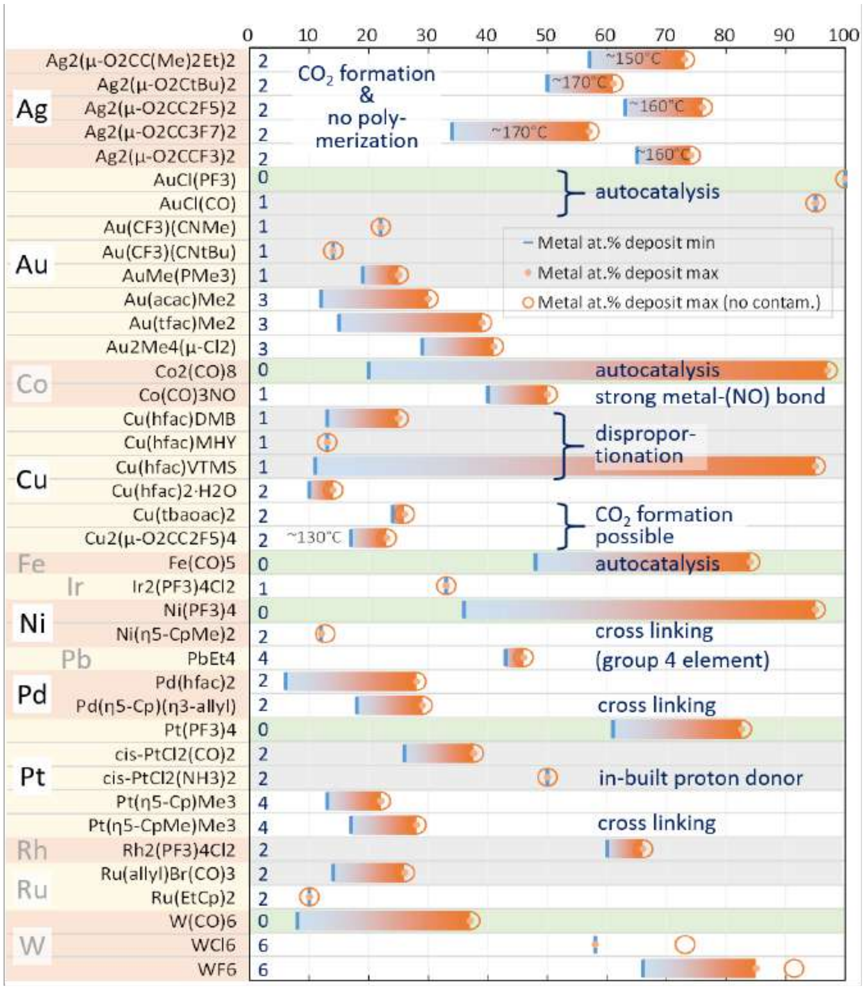

Fig. 2: Metal content (horizontal top axis) obtained by gas-assisted FEBID with various precursors. The metal content range reported in literature is given as blue-orange bars. The metal oxidation state is noted vertically next to the precursor names. Precursors are highlighted with ligands being all neutral (light green bars), mixed neutral & ionic (grey bars), or fully ionic (white). Specific FEBID conditions and precursor ligand peculiarities are noted within the graph. Note that the large ranges of FEBID metal content for the individual precursors found in literature point to thermal effects which can assist the non-thermal electron-induced adsorbate dissociation mechanism in the final formation of the FEB deposited material [2].

ALD for medical applications

J.R. van Ommen[1,*], **A.Y. Rwei**[1], **A.G. Denkova**[2], **V. van Steijn**[1]
[1]Delft University of Technology, Chemical Engineering, the Netherlands
[2] Delft University of Technology, Radiation Science & Technology, the Netherlands
e-mail: j.r.vanommen@tudelft.nl

While nanotechnology could potentially play an enormous role in the medical field, it is often not straightforward to make nanostructured materials for pharma and medical devices in a scalable manner. We will show that atomic layer deposition (ALD) can be used to make nanostructured materials for several health applications in a scalable way.

Modifying the surface of grains of powder – as used for example in dry powder inhalers for treating respiratory diseases – can increase the powder flowability while also adding a controlled release functionality. In this way, the powder is used more effectively and side-effects in the patient can strongly be reduced [1,2].

In targeted radionuclide therapy a major hurdle is the dependence on a very limited number of nuclear reactors worldwide to produce these radioisotopes. ALD can provide a way to prepare radionuclide generators, that can be placed in hospitals, providing on-site and on-demand supply. By modifying sorbent particles for isotope separation by ALD, we have made the first step towards 99Mo/99mTc radionuclide generators [3]. And by Lu ALD on nanoparticles, we have taken a step in producing 177Lu radionuclides [4].

We also apply ALD to other substrates than powders. Polydimethylsiloxane (PDMS) is a widely used material for lab-on-a-chip and organ-on-a-chip devices. It is very versatile, but the drawback is its low stability, especially when in contact with organic solvents. We will show that modifying the surface with ceramic oxide using ALD is a way to get much more durable microfluidic devices, usable for a range of health applications [5,6].

Summarizing, we can conclude that making nanostructured materials using ALD has a range of applications in the medical field. The combination of nanoprecision and scalability gives it a lot of potential.

References

[1] D. Zhang, D. La Zara, M.J. Quayle, G. Petersson, J.R. van Ommen, and S. Folestad, *ACS Applied Bio Materials*, **2**, 1518 (2019).

[2] D. La Zara, F. Sun, F. Zhang, F. Franek, K. Balogh Sivars, J. Horndahl, S. Bates, M. Brännström, P. Ewing, M.J. Quayle, G. Petersson, S. Folestad, and J.R. van Ommen, *ACS Nano*, **15**, 6684 (2021).

[3] J. Moret, J. Alkemade, T.M. Upcraft, E. Oehlke, H.T. Wolterbeek, J.R. van Ommen, and A.G. Denkova, *Applied Radiation and Isotopes*, **164**, 109266 (2020).

[4] J.L.T.M. Moret, M.B. Griffiths, J.E. Frijns, B.E. Terpstra, H.T. Wolterbeek, S.T. Barry, A.G. Denkova and J.R. van Ommen, J. R., *Journal of Vacuum Science & Technology A: Vacuum, Surfaces, and Films*, **38**, 022414 (2020).

[5] A. Santoso, M.K. David, P.E. Boukany, V. van Steijn, and J.R. van Ommen, *Chemical Engineering Journal*, **498**, 155269 (2024).

[6] A. Santoso, S. Trapp, I.M. Blommestein, S. Saedy, J.R. van Ommen, R.M. de Kruijff, and V. van Steijn, *Separation and Purification Technology*, **354**, 128865 (2025).

Session AM_1.2 PRECURSORS DESIGN I

Monday 2nd June 2025 | 11.00-12.30

Chair: **Elisabeth Blanquet** | Main Hall “Santo Mazzarino”

The First Non-Pyrophoric Precursor for the Low Temperature Deposition of Metallic Aluminium

Caroline E. Knapp[1]*

[1] Department of Chemistry, University College London, 20 Gordon Street, London, WC1H 0AJ
e-mail: caroline.knapp@ucl.ac.uk

The advancement of microelectronics on flexible plastic substrates has sparked a search for precursors capable of depositing conductive features at low temperatures.[1,2] However, there is limited research on aluminum (Al), as it is typically deposited using pyrophoric and highly air- and moisture-sensitive AlH_3 etherates or aminates.[3] By carefully selecting ligands, it is possible to enhance stability while still enabling the deposition of the desired materials. In this work, we have developed an aluminum complex that can be converted to Al(0) without a reductant at 100°C.

Our approach employed a multi-step synthetic strategy utilizing β-ketoiminate (acnac) bidentate ligands, $[Al(R\text{-acnac})_2Cl]$ (where R = Me, Et, ^{i}Pr, Ph, or Mes, **1**-**5**), which served as precursors to create aluminum hydride complexes: the polymeric amidoalane $Li[AlH_2(^i\text{Pr-Hacnac})AlH_3]_n$ (**6**) and the imidoalane cluster $[AlH_2AlH_2(\text{N-Mes})_3(AlH_2\text{–}Li(Et_2O)_2)_2]$ (**8**). When heated under vacuum at 100°C, complex **8** decomposes into aluminum metal, as confirmed by XRD, TEM, and XPS. This represents the first example of a low-temperature route to metallic aluminum using non-pyrophoric precursors.[4]

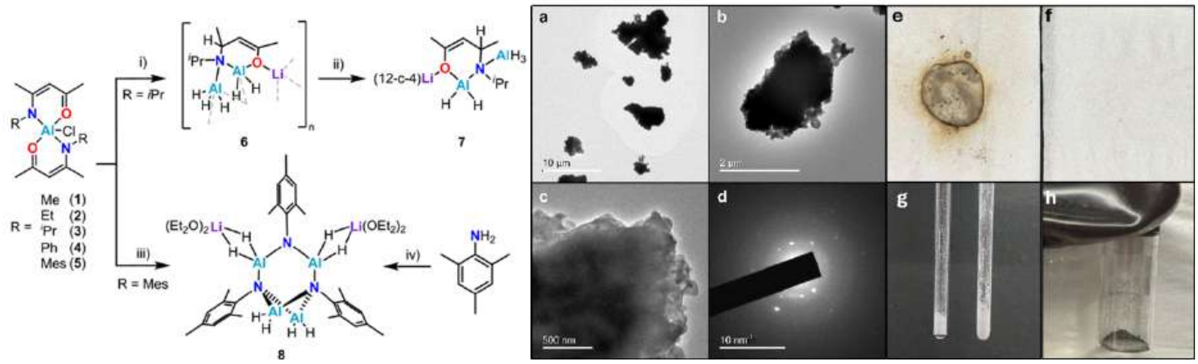

Fig. 1. Left: Synthesis of complexes **1**-**8**. Right: a-c TEM micrographs of dispersed Al powder from **8** heated under vacuum; d) selected area electron diffraction (SAED) of dispersed Al powder from **8** heated under vacuum; e) tissue after addition of hexane solution of DMEAA; f) and tissue after addition of a toluene solution of cluster **8**; g) precursor **8** before heating and h) grey powder containing metallic aluminium.

References

[1] S. P. Douglas, S. Mrig, and C. E. Knapp, *Chemistry–A European Journal*, **27**, 8062-8081 (2021).
[2] S. Mrig, M. A. Bhide, Y. Zhou, N. Staton, J. Wang, S.P. Douglas, H. R. Tinker, K.L. Mears, C. M. Bakewell and C. E. Knapp, *Small Methods*, **7**, 2300038 (2023)
[3] C. Knapp, E. N. de Faria, S. Douglas, S. Mrig, L. Santoni, D. Wilson, *Preprint on Research Square, Nature Portfolio,* (2025) https://doi.org/10.21203/rs.3.rs-5544055/v1
[4] S. P. Douglas, and C. E. Knapp, *ACS Appl. Mater. Interfaces*, **12**, 26193 (2020).

Understanding the decomposition mechanisms of the bis(2-dimethylamino propoxy) copper (II) precursor: total vapour pressure measurement using Kndsen effusion method

I. Nuta[1*], S. Fadloun[2], T.Mourrier[3], A.Mantoux[1], E.Blanquet[1]
[1] SIMaP, Univ. Grenoble Alpes, CNRS, Grenoble INP, 38000 Grenoble, France
[2]SPTS Technologies, 38330 Montbonnot St Martin, France
[3]CEA LETI, 38000 Grenoble, France
[*]e-mail: ioana.nuta@grenoble-inp.fr

The increased performance of integrated circuits (speed, power consumption) and their multidisciplinary nature, with the integration of heterogeneous functions, have been made possible by the evolution of interconnections and the emergence of TSVs: Through-Silicon Vias. Their micron-sized dimensions require metallization adapted to copper deposition, in particular by means of a so-called “seed layer” which acts as a conductive film needed to initiate the electroplating reaction for filling the TSVs, ensuring the routing of the electrical signal through the chip[1-4]. It is in this context that chemical deposition, and in particular MOCVD (Metal-Organic Chemical Vapor Deposition), is becoming a high-potential candidate for the metal coating of structures with complex geometries.

The success of metal thin film deposition by MOCVD is closely linked to the properties of the molecular precursors used. In general, precursors are chosen on the basis of their volatility and their ability to decompose into the desired material under an appropriate temperature regime. On the market many compounds readily available but they are not sufficiently volatile to make them suitable for CVD applications. Thus, prediction of their volatility linked to ligands and their molecular structure is much sought-after in order to determine the suitability of these compounds for the targeted application and processing conditions. This explains the importance of methods for determining the vapor pressure of a potential precursor for chemical thin-film deposition, as well as its optimum vaporization temperature.

Sublimation enthalpies can be determined by a number of techniques, most commonly by vapor pressure measurements using methods such as Knudsen effusion, TGA (Thermogravimetric Analysis) and DSC (Differential Scanning Calorimetry).

This work is devoted to characterizing the bis(dimethylamino-2-propoxy) copper (II) molecule as known as Cu(dmap)2 (Figure 1) as Cu precursor for MOCVD[5].

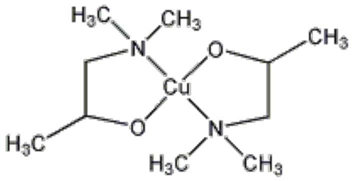

Figure 1. Bis(dimethylamino-2-propoxy) copper (II) molecule; $C_{10}H_{24}CuN_2O_2$, CAS 185827-91-2; Molar mass =267.86 g/mol

First, we will evaluate the vapor pressure of this precursor in order to determine its thermodynamic properties using the Knudsen method. We will then analyze the thermal stability of this compound, by means of a chemical composition analysis. By monitoring the decomposition of the molecular precursor via its loss of mass, we can determine its saturation vapor pressure. As a first step, we will determine the vapor pressure of the molecular precursor Cu(dmap)2: Bis(dimethylamino-2-propoxy)copper(II), min. 97%, from two different suppliers. The aim is to verify the properties of the molecule, while avoiding the specific synthesis methods used by each supplier.

The supplier of “Batch 1” Cu(dmap)2 gave us a vapour pressure value of Pvap = 6.67 Pa at 70°C. Our experimental point at 70°C gives a similar value, Pvap = 8.68 Pa. Its vapour pressure increases progressively with temperature. Our experimental point at 70°C indicates a similar value, Pvap = 8.68 Pa. Its vapour pressure increases progressively with temperature. Batch 2” of Cu(dmap)2 shows lower vapour pressure values than ‘Batch 1’, over the whole temperature range studied. Every precaution has been taken to ensure that all these measurements are carried out under the same conditions.

This work was carried out as part of the IRT Nanoelec program,a part of a joint project between CEA-Léti Minatec (Grenoble), SPTS Technologies (Newport, UK) and SIMaP (CNRS, Grenoble).
IN acknowledge for the French government grant managed by the Agence Nationale de la Recherche under the France 2030 program- reference ANR-22-PEXD-0017.

References

[1] T. Mourier, S. Minoret, S. Fadloun, L. Djomeni, S. Maitrejean, S. Burgess, A. Price, C. Jones, A. Roule, L. Vandroux, *Low temperature MOCVD TiN barrier deposition for high aspect ratio TSVs : A solution for 3D integration*, Additional Conferences (Device Packaging, HiTEC, HiTEN, and CICMT), 2013, 001322-001342, 10.4071/2013DPC-wp12, (2013).
[2] L. Djomeni, T. Mourier, S. Minoret, S. Fadloun, J.-P. Barnes, D. Rouchon, S. Burgess, A. Price, L. Vandroux, D. Mathiot, *Analysis of High Aspect Ratio through Silicon via (TSV) Diffusion and Stress Impact Profile during 3D Advanced Integration*, ECS Transactions, 61, 219, 10.1149/06103.0219ecst, (2014).
[3] L. Djomeni, T. Mourier, S. Minoret, S. Fadloun, F. Piallat, S. Burgess, A. Price, Y. Zhou, C. Jones, D. Mathiot, S. Maitrejean, *Study of low temperature MOCVD deposition of TiN barrier layer for copper diffusion in high aspect ratio through silicon vias*, Microelectronic Engineering, 120, 127-132, https://doi.org/10.1016/j.mee.2013.11.010, (2014).
[4] J.-P. Barnes, L. Djomeni, S. Minoret, T. Mourier, J.-M. Fabbri, G. Audoit, S. Fadloun, *Focused ion beam time-of-flight secondary ion mass spectroscopy tomography of through-silicon vias for 3D integration*, Journal of Vacuum Science & Technology B, 34, 10.1116/1.4947463, (2016).
[5] S. Fadloun, *Copper deposition by MOCVD for high form factor through silicon vias for 3D integration (fr. Etude d'un procédé de dépôt de cuivre par MOCVD pour la réalisation de vias traversants à fort facteur de forme pour l'intégration 3D)*, 2019GREAI075, Université Grenoble Alpes, https://theses.hal.science/tel-02475687, (2019).

Development of Precursors for Atomic Layer Deposition of p-Type Oxides

A. L. Johnson
Department of Chemistry, University of Bath, BA2 7AY, UK
e-mail: chsalj@bath.ac.uk

Owing to the tunable properties, high stability, and standardized fabrication process, metal oxides have become key materials in almost every electronic and energy application. In particular, oxide semiconductors possessing band gaps of 1–4 eV with controllable carrier densities and high mobilities have potentials to overcome cost, performance, and process limitations of semiconductors such as Si and GaAs.

A critical obstacle in the current development of thin film transistor (TFT)-based oxide electronics is the absence of good p-type oxide semiconductors; well-known p-type oxides such as NiO and Cu_2O are poor in performance or stability when compared to n-type counterparts such as ZnO, In_2O_3, and Ga_2O_3. Because of this deficiency, practical implementations TFT circuits using oxide semiconductors are confined to unipolar (NMOS) architectures. Development of high-performance p-type components would greatly expand the application area of oxide semiconductors by permitting, for example, energy efficient devices or sensors with new functionalities, as complementary (CMOS) architectures would be possible.

The fundamental reason underlying the scarcity of p-type oxides is well understood; firstly, valence bands of oxides are low in energy, and, therefore, holes are easily compensated by defects like oxygen vacancy and ubiquitous hydrogen, resulting in the low p-type dopability. Secondly, the valence band maximum mainly consists of localized oxygen 2p-orbitals, which leads to a large hole effective mass. Despite this challenge materials such as tin(II) oxide (SnO) and bismuth(III) oxide (Bi_2O_3) and materials containing these oxides have emerged as possible p-type semiconductor materials, for the fabrication of thin film transistors (TFTs) and complementary metal oxide semiconductors.

Atomic layer deposition (ALD) of SnO[1-4] and Bi_2O_3[5-6] has been reported for a range of ligand systems in conjunction with H_2O. However, many of the ‘state-of-the-art’ ALD processes suffer with chemical vapor deposition (CVD) pathways or contamination of higher oxide materials or metal, negatively impacting the electronic properties. Here, we report on our continuing work on the development potential ALD precursors for SnO and Bi_2O_3, with their synthesis, thermal stability and volatility discussed. The performance of devices deposited using the varying precursors, and delivery modes will also be discussed.

This work was supported by the EPRSC and Pragmatic Semiconductor.

References

[1] S. H. Kim, I. Baek, D. H. Kim, J. J. Pyeon, T. Chung, S. Baek, J. Kim, J. H. Han and S. K. Kim, *J. Mater. Chem. C.*, **5**, 3139-3145 (2017).

[2] a) A. Mameli, J. D. Parish, T. Dogan, G. Gelinck, M. W. Snook, A. J. Straiton, A. L. Johnson, A. J. Kronemeijer, Adv. Mater. Interfaces, 2022, 9, 2101278, b) D. E. Gomersall, K. M. Niang, J. D. Parish, Z. Sun, A. L. Johnson, J. L. MacManus-Driscoll and A. J. Flewitt, *J. Mater. Chem. C.*, **11**, 5740-5749 (2023).

[3] J. Heo, A. S. Hock and R. G. Gordon, *Chem. Mater.*, **22**, 4964-4973 (2010).

[4] N. Huster, R. Ghiyasi, D. Zanders, D. Rogalla, M. Karppinen and A. Devi, *Dalton Trans.*, **51**, 14970-14979 (2022).
[5] T. Hatanpää, M. Vehkamäki, M. Ritala and M. Leskeläa, *Dalton Trans.*, 2010,**39**, 3219-3226.
[6] M Vehkamäki, T. Hatanpää, Mikko Ritala and M. Leskeläa *J. Mater. Chem.*, 2004,14, 3191-3197

Ru metal CVD: The role of the precursor

J. Obenlüneschloß,[2] N. Huster,[2] D. Zanders,[2] H. Parala[1], M. Gock,[3] M. Unkrig-Bau,[3] A. Devi[1,2,4,5]
[1]Leibniz Institute for Solid State and Materials Research, Dresden, Germany
[2]Inorganic Materials Chemistry, Ruhr University Bochum, Germany
[3]Global Business Unit Heraeus Precious Metals, Heraeus Deutschland GmbH & Co. KG, Germany
[4]Dresden University of Technology, Germany
[5] Fraunhofer Institute for Microelectronic Circuits and Systems, Germany

e-mail: a.devi@ifw-dresden.de

As interconnects continue to scale down, resistance-capacitance (RC) delays have become a significant challenge for copper-based technologies. Copper interconnects require diffusion barriers to prevent intermixing with surrounding dielectrics, whereas ruthenium offers a promising alternative due to its superior resistance to electromigration and minimal scaling effects.[1] Ruthenium demonstrates high conductivity even at low film thicknesses, making it a suitable candidate for next-generation interconnects.[2] Interconnects current research focuses on the integration of ruthenium interconnects into advanced devices. To fully leverage its advantageous properties, precise control over ruthenium film thickness, purity, surface roughness, and low resistivity is essential. Vapor-phase deposition techniques, particularly chemical vapor deposition (CVD) and atomic layer deposition (ALD) are preferred for achieving these requirements. The choice of chemical precursors is critical, as they directly influence the deposition rate, film quality, and process efficiency.

To assess the influence the precursor choice has on the desired metal thin film, herein a comparative study on the CVD of Ru films is presented. Two different precursors namely, ruthenium(II) carbonyl acetamidinate [Ru(CO)$_2$(AMD)$_2$] and ruthenium(II) diazadienyl cymene [Ru(DAD)(Cym)] are investigated and compared for Ru film deposition.[3–4] The film properties, including structure, morphology, composition, and resistivity, were systematically analyzed employing XRD, XPS, RBS/NRA, SEM, and compared. Results revealed that both the deposition temperature and the choice of co-reactants, such as reducing agents like ammonia, had a significant impact on the resulting film characteristics. Notably, the use of reductively enhanced deposition chemistry proved to be a highly effective strategy in CVD, enabling the growth of high-quality ruthenium thin films with low resistivities.

This work was supported by Global Business Unit Heraeus Precious Metals, Heraeus Deutschland GmbH & Co. KG, Hanau, 63450, Germany.

References

[1] M. Hayes, M. A. Jenkins, J. Woodruff, D. F. Moser, C. L. Dezelah, J. F. Conley, *J. Vac. Sci. Technol. A* ***39***, 052402 (2021).
[2] Y. Kotsugi, S.-M. Han, Y.-H. Kim, T. Cheon, D. K. Nandi, R. Ramesh, N.-K. Yu, K. Son, T. Tsugawa, S. Ohtake, R. Harada, Y.-B. Park, B. Shong, S.-H. Kim, *Chem. Mater.* ***33***, 5639–5651 (2021).
[3] D. Zanders, J. Obenlüneschloß, J. Wree, J. Jagosz, P. Kaur, N. Boysen, D. Rogalla, A. Kostka, C. Bock, D. Öhl, M. Gock, W. Schuhmann, A. Devi, *Adv. Mater. Interfaces*, 2201709 (2022).
[4] R. G. Gordon, H. Li, T. Aaltonen, B. S. Lim, Z. Li, *Open Inorg. Chem. J.* ***2***, 11–17 (2008).

Tris(dimethylamino)phosphine as Phosphorous Precursor for Metal Phosphate ALD

R. Blomme[1], A. Chalishazar[1], L. Henderick[1], F. Munnik[2], J. Meersschaut[3], M. Minjauw[1], C. Detavernier[1], J. Dendooven[1]
[1]CoCooN Research Group, Department of Solid State Sciences, Ghent University, Belgium
[2]Helholtz-Zentrum Dresden-Rossendorf, Institue of Ion Beam Physics and Materials Research, Dresden, Germany
[3]Imec, Heverlee, Belgium

e-mail: rpblomme.blomme@ugent.be

Metal phosphates are highly promising materials with a broad range of applications, including lithium ion battery electrode coatings and water-splitting catalysts. Although various types of metal phosphate have been deposited using different deposition techniques, comparatively little is known for their deposition using ALD. Most existing ALD processes utilize trimethylphosphate (TMP) as the phosphorous precursor, with only a few alternative precursors reported. Moreover, the effect of variations in phosphate structure (e.g., orthophosphate, pyrophosphate) on functional properties is often not discussed.

In this work, we focus on a novel precursor, tris(dimethylamino)phosphine (TDMAP), which has so far been reported in two ALD studies [1-2], with the publication by Su et al. providing a comprehensive characterization of an ALD process for magnesium phosphate. To confirm the viability of TDMAP, additional studies are essential. Here, aluminum phosphate was chosen for characterization, employing TDMAP, O_2 plasma, and trimethylaluminum (TMA). TMA was selected due to its status as the most extensively studied ALD precursor, minimizing the uncertainties associated with introducing a new metalorganic precursor.

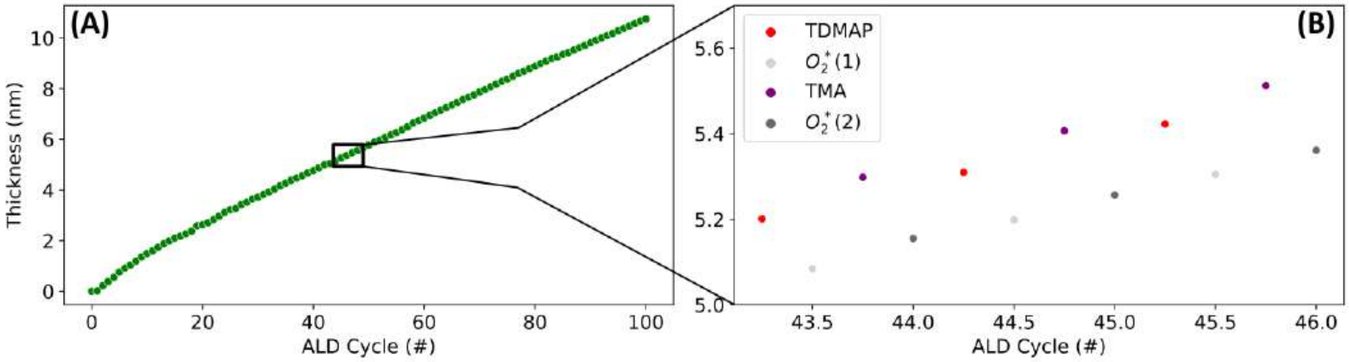

Figure 1 (A) In-situ ellipsometry data of the TDMAP-O_2-plasma-TMA-O_2-plasma process showing a linear trend. (B) Zoomed-In section showing the effect of each precursor step on the thickness of the film. The TDMAP and TMA add to the thickness while the O_2-plasma co-precursor steps detract from it.

By adopting a similar process sequence — TDMAP-O_2 plasma-TMA-O_2 plasma — a new process for depositing aluminum phosphates was successfully developed. This is evidenced by the ALD-like growth shown in Figure 1. The growth-per-cycle (GPC) of the material was determined to be 0.11 nm/cycle, and the composition of the as-deposited material was identified as $Al_1P_{0.51}O_{2.9}$.

By dividing our process into two distinct steps — PO (TDMAP-O_2 plasma) and AlO (TMA-O_2 plasma) — and increasing the relative number of PO cycles, the overall composition of the material could be tailored to incorporate more phosphorous. This approach allows for greater control over the type of phosphate material being deposited, ranging from phosphorous-doped metal oxides to ortho- or pyrophosphates.

The functionality of the material was evaluated using a known application of aluminum phosphate materials: their function as coating materials to enhance the long-term lifespan of batteries [3]. To conduct this test, very thin layers of the 1:1, 1:3, and 1:6 (AlO:PO) materials were deposited onto a TiO_2 thin film electrode. The results of the electrochemical experiments are presented in Figure 2. The data indicate the dependency of the performance on the phosphate structure and show the existence of an optimal phosphorus content for this application.

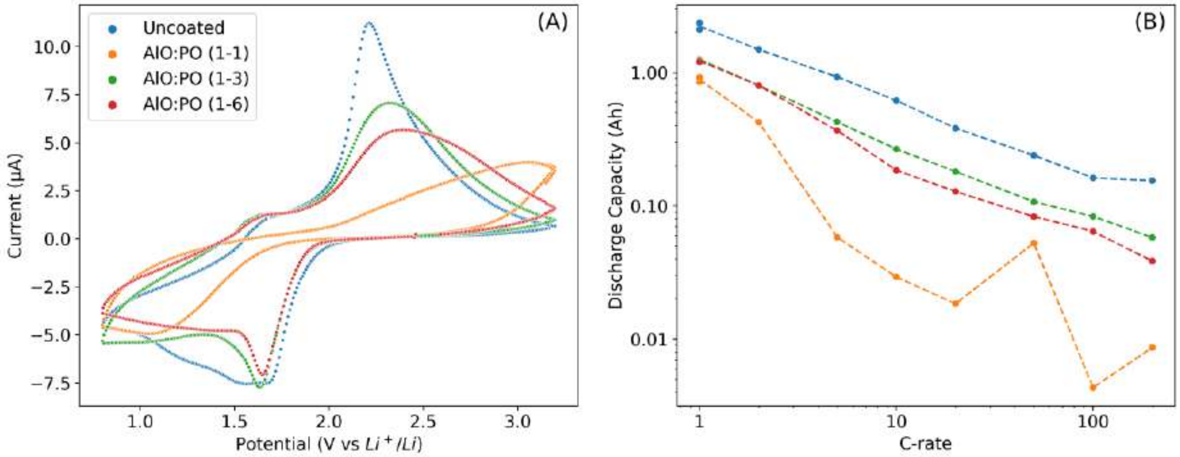

Figure 2 (A) Cyclic Voltammetry scans of TiO_2 materials coated with thin aluminum phosphate ALD films deposited with different AlO:PO ratio's. (B) Discharge capacities of the different films for different C-rates (1C = charging speed equal to the capacity of the battery).

This work shows that the library of metal phosphate ALD processes can be further extended and that optimization of the processes and the resulting material is essential to obtain optimal performance.

This work was supported by the Special Research Fund BOF of Ghent University (GOA-01G01019, Starting Grant 01N14319) and L.H. acknowledges FWO for a postdoctoral research grant (1254324N).

References

[1] V.E. Strempel et al., *Journal of Vacuum Science and Technology A*, **34**, 01A135 (2015).
[2] J. Su et al., *Chemistry of Materials*, **31**, 5566-5575 (2019).
[3] L. Henderick et al., *ACS Applied Materials and Interfaces,* **12**, 25949-25960 (2020).

Session PM_1.1 PIEZOELECTRICS

Monday 2nd June 2025 | 14.00-15.30

Chair: **Sven Van Elshocht** | Main Hall “Santo Mazzarino”

Advances and challenges in growth of $LiNbO_3$ thin films for acoustic and photonic devices

A. Bartasyte[1,2,3], **Z. Vieron-Lepoutre**[1], **N. Scheibel**[1,2], **G. Larger**[1,4], **V. Astié**[5], **N. Findling**[2], **L. Largeau**[2], **C. David**[2], **S. Margueron**[1], **and J.-M. Decams**[5]
[1]Institute FEMTO-ST, Université Marie et Louis Pasteur, ENSMM, Besançon, France
[2]C2N, Université Paris-Saclay, CNRS, Palaiseau, France
[3]Institut Universitaire de France
[4]Exail, Besançon, France
[5]Annealsys, Montpellier, France
e-mail: ausrine.bartasyte@femto-st.fr

Over the past five decades, the single crystals and thin films of $LiNbO_3$ (LN) and $LiTaO_3$ (LT) have been intensively studied for their outstanding acoustic, electro-optical, pyroelectric and ferroelectric properties. Today, single crystals of $LiNbO_3$ are considered in electro-optics as equivalent to silicon for microelectronics. In addition, about 70% of radio frequency (RF) filters, including those for mobile phones, using surface acoustic waves, are manufactured from these single crystals of LN and LT. LN and LT materials in the form of thin films preserving the crystalline properties of the bulk material, are necessary for the development of the new generation of high frequency and/or broadband and/or tunable frequency RF filters and integrated photonic devices suitable for the fifth generation (5G-6G) of infrastructures/networks/communications [1]. Currently, LN and LT thin films are fabricated from single crystals through top-down methods such as polishing (film thickness > 400 nm) or crystal ion slicing (300 nm < film thickness < 1 µm) and wafer bonding techniques. The polishing steps in top-down LN film fabrication induce difficulties in achieving uniform & controlled film thickness (≥ 3 % across the 6'' wafer), leading to inaccuracies in device response and irreproducibility making challenging their implementation for industrial-scale devices and requiring time consuming trimming steps.

The direct growth of LN films could offer better thickness control and homogeneity (≤ 1%), reduced costs in line with the ability to produce thicknesses < 250 nm overcoming limitations inherent in ion-slicing and polishing methods and to fabricate resonators with frequencies up to 24 GHz. The first reports on the growth of LN films appeared in the 70's [1]. Although LN films have been fabricated by different techniques, many electrical and electro-optical properties reported were not comparable to those of LN single crystals [1]. In general, the fabrication of high-quality alkaline niobate films is hindered by the difficulty to control the loss of volatile alkali metal oxides and consequently the composition and physical properties of the films. LN phase exists over the large compositional range (46.5 - 50.5 mol% of Li_2O) and LN physical and compositional properties are extremely dependent on the Li_2O nonstoichiometry [1]. Thus, the Li composition within the films must be controlled with precision 0.2 mol% to obtain reproducible physical properties (such as coercive field, acoustic velocity, K2, etc.) acceptable for the industrial applications [1]. The control of Li_2O stoichiometry and homogenous composition distribution are in particular difficult by means of physical deposition methods (pulsed laser deposition (PLD), RF sputtering, etc.) due to increased volatility at high vacuum conditions and scattering processes during the expansion regime of Li ions in the plasma [1]. Homogenous composition of such films can be much easier adjusted by changing the ratio between different element precursors in the case of chemical deposition methods. Additionally, Li is a very light element, and its composition is difficult to measure by direct analysis methods. In most of literature reports, authors claimed about the single phase and even stoichiometric films using compositional analysis methods with precision not better than 10% [1].

At FEMTO-ST, the state-of-the-art control/tuning/measurement of Li nonstoichiometry in deposited LN films were addressed for the first time and the stoichiometry homogeneity of <0.05 mol% /reproducibility of high-quality LN films at 4'' wafer scale (never demonstrated before) was attained by direct liquid injection (DLI) CVD in collaboration with Annealsys [2]. The Li content in the films is adjusted roughly by adjusting the Li/Nb ratio in the precursors and then the stoichiometry is finely tuned by varying other deposition conditions. Nearly stoichiometric LN films were deposited for the first time [2]. CVD growth also assured highly homogeneous thickness on the wafer scale. The epitaxial growth of LN films with unique orientations in the substrate plane (necessary for guided wave applications) in the case of X, Y, and Z orientations (according to IEEE convention) was optimized. The X and Z orientations are of particular interest for optical applications and the Y orientation for acoustic applications. In addition, we have succeeded in epitaxially growing new Y128° and Y52° orientations of LN with a single orientation in the plane of the substrate, this is the most used crystal orientation for RF SAW filters. We have shown an extremely high acoustical performance (K^2 up to 8% at 5.4 GHz) in SAW devices operating in the frequency range from 3.5 GHz up to 6 GHz [3].
In the literature, only the epitaxy/texture of the Z orientation, (not having good piezoelectric properties) on Si substrates has been successful. We have obtained the epitaxial growth of Y33°-LN (the orientation offering optimized electromechanical coupling for thickness mode) on the Si substrate using an intermediate layer of $SrTiO_3$ obtained by MBE [3]. Recently, we introduced high-overtone bulk acoustic wave resonators (HBARs) employing highly coupled Y33°textured LN thin films grown via DLI-CVD [4]. These films, with thicknesses ranging from 100 nm to 300 nm, achieved resonance frequencies between 4.5 GHz and 7.3 GHz [4]. The fabricated solidly mounted resonators (SMRs) based on grown LN films directly on sputtered (111) Pt and SiO_2/Ta_2O_5 mirror operated at 6.96 GHz and longitudinal mode presented K^2 of 6% [4]. Although, LN film orientation is defined only by the $LaNiO_3$ seed layer and any substrate/structure and electrode, able to withstand LN deposition conditions, can be used [5]. However, the Si substrate was replaced by sapphire substrate in these HBAR and SMR devices in order to reduce thermal stresses and to eliminate chemical interactions of LN with Pt adhesion layers (Ta, Ti, TiO_2) and SiO_2/Si. Further effort was done to stabilize the heterostructures based on grown LN layers, electrodes and Si substrates by introducing new adhesion layers for Pt electrode and by stress engineering. In order to bring epitaxial LN films towards the integrated photonic applications requiring single crystalline LN films on semiconductor platforms, the layer transfer process is under development. This includes epitaxial growth of LN films on LN substrates with sacrificial layer then bonding on freely chosen structure and liberation of LN film from the growth template by chemical etching.

This work was supported by the French RENATECH network and its FEMTO-ST technological facility and C2N micro nanotechnologies platform, the French national ANR project LINKS ANR-20-CE08-0025 and ANTARES ANR ANR-24-CE51-0541, and the graduate school EUR EIPHI contract ANR-17-EURE-0002.

References

[1] A. Bartasyte, S. Margueron, T. Baron, S. Oliveri, P. Boulet, Adv. Mater. Interfaces 1600998 (2017).
[2] Q. Micard et al., Proceedings IEEE IUS (2024).
[2] A. Almirall et al., Appl. Phys. Lett. 114, 162905 (2019).
[3] A. Bartasyte et al., Nanotechnology 35 (17), 175601 (2024).
[4] S. Boujnah et al., EFTF/IFCS, Toyama, Japan: IEEE, pp. 1–2, (2023) & Proceedings IUS (2024).
[5] A. Bartasyte, S. Kuprenaite, V. Astié, Layered solid element comprising a ferroelectric layer and a method for manufacturing the same, Patent EP20 305575 (2020).

Unraveling mechanisms to achieve singlecrystalline MoS_2 monolayer by metal organic chemical vapor deposition

I. Kandybka[1,2*], **P. Kumar**[2], **H. Medina Silva**[2], **B. Groven**[2], **A. Nalin Mehta**[2], **Y. Shi**[2,▲], **S. Banerjee**[2], **P. Morin**[2], **A. Delabie**[1,2*]

[1] KU Leuven, Department of Chemistry, Celestijnenlaan 200F, Leuven, 3001, Belgium
[2] imec, Kapeldreef 75, Leuven, 3001, Belgium
Current address ▲University of Science and Technology of China (USTC), School of Microelectronics
e-mail: iryna.kandybka@imec.be

Interest in 2D materials has been increasing over the years for various applications, and van der Waals epitaxy is proven to be a reliable method to deposit high-quality 2D monolayers. In this study, we present a method to achieve high-quality, single-crystalline MoS_2 monolayers using metal-organic chemical vapor deposition (MOCVD) with molybdenum hexacarbonyl ($Mo(CO)_6$) and dihydrogen sulfide (H_2S) on sapphire substrates at 1000°C. The MOCVD involves three simultaneous processes: sapphire surface morphological change (reorganization), MoS_2 growth, and domains (re)-crystallization (Figure 1). Sapphire surface reorganization during MOCVD does not affect the epitaxial relationship between bulk sapphire and MoS_2 crystals, though it can alter the shape of isolated crystals [1]. We can control MoS_2 growth kinetics by changing the metal precursor concentration, determining deposition rate and nucleation density. At concentrations of 0.6 ppm and lower, the adsorption rate is sufficiently low, allowing crystals to form the most favorable epitaxial alignment. As a result, a growth mode is enabled with the majority of MoS_2 isolated crystals oriented at 0° relative to the sapphire template, and minority at non-equivalent 60° rotation (so-called, twins). After the layer coalescence, recrystallization of 60° rotated grains within the closed 0° oriented monolayer happens during post-deposition annealing, provided that the majority of the layer is aligned in a single 0° orientation. The single-crystalline monolayers exhibit mobility as high as 48 $cm^2\ V^{-1}\ s^{-1}$, while the monolayers with the high grain boundary density demonstrate lower electrical performance. This study enhances the understanding of 2D TMD epitaxial growth on single-crystalline templates and demonstrates how optimizing MOCVD process conditions can achieve high-performance MoS_2 monolayers, applicable to other 2D materials.

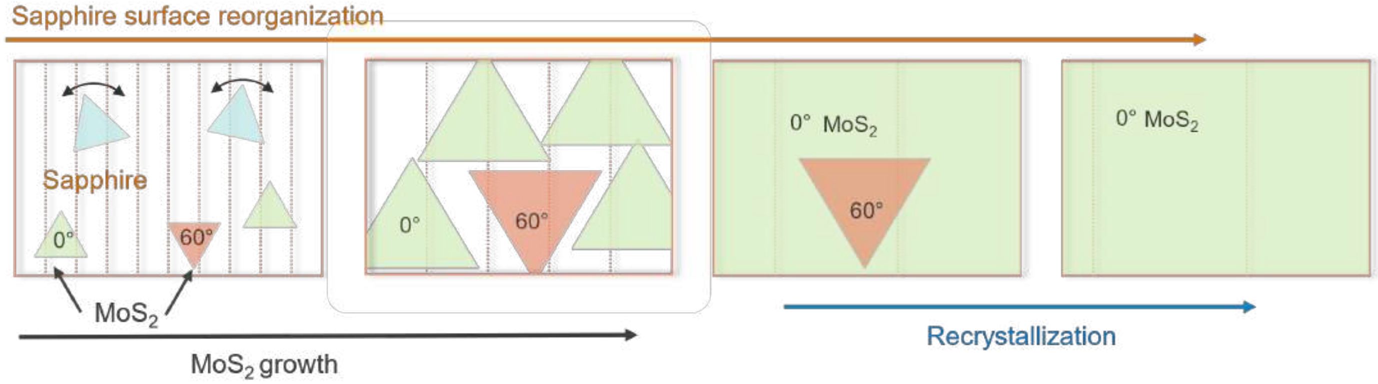

Fig. 1. The processes present during the MOCVD of MoS_2 monolayer on sapphire. Sapphire surface reorganization takes place thought the whole deposition process, however, does not affect the epitaxial alignment. The minimum energy orientations of MoS_2 towards sapphire are 0° (green) and 60° (red). When given enough time, the misoriented domains (blue) can reorient during the growth towards 0° or

60° orientation. After the layer coalescence, post deposition annealing enables recrystallization of the 60° rotated domains to form singlecrystalline MoS_2 monolater.

References

[1] I. Kandybka, B. Groven, H. Medina Silva, S. Sergeant, A. Nalin Mehta, S. Koylan, Y. Shi, S. Banerjee, P. Morin, A. Delabie, *ACS Nano*, **18**, 3173–3186 (2024).

Exploring Early-Stage ALD Growth Dynamics of LiNbO3 on NMC 811 Cathodes: An In Situ QCM Study for Artificial CEI Applications

Léo Lapeyre[1], Amit Sharma[1], Arnold Müller[3], Laszlo Pethö[1], Patrice Raynaud[2], Johann Michler[1], Ivo Utke[1]

[1] Empa, Feuerwerkerstrasse 39, CH3602 Thun, Switzerland
[2] PSI Center for Energy and Environmental Sciences, Paul Scherrer Institute, Villigen, Switzerland
[3] LAPLACE, Université de Toulouse, CNRS, INPT, UPS, 31062 Toulouse, France
e-mail: leo.lapeyreempa.ch

Atomic layer deposition (ALD) has emerged as cutting-edge technique for producing ultra-thin, conformal coatings, particularly on complex geometries such as Ni-rich cathodes making it a preferred method for fabricating artificial cathode-electrolyte interphase (CEI) layers to enhance the stability of high-energy-density lithium-ion batteries. Despite the widespread application of ALD, the fundamental understanding of its growth dynamics on battery materials remains limited, particularly in the early stages of film deposition, essential for nanometre-thick coatings.

In this study, we investigate the nucleation dynamics and early growth behaviour of lithium niobium oxide ($LiNbO_3$, LNO) on $LiNi_{0.8}Mn_{0.1}Co_{0.1}O_2$ (NMC811) cathodes using in situ quartz crystal microbalance (QCM) with NMC 811-coated QCM crystals, to achieve closer-to-application conditions, and employing complementary electron microscopy techniques. The results from Figure 1 reveal significant substrate inhibition and island growth during the initial ALD cycles (Fig. 1), leading to poor NMC 811 surface coverage at low ALD cycle number which implies limited protective efficiency. By analysing mass gain patterns from QCM, we determined the critical thickness for full film closure (island coalescence) to be approximately 15 nm. Transmission electron microscopy observations of LNO island coverage on NMC 811 supported the QCM study and provided a comprehensive view of the growth mechanism, enabling precise monitoring of surface coverage evolution, see Fig. 2. This critical threshold underscores the deviation from the ideal layer-by-layer growth paradigm commonly associated with ALD and highlights the strong influence of substrate-precursor interactions.

Further, we demonstrate that a tailored pulsing sequence with a 1Li:4Nb ratio effectively mitigates compositional gradients arising from the preferential adsorption of lithium precursor (LiO^tBu) over niobium precursor ($Nb(OEt)_5$) on the NMC 811 surface. This approach yields near-stoichiometric $LiNbO_3$ films with enhanced chemical homogeneity and uniformity.

Our findings emphasize the importance of optimizing ALD processes to address substrate-induced growth challenges, by providing a powerful method for optimizing ALD processes for NMC811 and other battery materials, enabling superior electrochemical performance and longevity in next-generation lithium-ion batteries.

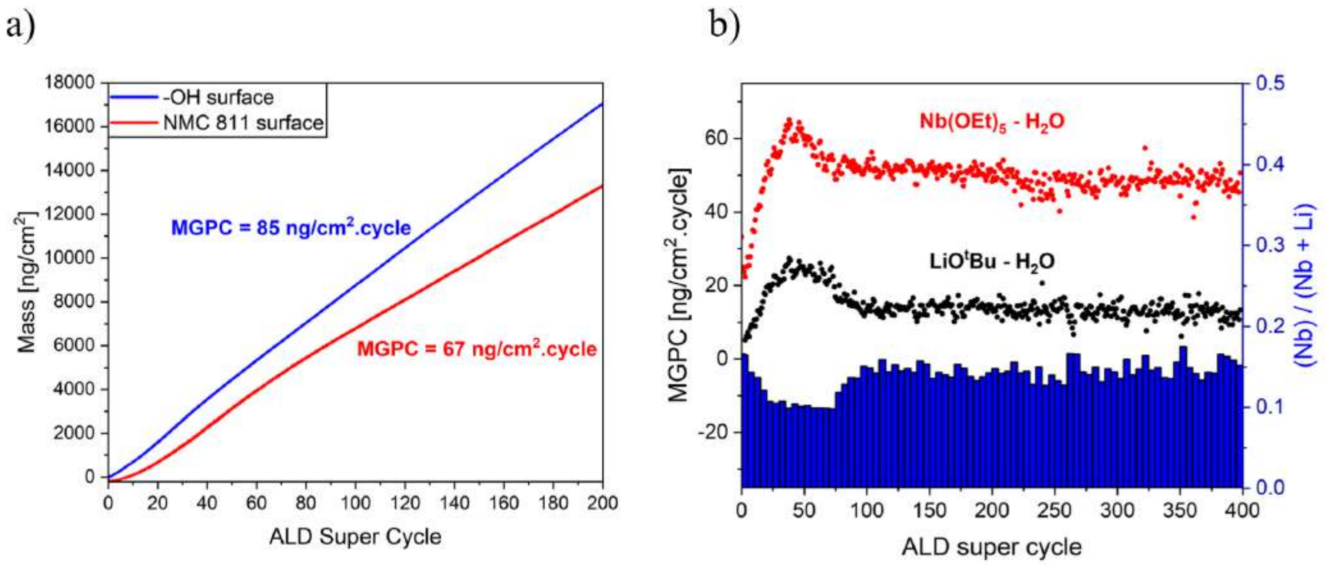

Fig.1 **a)** Deposited mass of LNO vs. ALD cycles for -OH terminated and NMC 811 surfaces. Displayed MGPC values were calculated from regions of linear growth, i.e. after 100 super cycles. MGPC stands here for mass gain per super cycle, i.e. a full LNO deposition super cycle. **b)** MGPC for the two sub-reactions on NMC 811 surface, extracted from mass evolution displayed in a). The bar plots describe the estimated cationic ratio averaged from intervals of 5 super cycles.

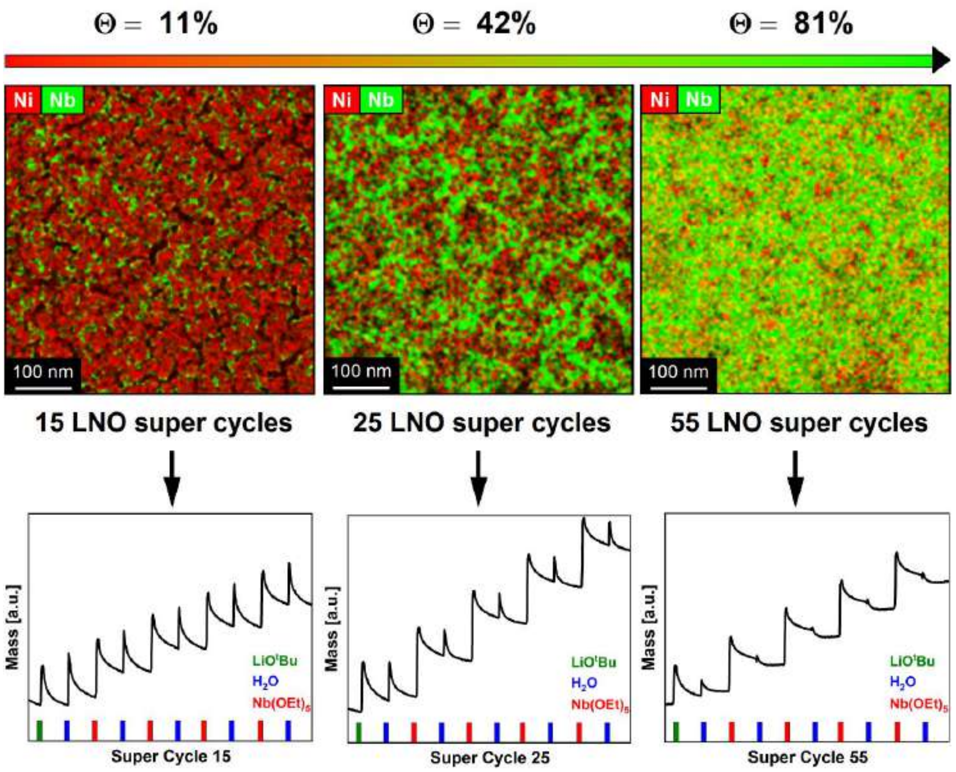
Θ = 11%
Θ = 42%
Θ = 81%
Ni
Nb
100 nm
15 LNO super cycles
25 LNO super cycles
55 LNO super cycles
Mass [a.u.]
LiO^{t}Bu
H$_2$O
Nb(OEt)$_5$
Super Cycle 15
Super Cycle 25
Super Cycle 55

Fig.2 TEM-EDX mapping of Nb (green) and Ni (red) signals representative of LNO and NMC 811 surfaces, respectively, for 15, 25 and 55 super-cycles of LNO. Note that the related QCM signal pattern changes with respect to LNO island surface coverage Θ extracted from TEM-EDX mapping.

Strain Modulation and Piezoelectric Response in Chemical Vapor Deposition Grown MoS_2 Monolayers

Sabir Hussain[1*], Lynette Keeney[1*]

[1] Tyndall National Institute, University College Cork, Lee Maltings Complex, Dyke Parade, Cork T12 R5CP, Ireland
e-mail: sabir.hussain@tyndall.ie; lynette.keeney@tyndall.ie

Abstract: Two-dimensional (2D) materials have garnered considerable attention for their potential in developing miniaturized, multifunctional devices. Among them, monolayer molybdenum disulfide (MoS_2), a transition metal dichalcogenide (TMDC), stands out due to its semiconducting properties, with a direct bandgap, and inherent piezoelectricity arising from broken inversion symmetry. These unique characteristics make MoS_2 a promising candidate for next generation piezoelectric applications. Achieving self-limited growth in monolayer MoS_2 is challenging due to thermodynamic instability and kinetic factors that promote multilayer formation. Additionally, precise strain control is difficult because of the complexities in controlling strain distribution without compromising structural integrity. These limitations impede the optimization of monolayer MoS_2 for applications such as piezoelectric devices and strain-engineered electronics. Consequently, experimental demonstrations of piezoelectricity in monolayer TMDCs have been relatively limited. In this study, we investigate the self-limited growth of MoS_2 monolayers using liquid-phase edge epitaxy via chemical vapor deposition, focusing on how strain modulation during synthesis influences their piezoelectric properties. The thermal expansion mismatch between the sapphire supporting substrate and the MoS_2 monolayers induces biaxial tensile strain, leading to a distinctive strain pattern characterized by a three-fold, hierarchical and vein-like structure (Fig. 1a). This domain morphology is influenced by the combined effects of thermal strain and the intrinsic structure of the MoS_2 layers. We employ Raman spectroscopy, photoluminescence, X-ray diffraction, X-ray photoelectron spectroscopy, and atomic force microscopy-based techniques (Fig. 1b, c) to analyze the strain-induced response. This strain modulates the piezoelectric properties of the monolayer, by distorting the bond lengths and angles between Mo and S atoms, thereby inducing electric polarization. Piezoresponse force microscopy (PFM) reveals enhanced piezoelectric effects, offering new insights into the tunability of piezoelectric properties (Fig. 1d). The findings demonstrate that structural rippling and corrugation can induce significant flexoelectric effects, with piezoresponse values more than doubling those previously reported in the literature, particularly in regions experiencing elevated stress. These findings offer critical insights for TMDCs-based devices, which could enable advancements in energy harvesting, flexible electronics, actuators, nanogenerators and piezoelectric sensors.

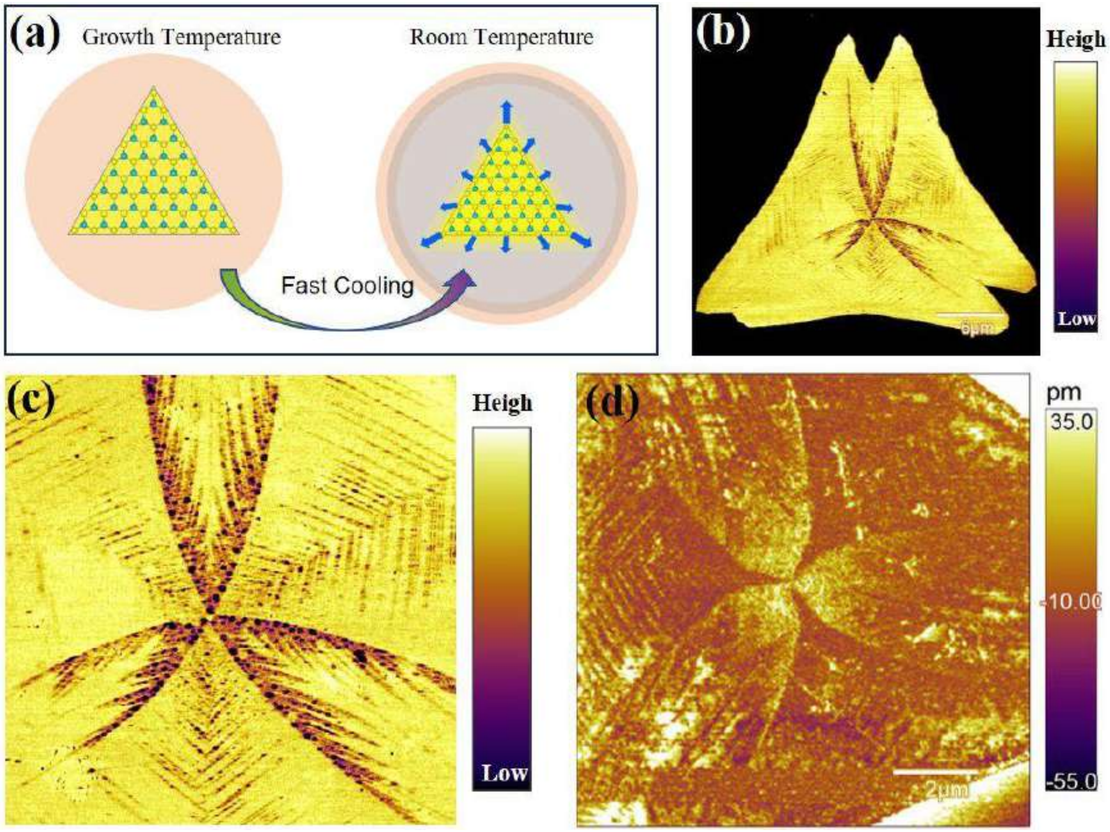
(a)
Growth Temperature
Room Temperature
Fast Cooling
(b)
Heigh
Low
6μm
(c)
Heigh
Low
(d)
pm
35.0
-10.00
-55.0
2μm

Fig. 1: (a) Schematic of the tensile strain generation through thermal expansion coefficient mismatch. (b, c) Lateral force microscopy with zoom-in images showing strain pattern inside the monolayer of MoS_2. (d) PFM image showing flexoelectricity response.

References

[1] S. Hussain, R. Zhou, Y. Li, Z. Qian, Z. Urooj, M. Younas, Z. Zhao, Q. Zhang, W. Dong, Y. Wu, X. Zhu, K. Wang, Y. Chen, L. Liu, and L. Xie, J. Am. Chem. Soc., **145**, 20, 11348-11355, (2023).

[2] S. Hussain, R. Xu, K. Xu, L. Lei, L. Meng, Z. Zheng, S. Xing, J. Guo, H. Dong, A. Liaqat, M. A. Iqbal, Y. Jun Li, Y. Sugawara, F. Pang, W. Ji, L. Xie, and Z. Cheng, Appl. Phys. Lett., **117**, 153102 (2020).

[3] D. Nandwana1 and E. Ertekin, J. App. Phys., **117**, 234304 (2015).

[4] W. Shi, Y. Guo, Z. Zhang, and W. Guo, J. Phys. Chem. Lett., **9**, 6841-6846 (2018).

Epitaxial $LiNbO_3$ thin films with controlled stoichiometry

Nelly SCHEIBEL[1,2], Vincent ASTIE[3], Léa LA SPINA[1], Grégoire LARGER[1,4], Elliott CREVON[1], Pascal BOULET[5], Samuel MARGUERON[1], Jean-Manuel DECAMS[3], Ausrine BARTASYTE[1,2,6]

[1] FEMTO-ST Institute, Université Marie et Louis Pasteur, ENSMM, 25030 Besançon, France
[2] C2N, Université de Paris-Saclay, CNRS (UMR 8622),91120 Palaiseau, France
[3] Annealsys, 34000 Montpellier, France
[4] Exail, 25000 Besançon, France
[5] Jean Lamour Institute, CNRS (UMR 7198), Université de Lorraine, 54011 Nancy, France
[6] Institut Universitaire de France

e-mail : nelly.scheibel@femto-st.fr

ABSTRACT

Single crystalline quality $LiNbO_3$ films were grown on the sapphire by means of the direct liquid injection CVD. Particular effort was done to achieve films with controlled and homogeneous Li_2O composition (± 0.05 mol%) over 4-inch wafers and to grow stoichiometric films. CVD growth also assured highly homogeneous film thickness on the wafer scale.

KEYWORDS: *$LiNbO_3$ films, CVD, epitaxy, Li stoichiometry*

1. INTRODUCTION

Over the past five decades, $LiNbO_3$ (LN) single crystals and thin films have been studied intensively for their exceptional acoustic, electro-optical, and pyroelectric and ferroelectric properties [1]. Today, LN single crystals in electro-optics are equivalent to silicon in electronics. LN thin films are needed urgently for the development of the next-generation infrastructures/networks/communications and the integration of LN films in guided nanophotonic devices will allow higher operational frequencies, wider bandwidth, and miniaturized optical devices in line with improved electronic conversion. However, the growth of high-quality LN films with reproducible physical properties is complicated by the difficulty in controlling volatile Li_2O incorporation into the film and of measuring its composition [1]. So far, large-scale production of deposited films with physical properties suitable for the targeted applications is not available. Here, the challenges and the achievements in the epitaxial growth of LN thin films and their integration with silicon technology and guided nanophotonic devices are discussed in detail.

2. RESULTS

Direct liquid injection metalorganic chemical vapor deposition (DLI-CVD, Annealsys) technique was used to grow LN thin films on various substrates using tetramethylheptanedionate precursors, Li(thd) and $Nb(thd)_4$. In the case of optical waveguiding applications, proper propagation axis and single-crystal quality films are demanded. Thus, particular effort was done to achieve growth of films with single crystallographic orientation. Epitaxial relationships and structural properties of the deposited films are investigated using X-ray diffraction and scanning electron microscopic techniques. Single crystalline quality films were obtained on sapphire substrates with the mosaicity comparable to that of the single-crystal. As lithium nonstoichiometry in $LiNbO_3$ films is critical parameter defining high acoustical performance, Li incorporation in the films was studied in details by varying deposition conditions. Li concentration in the films was estimated by means of Raman spectroscopy. Particular effort was done to achieve films with controlled Li_2O composition and stoichiometric composition [Figure 1a] and homogeneous composition (± 0.05 mol%) distribution over 4-inch wafers. CVD growth also assured highly homogeneous thickness on the wafer scale. Extremely high acoustic performance (quality factor, Q, up to 700, K^2 up to 8%) in SAW devices based on Z-$LiNbO_3$ thin films was achieved in the frequency range from 3.7 GHz to 5.3 GHz [2]. The deposited LN films presented e_{31} piezoelectric coefficient of -2.4 C/m^2 which as expected for clamped film was higher than that of the single crystal, confirming high quality of the grown films by DLI-CVD.

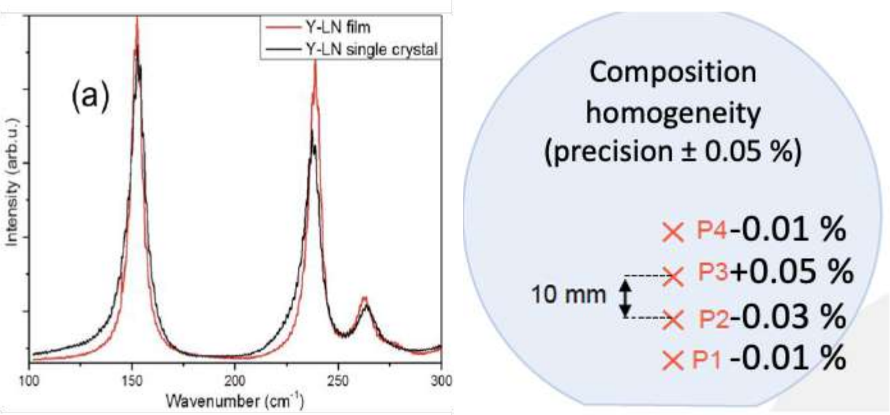

Fig.1. (left) Comparison of the Raman spectra of the LN layer with the almost stoichiometric composition and of the LN single crystal with the congruent composition. The width of the modes is dependent on the concentration of nonstoichiometry defects. (right) Li composition homogeneity in LN film, grown by DLI-CVD on 4-inch sapphire wafer.

CONCLUSIONS

High quality single crystalline quality $LiNbO_3$ films were grown on the sapphire substrates by means of the direct liquid injection CVD. The ability to control the Li composition in grown films with precision, to grow stoichiometric films and to attain the homogeneity of the Li stoichiometry better than ± 0.05 mol% on wafer scale was demonstrated for the first time.

This work was funded by French RENATECH network, and EUR EIPHI Program Grant No. ANR-17-EURE-0002 and French PEPR Electronic project.

REFERENCES

[1] A. Bartasyte, S. Margueron, T. Baron, S. Oliveri, P. Boulet, Adv. Mater. Interfaces, 1600998 (2017).

[2] A. Almirall, S. Oliveri, W. Daniau, S. Margueron, T. Baron, P. Boulet, S. Ballandras, S. Chamaly, A. Bartasyte, Appl. Phys. Lett., Vol. 114, 162905 (2019).

Session PM_1.2 SEMICONDUCTORS I

Monday 2nd June 2025 | 14.30-15.30

Chair: **Gloria Tabacchi** | Room “Coro di Notte”

Cl_2 etching selectivity for defects in two-dimensional transition metal dichalcogenides (TMDs)

P. Kumar[1*], N. Trainor[1,2,3], B. Groven[1], H. Medina[1], D. Vranckx[1], J. M. Redwing[2,3] A. Delabie[1,3], C.J. Lockhart[1], G.S. Kar[1], P. Morin[1]
[1] IMEC, Leuven, BE
[2]2D Crystal Consortium Materials Innovation Platform, Materials Research Institute, Penn State University, University Park, PA, USA
[3]Department of Chemistry, KU Leuven, Leuven, BE
*e-mail: pawan.kumar@imec.be

Two-dimensional (2D) semiconducting transition metal dichalcogenides (TMDs) are promising candidates for advanced electronic and optoelectronic devices. However, currently state-of-the-art deposition methods for growing wafer-scale TMDs layers suffer from undesirable defects.

Here we present the development of Cl_2-based etch process for 2D MoS2 monolayer on sapphire preferentially which perfectly correlated to the available defects. Before the etch process, epitaxial MoS_2 was grown by metal-organic chemical vapour deposition (MOCVD) process using molybdenum hexacarbonyl and hydrogen sulfide precursors on c-plane sapphire using an industry-standard 200 mm horizontal reactor. In comparison, the etch process was conducted ex-situ on 300 mm reactor using custom-made pocket wafers. The Cl2-based etching process is identified for the temperatures between 400°C and 700°C, where the different defect site-associated regions (like superficial islands, line defects, etc) are selectively reacted without noticeable damage to the 2D monolayer structure as observed with scanning electron microscopy (SEM), atomic force microscopy (AFM) and Raman spectroscopy. The etch process's selectivity can also be tuned by co-injecting S-containing species. Thermodynamic calculations are also validated for various H_2S and Cl_2-based reaction processes. Such reactions may also have the dual effect of depleting Cl_2 and generating etching by-products.

In addition to morphological changes, the Cl_2 etching caused changes in the Raman and photoluminescence (PL) response, which correlated with defectivity and doping into an atomic thin layer. The MoS2 Raman modes narrowed after Cl_2 exposure; however, this effect was reduced with the co-injection of H2S. With the PL response, the defectivity and doping behaviour are consistently modulated using the Chlorination chemistry.

References

[1] Q. Smets *et al.*, "Sources of variability in scaled MoS2 FETs," *2020 IEEE International Electron Devices Meeting (IEDM)*, San Francisco, CA, USA, 2020, pp. 3.1.1-3.1.4, doi: 10.1109/IEDM13553.2020.9371890.

[2] Y. Shi et al., "Superior electrostatic control in uniform monolayer MoS2 scaled transistors via in-situ surface smoothening," 2021 IEEE International Electron Devices Meeting (IEDM), San Francisco, CA, USA, 2021, pp. 37.1.1-37.1.4, doi: 10.1109/IEDM19574.2021.9720676.

Advances and challenges in gapfill oxides

VSK. Channam[1], **I. Belov, P. Dhakras, S. Tasneem, R. Chukka, A. Jourdain & A. Sepulveda**
[1] Imec Leuven, Belgium.
e-mail: sunil.kumar@imec.be

With the rapid advancement in semiconductor manufacturing, newer integration schemes in chip packaging—such as 3D heterogeneous die-to-wafer hybrid bonding schemes [1]—and complex transistor fabrication approaches like FinFET and CFET [2] have become critical. These methods necessitate the use of silicon oxide deposited by PECVD processes to enable void-free gapfill and encapsulation of large, micron-range gaps and trenches for wafer reconstitution and 3D stacking. Concurrently, there is a need for dielectric layer filling in high aspect ratio, narrow trenches with bottom-up conformal filling using techniques such as flowable CVD (FCVD) [3]. This article discusses the current state of the art for these diverse oxide deposition schemes and highlights challenges related to process conditions and oxide removal/planarization methods.
Keywords: PECVD, PEALD, FCVD, Gapfill Oxides

Die-to-wafer hybrid bonding is an advanced packaging technique combining the benefits of dielectric bonding (using materials like SiOx) with embedded metal (typically copper, Cu) to create interconnections. In this scheme, individual dies are bonded to a wafer, followed by depositing a thick layer of oxide to encapsulate the dies and fill the gaps between them. Figure 1 presents a schematic of the process, showing a trench depth of 25 µm and a spacing of 130 µm. Figure 2 depicts SEM images of two variations of thick oxide deposited by PECVD. To encapsulate the dies, a 30–50 µm thick oxide must be deposited. This oxide must exhibit low stress to prevent excessive wafer bowing. New metrology and oxide planarization processes are required to address the challenges of measuring and processing such thick oxides

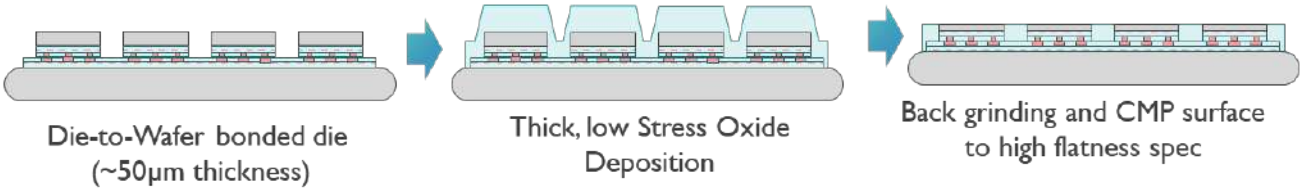
Die-to-Wafer bonded die
(~50µm thickness)
Thick, low Stress Oxide
Deposition
Back grinding and CMP surface
to high flatness spec

Figure 1: Schematic of thick oxide gap fill after die-to-wafer bonding

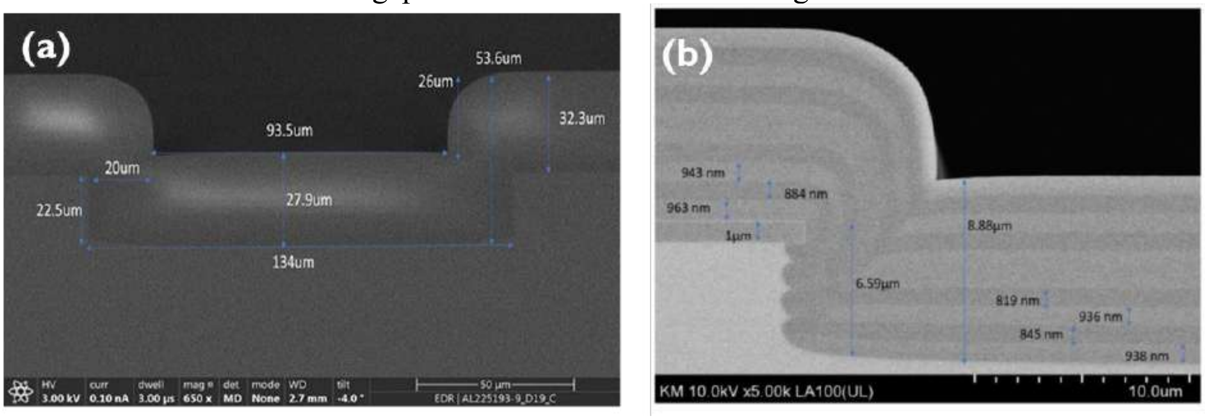
(a)
53.6um
26um
32.3um
93.5um
20um
22.5um
27.9um
134um
HV 3.00 kV
curr 0.10 nA
dwell 3.00 µs
mag 650 x
det MD
mode None
WD 2.7 mm
tilt -4.0°
50 µm
EDR | AL225193-9_D19_C
(b)
943 nm
884 nm
963 nm
1µm
8.88µm
6.59µm
819 nm
936 nm
845 nm
938 nm
KM 10.0kV x5.00k LA100(UL)
10.0um

Figure 2: (a) SEM image of 30 µm solid oxide deposition. (b) SEM image of a 9 µm laminated oxide with alternate tensile and compressive layers of 1 µm each.

STI Oxides in Transistor Fabrication

STI Oxides in Transistor Fabrication

In next-generation FinFET and CFET-based transistor fabrication, shallow trench isolation (STI) oxide is essential for device performance and reliability. STI oxide provides inter-layer isolation, separating vertically stacked nFET and pFET layers to reduce leakage and electrical interference. It also aids planarization, creating a flat surface essential for precise layer stacking during fabrication. Furthermore, STI oxide supports advanced scaling by maintaining robust isolation and structural integrity in compact geometries, while contributing to thermal management by mitigating heat dissipation challenges. Overall, STI oxide is indispensable for electrical isolation, structural support, and seamless process integration in CFET technology. FCVD [3] is one of the most effective techniques for achieving challenging oxide fills. Process optimization and post-deposition curing and annealing conditions are pivotal for obtaining high-quality oxides capable of withstanding further processing steps in CFET integration flows.
This study examines various levels of process optimization, including curing time, curing power, annealing conditions, and pre- and post-deposition treatments. These efforts aim to tailor FCVD processes for effective gap filling across different structures.

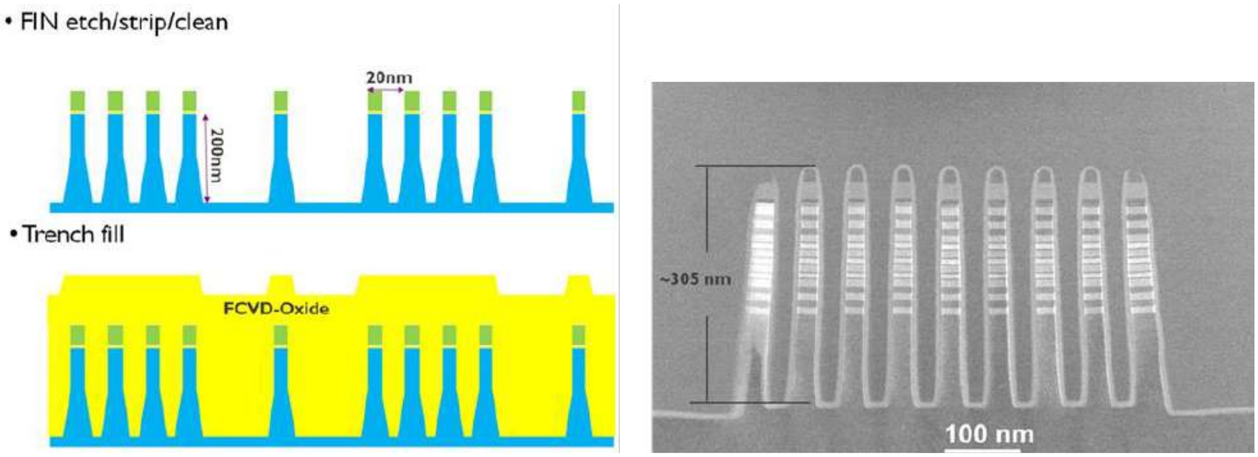

Figure 3: (Left) SEM image of a 500 nm oxide deposited in high aspect ratio structures, demonstrating void-free fill. (Right) Illustration of FCVD oxide deposition in trench filling

In conclusion we present the state of the art in depositing gapfill oxides for large-area gaps using PECVD processes (30–50 µm thick oxide) and demonstrates how narrow, high aspect ratio STI oxide fills can be achieved with FCVD. It also addresses deposition-related challenges in the rapidly evolving integration schemes of the semiconductor industry.

References

[1] Lin, Y., Bex, P., Kennes, K., Derakhshandeh, J., Dhakras, P., Suhard, S., ... & Beyne, E. 2024 IEEE 74th Electronic Components and Technology Conference (ECTC) (pp. 40-44). IEEE. (2024)

[2] Chiarella, T., P. Matagne, H. Mertens, M. Hosseini, X. Zhou, P. Eyben, H. Arimura et al. In 2024 8th IEEE Electron Devices Technology & Manufacturing Conference (EDTM), pp. 1-3. IEEE (2024).

[3] Mehta, Sanjay C., Richard Conti, Thamarai Devarajan, Matthew P. Wright, Yiping Yao, Stephan A. Cohen, Todd Ryan et al. In *Electrochemical Society Meeting Abstracts 230*, no. 27, pp. 1835-1835. The Electrochemical Society, Inc., (2016).

Exploring the Impact of Atomic Layer Deposition Processing on NiO Chemistry and Opto-electrical Properties

K. Mukherjee[1], T. Staps[1], C. van Helvoirt[1], C. H. L. Weijtens[2], M. Verheijen[1,3], M. Creatore[1,4]

[1] Eindhoven University of Technology, Department of Applied Physics and Science Education

[2] Eindhoven University of Technology, Molecular Materials and Nanosystems and Institute of Complex Molecular Systems

[3] Eurofins Materials Science BV

[4] Eindhoven Institute of Renewable Energy Systems (EIRES)

e-mail: k.mukherjee@tue.nl

Nickel oxide (NiO) is a promising p-type semiconductor widely researched for applications, amongst others, in solar cells, lithium-ion batteries, electrocatalysis, and gas sensors. Various NiO deposition techniques, including solution processing, magnetron sputtering, chemical vapour deposition, and atomic layer deposition (ALD), have been reported in the literature. [1] Among these, ALD has advantages such as scalability and the ability to deliver pinhole-free and conformal films, particularly of major interest when processed on textured substrates. In this study, we have compared three ALD NiO processing routes to unravel their effect on NiO chemistry, electrical and optical properties. To this purpose, nickel bis(N, N′-di-tert-butylyacetaminidate) ($Ni(^tBu\text{-}MeAMD)_2$)-based thermal ALD process (‘$NiO_{Bu\text{-}MeAMD}$’) [2], nickel bis-methylcyclopentadienyl ($Ni(MeCp)_2$)-based plasma-assisted ALD (PA-ALD) process (‘NiO_{MeCp}’) [3] and the newly developed PA-ALD process, based on the Alanis™ precursor (‘NiO_{Alanis}’), from Air Liquide, are compared.

The NiO_{Alanis} process exhibits a linear growth on *c*-Si with a growth per cycle (GPC) of 0.27 ± 0.02 Å/cycle, similar to the NiO_{MeCp} process, whereas the $NiO_{Bu\text{-}MeAMD}$ process is characterized by a higher GPC of 0.43 ± 0.01 Å/cycle. X-ray photoelectron spectroscopy reveals that the thermal $NiO_{Bu\text{-}MeAMD}$ films contain a larger impurity content, due to unremoved ligands, which can lead to the observed higher GPC value. The NiO_{Alanis} films have the lowest Ni-to-O ratio (0.82 ± 0.04), compared to NiO_{MeCp} (0.96 ± 0.04) and $NiO_{Bu\text{-}MeAMD}$ (0.94 ± 0.04). The presence of a relatively high content of excess oxygen in the NiO_{Alanis} films indicates the presence of a higher density of Ni^{3+} acceptor states. This is further corroborated by ultraviolet photoelectron spectroscopy (UPS) revealing a smaller energy gap between the valence band and work function of the NiO_{Alanis} films compared to the other films. The formation of Ni^{3+} states contributes to sub-bandgap absorption leading to a lower transmittance of the NiO_{Alanis} films (~79%) as compared to the NiO_{MeCp} (~84%) and $NiO_{Bu\text{-}MeAMD}$ films (~90%) in the visible range. In parallel, the resistivity of the NiO_{Alanis} films ($6 \pm 2\ \Omega\cdot cm$) is lower than NiO_{MeCp} ($66 \pm 33\ \Omega\cdot cm$) and $NiO_{Bu\text{-}MeAMD}$ films ($(1.7 \pm 0.1)\cdot 10^4\ \Omega\cdot cm$), supporting the presence of Ni^{3+} acceptor states. Moreover, transmission electron microscopy images reveal that the thermal ALD $NiO_{Bu\text{-}MeAMD}$ films have voids or low-density areas which can affect the carrier mobility and support the high electrical resistivity values. In contrast, the PA-ALD NiO films exhibit a higher density ($6.8 - 7.0 \pm 0.8\ g/cm^3$) than the thermal ALD $NiO_{Bu\text{-}MeAMD}$ films ($5.1 \pm 0.3\ g/cm^3$), due to the ion flux impinging on the film during the O_2 plasma half-cycle.

Our study demonstrates that the reactivity of the Ni-precursor with the co-reactant influences the stoichiometry as well as the morphology of the NiO film, ultimately impacting its electrical and optical properties. Additionally, it highlights the role of the Ni-precursor and co-reactant selection in tailoring NiO material properties for a specific application area, such as hole transport layers for metal halide perovskite photovoltaics.

This work was supported by the "New Energy and Mobility Outlook for the Netherlands" (*No: 17628*), the NWO Aspasia Program, the HORIZON 2020 projects Supertandem (*No: RT10422*) and PEPPERONI (*No: RT104150*). The authors also thank Air Liquide for providing the Alanis™ precursor.

References

[1] X. Yin, Y. Guo, H. Xie, W. Que and L. B. Kong, *Solar RRL*, **3**, 1900001 (2019).

[2] N. Phung, D. Zhang, C. van Helvoirt, M. Verhage, M. Verheijen, V. Zardetto, F. Bens, C. H. L. Weijtens, L. J. (Bart) Geerligs, W. M. M. Kessels, B. Macco and M. Creatore, *Solar Energy Materials and Solar Cells*, **261**, 112498 (2023).

[3] D. Koushik, M. Jošt, A. Dučinskas, C. Burgess, V. Zardetto, C. Weijtens, M. A. Verheijen, W. M. M. Kessels, S. Albrecht and M. Creatore, *Journal of Materials Chemistry C*, **7**, 12532 (2019).

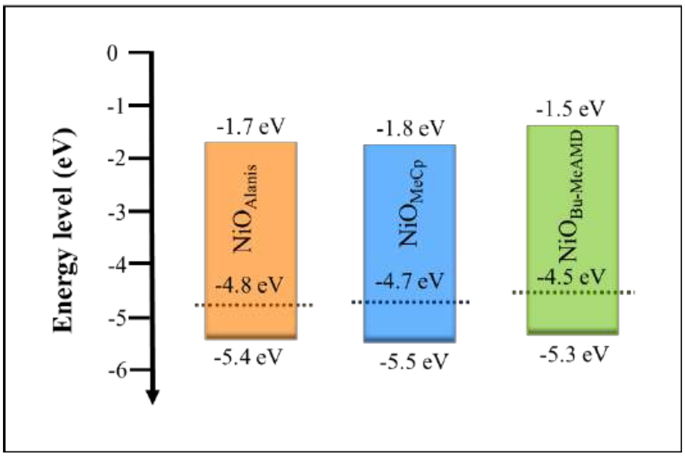

Fig. 1. Illustration of the energy levels with respect to the vacuum level, measured by UPS, of NiO$_{Alanis}$, NiO$_{MeCp}$ and NiO$_{Bu-MeAMD}$ films.

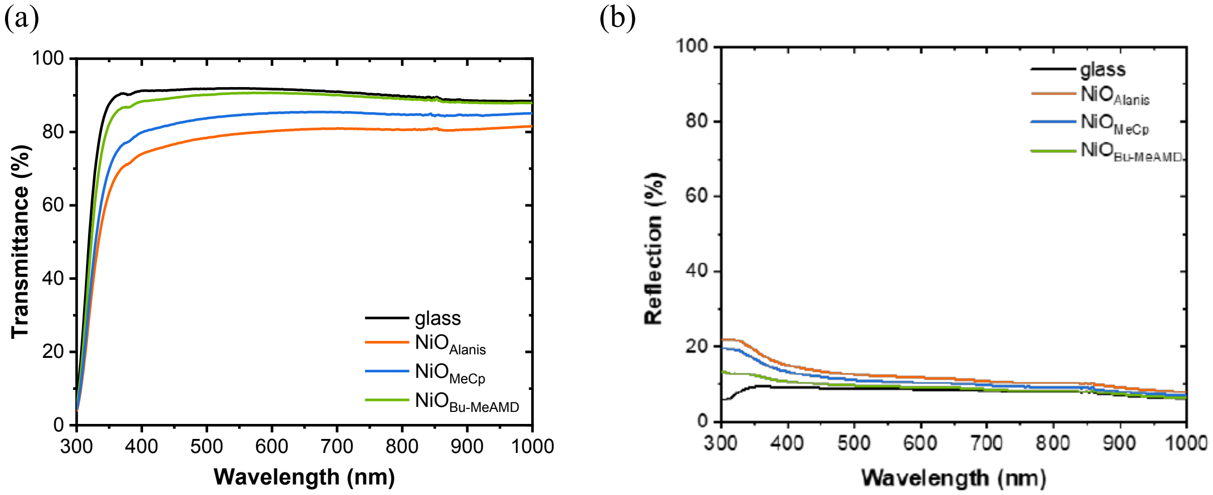

Fig. 2. (a) Transmittance and (b) reflectance of NiO$_{Alanis}$, NiO$_{MeCp}$ and NiO$_{Bu-MeAMD}$ films on glass. The thickness of the NiO films is ~9 nm.

In-situ-monitored Chemical Vapor Deposition of silicon oxynitride layers

P. Dubreuil[1], U. Legallois[1], O. Gauthier-Lafaye[1] and S. Calvez[1,*]
[1]Laboratoire d'Analyse et d'Architecture des Systèmes – Centre National de la Recherche Scientifique
e-mail: stephane.calvez@laas.fr

The ability to deposit optical thin films of controlled thickness and whose material linear and nonlinear refractive indexes can be adjusted over a wide range is an enabling technology in the fabrication of optical coatings [1,2] and of photonics integrated circuits [3,4]. In both cases, the applied coatings are often made by Plasma-Enhanced Chemical Vapor Deposition (PECVD) with calibrated and timed processes.

Following the implementation of in-situ monitoring systems in other types of deposition equipment [5,6], we report here the development of a combination of reflectometry and optical emission spectroscopy (OES) and its use on a Inductive-Coupled-Plasma PECVD tool to not only gain greater control on the deposited material compositions and thicknesses but also to help reduce the number of calibration runs.

The optical measurements are performed through a hole in the showerhead of an Oxford Plasmalab System 100 ICP-PECVD equipment used to deposit silicon oxynitride layers (SiO_xN_y) (see Figure 1 left). Both the plasma emission and sample reflection are collected in real time in a surface-normal direction with respect to the wafer under treatment.

In a first instance, we recorded the OES signal 10 seconds after the plasma strike, on a set of silicon samples where the layer SiO_xN_y composition was altered between SiO_x and SiN_y by changing the flux of NO_2 injected gas, all other parameters being kept constant. As shown on the right of Figure 1, the characteristic emission lines of oxygen-related species increase with the NO_2 flux while those that are nitrogen-related decrease, confirming the ability to monitor the deposited material content.

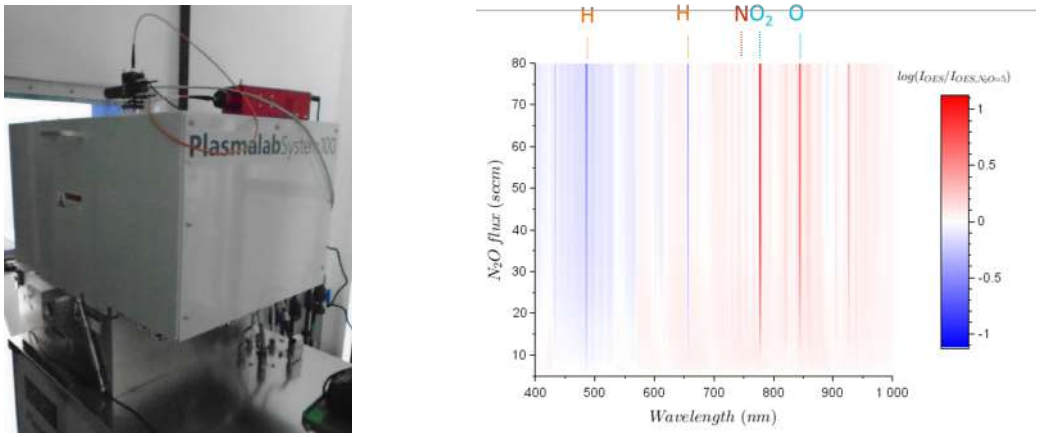

Figure 1: left : Photograph of the installed monitoring system.
right : Evolution of the OES signal as a function of the SiO_xN_y composition resulting from a variation of the injected NO_2 flux.

Subsequent work investigated the impact of the process conditioning on the deposited layer. As illustrated on the left part of Figure 2, both the plasma stabilization and deposition rate can be affected by the passivation condition of the chamber walls and the clamping system.

Finally, as it can be observed on the right part of Figure 2, the deposition of nanolaminates of SiO_x/SiN_y, which provide a digital way to fabricate layers of intermediary refractive index [7], is also successfully demonstrated and monitored.

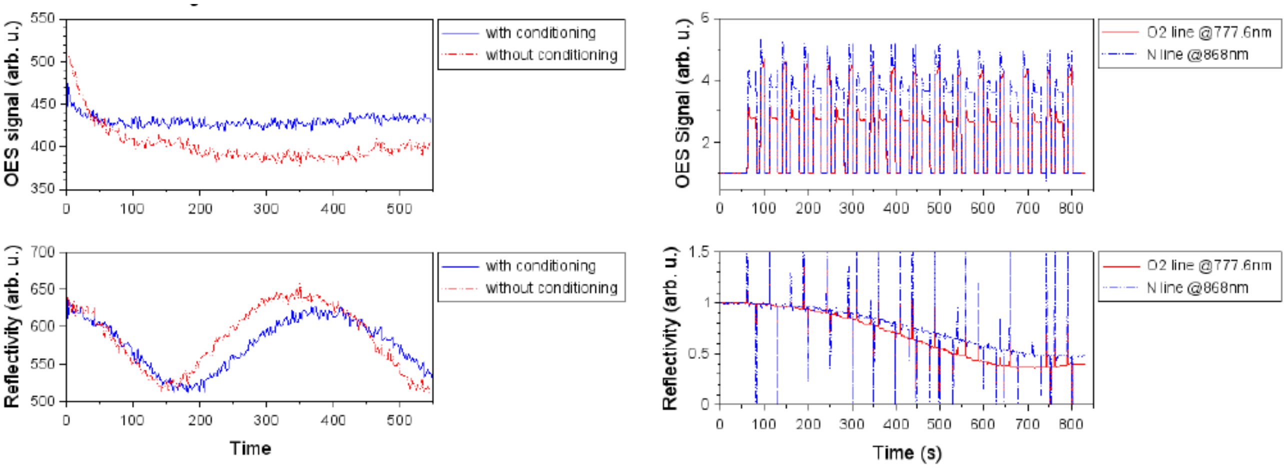

Figure 2: Time-dependence of the OES and reflectivity of Si substrates being coated
left: with a SiN_y layer with and without a 5-minute prior-conditioning step (measurements done at a wavelength of 532 nm).
right: with a 15-period digital SiO_x/SiN_y nanolaminate of total thickness of 134 nm and of refractive index at 790 nm of 1.65, an intermediary value between the ones of the constitutive binaries, 1.48 for SiO_x and 1.86 for SiN_y.

In conclusion, an in-situ monitoring system based on reflectometry and optical emission spectroscopy has been designed and installed on a PECVD equipment and it has been shown to provide real-time information that will facilitate the fabrication of single and multilayer thin films of controlled thickness and composition.

This work was supported by the ANR SCOPOL project (ANR-22-CE09-0019), by OPALE the joint laboratory between LAAS-CNRS and Essilor-Luxottica, and by the LAAS-CNRS micro and nanotechnologies platform, a member of the Renatech French national network.

References

[1] M. Jerman, Z. Qiao, D. Mergel, *Appl. Opt.*, **44** 3006 (2005).
[2] A. Farhaoui, A. Bousquet, R. Smaali, A. Moreau, E. Centeno, J. Cellier, C. Bernard, R. Rapegno, F. Réveret, E. Tomasella, *J. Phys. Appl. Phys.*, **50** 015306 (2017).
[3] C.J. Krückel, A. Fülöp, T. Klintberg, J. Bengtsson, P.A. Andrekson, V. Torres-Company, *Opt. Express*, **23** 25827 (2015).
[4] D.K.T. Ng, Q. Wang, T. Wang, S.-K. Ng, Y.-T. Toh, K.-P. Lim, Y. Yang, D.T.H. Tan, *ACS Appl. Mater. Interfaces*, **7** 21884–21889 (2015).
[5] W.G. Breiland, K.P. Killeen, *J. Appl. Phys.*, **78** 6726–6736 (1995).
[6] J. Zideluns, F. Lemarchand, D. Arhilger, H. Hagedorn, J. Lumeau, *Opt. Express*, **31** 9339 (2023).
[7] K. Kreuzer, P. Henning, M. Vergöhl, S. Bruns, T. Melzig, C. Patzig, R. Feder, *Appl. Opt.*, **63** 1641 (2024).

Session PM_1.3 SEMICONDUCTORS II

Monday 2nd June 2025 | 16.00-17.30

Chair: **Henrik Pedersen** | Main Hall “Santo Mazzarino”

How to help the planet – Parallel processing of free design complex objects

P. Hoffmann
Empa, Swiss Federal Laboratories for Materials Science and Technology; Laboratory for Advanced Materials Processing; Feuerwerkerstrasse 39, 3602 Thun, Switzerland
e-mail: Patrik.Hoffmann@empa.ch

Customization needs in industrial processing for small series fabrication as well as individual device production initiated a strong increase of attention to serial processing for fabrication generally called additive manufacturing (AM) in the past decades. Moving nozzle extrusion of (molten) material, nozzle printing (ink jet) scanning (laser, electron) beam induced sintering or melting of powders or wire feeding systems are examples. Different from these are in volume interacting processes which modify the materials properties locally in small volumes such as two-photon interaction in transparent materials to change solubility and result in complex 3-D structures and many more varieties of processing emerged. Many, if not all these processes, are serial processes in which every individual volume element (voxel) of every piece of final product has to be addressed individually at a certain moment in time by the beam, nozzle, or other. But the **shape design** is completely **free**, in other words any shape can be produced. Some technologies require so called support structures, which is sacrificial material to be removed after finalization of the process. This can be considered as compromise to the absolute freedom of design of the final workpiece.

In most of these processes the fact of serial individual addressing each voxel of a certain volume determines the total fabrication time, and therefore the fabrication cost per piece. This is probably the main reason for the slow industrial implementation of these processes lagging far behind expectations. The fabrication time can be reduced by increasing the voxel size, resulting in a decrease of precision or filigree shape of the final workpiece which is in many cases undesired. Furthermore post-processing is often needed for obtaining the final precision and surface smoothness.

Therefore the idea of a combination of serial and parallel processing for the fabrication of complex 3-D bodies is presented here. The method will work as follows: 1) slice the electronic body model into layers; 2) fabricate (in serial or partially serial and parallel processes) 2.5 D molds for each individual layer; 3) fill the mold with nanoparticle powder in solvent slurry of final material into mold; 4) dry to green bodies in the mold of the layers; 5) separate green body layer from mold; 6) assemble the green body layers to final stack and sinter to final product. In figure 1, the results of the technology used for large scale cost effective fabrication of very precise alumina stars after steps 2, 3, 4, 5 are presented as first results showing the feasibility of a few of the steps (the described layer on layer process is presently going on).

High impact products of this process are fluid flow optimized scaffold structures in metal or ceramic materials for improved efficiency of catalysts for heterogenous catalyzed gas or liquid reactions for hydrogen production, gas separation, creation of synthetic fuel from CO_2 and hydrogen, combined with membrane layers fuel cell fabrication, complex electrochemical multi-phase reactors or simply heat exchanger geometries could be imagined. The potential impact of the technology for helping to face todays challenges of our entire planet is enormous.

CO_2 reduction in the Carbon cycle – finalizing in graphite-fiber reinforcement in concrete; Heat exchangers with one order of magnitude size reductions (from chip cooling to computer cooling to nuclear power plant cooling); Energy reduction of catalytic chemical reactions (ammonia, methane synthesis) from hydrogen and air CO_2; Methane and higher alkane production, synthetic fuel (net zero);

Where is the link to Euro-CVD – ALD conference:

International conferences are ideal places for finding collaborations and putting consortia together for big world wide challenges. Euro-CVD brings together engineers and researchers with very complementary competences – from chemistry – chemical engineering – to fluid dynamics – simulation of processes and chemical reactions to materials science expertise of sintering processes to solid state physics.

The research challenges for realizing the layered fabrication are enormous and multi-disciplinary, complementary competences are required – many members of the CVD-ALD community are active in different application fields, from quantum computing to battery research - energy storage, photonics, macro- and micro- and nanofabrication, … . The here presented fundamental idea finds applications in all fields – the needed competences are complementary not competitive, the cake is so big, there is enough for everybody!

Some CVD researchers are active in catalyst research, therefore input for improvement of geometries for catalyst scaffolds and its realization in collaborations is of utmost importance;

Highly conformal gas phase coating processes are essential techniques needed for mold surface tailoring of wetting properties for slurry filling – and release; Low temperature coating methods (ALD), below sintering temperature will coat with functional materials (i.e. catalyst) before assembly;

As alternative, after sintering application of catalyst will need chemical reaction controlled deposition of catalytically active particles on the inner surface of complex scaffold structure;

Post-modification of scaffold geometries by gas-phase infiltration deposition; C infiltration for fabrication of reinforcement Carbon fiber scaffolds in concrete for construction work;

Other functional coatings of final products by ALD, CVD etc. modifying the ad- and desorption dynamics of reactants;

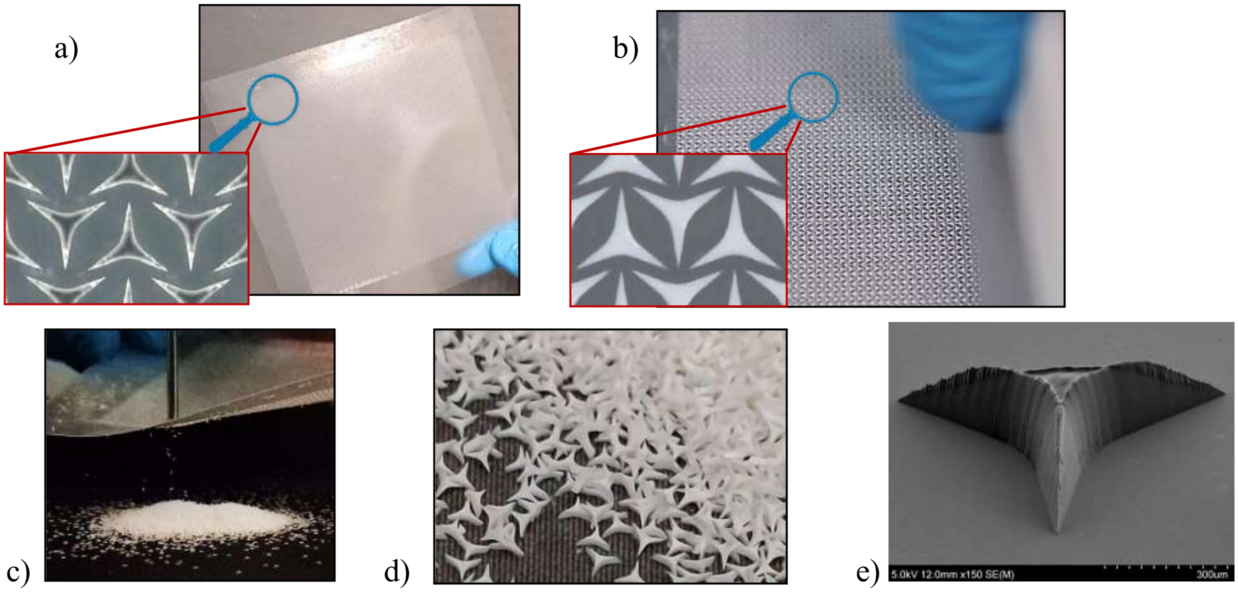

Fig. 1 Photos and inserted top view optical microscope pictures of a) polymer mold after mask projection direct laser ablation, b) ceramic nano-alumina filling in mold; c) photo of ultrasound separation of green particles from mold; d) photo of star shaped particles after sintering; e) SEM picture of PDMS replication of mold in a.

Fig. 1 Photos and inserted top view optical microscope pictures of a) polymer mold after mask projection direct laser ablation, b) ceramic nano-alumina filling in mold; c) photo of ultrasound separation of green particles from mold; d) photo of star shaped particles after sintering; e) SEM picture of PDMS replication of mold in a.

Life cycle assessment of CVD and ALD of GaN

H. Hafdi[1*], A. Carlson[2], H. Pedersen[1]
[1]Department of Physics, Chemistry and Biology, Linköping University, SE-581 83, Linköping, Sweden
[2]Department of Management and Engineering, Linköping University, SE-581 83, Linköping, Sweden

houyem.hafdi@liu.se

Gallium nitride (GaN) is one of the most widely used semiconductors, found in e.g. light emitting diodes and high-power devices. The most commonly used techniques for the deposition of GaN thin films are chemical vapor deposition (CVD) and Atomic Layer Deposition (ALD). CVD offers advantages such as high deposition rates and scalability, making it suitable for large-scale production. However, it is energy-intensive and may produce more waste and emissions including unreacted gases and byproducts. ALD provides precise control over film thickness and uniformity, and it uses lower temperatures, resulting in less energy consumption, and less emissions. However, ALD typically has slower deposition rates and may require more costly precursors. This combination of factors can affect the cost, scale of production, and environmental burden, particularly for large-scale manufacturing processes.

This study addresses the environmental impact of the deposition techniques CVD and ALD by using the Life Cycle Assessment (LCA) method. LCA is a systematic approach for evaluating the environmental impacts associated with all stages of a product's life cycle, from raw material extraction to manufacturing, use, and end-of-life disposal. It provides a comprehensive framework for assessing factors such as energy consumption, resource use, greenhouse gas emissions, waste generation, and potential environmental harm throughout the entire process. In this context, the LCA approach in this study quantifies the advantages and disadvantages of GaN CVD and ALD, i.e., assessing the environmental impact of each technique across all stages. This includes considering the acquisition of materials (such as gallium and nitrogen), the energy demands during the deposition process, the emissions associated with chemical reactions, and the disposal or recycling of waste byproducts. By integrating these aspects into the LCA framework, the study aims to provide a clear picture of the relative environmental impact of these techniques in GaN semiconductor manufacturing and highlighting the trade-offs between these two techniques. This will help to identify more sustainable options based on specific environmental criteria in GaN semiconductor production and highlight areas where improvements could be made to reduce environmental impact.

This work was supported by Formas under contract 2022-00831.

ZnO vapor phase infiltration into photo-patternable polyacrylate networks

L. Demelius[1], A. M. Coclite[2], M. Losego[1,2,*]

[1] Institute of Solid State Physics, NAWI Graz, Graz University of Technology,
Petersgasse 16, 8010 Graz, Austria
[2] Department of Phjysics, University of Bari, via Amendola 173, Bari, Italy
[3]School of Materials Science and Engineering, Georgia Institute of Technology,
Atlanta, Georgia 30332, USA
e-mail: annamaria.coclite@uniba.it

Photopatterning of polymers enables the microfabrication of numerous microelectronic, micromechanical, and microchemical systems. The incorporation of inorganics into a patterned polymer material can generate many new interesting properties such as enhanced stability, optical performance, or electrical properties. Vapor phase infiltration (VPI) allows for the creation of hybrid organic–inorganic materials by infiltrating polymers with gaseous metalorganic precursors.

In VPI, gas-phase inorganic precursors are sorbed into and diffuse throughout a polymer matrix, eventually becoming immobilized by either a chemical reaction with the polymer or loss of volatility, often due to reaction with a subsequently delivered co-reactant. Under ideal process conditions, a uniform distribution of inorganic species in the polymer matrix can be achieved that exhibits self-limiting saturation behavior akin to atomic layer deposition (ALD). At present, the library of photo-patternable polymers that have been studied for modification by VPI is fairly limited.

This study seeks to explore the potential of integrating VPI with existing photopatterning techniques to achieve top-down hybridization and property modification of polymer structures of different complexity. For this, VPI of diethylzinc (DEZ) is studied for four highly crosslinked acrylate networks that can be patterned by photolithography and two-photon polymerization (2PP): pentaerythritol triacrylate (PETA), pentaerythritol tetraacrylate (PETeA), trimethylolpropane triacrylate (TMPTA) and ethoxylated trimethylolpropane triacrylate (ETPTA). The findings show that for highly crosslinked polymer networks, VPI can be limited by slow precursor diffusion. However, by introducing flexible segments (e.g., ethoxylated chains), the polymer's free volume can be increased, and infiltration is accelerated, leading to faster infiltration times and higher and more uniform inorganic loading.

Finally, selective infiltration of ZnO into photolithographically patterned copolymer networks of TMPTA and ETPTA on non-infiltrating poly(methyl methacrylate) (PMMA) is demonstrated (see Fig. 1) illustrating the potential of VPI for advanced maskless patterning strategies.

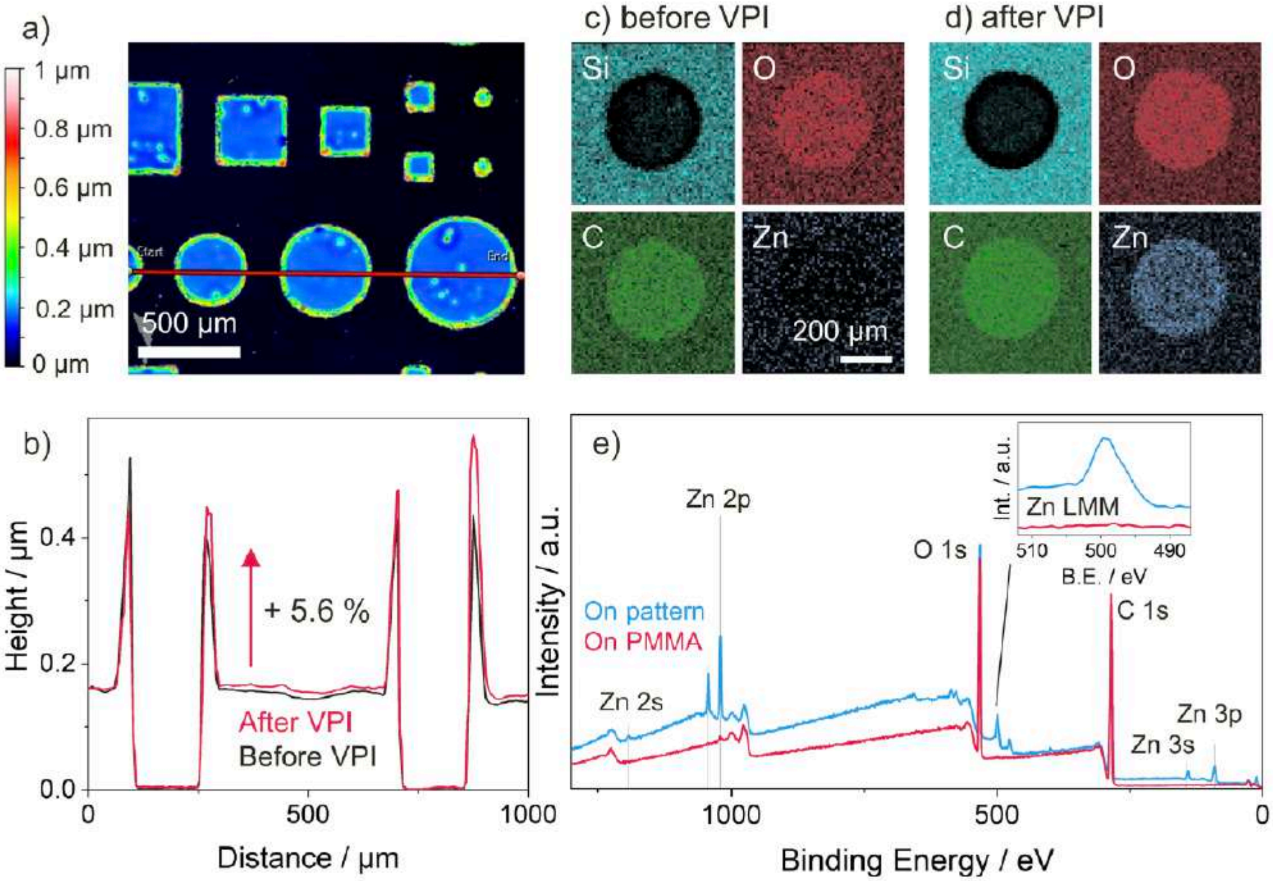

Fig. 1. Selective Zn infiltration (5 h DEZ, 120 1C) of a p(TMPTA-ETPTA) pattern on PMMA. (a) Optical Profilometry of the pattern before VPI, (b) height profile before and after VPI cut along pink line in (a), (c) and (d) EDX elemental maps of a p(TMPTA-ETPTA) feature on PMMA (c) before and (d) after VPI. (e) XPS survey scan of samples on the p(TMPTA-ETPTA) pattern and on PMMA after VPI. The inset shows a zoom on the Zn L$_3$M$_{4,5}$M$_{4,5}$ Auger peak

This work was supported by from the European Union's Horizon 2020 research and innovation programme under grant agreement no. 899349. L. D. acknowledges personal funding from the Austrian Marshall Plan Foundation for funding her research stay at Georgia Institute of Technology. The experimental part of this work was performed at the Georgia Tech Institute for Electronics and Nanotechnology, a member of the National Nanotechnology Coordinated Infrastructure (NNCI), which is supported by the National Science Foundation (ECCS- 2025462). Additional financial support was also supplied by the U.S. National Science Foundation under DMREF-1921873. Some measurements were also completed in Georgia Tech's Materials Innovation and Learning Laboratory (The MILL), an open-access research space for materials science and engineering.

References

[1] Demelius et a., *Materials Advances*, **5,** 8464-8474 (2024).

ALD Metal Oxide Monolayers on Si/SiO_2 Core-Shells Nanowires Enable High *p*-type Doping Without Mobility Deterioration

D. Hiller[1,*], **S. Nagarajan**[2], **I. Ratschinski**[1], **S. Shams**[1], **S. Shah**[1], **S. Schmult**[2,3], **S. Wirth**[4], **T. Mikolajick**[2,3], **D. König**[5], **J. Trommer**[2]
[1]Institute of Applied Physics (IAP), Technical University Bergakademie Freiberg, Germany
[2]Nanoelectronic Materials Laboratory (NaMLab) gGmbH, Dresden, Germany
[3]Institute of Semiconductors and Microsystems, TU Dresden, Germany
[4]Max Planck Institute for Chemical Physics of Solids, Dresden, Germany
[5]Research School of Physics, Australian National University (ANU), Canberra, Australia
e-mail: daniel.hiller@physik.tu-freiberg.de

Conventional impurity doping provides control over the charge carrier type and its density, and thereby over the conductivity, i.e., *the* key parameter for semiconductors. However, a high density of ionized dopants in a crystal lattice is known to deteriorate the charge carrier mobility via scattering. For transistor devices a low carrier mobility implicates mainly slower switching speeds and an increased ohmic resistance. Overall, electrical energy is lost via heat dissipation, which causes higher power demands, or for mobile devices, shorter battery lifetimes. Last but not least, integrated circuits have to be thermally optimized to avoid over-heating. The use of nanowires or nanosheets in modern gate-all-around (GAA) transistors is not relieving this problem, but in contrast, nano-size effects come into play and impede efficient impurity doping. Just to name a few: increased dopant formation and ionization energies by dielectric mismatch, quantum confinement and interaction with interface defects, as well as, statistical fluctuations due to the small number of dopant atoms in semiconductor nano-volumes.

In this contribution, we present a novel method to introduce holes as charge carriers into Si nanowires via an external source, i.e., metal atoms in the SiO_2-shell [1]. This so-called SiO_2-modulation acceptor doping relies on specific trivalent elements [2] incorporated into the amorphous SiO_2-network that provide unoccupied acceptor states located energetically below the valence band edge of Si. Via electron tunnelling induced by a short anneal during fabrication [3,4] these states become permanently ionized, providing – also permanently – holes as majority charge carriers. Hence, this *p*-type doping method provides charge carriers and increases the conductivity significantly [5], without the presence of mobility-deteriorating ionized dopants in the lattice. Moreover, the carriers cannot be frozen out by cryogenic temperatures [6], as shown in Fig. 1 and Tab. 1.

Here, we present how SiO_2-modulation acceptor doping can be realized by a few ALD-cycles of metal oxides on thermally-grown tunnel oxides, in combination with ALD capping layers of SiO_2 or the even high-k material HfO_2. Furthermore, the influence of the modulation acceptor element will be demonstrated by comparing Al with Ga, as well as the impact of multiple layers with acceptor states, in order to show the potential of this new ALD-based doping method.

This work was supported by the German Research Foundation (DFG) via project MADSiNano (456993281) and a Heisenberg grant (434030435).

References

[1] D. König et al., *Sci. Rep.* **7**, 46703 (2017)
[2] D. König et al., *Phys. Rev. Appl.* **10**, 054034 (2018)
[3] D. Hiller et al., *ACS Appl. Mater. Interfaces* **10**, 30495 (2018)
[4] D. Hiller et al., *J. Appl. Phys.* **125**, 015301 (2019)
[5] S. Nagarajan et al., *Adv. Mater. Interfaces* **11**, 2300600 (2023)
[6] S. Nagarajan et al., *Adv. Funct. Mater.* 2415230 (2024)

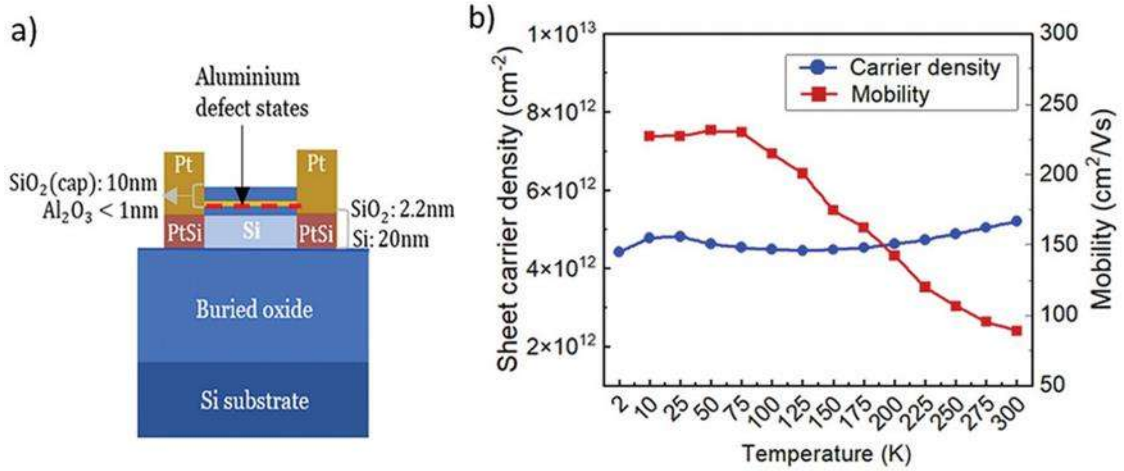

Fig. 1. (a) Schematic cross-section of SiO$_2$ modulation acceptor doped Si Hall-bar test devices on SOI substrates. (b) Hole sheet density (blue curve, left axis) and Hall mobility (red curve, right axis) of modulation acceptor doped Si as a function of temperature: The carrier freeze-out known from impurity doping is absent and charge carrier density remains nearly constant down 2 K. *Graphs adopted from [6].*

Tab. 1. Comparison of resistivity, carrier density, and mobility of impurity doped versus modulation doped *p*-type transport determined from Hall-bars at 300 K. *Graph adopted from Ref. [6]*

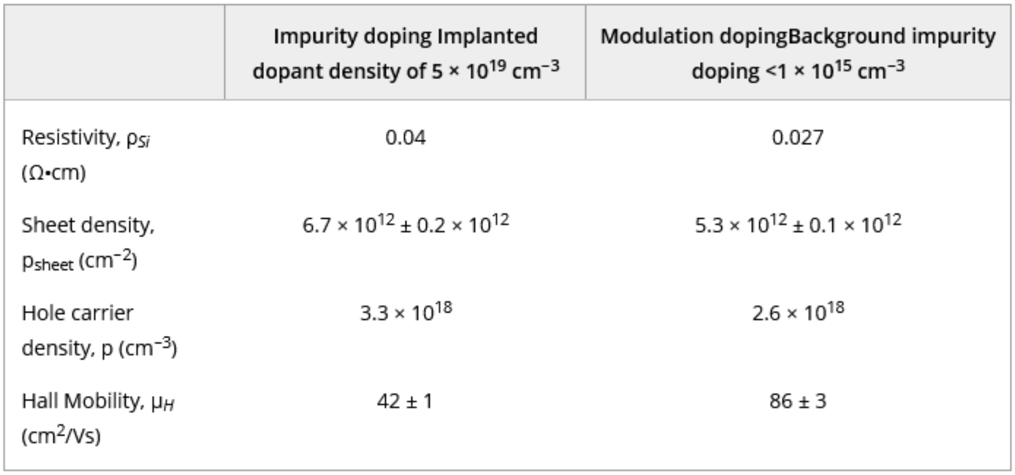

	Impurity doping Implanted dopant density of 5 × 10^{19} cm^{-3}	**Modulation dopingBackground impurity doping <1 × 10^{15} cm^{-3}**
Resistivity, ρ_{Si} (Ω•cm)	0.04	0.027
Sheet density, p_{sheet} (cm^{-2})	6.7 × 10^{12} ± 0.2 × 10^{12}	5.3 × 10^{12} ± 0.1 × 10^{12}
Hole carrier density, p (cm^{-3})	3.3 × 10^{18}	2.6 × 10^{18}
Hall Mobility, μ_H (cm^2/Vs)	42 ± 1	86 ± 3

Growth of p-type SnO by ALD and pulsed CVD using a diamidostannylene precursor

B. Peek, M. Werner and P.R. Chalker,
[1] University of Liverpool, School of Engineering, Liverpool, UK
e-mail: pchalker@liverpool.ac.uk

The development of oxide semiconductors films is underpinning to the drive towards all-oxide thin film transistor (TFT)-based electronics. The availability of n-type oxide-semiconductor TFTs, based on using channel materials such as α-IGZO and ZnO, is well developed through to commercial availability. However, the candidates for p-type oxide TFTs remain the subject of development and are a crucial element in the realization of oxide-based CMOS technology. Stannous oxide (SnO) is a leading candidate p-channel material and thin film deposition has been demonstrated widely using either physical vapor deposition techniques or atomic layer deposition (ALD). A range of tin (II) precursors is available for the ALD of semiconducting SnO, most notably this includes bis(1-dimethylamino-2-methyl-2-propoxy) tin(II) ($Sn(dmamp)_2$), which can be combined with water vapour [1] to achieve deposition at low temperatures. However, a precursor used in the synthesis of $Sn(dmamp)_2$, is a stannylene, which is also capable of SnO deposition with water [2], but has been researched less to date.

Here we report the use of the diamidostannylene, $[(Me_3Si)_2N]_2Sn$, ($Sn(hmds)_2$) to deposit p-type SnO via ALD and pulsed-CVD. The liquid precursor has been used to conformally deposit SnO thin films, in the so-called "ALD temperature window" between 150°C – 200°C, using water vapor as a co-reagent. By contrast, the pulsed CVD mode employs higher carrier gas flows and shorter purge times to achieve a CVD-like reaction, in contrast to the ALD-mode which uses conditions to ensure sequential surface reactions. Fig. 1(a) shows the achievement of growth rates of 0.35Å/cycle for the ALD mode and 2 Å/pulse for the CVD mode. An SEM of the pulsed-CVD SnO film deposited using 4000 pulses is shown in Fig. 1(b), illustrating the typical grain size and facetted crystalline features.

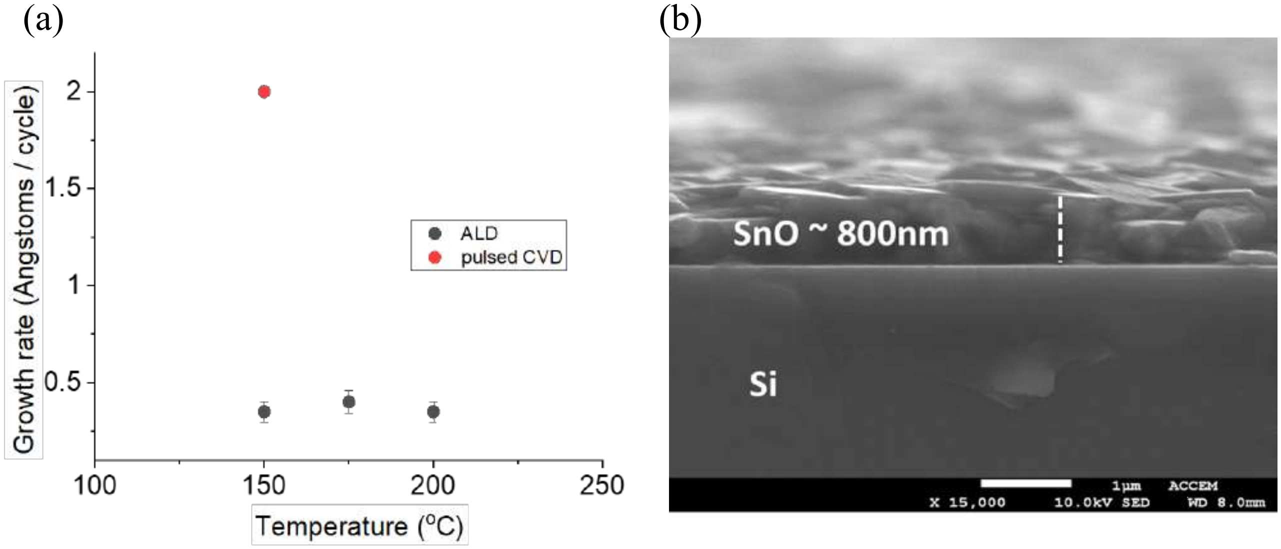

Fig. 1 (a) Growth rate of SnO films deposited via ALD and pulsed-CVD modes. (b) SEM of a cross section from an SnO film growth by the pulsed-CVD method.

Semiconductor devices, such as TFTs, require atomic-level control of the transistor channel over wafer-scale areas. To meet this challenge, ALD processes have been developed to deposit p-type SnO, which exploits the cyclical sequential surface reactions, show below.

$$\text{-OH}_{(ads)} + [(Me_3Si)_2N]_2Sn \quad \rightarrow \quad \text{-O-Sn}\ [(Me_3Si)_2N]_{(ads)} \ + \ (Me_3Si)_2NH_{(g)} \qquad (1)$$

$$\text{-O-Sn}\ [(Me_3Si)_2N]_{(ads)} \ + \ H_2O_{(g)} \quad \rightarrow \quad \text{-O-Sn-OH} \ + \ (Me_3Si)_2NH_{(g)} \qquad (2)$$

The $Sn(hmds)_2 – H_2O$ reaction was investigated using an in-situ quartz crystal microbalance (QCM) to monitor the surface chemistry of the ALD process in real time. Fig. 2 (a) shows the QCM frequency changes resulting from reactions (1) and (2) after deposition of 30 cycles of ALD alumina, using trimethyl aluminum and water. Details of sections of the alumina and SnO deposition are shown in Fig. 2 (b) and (c) respectively.

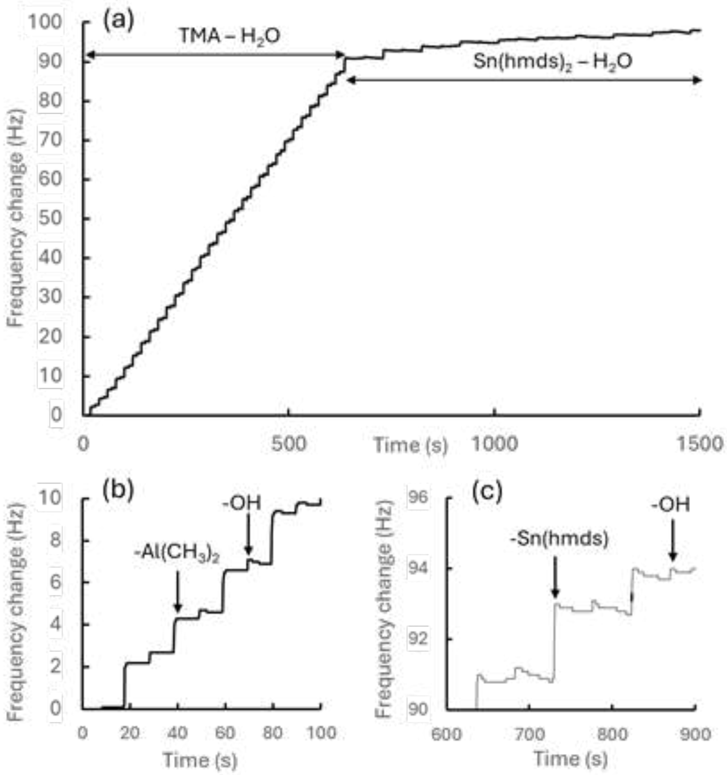

Fig. 2 (a) QCM frequency variation of $Sn(hmds)_2 – H_2O$ cycles on an ALD alumina buffer layer. (b) Details of the trimethyl aluminum - H_2O cycles. (c) Details of the $Sn(hmds)_2$ - H_2O cycles.

This presentation will report of microstructural and semiconducting properties of the SnO films deposited and their influence on p-type TFT's based on them.

This work was supported by the Innovate UK project 106098 and the EPSRC Prosperity Partnership EP/X025195/1.

References

[1] Jeong Hwan Han, *et.al.* Chem. Mater., 26, 6088−6091 (2014).
[2] Jere Tupala, *et. al.* Journal of Vacuum Science & Technology A 35, 041506 (2017)

Session PM_1.4 FERROELECTRICS & MULTIFERROICS

Monday 2nd June 2025 | 16.00-17.30

Chair: **Ausrine Bartasyte** | Room “Coro di Notte”

Epitaxial ALD of ε-Fe_2O_3 thin films to unlock scalable production of multiferroic thin films for next-generation spintronics

T. Jussila[1*], **L. Saltarelli**[1], **N. Dix**[2], **M. Gich**[2], **Maarit Karppinen**[1]
[1]Department of Chemistry and Materials Science, Aalto University, FI-00076 Aalto, Finland
[2] Institut de Ciència de Materials de Barcelona (ICMAB-CSIC), Campus UAB, 08193 Bellaterra, Catalonia, Spain
e-mail: topias.jussila@aalto.fi

Hard ferromagnetic thin films are essential for advanced spin-based technologies including high-density magnetic data storage, high-speed wireless communication devices, and sensing.[1] Materials exhibiting coupled magnetic and dielectric properties (i.e. multiferroics) can unlock novel technological solutions in the field of spintronics to enable novel device operations and higher efficiency compared to traditional electronics.[2] Such attractive materials are, unfortunately, of rare kind and typically composed of complex chemical compositions, their functional properties are limited to low temperatures, and their fabrication is often non-scalable. There is, however, one material that excels as a hard ferromagnet and multiferroic material: ε-Fe_2O_3, one of the seven known binary iron oxide crystal phases. The simple iron(III) oxide is composed of earth-abundant, non-toxic elements, and has a giant magnetic coercivity (hardness) of up to 20 kOe at room temperature which is higher than the widely used rare-earth based magnets. Moreover, the ε-Fe_2O_3 phase is ferroelectric and exhibits magneto-electric coupling even at room temperature making it a highly appealing candidate for spintronics applications.[3] The unmatched ferroic properties originate from the non-centrosymmetric orthorhombic crystal structure with four distinct non-equivalent iron sites (Fig. 1. inset). However, the synthesis of phase-pure ε-Fe_2O_3 is highly demanding due to its metastable nature and thus tendency to transform into the thermodynamically stable α-Fe_2O_3 (hematite) phase. The ε-phase only started to gain increasing scientific attention since the first successful synthesis of single-phase ε-Fe_2O_3 nanoparticles in 2004.[4] The first ε-Fe_2O_3 thin films were fabricated through epitaxial pulsed laser deposition (PLD) in 2010,[5] then through chemical vapor deposition (CVD) in 2013,[6] and finally through atomic layer deposition (ALD) in 2017.[7] The growth of ε-Fe_2O_3 in thin film form is the most essential for the microelectronic devices.

In our pioneering ALD process in 2017, the ε-Fe_2O_3 films were grown from $FeCl_3$ + H_2O precursors on Si(100) substrates at 260–300 °C.[7] The stable films presented relatively good crystallinity and hard room-temperature ferromagnetism until 481 K.[8] These films were, remarkably, grown on non-lattice matching substrates, thus opening possibilities towards optimization on various substrate materials. On the other hand, the most demanding requirements of next generation magnetic and spintronics devices such as highly anisotropic ferromagnetism and multiferroic properties could not be matched by the ε-Fe_2O_3/Si(100) films due to their polycrystalline structure. To address this issue, in the current work, we significantly improve the crystal quality and crystal orientation (magnetic anisotropy) of the ε-Fe_2O_3 thin films through epitaxial ALD. We use $FeCl_3$ + O_3 as the precursors and employ various epitaxial substrates and buffer layers to induce epitaxial growth of *(00l)* out-of-plane orientated ε-Fe_2O_3 thin films (Fig. 1). Yttrium stabilized zirconia (YSZ) (100), which has the lowest lattice mismatch with the ε-phase, is shown to produce phase-pure ε-Fe_2O_3 thin films with the excellent crystal quality and orientation. The film quality is substantially improved compared to the ε-Fe_2O_3/Si(100) thin films and is comparable to the PLD-based ε-Fe_2O_3 thin films. The ferromagnetic/electric properties are studied to evaluate the ferroic properties of the high-quality magnetic thin films. This work is a significant milestone towards production of epitaxial ferromagnetic thin films through an industrially appealing deposition route for next-generation spintronics.

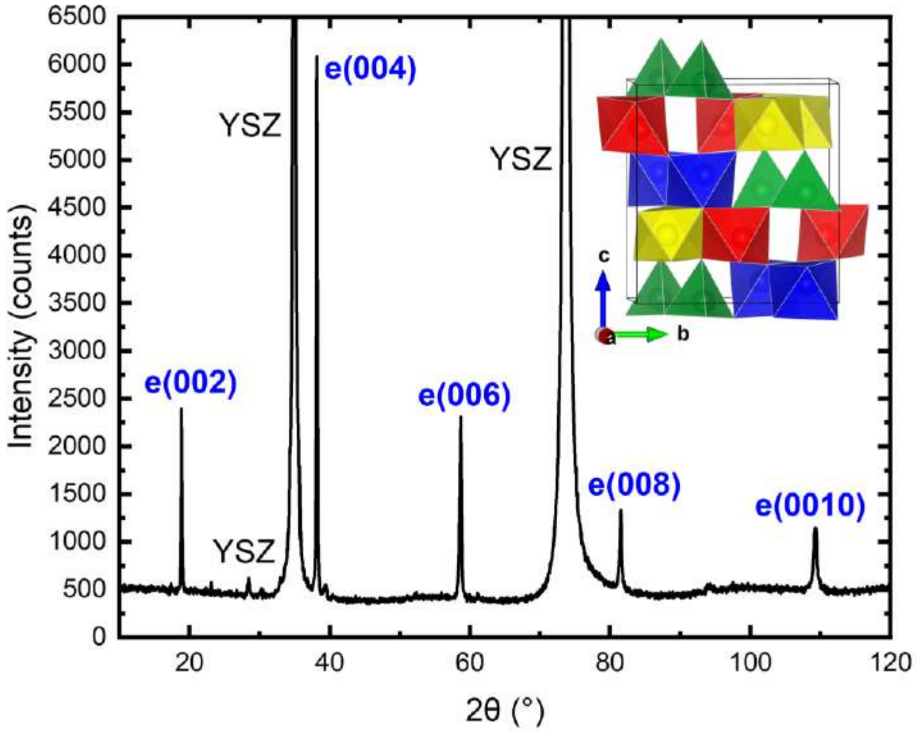

Fig. 1. θ/2θ XRD pattern of the epitaxial ε-Fe_2O_3 thin films grown via ALD @ 300 °C. The single-phase films presents highly oriented *(00l)* out-of-plane reflections. The polyhedral representation of the ε-Fe_2O_3 crystal structure is shown in inset: three octahedral Fe(III) (blue, red, yellow) and one tetrahedral Fe(III) (green) site.

This work was supported by European Union (ERC AdG, UniEnMLD, No. 101097815 and ERC CoG, FeMiT No. 819623). Views and opinions expressed are however those of the authors only and do not necessarily reflect those of the European Union or the European Research Council. Neither the European Union nor the granting authority can be held responsible for them. This work was also partly supported by Magnus Ehrnrooth Foundation, the Spanish Ministry of Science and Innovation and Universities through the Severo Ochoa Program for Centers of Excellence in R&D (CEX2019-000917-S), the project (PID2021-124734OB-C22) and Generalitat de Catalunya (2017-SGR-765).

References

[1] J. Tuček, R. Zbořil, A. Namai, and S.-i. Ohkoshi, *Chem. Mater.* **22**, 6483 (2010).
[2] B. Dieny, I. L. Prejbeanu, K. Garello, P. Gambardella, et al., *Nature Electronics* **3**, 446 (2020).
[3] M. Gich, I. Fina, A. Morelli, F. Sánchez, M. Alexe, J. Gàzquez, J. Fontcuberta, and A. Roig, *Adv. Mater.* **26**, 4645 (2014).
[4] J. Jin, S. Ohkoshi, and K. Hashimoto, *Adv. Mater.* **16**, 48 (2004).
[5] M. Gich, J. Gazquez, A. Roig, A. Crespi, J. Fontcuberta, J. C. Idrobo, S. J. Pennycook, M. Varela, V. Skumryev, and M. Varela, *Appl. Phys. Lett.* **96**, 112508 (2010).
[6] G. Carraro, D. Barreca, C. Maccato, E. Bontempi, L. E. Depero, C. de Julián Fernández, and A. Caneschi, *CrystEngComm* **15**, 1039 (2013).
[7] A. Tanskanen, O. Mustonen, and M. Karppinen, *APL Mater.* **5**, 056104 (2017).
[8] T. Jussila, A. Philip, J. Lindén, and M. Karppinen, *Adv. Eng. Mater.* **25**, 2201262 (2023).

Capping layers engineering for oxygen supply in solid and nanolaminate $Hf_xZr_{1-x}O_2$ for sub 10nm ferroelectric memory applications

H. Kim[1,2,*], **M. I. Popovici**[1], **G. De**[1,2], **D. S. Kwon**[1,3], **A. Pavel**[1], **G. Kim**[1,4], **H. Dekkers**[1], **L. Nyns**[1],
A. Delabie[1,5] **and J. Van Houdt**[1,2]
[1]IMEC : Interuniversity Microelectronics Centre
[2]KU Leuven, Department of Physics and Astronomy
[3]Sookmyung Women's University, Department of Chemical and Biological Engineering,
[4]Sungkyunkwan University, Department of Electrical and Computer Engineering
[5]KU Leuven, Department of Chemistry
e-mail: hyun-cheol.kim.ext@imec.be

Ferroelectric (FE) materials are promising candidates for emerging memory applications due to their intrinsic spontaneous polarization, which can be reversed by applying an electric field. In non-volatile random-access memory (RAM) applications, a ferroelectric gate stack utilizes this polarization within the gate structure. Recent advancements have highlighted the discovery of ferroelectricity in HfO_2, sparking new interest in this material. For low power application, a reduction of switching voltage is required, which can be implemented by reducing the physical thickness. In this work, an evaluation of crystallization behavior of 6 nm stoichiometric hafnium zirconium oxide (HZO) was investigated. The 6 nm thick films were grown by atomic layer deposition using metalorganic based Hf and Zr precursors and O_3 has been employed as oxidant in a TiN/HZO/TiN stack. The films deposited on TiN substrate appear amorphous in X-ray Diffraction (XRD) spectra even after crystallization anneal, likely due to small grain size. Therefore, functional layers acting as seed and capping layer were introduced at the interfaces with TiN electrodes. The functional layers acted mainly as O-supply source, enabling crystallization of HZO with ferroelectric behavior.[1] The XRD spectra show the presence of a peak around 2θ of ~30.5°, indicating that our HZO films are at least partially crystallized in polar-orthorhombic phase responsible for the ferroelectric character of the capacitor stack, which were manufactured by patterning the top electrode, as shown in Fig.1(a). Furthermore, we investigate the effects of capping layers serving as oxygen supply sources in solid and nanolaminate (NL) HZO. We define solid HZO as an alternation of single HfO_2 and ZrO_2 cycles, while the NL refer to several consecutive HfO_2 and ZrO_2 cycles, namely. The introduction of additional oxygen by applying capping layers facilitates the transition from the initial tetragonal (t-) to polar orthorhombic (o-) phase, which is crucial for enhancing ferroelectricity.[1,2] X-ray photoelectron spectroscopy (XPS) of various metal oxides investigated shows that the maximum oxidation state of each metal is changed, as result of their reducible character.[1] Although the most reducible oxide capping layers are effective oxygen donors, their compressive stress negatively impacts ferroelectric behavior, making them unsuitable as O donor candidates. To evaluate the effects of oxide capping layers, both having oxygen supply and tensile stress effect, on solid and NL HZO, we conducted additional measurements such as X-ray reflectivity (XRR) for thickness and density evaluation, and polarization-electrical field (P-E) measurements (Fig.1(b). Solid HZO without an oxide capping layer exhibited no ferroelectricity, consistent with XPS results. Even though the capping layers induce ferroelectricity, when comparing solid HZO and NL HZO we observed an opposite behavior in terms of the O-supply effect as reflected in remnant polarization ($2P_r$) and grain size evolution. Additionally, the sublayer thickness for NL HZO was varied to optimize ferroelectricity and reliability. Thicker sublayers reduce $2P_r$ due to insufficient crystallization of HfO_2 which requires higher anneal temperature as compared to ZrO_2 sublayer, resulting in less o-phase. However, ZrO_2 sublayers enhance the reliability of ferroelectric capacitors by suppressing V_O migration owing to a stable ZrO_2 barrier.[3] Based on the extracted o(111)/t(101) diffraction peak – $2P_r$ – grain size as a function of the type of capping layers, we were able to select which specific capping layers are the most suitable for solid HZO and NL HZO, respectively. In conclusion, capping layers facilitates HZO to have intermediate oxygen and tensile stress, resulting in improved ferroelectric characteristics. Accordingly, the technique of engineering capping layers opens pathways uniquely adaptable to sub-10 nm ferroelectric applications such as ferroelectric field-effect transistors and random-access memory.

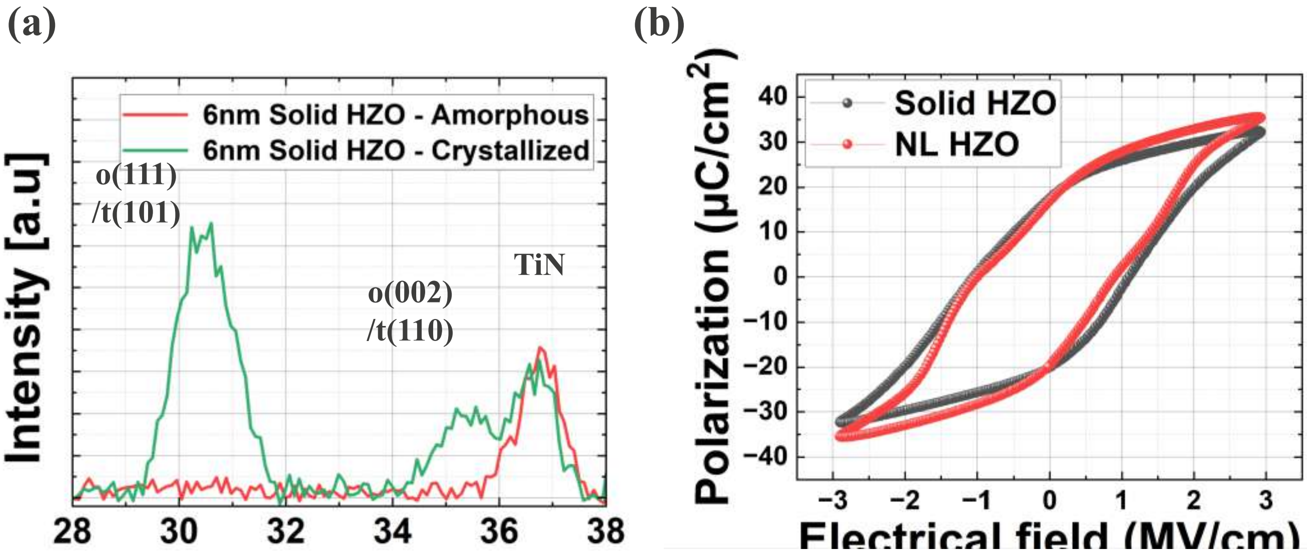

Fig.1 (a) XRD of amorphous(red) and crystallized(green) 6 nm solid HZO depending on capping layer (b) P-E curve of solid and NL 6nm HZO using same capping layer.

References

[1] M. I. Popovici and J. Bizindavy et al., *International Electron Devices Meeting,* (2022)
[2] Kwon, Dae Seon, et al. *ACS Applied Materials & Interfaces* **16.31,**41704 (2024)
[3] Chen, Meiwen, et al. *Nanomaterials* **13.10**, 1608 (2023)

Atomic layer deposition of preferentially c-axis oriented ferroelectric hafnium zirconium oxide thin films for enhanced ferroelectric response

G. De[1,2,*], **M. I. Popovici**[1], **P. K. Parida**[1], **D.S. Kwon**[3], **S. Mukherjee**[1,2], **H. Kim**[1,2], **G. Kim**[1,4], **O. Richard**[1], **P. Favia**[1], **A. Delabie**[1,5], **J. Van Houdt**[1,2]

[1]imec, Leuven, Belgium
[2]Department of Physics and Astronomy, KU Leuven, Leuven, Belgium
[3]Department of Chemical and Biological Engineering, Sookmyung Women's University, Seoul, Republic of Korea
[4]Department of Electrical and Computer Engineering, Sungkyunkwan University, Suwon, Republic of Korea
[5]Department of Chemistry, KU Leuven, Leuven, Belgium

e-mail: gourab.de@imec.be

Since the discovery of ferroelectricity in doped hafnium oxide in 2011[1], hafnium oxide based thin films are considered excellent candidates for next generation memory technologies like ferroelectric RAM (FeRAM), ferroelectric FET (FeFET) and ferroelectric tunnel junctions (FTJ)[2],[3]. Ferroelectricity in hafnium oxide based thin films arises due to stabilization of the non-centrosymmetric $Pca2_1$ orthorhombic phase (o_{III}-phase)[3],[4]. Although higher concentrations of o_{III}-phase will result in a higher remanent polarization ($2P_r$), the impact of other factors such as crystallite orientation has not been much explored. For example, a c-axis oriented o_{III}-phase crystallite (001) should result in a significantly higher polarization value due to the direction of the displacement of the oxygen atoms being aligned along the direction of the applied electric field[4]. In this work, we show that in 9 nm atomic layer deposited (ALD) stoichiometric hafnium zirconium oxide (HZO) films, the o_{III}-phase can be preferentially oriented along (002) direction by subjecting the ALD titanium nitride (TiN) bottom electrodes (BE) to different thermal treatments before deposition of the HZO layer. After deposition of the HZO layer and a TiN top electrode (TE), the stacks were subjected to post-metallization anneal (PMA) at 400 °C, in N_2 atmosphere for 1 hr to enhance the crystallinity of the layer, thereby stabilizing the o_{III}-phase. HZO films grown on treated TiN films exhibited smaller lateral grain size, as determined from top-view Scanning Electron Microscopy (SEM) analysis. This also coincided with promotion of (002) oriented o_{III}-phase crystallites of HZO on treated TiN BE (as observed from X-ray diffraction (XRD) spectra), which came at the expense of (111) oriented o_{III}-phase crystallites (Fig. 1(a)). Potential mechanisms driving the promotion of (002) orientation will be discussed. By improving the concentration of (002) oriented crystallites, an increase in pristine $2P_r$ by 84% was observed (Fig. 1(b)). This shows the critical role crystallite orientation plays in controlling $2P_r$, and we provide a pathway to engineer preferentially c-axis oriented ALD HZO films.

References:

[1] T. S. Böscke, J. Müller, D. Bräuhaus, U. Schröder and U. Böttger, *Applied Physics Letters*, **99**, 102903 (2011)

[2] M.I. Popovici, J. Bizindavyi, P. Favia, S. Clima, Md. Nur K. Alam, R.K. Ramachandran, A.M. Walke, U. Celano, A. Leonhardt, S. Mukherjee, O. Richard, A. Illiberi, M. Givens, R. Delhougne, J. Van Houdt and G.S. Kar, *2022 IEEE International Electron Devices Meeting (IEDM)*, 3-7 December, San Francisco, U.S.A., 6.4.1.-6.4.4

[3] D.S. Kwon, J. Bizindavyi, G. De, A. Belmonte, A. Delabie, L. Nyns, G.S. Kar, J. Van Houdt and M.I. Popovici, *ACS Applied Materials & Interfaces,* **16.31,** 41704–41715 (2024)

[4] T. Schenk, C.M. Fancher, M.H. Park, C. Richter, C. Künneth, A. Kersch, J.L. Jones, T. Mikolajick and U. Schroeder , *Advanced Electronic Materials*, **5**, 1900303 (2019)

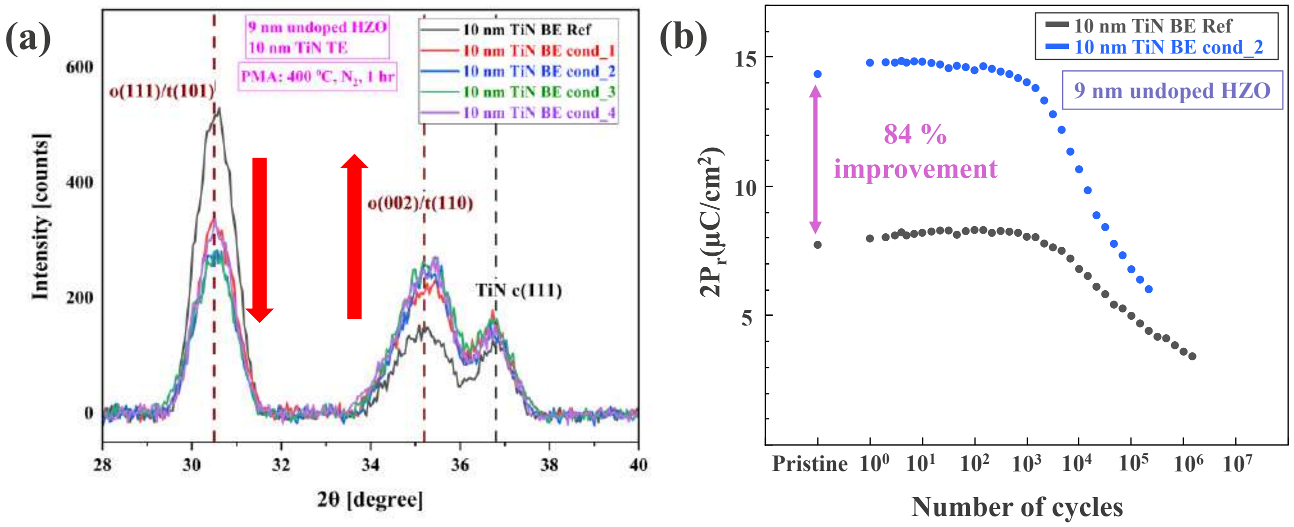

Fig. 1: (a) Grazing incidence X-ray diffraction (GIXRD) spectra showing promotion of $\mathrm{o_{III}}$-phase (002) oriented crystallites on TiN BE subjected to different thermal treatment conditions, (b) Evolution of remanent polarization over cycling at an electric field of 4 MV/cm for the HZO stacks. Reference HZO stack refers to HZO film being deposited on non-treated TiN BE.

Optimized Annealing and Seed Layer Processing of Zr-Doped HfO_2 Thin Films for Ferroelectric Applications

G. Kim[1,2*], **D. S. Kwon**[1,3], **G. De**[1,4], **H. Kim**[1,4], **L. Nyns**[1] **and M. I. Popovici**[1]

[1]IMEC: Interuniversity Microelectronics Centre, Leuven, Belgium
[2]Department of Electrical and Computer Engineering, Sungkyunkwan University, Suwon, Republic of Korea
[3]Department of Chemical and Biological Engineering, Sookmyung Women's University, Seoul, Republic of Korea
[4]Department of Physics and Astronomy, KU Leuven, Leuven, Belgium
e-mail: gwon.kim.ext@imec.be

Ferroelectric random access memory (FeRAM) has gained significant attention as a next-generation nonvolatile memory technology and is widely investigated as a potential replacement for Dynamic random access memory (DRAM) technology. One of the strongest advantages of FeRAM is its ability to provide nonvolatile data storage with superior energy efficiency, eliminating the need for periodic refreshing to retain data. Among the materials with ferroelectric characteristics, Zr-doped HfO_2 (HZO) thin films are particularly promising due to their strong ferroelectric properties at nanoscale thicknesses and compatibility with complementary metal-oxide-semiconductor (CMOS) processes. Despite extensive research on FeRAM capacitors for mass production in a one-transistor-one-capacitor (1T1C) structure, several challenges remain. Incorporating HZO thin films into aggressively scaled next-generation memory devices requires sub-5 nm film thicknesses, which intensifies concerns about stabilizing ferroelectric properties efficiently. To address these challenges, this study focuses on engineering 4 nm-thick HZO thin films optimized for ferroelectric properties. Fabrication processes are refined to suppress the tetragonal phase and promote the orthorhombic phase through optimized annealing processes, including post-deposition annealing (PDA) and post-metallization annealing (PMA), as well as pre-annealing of a seed layer [1]. PMA introduces mechanical stress to the HZO layer due to the confinement of the top electrode during annealing, unlike PDA which relies solely on thermal budget. Comparing these, the impact of the stress for the HZO layer is discussed in detail [2]. Additionally, a seed layer is employed to modulate the crystalline properties of the HZO layer. Among various candidates, ZrO_2 seed layer can affect the ferroelectric HZO layer by controlling the growth behavior of the HZO layer such as nucleation reactions, grain growth, and subsequent crystallization behavior [1,3,4]. The crystallization behaviors are examined using X-ray diffraction (XRD), enabling phase analysis and out-of-plane grain size estimation. Scanning electron microscopy (SEM) images are used to identify potential defects in the HZO film. Furthermore, the grain size distribution and median diameter are also estimated using SEM images and the watershed method in Gwyddion software (see Fig. 1). X-ray reflectivity (XRR) is employed to estimate the thickness, density, and roughness of the layers in each device (see Fig. 2). Based on various measurements, this study aims to identify combinations of ferroelectric properties suitable for FeRAM applications. These findings contribute to enhancing the ferroelectric performance of 4 nm-thick HZO films, meeting the stringent requirements for FeRAM applications.

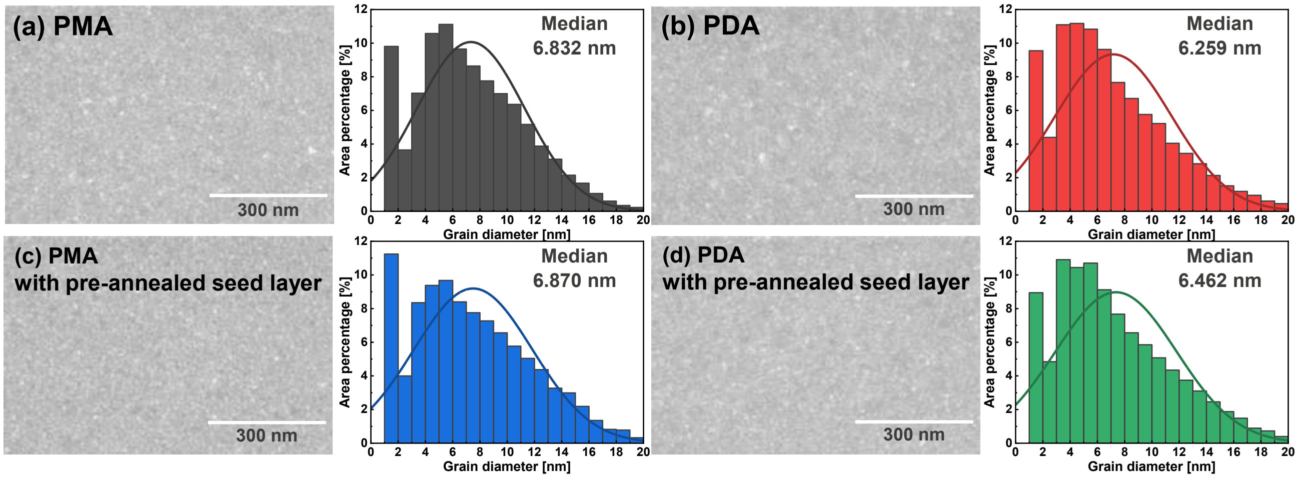

Fig. 1. HZO surface morphology and the distribution of the grain size (a-b) on the seed layer without annealing, and (c-d) on the pre-annealed seed layer. The surface morphology of the films was examined using SEM, and the grain size distribution was analyzed using the watershed method implemented in Gwyddion software.

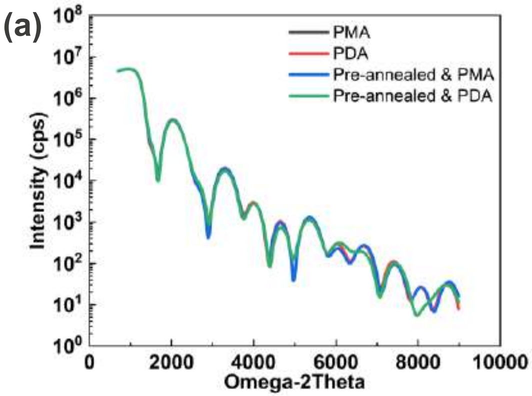

(b)

	TiN (Bottom)			ZrO_2			HZO			TiN (Top)		
	Thickness (Å)	Density (%)	Roughness (Å)	Thickness (Å)	Density (%)	Roughness (Å)	Thickness (Å)	Density (%)	Roughness (Å)	Thickness (Å)	Density (%)	Roughness (Å)
PMA	**82.00**	**82.68**	**0.14**	**16.85**	**79.33**	**8.78**	**39.06**	**96.54**	**5.12**	**89.48**	**84.17**	**6.19**
PDA	**86.48**	**85.52**	**6.49**	**12.45**	**78.39**	**6.38**	**40.28**	**94.49**	**3.15**	**87.26**	**84.63**	**6.77**
PMA with pre-annealed seed layer	**87.70**	**85.21**	**6.60**	**11.39**	**77.37**	**6.74**	**39.64**	**95.68**	**3.84**	**89.26**	**85.57**	**6.10**
PDA with pre-annealed seed layer	**85.93**	**85.40**	**1.53**	**12.82**	**80.08**	**5.27**	**40.38**	**96.17**	**2.49**	**87.63**	**86.21**	**6.71**

Fig. 2. (a) The XRR data of each device enables the measurement of the layer thickness. (b) Table summarizing the thickness, density, and roughness of the layers in each device.

References

[1] Popovici, Mihaela Ioana, et al. *ESSDERC 2023-IEEE 53rd European Solid-State Device Research Conference (ESSDERC). IEEE*, 11-14 Sept, Lisbon, Portugal, 121-124 (2023).
[2] Qin, Yixin, et al. *IEEE Transactions on Electron Devices,* **vol. 71**, no. 9, pp. 5618-5623 (2024).
[3] Kwon, Dae Seon, et al. *ACS Applied Materials & Interfaces* **16.31** (2024).
[4] Onaya, Takashi, et al. *Applied Physics Express* **10.8** (2017)

Session AM_2.1 FUNCTIONAL MATERIALS I

Tuesday 3rd June 2025 | 8.45-10.45

Chair: **Mato Knez** | Main Hall “Santo Mazzarino”

Chemical Vapour Deposition as the Key to Unlock Tailoring of Van der Waals Phase Change Materials

Maria Losurdo
Institute of Chemistry of Condensed Matter and of Technologies for Energy ICMATE-CNR
Corso Stati Uniti 4, Padova, Italy
e-mail: maria.losurdo@cnr.it

Chemical vapor deposition (CVD) is a powerful method which has been extensively used to to bring 2D compound materials and their heterostructures from the laboratory to industrial applications in recent years, despite several challenges remaining.

In this contribution, I will highlight recent advances in the controlled growth of unexpected and novel phases of Van der Waals (vdW) materials, with an emphasis on chalcogenides phase change materials (PCMs), taking chalcogenides of the III- and V-group elements, such as Sb_2S_3, Sb_2Se_3, GaS, InSe, etc... Those materials enable reconfigurable nanophotonic devices, offering the potential to create tunable and switchable nanophotonic systems through the modulation of their optical properties via external stimuli. I will provide insight into key technologies used to realize the of wafer-scale single crystal growth of continuous and homogeneous 2D films which are important for practical applications. Specifically, the key technology parameters that affect the CVD process, including non-metal precursor, metal precursor, substrate engineering, temperature, and gas flow, are systematically discussed, bringing to design of parametric space maps and diagrams for the controlled growth of the above vdW PCMs from amorphous to single crystalline layers. Meanwhile, strategies to design and grow various kinds of 2D material based heterostructures will be discussed, introduce some emerging methods in improving the quality of CVD-grown monolayers and few-layers vdW PCMs chalcogenides. The validated properties from structural to morphological and optical properties will be presented. Novel characterization approaches based on the combination of imaging ellipsometry and polarimetry with Raman spectroscopy also time-resolved is used to highlight the interplay of the structure-optical response in this novel vdW PCMs platform. The applications of the above CVD-grown van der Waals PCMs and their heterostructures in photonics such as optical switches, light modulators, broadband photodetectors, covering the range from near-infrared to visible, will also be discussed. Finally, I will suggest solutions to these challenges and ideas concerning future developments in CVD of structure-reversible chalcogenides materials with good controllability and high quality, laying the foundations for their potential applications.

This work was supported by the H2020 Future and Emerging Technologies (GA899598 – PHEMTRONICS)

Atomic/molecular layer deposition of copper ethenetetrathiolate thin films for thermoelectric applications

M. Heikkinen[1], **M. A. Francis**[1], **K. Meinander**[1], **G. C. Tewari**[1], **M. Nisula**[1], **M. Karppinen**[1]
[1]Aalto University, Department of Chemistry and Materials Science
e-mail: mari.heikkinen@aalto.fi

Thermoelectrics could potentially provide us means to tackle global challenges related to energy shortage, storage challenges, and increasing need for efficient cooling technologies. The focus of the research in this field has moved more and more towards materials composed of earth abundant and non-toxic elements, and as a result there is a rapidly growing interest in organic thermoelectrics. Coordination polymers based on 1,1,2,2-ethenetetrathiolate (ETT) exhibit excellent thermoelectric properties and they consist of relatively earth abundant and safe elements depending on the metal node chosen.[1] Metal-ethenetetrathiolate (M-ETT) with M = Cu or Ni in particular have shown promising thermoelectric properties as pressed pellets and composite films.[2] M-ETTs have been reported to exhibit both n- and p-type behavior depending on the metal used in the coordination polymer.[3,4] They are generally insoluble and the thin films are fabricated as composite films mixed with other polymer as a matrix material.[2]

The atomic/molecular layer deposition (ALD/MLD) has been proven to be a successful method for depositing complex materials through gas-surface reactions, and it is solvent free.[5] ALD/MLD has also been utilized in the fabrication of conductive coordination polymer films previously.[6] In this research, we have developed a novel three-step ABC type process to deposit M-ETT thin films. By using an intermediate alkali metal activation step, the otherwise unreactive organic precursor 1,3,4,6-tetrathiapentalene-2,5-dione (TPD) is first converted to an intermediate Li-ETT layer using lithium hexamethyldisilazide $LiN(SiMe_3)_2$ (Li-HMDS), followed by a transmetalation step with copper(II) acetylacetonate ($Cu(acac)_2$) to allow the end product Cu-ETT. The reaction scheme is given in Figure 1.

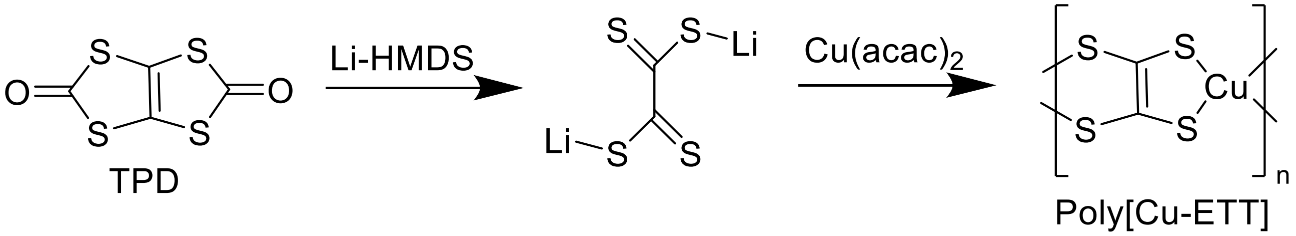

Figure 1. Reaction scheme of Cu-ETT thin films by ALD/MLD.

All the M-ETT thin-film depositions were carried out using an ASM Microchemistry F-120 flow-type hot-wall ALD reactor with base pressure of ~1 mbar. The depositions were carried out at a deposition temperature of 220 °C. The precursor temperatures used were 100, 65 and 130 °C for TPD, Li-HMDS and $Cu(acac)_2$, respectively. The pulse times for all precursors ranged between 4–6 s. The thin films were characterized with spectroscopic ellipsometry (SE) for film thickness, Fourier transform infrared spectroscopy (FTIR) and X-ray photoelectron spectroscopy (XPS) for film composition, grazing-incidence X-ray diffraction (GIXRD) for crystallinity and scanning electron microscope (SEM) for surface morphology. The thermoelectric properties (electrical resistivity and Seebeck coefficient) were measured using a physical property measurement system (PPMS; Quantum Design) and the results were compared to inhouse synthesized powder samples of Cu-ETT.

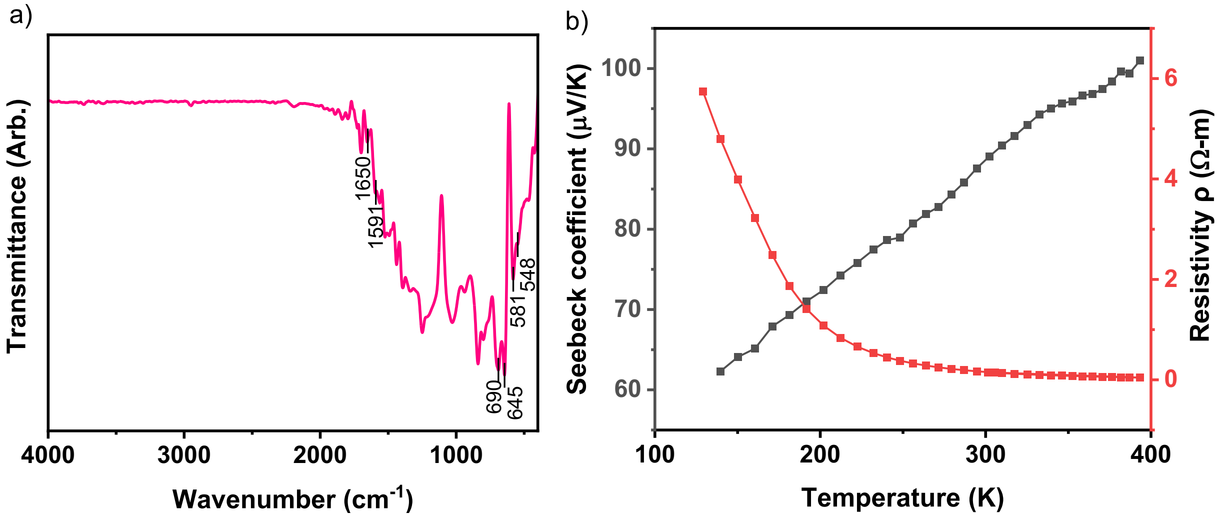

Figure 2. a) FTIR spectrum, and b) electrical resistivity and Seebeck coefficient of Cu-ETT thin film deposited at 220 °C for 200 cycles.

The results indicate that ALD/MLD like growth can be achieved with these precursors and the transmetalation happens between lithium and copper. All three precursors show surface saturation limited growth behavior. The saturation happens between 4–6 s for all precursors. The FTIR results in Figure 2a show the expected vibrations from bonding between Cu-S (640-690 cm^{-1}),[7] C-S (581 cm^{-1})[8] and C=C (1650 cm^{-1}). The FTIR spectrum also indicates that some additional bonds remain in the film, which can be attributed to unreacted Cu(acac)$_2$ ligands or unreacted ketone group from TPD. Another possibility for C-O (1325 cm^{-1}) bonds can arise from unreacted ligands or an undesired reaction with oxygen in TPD, in which the oxygen does not leave the film but reacts with copper on the film surface breaking the ketone group. Evidence for these impurities and additional bonding modes could also be seen by XPS and GIXRD. Aside from the impurities present in the film we show successful use of ion exchange in ALD/MLD depositions of Cu-ETT thin films, which also show electrical conductivity (Figure 2b).

This work was supported by FinnCERES.

References

[1] R. Tkachov, L. Stepien, R. Grafe, O. Guskova, A. Kiriy, F. Simon, H. Reith, K. Nielsch, G. Schierning, D. Kasinathane and C. Leyens, *Polym. Chem.*, **9**, 4543 (2018).
[2] A. K. Menon, R. M. W. Wolfe, S. R. Marder, J. R. Reynolds, and S. K. Yee, *Adv. Funct. Mater.*, **28**, 1801620 (2018).
[3] Y. Sun, P. Sheng, C. Di, F. Jiao, W. Xu, D. Qiu and D. Zhu, *Adv. Mater.*, **24**, 932–937 (2012).
[4] P. Sheng, Y. Suna, F. Jiaoa, C. Dia, W. Xua, and D. Zhu, *Synthetic Metals*, **193**, 1–7 (2014).
[5] J. Multia and M. Karppinen, *Adv. Mater. Interfaces*, **9**, 2200210 (2022).
[6] M. Nisula, A. J. Karttunen, E. Solano, G. C. Tewari, M. Karppinen, M. Minjauw, H. S. Jena, P. Van Der Voort, D. Poelman and C. Detavernier, *ACS Appl. Mater. Interfaces*, **13**, 10249−10256 (2021).
[7] L.Z. Pei, J.F. Wang, X.X. Tao, S.B. Wang, Y.P. Dong, C.G. Fan and Q.-F. Zhang, *Materials Characterization*, **62**, 354–359 (2011).
[8] A. B. D. Nandiyanto, R. Ragadhita and M. Fiandini, *Indonesian Journal of Science & Technology*, **8**, 113–126 (2023).

ALD Synthesis of Transition Metal Phosphides

Raul Zazpe[1,2], Jhonatan Rodriguez-Pereira[1,2], Jaroslav Charvot[3], Milan Klikar[3], Filip Bures[3] and Jan M. Macak[1,2]
[1]Center of Materials and Nanotechnologies, Faculty of Chemical Technology, University of Pardubice, Nam. Cs. Legii 565, 530 02 Pardubice, Czech Republic
[2]Central European Institute of Technology, Brno University of Technology, Purkynova 123, 612 00 Brno, Czech Republic
[3]Institute of Organic Chemistry and Technology, Faculty of Chemical Technology, University of Pardubice, Pardubice 532 10, Czech Republic

e-mail: raul.zazpe@upce.cz

The ever-increasing global energy demand together with the environmental issue originated from the use of fossil fuel, has triggered an intense search for sustainable and clean energy alternatives, such us hydrogen energy, biomass and solar energy among others. In this context, a pivotal key to deliver sustainable and superior energy systems lies on the rational design and development of high-quality and cost-effective catalyst offering enhanced stability, activity and selectivity. Consequently, intense efforts have been devoted in the search and synthesis of new catalyst materials to replace the scarce and expensive traditional noble metals (e.g. Pt, Pd, Au and Ru) for energy conversion and energy storage applications.

Among the recently explored novel catalyst materials, metal phosphides (MPs) have emerged in recent years, attracting significant attention thanks to their intriguing properties [1]. In particular transition metal phosphides (TMPs) exhibit striking properties. The moderately strong M−P bonds lend outstanding mechanical properties, high thermal stability and outstanding chemical resistance to chemical attack and oxidation in acidic and alkaline solutions. Additionally, Co, Ni, Mo-based phosphides demonstrated excellent catalytic and bifunctional properties, in particular towards water splitting as both hydrogen evolution reaction (HER) and oxygen evolution reaction (OER) [2,3].

Herein, we present the synthesis of TMPs by thermal Atomic Layer Deposition (ALD), including titanium phosphide [4], based on the use of different transition metal precursors combined with in-house synthesized P precursors. The physical and chemical properties of the resulting TMPs thin films were extensively characterized by different methods, including atomic force microscopy, X-ray photoelectron spectroscopy and X-Ray diffraction. The presentation will introduce and describe the synthesis of the TMPs and the corresponding characterization toward diverse applications.

[1] Z. Pu, T. Liu, I. S. Amiinu, R. Cheng, P. Wang, C. Zhang, P. Ji, W. Hu, J. Liu, S. Mu, *Adv. Funct. Mater.*, **30**, 2004009 (2020).
[2] C.C. Weng, J.T. Ren, Z.Y. Yuan, *ChemSusChem*, **13**, 3357-3375 (2020).
[3] C.-J. Huang, H.-M. Xu, T.-Y. Shuai, Q.-N. Zhan, Z.-J. Zhang, G.-R. Li, *Applied Catalysis B: Environmental*, **325**, 122313 (2023).
[4] R. Zazpe, J. Charvot, J. Rodriguez-Pereira, L. Hromádko, M. Kurka, K. Baishya, H. Sopha, F.Bureš, and J. M. Macak, submitted.

Emission peculiarities in MOCVD deposited undoped SnO_2 layers

Poting Liu[1, 2], Anjana Baby[1], Benjamin Dietzek-Ivanšič[1,2], Vaidas Klimkevičius[3], and **Vladimir Sivakov**[1]

[1] Department Functional Interfaces, Leibniz Institute of Photonic Technology, Albert Einstein Str. 9, 07745 Jena, Germany.
[2] Institute of Physical Chemistry, Friedrich Schiller University Jena, Helmholtzweg 4, 07743 Jena, Germany.
[3] Faculty of Chemistry and Geosciences, Vilnius University, Naugarduko Str. 24, 03225 Vilnius, Lithuania

email:vladimir.sivakov@leibniz-ipht.de

Tin dioxide (SnO_2), which is a direct bandgap semiconductor with a reported bandgap value of 3.6 eV, is widely used in various applications such as optoelectronics, photocatalysis, gas analysis, and energy conversion devices (e.g., perovskite solar cells) [1]. Due to its high electron mobility, SnO_2 thin film obtained by deposition techniques is commonly used as an electron-transport layer in optoelectronics, making it a key in these devices. Therefore, understanding the fundamental properties of SnO_2 thin films are essential for the further development of its functions and additional applications. In our previous studies, we reported the possibility of implementing nanoscale engineering to deposit unique Sn-based nanostructures using nanostructured and/or planar silicon surfaces [2-4]. In the current work, we report that a strong photoluminescence was observed in planar tin oxide layers deposited by metal-organic chemical vapor deposition (MOCVD). At the excitation wavelength of the system in the range of 250-325 nm, the deposited SnO_2 thin films exhibited broad red-orange photoluminescence with emission maximum above 600 nm and tunable emission intensity. Wide-ranging surface and bulk sensitive characterization techniques, such as electron microscopy, X-ray diffraction, X-ray photoelectron spectroscopy (XPS) and synchrotron radiation-based X-ray absorption near edge structure (XANES) spectroscopy, have been applied to study the atomic and electronic structure features of the deposited SnO_2 thin films. In the existing literature, blue-green (450-550 nm) emission associated with the presence of surface defects (oxygen vacancies) is widely reported for undoped 2D tin oxide layers. On the other hand, red-orange emission (580-650 nm) is poorly described and mainly observed for 1D SnO_2 nanowires and is explained as an effect of deeply trapped states associated with oxygen vacancies (not surface related) or tin interstitials. Our research can provide a deep fundamental understanding of the relationship between the structural features of SnO_2 thin film and its optoelectronic properties, enabling a theoretical basis for further applications of SnO_2 in various devices.

[1] P. Liu and V. Sivakov*, Nanomaterials* **13**(17), 2391 (2023).
[2] P. Liu, A. Schleusener, G. Zieger, A. Bochmann, M. A. van Spronsen, and V. Sivakov, *Small* **19**, 2206318 (2023).
[3] S. Turishchev, A. Schleusener, O. Chuvenkova, E. Parinova, P. Liu, Maxim Manyakin, S. Kurganskii, and V. Sivakov, *Small* **19**, 2206322 (2023).
[4] P. Liu, A. Makarova, K. Freiberg, D. C. Grinter, D. Sharma, P. Ferrer, O. Chuvenkova, T. Deckert-Gaudig, S.Turishchev, St. Lippmann, V. Sivakov, *Small* **20**, 2404508 (2024).

Synthesis of Lanthanum-based Perovskite Thin Films by Atomic Layer Deposition

S. Azpeitia[1*], **M. Knez**[1,2]
[1]CIC nanoGUNE. 20018 San Sebastián, Spain
[2]IKERBASQUE, Basque Foundation for Science. 48011 Bilbao, Spain
e-mail: s.azpeitia@nanogune.eu

Perovskites have proved to be highly interesting materials for diverse applications. This family of materials shares the ABX_3 formulation, where A and B represent cations of different sizes, and X is an anion such as oxygen or a halide bonded to both cations. The distortions in the crystal lattice of perovskites are closely related to the wide and varied range of physicochemical properties exhibited by the material. Currently, perovskite-based solar cells have emerged as a promising to conventional silicon-based photovoltaic technology, thanks to a high absorption coefficient, a wide spectral absorption range, and good charge transport. They have also showed a great potential photocatalysts, using solar radiation to transform water into fuel through the generation of H_2 and O_2, or for the reduction of CO_2, among others.

The photocatalytic activity and photoelectronic properties of perovskites will largely depend on their specific surface area, as the greater this is, the higher the number of active sites or centers for the reaction to occur in a catalyst. Thus, thin film formation methods would allow for the production of perovskites with a large specific surface area while reducing the amount of material used.

The aim of this work is the synthesis of lanthanum-based perovskite oxide thin films by atomic layer deposition (ALD) in different substrates. The excellent redox and oxygen mobility properties, as well as the surface acid−base character and good thermal stability, make La-based perovskite oxides ($LaBO_3$) very verstaile catalysts. This work describes the deposition of $LaAlO_3$ films using lanthanum bis(trimethylsilyl)amide $La(N(SiMe_3)_2)_3$, trimethylaluminium (TMA) as precursors and H_2O as a co-reactant in both cases. This ALD deposition is performed as a sequence of supercycles consisted by two alternating subcycles of $La(N(SiMe_3)_2)_3/H_2O$ and TMA/H_2O. This process enables a better control of the stoichiometry in the final perovskite structrure. To achieve the formation of the final perovskite structure, the samples deposited by ALD are calcined to allow the monolayers of both oxides La_2O_3 and Al_2O_3 integrate to adopt the $LaAlO_3$ structure.

The deposited thin films were characterized by X-ray diffraction (XRD), X-ray photoelectron spectroscopy (XPS) and transmission electron microscopy (TEM) among other techniques, to confirm the final $LaAlO_3$ structure formation.

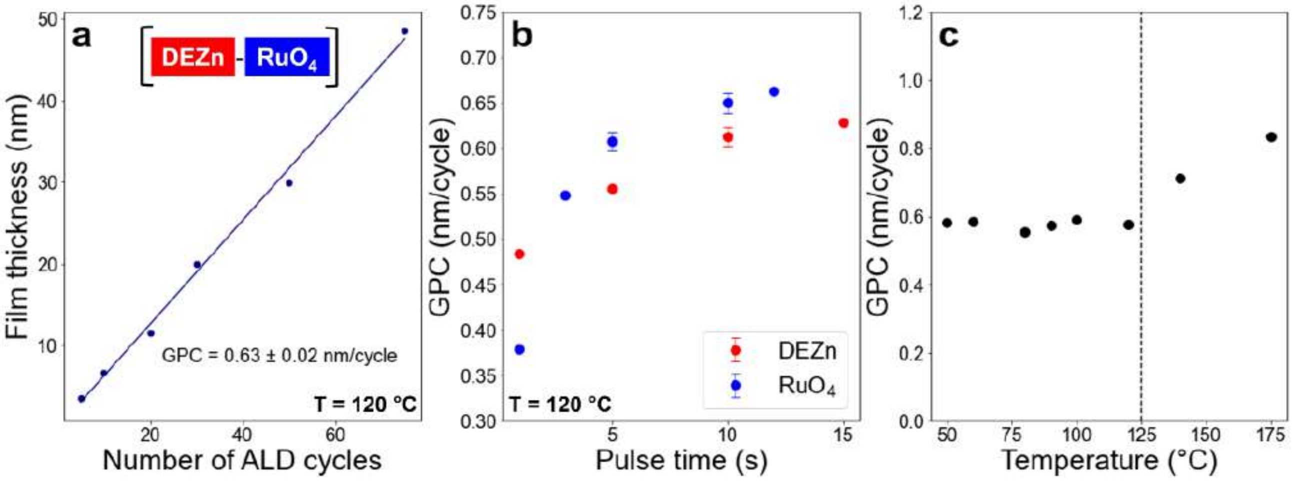

Figure 1. (a) Film thickness obtained from XRR against the number of ALD cycles, showing a linear growth behaviour. (b) Saturation conditions and (c) temperature window of the DEZn/RuO_4 process.

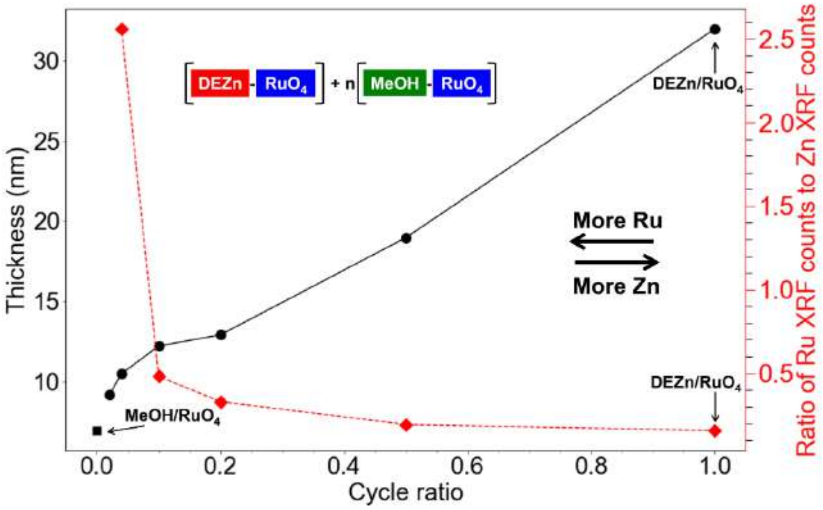

Fig 2. Film thickness (illustrative of the growth) and the ratio of the Ru to Zn XRF counts, as a function of the cycle ratio of the process [[DEZn – RuO_4] + n×[MeOH – RuO_4]]×c with n and the cycle amount c such that (1 + n) × c = 50 to keep a fixed number of RuO_4 pulses in each process. The cycle ratio is 1 / (1 + n). The Ru L and the Zn K XRF lines are used for analysis.

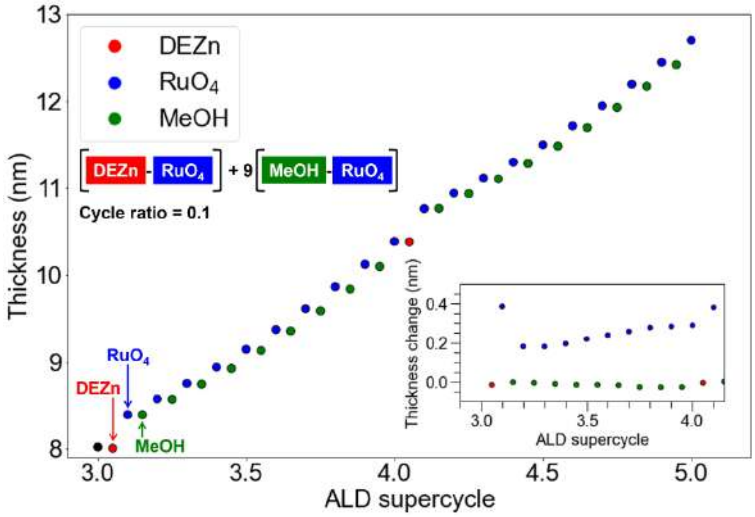

Fig 3. *In situ* film thickness as a function of ALD supercycle in the process [[DEZn – RuO_4] + 9×[MeOH – RuO_4]]×5, with the thickness variation as inset, for a cycle ratio of 0.1, as defined in the caption of Fig 2.

Pulsed-Liquid Injection MOCVD of epitaxial Ga_2O_3 thin films

M. Velasco Enriquez[1,2], I. Gelard[1], C. Jimenez[1], H. Roussel[1], S. Ortega[1], L. Rapenne[1], P. Ferrandis[2], E. Sarigiannidou[1], and V. Consonni[1]
[1]Univ. Grenoble Alpes, CNRS, Grenoble INP, LMGP, Grenoble, France
[2]Univ. Grenoble Alpes, CNRS, Grenoble INP, Institut Néel, Grenoble, France
e-mail: marielena.velasco-enriquez@grenoble-inp.fr

The epitaxial growth of Ga_2O_3 thin films has emerged as a critical topic for power electronics due to its promising properties (ultra-wide bandgap of 4.8-4.9 eV, breakdown field of 8MV/cm, etc.). Among several growth methods, MOCVD is a great technique for industrial-scale production as it can achieve high growth rates compared to their counterparts [1]. Gallium oxide can exist in several polymorphs: β, α, γ, δ, κ, with the monoclinic β-phase being the most thermodynamically stable one. The influence of MOCVD growth parameters were reported not only to improve growth rates (with tradeoff in crystal quality) of β-Ga_2O_3 on sapphire [2], but also to optimize the presence other polymorphs, for instance κ-Ga_2O_3 [3], [4], [5].

Beyond metal-organic chemical vapor deposition (MOCVD) equipped with a bubbler system for introducing the chemical precursors, the pulsed–liquid injection MOCVD technique comprises a vaporizer allowing the utilization of low vapor pressure and thermally unstable chemical precursors : these precursors are introduced in micro-amounts into the evaporator using pulses [6]. In-house studies have shown some key advantages of using this innovative technique in the growth of different materials, as it prevented accumulation of condensed precursor of high-k oxides [7] and it allowed a more controlled morphology and polarity transitions of ZnO [8].

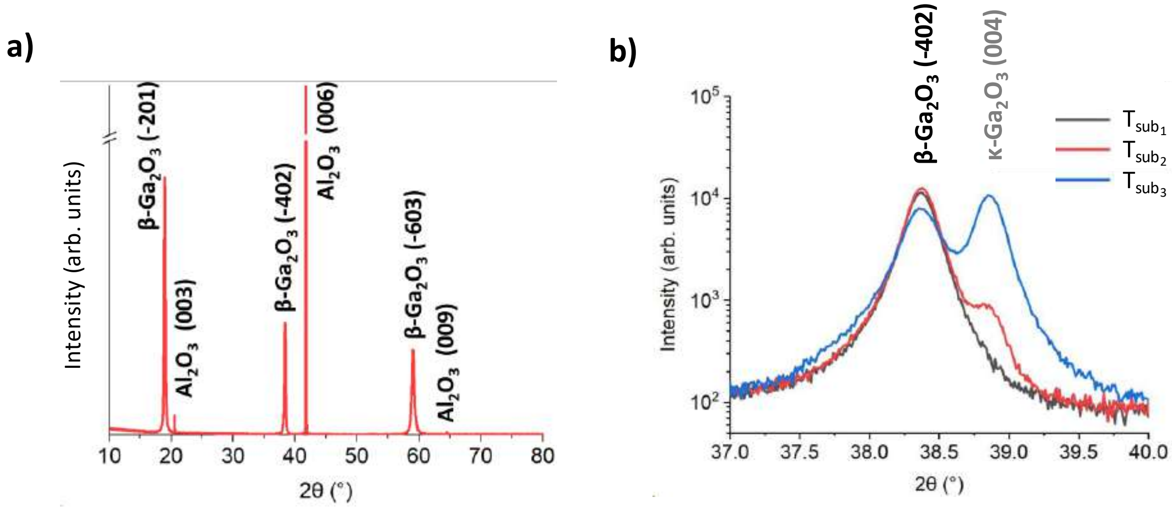

Fig. 1. XRD patterns of (a) β-Ga_2O_3 and (b) β(/κ)-Ga_2O_3 thin films grown at different substrate temperatures by PLI-MOCVD on sapphire.

In this work, we grow Ga_2O_3 thin films on c-plane sapphire by PLI-MOCVD using a semi-industrial ANNEALSYS MC200 reactor with triethyl Gallium (TEGa) and O_2 gas. The presence of pure β- or mixed β/κ-Ga_2O_3 (Fig. 1) was achieved by varying the substrate temperature, and VI/III ratio. Additionally, the epitaxial quality, nature of defect levels, and interface properties were characterized by SEM, AFM, XPS, TEM, X-ray diffraction, Raman spectroscopy, and cathodoluminescence spectroscopy. The present findings open perspectives for the growth of epitaxial Ga_2O_3 thin films with a high quality using PLI-MOCVD.

This work was supported by the French National Research Agency in the framework of the "Investissements d'avenir" program (ANR-15-IDEX-02)

References

[1] A. Waseem, Z. Ren, H.-C. Huang, K. Nguyen, X. Wu, and X. Li, "A Review of Recent Progress in β-Ga ₂ O ₃ Epitaxial Growth: Effect of Substrate Orientation and Precursors in Metal–Organic Chemical Vapor Deposition," *Physica Status Solidi (a)*, vol. 220, no. 8, p. 2200616, Apr. 2023, doi: 10.1002/pssa.202200616.

[2] F. Alema, B. Hertog, A. Osinsky, P. Mukhopadhyay, M. Toporkov, and W. V. Schoenfeld, "Fast growth rate of epitaxial β–Ga2O3 by close coupled showerhead MOCVD," *Journal of Crystal Growth*, vol. 475, pp. 77–82, Oct. 2017, doi: 10.1016/j.jcrysgro.2017.06.001.

[3] Y. Zhuo, Z. Chen, W. Tu, X. Ma, Y. Pei, and G. Wang, "β-Ga2O3 versus ε-Ga2O3: Control of the crystal phase composition of gallium oxide thin film prepared by metal-organic chemical vapor deposition," *Applied Surface Science*, vol. 420, pp. 802–807, Oct. 2017, doi: 10.1016/j.apsusc.2017.05.241.

[4] Y. Chen, X. Xia, H. Liang, Q. Abbas, Y. Liu, and G. Du, "Growth Pressure Controlled Nucleation Epitaxy of Pure Phase ε- and β-Ga2O3 Films on Al2O3 via Metal–Organic Chemical Vapor Deposition," *Crystal Growth & Design*, vol. 18, no. 2, pp. 1147–1154, Feb. 2018, doi: 10.1021/acs.cgd.7b01576.

[5] E. Dobročka *et al.*, "Structure and Thermal Stability of ε/κ-Ga2O3 Films Deposited by Liquid-Injection MOCVD," *Materials*, vol. 16, no. 1, Art. no. 1, Jan. 2023, doi: 10.3390/ma16010020.

[6] "PROCEDE ET DISPOSITIF D'INTRODUCTION DE PRECURSEURS DANS UNE ENCEINTE DE DEPOT CHIMIQUE EN PHASE VAPEUR (Brevets) - Data INPI." Accessed: Nov. 27, 2023. [Online]. Available: https://data.inpi.fr/brevets/FR2707671?q=#FR2707671

[7] C. Dubourdieu *et al.*, "Pulsed liquid-injection MOCVD of high-K oxides for advanced semiconductor technologies," *Materials Science and Engineering: B*, vol. 118, no. 1–3, pp. 105–111, Apr. 2005, doi: 10.1016/j.mseb.2004.12.019.

[8] Q. C. Bui *et al.*, "Morphology Transition of ZnO from Thin Film to Nanowires on Silicon and its Correlated Enhanced Zinc Polarity Uniformity and Piezoelectric Responses," *ACS Appl. Mater. Interfaces*, vol. 12, no. 26, pp. 29583–29593, Jul. 2020, doi: 10.1021/acsami.0c04112.

ALD of Zinc Ruthenate using RuO_4 as a Multiconstituent Reactant

B. Van Neste[1], **M. M. Minjauw**[1], **A. Chalishazar**[1], **C. Detavernier**[1], **J. Dendooven**[1]
[1]CoCooN Research Group, Department of Solid State Sciences, Ghent University, Belgium
e-mail: Brent.VanNeste@UGent.be, Jolien.Dendooven@UGent.be

Ruthenium (Ru) and compounds containing Ru are employed in a variety of applications, including electrochemical, catalytic, and electrical processes. For example, Ru is used as a seed for electroplating, and Ru and RuO_2 are suitable electrode materials for DRAM capacitors [1-2]. Ternary ruthenium oxides or ruthenates are promising electrocatalysts for the oxygen evolution reaction in terms of efficiency, overpotential and corrosion resistance [3], as well as lowering material costs.

The sequential and self-limiting nature of the reactions in ALD can be exploited for depositing ternary materials with tuneable compositions. The most common method for depositing ternary thin films is by combining different ratios of two binary ALD processes into supercycles, but possible challenges include differences in temperature windows and nucleation behaviours [4]. Another approach for the deposition of ternary materials is based on the incorporation of two elements by a single reactant, which is referred to as a multiconstituent reactant. Recent work from our group explored RuO_4 as a source of both Ru and O to deposit ternary ruthenium oxide films containing Al or Pt at low temperatures (50-120 °C) and with a high growth per cycle (GPC, 0.5-0.8 nm/cycle) [5]. However, tuning of the thin film stoichiometry with this approach was not demonstrated.

In this work, we first expand the library of ternary ruthenium oxide ALD processes by depositing zinc ruthenate ($ZnRuO_x$) on Si substrate using sequential exposures of diethylzinc (DEZn) and RuO_4.The ruthenate layers grow linearly with a GPC of 6.3 Å/cycle under saturated conditions (Fig 1a,b). *In situ* ellipsometry data (not shown) revealed a negligible nucleation delay. A limited temperature window of 50-120 °C is found for deposition of the $ZnRuO_x$ films (Fig 1c), with higher temperatures causing decomposition of RuO_4. We hypothesize that the high GPC of 6.3 Å/cycle is due to a high reactivity of the strongly oxidizing RuO_4 and strongly reducing DEZn reactants [2]. Analysis of the film composition by XPS showed a stoichiometry of $Zn_{2.33}Ru_1O_{3.44}$ suggesting the deposition of a Ru-doped ZnO film.

We further explore tuning the Ru/Zn ratio using a supercycle approach in which the DEZn/RuO_4 process for $Zn_{2.33}Ru_1O_{3.44}$ is combined with the MeOH/RuO_4 process for RuO_2 [2]. It is found that the Ru/Zn ratio can be tuned by varying the cycle ratio, but incorporating extra Ru comes at the cost of a decrease in GPC (Fig 2). Ellipsometry data reveal a larger thickness increase with RuO_4 dosing after a DEZn dose compared to after a MeOH dose (Fig 3). DEZn being a strong reductant, we hypothesize that the reaction with DEZn will lead to a more strongly reduced $ZnRuO_x$ surface, allowing for more oxidation, and hence deposition of Ru and O, during the subsequent RuO_4 dose. Following the first RuO_4/MeOH cycle after a DEZn dose, the thickness increase per RuO_4 dose first drops and then slowly increases with subsequent RuO_4/MeOH cycles (Fig 3 inset). These initial growth effects impact the overall growth and the Ru/Zn ratios observed for the $ZnRuO_x$ films, while also highlighting the important balance between oxidation and reduction reactions when using RuO_4 as a multiconstituent reactant.

References

[1] J. M. Hwang, S. Han, et al., *Journal of Materials Chemistry C*, **11**, 3820-3825 (2021)
[2] N. Poonkottil, M. Minjauw, et al., *Chemistry of Materials*, **34**, 8946-8958 (2022)
[3] Z. Shi, J. Li, et al., *Nature Communications*, **14**, 843 (2023)
[4] A. Mackus, J.R. Schneider, et al., *Chemistry of Materials*, **31**, 1142-1183 (2018)
[5] M. Minjauw, J. Feng, et al., *Dalton Transactions,* **51**, 10721-10727 (2022)

Session AM_2.2 PRECURSORS DESIGN II

Tuesday 3rd June 2025 | 9.15-10.45

Chair: **Anjana Devi** |Room “Coro di Notte”

Innovative Fluorinated Aminoalkoxide Precursors for DLI-CVD Growth of High-Quality LiNbO₃ and KNbO₃ Thin Films

A. Tacnet[1*], **A, Bartasyte**[2], **J.M. Decams**[3], **V. Astie**[3], **S. Daniele**[1]
[1] CP2M CPE Lyon, University Claude Bernard Lyon 1, CNRS-UMR 5128 [2] FEMTO-ST Institute, University of Bourgogne-Franche-Comté, CNRS-UMR 6174 [3] Annealsys, 139 Rue des Walkyries, 34000 Montpellier, France
e-mail: anthony.tacnet@etu.univ-lyon1.fr

Achieving the full potential of 5G mobile telecommunications and component miniaturization necessitates breakthroughs in advanced piezoelectric thin films for high-frequency RF acoustic filters. The miniaturization of both devices and their piezoelectric layers is critical to enhancing performance. However, developing ultra-thin piezoelectric layers poses significant challenges, particularly in maintaining homogeneity and crystalline integrity at extreme dimensions **[1]**.

Traditional fabrication methods for alkali niobate thin films, such as bonding, ion slicing, or polishing of single-crystal wafers, often struggle with precise thickness control. Alternative approaches, including capillary liquid epitaxy, RF magnetron sputtering, spin-coating, and metal-organic chemical vapor deposition (MOCVD), have shown promise but remain hindered by a limited selection of suitable alkali metal precursors for vapor-phase processes like MOCVD and atomic layer deposition (ALD) **[2-4]**. To address these limitations, we developed a series of innovative fluorinated aminoalkoxide precursors designed for the growth of alkali niobate $MNbO_3$ (M = Li or K) thin films using DLI-MOCVD techniques. Through a controlled synthesis approach, we successfully produced high-purity lithium and potassium precursors. These were used to deposit $MNbO_3$ thin films with precisely controlled thicknesses of 150 nm. Optimization of deposition parameters yielded films with a single, well-defined crystalline orientation and minimized parasitic phases. Figure 1 highlight the thermal properties of these precursors, demonstrating their compatibility with DLI-CVD processes and XRD patterns confirming the high phase purity and controlled crystalline orientation of $LiNbO_3$ thin films deposited using such precursor.

Our results underscore the potential of fluorinated aminoalkoxide ligands as next-generation precursors for scalable deposition of high-quality alkali niobate thin films, offering precise control over thickness, orientation, and stoichiometry.

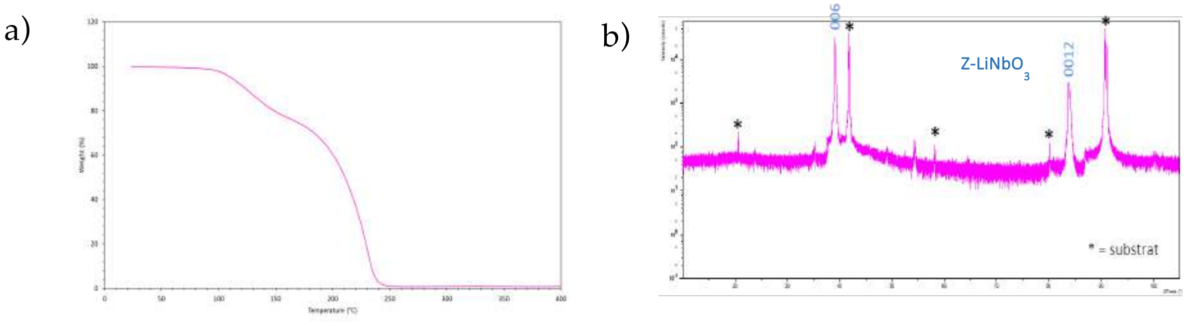

Fig. 1. a) TGA curve of one synthesized lithium precursor, b) X-ray diffraction (XRD, θ -2 θ) pattern of a $LiNbO_3$ thin film deposited on C-sapphire

References: **[1]** V. Astié, *Ph.D. thesis*, University of Franche-Comté (2020). **[2]** A. Bartasyte, S. Margueron, T. Baron, S. Oliveri, P. Boulet, *Advanced Materials Interfaces*, **4**, 1600998 (2017). **[3]** D. Saulys, V. Joshkin, M. Khoudiakov, T. Kuech, A. Ellis, S. Oktyabrsky, L. McCaughan, *Journal of Crystal Growth*, **217**, 287–301 (2000). **[4]** D. Tsymbarenko, I. Korsakov, A. Mankevich, G. Girichev, E. Pelevina, A. Kaul, *ECS Transactions*, **25**, 633–638 (2009).

Deposition of copper from copper triazenide precursor and plasma electrons

P. Promdet[1,2], P. Niiranen[1], P. Bagherzadeh[1], D. Lundin[1], and H. Pedersen[1,2,*]

[1]Department of Physics, Chemistry and Biology, Linköping University, SE-581 83 Linköping, Sweden
[2] Wallenberg Initiative Materials Science for Sustainability, Department of Physics, Chemistry and Biology,
Linköping University, SE-581 83 Linköping, Sweden
e-mail: henrik.pedersen@liu.se

We have recently demonstrated how films of elemental metals can be deposited using free electrons from a plasma discharge as reducing agents.[1] We refer to this process as electron CVD (e-CVD). Our recent study on e-CVD of copper from $Cu(hfac)_2$ and $Cu(acac)_2$ show that the deposition chemistry appears to be self-limiting, suggesting that this could be a novel e-ALD process. We will here demonstrate e-CVD and e-ALD of Cu using plasma electrons and a newly developed Cu precursor; Cu(I)1,3-di-*tert*-butyltriazenide.[2]

Film deposition by e-CVD was performed either in continuous mode, where the precursor was continuously supplied to the substrate with a constant plasma discharge, or in pulsed mode, where the precursor and plasma were introduced simultaneously, followed by argon purges between the cycles as shown in **Fig. 1** (**a** and **b**, respectively). In e-ALD, the precursor and plasma were introduced in sequential pulses, with each pulse separated by argon purges (**Fig. 1c**). The deposition was monitored in situ by a quartz crystal microbalance (QCM) sensor specially developed for e-CVD.[3] QCM results reveal the mass gain evolution over time during the deposition of copper films, offering insights into precursor adsorption and surface chemistry through the time-resolved electron deposition method.

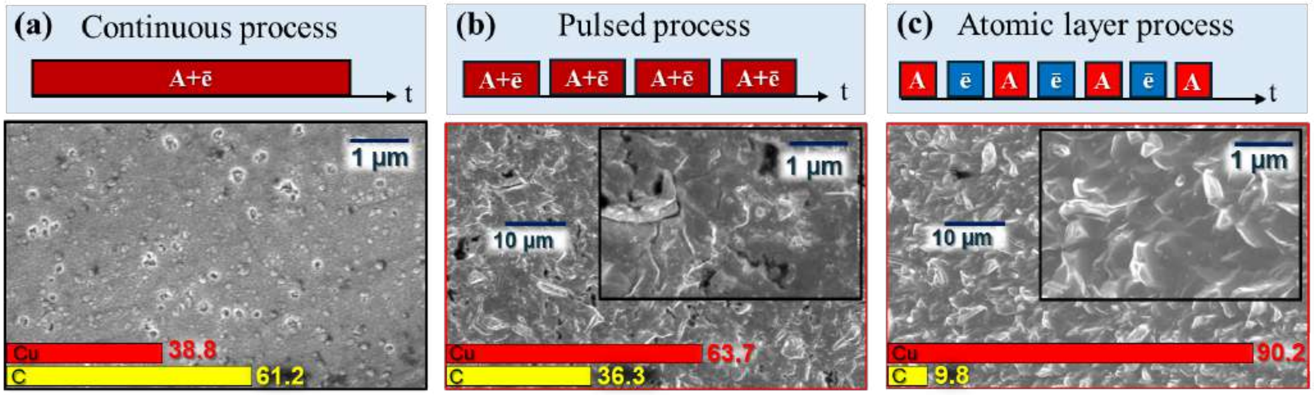

***Fig.1**. SEM images and Cu/C atomic ratio from XPS analysis of films deposited in (a) a continuous process, (b) a pulsed process, and in (c) an atomic layer process. All depositions were conducted at a plasma power of 20 W and a substrate bias voltage of +60 V. The elemental composition was derived from XPS measurements after 300 seconds of sputter cleaning using Ar ions accelerated to 0.5 keV.*

X-ray photoelectron spectroscopy (XPS) reveals the formation of copper films with a Cu/C atomic ratio of 9.20 for films deposited by the e-ALD process. This suggests a higher degree of precursor fragmentation and reduced ligand redeposition compared to the e-CVD processes, which provide Cu/C atomic ratios of 1.75 in pulsed mode and 0.63 in continuous mode. We found that plasma density significantly influenced film growth. Low plasma power resulted in a low growth rate, likely due to incomplete reactions caused by insufficient plasma electron density. Conversely, excessively high plasma power led to no film growth, possibly due to precursor desorption. A plausible explanation, supported by optical emission spectroscopy and surface morphology, is provided for the formation of active species in plasma volume and the growth process in different deposition parameters.

This work was supported by the Wallenberg Initiative Materials Science for Sustainability (WISE) funded by the Knut and Alice Wallenberg Foundation. Financial support from the Swedish Research Council (VR) under contract 2019-05055 and from the Swedish Government Strategic Research Area in Materials Science on Functional Materials at Linköping University (Faculty Grant SFO-Mat-LiU No. 2009-00971) is gratefully acknowledged.

References

[1] H. Nadhom, D. Lundin, P. Rouf, and H. Pedersen, *J. Vac. Sci. Technol. A Vacuum, Surfaces, Film*, **38**(3), 033402 (2020).
[2] R. Samii, A. Fransson, P. Mpofu, P. Niiranen, L. Ojamäe, V. Kessler, and N.J. O'Brien, *Inorg. Chem*, **61**(51), 20804–20813 (2022).
[3] P. Niiranen, H. Nadhom, M. Zanáška, R. Boyd, M. Sortica, D. Primetzhofer, D. Lundin, and H. Pedersen, *Rev. Sci. Instrum*., **94**(2), 023902–9 (2023).

Single-Source Precursors for the Aerosol Assisted Chemical Vapour Deposition of Tantalum Oxides and Tantalum Oxynitrides

J. Buckingham[1], **F. De Leeuw** [2], **A. L. Johnson**[1*]
[1]University of Bath, Department of Chemistry
[2]University of Amsterdam, Department of Chemistry
e-mail: jdb72@Bath.ac.uk and chsalj@bath.ac.uk

Single-source precursors for the Aerosol Assisted Chemical Vapour Deposition (AACVD) of tantalum-based materials were prepared as a possible route to stable and low recombination photoelectrochemical water splitting materials.[1] A readily synthesisable tri-tert-butanolamine ligand was employed to create tantalum alkoxide precursors as well as a tantalum oxo-bridged tetramer **1** and a tantalum imido species **2.** These are capable of decomposition into tantalum oxide and tantalum oxynitride respectively, as verified by thermogravimetric analysis.

Successful depositions of the tetramer **1** were performed in a hot wall AACVD reactor to yield tantalum oxide on a range of substrates. It was shown that higher deposition and annealing temperatures of up to 500 and 900 degrees Celsius improved the degree of order and microstructure in thin films, in accordance with literature.[2] The thin films produced were found to be amorphous, forming into large spherical nodule 'tower' structures as displayed in Figure **1** and possessing a band gap of ca. 4.7 eV.

Single-source precursors for tantalum oxide dopant elements such as nitrogen, aluminium and manganese have also been synthesised. An electric and magnetic field assisted AACVD reactor has also been constructed as part of the work which may be used to further alter material properties.[3]

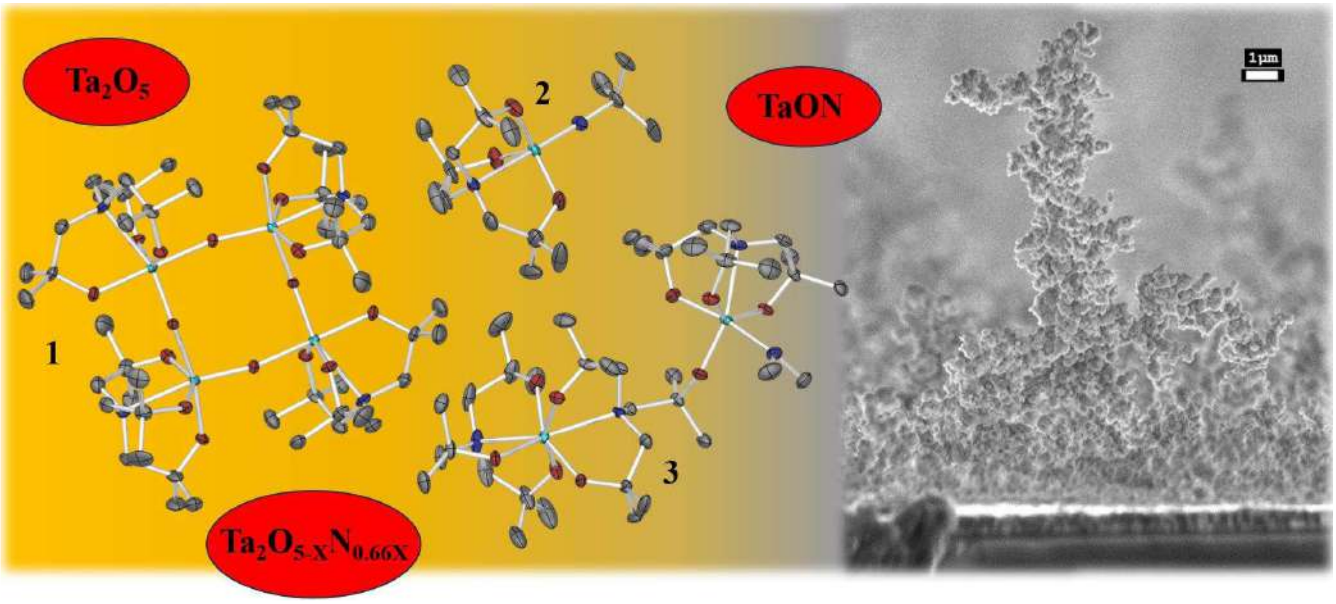

Fig. 1. To the left - tantalum oxide and oxynitride single source precursors prepared for deposition. to the right – A 'tower' of tantalum oxide, height ca. 15µm, grown from fluorine doped tin oxide.

References

[1] T.-P. Ruoko, A. Hiltunen, T. Iivonen, R. Ulkuniemi, K. Lahtonen, H. Ali-Löytty, K. Mizohata, M. Valden, M. Leskelä and N. V. Tkachenko, *J. Mater. Chem. A*, **7**, 3206–3215 (2019).

[2] I. Perez, V. Sosa, F. Gamboa, J. T. Elizalde Galindo, J. L. Enríquez-Carrejo, R. Farías and P. G. Mani González, *Appl. Phys. A*, **124**, 792 (2018).

[3] M. E. A. Warwick and R. Binions, *Sol. Energy Mater. Sol. Cells*, **143**, 592–600 (2015).

Molecularly engineered yttrium precursors for deposition of yttrium(III) oxide thin films

M. Schmickler[1], **H. Parala**[1], **A. Devi**[1,2,3]
[1]Leibniz Institute for Solid State and Materials Research, IFW, Dresden, Germany
[2]Dresden University of Technology, TUD, Dresden, Germany
[3] Fraunhofer Institute for Microelectronic Circuits and Systems, IMS, Duisburg, Germany
m.schmickler@ifw-dresden.de

The intriguing properties of yttrium(III) oxide (Y_2O_3), such as the high chemical resistance, mechanical strength, melting point as well as high dielectric constant and good transparency make this material suitable for a wide range of applications such as protection layers, antireflection coatings and gate dielectrics [1-2, 7]. The processing of Y_2O_3 thin films using metalorganic chemical vapor deposition (MOCVD) and atomic layer deposition (ALD) has gained significant attention as these methods possess several advantages in terms of conformal coatings, high density layers and moreover they are industry compatible in terms of scale-up. Both methods rely on metalorganic complexes as precursors to obtain films of high quality. Among the yttrium precursors for both methods are the commonly used yttrium tris-β-diketonates, especially those bearing the 2,2,6,6-tetramethyl-3,5-heptanedione (thd) ligand system. However, the low reactivity of those complexes results in a need for strong oxidizers and the growth rates are relatively low for ALD applications [3]. Alternatively, known precursors include cyclopentadienyl derivatives and, in the context of MOCVD bis(trimethylsilyl)amides [4].

In our studies, all nitrogen-coordinated precursors, specifically acetamidinates, guanidinates, and formamidinates, have been thoroughly investigated regarding their thermal properties and employed in MOCVD and ALD applications [4-7]. Particularly for ALD, the highly reactive metal-nitrogen bond is advantageous for the compounds to be reactive with mild oxidizing co-reactants such as water, while the bidentate nature and the delocalized π-system of the backbone provide thermal stability. The synergy created by this combination enables the deposition of crystalline thin films with high density and purity both via MOCVD and ALD. This presentation illustrates the impact of precursor design on the physicochemical properties of the yttrium precursor and its impact on the MOCVD deposition process.

References

[1] R. Gaboriaud, F. Pailloux, P. Guerin and F. Paumier, *Thin Solid Films*, **400**, 106-110 (2001).
[2] J. J. Araiza, M. A. Aguilar-Frutis, C. Falcony, *J. Vac. Sci. Technol. B*, **19**, 2206-2211 (2001).
[3] M. Putkonen, T. Sajavaara , L.-S. Johansson and L. Niinistö, *Chem. Vap. Deposition*, 7, 44-50 (2001).
[4] A. Milanov, K. Xu, S. Cwik, H. Parala, T. de los Arcos, H.-W. Becker, D. Rogalla, R. Cross, S.Paul and A. Devi*, Dalton Trans.,* **41**, 13936-13947 (2012).
[5] S. Karle, V.-S. Dang, M. Prenzel, D. Rogalla, H.-W. Becker and A. Devi, *Chem. Vap. Deposition*, **21**, 335-342 (2015).
[6] L. Mai, N. Boysen, E. Subasi, T. de los Arcos, D. Rogalla, G. Grundmeier, C. Bock, H.-L. Lu and A. Devi, *RSC Adv*., **8**, 4987-4994 (2018).
[7] S. Beer, N. Boysen, A. Muriqi, D. Zanders, T. Berning, D. Rogalla, C. Bock, M. Nolan and A. Devi, Dalton Trans., **50**, 12944–12956 (2021).

Unraveling the Steric Link to Copper Precursor Decomposition: A Multi-Faceted Study for the Printing of Flexible Electronics

Shreya Mrig[a], Caroline E. Knapp[a]*

[a] Department of Chemistry, University College London, 20 Gordon Street, London, WC1H 0AJ
[*] Corresponding author e-mail: caroline.knapp@ucl.ac.uk

With the global market for printed flexible electronics predicted to reach $12 billion by 2033, advances in the manufacture of large-scale flexible electronics has resulted in the efficient, environmentally friendly roll to roll process, employing inkjet printing. This leap in technology has come hand-in-hand with the requirement for precursors that will decompose cleanly, at low temperature and high speed. The Knapp group are working to create 'metal-organic decomposition (MOD) inks' that can be deposited in air, then treated at temperatures below 200 °C, to give conductive metallic features.[1]

Recent work has highlighted that the careful selection of ligands can aid reduction of the metal complexes to leave conductive metals (e.g. Cu, Ag, Al).[2-5] Facile formulation of these compounds into inks allows for inkjet printing and subsequent low temperature reduction (via thermal sintering) yielding highly conductive features which can be incorporated into electronic devices. MOD inks are an emerging alternative to the industrial standard nanoparticle (NP) inks.

Here we discuss the chemistry of copper precursor development and report our work on printed copper metal tracks. Using careful ligand design we attuned the properties of the copper precursors at the molecular level, making functionality fully adjustable. We describe the synthesis and characterisation of three novel copper compounds; and their subsequent deposition and inkjet printing onto flexible substrates to yield conductive copper tracks *via* thermal sintering.

References

[1] S. P. Douglas, S. Mrig, and C. E. Knapp, *Chemistry–A European Journal*, **27**, 8062-8081 (2021).
[2] S. Mrig, M. A. Bhide, Y. Zhou, N. Staton, J. Wang, S.P. Douglas, H. R. Tinker, K.L. Mears, C. M. Bakewell and C. E. Knapp, *Small Methods*, **7**, 2300038 (2023)
[3] S. P. Douglas, and C. E. Knapp, *ACS Appl. Mater. Interfaces*, **12**, 26193 (2020).
[4] C. E. Knapp, E. A. Metcalf, S. Mrig, C. Sanchez-Perez, S. P. Douglas, P. Choquet, and N. D. Boscher, *Chem. Open*, **7**, 850 (2018). Cover feature.
[5] C. E. Knapp, J.-B. Chemin, S. P. Douglas, D. Abessolo Ondo, J. Guillot, P. Choquet, and N. D. Boscher, *Advanced Mater. Technol.*, **3**, 1700326 (2018).

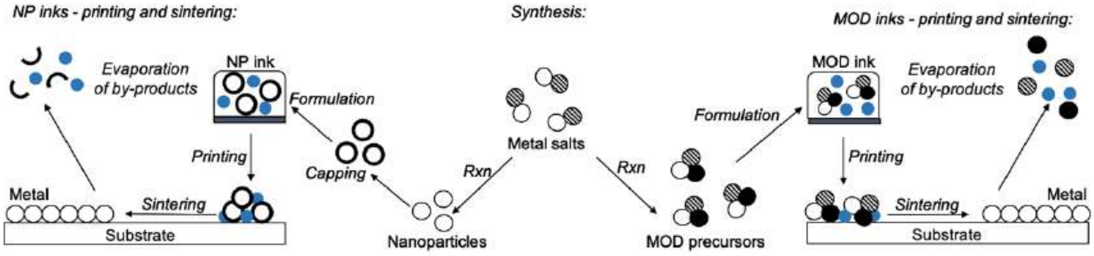
NP inks - printing and sintering:
Evaporation of by-products
NP ink
Formulation
Printing
Capping
Metal
Sintering
Substrate
Synthesis:
Metal salts
Rxn
Nanoparticles
Rxn
MOD precursors
MOD inks - printing and sintering:
MOD ink
Evaporation of by-products
Formulation
Printing
Sintering
Metal
Substrate

Fig. 1. MODs vs. NP: From the centre, schematic illustration showing the different synthetic routes to either NP (to the left) or MOD precursors (to the right), bookended by the process involved in printing and sintering metal coatings.[1]

The role of lithium precursors in tuning Lithium-terephthalate thin film properties.

Anish Philip[1], **Milad Madadi**[1], **Eero Haimi**[1], **and Maarit Karppinen**[1]
[1]Aalto University, School of Chemical Engineering, FI-00076, Espoo, Finland.
e-mail: anish.philip@aalto.fi

Lithium-terephthalate (Li-TP) is recognized as a highly promising anode material for lithium-ion batteries.[1] The advantages of atomic/molecular layer deposition (ALD/MLD) technique have enabled the realization of Li-TP thin films in a highly controllable manner needed for its use in thin-film micro battery configuration.[2] However not much attention has been paid to understanding the importance of selecting an appropriate lithium precursor for controlling the thin film properties and conformality, even though Li-TP materials are highly desirable from the battery application point of view. Given their potential application in 3D thin-film microbatteries, understanding both conformality and thin-film coverage (penetration depth) are also crucial.

In this research, we investigated the impact of different lithium precursors on the film roughness, conformality and penetration depth (PD) of Li-TP thin films. For these studies, we selected both lithium tert-butoxide (LiOtBu) and lithium bis(trimethylsilyl)amide (Li-HMDS) precursors in addition to the previously used Li(thd) (thd = 2,2,6,6-tetramethyl-3,5-heptanedionate). For conformality measurements, we utilized lateral high-aspect-ratio (LHAR) PillarHall [3] structures and a novel imaging ellipsometry technique. The need for cross-sectional sampling in the conventional high-aspect ratio approach of conformality measurements can be circumvented by utilizing LHAR PillarHall test structures. The use of imaging ellipsometry for such conformality studies is itself innovative, and the conformality data for ALD/MLD-grown thin films is scarce. The results (Figure 1) reveal that the choice of lithium precursor plays a critical role in determining both the conformality and film roughness. Our studies indicate that LiOtBu is the best choice among the lithium precursors tested when smoother films with higher film coverage (PD = 66 µm) are desired on 3D substrates. The conformality data obtained with the three different lithium precursors highlights the role of ligands [4] in controlling the conformality of the resulting Li-TP thin films, with the bulkier Li-(thd) showing the lowest PD (9 µm).

This work was supported by Business Finland (CHEMI-SEMI Co-Innovation project) and the European Union (ERC AdG, UniEn-MLD, No. 101097815).

References

[1] M. Armand, S. Grugeon, H. Vezin, S. Laruelle, P. Ribière, P. Poizot and J. M. Tarascon, *Nat Mater*, **8**, 120–125, 2009.
[2] M. Nisula and M. Karppinen, *Nano Lett.*, **16**, 1276–1281, 2016.
[3] A. Philip, T. Jussila, J. Obenlüneschloß, D. Zanders, F. Preischel, J. Kinnunen, A. Devi and M. Karppinen, *Small*, **20**, 2402608, 2024.
[4] M. Madadi, M. Heikkinen, A. Philip and M. Karppinen, *ACS Appl. Electron. Mater.*, **6**, 1574-1580, 2024.

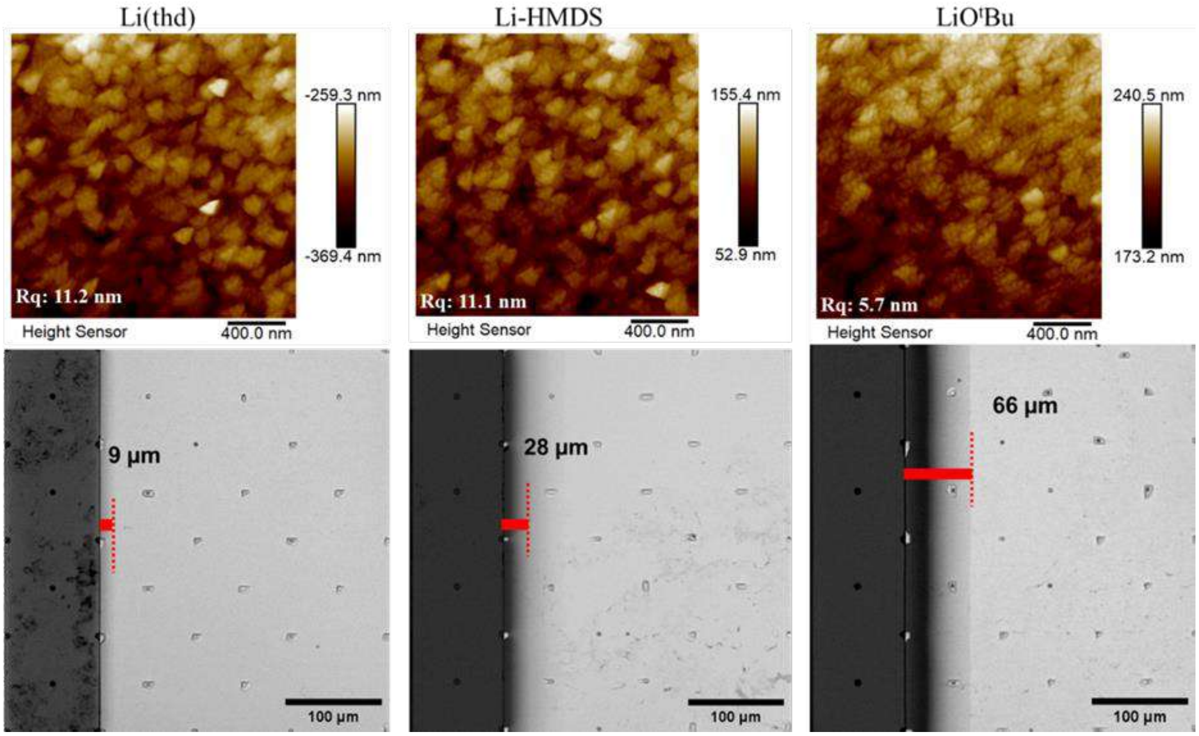
Li(thd)
Li-HMDS
LiO^{t}Bu
-259.3 nm
-369.4 nm
155.4 nm
52.9 nm
240.5 nm
173.2 nm
Rq: 11.2 nm
Rq: 11.1 nm
Rq: 5.7 nm
Height Sensor
400.0 nm
9 µm
28 µm
66 µm
100 µm

Fig. 1. AFM (top row) and SEM images (bottom row) of Li-TP deposited with 250 cycles of ALD/MLD. The lithium precursor used is indicated. The RMS roughness (Rq) is provided in the AFM images, while the penetration depth values are marked in the SEM images.

Session AM_2.3 HIGH-K DIELECTRICS

Tuesday 3rd June 2025 | 11.15-12.45

Chair: **Patrik Hoffmann** | Main Hall “Santo Mazzarino”

HfO_2 thin layers by low temperature thermal ALD processes for neuromorphic and spintronics applications: challenges and opportunities.

A. Lamperti[1,*], **A. Cataldo**[1], **G. Tallarida, C. Wiemer**[1]
[1]CNR-IMM, Unit of Agrate Brianza
e-mail: alessio.lamperti@cnr.it

Hafnium oxide (HfO_2) is widely used in modern electronics, in particular as transistor dielectric for microprocessors, due to its remarkable properties: dielectric constant k of 18–25, bandgap of 5.5–6.0 eV, dielectric breakdown field of 3.9–9 MV/cm, and good thermal stability. Among the various available deposition techniques to grow HfO_2, atomic layer deposition (ALD) emerged as the dominant method thanks to its atomic-scale thickness controllability, reproducibility, low defect density and cost effectiveness. Thermal ALD (TALD) processes are historically and nowadays commonly used to deposit HfO_2 but are prone to retain certain amounts of defectivity in the grown layers, which are controlled by transistor architecture optimization [1-3]. Further, because of the elevated temperature (>250 °C) needed for typical TALD processes, patterned dielectrics are commonly realized by first depositing an unstructured layer onto the substrate and subsequent structuring by lift-off etching because of photoresists damage and outgassing at such growth temperatures. To overcome such limitations, optimization of HfO_2 TALD deposition processes is needed, targeting low growth temperatures as low as possible, down to 100 °C or even room temperature, while preserving the ALD regime. Moreover, low temperature ALD enabled the integration of HfO_2 in the emerging fields of neuromorphic and magnetoionic based electronics, targeting synaptic and neural artificial architectures [4, 5].

In recent years, several attempts have been made to grow HfO_2 at such low temperatures, with both TALD and plasma enhanced (PE) ALD, considering different precursors both for the delivery of Hf and Oxygen [6, 7]. Despite PEALD being particularly considered for the growth at low temperature, plasma generated reactive species used in such deposition processes can also cause unintended modifications to composition or structure of sensitive surfaces [8]. Here, we focus on recent research efforts on TALD processes at growth temperature > 200 °C, especially considering tetrakis(ethylmethylamido)hafnium (TEMAHf) as Hf precursor and H_2O or O_3 as oxidizer. We show how the interplay between growth temperature and Oxygen source employed in the TALD process influences the process kinetics and the properties of the so-grown HfO_2 layer. For instance, considering a growth temperature at 200 °C, the resulting growth per cycle (GPC) is 1.40 Å/cy when using O_3, while reduces at 0.92 Å/cy by using H_2O (Fig. 1, left). On the HfO_2 side, the residuals from precursors are also affected, typically C, OH and CN, which appear lower in the growth with H_2O as oxidizer with respect to O_3, as shown by time-of-flight secondary ion mass spectrometry (ToF-SIMS) depth profiles in Fig.2. Moreover, we show how the GPC is dependent on the growth temperature, as shown in Fig 1 (right) in the case of using O_3, where the GPC spreads in the range 1.40-1.52 92 Å/cy. We also show additional results on the effect of optimization of the ALD cycle at 100 °C and its influence on HfO_2 properties with thickness scaling down to 3 nm, including examples of successful integration in magnetoionic stacks.

This work was partially supported by the European Union Horizon Europe programme, through the European Innovation Council (EIC) Pathfinder project METASPIN "Metaplastic Spintronics Synapses", grant n. 101098651.

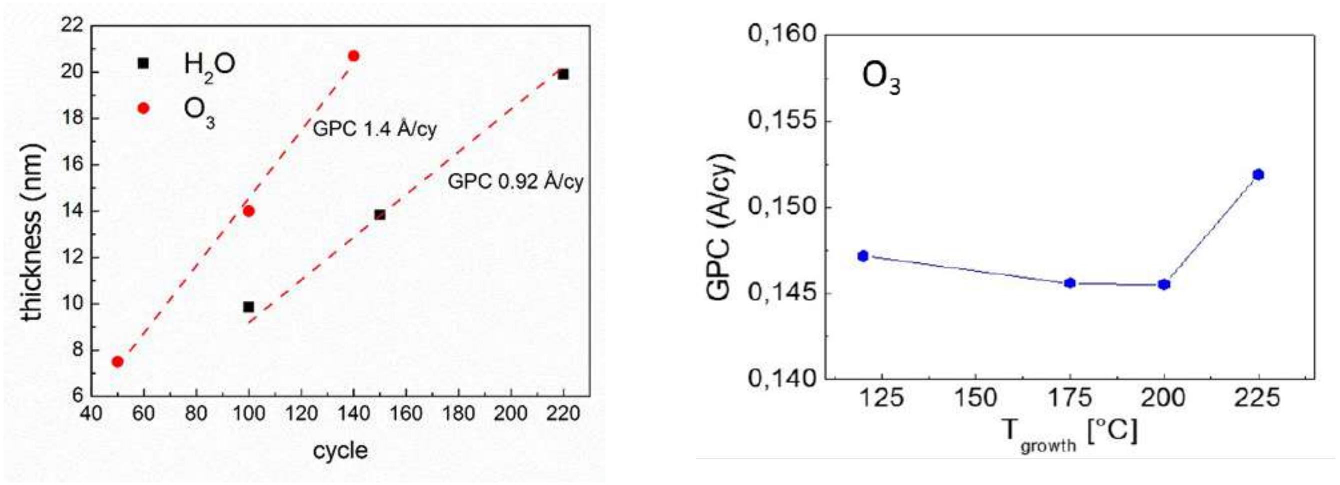

Fig. 1 Left: GPC from TALD at 200 °C using TEMAHf and H_2O or O_3; right: GPC as function of temperature for processes using TEMAHf and O_3.

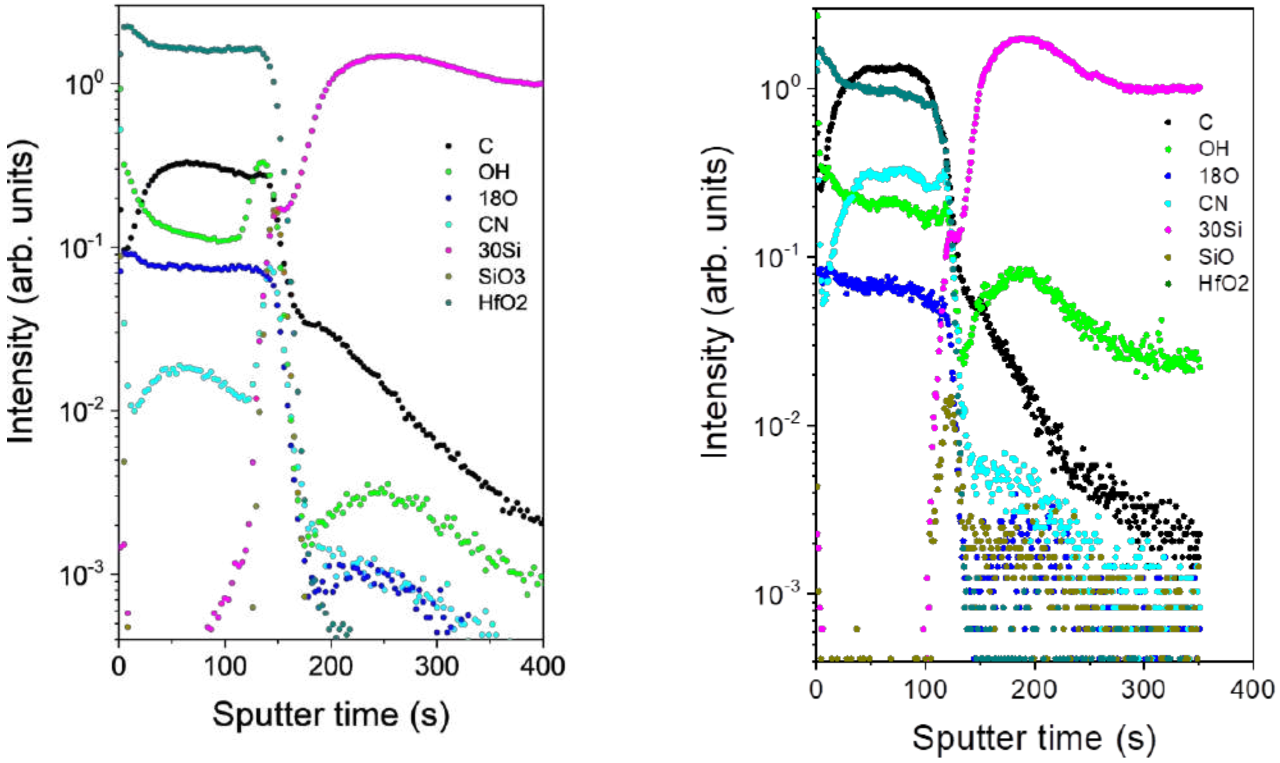

Fig. 2 ToF-SIMS depth profile of HfO_2 layer grown on SiO_2/Si at 200 °C from TEMAHf and H_2O (left) or O_3 (right)

References

[1] G. He, X. Chen, Z. Sun, *Surf. Sci. Rep.*, **68**, 68−107 (2013).
[2] J.H. Choi, Y. Mao, J.P. Chang, *Mater. Sci. Eng. R Rep.*, **72**, 97–136 (2011).
[3] S. Spiga et al., *ACS Appl. Nano Mater.*, **1**, 4633−4641 (2018).
[4] S Brivio, S Spiga, and D Ielmini, *Neuromorph. Comput. Eng.*, **2**, 042001 (2022)
[5] T. Bhatnagar-Schöffmann et al., *Adv. Mater. Interfaces*, **11**, 2300955 (2024)
[6] P. Shekhar et al., *ACS Appl. Mater. Interfaces*, **14**, 33960−33967 (2022).
[7] M.A. Martínez-Puente et al., *Materials Science and Engineering B*, **285**, 115964 (2022).
[8] H.C.M Knoops et al., *Journal of Vacuum Science & Technology A*, **37**, 030902 (2019).

Comparison between ALD and PE-ALD growth of Al_2O_3/AlN dielectric stacks on silicon carbide by In-Situ Spectroscopic Ellipsometry

R. Lo Nigro[1*], **B. Galizia**[1,2], **E. Schilirò,** [1,] **S. Peters,**[3] **J. Zessin,**[3] **F. Roccaforte**[1]
[1]Consiglio Nazionale delle Ricerche - Istituto per la Microelettronica e Microsistemi (CNR-IMM), Strada VIII n. 5 - Zona Industriale, 95121, Catania, Italy
[2]Dipartimento di Scienze Chimiche, Università di Catania, Viale A. Doria 6, 95125, Catania, Italy
[3]SENTECH Instruments GmbH, Schwarzschildstraße 2, 12489 Berlin, Germany
e-mail: raffaella.lonigro@imm.cnr.it

Silicon carbide (4H-SiC) is a wide band gap semiconductor suitable for high-power applications due to its superior properties compared with silicon [1,2]. Nevertheless, the replacement of the silicon oxide as gate dielectric in metal-oxide-semiconductor-field effect-transistors is still one of the open topics related to the full implementation SiC based technology. In fact, the traditionally used SiO_2 dielectric suffers from low dielectric constant (≈3.9) compared to the one of 4H-SiC (≈9.7), so that, according to Gauss' law, the high breakdown field of 4H-SiC (3 MV/cm) cannot be fully exploited because of the earlier breakdown of SiO_2 layer.

In the last years, the Al based materials have been considered as alternative to silicon oxide since in principle they possess quite ideal dielectric properties [3]. However, despite the aluminum oxide (Al_2O_3) has high dielectric constant value (κ ~9) and high critical electric field (~9-10 MV/cm), it did not demonstrate a better interface quality than SiO_2 layers. In this context, another high-κ insulator of interest is the aluminum nitride (AlN) having a low lattice mismatch to 4H-SiC (~0.9%), so that its implementation could improve the interface quality if epitaxially grown on (0001)4H-SiC.

In this work, Al_2O_3/AlN bilayer is proposed [4] as a new solution and two different stacks were fabricated on 4H-SiC via ALD methods (Fig.1). In particular, thermal-ALD and plasma enhanced-ALD processes of Al_2O_3 layers on AlN thin interfacial layer [5] have been compared and in-situ spectroscopic ellipsometry has been proposed as a non-destructive characterization technique for real-time monitoring. In fact, during the growth of Al_2O_3 films on AlN layer, some interaction phenomena may occur, such as the oxygen diffusion. By modeling the AlN optical properties, the oxygen content was progressively monitored and correlated with the measured, real-time variation of the AlN refractive index.

Incremental oxygen inclusion has been observed during the growth Al_2O_3 by both thermal and PE-ALD processes, but during this last process the oxygen plasma caused greater shift of the measured AlN refractive index towards values typical of the formation of an oxynitride mixed layer (Fig. 2). These findings were consistent with complementary ex-situ STEM-EDS analysis. In particular, the presence of degradation at the interface between plasma-deposited Al_2O_3 and AlN has been easily detected and effected also the electrical properties of the PE-ALD Al_2O_3/AlN stacks, which demonstrated to be leaky. Indeed, a moderate interaction occurs during the thermal ALD growth of the Al_2O_3 films and a quite good insulating behavior has been observed.

These results pave the way for the use of in-situ spectroscopic ellipsometry as a valuable tool in the processing of power electronics devices, particularly for the ALD high-κ dielectric integrations.

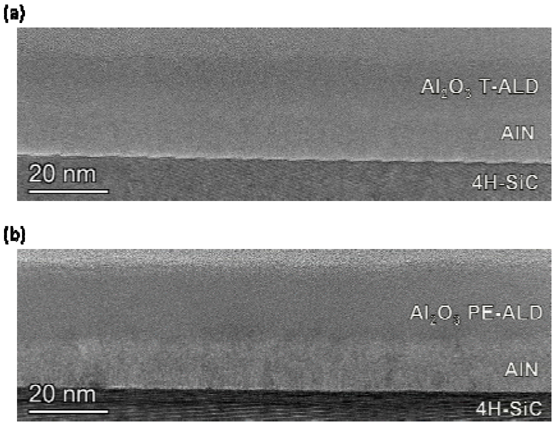

Fig. 1. STEM images of the two different dielectric stacks deposited on 4H-SiC using (a) thermal and (b) plasma enhanced ALD processes.

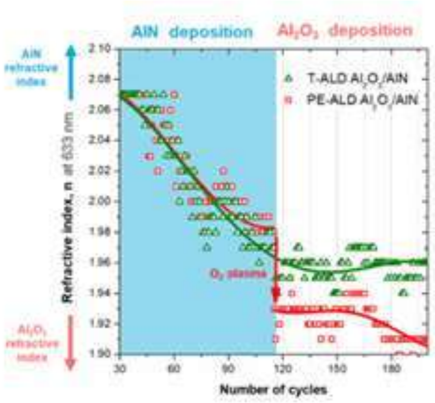

Fig. 2. Evolution of the refractive index at 633 nm upon increasing the number of ALD cycles for thermal (green triangles) and plasma enhanced ALD (red squares) processes.

This work was supported by European Union (NextGeneration EU), through the MUR PNRR project SAMOTHRACE (Grant Nos. PNRR-M4C2 and ECS00000022)

References

[1] F. Roccaforte, P. Fiorenza, G. Greco, R. Lo Nigro, F. Giannazzo, F. Iucolano, and M. Saggio, *Microelectronic Eng.* **66**, 187–188, (2018).

[2] J. Millán, P. Godignon, X. Perpiñà, A. Pérez-Tomás, and J. Rebollo, *IEEE Transactions on Power Electronics* **29**, 2155 (2014).

[3] R. Lo Nigro, P. Fiorenza, G. Greco, E. Schilirò, and F. Roccaforte, *Materials* **15**, 3 (2022).

[4] B. Galizia, P. Fiorenza, E. Schilirò, B. Pecz, Z. Fogarassy, G. Greco, M. Saggio, S. Cascino, R. Lo Nigro and F. Roccaforte, Mater. Sci. Semicond. Process. **174**, 108244 (2024)

[5] B. Galizia, P. Fiorenza, C. Bongiorno, B. Pécz, Z. Fogarassy, E. Schilirò, F. Giannazzo, F. Roccaforte, and R. Lo Nigro, *Microelectron. Eng.* **283**, 112103 (2024)

Optimization of High-*k* Gate Insulators for Amorphous IGZO channel-based 3D DRAM: Materials and Process Development

Seonyeong Park[1], Jisang Yoo[1], Jeongwoo Park[2], Pilsang Yun[2], Daewon Ha[2], Hyungjun Kim[1,*]
[1]School of Electrical and Electronic Engineering, Yonsei University, Seodaemun-Gu, Seoul 03722, Korea
[2]Semiconductor R&D Center, Samsung Electronics Co. Ltd., Hwaseong-si, Gyeonggi-do, Korea
e-mail: hyungjun@yonsei.ac.kr

As device scaling accelerates, the conventional planar dynamic random access-memory (DRAM) structures are transitioning to 3D DRAM architectures [1]. Various issues arise while converting the traditional Si-based transistors to 3D structures. In the case of using single crystal Si, over 100 layers of Si/SiGe epitaxial growth are required, but the high process difficulty in 3D stacked structures makes it unfavorable for mass production. Polycrystalline Si, which has been used in V-NAND for mass production, has been criticized for issues such as leakage current and degradation between cells due to grain boundaries. Amorphous Si, while advantageous for process manufacturability, has significant drawbacks related to electron mobility and defects [2].

As a result, amorphous oxide semiconductors (AOS) have recently gained attention as new channel materials. Among these, amorphous Indium Gallium Zinc oxide (a-IGZO) is particularly notable because it can be deposited using various techniques such as physical vapor deposition (PVD) and atomic layer deposition (ALD), which makes it favorable for mass production. Additionally, compared to polycrystalline and amorphous Si, a-IGZO has fewer issues with leakage current and degradation, and it can satisfy the electron mobility requirements of 2~10 cm^2/Vs needed for 3D DRAM [3]. However, research on a-IGZO itself has been focused mainly on the channel material, and studies on the gate insulator (GI) and source/drain (S/D) contact materials and processes are relatively underdeveloped. In particular, ALD-based GI, which are preferred for their conformal deposition capability in 3D structures, face limitations in terms of the material itself.

In ALD-based GI processes, the direct deposition of ultrathin high-k GIs on a-IGZO is a critical consideration. Traditional high-k GIs, when combined with a-IGZO channels, have caused issues such as high leakage current due to a low conduction band offset. Furthermore, direct reactions between a-IGZO channel and ALD precursors can induce trap states (oxidant vacancy, V_O) in the channel or channel interface [4].

Therefore, we have aimed to directly deposit high-k GI on a-IGZO channels, comparing and analyzing various oxide materials and precursor-oxidant combinations. Through various combinations, we tried to identify the optimal process for reducing leakage current and increasing device performance. After confirming the basic ALD growth characteristics, we characterized the thin film properties using XPS, XRD, and other techniques. Subsequently, we fabricated metal-oxide-silicon (MOS) capacitor and a-IGZO channel field effect transistor (FET) to evaluate their performance.

This work was supported by Samsung Electronics Co. Ltd. (IO240814-10717-01).

References

[1] Applied Materials, *Memory Mater Class Presentation*, May 5th (2021).
[2] A. Belmonte et al., *IEEE IEDM*, December 12th-18th, 28.2.1-28.2.4 (2020).
[3] S. Lee, *A Study on the Properties of a-IGZO according to the Substrate and the Electrode for 3D DRAM*, Seoul National University, Korea (2023).
[4] Y. Guan et al., *Applied Surface Science*, 625, 157177.1-157177.7 (2023).

Atomic Layer Deposition of Al_2O_3 as gate insulator in GaN-on-GaN capacitors and effect of annealing treatments on the film quality

E. Schilirò[1], G. Greco[1], P. Fiorenza[1], S. E. Panasci[1], S. Di Franco[1], R. Lo Nigro[1], F. Giannazzo[1], F. Roccaforte [1]
[1] Consiglio Nazionale delle Ricerche - Istituto per la Microelettronica e Microsistemi
(CNR-IMM), Strada VIII 5, Zona industriale – 95121 Catania, Italy
e-mail: emanuela.schiliro@imm.cnr.it

The development of ~~a~~ vertical GaN devices passes also through the availability of a suitable dielectric to guarantee high channel mobility and device reliability. Unfortunately, GaN has no good quality native oxide suitable as gate dielectric, thus deposited oxides must be adopted. Al_2O_3 is a particularly promising dielectric due to its relatively high κ (κ =8), high breakdown strength (7-8 MV/cm), and suitable conduction band offset to GaN (1.6 eV). Atomic layer deposition (ALD), with its nanometric thickness control, uniformity, and conformity, is undoubtedly the ideal technique to growth dielectric layers inside the grooved vertical GaN trench devices [1]. However, as deposited ALD-Al_2O_3 on GaN is known to suffer from the presence of charges and interface traps, which affects the electrical behavior of metal/Al_2O_3/GaN metal–insulator–semiconductor (MIS) devices both in terms of flat-band voltage (V_{FB}) shift and stretching of the capacitance-voltage (C-V) characteristics. To mitigate these issues, thermal annealing processes at different stages of the device fabrication, either after the ALD deposition (Post-Deposition-Annealing, PDA) and after the deposition of the metal gate (Post-Metallization-Annealing, PMA), have been investigated by several research groups. However, they only focused on the Al_2O_3 layer and Al_2O_3/GaN interface properties, without investigating the possible effects that PMA approach can have on the metal and on the metal/Al_2O_3 interface of the MIS structure.

In this work, Al_2O_3 layers have been growth using a Plasma Enhanced-ALD process as schematized in fig.1. The direct comparison between PDA and PMA has been evaluated on Al_2O_3/GaN MIS capacitors, of which schematic and optical image are reported in Fig 2 (a) and (b), respectively. The annealing approaches have been investigated using metal gate contacts with different work-functions (Nickel (Ni), Molybdenum (Mo), and Tantalum (Ta)) to investigate the charge-trapping phenomena occurring inside the dielectric and at dielectric/semiconductor interface but also the annealing treatment effect on the metal/dielectric interface as a function of the metal nature. Both PDA and PMA showed similar improvements of the Al_2O_3/GaN interface quality, by reducing the Dit values, but also of the dielectric quality, decreasing the hysteresis. However, differently from PDA, the PMA treatment gives an additional beneficial effect on the metal/dielectric interface. In fact, PMA approaches have been found able to stabilize the V_{FB}, shifting this toward the theoretical value (fig.2 (c), (d), (e)). We attribute this beneficial effect to the possible chemical reactions activated by the annealing process at metal/dielectric interface, which can perturb the known metal/dielectric dipole responsible for Fermi-level pinning phenomena, and consequently of the V_{FB} shift than theoretical value [2]. Moreover, the response to PMA treatment is a function of the metal gate nature. In particular, we found that the Ni metal gate, characterized by higher work function than Mo and Ta, does not reach the theoretical V_{FB} even after longer PMA treatments. This could be due to its lower tendency to react with the underlying oxide during the annealing process [3].

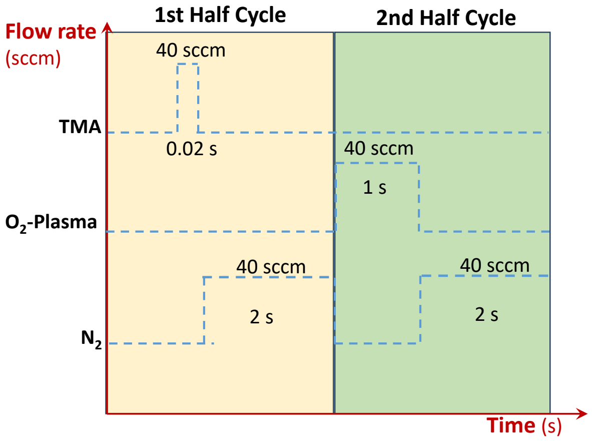
1st Half Cycle
2nd Half Cycle
Flow rate
(sccm)
40 sccm
TMA
0.02 s
40 sccm
1 s
O₂-Plasma
40 sccm
2 s
40 sccm
2 s
N₂
Time (s)

Fig. 1: ALD cycle of Al_2O_3 growth by Plasma-Enhanced process.

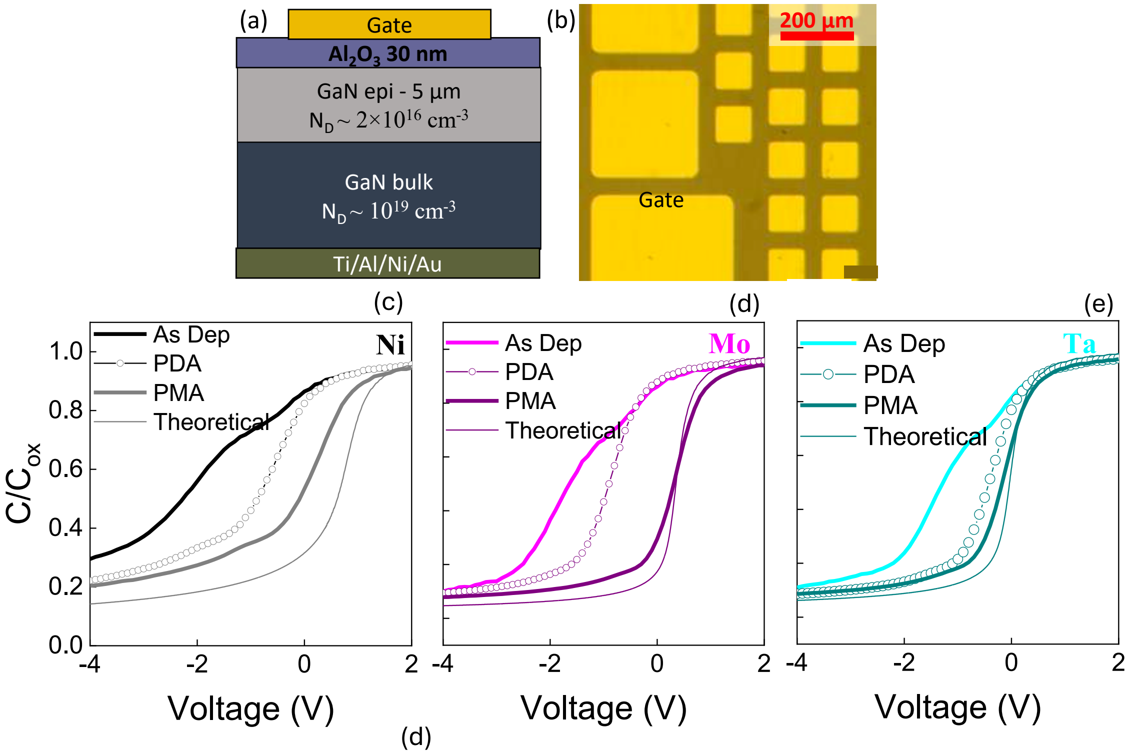

Fig. 2: Schematic cross-section of the Metal/Al2O3/GaN-on-GaN MIS (a) and top-view microscopy image of different size MIS (b). C-V curves of AsDep (solid line), PDA (circle line) and PMA (dashed line) Metal/Al2O3/GaN-on-GaN capacitors with Ni (c), Mo (d) and Ta (e) as metal gate. Summary of the C-V hysteresis amount between the different treatments and metals (d)

This work has been carried out in the framework of the ECSEL-JU Project GaN4AP (Gallium Nitride for Advanced Power Applications) - Grant Agreement No.101007310 and of the MUR-PNRR project SAMOTHRACE (NextGeneration EU, Nos. PNRRM4C2 and ECS00000022).

References

[1] M. Sun, et al. , *IEEE Electron Device Lett.* **38**, 509 (2017).
[2] Z. C. Yang, et al., *IEEE Electron Dev. Lett.*, **31**,10, (2010).
[3] E. Schilirò, et al., *AIP Advances* **14,** 105109 (2024)

Exploring low-k/high-k multilayers for improved dielectric performances in MIM capacitors

Julie Chaussard[1], Chloé Guérin[1], Aude Lefèvre[1], Patrice Gonon[2], Vincent Jousseaume[1]
[1] Univ. Grenoble Alpes, CEA, Leti, F-38000 Grenoble, France
[2] Univ. Grenoble Alpes, CNRS, LTM, F-38000 Grenoble, France
e-mail: julie.chaussard@cea.fr

In power electronics, passive components like capacitors are crucial for protecting GaN transistors from voltage fluctuations during switching phases. Usually, a capacitor and a resistor are connected in series and placed in parallel with a transistor to form a snubber network. Downsizing these capacitors remains a challenge. To this aim, researches on 3D architectures have been done using stacks of alternating silicon oxide and nitride layers (ONO structures) [1]. While promising high breakdown voltages have been demonstrated, the thicknesses required to withstand high voltages result in high internal stresses, which are not suitable.

One alternating approach is to integrate high-k/low-k multilayers into a MIM (=Metal-Insulator-Metal) capacitor. In this work, the realization of multilayers combining an organosilicate (SiOCH) as the low-k and HfO_2 as the high-k has been investigated. Two deposition processes have been used: PECVD (Plasma-Enhanced Chemical Vapor Deposition) for the low-k layers and ALD (Atomic Layer Deposition) for the high-k layers. To evaluate the impact of interfaces on dielectric properties in the multilayers, complex structures have been achieved from a single layer of SiOCH to seven alternating layers of low-k and high-k. The growth of HfO_2 on the hydrophobic surfaces of SiOCH has been studied carefully using chemical and physical characterizations. X-ray reflectometry (XRR) analysis was performed to estimate thickness, density and roughness of the layers. Combining XRR and ellipsometry data, HfO_2 growth seems to follow the same growth kinetics on SiOCH as on Si (Fig. 1). Grazing incidence X-ray diffraction (XRD) was carried out on different HfO_2 thicknesses to evaluate crystallinity. HfO_2 crystallinity appears to improve with thickness (Fig. 2), although the large peak suggests that layers remain mostly amorphous. The addition of more layers further increases the crystallinity of high-k layers, probably due to the thermal budget provided by the low-k deposition and curing (400°C). Fourier transform infrared spectroscopy (FTIR) was used to analyze the composition of the layers.

Finally, various thicknesses and stacks were fully integrated into MIM capacitors on 200 mm Si wafers for electrical characterizations (Fig. 3). Electrical parameters such as dielectric permittivity, dielectric losses, leakage current and breakdown voltage were measured. Electrical characterization reveals introducing a very thin HfO_2 layer (15 nm thick) between SiOCH layers (50 nm thick) enhances the dielectric constant by up to 13%. For the low-k monolayer, Weibull distribution shows a significant reduction in breakdown voltage as the capacitor area increases. However, the addition of a thin HfO_2 layer leads to an exceptional reduction in the dispersion of the breakdown field as shown in Fig. 4. This approach combining low-k and high-k appears promising for the development of high-voltage 3D capacitors on Si.

[1] F. Krach *et al.*, *J. Vac. Sci. Technol. B* **2015**, *33* (1), 01A112

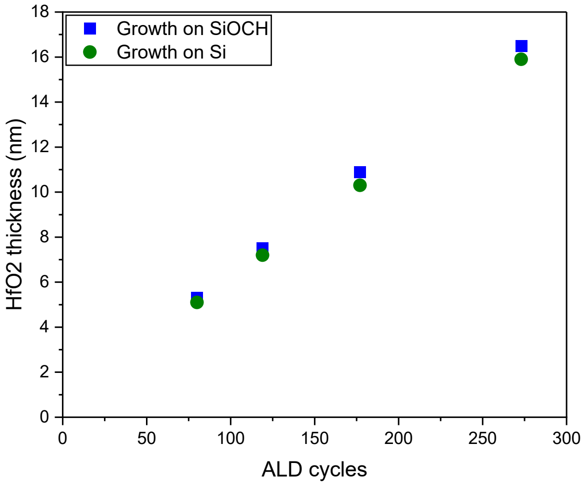

Figure 1: XRR data of HfO_2 growth on SiOCH and Si as a function of the number of ALD cycles

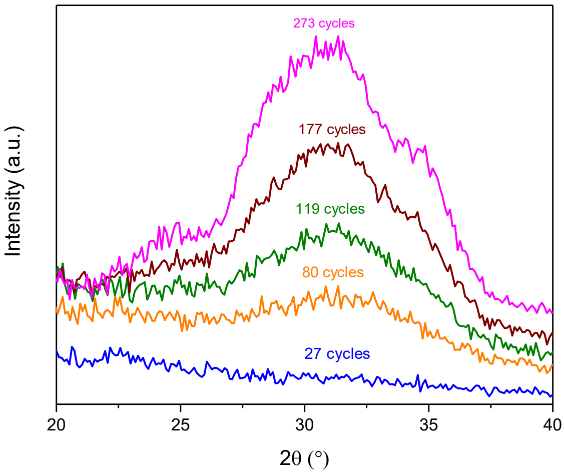

Figure 2: XRD data of HfO_2 on SiOCH as the number of ALD cycles increases

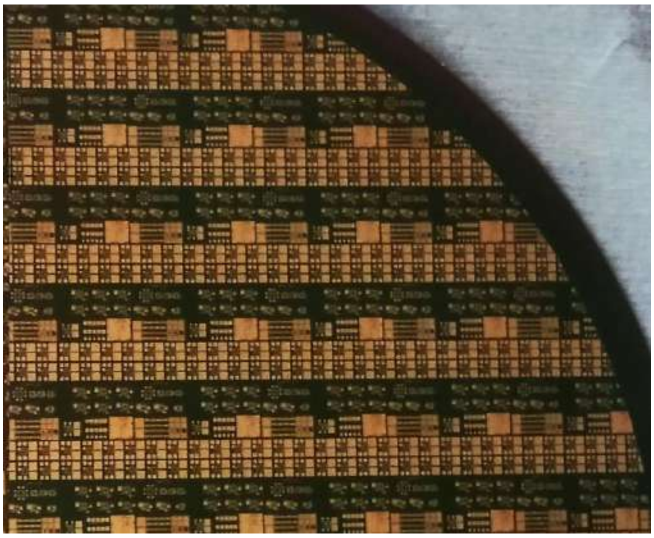

Figure 3 : MIM capacitors on 200 mm Si wafers for electrical characterizations

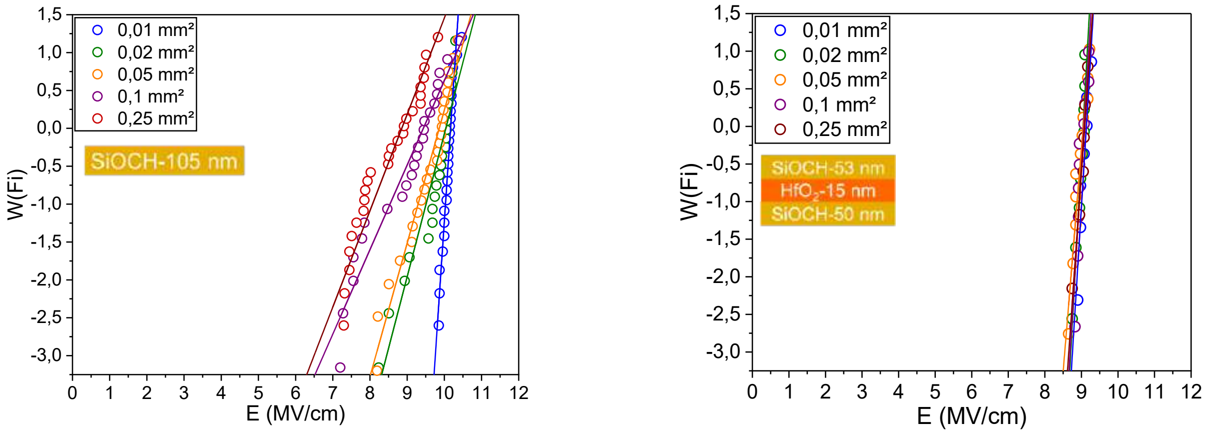

Figure 4: Evolution of the breakdown voltage as a function of capacitor surface area for a low-k monolayer and the impact of adding a thin high-k layer

Session AM_2.4 MATERIALS FOR ENERGY: PHOTOCATALYSIS

Tuesday 3rd June 2025 | 11.45-12.45

Chair: **Angel Barranco** | Room “Coro di Notte”

Self-assembled silver-decorated titania and zinc oxide nanowires by MS-ALD for photocatalytic dye degradation

M. Ziegler[1]*, Valentin Ripka[1], Anke Drewitz[2], Marco Diegel[1], Martin Kühnel[1], and Uwe Hübner[1]
[1]Leibniz Institute of Photonic Technology Jena (IPHT), Albert-Einstein-Str. 9, 07745 Jena, Germany
[2]GMBU e.V., Photonics and Sensor Technology, Felsbachstr. 7, 07745 Jena, Germany
e-mail: mario.ziegler@leibniz-ipht.de

Fast fashion and expanding to new markets, mainly in Asia have led to a drastic increase in demand for dyes, with a large proportion of toxic dyes released to the environment unfiltered causing severe damages such as disrupt photosynthesis or respiration of water organism even at low concentrations of 1 mg/l. Over the past few decades, a number of methods have been developed to filter or neutralize these dyes. The three subcategories of those strategies are chemical, biological, and physiochemical separation [1]. Photocatalysis is a chemical separation technique, which will be taken into consideration for the removal of dyes from waste water as it can operate at ambient temperatures and pressures, while lowering the overall operating costs[2]. Photocatalysts generate highly reactive oxygen species (ROS) in aqueous ambient under the illumination of light such as hydroxyl radicals (•OH) or hydrogen peroxide. Those reagents can be utilized to decompose dyes into inorganic salts, carbon dioxide or other non-toxic compounds [3].

Because of their superior optical qualities, high oxidative power, high chemical and thermal stability, and non-toxicity, zinc oxide (ZnO) and titanium dioxide (titania, TiO2) are the most researched photocatalytic materials for dye degradation. Unfortunately, both materials reveal a rather high band gap of 3.0-3.2 eV and 3.37 eV for ZnO and TiO_2, respectively. The high band gap enables photocatalytic activity only under UV illumination [3].

This study presents a novel method for creating silver-nanoparticle-decorated titania and zinc oxide nanostructures with broad band absorption (200–2500 nm) that is based on well-established deposition techniques. Using a self-assembly technique, metastable ALD (MS-ALD) makes it possible to create intricate 3D nanostructures without the use of pre-structured or pre-defined 3D substrates [4]. Former, optimized structures based on silver decorated silica nanowires (Ag-NP@SiO_2) revealed superior optical absorption above 99 % from 220 nm up to 2500 nm [5]. By adjusting the corresponding MS-ALD process parameters, the morphology of the structures could be easily changed. Here, we introduce the growth behavior of two common precursors for the MS-ALD approach to 3D structure formation: diethylzinc (DEZ) and titanium (IV) isopropoxide (TTIP). The resulting structures consisted of silver nanoparticles (Ag-NP) and TiO_2 or ZnO nanostructures (see **Fig. 1**). A planar silver film will be used as the substrate and oxygen plasma as the co-reactant for the MS-ALD process. To find promising high absorption structures, dose times were adapted and formed structures were analyzed by cross-section SEM and their optical performance was determined. X-ray diffraction was conducted to determine the crystal phases of TiO_2 and ZnO. Promising structures were tested for the degradation of a model dye (acid orange 7) in an aqueous solution under 3h UV illumination and compared with a model catalyst TiO_2 P25 (see **Fig. 2**).

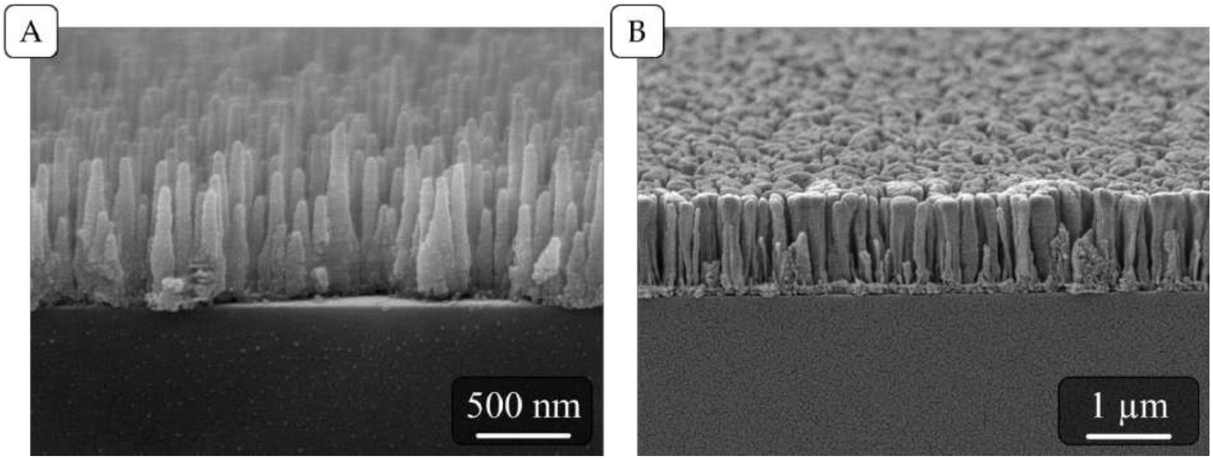

Fig. 1. Exemplary SEM images of structures formed using DEZ (A) and TTIP (B) as precursor for the formation of photocatalytic silver-decorated 3D nanostructures.

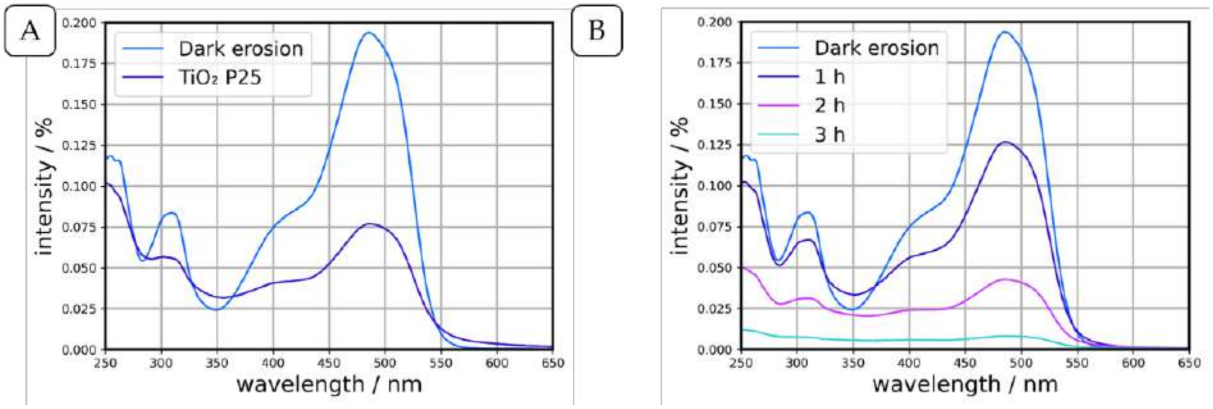

Fig. 2. Absorption spectra of the dye acid orange (AO7) diluted in water degraded under UV illumination on (A) immobilized P25 TiO_2 nanoparticles for 3 hours and (B) ethanol exposed ZnO structures (ZAE) formed at 225 cycles of 10 ms DEZ and 12 s O_2-plasma.

References

[1] A. Srinivasan, T. Viraraghavan, Journal of environmental management 91 (2010) 1915–1929.
[2] N. Madkhali, C. Prasad, K. Malkappa, H.Y. Choi, V. Govinda, I. Bahadur, R.A. Abumousa, Results in Engineering 17 (2023) 100920.
[3] D.-E. Lee, M.-K. Kim, M. Danish, W.-K. Jo, Catalysis Communications 183 (2023) 106764.
[4] M. Ziegler, S. Thamm, H.L.K. Stolle, J. Dellith, U. Hübner, D. Wang, P. Schaaf, Applied Surface Science 514 (2020) 145770.
[5] M. Ziegler, A. Dathe, K. Pollok, F. Langenhorst, U. Hübner, D. Wang, P. Schaaf, ACS Nano 14 (2020) 15023–15031.

Nanoengineering Of Chitosan Sponges Via Atomic Layer Deposition Of ZnO For Water Remediation Technologies

S. Lotito[a,d], D. Cignolo[a], J. Gubitosa[a,d], G. Barucca[b], P. Mengucci[b], M. Striccoli[c], F. Palumbo[d], P. Cosma[a], P. Fini[c], S. Murgolo[e], V. Rizzi[a] , A. Milella, A. Perrotta[d*]

a Dipartimento di Chimica, Università Degli Studi di Bari “Aldo Moro”, 70126 Bari, Italy
b Dipartimento di Scienze e Ingegneria della Materia, dell'Ambiente ed Urbanistica, Università Politecnica delle Marche & UdR INSTM, 60131 Ancona, Italy
c CNR IPCF: Istituto per i Processi Chimico-Fisici - Sede Secondaria di Bari- c/o Dipartimento di Chimica, Università degli Studi di Bari “Aldo Moro”, 70126 Bari, Italy
d CNR NANOTEC – Istituto di Nanotecnologia – Sede Secondaria di Bari c/o Dipartimento di Chimica, Università degli Studi di Bari “Aldo Moro”, 70126 Bari, Italy
e CNR IRSA – Istituto di Ricerca sulle Acque – Sede Secondaria di Bari, 70132 Bari, Italy
e-mail: alberto.perrotta@cnr.it

Water pollution is a pressing global challenge, necessitating innovative materials for effective remediation. This study addresses this issue by developing cost-effective, multifunctional, millimeter-thick chitosan sponges nanoengineered via atomic layer deposition (ALD) with ZnO. These advanced materials are designed for dual purposes: pollutant removal and material regeneration through solid-state photocatalysis, targeting applications in industrial wastewater treatment, pharmaceutical pollutant degradation, and sustainable water purification systems.

Non-porous chitosan films were initially employed as model systems to investigate the growth behavior and infiltration of ZnO. Using ALD, ZnO layers with controlled thicknesses of 5-30 nm were deposited on the films at 100°C, resulting in strong chemisorptive interactions between ZnO and the chitosan amino groups. Spectroscopic ellipsometry (SE) modeling confirmed a reaction-limited growth mechanism, with ZnO infiltration extending up to 10-20 nm into the polymer matrix. Photoluminescence (PL) measurements of these films revealed defect-induced emission properties, with a prominent broad red-region emission associated with surface defects and hydroxyl groups. These findings underscore the suboptimal crystallinity of ZnO grown on chitosan but highlight the enhanced photocatalytic potential arising from defect-mediated optical properties.

Building on these findings, porous chitosan sponges were engineered to achieve uniform ZnO infiltration up to several hundred microns within their 3D structure. XPS analysis revealed a stoichiometric ZnO coating with an O/Zn atomic ratio of ~1.1 after 100 ALD cycles. The ALD-modified sponges demonstrated significantly enhanced performance in adsorption experiments using Direct Blue 78 (DB78), a textile dye. Adsorption capacity reached a maximum of 2000 mg/g, compared to 20 mg/g for pristine chitosan sponges (Fig. 1). This enhancement was attributed to the combination of reduced swelling (from ~8000% for pristine sponges to ~1000% for ZnO-coated sponges) and electrostatic interactions between the dye’s sulfonate groups and the protonated amino moieties of the chitosan. The ZnO coating imparted water stability to the sponges, preventing dissolution and preserving their structural integrity during extended contact with aqueous solutions.

Photocatalytic tests using Naproxen, a pharmaceutical pollutant, further demonstrated the hybrid material’s potential for environmental remediation (Fig. 1). Under UV light, ZnO-modified sponges achieved significant degradation of Naproxen, as evidenced by UV-Vis absorbance reduction and the identification of multiple degradation products via high-resolution mass spectrometry. In contrast, pristine chitosan sponges exhibited negligible photodegradation of Naproxen.

This study demonstrates the synergy between adsorption and photocatalysis in ALD-engineered chitosan-ZnO sponges, providing an eco-friendly, scalable solution for water treatment. The results highlight ALD as an effective tool for creating multifunctional, bio-based materials with the potential to remove a wide range of aqueous pollutants, addressing key challenges in environmental remediation.

This work was supported by the European Union - Next Generation EU within the project PRIN-BECOMEH2 (grant n. P2022XHMRY).

References

[1] S. Lotito, D. Cignolo, J. Gubitosa, G. Barucca, P. Mengucci, M. Striccoli, F. Palumbo, P. Cosma, P. Fini, S. Murgolo, V. Rizzi , F. Fracassi, A. Milella, A. Perrotta, *Advanced Materials Interfaces*, accepted (2024)

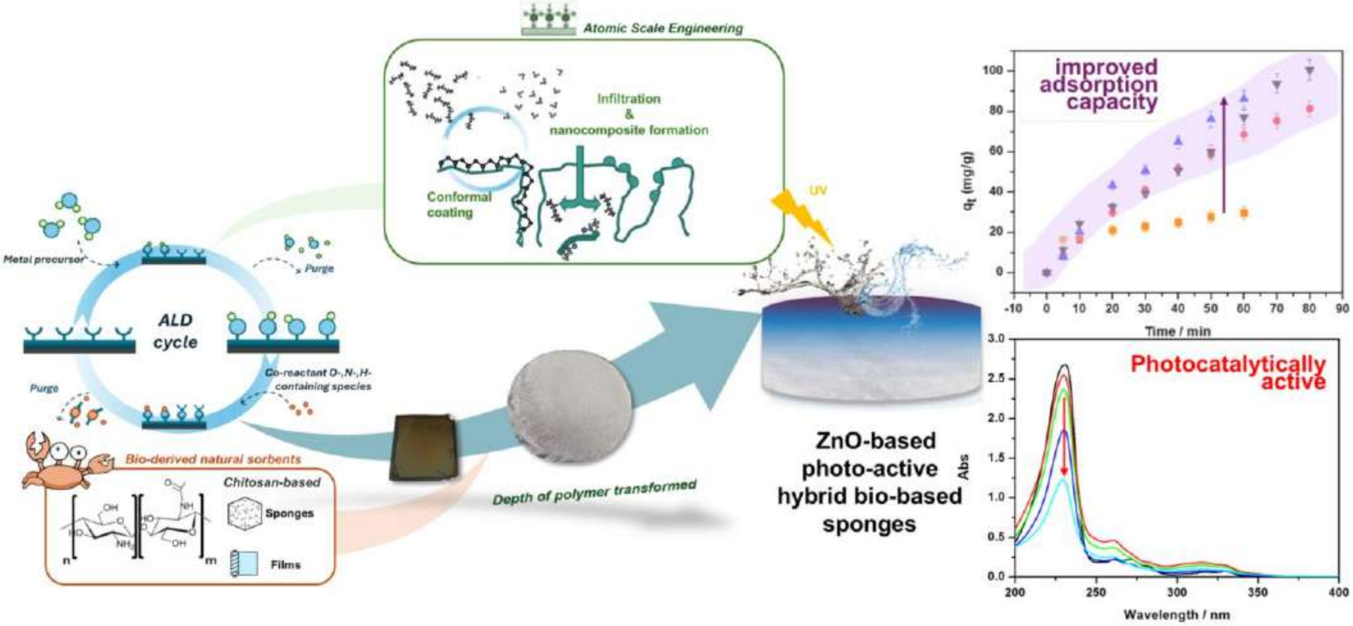
Atomic Scale Engineering
Infiltration & nanocomposite formation
Conformal coating
Metal precursor
Purge
ALD cycle
Co-reactant O-,N-,H- containing species
Purge
Bio-derived natural sorbents
Chitosan-based
Sponges
Films
Depth of polymer transformed
UV
ZnO-based photo-active hybrid bio-based sponges
improved adsorption capacity
q_t (mg/g)
Time / min
Photocatalytically active
Abs
Wavelength / nm

Fig. 1. Concept of the nanoengineering of the chitosan sponges. On the left, the improved adsorption capacity of the modified sponges is illustrated, along with proof of their photocatalytic activity for removing emerging contaminants..

The photocatalytic properties of microstructured TiO_2 coatings grown by MOCVD as ecofriendly antibiofouling solutions

Carmen Jiménez[1] **Lisa Deblock**[1,2], **Lylia Fellah**[3], **Christèle Poggi**[1], **Claire Hellio**[2], **Marianne Weidenhaupt**[1], **Fabienne Faÿ**[3]

[1] Univ. Grenoble Alpes, CNRS, Grenoble INP, LMGP, 38000 Grenoble France.
[2] Univ Brest, BIODIMAR/LEMAR, CNRS, UMR 6539, F-29200 Brest, France
[3] LBCM, Université Bretagne Sud, EMR CNRS 6076, IUEM, 56100 Lorient, France

Since 2003, the use of tributyltin (TBT) in antifouling coatings is prohibited because of its toxicity towards marine environments. The tightening of regulations on toxic marine antifouling solutions is driving the demand for new and more environmentally friendly antifouling coatings [1]. Combined with a non-toxic, corrosion-resistant character and good chemical stability in saline conditions, the photocatalytic properties of TiO_2 make this oxide a good, eco-friendly antibiofouling alternative for marine environments.

In this work, two kinds of TiO_2 photocatalytic surfaces consisting in thin films and microstructured films (see Fig 1) were synthesized by Aerosol Assisted Metal Organic Chemical Vapor Deposition (AA-MOCVD). Using precise parameters, nanometric petal assemblies, forming hierarchical microflower-like structures, are obtained. The microstructured films are characterized by the presence, on the top of TiO_2 thin films, of hierarchical hemispherical microstructures formed by nanosheets and described as microflowers. Both thin films and microstructured films present a crystallization in TiO_2 anatase phase.

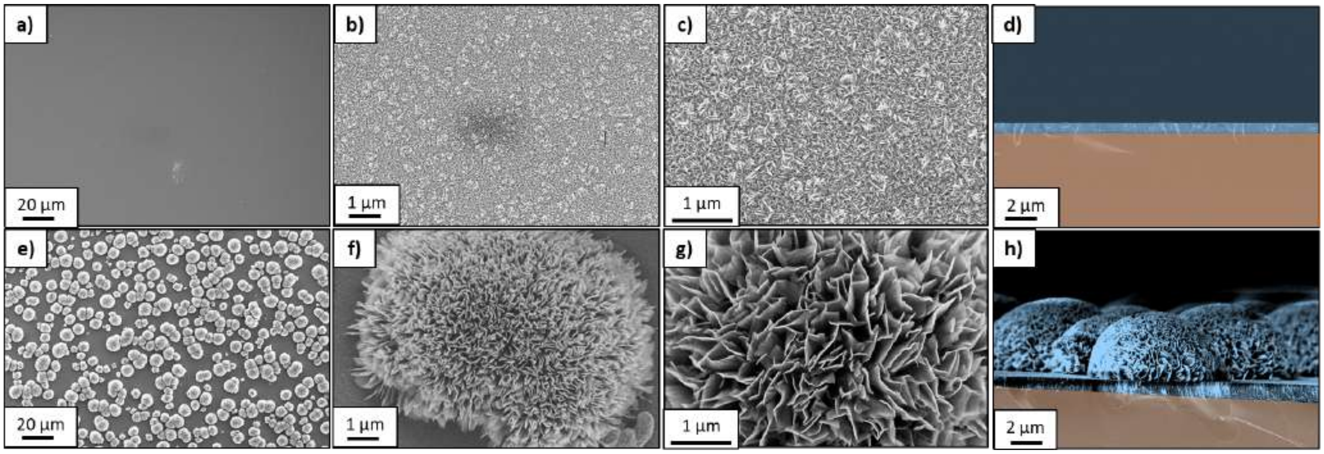

Fig. 1. *SEM Images of TiO2 thin films (a, b, c, and d) and* TiO_2 *microstructured films (e, f, g and h) Images a and e shows the dark grey plane thin film in the absence (a) or in the presence of round structures of micrometric dimension (light grey on e), b and c show the nanometric grains that forms the thin film and f and g the assembly of randomly-oriented* TiO_2 *nanosheets that form the microstructures (also called microflowers). Images d and h respectively show a side view of both samples. The semi-spherical shape of the microstructures can be observed on image h.*

The developed surface of these microflowers enhances the specific reactive surface of the material and thus its photocatalytic properties, by a factor of 10 in the presence of microflowers. The photocatalytic properties of TiO_2 enable local generation of Reactive Oxygen Species (ROS) such as OH° or H_2O_2, which can directly or indirectly damage cells [2]. The photocatalytic mechanisms of the films are investigated using specific ROS detection assays with fluorescence and luminescence readouts.

The antifouling properties of TiO_2 thin films and microstructured TiO_2 films were tested for the adhesion and biofilm formation of *Vibrio harveyi*, a marine pathogen responsible for marine fouling. The role of the photocatalytic activity was established by comparing the *V. harveyi* bacterial adhesion and biofilm maturation when exposed to these TiO_2 surfaces under illumination or in darkness conditions.

For both surfaces, a bactericidal efficacy and a limited biofilm formation was observed under illumination, the presence of TiO_2 microstructures enhancing the inhibition of the development of *V. harveyi*.

This work has been financed by the Coatinsea project of the MITI80 CNRS program (PhD grant to LD) and by the Cleansea ANR project (ANR-22-CE08-0006).

References

[1] Vellwock, A. and Yao, H. *Bioinspiration & Biomimetics*, *16(4),* 041003A (2021).
[2] Wang X., Li, S., Chen P. , Li F., Hu X., Hua T., *Materials Today Chemistry*, **23**, 100650 (2022).

ZnO deposited on hemp shives by ALD for a sustainable wastewater remediation

C. Laferrera[1*], M. Zimbone,[1] G. Sfuncia[2], G. Nicotra[2], L. Vitiello[3], S. C. Carroccio[3], G. Impellizzeri[1]

[1]National Research Council (CNR) – Institute for Microelectronics and Microsystems (IMM),
Via Santa Sofia 64, 95123 Catania, Italy
[2]National Research Council (CNR) – Institute for Microelectronics and Microsystems (IMM),
Z.I. VIII Strada, 95121 Catania, Italy
[3]National Research Council (CNR) – Institute of Polymers, Composites and Biomaterials (IPCB),
Via Paolo Gaifami 18, 95126 Catania, Italy
e-mail corresponding author: chiara.laferrera@dfa.unict.it

Zinc oxide has rapidly attracted increased attention because of its significant properties. It has a wide and direct band-gap energy ($E_g \sim 3.3$ eV at 300 K) in the near-UV spectral region, a strong oxidation ability, a great photocatalytic property, and a large free-exciton binding energy so that exciton emission processes can persist at or even above the room temperature. In addition, ZnO is an environmentally friendly material as it is compatible with living organisms, which lends itself nicely to a broad range of applications that will not leave any risks to human health or environment. The ZnO has a relatively low-cost, it is easy to grow, and its thermodynamically stable phase is the hexagonal wurtzite structure [1-2]. In particular, the use of atomic layer deposition (ALD) offers unique advantages such as precise thickness control, uniformity, conformality, and scalability. Indeed, the ALD process is highly reproducible and easily scalable to the industrial process level [2].

Hemp shives are the by-product of the hemp fiber production obtained from the woody inner portion of the hemp stalk. Hemp shives contain about 45% cellulose, 27% hemicellulose, 22% lignin and 6% other elements. Shiv is an insulating material that finds its main application in green building. It is a renewable resource with minimal environmental impact, making it an attractive alternative to traditional materials in various industries.

In this work, we originally coated hemp shive powders with ZnO by ALD, for photocatalytic application in wastewater treatment.

The hemp was ground to a fine powder, hereinafter referred to as "fibers", by using a Retsch cutting mill. The so-obtained fibers were in the form of cylinders with an average length of 376 ± 181 µm. Their density, measured with a helium pycnometer, was 1.51 g/cm³ [3]. The fibers were coated with thin layers of ZnO by ALD using a Picosun R-200 Advanced reactor equipped with a POCA system. The POCA is a powder coating solution, consisting of a quartz glass with a porous sector. The deposition was performed at 80 °C. The deposition temperature was fixed because of a previous study aimed to optimize the photocatalytic response of ALD ZnO [2]. Diethyl zinc (DEZ, purity 99,9999%) and de-ionized water were used as precursors, while N_2 was used as carrier and purge gas (purity ≥ 99.999%). Three different cycles were set so to obtain three different ZnO film thicknesses: 10, 30 and 90 nm. The film thickness was first evaluated by ellipsometry on Si substrates where the same thickness of ZnO was deposited. The obtained composites were characterized using a range of techniques: scanning and transmission electron microscopy (SEM and TEM) for the morphological and chemical analyses, thermogravimetric (TGA) analysis to evaluate the ZnO content, Raman spectroscopy to assess the structural properties, Z-potential analysis to determine the surface charge, Brunauer–Emmett–Teller (BET) analysis for the evaluation of the surface area and porosity, and UV-vis spectroscopy.

Figure 1 reports the results of the TEM analyses. In detail, Figure 1(a) presents a scanning TEM (STEM) image of a hemp shive powder sample with 90 nm of ZnO deposited on it. Figure 1(b) reports a graph confirming that the deposited thickness is approximately as expected. Figure 1(c) presents the chemical analysis obtained by electron energy loss spectroscopy (EELS), revealing the presence of ZnO and the conformal coating of the hemp shives by the ZnO.

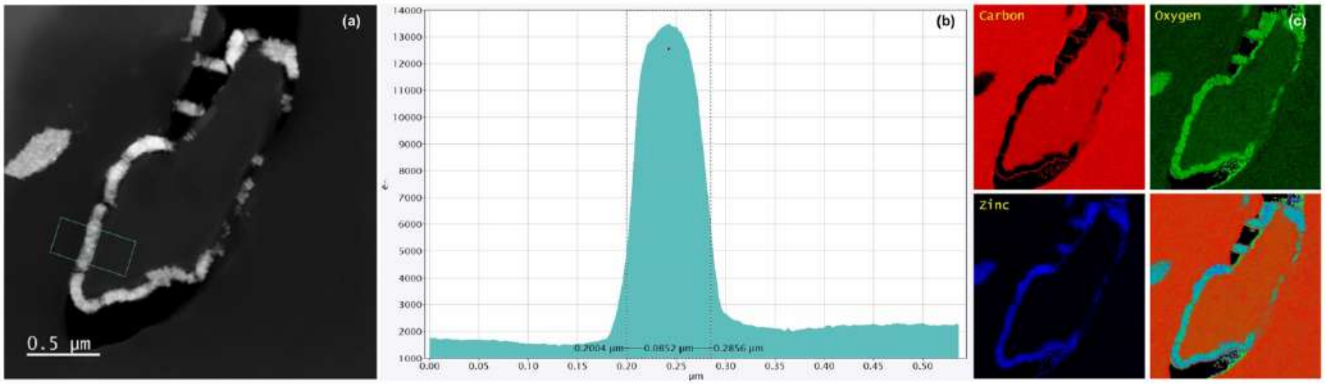

Fig. 1. STEM image (a), ZnO thickness (b), and EELS analysis (c) of 90 nm ZnO-hemp shive powder.

The photocatalytic properties of the composites were proved by the photo-degradation of methylene blue dye in water under UV-light irradiation. The photocatalysis was studied as a function of the ZnO thickness to optimize the material preparation-protocol for this peculiar application.

In conclusion, we deposited ZnO with different thicknesses on hemp shive powders by ALD technique. TEM analyses confirmed both the thickness found by spectroscopic ellipsometer after the depositions and the conformal coating of the shives by the ZnO. The materials were fully characterized, and the photocatalytic activity was proved by the degradation of methylene blue dye as a function of the film thickness. The present results demonstrate that the ALD can be employed as a simple method to realize functional composites that can find applications in photocatalysis, especially for wastewater treatment.

This work was supported by NextGeneration EU through the MUR-PNRR project SAMOTHRACE (ECS00000022), MUR-PRIN 2022 project WATERONIC (CUP: B53D23015190006), and MUR-PRIN 2022 GREENCO project (grant number: 20223LWKTC).

References

[1] A. Di Mauro, M. E. Fragalà, V. Privitera, G. Impellizzeri, *Materials Science in Semiconductor Processing*, **69**, 44 (2017).
[2] A. Di Mauro, M. Cantarella, G. Nicotra, V. Privitera, G. Impellizzeri, *Applied Catalysis B: Environmental*, **196**, 68 (2016).
[3] L. Vitiello, S. C. Carroccio, V. Ambrogi, E. Podda, G. Filippone, M. Salzano de Luna, *Composites Science and Technology*, **257**, 110806 (2024).

Session PM_2.1 MATERIALS FOR ENERGY: WATER SPLITTING

Tuesday 3rd June 2025 | 14.00-15.30

Chair: **Mariadriana Creatore** | Main Hall “Santo Mazzarino”

Nanoarchitectonics of multi-functional metal oxide systems: a multi-purpose toolbox for human/environmental protection and sustainable energy production

D. Barreca[1,*], **A. Gasparotto**[1,2], **G. A. Rizzi**[1,2,], **C. Maccato**[1,2]
[1]CNR-ICMATE and INSTM, Department of Chemical Sciences, Padova University, 35131 Padova, Italy
[2]Department of Chemical Sciences, Padova University and INSTM, 35131 Padova, Italy
e-mail: davide.barreca@cnr.it

Over the last decades, the progressively increasing concern in the protection of both human health and environment has triggered numerous research activities aimed at the detection of flammable/toxic chemicals, the purification of both water and air, and the carbon-free energy generation. The *trait d'union* that could substantially accelerate significant advancements in such fields is the engineering of efficient, green, and economically viable multi-functional catalytic platforms endowed with optimized activity, selectivity and time stability [1]. Despite the efforts undertaken globally, the implementation of active systems simultaneously meeting these requirements remains an open and challenging task.

Among the possible candidates under scrutiny, metal oxide-based-nanosystems represent an endless source of functionalities, since they join together the variety of features of inorganic materials and the unique properties of nanostructures [2]. The modulation of their characteristics offers attractive perspectives in the framework of nanoarchitectonics, an emerging paradigm in nanomaterials science based on the combination of nanotechnologies, as concerns controllable nanomaterial construction from nanosized units, with other specific disciplines, to yield systems endowed with tailored information [1].

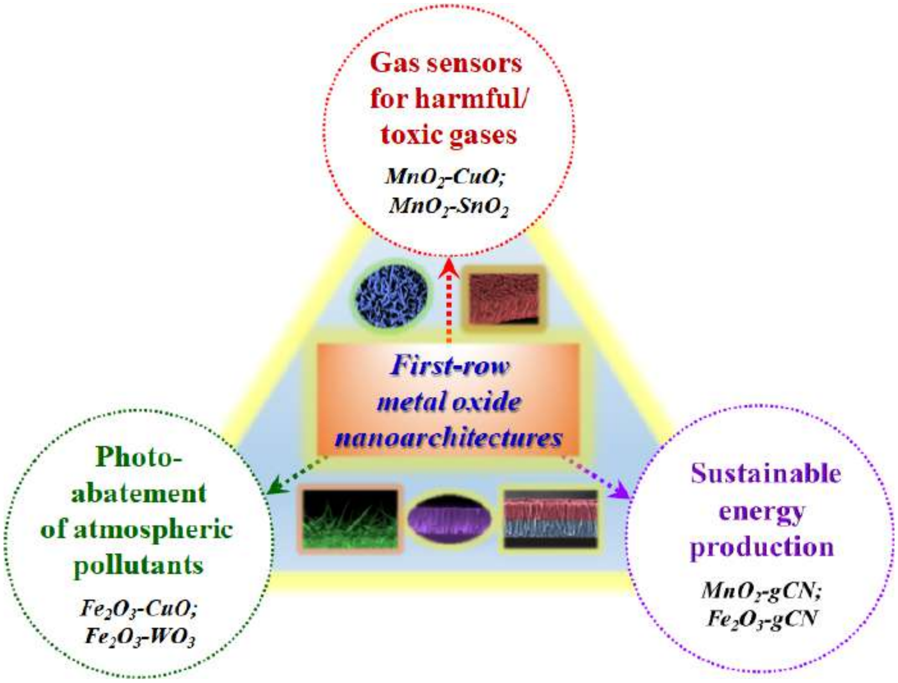
Gas sensors for harmful/ toxic gases
MnO_2-CuO; MnO_2-SnO_2
First-row metal oxide nanoarchitectures
Photo-abatement of atmospheric pollutants
Fe_2O_3-CuO; Fe_2O_3-WO_3
Sustainable energy production
MnO_2-gCN; Fe_2O_3-gCN

Fig. 1. Overview of the materials dealt with in this presentation and related functional applications.

The control of the system behavior is directly dependent on the availability of suitable processing strategies enabling to tailor their structure, chemical composition and nano-organization. To this aim, chemical vapor deposition, eventually plasma-assisted (CVD, PA-CVD) and radio frequency- (RF-) Sputtering, are endowed with numerous degrees of freedom, allowing to conveniently modulate the system characteristics as a function of specific applications. Additional perspectives are offered by the combination of these techniques with liquid-phase routes in the framework of hybrid synthesis processes, yielding material properties hardly accessible by means of conventional preparation routes.

In this context, the present talk will provide an overview of our recent results on the processing of nanoarchitectures based on first-row transition metal oxides, eventually functionalized with dispersed activators, aimed at safety-, environment- and clean energy-related applications The most important issues related to the engineering of the target nanomaterials will be highlighted and critically discussed in relation to the following case studies (Fig. 1):

- detection of flammable/toxic analytes, for safety applications [3,4];
- photocatalytic abatement of gaseous pollutants, for air purification [5,6];
- photoactivated splitting of freshwater and seawater, a largely available natural resource, to yield green hydrogen, a strategically appealing energy vector [7-11].

The outcomes of a comprehensive experimental characterization by forefront analytical tools validate our synthetic strategies as amenable and flexible routes to multi-functional oxide-based active materials. These issues represent important starting points paving the way to additional steps forward eventually enabling the construction of functional platforms by design and the valorization of natural capital in a greener perspective.

This work was supported by CNR (Progetti di Ricerca @CNR—avviso 2020—ASSIST), Padova University (P-DiSC#04BIRD2020-UNIPD EUREKA, P-DiSC#02BIRD2023-UNIPD RIGENERA), INSTM Consortium (INSTM21PDGASPAROTTO-NANO^{MAT} and INSTM21PDBARMAC-ATENA), and PRIN 2022474YE8 (SCI-TROPHY project).

References

[1] D. Barreca and C. Maccato, *CrystEngComm*, **25**, 3968 (2023).

[2] D. Barreca and C. Maccato (eds.), *Tailored Functional Oxide Nanomaterials: From Design to Multi-Purpose Application*, Wiley-VCH (2022).

[3] L. Bigiani, D. Zappa, C. Maccato, E. Comini, D. Barreca, and A. Gasparotto, *Appl. Surf. Sci.*, **512**, 145667 (2020).

[4] L. Bigiani, C. Maccato, D. Barreca, and A. Gasparotto, *Surf. Sci. Spectra*, **27**, 024005 (2020).

[5] J. Fragoso, D. Barreca, L. Bigiani, A. Gasparotto, C. Sada, O.I. Lebedev, E. Modin, I. Pavlovic, L. Sánchez, and C. Maccato, *Chem. Eng. J.*, **430**, 132757 (2022).

[6] C. Maccato, L. Bigiani, D. Barreca, and A. Gasparotto, *Surf. Sci. Spectra*, **28**, 024003 (2021).

[7] D. Barreca, G. Carraro, A. Gasparotto, and C. Maccato, *Metal oxide electrodes for photo-activated water splitting*, in *Multifunctional Photocatalytic Materials for Energy*, Z. Lin, M. Ye, and M. Wang (eds.), Elsevier WP - Woodhead Publishing (2018).

[8] M. Benedet, A. Gallo, C. Maccato, G.A. Rizzi, D. Barreca, O.I. Lebedev, E. Modin, R. McGlynn, D. Mariotti, and A. Gasparotto, *ACS Appl. Mater. Interfaces*, **15**, 47368 (2023).

[9] M. Benedet, A. Gasparotto, G.A. Rizzi, C. Maccato, D. Mariotti, R. McGlynn, and D. Barreca, *Surf. Sci. Spectra*, **30**, 024018 (2023).

[10] M. Benedet, G.A. Rizzi, O.I. Lebedev, V. Roddatis, C. Sada, J.-L. Wree, A. Devi, C. Maccato, A. Gasparotto, and D. Barreca, *J. Mater. Chem. A*, **11**, 21595 (2023).

[11] M. Benedet, D. Barreca, G.A. Rizzi, C. Maccato, J.-L. Wree, A. Devi, and A. Gasparotto, *Surf. Sci. Spectra*, **30**, 024021 (2023).

Atomic Layer Deposition of Heterostructure of Tantalum Oxide and Tantalum Nitride on CNTs for Photoelectrochemical Water Splitting

MA. Khan[1], D. Martinez Martinez[1], N. Boscher[1]
Luxembourg Institute of Science and Technology (LIST)
Muhammad.khan@list.lu; diego.martinez-martinez@list.lu; nicolas.boscher@list.lu.

To counter the issue of CO_2 emissions and climate change there is a very significant shift from conventional fossil fuels to Hydrogen, whose demand soared up to 100 Mt in 2024 [1]. Photoelectrochemical water splitting (PEC WS) has the proven ability to produce green H_2 by utilizing solar energy, but this process is still limited by some thermodynamic and kinetic constraints. Thermodynamically, the bandgap of photo-electrocatalysts should cover the redox potential of water and also absorb large parts of the solar spectrum. Kinetically, it is essential to overcome the slow charge carrier dynamics and surface reaction kinetics in the rate limiting oxygen evolution reaction (OER). Therefore, to overcome the limitations of PEC, a heterojunction photo-electrocatalysts is proposed.

In this work, a heterojunction of tantalum-based oxides and nitrides on carbon nanotubes is implemented. The rationale for this heterojunction is that, in the one hand, the bandgap of tantalum nitride is found to be 2.1 eV, while the theoretical solar to hydrogen efficiency (STH) and theoretical current density are reported to be 15.25 % and 8.1 mA cm^{-2}, respectively [1][2]. In the other hand, the CNTs core-shell acts as an electron channel. Therefore, the combination of these two materials would address the thermodynamic and kinetic limitations. However, the higher aspect ratio of CNTs, and the short mean free diffusion length of holes (~30-50 nm) poses a fabricating challenge [3]. To solve these issues, the use of atomic layer deposition (ALD) is explored to ensure controlled thin (up to 50 nm) and conformal coatings.

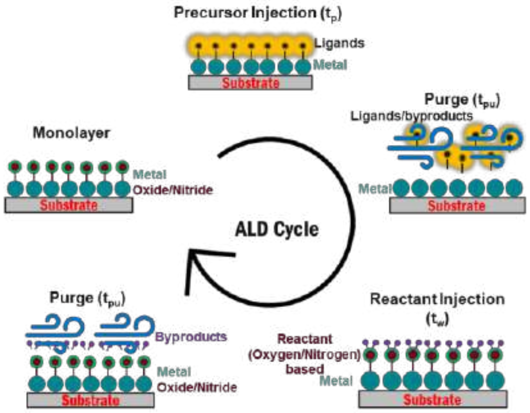

Fig 2. Schematics of ALD of Tantalum Oxide

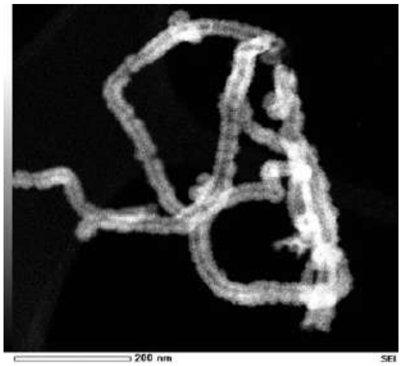

Fig 1. TEM of Ta_2O_5 on CNTs

Tantalum nitride is known to have a limited stability [ref]. Therefore, the final goal of our project would be the deposition of a Ta oxynitride with enhanced stability and good optical and electrochemical properties. In that regard, the deposition of Ta oxide was selected as the first system to be explored.

Thus, the optimization of process parameter was done to attain controlled self-limiting growth of Tantalum oxide. Pentakis (dimethyl amino) tantalum (PDMAT) and water were sequentially used as a precursor for tantalum and oxygen, respectively (cf. Fig. 1). The growth behavior was recorded using *insitu* ellipsometry. Self-limiting growth of about 0.5 Å/cycle was observed at the precursor and water pulse time in a window above 4 s and above 40 ms, respectively, while the purge time between the sequential exposure of precursor and water was 200 sccm. Cross sectional analysis of the obtained thin films of tantalum oxide performed by FESEM and profilometry confirmed the different thicknesses obtained by *in situ* ellipsometry. The XRD measurements showed an amorphous structure of tantalum oxide and the XRR showed a high density i.e., about 6.4 g/cm^3, XPS analysis confirmed the presence of tantalum oxide with less than 5% carbon impurity. The electronic and optical band gap evaluated by REELS and UV-VIS were found to be around 4 eV. Using optimized parameters, the tantalum oxide was then deposited on carbon nanotubes. Fig. 2 shows the TEM analysis indicating conformal and uniform growth of tantalum oxide on the CNTs.

This work was supported by Fonds National de la Recherche (FNR).

References

[1] *Global Hydrogen Review,* International Hydrogen Agency (IEA), Paris, 2024.

[2]Nandal, V., Pihosh, Y., Higashi, T., Minegishi, T., Yamada, T., Seki, K., Sugiyama, M., & Domen, K. *Energy & Environmental Science*, *14* (7), 4038–4047 (2021).

[3] Ela Nurlaela, Mamiko Nakabayashi, Yuji Kobayashi, Naoya Shibata, Taro Yamada and Kazunari Domen, *Sustainable Energy Fuels,*4, 2293-2300, (2020).

[4] Hamed Hajibabaei, Daniel J. Little, Ayush Pandey, Dunwei Wang, Zetian Mi, and Thomas W. Hamann *ACS Applied Materials & Interfaces, 11, 17, 15457–15466, , (2019).*

Aerosol-Assisted Chemical Vapour Deposition of α-Fe_2O_3 and $BiFeO_3$ as effective Photoanodes for Photoelectrochemical Water Splitting

Charlie Brown[1,2], Quan Yee Tey[3] Matthew K. Surman[1], Frank Marken[1], Andrew L. Johnson[1]
[1]Department of Chemistry, University of Bath, Claverton Down, Bath, BA2 7AY, UK
[2]School of Chemistry, Monash University, Clayton, Vic 3800, Australia
[3]School of Engineering, Monash University, Bandar Sunway Selangor DE 47500
Malaysia
e-mail: ceb95@bath.ac.uk

Photoelectrochemical (PEC) water splitting shows promising potential for green hydrogen production. However, it currently lacks the technological readiness to allow commercialisation due to limitations in material performance, particularly in developing a scalable, efficient photoanode. α-Fe_2O_3 and $BiFeO_3$ are semiconductor photoanode materials with great potential due to their desirable bandgap sizes and positionings. These materials however face issues to varying degrees with charge carrier dynamics, which is significantly influenced by their phase purity and morphology[1]. Developing a scalable fabrication technique that promotes high phase purity and favourable morphology is therefore essential. Aerosol assisted chemical vapour deposition (AACVD) is a method of depositing semiconductor thin films that has had relatively little reporting in the field of PEC. Unlike other classes of chemical vapour deposition, AACVD does not require volatile precursors, thus allowing precursors to be more tailored towards producing highly efficient, specifically designed photoelectrodes[2]. Herein, we report some of the first instances of depositing phase pure α-Fe_2O_3 and $BiFeO_3$ via a 'Universal' precursor approach, in which a common ligand framework based upon an amino-tris alcohol was utilised on various metal centres.

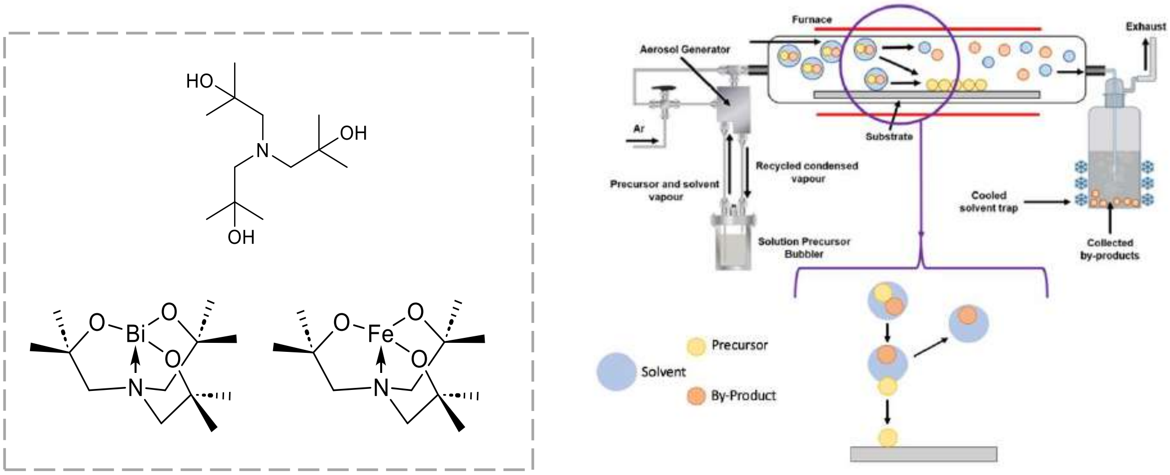

Fig. 1. *Left*: 'Universal' ligand and precursors utilised in this study. *Right* Schematic Diagram of an AACVD setup and theorised deposition mechanism

By aligning precursors at molecular level, complementary decomposition pathways could be achieved, enabling the development of dual-source precursors to deposit mixed metal oxides of high phase purity. Each precursor's structure was confirmed via single-crystal X-ray diffraction, ^1H NMR, ^{13}C NMR, and elemental analysis. The suitability of each compound as an AACVD precursor was assessed using thermogravimetric analysis (TGA). By studying TGA results, our dual-source precursors were effectively matched together based on compatibility/overlap in decomposition pathway. Successful deposition of phase pure films of **α**-Fe_2O_3 and $BiFeO_3$ was confirmed using powder X-ray diffraction, Raman spectroscopy, and energy dispersive X-ray spectroscopy. In addition, scanning electron microscopy revealed favourable morphologies: **α**-Fe_2O_3 formed as nanoflakes, while $BiFeO_3$ grew as high-surface-area nanorods. Our films displayed the highest photoactivity reported to date for **α**-Fe_2O_3 and $BiFeO_3$ films produced via AACVD, suggesting that the high phase purity and optimised morphologies of AACVD-derived photoanodes enhances charge carrier dynamics, leading to improved PEC performance.

This work was supported by the Institute of Sustainability and Climate change at Bath University, and their joint Bath-Monash PhD programme.

References

[1] A. Thakur, D. Gosh, P. Devi, K. Kim, and P. Kumar*, Chemical Engineering Journal*, **397**, 125415 (2020).

[2] P. Marchand, I. A. Hassan, I. P. Parkin and C. J. Carmalt, *Dalton Transactions*, **42**, 9406–9422 (2013).

Ultrathin Overlayers for Anode Protection in Offshore Green Hydrogen Production via Saline Water Electrolysis

K. Encalada[1,*], J.R. van Ommen[2], R. Kortlever[1]
[1]Delft University of Technology, Process and Energy Department
[2]Delft University of Technology, Chemical Engineering Department
e-mail[*]: k.s.encaladaflores@tudelft.nl

Water electrolysis is the electrochemical process that splits water into gaseous hydrogen and oxygen when a certain electrical potential is applied to the electrodes submerged in an aqueous electrolyte. Electrochemical water splitting for green hydrogen production is a targeted technology for the energy transition toward fossil-free energy [1]. Green hydrogen is produced by water-splitting using electrical energy from renewable sources as input to power up the electrochemical conversion unit, the electrolyzer. This redox process involves two half-cell reactions: hydrogen is generated at the cathode and oxygen at the anode. The hydrogen evolution reaction (HER) provides the commercially valuable product, hydrogen. However, the HER is inherently linked to the oxygen evolution reaction (OER), as they are part of the global redox reaction. The OER is the limiting step of the process as it is a sluggish reaction involving a four-electron transfer as opposed to the HER requiring only a two-electron transfer [2]. This explains the relevance of studying the OER at the anode in the context of water splitting.

The current commercially available and more mature electrolyzer technologies for water electrolysis are alkaline water electrolysis (AWE) and proton exchange membrane electrolysis (PEM) [3]. These technologies have been developed based on a highly pure water feedstock. Nonetheless, saline water electrolysis offers a promising pathway for green hydrogen production, particularly in offshore applications where water is sourced from ship-based desalination units. Typically relying on reverse osmosis, these units produce water with reduced but significant chloride concentrations. The presence of chloride ions, even at lower levels, presents technical challenges due to their competing role with OER and potential material degradation at the anode side. Previous studies showed that MnO_x and SiO_2 act as permeable overlays and selectively suppress the competing anode's chlorine evolution reaction (CER). However, the overlayer´s liquid deposition techniques resulted in non-uniform thickness and poor stability [4].

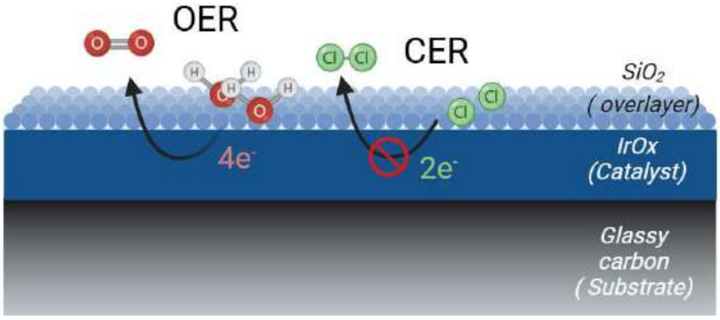

Fig. 1. Representation of OER vs. CER competing reactions at the anode in acidic chloride-containing electrolyte during saline water electrolysis.

This presentation explores the effectiveness of a SiO_2 overlayer deposited by atomic layer deposition (ALD) on a carbon-supported IrO_x catalyst to suppress the CER competing reaction during water electrolysis in an acidic chloride-containing electrolyte. The IrO_x catalyst was prepared by electrodeposition, while the SiO_2 overlayer was made using ALD in two different setups: atmospheric and vacuum ALD. $SiCl_4$ and water/ozone were used as reactants for the atmospheric ALD at 150 °C reaction temperature. Similarly, BDEAS and O_2 plasma were used for the vacuum ALD process at 100 °C. Comparative electrochemical measurements were conducted with and without the SiO_2 overlayer on the IrO_x|GC catalyst. The ratio between OER vs. CER is quantified using a rotating ring disk electrode setup that simultaneously measures the oxidation (disk) and reduction (ring) currents within a potential range using 0.5 M H_2SO_4 + 30 mM KCl as electrolyte. Both competing reactions are performed at the disk (IrO_2|GC) by sweeping the potential from 1.1 V to 1.55 V vs RHE. In this first step, water molecules and chloride ions oxidize, forming O_2(g) and Cl_2(g), respectively. The second simultaneous step involves selective reduction at the ring (Pt) of the previously formed Cl_2(g), allowing quantification.

Results show that a layer of 20 cycles of SiO_2 by atmospheric ALD induces an initial suppression of CER compared to OER. However, repetitive cyclic voltammograms cause the CER suppression to partially revert to the uncoated IrO_x behavior, suggesting instability of the SiO_2 overlayer, likely due to physical detachment. Conversely, the vacuum ALD process demonstrates more stable SiO_2 coating layers, although at 20 cycles, the underlying catalytic performance is negatively affected, and the OER performance signal becomes negligible. These findings highlight the critical role of the deposition method in tailoring the permeability and stability of the SiO_2 overlayer, emphasizing the need for further optimization to balance stability and catalytic performance.

This work was supported by The Rijksdienst voor Ondernemend Nederland (RVO) in collaboration with the OFFSET-MOOI consortium, which comprises SwitcH2, BW Offshore, MARIN, TU Delft, and Strohm B.V.

References

[1] E. Asghari, M. I. Abdullah, F. Foroughi, J. J. Lamb, and B. G. Pollet, “Advances, opportunities, and challenges of hydrogen and oxygen production from seawater electrolysis: An electrocatalysis perspective,” *Current Opinion in Electrochemistry*, vol. 31, p. 100879, Feb. 2022, doi: 10.1016/j.coelec.2021.100879.
[2] J. Mohammed-Ibrahim and H. Moussab, “Recent advances on hydrogen production through seawater electrolysis,” *Materials Science for Energy Technologies*, vol. 3, pp. 780–807, 2020, doi: 10.1016/j.mset.2020.09.005.
[3] B. A. Horri and H. Ozcan, “Green Hydrogen Production by Water Electrolysis: Current Status and Challenges,” *Current Opinion in Green and Sustainable Chemistry*, p. 100932, May 2024, doi: 10.1016/j.cogsc.2024.100932.
[4] J. G. Vos, A. A. Bhardwaj, A. W. Jeremiasse, D. V. Esposito, and M. T. M. Koper, “Probing the Effects of Electrode Composition and Morphology on the Effectiveness of Silicon Oxide Overlayers to Enhance Selective Oxygen Evolution in the Presence of Chloride Ions,” *J. Phys. Chem. C*, vol. 126, no. 48, pp. 20314–20325, Dec. 2022, doi: 10.1021/acs.jpcc.2c07116.

Innovative protective coatings prepared by Atomic Layer Deposition (ALD) and Direct Liquid Injection Metal-Organic Chemical Vapor Deposition (DLI-MOCVD) for Solid Oxide Electrolyzer Cells (SOEC) interconnects

J. Delbreuve[1,2], **R. Chanson**[1], **D. Coutancier**[2], **F. Miserque**[1], **L. Artaud**[3], **I. Nuta**[3], **F. Rouillard**[1], **N. Schneider**[2]
[1]Université Paris-Saclay, CEA, Service de recherche en Corrosion et Comportement des Matériaux, 91191 Gif Sur Yvette, France
[2]Institut Photovoltaïque d'Île de France (IPVF), UMR CNRS 9006, 18 boulevard Thomas Gobert, 91120 Palaiseau
[3]Science et Ingénierie des Matériaux et Procédés (SIMaP), 1130 rue de la piscine, 38402 Saint-Martin d'Hères
e-mail: juliette.delbreuve@cnrs.fr

In the energy transition, producing decarbonized hydrogen (H_2) is a key challenge. Low-emission H_2 can be generated through high-temperature water electrolysis using Solid Oxide Electrolyzer (SOE). This SOE contains ferritic stainless-steel interconnects facing two major issues: (i) the O_2 side undergoes high-temperature oxidation, forming a low-conductive chromia (Cr_2O_3) layer that reduces the electrical current and releases poisoning Cr^{+VI} species; (ii) on the H_2/H_2O side, H_2 permeation can exacerbate the oxidation on the O_2 side, leading to "catastrophic" oxidation (see Fig. 1.). To prevent these issues, protective coatings are needed on both sides of the interconnects. Previous research for coating on the O_2 side identified spinel cobalt oxide (Co_3O_4) for its good electrical property and Cr diffusion barrier property, and rare-earth oxides such as cerium oxide (CeO_2) for its reducing effect on the chromia layer growth rate [1, 2]. Multilayer coatings could be a solution to benefit from both materials. As recently shown [3], alumina (Al_2O_3) could be a solution as well on both sides for its protection against H_2 permeation.

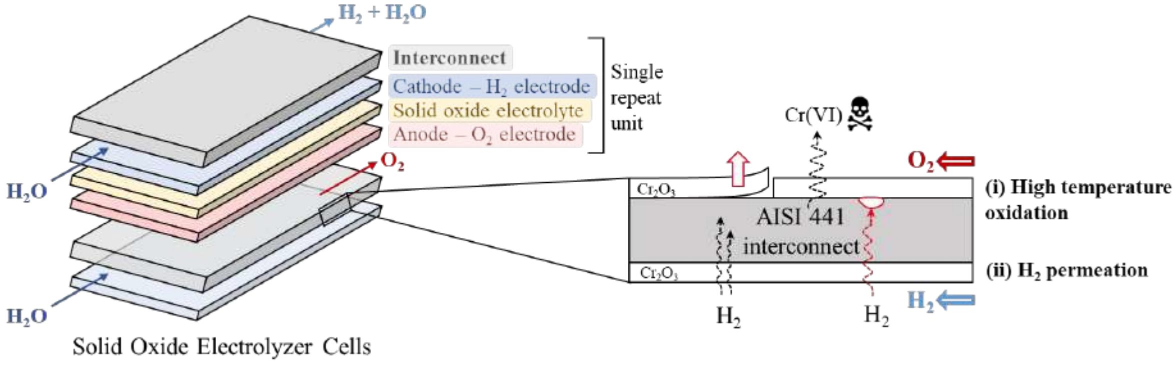

Fig. 1. Composition of SOE cells and schematic view of the different phenomena happening at the interconnect's surfaces.

In that context, we decided to deposit these oxides by two deposition techniques: Atomic Layer Deposition (ALD) on one hand, for its ability to grow thin films with excellent thickness control and conformality; and Direct Liquid Injection Metal-Organic Chemical Vapor Deposition (DLI-MOCVD) on the other hand, for its versatility and faster deposition rate, making it more suited to thicker films deposition. Chemical precursors for cobalt and cerium oxides were chosen following the outcome of our "home-made" selection method based on four major criteria: the availability of the precursor, its reactivity towards oxidants, its thermal properties and the robustness of the process. The thermal properties of these precursors were determined by ThermoGravimetric Analyses (TGA). The ALD and DLI-MOCVD tests were conducted on silicon wafers and AISI 441 stainless steel samples. The ALD tests were monitored using in-situ Quartz Crystal Microbalance (QCM) and the gas phase was analyzed by Quadrupole Mass Spectroscopy (QMS). Complementary ex-situ analyses were carried out on the coated samples: samples weighing, ellipsometry, Grazing Incidence X-Ray Diffraction (GIXRD), X-Ray Reflectometry (XRR) and X-ray Photoelectron Spectrometry (XPS). The electrical performance (Area Specific Resistance, ASR) of coated samples under operating conditions (high temperature 700 - 850 °C, thousands of hours) was measured in a home-built set-up called RESIST (see Fig. 2.). Post mortem analyses were conducted by a set of characterization (Scanning Electron Microscopy, X-Ray Diffraction, Raman Spectroscopy), and compared to bare AISI 441 samples to identify degradation mechanisms.

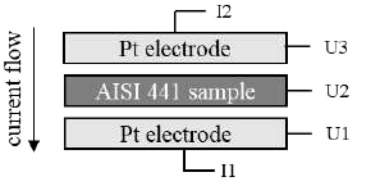

$$ASR = \frac{\Delta U}{I} * S$$

with S, sample surface

Fig. 2. Scheme of the RESIST set-up and formula for the calculation of the Area Specific Resistance (ASR) of AISI 441 coated samples.

First ALD experiments of cobalt oxide were conducted using [bis(cyclopentadienyl)cobalt(II)] $Co(Cp)_2$ and O_3, [4] and highlighted the strong influence of the precursor's volatility on the growth of the film. The deposited films were amorphous (GIXRD) with a Co_3O_4 stoichiometry (XPS). Cerium oxide deposition tests were carried out using DLI-MOCVD with [tetrakis(tetramethylheptandionate)cerium(IV)] $Ce(tmhd)_4$ in p-xylene and O_2. The influence of several deposition parameters (deposition pressure, deposition temperature, O_2 percentage) on the film properties (thickness, composition, morphology, uniformity) was explored.

Finally, Al_2O_3 was deposited by ALD using trimethylaluminum (TMA) and H_2O, and thermally annealed under various atmospheres (N_2, Ar/H_2, pure H_2). The evolution of the ASR was monitored for samples with a single layer (cobalt oxide, cerium oxide or alumina) or with multilayer coatings (cerium and cobalt oxides) in our RESIST set-up for thousands of hours.

This project is part of the PEPR DIADEM and benefits from a fund given by the national French research agency (Agence Nationale de la Recherche) with the reference ANR-22-PEXD-0017.

References

[1] J. Froitzheim and J.-E. Svensson, "Multifunctional Nano-Coatings for SOFC Interconnects," *ECS Transactions*, vol. 35, no. 1, p. 2503, 2011.

[2] T. Dejob, "Dépôt de couches minces multiéléments par pulvérisation HiPIMS réactive pour l'électrolyse à haute température," Université de Troyes, CEA Paris-Saclay, 2024.

[3] M. Tomas, J.-E. Svensson, and J. Froitzheim, "Hydrogen-barrier coatings against dual-atmosphere corrosion for IT-SOFC interconnect applications," *International Journal of Hydrogen Energy*, vol. 58, pp. 852–862, 2024.

[4] M. Diskus, O. Nilsen, and H. Fjellvåg, "Thin Films of Cobalt Oxide Deposited on High Aspect Ratio Supports by Atomic Layer Deposition," *Chemical Vapor Deposition*, vol. 17, no. 4–6, pp. 135–140, 2011.

Session PM_2.2 DIELECTRICS

Tuesday 3rd June 2025 | 14.30-15.30

Chair: **Alessio Lamperti** | Room “Coro di Notte”

Nucleation of ALD Grown Gate Dielectrics on WS_2 using Low Temperature Oxygen Plasma Pretreatment

R.K. Grubbs[1], **T. van Pelt**[1], **S. Nemeth**[1], **D. Cott**[1], **B. Groven**[1], **P. Morin**[1], **C Lockhart de la Rosa**[1], **G. Sankar Kar**[1], **J. Swerts**[1]

[1]IMEC, Leuven, Belgium

abstract

Due the ever decreasing device size driven by the electronics industry, the future of channel materials for small transistors is heading toward the use of two dimensional transitional metal dichalcogenide (2d TMD) materials. 2d TMDs are beneficial in the short channel regime because of their potential high on-to-off current ratios and because of their potentially high channel mobilities, or conductance, between the source and the drain. Beyond TMD electrical and structural quality, two large challenges exist for the implementation of TMDs into transistors. First is the electrical contact of source and drain metals to the TMD and second is the deposition of a nanometer thin, high quality, high κ, defect free dielectric material on top of the TMD to form the critical transistor gate dielectric. To tackle the second challenge, the surface of WS_2 TMD was functionalized with a low temperature remote oxygen plasma which enabled nucleation sites to form on the surface of multi-layer WS_2 without catastrophic destruction of the long-range order of the WS_2. From these nucleation sites, ALD HfO_2 and Al_2O_3 using TMEAH (tetrakis(methylethylamido)hafnium)/H_2O and TMA (trimethylaluminum)/H_2O at 200C was deposited as the gate dielectric and a 5 nm thin layer with 100% coverage could be achieved at increased oxygen plasma exposures. This WS_2 functionalization / nucleation process was explored by measuring the effects of oxygen exposure and temperature and their resulting effect on the ALD deposited gate dielectric film. The ALD gate dielectric coverage and its effects on the underlying 2D material was quantified with AFM, XPS, photoluminescence and Raman spectroscopy. This research has led to a process where multi-layer WS_2 can be functionalized and a high-quality gate dielectric can be successfully deposited on the TMD channel materials.

Resistive switching in hafnium-titanium-oxide thin films grown by atomic layer deposition

Toomas Daniel Viskus, Joonas Merisalu, Markus Otsus, Jaan Aarik, Aarne Kasikov, Hugo Mändar, Lauri Aarik, Kaupo Kukli

University of Tartu, Institute of Physics, W. Ostwaldi 1, 50411 Tartu, Estonia

e-mail of presenting author: toomas.daniel.viskus@ut.ee

Resistive switching has, to date, been studied in metal-insulator-metal (MIM) structures based on both titanium oxide [1] and hafnium oxide [2]. Devices utilizing a TiO_2/HfO_2 bilayer have also been studied [3].

In this work we investigate the resistive switching properties of devices where $TiO_2:HfO_2$ mixed oxide dielectric layers were deposited on RuO_2 bottom electrodes with Pt top electrodes forming MIM-like structures. The top electrodes were deposited using electron beam evaporation and the mixed oxide thin films were prepared using atomic layer deposition (ALD). ALD was carried out at 350 °C. The precursors used were $HfCl_4$, $TiCl_4$, H_2O, whereby N_2 was employed as a carrier gas. Multiple samples with a varying ratio of TiO_2 to HfO_2 ALD cycles were prepared. For each ratio, both as-deposited samples and samples annealed for 30 minutes at 400 °C were evaluated.

Grazing incidence X-ray diffractometry (GIXRD) measurements showed that with the growing $HfO_2:TiO_2$ ALD cycle ratio, transition from the TiO_2 rutile phase to the $HfTiO_4$ orthorhombic phase took place and was followed by a transition from the orthorhombic phase to the monoclinic HfO_2 phase.

Electrical measurements were carried out using a Cascade Microtech EPS-150 probe station and a Keithley 2636A source-meter. All studied samples demonstrated resistive switching behavior (Fig. 1 a). As-deposited devices with the $HfTiO_4$ orthorhombic phase and $HfO_2:TiO_2$ ratio of 1:3 showed a ratio between the low resistance state (LRS) and high resistance state (HRS) about 10 with an endurance measurable in thousands of cycles (Fig. 1 b). Retention for these samples was stable for six hours at 110 °C (Fig. 2). Some samples demonstrated appreciably stable memory window, that is HRS:LRS ratio during 6 hours, even at measurement temperatures as high as 140 °C. Independently from the measurement temperatures, selected samples were subjected to annealing procedures where the samples with electrodes were heat-treated at 300 or 400 °C. Preliminary device-to-device repeatability tests were also carried out and showed that annealed devices tended to show better repeatability when compared with unannealed devices.

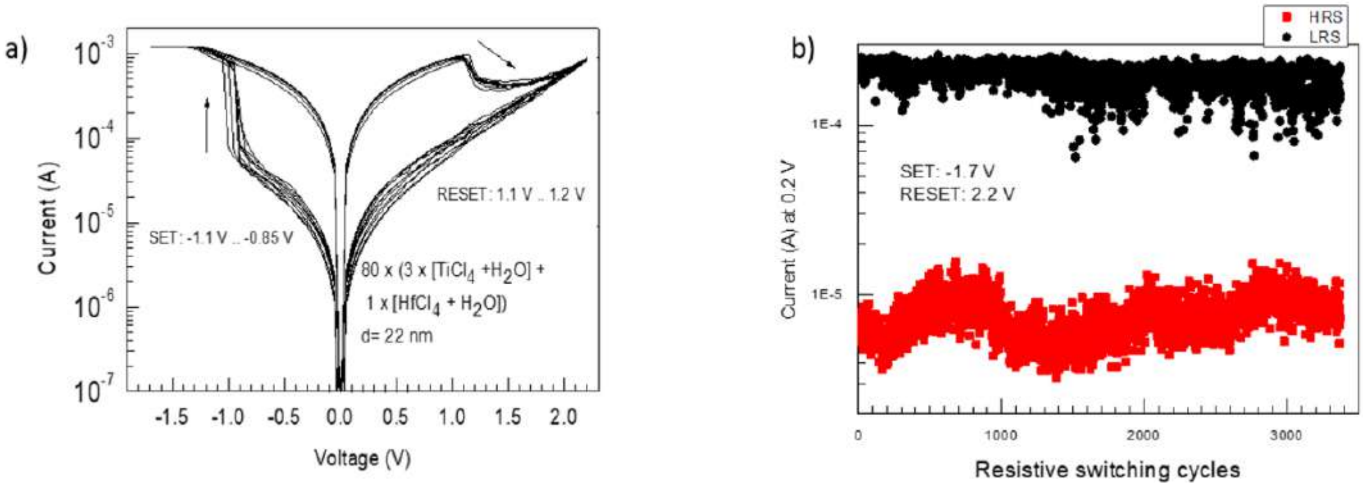

Fig 1. I-V and endurance graphs for samples where the HfO_2:TiO_2 thin film was deposited using 80 × 1 HfO_2 : 3 TiO_2 ALD cycles.

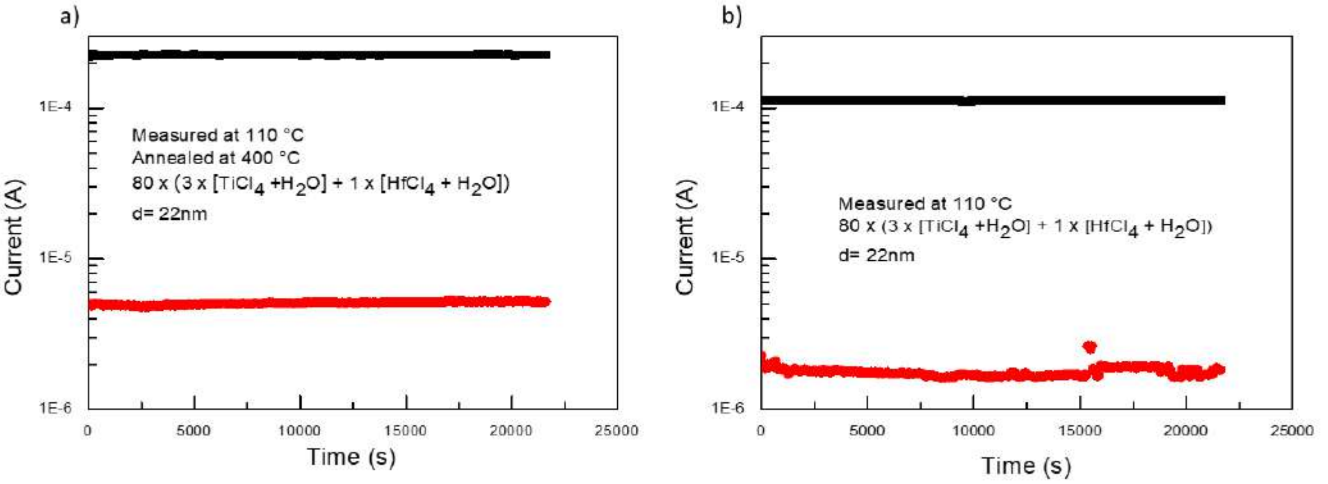

Fig 2. Retention graphs measured at 110 °C for both annealed (a) and unannealed samples (b)

This work was supported by Estonian Science Foundation grants PRG448 and PRG753.

References:

[1] S. C. Oh, H. Y. Jung, and H. Lee, ‘Effect of the top electrode materials on the resistive switching characteristics of TiO2 thin film’, *Journal of Applied Physics*, vol. 109, no. 12, p. 124511, Jun. 2011, doi: 10.1063/1.3596576.

[2] A. S. Sokolov *et al.*, ‘Influence of oxygen vacancies in ALD HfO2-x thin films on non-volatile resistive switching phenomena with a Ti/HfO2-x/Pt structure’, *Applied Surface Science*, vol. 434, pp. 822–830, Mar. 2018, doi: 10.1016/j.apsusc.2017.11.016.

[3] C. Ye *et al.*, ‘Enhanced resistive switching performance for bilayer HfO $_2$ /TiO $_2$ resistive random access memory’, *Semicond. Sci. Technol.*, vol. 31, no. 10, p. 105005, Oct. 2016, doi: 10.1088/0268-1242/31/10/105005.

Bottleneck-Effect on High Aspect Ratio ALD Thin-Film Conformality

J. Kinnunen[1,*], **A. Philip**[2], **F. Gao**[1], **J. Karttunen**[1], **M. Utriainen**[1]
[1]Chipmetrics Ltd, Finland
[2]Aalto University, School of Chemical Engineering, Finland
e-mail: Jussi.kinnunen@chipmetrics.com

Atomic Layer Deposition (ALD) enables conformal deposition into High Aspect Ratio (HAR) structures making it critical technology for fabrication of advanced 3D semiconductor device architectures as well as other application areas such batteries and capacitors. Achieving conformal thin-film deposition in complex geometries is challenging. As the structures or design become more complex the narrow dimensions create bottlenecks that presumably affect the conformal film formation. Proper control of the ALD process is crucial for the device performance and reliability. Understanding how bottlenecks affect the film formation is the basis of ALD process control and process optimization.

In this study, we show how the PillarHall® lateral high-aspect ratio (LHAR) test structure offers a robust framework for studying bottleneck effects by precisely controlling cavity entry dimensions, enabling the evaluation of how geometry influences film penetration and refining ALD processes. Thermal ALD experiments for Al_2O_3 on three LHAR test structures and one VHAR (Vertical High Aspect Ratio) was performed. One of the LHAR test structures acted as a reference without a bottleneck (Gap height 500 nm). Two LHAR structures gap height was reduced from 500 nm to 400 nm by a 50 nm deposition at the trench opening, covering both the floor and the top of the opening. The two bottlenecks were generated with non-conformal process of Al_2O_3 and TiO_2. The VHAR1 structure is a hole design with a native bottleneck at the entry point.

For LHAR structures, we observed penetration depth of 152 μm without bottleneck (Fig. 1a), which reduced to 133–135 μm in the presence of bottleneck (Fig. 1b & 1c)) regardless of the bottleneck material. The PillarHall test structures were measured using a line-scanning reflectometry. The optical method enables separation of different thin films in the stack when the bottleneck is TiO_2 (Fig. 1b). These results align with theoretical models by Gordon et al. [1], which predict diffusion-limited deposition in constrained geometries. The theoretical model was used to compare the LHAR results with VHAR results. Building on these findings, it is possible to create application-specific bottleneck structures using various deposition methods. These structures will support the development of refined physical models to better predict deposition behavior in complex geometries, including cases with multiple bottlenecks.

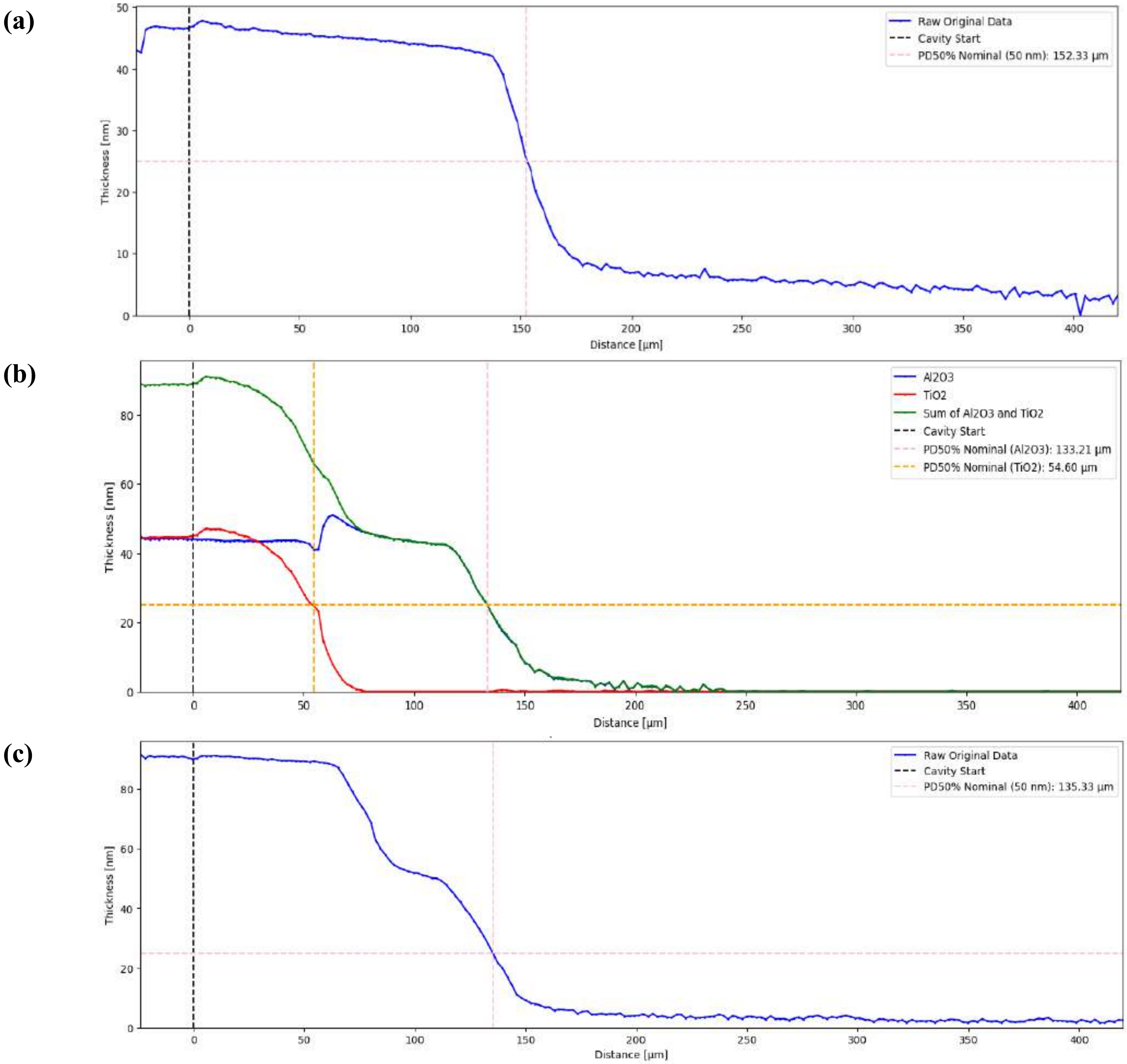

Fig. 1. The film penetration depth profile of Al_2O_3 ALD deposition into the horizontal trench with constant gap height of 500nm (a). The effect of the reduction of the penetration depth based on the 400nm trench opening (50nm pre-deposition on top and on bottom of the opening) after TiO_2 (b) and Al_2O_3 (c) ALD pre-deposition. The material stack can be separated in the thin film measurement of TiO_2 (b).

References

[1] R.G. Gordon, D. Hausmann, E. Kim, and J. Shepard, Chem. Vapor Deposition, 9, 73 (2003).

Deposition and Characterization of ALD Ta_2O_5 Coatings for Gravitational Wave Detectors

J. De Bolle[1], M. Granata[2], J. Steinlechner[3,4], J. Dendooven[1], C. Detavernier[1]
[1]CoCooN Research Group, Department of Solid State Sciences, Ghent University, Belgium
[2]Université Claude Bernard Lyon 1, CNRS, Laboratoire des Matériaux Avancés (LMA), IP2I Lyon / IN2P3, UMR 5822, F-69622, Villeurbanne, France
[3]Maastricht University, 6200 MD Maastricht, Netherlands
[4]Nikhef, 1098 XG Amsterdam, Netherlands
e-mail: jorden.debolle@ugent.be

Gravitational waves are detected with km-scale interferometers. One of the most critical components of these extremely sensitive detectors are the highly reflective mirror coatings, since these contribute a large fraction to the total detector noise [1]. The coatings operate as Bragg reflectors and currently consist of alternating layers of SiO_2 and Ti-doped Ta_2O_5, deposited on fused silica by ion beam sputtering (IBS) [2]. For future detectors, atomic layer deposition (ALD) is under investigation as an alternative deposition technique for the mirror coatings, since it offers interesting advantages such as the precise thickness control and superior uniformity. The ALD deposition of Ta_2O_5 with PDMAT as precursor and H_2O or O_2-plasma as co-reactant have been studied before [3, 4, 5, 6]. In this work, we study the ALD growth of Ta_2O_5 films from PDMAT and three different co-reactants (H_2O, O_2-plasma and O_3). Furthermore, some critical properties to determine the applicability of the obtained coatings in gravitational wave detectors are evaluated.

The growth characteristics under different deposition conditions for all three co-reactants were studied using in-situ spectroscopic ellipsometry. For the application as mirror coatings in gravitational wave detectors, dense and pure coatings with an as high as possible refractive index should be obtained. Ex-situ spectroscopic ellipsometry was used to determine the refractive indices, XPS was used to check for impurities, XRR and XRF were combined to study the coating density, and the stoichiometry was determined from ERD measurements. Furthermore, the morphology of the surface was studied with SEM, mainly to check for damage originating from the O_2-plasma, and in-situ XRD was used to study crystallization behavior. Finally, the local atomic structure was investigated with synchrotron-based grazing incidence total X-ray scattering, since this can be correlated with the coating thermal noise [7].

It is shown that the co-reactant and deposition conditions strongly influence the growth characteristics of the Ta_2O_5 coatings (Fig. 1). These differences are also reflected in the coating properties, for example very different refractive indices are obtained (Fig. 2). Our results suggest that the co-reactant and deposition conditions must be carefully chosen to obtain coatings with the desired properties for the envisioned application.

This work was supported by the Research Foundation Flanders (FWO) through PhD Fellowship 11PRJ24N.

References

[1] J. Steinlechner, *Phil. Trans. R. Soc. Lond. A*, **376**, 2120 (2018).
[2] M. Granata et al., *Class. Quantum Grav.*, **37**, 095004 (2020).
[3] W. J. Maeng et al., *Electrochem. Solid-State Lett.,* **9,** G191(2006).
[4] W. J. Maeng et al., *J. Vac. Sci. Technol. B*, **24**, 2276–2281 (2006)
[5] S. B. S. Heil et al., *J. Vac. Sci. Technol. A*, **26**, 472–480 (2008).
[6] S. E. Potts et al., *J. Electrochem. Soc.*, **157**, 66 (2010).
[7] K. Prasai et al., *Phys. Rev. Lett.*, **123**, 045501 (2019).

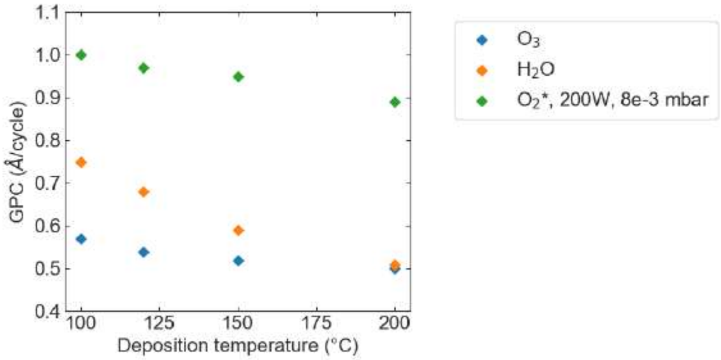

Fig. 1. The growth rate of the PDMAT/H_2O, PDMAT/O_2-plasma and PDMAT/O_3 processes for different deposition temperatures.

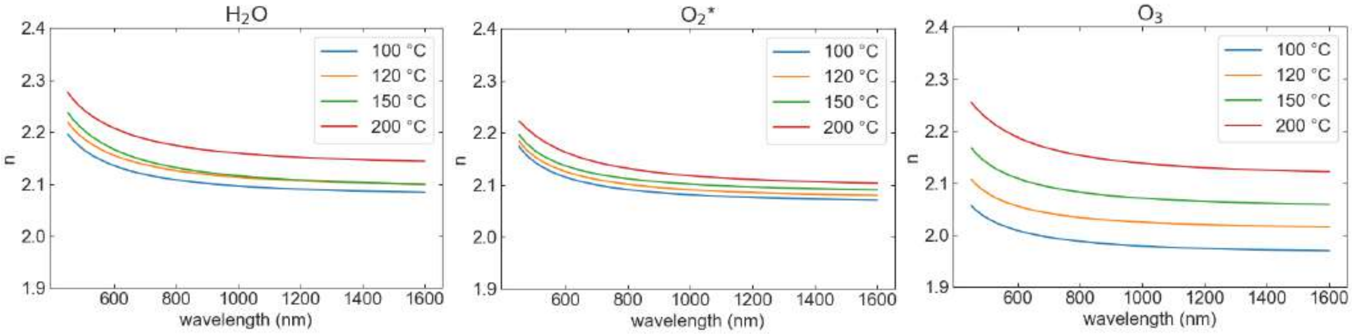

Fig. 2. The refractive index of the Ta_2O_5 coatings obtained from the different ALD processes at different deposition temperatures, determined from ex-situ spectroscopic ellipsometry. For the O_2-plasma, a power of 200W and a plasma pressure of 8e-3 mbar were used.

Session PM_2.3 MATERIALS FOR ENERGY: PHOTOVOLTAICS

Tuesday 3rd June 2025 | 16.00-17.30

Chair: **David Muñoz-Rojas** | Main Hall “Santo Mazzarino”

ALD layers and interfaces in metal halide perovskite-based photovoltaics

Y. Salimi[1], A.E.A. Bracesco[1], K. Mukherjee[1], C. van Helvoirt[1], P. Gnanasambandan[1], V. Zardetto[2],
M. Creatore[1]
[1]Department of Applied Physics and Science Education, Eindhoven University of Technology, the Netherlands
[2]TNO, Eindhoven, the Netherlands
e-mail: m.creatore@tue.nl

Innovation in thin film and interface engineering has played an essential role in pushing the conversion efficiency of the most widespread photovoltaic (PV) technology, i.e. crystalline silicon-based (c-Si), towards its thermodynamic limit. In this respect, ultra-thin, conformal, high-purity Al_2O_3 thin films synthesized by ALD are key in c-Si PV manufacturing industry as they passivate the c-Si surface, thereby suppressing a major channel of electron-hole pair recombination.

In the past years we have explored the ALD synthesis of thin films and interfaces in metal halide perovskite- based PV. The latter has recently surpassed the conversion efficiency of 26% and, when coupled with c-Si PV in a tandem device, presently leads to efficiencies beyond 34%.

In this contribution the merits which ALD offers to perovskite-based PV will be discussed by focusing on NiO-based hole transport layers and SnO_2 buffer layers. Specifically, we have synthesized by ALD thin (< 10 nm) NiO layers which enable homogeneous anchoring (Fig.1) of self-assembled monolayers (SAMs) for “lossless” (i.e. in terms of suppression of charge recombination) SAM/perovskite interfaces and narrow spread in conversion efficiency of perovskite [1] and tandem perovskite/c-Si devices [2]. Presently, our studies include the appropriate selection of the ALD Ni-precursor and co-reactant for accurate control over film stoichiometry, Ni oxidation state and layer resistivity, leading to careful engineering of NiO/(SAM)/perovskite interfaces in both wide- and narrow-band gap perovskites for all-perovskite tandem devices.

We will also address the case study of ALD SnO_2, as presently implemented in perovskite PV R&D and industry as buffer layer. The latter imparts thermal and environmental stability to the device, while protecting the perovskite absorber and fullerene electron transport layer from the sputtering of the transparent top contact. More recently, ALD SnO_2 is explored as solvent barrier layer in the tunnel recombination junction of perovskite/perovskite tandem PV, to prevent the damage of the wide-gap perovskite absorber when processing the narrow- band gap perovskite cell.

Although we can conclude that several ALD merits are already extensively acknowledged by the PV community, studies addressing ALD film growth on challenging substrates such as fullerenes and metal halide perovskites are rarely reported in literature. We are convinced that these studies provide the needed rationale to implement more efficiently these layers at device level and promote process upscaling. Therefore, this contribution will also highlight the adoption of *in situ* diagnostics, namely spectroscopic ellipsometry and IR spectroscopy, to characterize the ALD SnO_2 growth on two commonly adopted fullerenes, C60 and [6,6]-phenyl-C61-butyric acid methyl ester (PCBM). Our studies [3] show that a substrate-inhibited growth occurs in the case of PCBM and, to a minor extent, in the case of C60, with respect to c-Si. Moreover, IR spectroscopy highlights the loss of vibrational features of the ester group in PCBM upon SnO_2 growth, whereas C60 is chemically unaffected. We conclude that the delayed film growth and chemical modifications detected on PCBM are responsible for the consistently lower device performance when ALD SnO_2 is grown on PCBM instead of C60.

References

[1] N. Phung *et al.*, *ACS Applied Materials & Interfaces* **14**, 2166 (2021)
[2] N. Phung *et al.*, *Solar Energy Mat. Solar Cells* **261**, 112498 (2023)
[3] A.E.A. Bracesco *et al.*, *ACS Applied Mat. Interfaces* **16**, 59468 (2024)

Figures

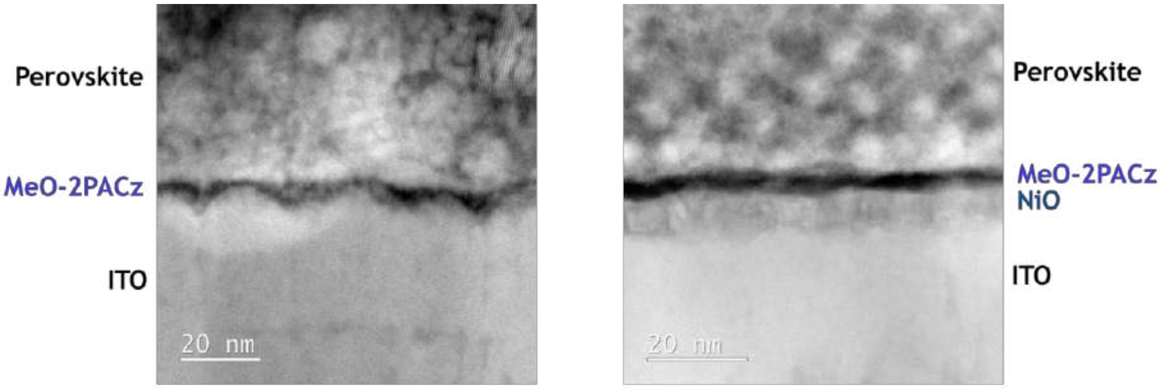

Inhomogeneous SAM coverage on ITO **Homogeneous** SAM coverage on ITO+NiO

Fig.1: TEM analysis of (left) ITO/SAM (MeO-2PACz) and (right) ITO/ALD NiO/SAM (MeO-2PACz) interfaces showing the homogeneous coverage of the SAM layer in the presence of NiO. The SAM coverage affects the perovskite device performance in terms of yield as shown in [1,2].

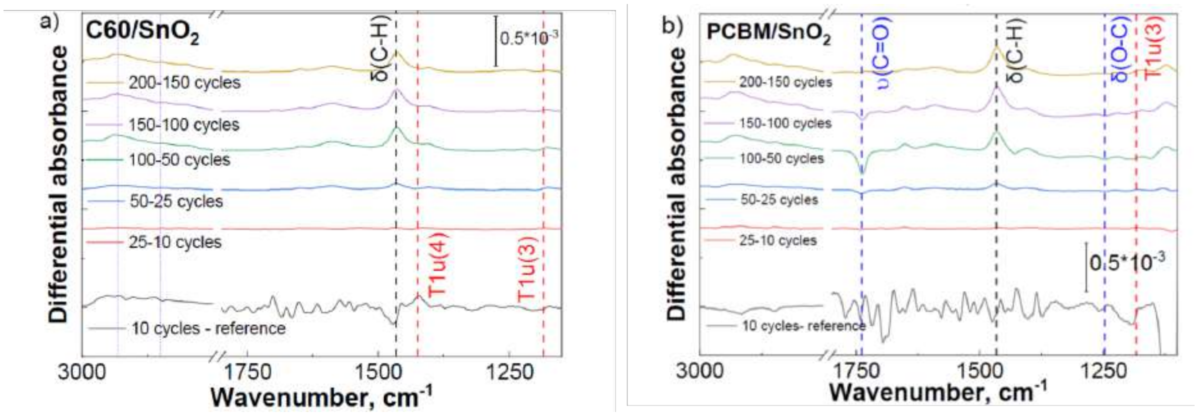

Fig.2: *In situ* IR spectroscopy studies on fullerene (left-C60 and right-PCBM) during the growth of several ALD SnO_2 cycles: positive absorption features point out to the growth of SnO_2 (as monitored by the δ mode of C-H bonds of the metalorganic Sn-precursor), while negative absorption features indicate the chemical modification of the fullerene (υ mode of the C=O bond belonging to the ester group in PCBM), as shown in [3].

Detailed investigation of earth abundant nanostructures for PV

Spadaro M. C.[1,2], Rabelo-Freitas H.[2], Salutari F.[2], Urbonavicius A.[4], Hagger T.[3], Lemerle R.[3], Escobar Steinvall S.[4], Fontcuberta i Morral A.[3], Dick K. A.[4], Arbiol J.[2,5].

1. Department of Physics and Astronomy "Ettore Majorana", University of Catania and CNR-IMM, Via S. Sofia 64, 95123 Catania, Italy
2. Catalan Institute of Nanoscience and Nanotechnology (ICN2), CSIC and BIST, Campus UAB, Bellaterra, 08193 Barcelona, Catalonia, Spain.
3. Laboratory of Semiconductor Materials, Institute of Materials & Institute of Physics EPFL, Lausanne, Switzerland
4. Center for Analysis and Synthesis and NanoLund, Lund University, Box 124, 221 00 Lund, Sweden
5. ICREA, Pg Lluis Companys 23, 08010 Barcelona, Catalonia, Spain.

Nowadays, the need of clean energy and smart electronic accessories rose research attention towards nanostructured photovoltaics panel that can be easily implemented in our everyday life. In this scenario zinc phosphide (Zn3P2) is an ideal candidate thanks to its direct bandgap, earth-abundance, and optoelectronic characteristics, although it has not been widely investigated due to limitations in the fabrication of high-quality material. It is possible to overcome these factors by growing the material into nanoscale objects, exploiting the selected area epitaxy approach (SAE), opening up new elastic strain relaxation mechanisms and minimizing the interface area [1].

Here we present our latest results for Zn3P2 nanowire-like structures grown on different substrate, including InP and Si, via Molecular Beam Epitaxy (MBE) and Metal Organic Chemical Vapor Deposition (MOCVD). Different NW-substrate mutual orientations are presented to obtain a full picture of the main mechanism involved during the growth. By combining scanning transmission electron microscopy in high angle annular dark field (HAADF-STEM) mode, with modelling and simulation we could recognize the presence of rotated crystal domains coexisting in the same nanowire structure. We deeply investigated these defects' structure to address their formation mechanism and potential role on the electronic properties in the final PV device [2]. These results represent a breakthrough for the utilization of earth-abundant compound for sustainable PV technology, evidencing the high potential of SAE approach for the growth of high-quality material.

References

1. S. Escobar Steinvall et al. Nanoscale Advances, 3, 326 (2020).

2. M. C. Spadaro, S. Escobar Steinvall et al. Nanoscale, 13, 18441-18450 (2021).

Structural and Luminescent Characterization of Eu-Doped BaF_2 Thin Films Deposited via MOCVDù

Francesca Lo Presti[1], Anna Lucia Pellegrino[1], Emil Milan[2], Eros Radicchi[2], Adolfo Speghini[2], and Graziella Malandrino[1]*

1.Dipartimento di Scienze Chimiche, Università di Catania and INSTM UdR Catania V.le A. Doria 6, 95125 Catania Italy.
2. Nanomaterials Research Group, Dipartimento di Biotecnologie, Università di Verona and INSTM UdR Verona, Strada le Grazie 15, 37134 Verona, Italy.
*E-mail: graziella.malandrino@unict.it

In recent years, there has been a pronounced push toward the development of advanced functional materials, driven by the necessity to enhance the efficiency of photovoltaic (PV) devices while optimizing the exploitation of solar radiation [1]. An innovative strategy to improve PV system performance refers to the conversion of photons with energies beyond the absorption capabilities of conventional photoactive materials, such as silicon, into a more favorable optical region. Within this context, lanthanide (Ln)-doped fluoride materials have emerged as highly promising candidates for energy conversion (EC) applications due to their distinctive luminescent properties under light irradiation [2,3].

It is know that fluoride compounds serve as superior inorganic hosts for EC processes when compared to alternative inorganic matrices. Among these, BaF_2 has garnered attention as an optimal host for the incorporation of luminescent Ln^{3+} ions. This is attributed to its exceptionally low phonon energy, alongside its high chemical stability, broad transparency range, and versatile synthesis techniques [4]. Furthermore, the lattice matching requirements between the host material and Ln^{3+} dopant ions facilitate the seamless integration of trivalent lanthanides into the crystalline structure of alkaline-earth fluorides due to their similar coordination environments. Nevertheless, the substitution of trivalent Ln dopants for divalent alkaline-earth ions necessitates a charge compensation mechanism to mitigate the resulting charge imbalance. Among the lanthanides, Europium has attracted significant scientific interest, particularly in its +3 oxidation state, owing to its unique chemical and luminescent properties.

This study focuses on the fabrication of Europium-doped BaF_2 thin films via the metalorganic chemical vapor deposition (MOCVD) technique, emphasizing the synthesis process and the downshifting (DS) luminescent properties of these films (refer to the schematic in Figure 1). The preparation of BaF_2 thin films doped with Eu^{3+} involves the utilization of a multicomponent mixture of metalorganic adducts in a carefully controlled molar ratio, employed as a single molten source.

By modulating the composition of the precursor mixture—specifically the Ba:Eu ratio in the multicomponent source—it is possible to precisely adjust the chemical composition of the resulting films and optimize the associated energy transfer processes. Comprehensive structural, morphological, and compositional analyses were conducted using X-ray diffraction (XRD), field-emission scanning electron microscopy (FE-SEM), and energy-dispersive X-ray spectroscopy (EDX). The functional properties of the films were further evaluated through luminescence spectroscopy.

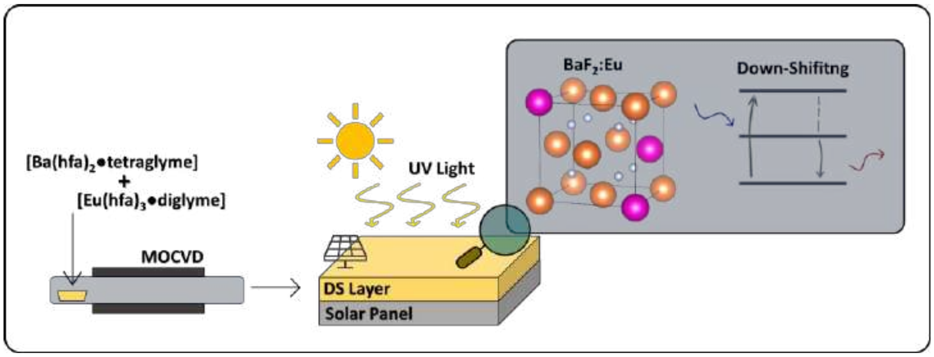
[Ba(hfa)$_2$•tetraglyme]
+
[Eu(hfa)$_3$•diglyme]
MOCVD
UV Light
DS Layer
Solar Panel
BaF$_2$:Eu
Down-Shifitng

Figure 1 : MOCVD approach adopted to produce inorganico Eu-doped inorganic fluoride thin film and study of the downshifting properties.

.

This work has been partially funded by the European Union, through the MUR-PNRR project SAMOTHRACE (ECS00000022).

References

[1] G. W. Crabtree and N. S. Lewis, *Phys. Today*, **60**, 37–42 (2007).
[2] X. Huang, S. Han, W. Huang and X. Liu, *Chem. Soc. Rev.*, **42**, 173–201 (2013).
[3] N. Kumam, L. P. Singh, K. Srivastava and N. R. Singh, *J. Lumin.*, **203**, 59–66 (2018).
[4] R. K. Sharma, S. Nigam, Y. N. Chouryal, S. Nema, S. P. Bera, Y. Bhargava and P. Ghosh, *ACS Appl. Nano Mater.*, **2**, 927–936 (2019).

Hight throughput solution towards roll-to-roll S-ALD coatings for packaging , batteries and flexible PV applications

A. Ghazy[1], D. Spee[1]
[1]Kalpana Systems, Rotterdam, the Netherlands

ALD is currently the state-of-the-art thin film fabrication technology. While ALD has built a well-established reputation in the semiconductor industry and crystalline silicon solar cell, it is currently being researched for several industries, such as batteries, solar cells, and optoelectronics .[1] However, the long processing times in temporal ALD presents a serious hinderance to adoption of ALD in high-throughput industrial applications. This has paved the way for the creation of spatial ALD (S-ALD) with significantly faster processing times.[2] Nevertheless, scaling up ALD to a roll-to-roll (R2R) with high throughput has been so far challenging. As flexible substrates are becoming key to several applications such as batteries, low load-bearing PV and packaging.[3]

Kalpana Systems has developed equipment (K300) that aims to fill this gap in the industrial applications of ALD. Combining a 3D answer to the question of how to increase the substrate speed while maintaining the precursor separation, Thus, achieving a high throughput S-ALD solution for coating flexible substrates. In this work, we will show the initial results of our equipment in ALD process development, on various substrates. We will also present the potential of K300 towards various applications such as coating battery electrodes for enhancing battery performance, or production of barrier layers for packaging materials and flexible PV applications.

References

[1] V. Zardetto *et al.*, "Atomic layer deposition for perovskite solar cells: Research status, opportunities and challenges," *Sustainable Energy and Fuels*, vol. 1, no. 1. Royal Society of Chemistry, pp. 30–55, Mar. 01, 2017. doi: 10.1039/c6se00076b.

[2] P. Poodt *et al.*, "Spatial atomic layer deposition: A route towards further industrialization of atomic layer deposition," *J. Vac. Sci. Technol. A Vacuum, Surfaces, Film.*, vol. 30, no. 1, Jan. 2012, doi: 10.1116/1.3670745/100584.

[3] K. Ali, K. H. Choi, and N. M. Muhammad, "Roll-to-Roll Atmospheric Atomic Layer Deposition of Al2O3 Thin Films on PET Substrates," *Chem. Vap. Depos.*, vol. 20, no. 10-11–12, pp. 380–387, Dec. 2014, doi: 10.1002/CVDE.201407126.

Study of gas diffusion mechanisms within ALD and SALD (Spatial ALD) thin films for the encapsulation of perovskite-based photovoltaic cells.

Aubin Parmentier[1,2], Damien Coutancier[1], Stéphane Cros[3], Timéa Bejat[3], Marc Fivel[4], José Alvarez[1], Jean-Paul Kleider[1], David Muñoz-Rojas[2], Nathanaelle Schneider[1]

[1]Institut Photovoltaïque d'Île de France (IPVF), UMR CNRS 9006, 91120 Palaiseau, France
[2]Université Grenoble Alpes, CNRS, Grenoble INP, LMGP, 38000 Grenoble, France
[3]Univ. Grenoble Alpes, CEA, Liten, INES, 73375 Le Bourget du Lac, France
[4]Univ. Grenoble Alpes, CNRS, Grenoble INP, SIMAP, 38000 Grenoble, France.
e-mail: aubin.parmentier@cnrs.fr

In the context of decarbonization of energy production, new types of photovoltaic solar cells are elaborated to achieve higher power conversion efficiencies at lower manufacturing costs. Perovskites based solar cells (PSC) are one of the most promising technologies currently, in particular tandem silicon-perovskite cells that have reached 33.9 % efficiency compared to current standard silicon-based cells at 27.6 % [1]. However, those new architectures come with new challenges: for example, perovskite materials are highly sensitive to humidity permeation, which severely limits their long-term stability. One possible solution to protect them from that extrinsic degradation is the use of efficient encapsulation layers [2].

Thin Film Encapsulation (TFE) is a powerful method to meet the encapsulation needs of perovskite-based cells, namely, i) to achieve WVTRs (physical quantity, Water Vapor Transmission Rate, used to quantify barrier properties [3]) values between 10^{-4} and $10^{-6}\ g.m^{-2}.d^{-1}$ [4]; ii) to offer laminated films with high flexibility (Young's modulus $\leq 20\ MPa$ at 25 °C [4]); and iii) to ensure good light transmission between 400 and 1100 nm (> 80% [4]). In addition, due to the sensitivity of PSC, encapsulation solutions must be elaborated under soft conditions (deposition temperature $\leq$ 100 °C). Among the various thin film deposition methods available, Atomic Layer Deposition (ALD) is an attractive technique since it enables the deposition of uniform and dense [5] thin films of controlled thickness (nm-scale), with low pinhole defect densities and at low temperature ($\leq$ 100 °C) thus avoiding damage to the perovskite materials [6].

In fact, one of the most important factors in guaranteeing optimum resistance to gas permeation is a low density of voids of other defects such as cracks, which are preferential permeation paths, and small diameter defects. Void defects within thin films can be linked to the detachment of particles initially present on the substrate, or to pinholes inherent to the morphology of the layer, this latter resulting from the growth mechanism.

These explain the large efforts, from both academia and industry to produce nanolaminated films composed of multilayers that allow pinholes to be misaligned, thereby lengthening the diffusion paths of gaseous species within the films [7].

Thus, inorganic or organic-inorganic hybrid nanolaminate structures synthesized by ALD have been made, with WVTRs reaching values close to $10^{-6}\ g.m^{-2}.d^{-1}$ [6]. Concerning the nature of the nanolaminates, there are many candidate materials, most of which are metal oxides (e.g. Al_2O_3, TiO_2). They are often combined in nanolaminate structures with their "metalcones" counterparts, which are organic-inorganic hybrid materials typically synthesized by ALD-MLD (ALD-Molecular Layer Deposition) using metal precursors and various organic coreactants that yield metal alkoxide films [8]. For this reason, ALD is the method of choice for nanolaminates: thanks to the precise thickness control it provides, any multilayer structure can be envisaged. This makes the determination of an optimal structure achievable at the cost of an almost infinite number of possibilities.

In this study, we first screened metal oxides and hybrid materials - such as alucones deposited by ALD from trimethylaluminium (TMA) and ethylene glycol (EG) - gas permeation resistance properties using helium permeation measurements which are less time-consuming than water permeation measurements. Establishing the Barrier Improvement Factor (BIF) - described as the ratio between the Helium Transmission Rates (HeTRs) of the substrate and the thin film, makes it possible to select the best candidates for integration into nanolaminated multilayers effective against gas permeation (classification shown in *Figure 1*). Then, we propose to study the role of the different types of void defects existing within encapsulating films which are due to initial particulate contamination (large-diameter) or inherent to growth pinholes (little-diameter) with optical microscopy techniques and electrical atomic force microscopy (AFM) methods.

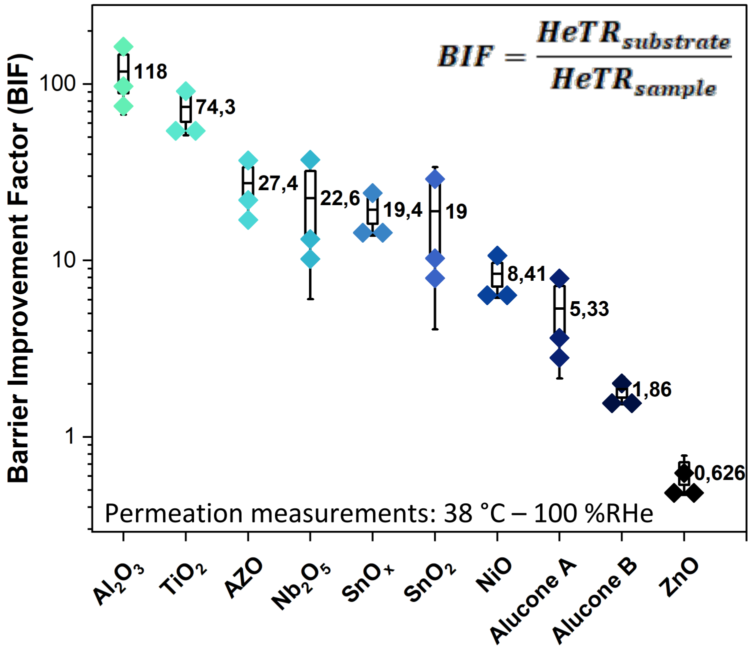

Fig. 1. Helium BIF of several ALD-materials of 15 nm deposited at 100 °C.

This work was supported by the French National Research Agency (ANR) via the project SMART4MODULE (ANR-22-PETA-0006).

References

[1] NREL Cell-Efficiency Page. https://www.nrel.gov/pv/cell-efficiency.html (accessed 2024-12-12).
[2] Jeong. E. G. et al, *Journal of Information Display*, **21** (1), 19-32 (2020).
[3] Crank, J., *The Mathematics of Diffusion*, Clarendon Press, Oxford (1975).
[4] Xiang, Ling et al, *Organic Electronics*, **106**, 106515 (2022).
[5] Gupta, B. et al, *Advanced Functional Materials*, **32** (3), 2109105 (2022).
[6] Ramos, F. J. et al, *Sustainable Energy Fuels*, **2** (11), 2468–2479 (2018).
[7] Yun Li et al, *Journal of Materials Research*, **35** (7), 681-700 (2020).
[8] Wang, L. et al, *J. Mater. Chem. C*, **5** (16), 4017–4024 (2017).

Session PM_2.4 INNOVATIVE PLASMA ASSISTED PROCESSES

Tuesday 3rd June 2025 | 16.30-17.30

Chair: **Maria Losurdo** | Room “Coro di Notte”

Strategy to produce boron-containing ALD thin films using a combined plasma approach

A. Dhara[1], A. Werbrouck[1], J. Li[1] , T. Verhelle[1], M. Minjauw[1], J. Meersschaut[2], L. Henderick[1], J. Dendooven[1], C. Detavernier[1,*]
[1]CoCooN Research Group, Department of Solid State Sciences, Ghent University, Belgium
[2]Imec, Leuven, Belgium
e-mail: Christophe.detavernier@ugent.be

Atomic layer deposition of boron-containing thin films holds potential for various applications, such as semiconductor doping, neutron detection and protective coatings for lithium-ion batteries. Despite the availability of highly volatile precursors, such as trimethylborate (TMB), the boron incorporation is often insufficient due to the precursor's low reactivity. [1] In this work, we demonstrate different ALD strategies to deposit aluminum borate with TMB as the boron source (Fig. 1a).

First, a thermal ALD process (TMA – H_2O – TMB – H_2O) demonstrated a growth rate of 1.4 Å/cycle (Fig. 1b). The process required long TMB exposures and still could not reach full saturation. This process resulted in only 4 at.% B incorporation with significant C (2.5 at.%) and H (>10 at.%) impurities. An O_2 plasma-assisted process (TMA–O_2*–TMB–O_2*) resulted in a growth rate of 1.8 Å/cycle (Fig. 1b) and achieved a slightly higher B incorporation of 6 at.%. Moreover, it reduced C impurities to below 1 at.%, although H impurities remained above 5 at.%. Despite these advances, the B incorporation remains insufficient, underscoring the need for a more effective approach.

A similar challenge has been observed for ALD of phosphates, where our group has addressed this issue using trimethylphosphate (TMP) plasma. [2] This approach relied on in-situ polymerization of the TMP molecule, leading to a significantly larger phosphorus incorporation and improved growth rates.

Inspired by this success, we explored a similar strategy for TMB. Dosing only TMB plasma (without other reactant) resulted in non-self-limiting growth across the wide range of substrate temperatures studied (Fig. 2a). When co-dosing H_2O during the plasma, self-limiting growth could be obtained from 250°C onwards (Fig. 2b). We hypothesize that TMB undergoes a similar polymerization during the plasma as the TMP molecule. In absence of H_2O, the polymerized species keep accumulating on the surface, resulting in the observed continuous growth. In combination with H_2O, the available OH radicals present in the plasma can assist in hydrolysing surface groups and thereby terminate the polymerization process. The resulting combined plasma approach (TMA – (TMB + H_2O)* - H_2O*) achieved a growth rate of 3.4 Å/cycle and an increased B incorporation of 7.7 at.%, while reducing C and H impurities to below 1 at.% and 5 at.%, respectively.

The combined plasma approach not only overcomes the challenges of low boron incorporation but also results in thin films of higher quality. Through in-vacuo XPS and in-situ transient mass spectrometry, we propose a detailed reaction mechanism underlying this process (Fig. 3). Our findings demonstrate that this strategy is a promising route to deposit boron-containing thin films with enhanced incorporation and minimal impurities, opening new possibilities for advanced ALD applications.

[1] Mattelaer F., *Chem. Mater.*, **32**, 4152–4165 (2020)
[2] Dobbelaere T., *Chem. Mater.*, **26**, 6863–6871 (2014)

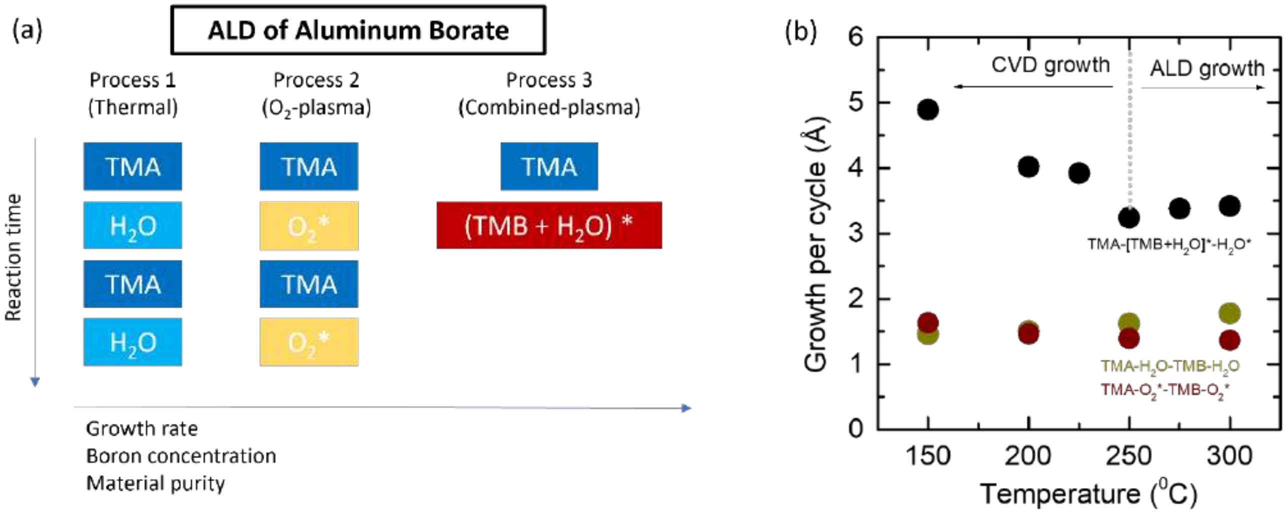

Fig 2: (a) Different ALD strategies to deposit aluminum borate studied in this work. (b) Growth per cycle of the different ALD processes against substrate temperature.

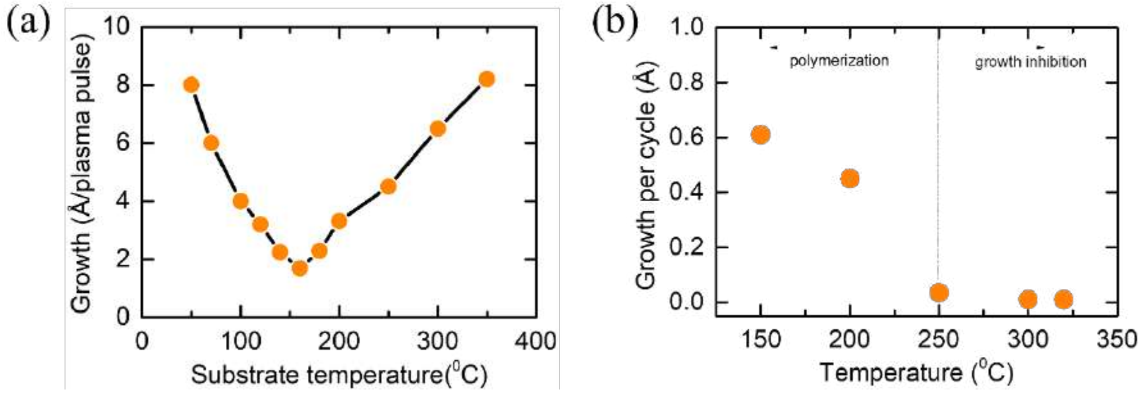

Fig 1: Growth vs substrate T for a 10s (a) TMB plasma and (b) combined (TMB + H_2O) plasma pulse.

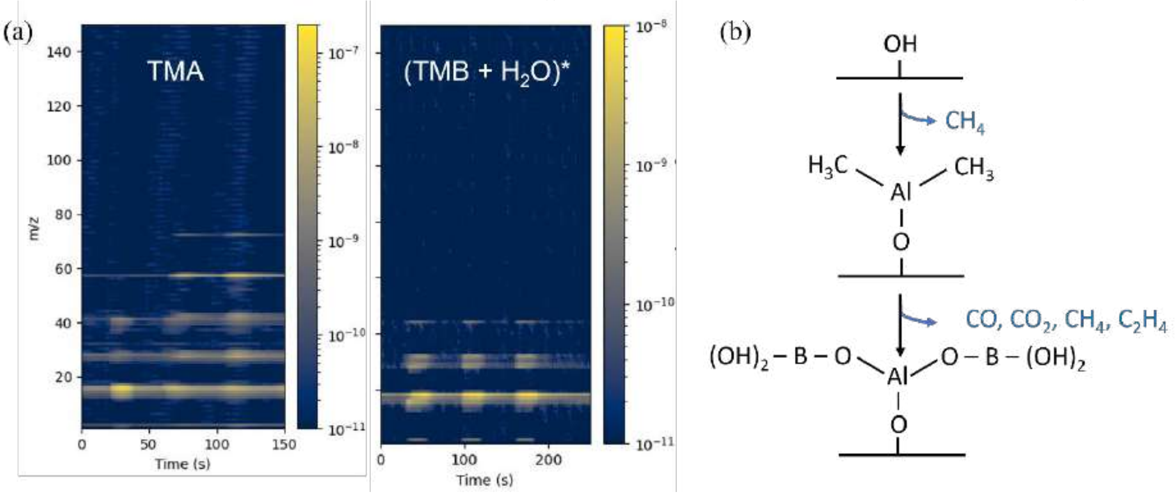

Fig 3: (a) In-situ mass spectrometry data recorded during a TMA - (TMB + H_2O)* process. (b) Proposed reaction mechanism.

Controlled growth of nanostructured NiO by plasma assisted-chemical vapor deposition

C. Maccato[1,2*], **E. Scattolin**[1], **D. Barreca**[2], **A. Gasparotto**[1,2], **L. Signorin**[1],
N. El Habra[2], **A. Šuligoj**[3,4], **U. Lavrenčič Štangar,**[4] **G. A. Rizzi**[1,2]
[1]Department of Chemical Sciences, Padova University and INSTM, 35131 Padova, Italy
[2]CNR-ICMATE and INSTM, 35127 Padova, Italy
[3]National Institute of Chemistry, Ljubljana SI-1000, Slovenia
[4]Faculty of Chemistry and Chemical Technology, University of Ljubljana, Ljubljana SI-1000, Slovenia.
* e-mail: chiara.maccato@unipd.it

Nanomaterials based on NiO, a multi-functional *p*-type semiconductor, have been the focus of various studies thanks to their use in a broad range of applicative fields, ranging from electrochromic devices, solar cells, and heterogeneous catalysts for the removal of organic pollutants from wastewaters. In addition, NiO systems stand as attractive option for protection against corrosion, offering also self-cleaning, anti-fouling, and frost-prevention characteristics [1,2].

The present study reports on an original plasma assisted vapor phase route for the growth of supported NiO nanostructures on conductive glasses (fluorine-doped tin oxide, FTO), in which $Ni(tfa)_2TMEDA$; [tfa = 1,1,1-trifluoro-2,4-pentanedionate; TMEDA = *N,N,N',N'*-tetramethylethylenediamine) [3] was used for the first time as a molecular precursor. The target systems have been fabricated at a growth temperature of 100°C, the lowest ever reported in analogous processes, at different deposition times [2].

The unique plasma activation mechanisms resulted in the obtainment of phase-pure nickel(II) oxide nanostructures endowed with an inherent oxygen defectivity, whose properties, with particular regard to their actual morphology, could be modulated by simple variations of the sole process duration as testified by field emission-scanning electron microscopy (FE-SEM) analyses (Fig. 1). In particular, tailoring of grain dimensions and deposit thickness directly affect material properties not only in terms of NiO wetting behavior, but also its photodegradation efficiency towards aqueous diclofenac {DCF; 2-[2-(2,6-dichloroanilino)phenyl]acetic acid}, a persistent pharmaceutical pollutant, whose removal has never been reported so far by NiO materials.

This work demonstrates an attractive preparation route to NiO nanostructures with modular properties, that can be extended even to thermally labile substrates. The system surface hydrophobicity can be eventually exploited for the obtainment of catalysts with improved activity and selectivity, and the flexible control over thickness and morphology paves the way to additional (photo)catalytic applications, including water splitting to yield green hydrogen.

References

[1] M. Benedet, C. Maccato, G. Pagot, C. Invernizzi, C. Sada, V. Di Noto, G.A. Rizzi, E. Fois, G. Tabacchi, and D. Barreca, *J. Phys. Chem. C*, **127**, 22304 (2023).

[2] D. Barreca, E. Scattolin, C. Maccato, A. Gasparotto, L. Signorin, N. El Habra, A. Šuligoj, U. Lavrenčič Štangar, G. A. Rizzi, *ChemComm* (2025) - https://doi.org/10.1039/d4cc06548d.

[3] M. Benedet, D. Barreca, E. Fois, R. Seraglia, G. Tabacchi, M. Roverso, G. Pagot, C. Invernizzi, A. Gasparotto, A.A. Heidecker, A. Pöthig, E. Callone, S. Dirè, S. Bogialli, V. Di Noto, and C. Maccato, *Dalton Trans.*, **52**, 10677 (2023).

The present work was financially supported by CNR (Progetti di Ricerca @CNR—avviso 2020—ASSIST), Padova University (P-DiSC#02BIRD2023-UNIPD RIGENERA), INSTM Consortium (TRI.25/013-CIMENTO), and PRIN 2022474YE8 (SCI-TROPHY project).

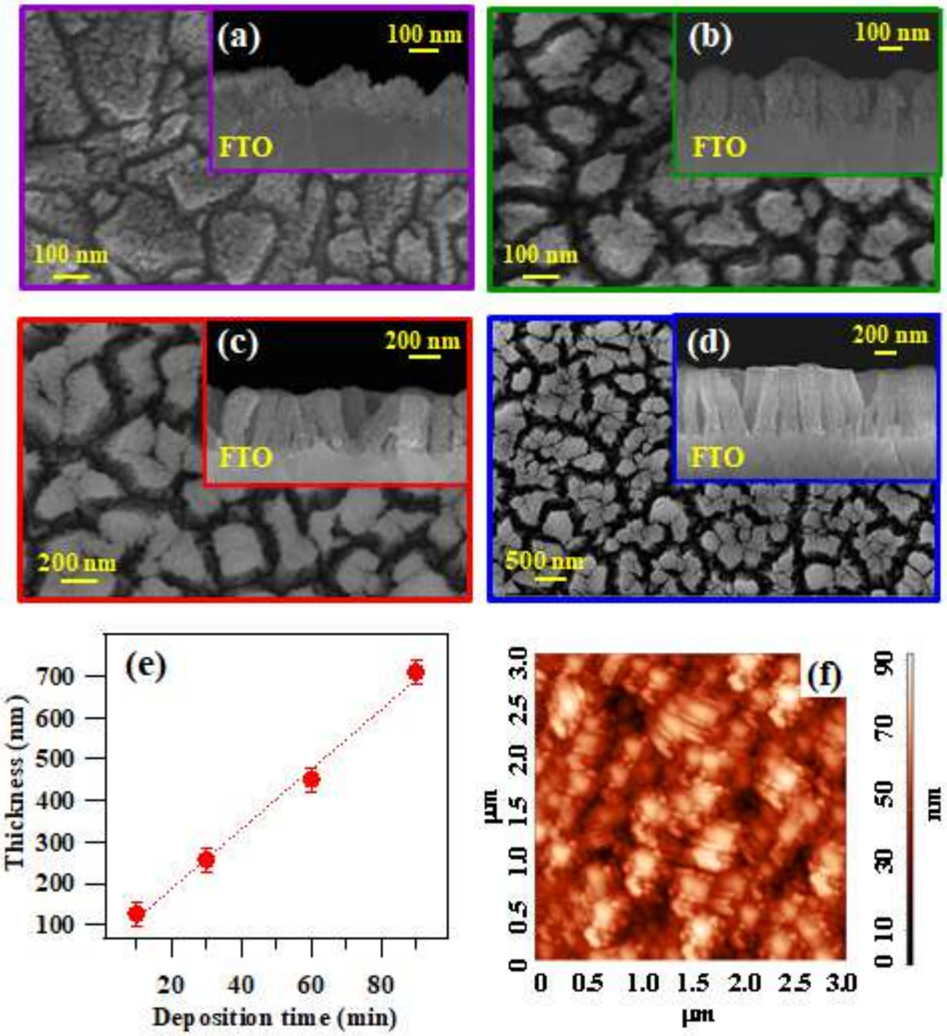
(a)
100 nm
FTO
100 nm
(b)
100 nm
FTO
100 nm
(c)
200 nm
FTO
200 nm
(d)
200 nm
FTO
500 nm
(e)
Thickness (nm)
100
200
300
400
500
600
700
20
40
60
80
Deposition time (min)
(f)
μm
0
0.5
1.0
1.5
2.0
2.5
3.0
0
0.5
1.0
1.5
2.0
2.5
3.0
μm
0
10
30
50
70
90
nm

Fig. 1. Representative plane-view and cross-sectional (inset) FE-SEM micrographgs for NiO specimens supported on FTO, obtained @: a) 10’; b) 30’, c) 60’; d) 90’. (e) Deposit thickness oas a function of deposition time. (f) AFM micrograph for a NiO specimen obtained for 10 min (root-mean-square roughness ≈ 16 nm).

Tailored waveform biasing for precise ion-energy control during plasma-enhanced ALD of AlN

A.A. de Jong[1], **S.A. Peeters**[1], **W.M.M. Kessels**[1], **A.J.M. Mackus**[1]
[1]Eindhoven University of Technology, Department of Applied Physics and Science Education
e-mail: a.a.d.jong@tue.nl

Controlling the ion energy during plasma-enhanced atomic layer deposition (PEALD) allows for tunable material properties such as the refractive index, material composition and crystallinity [1]. The ion energy is traditionally controlled by radiofrequency (RF) biasing at 13.56 MHz. However, this biasing technique results in a broad ion flux energy distribution function (IFEDF) [2]. In the current work, a novel 200 kHz tailored waveform (TW) biasing generator was installed on a commercial PEALD reactor (Fig. 1). By applying TW biasing, narrow IFEDFs were obtained during a N_2-H_2 plasma (Fig. 2). This more precise ion energy control can enable better control over the material properties. The N_2-H_2 plasma was used as coreactant for AlN PEALD at 350°C using trimethylaluminum (TMA) as the precursor.

The growth per cycle (GPC) and refractive index of AlN after 500 PEALD cycles as function of the ion energy are shown in Fig. 3A. The GPC decreased slightly when enhancing the ion energy, and increases again for higher ion energies. A significant improvement in refractive index was observed at the intermediate ion energies, while a low index was obtained for higher ion energies. The O contamination as determined by X-ray photoelectron spectroscopy is shown in Fig. 3B. By using TW biasing, the O contamination was decreased from 6.4 to 3.5 at.% if ion energies larger than 36 eV were used. The crystallinity was investigated using grazing-incidence X-ray diffraction (Fig. 3C) and it only changes for ion energies larger than 36 eV. At intermediate ion energies, a notable peak shift is observed, suggesting an enhanced compressive stress. Higher ion energies eventually result in a reduction of the crystalline signal. Such behaviour of the material properties as function of the ion energy is typically also observed when applying the established RF biasing, indicating the validity of TW biasing for ion energy control during PEALD.

The aforementioned results suggest the existence of ion energy thresholds between 36 and 55 eV for reducing the O contamination and altering the crystallinity of AlN. Meanwhile, the threshold for activating mechanisms increasing the refractive index is lower. The narrower IFEDFs from TW biasing are beneficial for investigating ion energy thresholds for modifying material properties during plasma-enhanced deposition. These narrow IFEDFs can be controlled to be precisely in between such thresholds. Thereby, TW biasing can enable the deposition of thin films with accurately tailored material properties.

This work was supported by the European Research Council and the Netherlands Organization for Scientific Research NWO.

References

[1] K. Arts, S. Hamaguchi, T. Ito, K. Karahashi, H. C. M. Knoops, A. J. M. Mackus, W. M. M. Kessels*,* *Plasma Sources Sci Technol*, **31**, 103002 (2022).
[2] T. Faraz, Y. G. P. Verstappen, M. A. Verheijen, N. J. Chittock, J. E. Lopez, E. Heijdra, W. J. H. van Gennip, W. M. M. Kessels, A. J. M. Mackus, *J Appl Phys*, **31**, 213301 (2020).

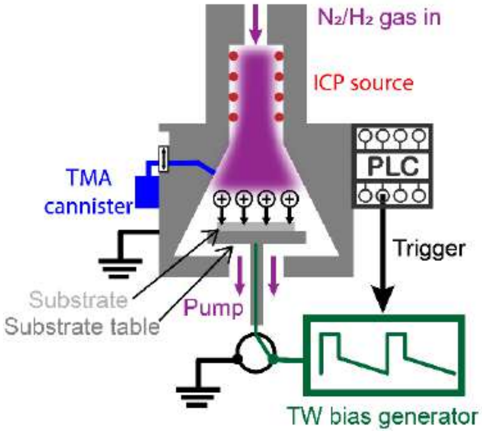
N₂/H₂ gas in
ICP source
TMA cannister
PLC
Trigger
Substrate
Substrate table
Pump
TW bias generator

Fig. 1. Schematic of the ALD reactor equipped with a remote inductively coupled plasma and a tailored waveform (TW) biasing generator.

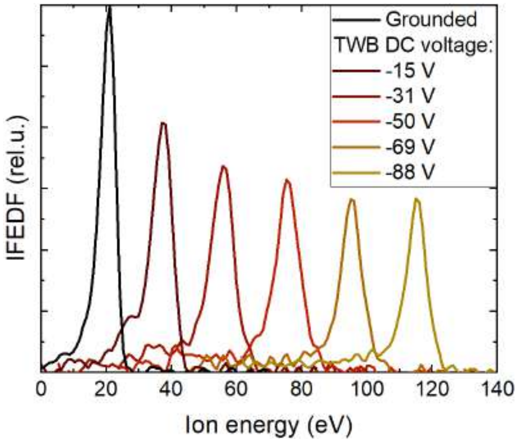

Fig. 2: Ion flux energy distribution functions of the N_2-H_2 plasma for a grounded substrate and various TW biasing settings.

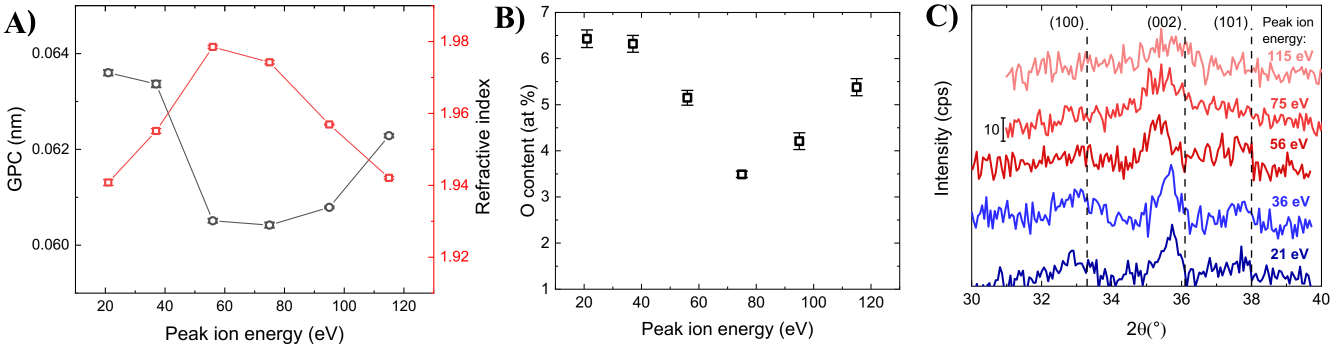

Fig. 3. Material properties of AlN deposited using various peak ion energies controlled by TW biasing: A) GPC and refractive index as determined by ex-situ spectroscopic ellipsometry. The refractive index can be increased using very low ion energies. B) The oxygen contamination obtained from X-ray photoelectron spectroscopy reveals that ion energies larger than 36 eV are required to decrease the oxygen contamination. C) Grazing incidence x-ray diffraction spectra of AlN, including expected peak positions. The induction of more stress and eventually amorphization occurs for ion energies larger than 36 eV.

Protection of Transparent Electrodes based on metallic nanowires by nitrides deposited by Plasma-Enhanced ALD

Ma. Del Mar Rodriguez[1, *], **Alexandre Crisci**[1], **Marc Fivel**[1], **David Muñoz-Rojas**[3], **Arnaud Mantoux**[1], **Marceline Bonvalot**[2], **Daniel Bellet**[3], **Elisabeth Blanquet**[1]
[1]Univ. Grenoble Alpes, CNRS, Grenoble INP, SIMaP, 38000 Grenoble, France
[2]Univ. Grenoble Alpes, CNRS, LTM, 38000 Grenoble, France
[3]Univ. Grenoble Alpes, b CNRS, Grenoble INP, LMGP, 38000 Grenoble, France
e-mail : maria-del-mar.rodriguez-robles@grenoble-inp.fr

Transparent electrodes (TEs) are critical components of many devices in daily life, such as displays, wearable electronics, solar cells, sensors, light-emitting diodes, and many more [1]. They consist of a transparent conductive material (TCM) deposited on a transparent substrate; the main requirement is to exhibit a high optical transmittance and a low sheet resistance. Other essential features like stability, flexibility, uniformity, and cost-effectiveness must be considered. The most studied and used TCM in the last four decades is indium tin oxide (ITO), an n-type semiconductor with 80 % transparency in the visible range and low electrical resistivity (~10^{-4} Ω·m) [2], nevertheless, its ceramic nature and scarcity in the Earth's crust have driven an ongoing race to develop alternative ITO-free TEs for the next generation of flexible electronic devices. In response to this scenario, silver nanowires (AgNWs) assembled within a percolation network are a promising contestant, not only because their physical performance is nearly comparable to ITO but also due to their high mechanical flexibility and compatibility with cost-effective solution-based techniques. However, their performance and integration into devices are limited by their morphological instability caused by the high surface effects [3].

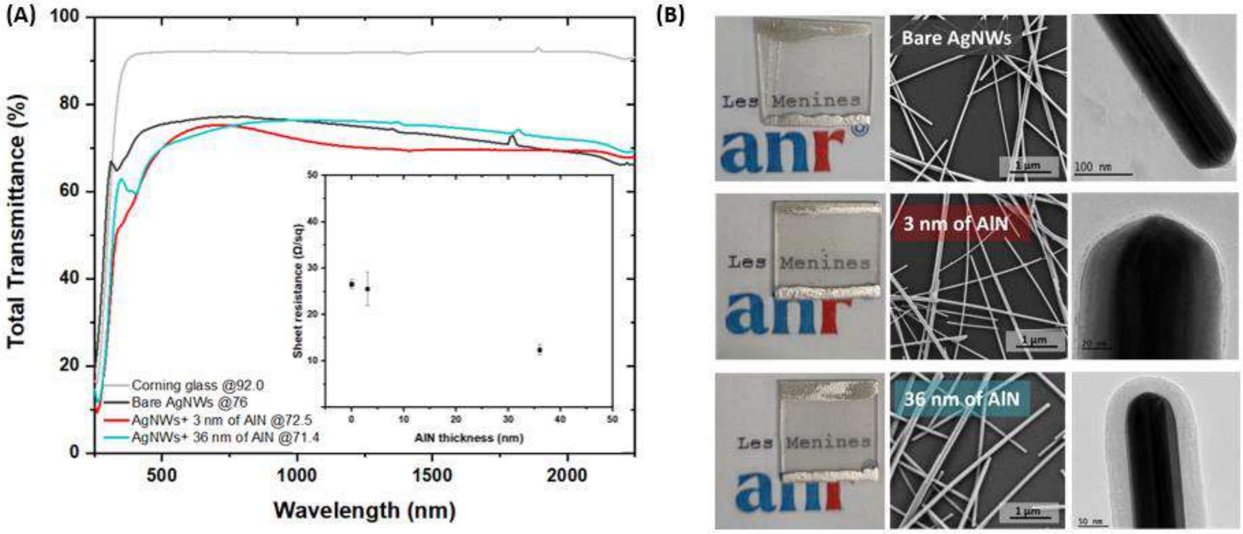

Fig. 1. (A) Total transmittance (with substrate contribution) in UV-visible-NIR region of the bare and AlN-coated AgNW networks. The inset corresponds to the sheet resistance vs the AlN thickness. (B) Photograph, SEM and TEM of the TEs based on bare and AlN- coated AgNWs (from left to right).

In a previous work, we have investigated the possibility of coating such Ag nanowires with a robust and stable AlN diffusion barrier by Plasma-Enhanced ALD (PEALD) at 250 °C [4] to prevent the reaction of silver atoms with the environment and their surface diffusion. The current work intends to continue the research at a lower deposition temperature (200°C) and higher growth per cycle (GPC) for a cost-effective approach. The temperature and plasma power were optimized to obtain a GPC of 0.08 nm/cycle for a (TMA/purge/NH_3 plasma/ purge) pulse sequence, while the work presented in [4] uses H_2 plasma and subsequent exposure of NH_3 (TMA/purge/H_2 plasma/purge/NH_3/purge) with a GPC of 0.05 nm/cycle.

The results show that an optimal coating thickness of 3 nm of AlN can resist thermal stress up to 400 °C and electrical stress of 11 V, while the bare nanowires present an irreversible morphological change after 300 °C and 6 V respectively. Regarding the adhesion to the substrate, the bare ones can be easily removed with a force of only 10 mN, in comparison the coated ones remain in the glass substrate even after an applied force of 6 N. Additionally, no optical transmittance loss was exhibited as observed in Fig.1, due to the high optical bandgap of AlN (6.42 Ev), a remarkable asset of this approach.

In addition, AlN was also deposited by Physical Vapor Deposition (PVD) using a similar deposition temperature (180°C) to compare the properties and stability of the AlN-coated AgNWs by using different coating techniques. The thermal and electrical stability performance presents a lower enhancement but is comparable to the one obtained by PEALD; in terms of mechanical stability, the nanowires were still peeled off. This comparison justifies the use of ALD techniques to fabricate a TE with nitride-coated silver nanowire networks to integrate them into transparent heaters or low-emissivity coatings.

This work was supported by the Project ANR-23-CE51-0038 of the French National Research Agency (ANR).

References:

[1] Nguyen, Viet Huong, et al., *Small*, **18.19,** 2106006 (2022).
[2] Papanastasiou, Dorina T., et al., Advanced Functional Materials, **30.21**, 1910225 (2020).
[3] Morales‐Masis, Monica, et al., Advanced Electronic Materials, **3.5**, 1600529 (2017).
[4] Papanastasiou, Dorina T., et al., ACS Applied Nano Materials (2024).

Session AM_3.1 INNOVATIVE PROCESSES: SALD AND AREA-SELECTIVE DEPOSITION

Wednesday 4th June 2025 | 8.30-10.30

Chair: **Maarit Karppinen** | Main Hall “Santo Mazzarino”

New processes for the Spatial Atomic Layer Deposition (SALD) of functional materials

David Muñoz-Rojas
Univ. Grenoble Alpes, CNRS, Grenoble INP, LMGP, 38000 Grenoble, France
e-mail : david.munoz-rojas@grenoble-inp.fr

Spatial Atomic Layer Deposition is a variant of ALD offering the same unique assets but at deposition rates up to two orders of magnitude faster, thus being more appealing for industrial mass production. This is achieved by having a continuous injection of precursors in different regions of the reactor separated by inert gas regions. SALD can be performed using many different engineering approaches and both at low and atmospheric pressure, and even in the open air, i.e. without the need of a deposition chamber, when using close proximity manifold approaches. While common ALD precursors are in principle suitable for SALD, when working at atmospheric pressure, some precursors may lack sufficient volatility or stability. Additionally, in the case of open-air approaches the use of highly-reactive, pyrophoric or highly-toxic precursors can seriously jeopardize the transfer of SALD processes form lab to fab.
In my talk I will provide a brief introduction to our close proximity SALD approach and our activities. I will then present in detail several examples of successful SALD processes achieved using alternative precursors. Finally, I will show how laser processing can be used to tune the transport properties of the deposited films.

This work was supported by the ANR/DFG project REACTIVE (ANR-21-CE08-0047; DFG-490773082) and EU project SPRINT (H2020-FETOPEN 801464), the Spanish MCIN/AEI/10.13039/501100011033 (project PID2020-113034RB-I00) and from the Gobierno de Aragn (research group T54_23R)

References

[1] A. Author, B. Author, and C. Author*, Journal*, **Volume**, Page (Year).
[2] A. Author, *Title of Book*, Publisher, City (Year).
[3] A. Author and B. Author, *Conference,* Dates, City, Country, Page (Year).

Recent Advances for Spatial Atomic Layer Deposition Process: Microreactor Direct Atomic Layer Processing (μDALP™)

Maksym Plakhotnyuk [a,*], Atilla C. Varga,[a] Ivan Kundrata [a] and Julien Bachmann [a,b]

[a] ATLANT 3D, Taastrup, Denmark

[b] Friedrich-Alexander Universität Erlangen-Nürnberg, Germany

*mp@atlant3d.com

Topic AM2 or AS3:

In parallel to additive manufacturing leading the revolution in traditional manufacturing, the same principles can revolutionize traditional thin film deposition techniques. Where lithography and vapor phase deposition techniques struggle, for example, with rapid iterations for prototyping or incompatibility with the used chemistry, additive manufacturing can shine. Indeed, several approaches are in development for 3D nanopriting[1,2,3].

Atomic Layer Deposition, and in more general Atomic Layer Processing, offers a unique opportunity for localized 3D processing/printing due to its two-step process. While simple in theory, due to well-developed examples of Spatial Atomic Layer Deposition (SALD), in practice miniturization of SALD requires substantial effort into the creation of suitable micro-nozzles. Uniquely, ATLANT 3D has developed proprietary Spatial ALD micronozzles, naming the process microreactor Direct Atomic Layer Processing - μDALP™.

In recent years, the team at ATLANT 3D has been able to significantly develop the technology to reduce the μDALP™ resolution, increase material capabilities, assessable morphologies, and new instruments. Giving one example of recent development in morphologies; films deposited with μDALP™ have conformal coverage of gratings, microchannels and trenches up to a depth of 25 μm using a Platinum deposition process (**Figure 1**). Substrates with a surface roughness including Carbon nanograss (**Figure 2**), black silicon and anodized Aluminum Oxide membranes were also conformally coated with roughness up to an aspect ratio of 1:25 again with Platinum and TiO_2. Our results demonstrate how a given ALD material process (in this case, Pt and TiO_2) can be used with ATLANT 3D technology to deposit localized area conformal coatings of complex surfaces with an aspect ratio of 1:25. The μDALP™ technology enables rapid prototyping and manufacturing for an array of applications from sensors (temperature, pressure, gas sensing and capacitive) to optics, all with sensitivities that meet or exceed those of devices made using conventional vapor phase deposition techniques.[4] In addition, rapid localized processing facilitated by ATLANT 3D technology of such devices enables design innovation and optimization not possible with other thin film deposition techniques and lithography.

[1] Kundrata I. et al., *ALD/ALE 2022 [Int. Conf.],* **2022**
[2] de la Huerta C. A. M. et al., *arXiv*, **2020**, 0523.
[3] Winkler, R. et al., *J. Appl. Phys.*, **2019**, *125*, 210901
[4] Kundrata I., et al., *Small Methods.*, **2022**, *6* ***(5)***, 2101546

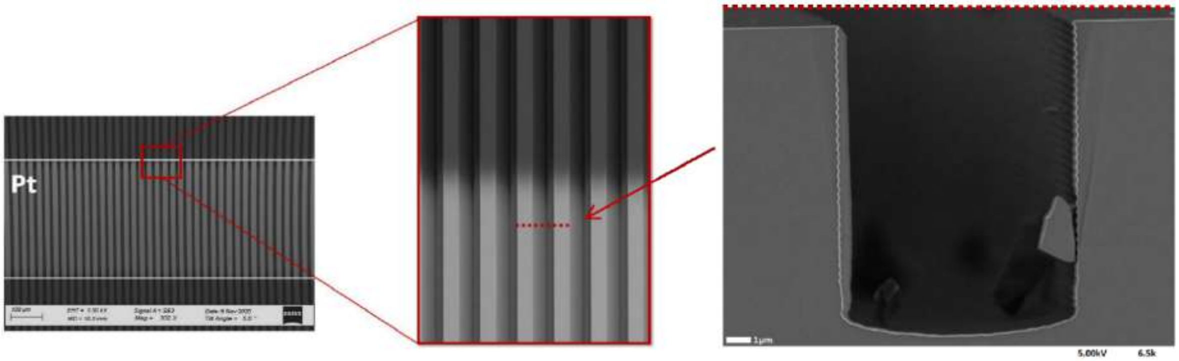
Pt
1µm
5.00kV
6.5k

Figure 1. SEM images of conformal deposition of Pt on 20 μm wide, 15 μm deep Silicon microchannels using μDALP™. Aspect ratio of 1:25.

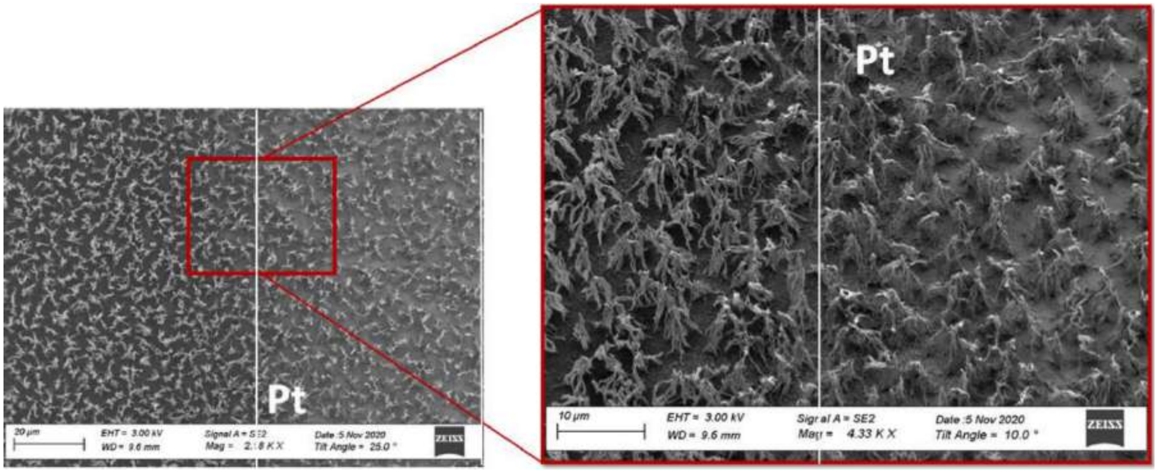
Pt
20 µm
EHT = 3.00 kV
WD = 9.6 mm
Signal A = SE2
Mag = 2.18 K X
Date :5 Nov 2020
Tilt Angle = 25.0 °
Pt
10 µm
EHT = 3.00 kV
WD = 9.6 mm
Signal A = SE2
Mag = 4.33 K X
Date :5 Nov 2020
Tilt Angle = 10.0 °

Figure. 2. SEM images showing the edge of deposited Pt line using μDALP™ showing conformally coated Carbon nanograss with an aspect ratio of 1:10.

Towards Low Temperature Spatial Atomic Layer Deposition of Moisture Barriers using a Synergystic Co-reactant Dosing Approach

H.W. de Vries[1], **I. Aretz, J. Bolding**[1], **F. Souren**[1]
[1]SALD B.V.
e-mail: hindrik.devries@spatialald.com

High performance moisture barrier coatings have been demonstrated by many groups using vacuum gas phase deposition techniques operated in PVD [1] or PECVD [2] reactors. These moisture barrier are deposited as nano-layers or as dyads [3] consisting of alternating inorganic and organic coatings to reach very low permeabilities. An important challenge in depositing moisture barrier films on polymer substrates is to achieve sufficiently high throughput while maintaining the same barrier functionality. Moreover, it is preferred to process the polymer substrate at low temperatures and remain below the softening point of the polymer substrate.

Here, we deposit Al_2O_3 at 75°C using the atmospheric spatial atomic layer deposition technique. It is well known that below a processing temperature of 100°C the co-reactant dosing of H_2O leads to condensation, or multi-layer physisorption which leads to inferior barrier properties. To some extent the condensation effect can be controlled by significantly reducing the H_2O concentration [4] albeit at the expense of uniformity and throughput.

To deposit Al_2O_3, well below 100°C, O_3 can be used as the co-reactant. Although a high concentration of O_3, up to 13 wt%, can be produced by the ozone generator, it is observed that increasing the deposition speed (or decreasing the exposure time) leads to sub-saturation of the oxidation step. This is attributed to the complex reaction kinetics of O_3 [5-7] compared to the direct ligand exchange reaction in the TMA / H_2O reaction.

Hence, we use a novel solution by co-dosing O_3 and H_2O simultaneously. The co-dosing approach is compatible with atmospheric spatial ALD. The main advantage of this approach is that, at constant exposure time, addition of H_2O to the O_3 results in saturated ALD growth (1 monolayer per cycle) whereas the film growth remains clearly unsaturated using O_3 alone. Films have been characterized on thickness and refractive index using spectroscopic ellipsometry.

To determine the layer quality a series of Al_2O_3 films are deposited on 100 µm PET film. Extrinsic moisture barrier properties are characterized using a Technolox Deltaperm apparatus operated accelerated conditions of 38°C and 90%RH. A solvent penetration test is adopted to assess the pinhole density. We show excellent moisture barrier performance of Al_2O_3 films of 20 nm film thickness having a barrier improvement factor of more than 500, see Fig. 1. The solvent penetration analysis reveals that the permeation of moisture is defect controlled. Thus, in order to further improve the barrier performance of the films, the cleanliness of the substrate and the process environment must be improved. Finally, we hypothesize a mechanism to explain the synergy in the surface chemistry between simultaneous dosing of the co-reactants O_3 and H_2O.

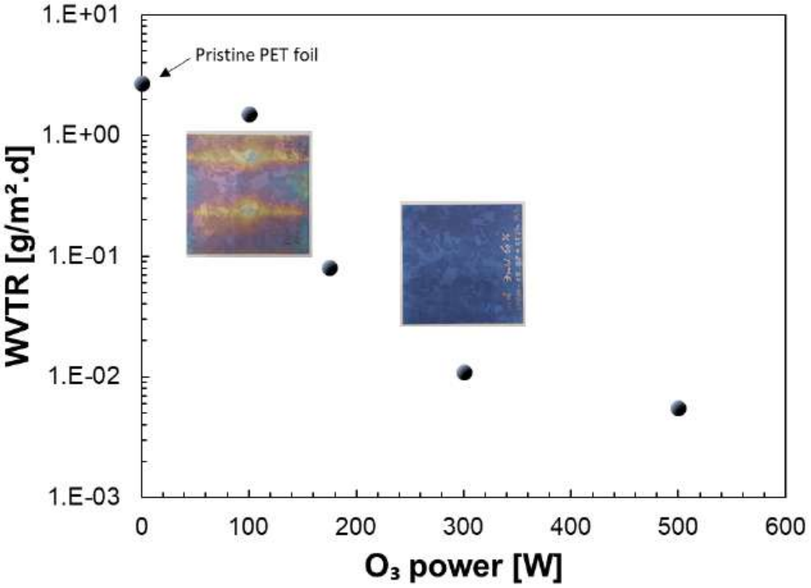

Fig. 1: Water vapour transmission rate (WVTR) as a function of the O_3 power using a constant bubbler flow of 0.5 slm H_2O. At low O_3 power output (100 W) the Al_2O_3 growth is dominated by the H_2O bubbler flow reflected in a non-uniform CVD-like Al_2O_3 coating whereas at higher O_3 concentration (300 W) a uniform ALD-like Al_2O_3 layer is obtained with significantly improved barrier properties.

This work was supported by NEXTGEN HIGHTECH Energy02

References

[1] H. Chatham, *Surface and Coatings Technology* 78, nr. 1: 1-9 (1996).

[2] M. Creatore, M., F. Palumbo, and R. d'Agostino. *Pure and applied chemistry* 74, nr. 3: 407-12 (2002).

[3] J.D. Affinito, S. Eufinger, M. E. Gross, G. L. Graff, and P. M. Martin. *Thin Solid Films* 308 19-25 (1997).

[4] P. Poodt, R. Knaapen, A. Illiberi, F. Roozeboom, and A. van Asten. *Journal of Vacuum Science & Technology A: Vacuum, Surfaces, and Films* 30, nr. 1: 01A142 (2012).

[5] D.N. Goldstein, J.A. McCormick, and S.M. George. *The Journal of Physical Chemistry C* 112, nr. 49: 19530-39 (2008).

[6] V.R. Rai, V. Vandalon, and S. Agarwal. *Langmuir* 28, nr. 1: 350-57 (2012).

[7] J.W. Choi, Y. Min, and K. C. Kim. *Ind. & Eng. Chem. Res.* 61, nr. 27: 9695-9702 (2022).

Inherent Area-Selective Atomic Layer Deposition of Copper on Metal-Patterned Silicon Substrates

Camilla Minzoni[1-2], Caroline Hain[1], Krzysztof Mackosz[1], Aleksandra Figura-Jagoda[3], Aleksandra Szkudlarek[3], Sylwia Klejna[3], Marcin Sikora[4], Esko Kokkonen[5], Patrik Hoffmann[2], Ivo Utke[1]

[1] Empa, Feuerwerkerstrasse 39, CH-3602 Thun, Switzerland
[2] EPFL, Rte Cantonale, 1015, Lausanne, Switzerland
[3] AGH University of Krakow, Academic Center for Materials and Nanotechnology, al. A. Mickiewicza 30, Krakow, 30-059, Poland
[4] SOLARIS Centre, Jagiellonian University, ul. Czerwone Maki 98, Krakow, 30-392, Poland
[5] MAX IV Laboratory, Lund University, Fotongatan 2, 224 84 Lund, Sweden
e-mail: camilla.minzoni@empa.ch

Selective Atomic Layer Deposition (SALD) represents a promising "bottom-up" approach for the fabrication of next-generation semiconductor materials. In contrast to traditional fabrication methods, which rely on deposition followed by selective removal through costly chemical etching and photolithography steps, SALD enables direct, targeted material growth only in specific areas. [1-2]
Conventionally, SALD has employed various modification approaches, including surface passivation with polymers, self-assembled monolayers (SAMs) and chemical molecular inhibitors. However, these methods often show limitations, including long passivation times and limited layer stability. A more efficient alternative approach to SALD exploits the differences in nucleation times of various surface materials during ALD film growth. [3-4]

Copper ALD has been extensively studied for several advanced technologies thanks to the Cu properties as a conducting material. With the increasing demand for precise copper patterning in microelectronics, developing selective deposition methods for copper has become particularly crucial. [5]
The current work focuses on studying the selective deposition of ultrathin copper layers on metal/SiO_2 and metal/Si_3N_4 substrates by exploiting the inherent differences in precursor adsorption.

The Cu samples were fabricated via ALD using dehydrated copper(II) hexafluoroacetylacetonate $Cu(hfac)_2$ ($CuC_{10}H_2F_{12}O_4$) as Cu source and diethylzinc DEZ ($Zn(C_2H_5)_2$) as reducing agent.
Figure 1 confirms selective Cu deposition, with preferential growth on oxide and nitride surfaces while exhibiting growth inhibition on metal surfaces such as platinum and gold.
Detailed *in-situ* XPS analysis performed at the SPECIES beamline at MAX IV Synchrotron (Lund, Sweden) revealed reduced adsorption of $Cu(hfac)_2$ on Pt surfaces compared to SiO_2 substrate, as shown in Figure 2. This direct observation suggests different chemisorption mechanisms. Growth occurs on oxide and nitride surfaces through ligand exchange reactions with surface hydroxyl (-OH) and amino (-NH_2) groups. In contrast, on metallic substrates the precursor chemisorbs poorly through ligands transfer reactions, resulting in a passivation layer.
Supporting these results, temperature-dependent studies of Girolami et al. [6] revealed peak intensity reductions and peak shifts in the XPS spectra, demonstrating precursor decomposition at temperatures as low as 100°C on metal surfaces, which prevents further growth.

These results demonstrate that the inherent differences in precursor-surface interactions can be strategically exploited to achieve selective copper growth, providing a simplified approach to area-selective deposition without the need for additional surface modification steps.

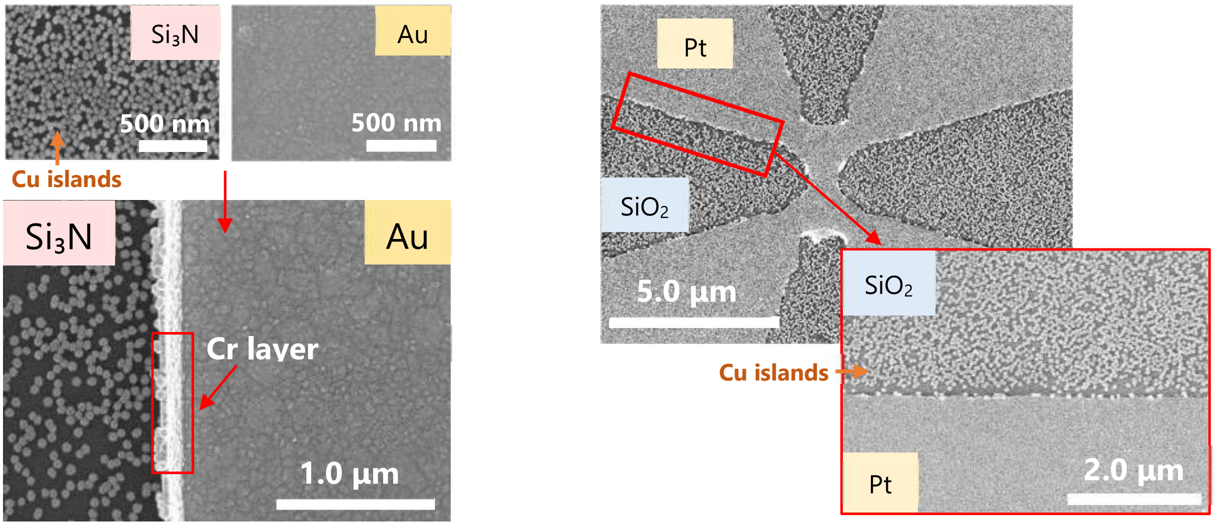

Fig. 1. Early-stage SALD of Cu: (left) on Si_3N_4 surface with growth inhibition on Au and (right) on SiO_2 surface with growth inhibition on Pt.

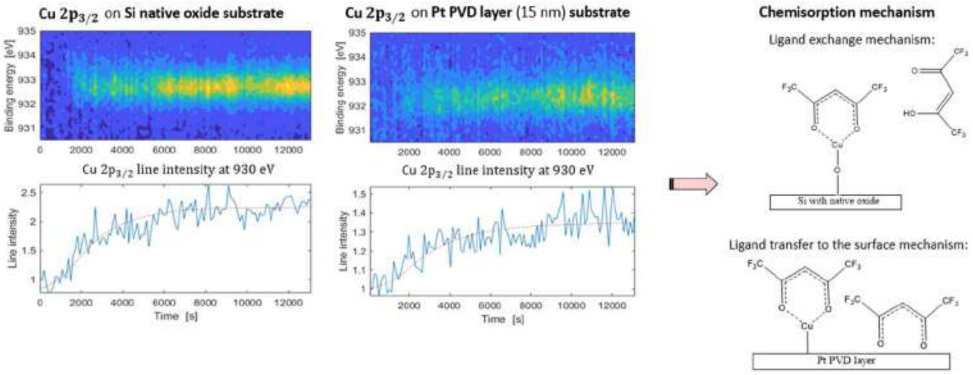

Fig. 2. Results of time-resolved XPS measurements at Cu $2p_{3/2}$ line, showing the adsorption curves of $Cu(hfac)_2$ on SiO_2 and Pt surfaces. Comparison of the XPS suggests that $Cu(hfac)_2$ adsorbs in greater amounts on the SiO_2 surface, as indicated by the higher intensity of the Cu $2p_{3/2}$ line at saturation.

References

[1] A. J. M. Mackus, M. J. M. Merkx and W.M. M. Kessels, *Chem. Mater.*, **31**, 2-12 (2019).
[2] C. Kim, M. Choi, J. Sim, H. Kim and C. Cho, *Applied Surface Science*, **663**, 160033 (2024).
[3] YC. Li, K. Cao, YX. Lan, JM. Zhang, M.Gong, YW. Wen, B. Shan and R. Chen, *Molecules,* **26**, 3056 (2021).
[4] Q. Tao, G. Jursich, C and Takoudis, *Appl. Phys. Lett.,* **96**, 192105 (2010).
[5] M. George, *Chem. Rev.,* **110**, 111-131 (2010).
[6] G. S. Girolami, P. M. Jeffries and L. H. Dubois, *J. Am. Chem. Rev.,* **115**, 1015-1024 (1993).

Evaluation of the Infiltration Capability Improvement for a Very Low-Pressure SiC CVI Process

B.Cossou[1], C. Descamps[1]
[1]Safran Ceramics
e-mail: benjamin.cossou@safrangroup.com

Safran is one of the global pioneers in the field of Ceramic Matrix Composites (CMC), materials developed to withstand high-temperature conditions under significant stress. A key process for the formation of these materials is the chemical vapor infiltration of Silicon Carbide (CVI).

This CVI process is typically carried out using CH_3SiHCl_3 at moderate temperatures (950 to 1150°C) and low pressures (100 mbar). The potential benefits of exploring even lower pressures (10 mbar) to enhance infiltration are theoretically assessed and then compared with the actual deposition profiles measured on model pores with openings of 2 and 0.5 mm.

The chamber of an isothermal isobaric CVI reactor is controlled in terms of temperature and pressure (T and P). The precursor injected into this chamber undergoes decomposition, with the nature and proportions of the by-products depending primarily on these two parameters (T, P)[1], [2], [3]. The resulting molecules then combine through the energetically most favorable pathways to form a solid deposit.

According to the literature, no modification in the reaction mechanism is expected when reducing the operating pressure by a factor of ten. This is corroborated by the observed CVD kinetics under both conditions.

The deposition gradient within a porous medium results from a competition between the reaction rate and the effective diffusion of the precursor through the porosity. It is possible to chart the trends in the evolution of the diffusion coefficient D by considering the undecomposed MTS molecule diffusing in a highly diluted hydrogen medium, and to deduce the expected impact on the deposition profile.

For this purpose, the approximation of a simple first-order reaction preceded by a diffusion step through a boundary layer is used. Theoretical profiles are then compared to the actual values obtained for the 2, 0.5 mm pores, demonstrating the benefits of this approach in these conditions.

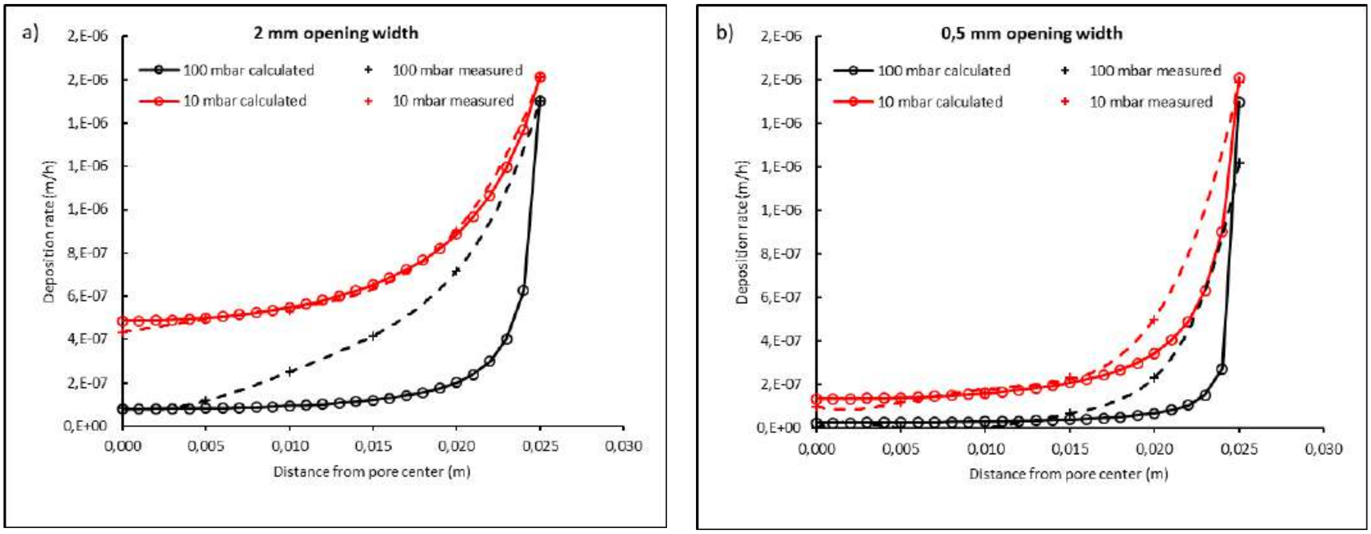

Fig. 1. Deposition rates calculated and measured at 100 and 10 mbar in model pores with a) 2 mm opening width b) 0.5 mm opening width

References

[1] F. Loumagne, F. Langlais, R. Naslain, *Journal of Crystal Growth*, **155**, 205-213 (1995).
[2] G. Laduye, *PHD Thesis*, Université de Bordeaux (2016).
[3] A. Desenfant, *PHD Thesis*, Université de Bordeaux (2018).

Area Selective Chemical Vapor Deposition of Gold by Electron Beam Seeding

A. Tsarapkin[1], K. Maćkosz[2], C.S. Jurredy[2], I. Utke[2], K. Höflich[1]
[1] Ferdinand-Braun-Institut (FBH), Berlin, Germany
[2] Empa - Swiss Federal Laboratories for Materials Science and Technology, Thun, Switzerland
e-mail: aleksei.tsarapkin@fbh-berlin.de, katja.hoeflich@fbh-berlin.de

Gold is a key metal in microelectronics due to its low resistivity, resistance to electromigration and chemical inert-ness making it an excellent choice for stable and reliable electrical contacts. Chemical vapor deposition (CVD) is a technologically significant option for fabricating gold contacts or other metallic functional structures. CVD utilises the thermal decomposition of precursor molecules in a gaseous state. Molecules reaching the surface are thermally decomposed, leaving the central metal atom on the surface. If the decomposition is favored kinetically or thermodynamically on certain surfaces compared to others, the ensuing variation in reaction rates can be exploited for area selective deposition.

This work presents a novel maskless patterning technique that enables area selective CVD of gold [1], see Fig. 1 for a schematic representation of the process. A focused electron beam is used to decompose the metal-organic precursor $Au(acac)Me_2$ locally [2], thereby creating an autocatalytically active seed layer for subsequent CVD with the same precursor. The procedure can be included in the same CVD cycle without the need for clean room lithographic processing. Moreover, it operates at low temperatures of 80 °C, over 200 K lower than standard CVD temperatures for this precursor, reducing thermal load on the specimen. Given that electron beam seeding operates on any even moderately conductive surface, the process does not con-strain device design. This is demonstrated by the example of vertical nanostructures with high aspect ratios of around 40:1 and more. Written using a focused electron beam and the same precursor, these nanopillars exhibit catalytically active nuclei on their surface. Furthermore, they allow for the first time the precise determination of the local temperature increase caused by the writing of nanostructures with an electron beam.

To summarise, this work presents a new, technologically powerful and easy to implement approach to area selective gold deposition. The low temperature necessary makes it highly suitable for processing innovative flexible devices that rely on heat-sensitive polymers, including flexible electronics and flexible solar cells. In addition, the maskless direct write seeding is possible on 3D architectures, which provides the potential to fabricate nanostructures or localized electric contacts on intricate 3D devices.

This work was supported by the German Research Foundation (DFG) under grant no. HO 5461/3-1

References

[1] A. Tsarapkin, K. Maćkosz, C.S. Jurredy, I. Utke, and K. Höflich, *Adv. Mater.* **36**, 2313571 (2024)
[2] I. Utke, P. Swiderek, K. Höflich et al., *Coord. Chem. Rev.* **458**, 213851, (2022).

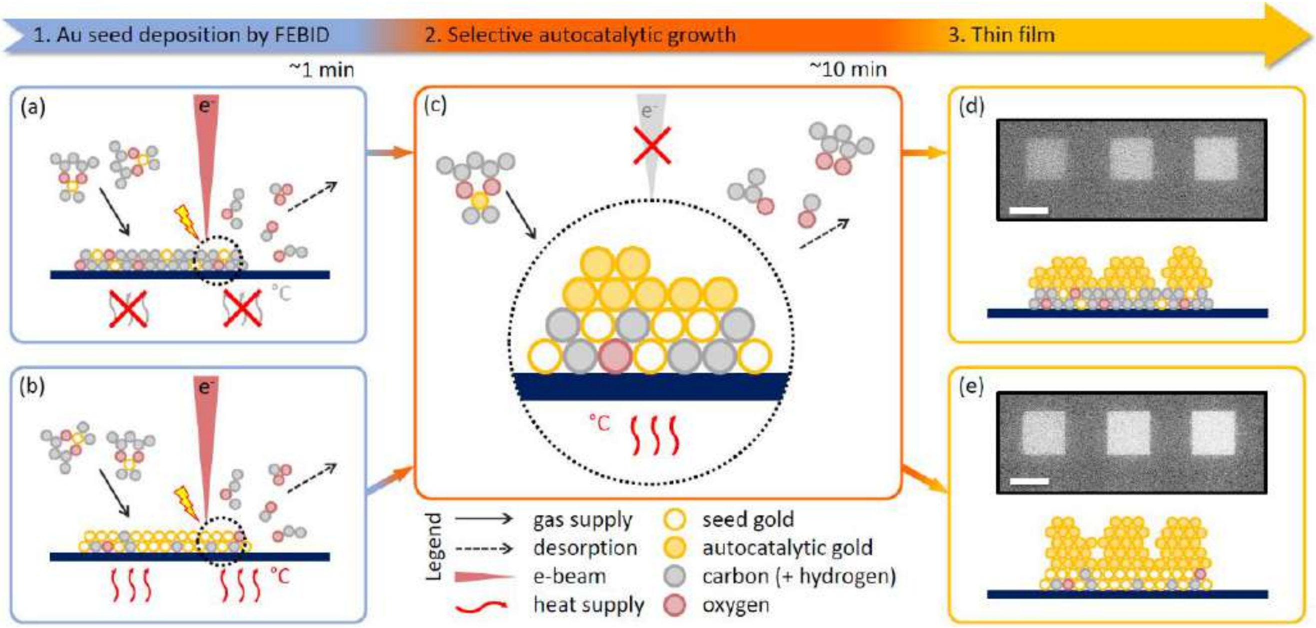
1. Au seed deposition by FEBID
2. Selective autocatalytic growth
3. Thin film
~1 min
~10 min
(a)
(b)
(c)
(d)
(e)
e⁻
°C
Legend
gas supply
desorption
e-beam
heat supply
seed gold
autocatalytic gold
carbon (+ hydrogen)
oxygen

Fig. 1. Schematic of the area-selective autocatalytic film growth. A seed layer is deposited using a focused electron beam to locally decompose the precursor on a substrate a) at room temperature (30 °C) or b) at elevated substrate temperatures. c) After seeding the precursor is decomposed at the deposited Au nuclei without further electron-beam assistance. SE micrographs show the resulting gold films for d) room-temperature seeding and e) seeding at elevated substrate temperatures, both proving the area-selectivity of the process. Scale bars represent 2 µm.

7Area Selective Infiltration of polymers with inorganics

S. Mirallas García[1,*], **G. Botta**[1], **A. Álvarez Yenes**[1], **M. Borraz Casanova**[1], **S. Azpeitia Coscarón**[1], **M. Knez**[1,2,*]

[1] CIC nanoGUNE BRTA, San Sebastián, Spain
[2]Ikerbasque, Basque Foundation for Science, Bilbao, Spain
e-mail: s.mirallas@nanogune.eu, m.knez@nanogune.eu

Hybrid materials combine two or more distinct components, often merging organic and inorganic constituents. Their properties are not solely determined by the individual components but also by their nanoscale arrangement, which can significantly influence their behaviour, enabling enhanced or entirely novel physical and chemical functionalities. Properly nanostructured hybrid materials have broad applications, including energy storage, biomedical devices, environmental remediation, and flexible electronics.

This work focuses on developing and characterizing area-selective infiltration using vapor phase infiltration (VPI) combined with lithographic processes for advanced device design and fabrication. Zinc oxide (ZnO) was selected as the inorganic infiltrant due to its tunable semiconducting properties, high electron mobility, and excellent thermal conductivity. Polyethylene terephthalate (PET) was chosen as the organic matrix for its notable thermal stability, chemical resistance, dimensional stability, and durability, alongside its lightweight and cost-effective properties. Together, these materials form a non-toxic and economically viable combination suitable for a wide range of applications across consumer and industrial sectors.

The VPI process was conducted on patterned substrates, varying pulse, exposure, and purge times to optimize infiltration and coating. Diethylzinc (DEZ) and water were employed as precursors to deposit ZnO, with two primary temperatures investigated: 60 °C (below PET's glass transition temperature) and 140 °C (above the glass transition temperature). Elemental composition analysis via EDX detected Zn, O, and C in the samples, while thickness and growth rates measured using XRR revealed ZnO deposition levels and suggested further optimization of pulse times. XRD data confirmed the presence of ZnO in its wurtzite phase.

Cross-sectional analysis of processed samples demonstrated area-selective infiltration when the process was conducted above the glass transition temperature of PET. In contrast, samples processed below this temperature exhibited only surface coating. The samples maintained structural integrity throughout the process, including exposure to lasers, chemicals, and high temperatures.

This study successfully demonstrates area-selective infiltration for the first time, representing a foundational step toward device design and fabrication based on selectively embedded inorganic materials within polymers.

Session AM_3.2 INNOVATIVE PROCESSESS II

Wednesday 4th June 2025 | 9.00-10.30

Chair: **Anna Maria Coclite** | Room “Coro di Notte”

Incorporation of Dopants into CVD and ALD grown MoS_2

Jun Lin, James Connolly, and Ian M. Povey
Tyndall National Institute, University College Cork, Cork, T12R5CP, Ireland
e-mail: jun.lin@tyndall.ie

MoS_2 is a 2D transition metal dichalcogenides that has received extensive research attention in recent years due to its tunable bandgap that enables the potential to diversify functionalities at the back-end-of-line (BEOL) of complementary metal-oxide-semiconductor (CMOS) circuitry. Flakes of MoS_2 achieved from mechanical exfoliation have been shown to perform successfully in logic functionality (i.e., field-effect transistors) [1]. With the current technique constraints, large-area, directly grown MoS_2 with device-grade electrical properties has yet to be demonstrated.

Chemical vapor deposition (CVD) is a leading candidate for wafer-level growth of MoS_2 thin films. Fig. 1 illustrates an example of MoS_2 grown by CVD at 550 °C for 2.5 hours by our group in a manufacturing-compatible 300 mm Applied Materials reactor [2]. Our CVD thermal budget (temperature + time) approximates to the BEOL thermal budget limit of CMOS processes [3]. No pre-/post-deposition anneal has been performed. The formation of MoS_2 by CVD is confirmed by structural/chemical analysis (see Fig. 1-3). Moreover, our CVD process has demonstrated continuous and uniform 300 mm wafer-level growth, with a high degree of repeatability, at temperatures as low as 300°C.

A trade-off exists between BEOL thermal compatibility and quality of the MoS_2 thin films, which is manifested by its poor electrical properties. It is noted that, in the literature, the majority of CVD of MoS_2 and pre-/post-deposition anneal processes are performed at 600-1100 °C [2]. Our CVD-grown nominally undoped MoS_2 demonstrates a high resistivity and low carrier concentration ($10^{14} – 10^{15}$ cm^{-3}). This is due to the restricted BEOL thermal budget, leading to small grains and therefore a high density of grain boundaries. These grain boundaries introduce defect states in the MoS_2 bandgap, which act as trapping sites that capture free carriers, resulting in such a low carrier concentration and limiting the lateral transport of carriers.

The solution to improving the electrical properties of CVD-grown MoS_2 within the BEOL thermal budget is doping. Potential dopants include aluminum/niobium as p-type dopants and iron/rhenium as n-type dopants. It is expected that sufficient dopants will firstly saturate the grain boundary defects, beyond which free carriers become available for transporting. This is similar to the early work on polycrystalline silicon, where dopant saturation of grain boundary defects was required to achieve controlled semiconductor or pseudo-metallic behavior [4].

Here we use both CVD and plasma enhanced ALD (VEECO Fiji 200 mm tool) to optimize grain size and study the impacts of both p and n dopants aluminum and iron respectively. In our investigation, in addition to a standard chemical/structural study, we perform an in-depth electrical characterization on thin films and devices, illustrating how doping can overcome the limitations of directly grown low temperature MoS_2 without the need for high temperature anneals and subsequent layer transfer.

This work was supported by Science Foundation Ireland (SFI) under Grant Number SFI 12-RC-2278_P2.

References

[1] Desai S B et al., *Science,* **354**, 99–102 (2016).
[2] Lin J et al., 2D Mater. **8**, 025008 (2021).
[3] Fenouillet-Beranger C et al., IEEE IEDM (San Francisco, CA, USA, 15–17 December) pp 27.5.1–4 (2014).
[4] Seto, John YW, *J. Appl. Phys.*, **46**, 5247–5254 (1975).

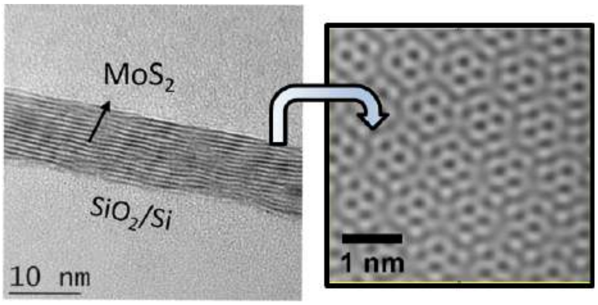

Fig. 1: 2D layered and polycrystalline MoS_2 grown at 550 °C for 2.5 hours by chemical vapor deposition in a 300 mm chamber by our group [1].

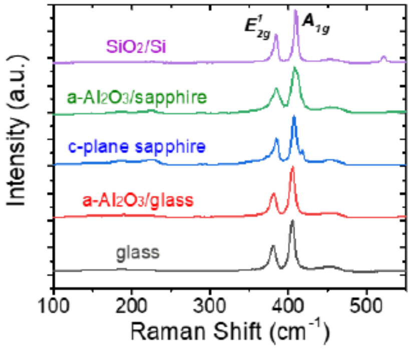

Fig. 2: Raman of CVD-grown MoS_2 (550 °C, 2.5 hours) on a variety of substrates.

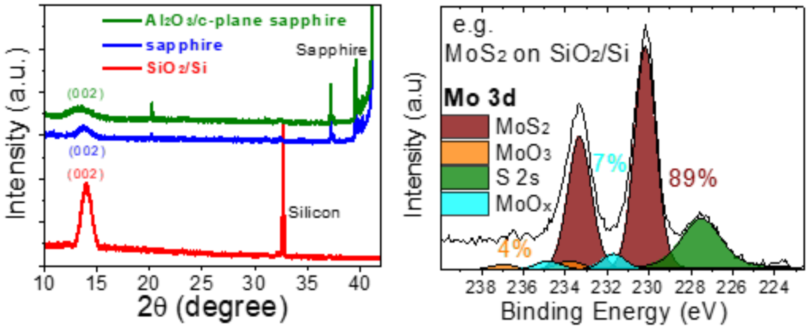

Fig. 3: X-ray diffraction and x-ray photoelectron spectroscopy of CVD-grown MoS_2 (550 °C, 2.5 hours), confirming formation of MoS_2.

Innovative Approaches to Coating Systems for Stone Heritage Conservation

Ancy Mini Vibin Lal Nayakom Mini[1], Gabriele Botta[1], Susana De la Rosa-García[2], Sergio Gómez-Cornelio[3, 4], Mato Knez[1,5], Aranzazu Sierra-Fernández[1*]

[1] CIC nanoGUNE, Tolosa Hiribidea 76, E-20018 Donostia-San Sebastián, Spain
[2] Laboratorio de Microbiología Aplicada, División Académica de Ciencias Biológicas, Universidad Juárez Autónoma de Tabasco, Villahermosa 86000, Tabasco, Mexico
[3] Universidad Politécnica del Centro, Tumbulushal, Centro, 86290 Villahermosa, Tabasco, Mexico
[4] Laboratorio de Nanotecnología-CICTAT, División Académica de Ingeniería y Arquitectura, Universidad Juárez Autónoma de Tabasco, Cunduacán, Tabasco 86690, Mexico
[5] IKERBASQUE, Basque Foundation for Science, Plaza Euskadi 5, E-48009 Bilbao, Spain

*E-mail: a.sierra@nanogune.eu

The preservation of stone cultural heritage (CH) materials faces escalating challenges due to the compounded effects of harsh environmental conditions and biological colonization, particularly in the context of climate change. Extreme weather, fluctuating humidity, and elevated temperatures accelerate material degradation, while pollution and microbial activity further exacerbate the damage. This study addresses these pressing issues by developing advanced self-healing coatings specifically designed to repair microdamage and extend the functional lifespan of stone substrates. Using Atomic Layer Deposition (ALD), we fabricated protective systems with tailored functionalities to enhance durability, adaptability, and resilience.

A central focus of this work is surface functionalization using metal oxides, which promotes mineral growth in damaged regions, mimicking natural self-healing mechanisms. Furthermore, this functionalization creates chemically reactive surfaces that improve the compatibility of coatings with porous stone substrates, enhancing both cohesion and the overall mechanical stability of the system under stress. These advancements establish a robust platform for protective layer deposition and long-term material conservation.

To complement the self-healing functionality, zinc oxide (ZnO) layers of varying thicknesses were incorporated to explore their potential for antimicrobial integration. These coatings were specifically tested against *Phoma euphyren*a and microcolonial fungi, both of which are notorious for their aggressive biodeterioration of stone heritage materials. The results demonstrate the ability of ZnO layers to effectively inhibit fungal colonization, with antifungal efficacy strongly influenced by the thickness of the deposited layers. This highlights the potential of ZnO as both a protective and active component within multifunctional coatings.

This dual approach—integrating self-healing capabilities with antimicrobial properties—marks a significant advancement in CH conservation technologies. By addressing both mechanical degradation and biodeterioration, this research establishes a versatile and sustainable framework for the long-term protection of stone heritage materials. The application of advanced ALD systems and multifunctional coatings provides a transformative pathway to overcome the challenges posed by environmental and biological stressors in cultural heritage preservation.

The projects that gave rise to these results received the support of a fellowship from ‘‘la Caixa” Foundation (LCF/BQ/PI23/11970025), and by the project ASSIST (PID2023-147532OA-I00) from the MICIU/AEI/10.13039/501100011033.

Next generation ALD functionalization of lead-free high-gain microchannel plates for photomultiplier tubes

S. Cwik[1], M. J. Aviles[1], S. M. Clarke[1], C. J. Hamel[1], A. V. Lyashenko[1], M. A. Popecki[1], J. W. Elam[2], T. Curtis[3], A. Tremsin[3], O. H. Siegmund[3], M. J. Minot[1,*]
[1]Incom Inc., Research & Development
[2] Argonne National Laboratory, Applied Materials Division
3 UC Berkeley, Space Science Laboratory
e-mail: scwik@incomusa.com, mjm@incomusa.com

Microchannel plates (MCPs) find application in image intensifier tubes of night vision goggles, in spectrometers and in photo multiplier tubes (PMTs) based on their high resolution, ultra-fast timing and high gain. Conventional lead glass MCPs have been the industry standard since the 1960s. The manufacture includes a hydrogen firing step in which lead oxide gets reduced to bring the plate to target resistance and to generate the electron emission layer at the same time. This functionalization limits the adjustability of the MCP to target applications.

Incom Inc. has commercialized the ALD-GCA-MCP technology, applying ALD technology from Argonne on Incom's glass capillary arrays (GCAs). The physically and chemically robust silicate glass allows the fabrication of large area GCAs up to 203x203 mm and the high resistance of the GCAs enables functionalization with ALD. The functionalization of the GCA is conducted with a resistive and an emissive layer (Fig. 1 left). The tunable resistive layer is a nanocomposite of conductive and insulating materials and defines most electrical characteristics of the MCP since it serves as strip layer to recharge the emissive layer. The emissive layer is comprised of a high secondary electron yield (SEY) material like MgO or Al_2O_3 to provide maximum gain for intensifier applications.

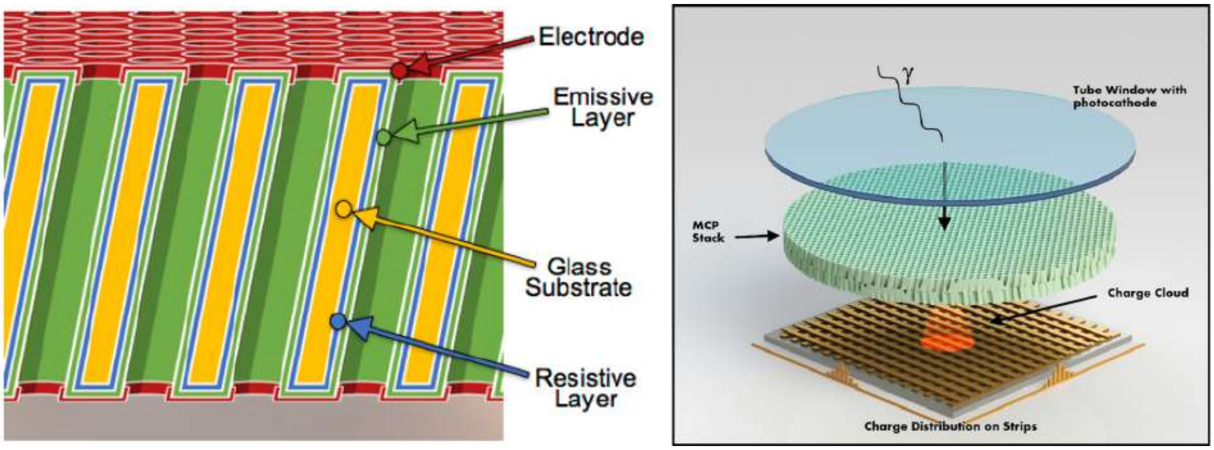

Fig. 1. Schematic of ALD-GCA-MCP (left) and the application as chevron pair in a photodetector (right)

Incom's 1st generation MCPs rely on the combination of Chem1 and MgO, which provide high gain for both sealed PMTs (see Fig. 1 right) and open MCP applications [1]. While both high gain, and durability of Chem1-MgO MCPs fulfill the standards of conventional MCPs, characteristics like the thermal coefficient of resistance (TCR) and the after-pulsing of MCPs should be improved to enhance device performance and life-time.

The negative TCR of MCPs, i.e. decreasing resistance at increasing temperature can lead to thermal runaway and potentially break-down of the device. In contrast to conventional MCPs, this can be directly addressed by tailoring the resistive layer, which allowed to reduce the TCR of Chem1-MgO from -0.03 K^{-1} to -0.02 K^{-1} by optimizing the Chem1 composition.

In the efforts to optimize the performance of ALD-GCA-MCPs, the alternative Chem5 resistive layer was transferred from Argonne to Incom to allow the fabrication of halide free MCPs. The optimization of Chem5-MgO MCPs [2] with respect to gain uniformity allowed the upscaling to 108x108 mm format, that are used in Incom's 10 cm detectors, the HRPPD (High rate picosecond photo detector, fig 2 left). While the TCR of the current version of Chem5-MgO is only at -0.03 K^{-1}, the resistive coating Chem5 revealed outstanding electrical performance. Especially, the extraordinary current stability of over 1 mA as determined for a chevron pair of 33 mm Chem5-MgO MCPs at 150 °C (0.8 MΩ in operation at 1 kV), exceed both Chem1 and conventional MCPs. The high current stability reduces the risk of thermal runaway as the plates get exposed to increasing temperatures despite a higher TCR.

For the application in sealed PMTs, high MCP gain is critical to allow for the operation at reduced MCP voltages. When the MCPs release ions in operation, the acceleration towards the photocathode is defined by the electrical field. This after-pulsing can deteriorate the photocathode, especially when the ions impact with high velocity. Chem5-MgO MCPs were integrated in HRPPDs, to determine the performance in sealed environment which revealed a significant improvement in gain. This reduces the operational voltages by 200 V to 650 V per MCP. While the corresponding device lifetimes measurements are ongoing, Incom Inc. is transitioning the full scale LAPPD (Large area picosecond photo detector) [3] to 2nd generation Chem5-MgO MCPs in 2025.

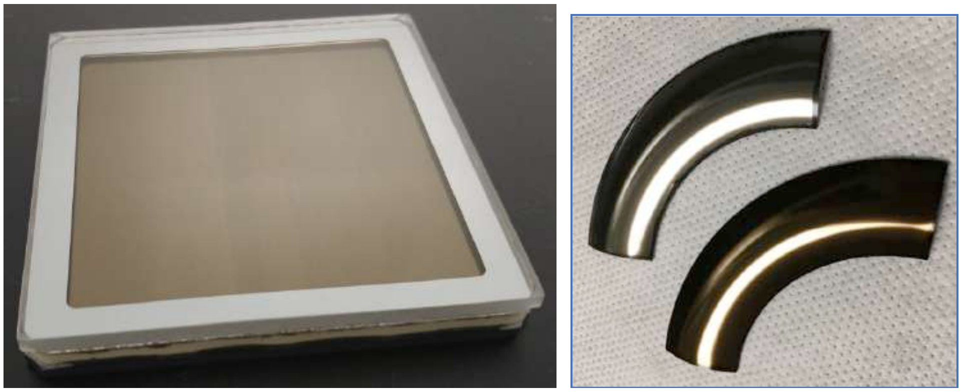

Fig. 2. High Rate Picosecond Photodetector (left) and custom curved ALD-GCA-MCPs (right)

This work was supported by the US Department of Energy (National Nuclear Security Administration), Award number: #DE-SC0018778

References

[1] A. U. Mane, and J. W. Elam, *Material Matters*, **13**, 45 (2018).

[2] S. Cwik, J. W. Elam, M. Aviles, S. M. Clarke, C. Hamel, A. Lyashenko, M. J. Minot, M. A. Popecki, US Patent Provisional application: 18/962,346 (2024)

[3] S. Shin, M. Aviles, S. M. Clarke, S. Cwik, M. Foley, C. Hamel, A. Lyashenko, D. Mensah, M. Minot, M. Popecki, and M. Stochaj, *Journal of Instrumentation,* **19**, P06040 (2024).

Low Temperature Atomic Layer Deposition of (00*l*)-Oriented Elemental Bismuth

J.L. Vazquez-Arce[1], A. Bahrami[1*], S. Lehmann[1] and K Nielsch[1,2]

[1.] Leibniz-Institute for Solid State and Materials Research Dresden, Helmholtzstraße 20, 01069 Dresden, Germany

[2.] Institute of Materials Science, Technische Universität Dresden, Helmholtzstraße 7, 01062 Dresden, Germany

e-mail: a.bahrami@ifw-dresden.de

Abstract.
This study presents the first successful demonstration of growing elemental bismuth (Bi) thin films via thermal atomic layer deposition (ALD) using $Bi(NMe_2)_3$ as the precursor and $Sb(SiMe_3)_3$ as the co-reactant. The films were deposited at a relatively low temperature of 100 °C, with a growth per cycle (GPC) of 0.31-0.34 Å/cycle. Island formation marked the initial growth stages, with surface coverage reaching around 80% after 1000 cycles and full coverage between 2000 and 2500 cycles. Morphological analysis revealed that the Bi grains expanded and became more defined as the number of ALD cycles increased. This coalescence is further supported by X-ray diffraction (XRD) patterns, which show a preferential shift in growth orientation from the (012) plane to the (003) plane as the film thickness increases. X-ray photoemission spectroscopy (XPS) confirmed the presence of metallic Bi with minimal surface oxidation. Temperature-dependent sheet resistance measurements highlight the semimetallic nature of Bi, with a room temperature resistivity of ≈200 μΩcm for the 2500 cycles Bi. Temperature-dependent sheet resistance was also associated with a transition in carrier-type dominance from electrons at higher temperatures to holes at lower temperatures.

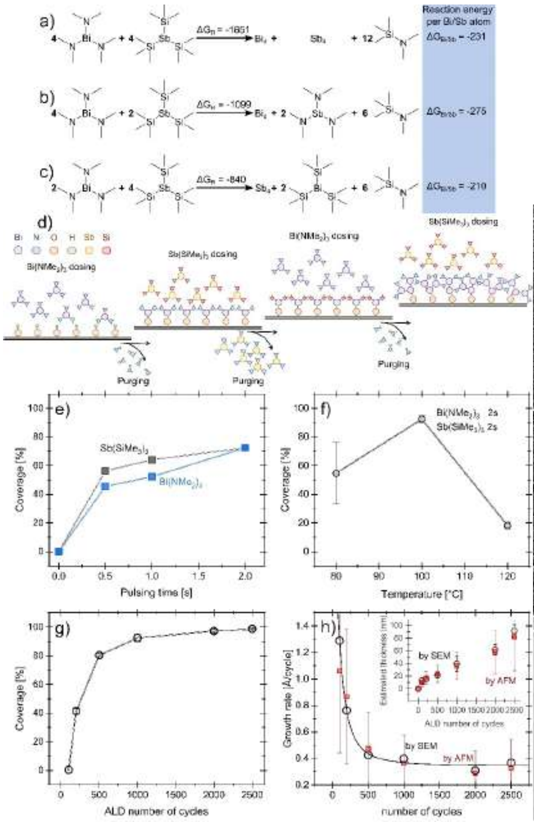
a)
b)
c)
Reaction energy per Bi/Sb atom
ΔG = -1651
ΔG = -231
ΔG = -1099
ΔG = -275
ΔG = -840
ΔG = -210
d)
Bi N C H Sb Si
Bi(NMe2)3 dosing
Sb(SiMe3)3 dosing
Bi(NMe2)3 dosing
Sb(SiMe3)3 dosing
Purging
Purging
Purging
e)
Sb(SiMe3)3
Bi(NMe2)3
Coverage [%]
Pulsing time [s]
f)
Bi(NMe2)3 2s
Sb(SiMe3)3 2s
Coverage [%]
Temperature [°C]
g)
Coverage [%]
ALD number of cycles
h)
Growth rate [Å/cycle]
Estimated thickness [nm]
by SEM
by AFM
ALD number of cycles
number of cycles

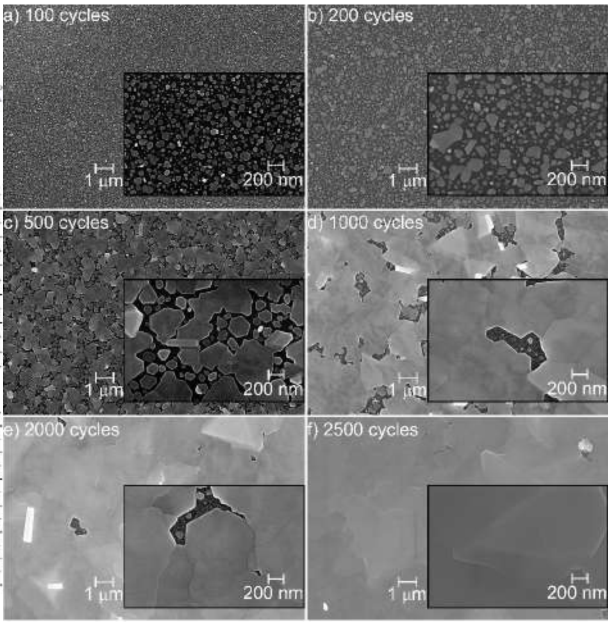
a) 100 cycles
b) 200 cycles
c) 500 cycles
d) 1000 cycles
e) 2000 cycles
f) 2500 cycles
1 µm
200 nm

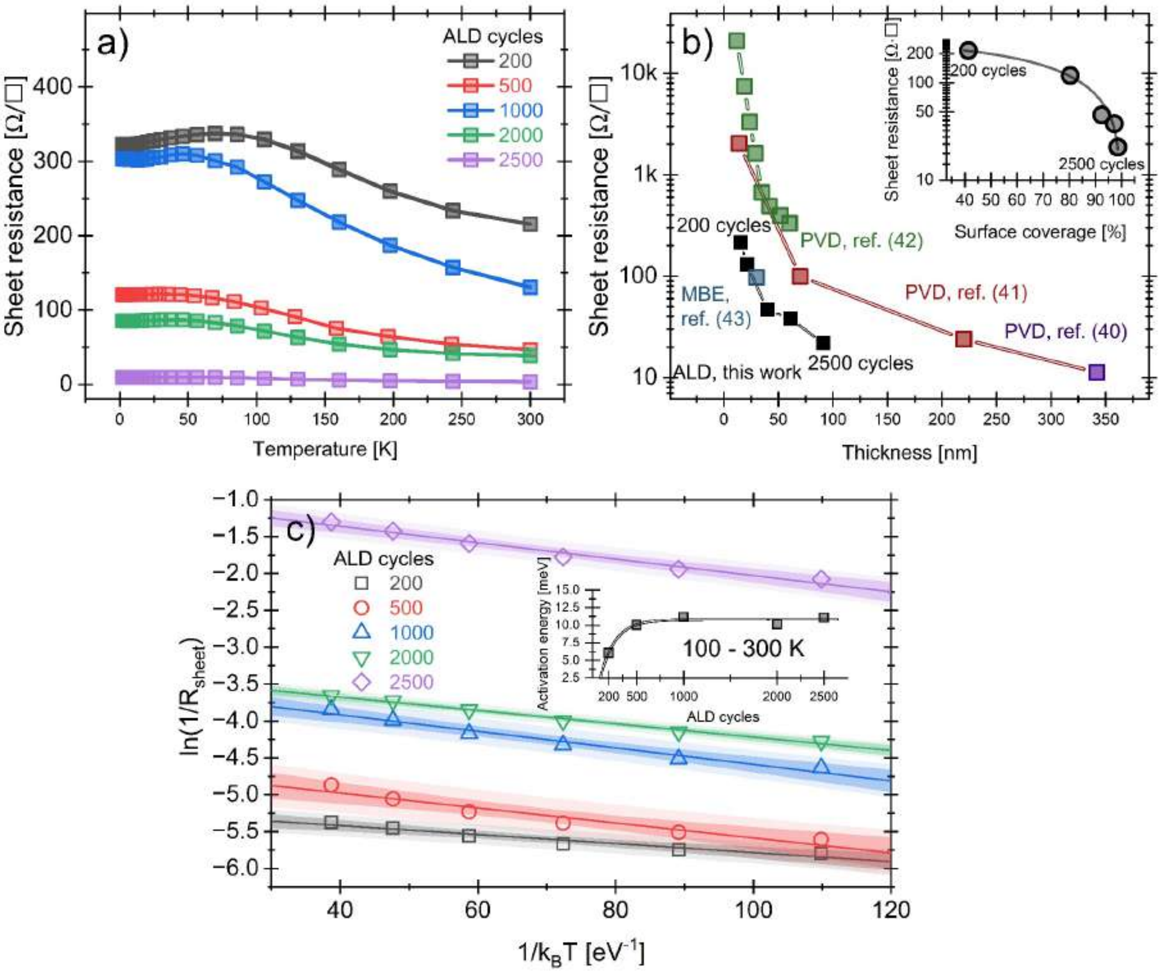
a)
ALD cycles
200
500
1000
2000
2500
Sheet resistance [Ω/□]
Temperature [K]
b)
Sheet resistance [Ω/□]
Thickness [nm]
200 cycles
2500 cycles
Surface coverage [%]
PVD, ref. (42)
PVD, ref. (41)
PVD, ref. (40)
MBE, ref. (43)
ALD, this work
c)
ALD cycles
200
500
1000
2000
2500
ln(1/R_sheet)
1/k_BT [eV^-1]
Activation energy [meV]
100 - 300 K
ALD cycles

References

Surface chemistry in the early growth stages of TiN ALD using operando APXPS

P. Mpofu[1,*], P. Promdet[1], H. Hafdi[1], J. Lauridsen[2], O. Alm[2], T. Larsson[2], E. Kokkonen[3], J. Schnadt[3,4,5], H. Pedersen[1]

[1]Linköping University, Department of Physics, Chemistry and Biology, Linköping, 58183, Sweden
[2]Seco Tools AB, SE-737 82, Fagersta, Sweden
[3]MAX IV Laboratory, Lund University, Box 118, 221 00 Lund, Sweden
[4]Division of Synchrotron Radiation Research, Department of Physics, Lund University, Box 118, 221 00 Lund, Sweden
[5]NanoLund, Lund University, Box 118, 221 00, Lund, Sweden
e-mail: pamburayi.mpofu@liu.se

Studying the surface chemistry of the first few cycles of atomic layer deposition (ALD) using *in-situ* and *operando* techniques is attractive for realizing, understanding and obtaining true mechanistic information during a deposition. One way to do this is by using *operando* ambient pressure X-ray photoelectron spectroscopy (APXPS) to monitor the chemical environment of the substrate and film surface while pulsing the ALD precursors. In this *operando* approach, XPS is conducted concurrently with the dosing of the precursor, as opposed to the more common *in-situ* XPS experiments that are performed after ALD half-cycles.[1]–[3] The initial growth stages of materials such as titanium nitride (TiN) is a crucial factor for very thin films, as the nucleation process significantly affects the material properties and functionality.[4] TiN has numerous applications in the protective hard coatings industry, semiconductor device manufacturing, including aluminium diffusion barriers, seed layers for copper plating, metal gates, and electrodes in high-density capacitors.[5]

Here we present, for the first time, a surface-chemistry investigation through a comprehensive *operando* ambient pressure XPS study of the initial growth of TiN, at different process temperatures, during an ongoing thermal ALD process using tetrakis(dimethylamido)titanium(IV) (TDMAT) and ammonia (NH_3). The core level spectra of Si 2p, C 1s, O 1s, N 1s, and Ti 2p were recorded at different stages during deposition. We found that growth occurs immediately on silicon dioxide surface due to the ready reaction of TDMAT with the surface hydroxyl (OH) groups, which means that initial Ti nucleation is governed by the available OH groups. Thereafter, we have a resulting delay in nucleation on a supposedly NH_2-terminated surface, after which the intensity begins to increase as shown by the surface becoming coated with Ti and N atoms and no Si signals are observed with time. We believe that ligand exchange reactions take place before transamination and more chemical reactions kick in at a later stage.[6] This was verified using the periodic changes of the above-mentioned spectra concentration and peak positions. These results can help with insights into the ALD surface growth of not only TiN but also other metal nitrides.

References

[1] R. Jones *et al.*, *Surf. Sci.*, **753**, 122656, (2025).
[2] R. Jones *et al.*, *J. Vac. Sci. Technol. A*, **42**, 022404, (2024).
[3] E. Kokkonen *et al.*, *J. Vac. Sci. Technol. A*, **42**, 062406, (2024).
[4] E. Langereis *et al.*, *Phys. Status Solidi C Conf.*, **2**, 3958–3962, (2005).
[5] H. Kim, *J. Vac. Sci. Technol. B Microelectron. Nanom. Struct. Process. Meas. Phenom.*, **21**, 2231–2261, (2003)
[6] P. Mpofu *et al.*, *Mater. Adv.*, **5**, 9259–9269, (2024).

Influence of different oxidants in the growth of Al_2O_3 elaborated by atomic layer deposition on cellulose

Hugo Patureau[a], Thierry Encinas[b], Alexandre Crisci[a], Frederic Mercier[a], Erwan Gicquel[c], Arnaud Mantoux[a], Elisabeth Blanquet[a]

[a] Univ. Grenoble Alpes, CNRS, Grenoble INP, SIMaP, 38000 Grenoble, France
[b] Consortium des Moyens Technologiques Communs, Grenoble INP, CMTC, 38000 Grenoble, France
[c] CILKOA, 38330 Montbonnot Saint Martin, France
hugo.patureau@grenoble-inp.fr

With the gradual ban on single use plastics, cellulosic products have emerged as suitable candidates to replace plastics in the packaging industry. Cellulose is biodegradable, recyclable and possesses good mechanical properties. To be viable for packaging, especially in the food industry, cellulose surfaces need to be functionalised to obtain additional properties, such as wettability, oxygen/water barriers and mechanical resistance in humid conditions.

In this context, aluminium oxide films elaborated by atomic layer deposition on cellulosic substrate have been investigated in order to improve the barrier properties while keeping its biodegradability and recyclability.

While the reactivity of the precursors trimethylaluminium (TMA) and H_2O to form Al_2O_3 on silicon are well established, the same cannot be said of cellulosic substrates due to their complex structure. In this presentation, a study on the growth of ALD Al_2O_3 on cellulose is conducted, as per the experimental setup in figure 1a. Different precursors for the oxidation of TMA are studied: H_2O, Ethanol and O_2 plasma. Such precursors have already been studied for the ALD growth of Al_2O_3 on silicon substrates [1][2]. Saturation curves and the effect of deposition temperature are established for these precursors. In order to understand the effect of the precursors and the temperature on the deposition of Al_2O_3 on cellulose, X-ray fluorescence (XRF) on cellulose is developed and implemented to quantify the amount of aluminium deposited. Additionally, the composition of the films is characterised using X-ray photoelectron spectroscopy (XPS). Figure 1b and 1c give example of evolution of the growth rate and composition with deposition temperature by using XRF and XPS.

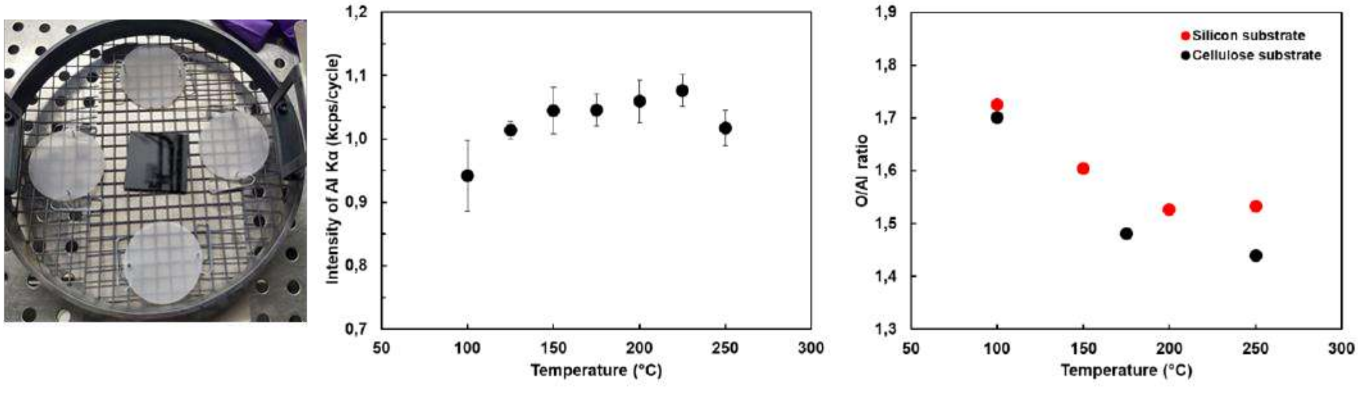

Figure 1: (a) Experimental set up. (b) Impact of the temperature on the Al intensity for alumina deposited on cellulose, measured by XRF (c) Impact of temperature on the O/Al ratio for alumina on cellulose measured by XPS.

[1] Heil SBS, Van Hemmen JL, Van De Sanden MCM, Kessels WMM. Reaction mechanisms during plasma-assisted atomic layer deposition of metal oxides: A case study for Al_2O_3. Journal of Applied Physics. 2008 May 15;103(10):103302.

[2] Seo S, Woo WJ, Lee Y, Yoon H, Kim M, Oh IK, et al. Reaction Mechanisms of Non-hydrolytic Atomic Layer Deposition of Al_2O_3 with a Series of Alcohol Oxidants. J Phys Chem C. 2021 Aug 26;125(33):18151–60.

Session AM_3.3 MODELING

Wednesday 4th June 2025 | 11.00-12.30

Chair: **Davide Barreca** | Main Hall “Santo Mazzarino”

An atomistic viewpoint on Chemical Vapour Deposition precursors, processes and applications

G.Tabacchi[1*], E. Fois[1], C. Invernizzi[1], D. Barreca[2,3], A. Gasparotto[2], C. Maccato[2]
[1]University of Insubria, Department of Science and High Technology, and INSTM.
[2]University of Padova, Department of Chemistry, and INSTM
[3]CNR-ICMATE and INSTM– Department of Chemical Sciences

e-mail: gloria.tabacchi@uninsubria.it

The relevance of theoretical methodologies for the science and technology of oxide-based materials – from fabrication processes to functional applications - has experienced a steady growth in the last decades. In particular, approaches based on Density Functional Theory (DFT) have been fruitfully exploited to study the reactivity of molecular precursors for chemical vapor deposition (CVD) of metal oxides [1-3], as well as to characterize structural and electronic properties of the fabricated nanomaterials at atomistic detail [4]. As a result, a deeper understanding of CVD processes and fabricated nanosystems has been accomplished by combining an accurate, multi-technique experimental characterization of the target systems with molecular-level insight gathered from first-principles computational modeling, which is difficult to achieve from experiments [3,4].

The aim of this contribution is to highlight how theoretical modeling may be used not only to complement experimental data, but also to provide a thorough atomistic-level understanding able to guide the design and fabrication of new nanostructured oxide materials via vapor deposition techniques, as well as to enhance the application scopes of the fabricated functional materials. Additionally, the presented case studies will highlight open challenges in the simulation of nanostructured oxide materials. The atomistic details of the complex chemical processes occurring in CVD routes, including the decomposition mechanisms of the precursor molecules, are, in general, not fully undersood yet [3,4].

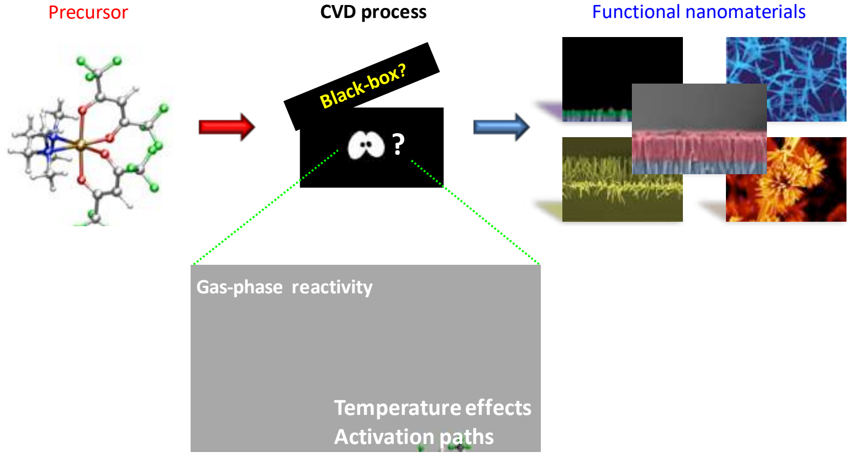

Fig. 1: Scheme illustrating the molecule-to-material conversion in thermal CVD. Relevant open questions at the microscopic level on gas-phase and surface reactivity are highlighted.

Herein, we select as case study a family of β-diketonate-diamine adducts of first-row transition metal(II) cations, of general formula [M(L)$_2$TMEDA] (M= Mn, Fe, Co, Ni, Cu, Zn; L=β-diketonate ligand; TMEDA= *N*,*N*,*N*′,*N*′-tetramethylethylenediamine), utilized as molecular precursors for the vapor phase deposition of the corresponding metal oxides [5-7]. Computational studies on the properties and reactivity of these compounds have contributed to enhance the atomistic-level knowledge of the mechanistic aspects of precursor activation [8,9] (*i.e.* adsorption of the precursor complex, early stages of the reactivity at the substrate surface, and physisorption/bonding to the surface), which require a proper theoretical modeling of both high-temperature effects and bond breaking/forming events.

A thorough atomistic knowledge of the oxide nanomaterials obtained through vapor deposition routes has not been accomplished yet. Specifically, the role of the surface defects, which are ubiquitous on the deposited samples, in affecting the electronic properties of the resulting nanosystems, is still an open question, due also to the inherent experimental difficulties in gathering atomistic insight on the structural details of surface defects. Modeling the influence of different types of defects on the electronic properties of fabricated NiO nanomaterials revealed important structure-properties relationships which could enable to tune nanosystem functional properties towards specific applications [10].

Oxide nanomaterials decorated with metal nanoparticles are relevant for real-world uses such as sensing and electrocatalysis. In these applications, molecular species interact with oxide materials surfaces. Yet, many aspects of the detailed mechanisms involving adsorption and reactivity at the molecule-material interface are not clarified. Insight gathered through modeling can shed light on the atomistic origins of the excellent performances in sensing [11] and electrocatalysis [12] of Au-decorated manganese oxide nanosystems, providing solid bases for the improvement of these applications via a knowledge-based approach.

This work was supported by Insubria University (FAR 2023)

References

[1] L. McElwee-White, *J. Chem. Soc. Dalt. Trans.*, **45**, 5327 (2006)
[2] H. Pedersen, and S.D. Elliott, *Theor. Chem. Acc.*, **133**, 1 (2014)
[3] G. Tabacchi, E. Fois, D. Barreca, and A. Gasparotto, *Int. J. Quantum Chem*., **114**, 1 (2014)
[4] E. Fois, and G. Tabacchi, in: *Tailored Functional Oxide Nanomaterials: From Design to Multi-Purpose Applications* (eds C. Maccato and D. Barreca), pp. 111-136, Wiley-VCH GmbH, Weinheim, Germany (2022)
[5] G. Tabacchi, E. Fois, D. Barreca and A. Gasparotto, *Phys. Status Solidi A*, **211**, 251 (2014)
[6] M. Klotzsche, D. Barreca, L. Bigiani, R. Seraglia, A. Gasparotto, L. Vanin, C. Jandl, A. Pöthig, M. Roverso, S. Bogialli, G. Tabacchi, E. Fois, E. Callone, S. Dirè and C. Maccato, *Dalton Trans.*, **50**, 10374 (2021)
[7] M. Benedet, D. Barreca, E. Fois, R. Seraglia, G. Tabacchi, M. Roverso, G. Pagot, C. Invernizzi, A. Gasparotto, A. A. Heidecker, A. Pöthig, E. Callone, S. Dirè, S. Bogialli, V. Di Noto, and C. Maccato, *Dalton Trans.*, **52**, 10677 (2023)
[8] E. Fois, G. Tabacchi, D. Barreca, A. Gasparotto, E.Tondello, *Angew.Chem.Int. Ed.*, **49**, 1944 (2010)
[9] D. Barreca, E. Fois, A. Gasparotto, C. Maccato, M. Oriani,G. Tabacchi, *Molecules*, **26**, 1988 (2021)
[10] E Fois, C Maccato, D Barreca, C Invernizzi, and G Tabacchi, *Dalton Trans.*, DOI: 10.1039/D4DT03340J (2025)
[11] L. Bigiani, D. Zappa, D. Barreca, A. Gasparotto, C. Sada, G. Tabacchi, E. Fois, E. Comini and C. Maccato, *ACS Appl. Mater. Interfaces*, **11**, 23692 (2019)
[12] L. Bigiani, T. Andreu, C. Maccato, E. Fois, A. Gasparotto, C. Sada, G. Tabacchi, D. Krishnan, J. Verbeeck, J. R. Morante, and D. Barreca, *J. Mater. Chem.*, **8**, 16902 (2020)

Analytical Model for 3D Island Growth Mode in ALD

W. Szmyt[1,2,*], **L. Lapeyre**[3], **I. Utke**[3]
[1]Advanced Materials Processing Laboratory, Empa Swiss Federal Laboratories for Materials Science and Technology, CH-3603 Thun, Switzerland
[2]Laboratory for Photonic Materials and Characterization, EPFL École Polytechnique Fédérale de Lausanne, CH-1015 Lausanne, Switzerland
[3]Mechanics of Materials and Nanostructures Laboratory, Empa Swiss Federal Laboratories for Materials Science and Technology, CH-3603 Thun, Switzerland
e-mail: Wojciech.Szmyt@empa.ch

The behavior of initial stages of growth in ALD is determined by surface phenomena on the substrate upon exposure to ALD precursors. Particularly, if reactivity of substrate surface with given precursor compounds is limited, the film growth originates at sparsely-distributed nucleation sites, typically corresponding to surface defects. These conditions result in a heterogeneous island growth mode. In such a case, islands continue to grow in a 3D fashion, until island coalescence occurs, when a transition to a homogeneous 2D growth is observed, as in classical idealized ALD. This characteristic growth behavior is directly reflected in measurements of mass uptake by Quartz Crystal Microbalance technique (QCM), as well as in other measurements of the amount of material deposited. Modelling the phenomenon accurately is a key to understanding the process and its optimization with respect to achieving ultrathin compact films as needed for energy conversion applications, for example.

There have been several attempts to model the island mode growth in ALD, both analytical and purely numerical. Analytical models assume nucleation sites on regular periodic lattices [1-3], which limits model accuracy, while realistically the nucleation site distribution is random in nature in most cases. An advantage of the analytical models is an instant model evaluation and a possibility to fit it directly to the measurement data at a low computational effort. Furthermore, in analytical models the influence of physical parameters on the model output is transparent, seen directly in the equations. The numerical simulations, on the other hand, are highly flexible [4,5] – they may assume virtually any arbitrary shape and distribution of growing islands, however a high model complexity results in a long computation time, which is a strong limitation in model fitting. Also, the influence of physical parameters on the output of numerical simulations is relatively obscured and typically requires multiple simulation runs and in-depth analysis to reliably reveal the dependencies.

We are proposing an analytical model derived from basic geometrical and statistical principles that can be fitted to measurement data of growth per cycle or total mass uptake, as exemplified in Fig. 1. The model assumes islands of a spherical dome shape randomly distributed on a flat substrate surface, see Fig. 2. The width to height ratio of an island reflects the substrate activation in the vicinity of an island. Moreover, the model allows for continuing spontaneous island nucleation during process in parallel to advancing island growth, i.e. increasing nucleation density. A successful model fit gives an estimate of characteristic parameters of film nucleation in ALD: initial density of nucleation sites, spontaneous island nucleation rate, lateral island growth rate enhancement factor due to substrate activation, film surface roughness, and island coalescence. This provides an insight into the phenomena governing initial stages of growth. Owing to the analytical nature of the model, scaling laws of the process emerge, elucidating how the physical process parameters determine the island growth behavior.

This work presents, to the best of the authors' knowledge, the first analytical model for island growth mode ALD that accounts for randomly distributed nucleation sites on the substrate surface. This advancement enhances the accuracy of growth modeling and deepens our understanding of the process.

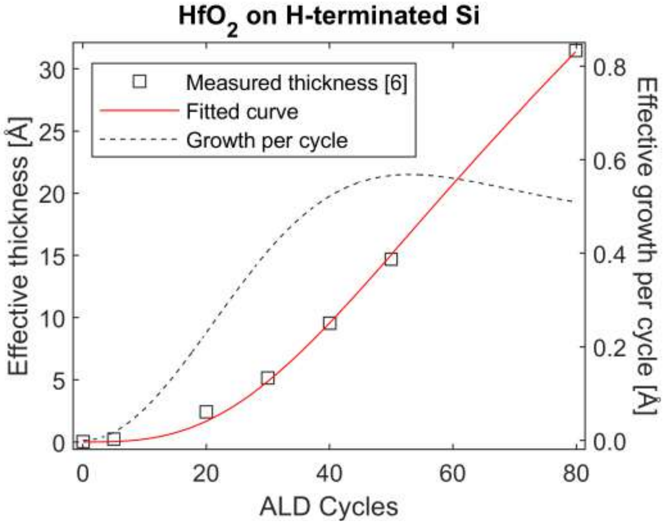

Fig. 1. Example of a model fit to experimental data. Effective thickness is the volume of the material deposited divided by the surface area of the substrate. Additionally, the effective growth per cycle, evaluated based on the model fit, is shown with a dashed line. The measurement data comes from Ref. [6], where the amount deposited was given in number of Hf atoms per unit area, measured using Rutherford Backscattering Spectrometry. Here, we scaled it assuming the density of HfO_2 as 9.68 g/cm^3.

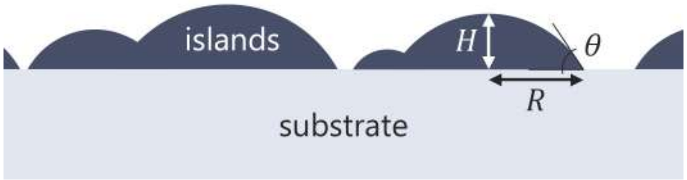

Fig. 2. Side-view schematic illustration of island growth modelled in the presented work. Notice, islands may have different heights H due to the spontaneous nucleation during the growth process. All islands have a spherical dome shape and due to substrate activation they may grow laterally at an enhanced rate, resulting in a contact angle $\theta \leq 90°$ and the radius $R \geq H$.

References

[1] R. L. Puurunen and W. Vandervorst, *J. Appl. Phys.*, **96**, 7686 (2004).
[2] E. V. Skopin, L. Rapenne, H. Roussel et al., *Nanoscale*, **10**, 11585 (2018).
[3] G. P. Gakis, C. Vahlas, H. Vergnes et al., *Appl. Surf. Sci.*, **492**, 245 (2019).
[4] Y. Wen, Y. Lan, H. Li et al., *J. Phys. Chem. C*, **128**, 9915 (2024).
[5] D. K. LaFollette, K. L. Canova, Z. V. Zhang et al., *J. Vac. Sci. Technol. A*, **40**, 023403 (2022).
[6] R. L. Puurunen, *J. Appl. Phys.* **95**, 4777 (2004).

On the fragmentation of Ni(II) β-diketonate-diamine complexes as molecular precursors for NiO films: a theoretical and experimental investigation

C. Invernizzi[1], **G. Tabacchi**[1,*], **R. Seraglia**[2], **M. Benedet**[2,3], **M. Roverso**[2,3], **C. Maccato**[2,3], **S. Bogialli**[2,3], **D. Barreca**[2,*], **E. Fois**[1]
[1] Department of Science and High Technology - Insubria University and INSTM, 22100 Como, Italy
[2] CNR-ICMATE and INSTM, Department of Chemical Sciences, Padova University, 35131 Padova, Italy
[3] Department of Chemical Sciences, Padova University and INSTM, 35131 Padova, Italy
e-mail: gloria.tabacchi@uninsubria.it; davide.barreca@unipd.it

Thin films and nanosystems based on NiO (Nickel Oxide), a prototype p-type transparent semiconductor featuring a good chemical stability and a wide band gap (E_{gap} = 3.5 eV), are critical materials for various technological applications, including resistive random-access memories, sensors, solar cells, displays and light-emitting diodes. Among the various preparation routes for the growth of NiO films/nanoarchitectures, Chemical Vapor Deposition (CVD) represents the favorable option thanks to its advantage to control material features under non-equilibrium conditions by a suitable choice of experimental parameters and starting precursors. On this subject, in our previous work [1,2] we have focused on the preparation and characterization of three different Ni(II) β-diketonate-diamine precursors, denoted $Ni(L)_2TMEDA$: $Ni(tfa)_2TMEDA$ (**1**), $Ni(fod)_2TMEDA$ (**2**), and $Ni(thd)_2TMEDA$ (**3**), where TMEDA stands for N,N,N',N'-tetramethylethylenediamine and L represents the β-diketonate ligands: tfa (Htfa = 1,1,1-trifluoro-2,4-pentanedione), fod (Hfod=2,2-dimethyl-6,6,7,7,8,8,8-heptafluoro-3,5-octanedione) and thd (Hthd = 2,2,6,6-tetramethyl-3,5-heptanedione), respectively. The results of a comprehensive experimental and theoretical investigation highlighted that these compounds offer several amenable characteristics as CVD precursors of NiO films with modular properties. In order to obtain more information regarding the reactivity of these precursors under the same reaction conditions, in the present work, the fragmentation behavior of the three Ni(II) β-diketonate-diamine complexes (1, 2 and 3), is investigated by electrospray ionization-high resolution mass spectrometry (ESI-HRMS), ESI-MS^n experiments and theoretical investigations.

Based on experimental data obtained through electrospray ionization-high resolution mass spectrometry (ESI-HRMS) and ESI-MS^n experiments [3], a detailed computational study based on density functional theory (DFT) calculations was performed [3], aiming to elucidate the molecular and electronic structure of $Ni(L)_2TMEDA$-derived fragments. The obtained data provides a valuable picture of the gas-phase fragmentation mechanism of such compounds as function of the ligand nature. Initially, the DFT approach was employed to optimize the molecular structures of the neutral complexes 1, 2 and 3. Calculations revealed that, in all three complexes, Ni exhibits a slightly distorted octahedral coordination environment with slight differences in some structure parameters (bond angles and distances). Nonetheless, both molecular geometry and electronic structure underlying the metal-ligand bonding scheme show a strong similarity in the three compounds. This result might rationalize the similar fragmentation behavior of the target complexes, in particular the presence of $[M-L]^+$ fragments (where M = $Ni(L)_2TMEDA$ and "-L" stands for the loss of one β-diketonate ligand) as the base peak in all the experimentally obtained ESI-HRMS spectra. Similar observations hold for the minimum energy structures calculated for such $[M-L]^+$ fragments, all characterized by very similar geometric arrangements and metal-ligand bonding schemes (square-planar geometry). This finding is supported by

Natural Bond Orbital (NBO) analysis performed on the electronic structure of the three fragments, which shows that all NBOs, localized on the metal-ligand bonds, have σ -character (single bond). Such a close similarity in the electronic structure suggests that all three ions possess an analogous stability and may all easily form in ESI-HRMS conditions. A useful feature of NBO analysis is the opportunity to provide insights into the charge distribution within a given molecule. Indeed, upon fragmentation (from M to $[M-L]^+$), one can notice an evident electronic charge donation from L and TMEDA to Ni due to the loss of a diketonate ligand. This result indicates that all $[M-L]^+$ species are stabilized by a strong electronic density donation from ligands towards Ni. Also MS^2 spectra of the three cations presents common features, in particular the formation of $[M-L]^+$ - $NH(CH_3)_2$ species, obtained from the subsequent fragmentation of $[M-L]^+$. Theoretical calculations performed on these species revealed that also these cations have very similar geometries and Ni-ligands bonding patterns. Whereas the diketonate remains coordinated to Ni with both its O atoms, only one N atom (the one survived to the fragmentation) is linked to the metal center. Nevertheless, Ni maintains its nearly square-planar coordination geometry thanks to the interaction with a double C=C bond formed upon - $NH(CH_3)_2$ release. The loss of a $-CH_3CH_2N(CH_3)_2$ group was observed only for fluorinated $[M-L]^+$ species derived from 1 and 2. In these cations the bonding pattern around Ni is practically the same as in $[M-L]^+$ - $NH(CH_3)_2$ species. Further evidence of common features in the three complexes' fragmentation was obtained from Bader charges analysis. The latter revealed an electron displacement from ligands to the Ni center, whose positive charge is significantly depleted during the fragmentation, in line with the findings obtained from NBO analysis.

In conclusion, the gas-phase fragmentation mechanisms as a function of the ligand nature were evaluated both experimentally and computationally. The outcomes revealed common features in the fragmentation pattern of the target compounds: i) in the first-fragmentation, the three complexes yield analogous base-peak cations by losing a negatively charged diketonate moiety; in these cations, Ni-O and Ni-N interactions are stronger, and the Ni positive charge is lower, than in the parent neutral complexes; ii) the tendency of ligand electronic charge to migrate towards Ni further increases in the subsequent fragmentation, leading to the formation of a tetracoordinated Ni environment featuring an interesting cation-π intramolecular interaction.

References

[1] M. Benedet, D. Barreca, E. Fois, R. Seraglia, G. Tabacchi, M. Roverso, G. Pagot, C. Invernizzi, A. Gasparotto, A.A. Heidecker, et al., *Dalton Trans.*, **52**, 10677-10688 (2023)

[2] M. Benedet, C. Maccato, G. Pagot, C. Invernizzi, C. Sada, V. Di Noto, G.A. Rizzi, E. Fois, G. Tabacchi, D. Barreca, *J. Phys. Chem. C*, **127**, 22304-22314 (2023)

[3] C. Invernizzi, G. Tabacchi, R. Seraglia, M. Benedet, M. Roverso, C. Maccato, S. Bogialli, D. Barreca, E. Fois, *Molecules*, **29**, 642 (2024)

Advancing the *operando* study of ALD chemistry with time-resolved ambient pressure x-ray photoelectron spectroscopy

R. Jones[1,2,3], E. Kokkonen[1*], J. Schnadt[1,2,3]
[1]MAX IV Laboratory, Lund University, Lund, Sweden
[2]Division of Synchrotron Radiation Research, Department of Physics, Lund University, Lund, Sweden
[3]NanoLund, Lund University, Box 118, 221 00, Lund, Sweden
e-mail: esko.kokkonen@maxiv.lu.se

The cyclic nature of thin film growth using atomic layer deposition (ALD) provides an especially interesting testbed for extracting useful time-resolved information on the exact role of the surface states during the deposition process. Ambient pressure x-ray photoelectron spectroscopy (APXPS) allows acquiring such surface sensitive data on many ALD processes. Combining APXPS data acquisition with advanced time-resolved data analysis techniques enables obtaining accurate time-resolved data on the deposition mechanisms from the raw oscillatory surface data. By averaging data from several ALD cycles together it becomes possible to resolve information from the data even with low signal-to-noise ratio. Another advanced data analysis technique is treating it by using Fourier transform (FT) analysis which allows to focus only on the oscillating (changing) portion of the surface data.

Data averaging or FT approaches are commonplace in many techniques, but in XPS analysis, they have only seen limited use. Here, we apply these techniques to study the growth of TiO_2 using titanium(IV) isopropoxide (TTIP) and H_2O process, which is a well-understood and -studied method. The TiO_2 films were grown on Si substrates with native oxide. With APXPS we can make continuous XPS measurements on interesting surface core levels and plot such data as a function of time. After the initial deposition is done, the created film is thick enough to completely obscure the bulk signal when measuring XPS with high surface sensitivity. Therefore, in this so-called steady-growth regime, the XPS signals are completely reversible from one ALD cycle to another, allowing to sum together the data from many cycles in order to increase the signal-to-noise ratio, or to use FT methods.

This study focused on the Ti 2p, O 1s, and C 1s core levels which are all measured at a photon energy which yields high surface sensitivity. In addition, the Si 2p core level was used to confirm the disappearance of the bare substrate signal. We have recorded XPS continuously while pulsing the TTIP and H_2O precursor into the experimental setup with a specific pulsing pattern. The data from several ALD cycles was later averaged together, in order to probe weaker signals that are not typically visible in just one ALD cycle due to low statistics. In addition, by taking a special look into the gas phase products just above the substrate surface using XPS, it is possible to identify minority, short-lived, products that are not possible to detect with other methods. For example, we can identify residual water vapour signal after the TTIP half-cycle which coincides with a changed surface chemistry and is therefore at a slightly different binding energy. Furthermore, clear signals from the intact TTIP molecule from the -O-CH, methyl, and -OCH= components in the O 1s and C 1s regions can be seen.

The FT analysis allows us to further dive into the data to obtain more detailed information. For example, the FT analysis on the C 1s region only shows the components which oscillate with time, e.g. the methyl and -OCH= components which get adsorbed on the surface and removed with each TTIP water half-cycle, respectively. FT analysis neatly removes any surface contamination peaks from the C 1s region, because they are constant and do not oscillate with time. Similarly, the O 1s spectra show the TiO_2 peaks that oscillate out of phase with each other i.e. with each TTIP and H_2O pulse, respectively.

References

[1] R. Jones, et al., *Surface Science*, **753**, 122656 (2025)
[2] J. Knudsen, et al., *Nature Communications*, **12**, 6117 (2021)
[3] E. Kokkonen, et al., *Review of Scientific Instrumentation*, **93**, 013905 (2022)

Experimental verification of kinetic growth model of ALD TiO_2 using Titanium isopropoxide and water

M. Pecz, A. Seifertová, and B. Hudec
Institute of Electrical Engineering, Slovak Academy of Sciences, 841 04 Bratislava, Slovakia
e-mail: boris.hudec@savba.sk

In Atomic layer deposition (ALD), thin films are grown by two or more alternating chemical reactions. Alternation of different precursors, substituted by purging steps separates and self-limits these processes. Pulse and purge timings are usually set in ways where saturation is achieved and further pulse time variation would result in no change in growth. Expectation for process is normally to run in so called ALD window, a temperature range where growth per cycle (GPC) is more-less independent of temperature. Because of different reactor designs utilized, measured GPC values can vary wildly [2],[3]. Therefore it is very useful to have theoretical simulations, based on simple input parameters represented by condition on sample freed from factors of reactor geometry. A lot of models are however often working only under ideal conditions, and do not offer insides into all possible outcomes. Successful prediction of effective GPC and its character can save a lot of unnecessary experiments and trials and errors, especially with newly developed precursors. For this purpose, kinetic model utilized by M. Reinke [3] was used for TiO_2 deposition based on reaction of titanium isopropoxyde (TTIP) and water. The model describes all processes as reactions with Arrhenial factors, where molecules of both precursors can get adsorbed on surface in monoatomic layer. Each molecule has certain probability for desorption, or if both precursors meet, for synthesis of final material and emptying of reaction sides. The equations representing the model and its growth components are shown in Fig. 1a.

Model also predicts unwanted pyrolytical process in higher temperatures, where precursor decomposes and interacts with itself (TTIP molecule contains oxygen) to form TiO_2. This process is however supposedly responsible for apparently flat ALD window of the TTIP + H_2O process (Fig. 1b).

In this study, numerous experiments with varying temperatures, pulse times and purge times of TTIP and H_2O were conducted and measured using in-situ ellipsometry. Ellipsometry was used after every 50 ALD cycles and every process parameters were kept constant for 150 cycles. Results were quantitatively compared to verify the viability of the model. Beneq TFS-200 ALD tool was used for all of our experiments, equipped wih in-situ ellipsometer Film Sense FS-1.

All variation of parameters was conducted on already pre-grown ALD TiO_2 film of 20 nm, to eliminate the effects of nucleation, amorphous growth with lower GPC present during first 10 nm and and uncertainty of ellipsometry at lower thicknesses. As shown in Fig. 3 When TTIP pulses are prolonging , GPC grows linearly with time, with speed of this unsaturated growth dependent on temperature. Fig. 4 confirms, that to receive ALD window increasing amount of water must be added with cooler process. Reaction is both limited by amount of precursor and speed of reaction at 0.12s H_2O pulse.

This work was supported by national grants VEGA 2/0162/22 and APVV-20-0111.

References

[1] M. Ritala, et. al, Chem. Mater., vol. 5, no. 8, pp. 1174–1181, doi: 10.1021/cm00032a023.
[2] J. Aarik, et. al, Appl. Surf. Sci., vol. 161, no. 3–4, pp. 385–395, doi: 10.1016/S0169-4332(00)00274-9.
[3] M.Reinke, et. al J. Phys. Chem. C, vol. 120, no. 8, pp. 4337–4344, doi:0.1021/acs.jpcc.5b10529.

$$\frac{d\Gamma_{TTIP}}{dt} = \overbrace{J_{TTIP}s_{TTIP}\left(1-\frac{\Gamma_{TTIP}}{\Gamma^{0}_{TTIP}}\right) - k^{des}_{TTIP}\Gamma_{TTIP}}^{\text{precursor adsorption and desorption}} \overbrace{- k^{(2)}_{pyrolysis}\Gamma_{TTIP}^{2}}^{\text{pyrolytic decomposition}} \overbrace{- k_{hydrolysis}\Gamma_{TTIP}\Gamma_{H_2O}}^{\text{hydrolytic decomposition}}$$

$$\frac{d\Gamma_{H_2O}}{dt} = J_{H_2O}s_{H_2O}\left(1-\frac{\Gamma_{H_2O}}{\Gamma^{0}_{H_2O}}\right) - k^{des}_{H_2O}\Gamma_{H_2O} - k_{hydrolysis}\Gamma_{TTIP}\Gamma_{H_2O}$$

Fig.1. Differential equations of kinetic model [1] for TTIP and for H_2O

Γ- number of reaction sites,

k - arhenian reaction rate, J - flow of molecules,

s – sticking probability,

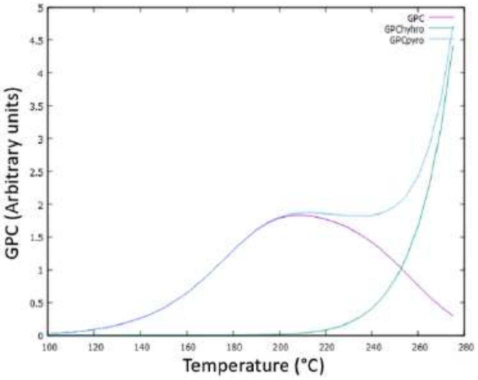

Fig.2 Division of total GPC to ALD and pyrolytic CVD component

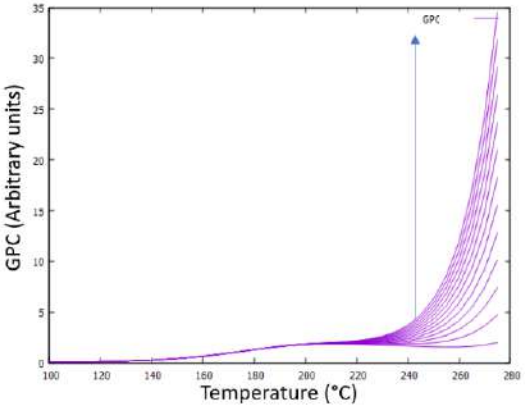

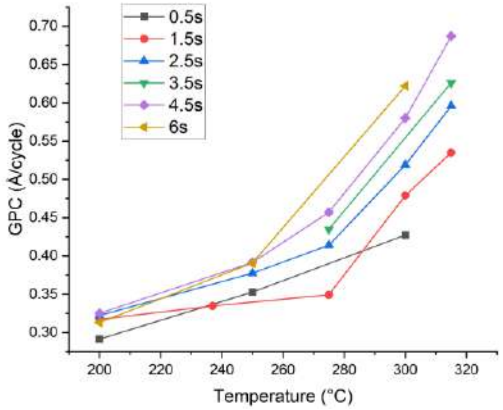

Fig. 3 **left** - Model prediction of GPC for growing TTIP pulse in arrow direction, **right** - Experimental GPC temperature curves with changing TTIP pulse. Both experiment and prediction shows unsaturated growth at higher temperatures

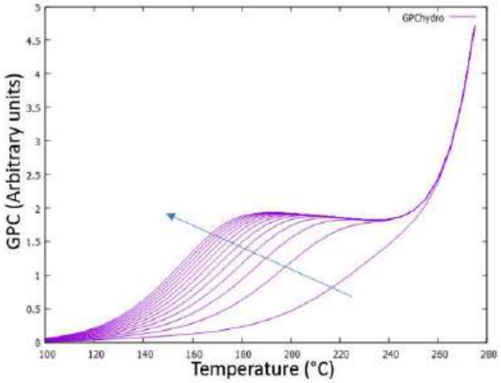

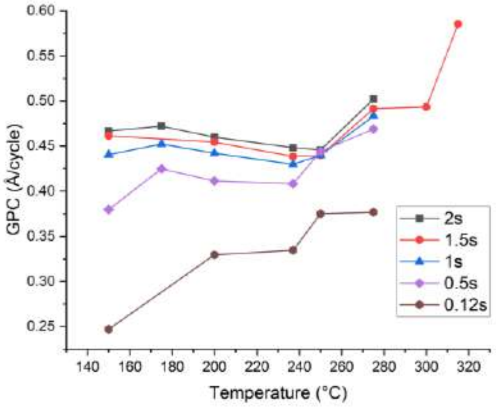

Fig. 4 **left -** Model prediction of GPC for growing H_2O pulse in arrow direction, **right -** Experimental GPC temperature curves with changing H_2O pulse. Both prediction and experiment show need for longer H_2O pulses, to stay in ALD window at lower temperatures.

Session AM_3.4 FUNCTIONAL MATERIALS II

Wednesday 4th June 2025 | 11.30-12.30

Chair: **Caroline E. Knapp** | Room “Coro di Notte”

On the epitaxial growth in ALD Co_3O_4- and NiO-based bilayers

R.T.M.. van Limpt[1*], C.A.A. van Helvoirt[1], M. Lao[2], M. Creatore[1,3], M.N. Tsampas[2], M.A. Verheijen[1,4]
[1]Eindhoven University of Technology, Department of Applied Physics and Science Education
[2]Dutch Institute For Fundamental Energy Research (DIFFER)
[3]Eindhoven Institute for Renewable Energy Systems (EIRES)
[4]Eurofins Materials Science Netherlands
e-mail: r.t.m.v.limpt@tue.nl

NiO and Co_3O_4 are versatile materials with applications in photovoltaics and chemical and electrical storage. Combining these materials is furthermore shown to benefit the aforementioned applications.[1-3] A key property influencing their performance in these domains is the crystal orientation in polycrystalline films and the associated atomic configuration at the surface. Typically, achieving texture, i.e. a preferential growth orientation, requires hetero-epitaxial growth on single-crystalline substrates, which are often incompatible with the application requirements.

This work[4] demonstrates a novel approach to texture control, through the combination of NiO and Co_3O_4 in heterostructures, retaining the possibility to work with more versatile substrates. ALD films prepared with cyclopentadienyl precursors and an oxygen plasma exhibit strongly textured <100> rock-salt NiO and <111> spinel Co_3O_4, both characterized by a columnar morphology. In the heterostructures, Co_3O_4 adapts its growth direction to align with the <100> texture of NiO, while NiO similarly mimics the <111> textured Co_3O_4 (Fig. 1, 2). XPS reveals that the films crystallize directly in their own stable crystal structure with corresponding metal atom coordination, while conforming to the crystal orientation of the template material.

Variations in the ALD process parameters of NiO reveal that the crystal orientation of NiO on *c*-Si is independent of the precursor or temperature but depends on the choice of co-reactant. Switching co-reactant from O_2 plasma to H_2O shifts the NiO texture from <100> to <111>. However, the epitaxial relation in the heterostructure is more sensitive to ALD parameters. Lowering the substrate table temperatures from 300°C to 150°C results in a partial loss of <111> texture, allowing <100> oriented grains to develop in thicker films. This effect is more pronounced for $Ni(^{t}Bu\text{-}MeAMD)_2$-based films as compared to $Ni(^{Me}Cp)_2$, potentially due to nitrogen impurities in the film. No epitaxial growth is observed for H_2O-based process.

The benefit of this approach was demonstrated for the oxygen evolution reaction, where the current density was doubled for the Co_3O_4/NiO stack as compared to the individual oxides (Fig. 3). This work therefore highlights an additional merit of ALD, beyond its well-established benefits of thickness control, precise composition tuning, and excellent uniformity and conformality, expanding the ALD toolbox to include crystallographic control, opening new opportunities for the design and engineering of thin films.

This work was supported by the SCALE project SCALE Project (No. NWA.1237.18.001)

References

[1] R.T.M. van Limpt, M. Lao, M.N. Tsampas and M. Creatore *Advanced Science* **11** 2405188 (2024)
[2] J. Zhang, J. Qian, J. Ran, P. Xi, L.Yang, and D. Gao *ACS Catalysis* **10** 12376-12384 (2020)
[3] C. Lou, H.; Pan. H. Mei, G. Lu, X. Liu, J. Zhang *Chemical Engineering Journal* **448** 137641 (2022)
[4] R.T.M. van Limpt, C.A.A. van Helvoirt, M. Creatore, and M.A. Verheijen J*ournal of Materials Chemistry A,* submitted

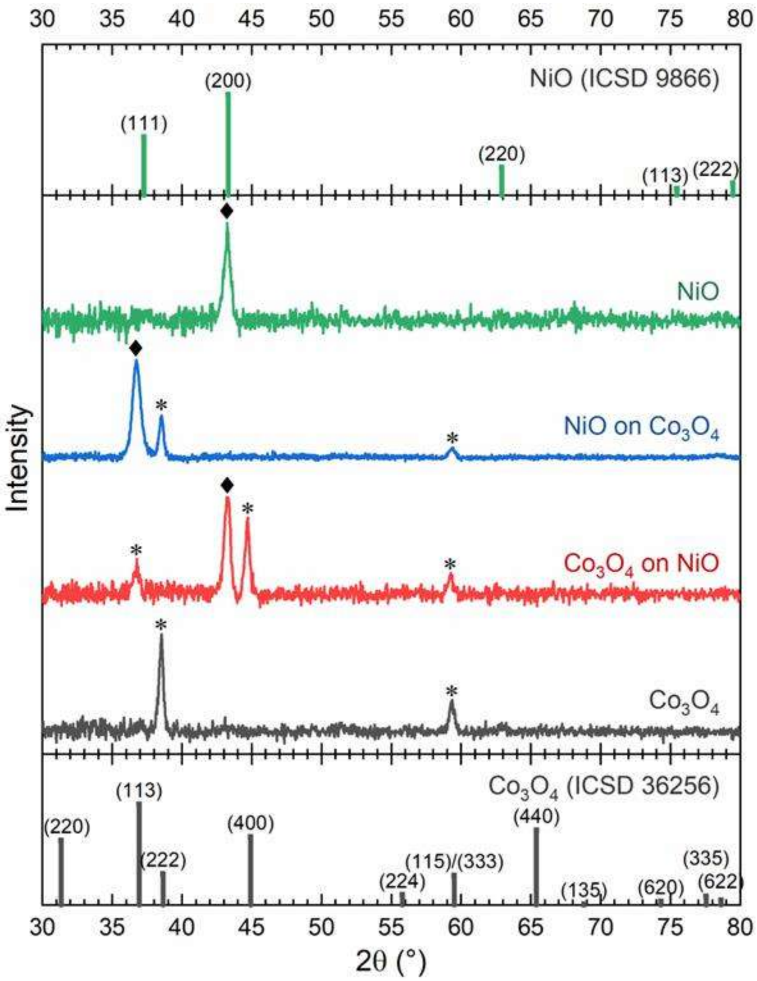

Fig. 1. Gonio X-ray diffractograms of NiO, Co_3O_4, NiO/Co_3O_4 and Co_3O_4/NiO stacks. Peaks associated with the NiO rock salt structure are indicated by ♦ and peaks associated with the spinel phase of Co_3O_4 by *. ICSD reference measurements of both NiO and Co_3O_4 are provided.

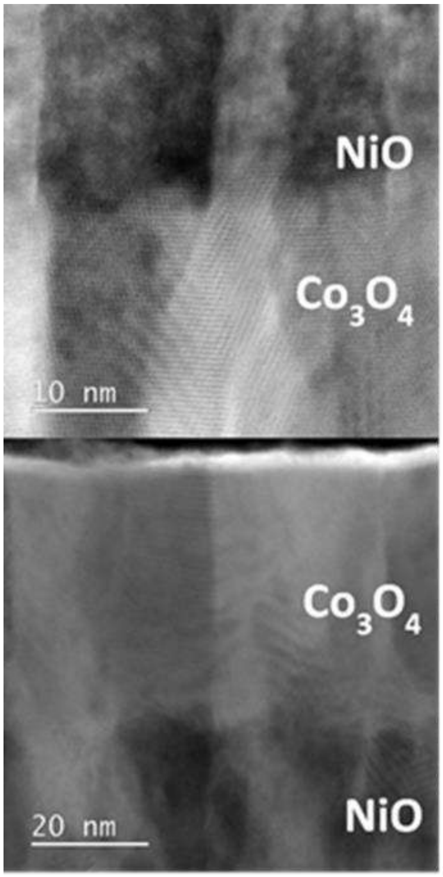

Fig. 2. Complementary cross-sectional bright-field scanning transmission electron microscopy images of both stacks, showing the continuation of the crystals across the interface.

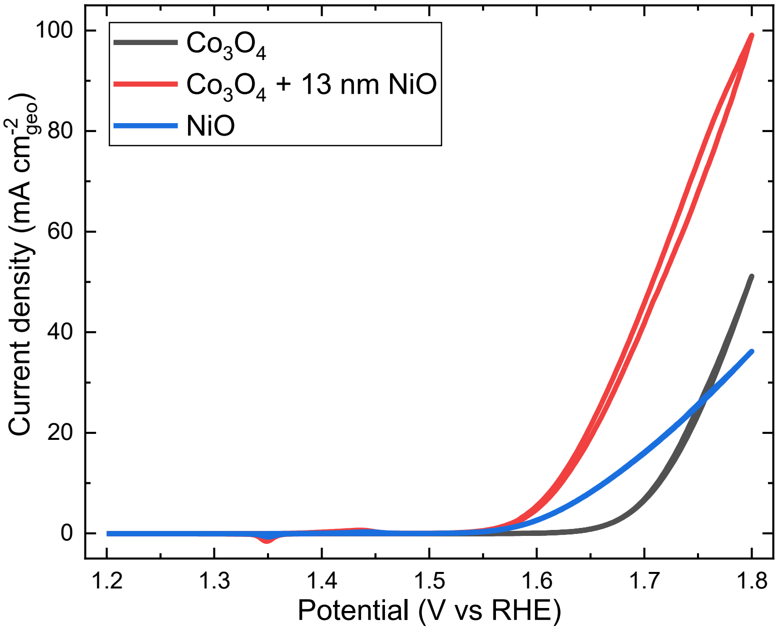

Fig. 3. Cyclic voltammetry data of activated NiO, Co_3O_4 and NiO on Co_3O_4 on FTO in 1M KOH showing the enhanced Oxygen Evolution Reaction activity for the stack as compared to the single oxide layers.

Atomic layer deposition of crystalline NiS thin films from elemental sulphur

J. Linjala[1]**, Y. Singh**[1]**, G. C. Tewari**[1]**, T. Tripathi,**[2] **M. Karppinen**[1]

[1]Aalto University, Department of Chemistry and Materials Science
[2]Aalto University, Low Temperature Laboratory, OtaNano
e-mail: juha.linjala@aalto.fi

Historically, metal sulfide thin films have been one of the important targets in atomic layer deposition (ALD) research. In recent years the interest in ALD-grown metal sulphide films has increased especially due the development of sensors, solar cells, solar selective coatings, photodiode arrays, and photoconductors with many different application variations in (opto)electronics has garnered significant attention due to its metal-insulator transition in the hexagonal phase, making it a promising candidate for crit applications in catalysis, solar cells, supercapacitors, and batteries. Most ALD sulfide processes rely on H_2S owing to its high volatility and strong reactivity with metalorganic precursors.[1] However, incorporating H_2S in ALD poses significant challenges. H_2S is a flammable, corrosive, and toxic gas, and thus the design of an ALD reactor for hydrogen sulfide compatibility must be ensured.[3] Another drawback of the H_2S-based processes is their characteristically slow growth rates which leads to longer process times.[4] Hence, there is a clear demand for a new simple, yet efficient ALD process to produce highly crystalline NiS thin films.

Here we report a simple and efficient ALD process for the deposition of high-quality electrically conducting NiS thin films from nickel(II) acetylacetonate and elemental sulphur precursors to tackle the challenges discussed above. Although some early ALD processes utilized elemental sulphur instead of H_2S as the sulfur source,[4-8] to the best of our knowledge, no sulphur-based ALD processes have been reported for nickel sulfide films. All the depositions were carried out in a commercial flow type F-120 reactor manufactured by ASM Microchemistry Ltd (Espoo, Finland). The sublimation temperature of sulphur was set to 120 ^{o}C and for nickel(II) acetylacetonate to 160 ^{o}C. The precursor vapors were consecutively pulsed into the reactor while high purity (99.999%) nitrogen was used as a carrier and purging gas. We used commercially available precursors: elemental sulfur from Sigma-Aldrich (purity 99.999%) and nickel(II) acetylacetonate from Merck-Schuchardt. The pulse length varied between 3 to 11 s for nickel(II) acetylacetonate and between 4 to 7 s for elemental sulphur, while the purge length varied between 4 to 15 s.

Crystallinity and phase composition of the films were investigated with grazing incidence X-ray diffractometer (GIXRD) (Rigaku SmartLab X-ray diffractometer; CuK α radiation). The same diffractometer was used for the XRR measurements. GIXRD pattern of NiS is displayed with a reference in Fig. 1a. The sharp peaks manifest the high degree of crystallinity of the films. No impurity peaks were seen. The XRR pattern, seen in Fig 1.b., shows a fringe pattern even for a sample which was deposited at high temperature. This is an interesting observation as e,g, for copper sulphide films deposited from elemental sulphur no fringes were seen.[4] This observation implies that the surface of our thin films is smoother compared to the copper sulphide films reported in our previous study.[4]

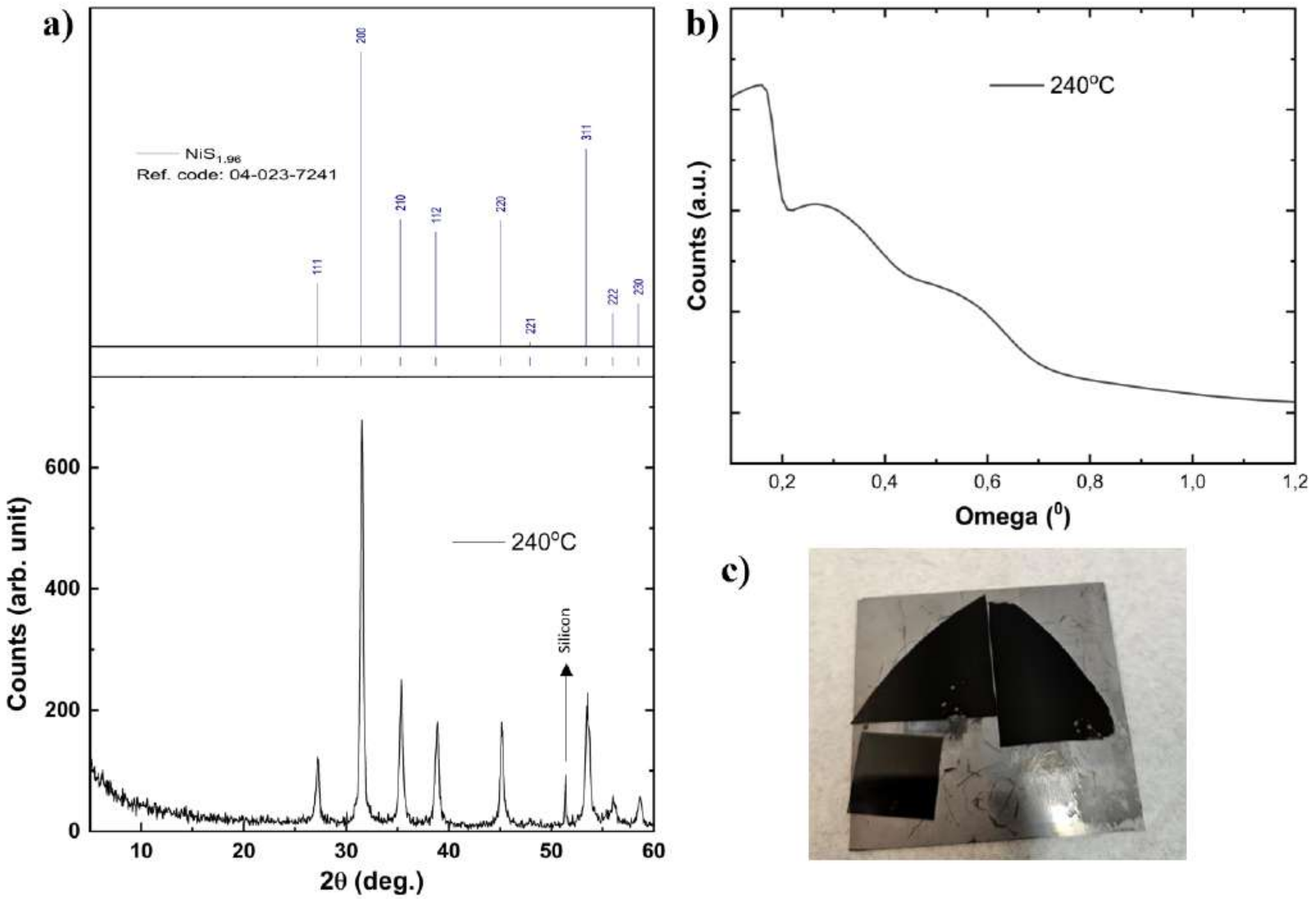

Fig. 1. a) GIXRD patterns for the nickel sulphide thin films deposited at 240 °C. Above reference for $NiS_{1.96}$.[9] b) XRR pattern for the nickel sulphide thin films deposited at 240 °C. c) Image of the nickel sulphide thin film samples.

References

[1] N. P. Dasgupta, X. Meng, J. W. Elam, A. B. F. Martinson, *Accounts of Chemical Research*, **48**, 341-348 (2015).

[2] R. Singh, M. M. Ayyub, *ACS Applied Electronic Materials*, **3**, 1912-1919 (2021).

[3] N. P. Dasgupta, J. F. Mack, M. C. Langston, A. Bousetta, F. B. Prinz, *Review of Scientific Instruments*, **81**, 044102 (2010).

[4] T. S. Tripathi, J. Lahtinen, M. Karppinen, *Advanced Materials Interfaces*, 5, 1701366 (2018).

[5] W. Faschinger, P. Juza, S. Ferreira, H. Zajicek, A. Pesek, H. Sitter, K. Lischka, *Thin Solid Films*, **225**, Issues 1-2, 270-274 (1993).

[6] T.Tadokoro, S. Ohta, T. Ishiguro, Yukio Ichinose, S. Kobayashi, *Journal of Crystal Growth*, **148**, Issue 3, 223-231 (1995).

[7] Yu. K. Ezhovskii, N. V. Zakharova, *Russian Microelectronics*, **45**, 18-25 (2016).

[8] Yu. K. Ezhovskii, N. V. Zakharova, *Physical Chemistry of Surface Phenomena*, **90**, 647-651 (2016).

[9] R. Otero, J.L.M. de Vidales, C. De las Heras, *Journal of Physics: Condensed Matter*, **10**, 6919, (1998).

ALD of epitaxial Ga_2O_3 thin films on c-plane sapphire

A. Séguret [1, 2,*], **I. Jellal** [1], **M. Weber** [1], **H. Roussel** [1], **I. Gélard** [1], **H. Okuno** [3], **L. Rapenne** [1], **E. Sarigiannidou** [1], **E. Monroy** [2], **V. Consonni** [1].

[1]Université Grenoble Alpes, CNRS, Grenoble INP, LMGP, 38000 Grenoble, France
[2]Université Grenoble-Alpes, CEA, Grenoble INP, IRIG, PHELIQS, 38000 Grenoble, France
[3]Université Grenoble-Alpes, CEA, Grenoble INP, IRIG, MEM, 38000 Grenoble, France

*Corresponding author(s).

Email: andy.seguret@grenoble-inp.fr (A.Séguret)

With the increasing demand for power electronics, ultra-wide bandgap (UWBG) semiconductors such as diamond, AlN and Ga_2O_3 are emerging as strong contenders to obtain performance beyond the limits of SiC and GaN. Monoclinic β-Ga_2O_3 and orthorhombic κ-Ga_2O_3 are particularly interesting, with a 4.9 eV bandgap energy and a high breakdown electric field, which leads to large figures of merit for power electronics [1]. Atomic Layer Deposition (ALD) as a self-limiting growth method, results in the elaboration of conformal thin films with low surface roughness, using a low thermal budget. In contrast to other vapor phase deposition techniques, the ALD of Ga_2O_3 has been much less explored and studies have mainly been limited to the use of precursor combinations such as trimethylgallium (TMGa) & ozone (O_3) or triethylgallium (TEGa) & oxygen (O_2) plasma [2–4]. In particular, the ALD of Ga_2O_3 using TEGa and O_3 precursors has not yet been thoroughly investigated on the substrates that are widely used in the semiconductor industry.

In this study, Ga_2O_3 thin films are grown by ALD on sapphire(0001) in the temperature range from 150°C to 450°C using TEGa and O_3 precursors. The ALD window is found to lie between 250°C and 400°C, with a growth rate of approximately 0.4 Å/cycle. The number of cycles is varied between 400 and 2000 to tune the thickness of Ga_2O_3 thin films in the range from 16 nm to 80 nm.

The surface morphology of the films and its dependence on the deposition temperature and number of cycles is determined using atomic force microscopy (AFM). The crystalline structures of the films are investigated by performing Raman spectroscopy and X-ray diffraction (XRD) measurements. XRD data indicates that Ga_2O_3 films grown at temperatures below 300°C are amorphous, whereas those grown between 300°C and 350°C show a start of the crystallization process. In contrast, XRD θ-2θ scans of Ga_2O_3 films grown on sapphire in the 350-400°C range show clear and sharp diffraction peaks that can be attributed to either (-201)β-Ga_2O_3 or (002)κ-Ga_2O_3. In-plane XRD (φ-$2\theta_\chi$) is performed to further investigate the orientation relationship between the sapphire substrate and the Ga_2O_3 film, and determine the phase grown. Transmission electron microscopy (TEM) is also achieved to assess the crystalline quality of the films, as well as the nature of the interface between the substrate and the Ga_2O_3 layers. Finally, XPS measurements are collected on the samples in order to evaluate film quality and stoichiometry. These results show the high potential of ALD to obtain epitaxial Ga_2O_3 thins films with a high crystalline quality at relatively low temperatures.

This work was supported by the Université Grenoble Alpes via the IRGA-DEFI2 grant.

References

[1] Zhou H, Zhang J, Zhang C, Feng Q, Zhao S, Ma P and Hao Y 2019 A review of the most recent progresses of state-of-art gallium oxide power devices *J. Semicond.* **40** 011803

[2] Rafie Borujeny E, Sendetskyi O, Fleischauer M D and Cadien K C 2020 Low Thermal Budget Heteroepitaxial Gallium Oxide Thin Films Enabled by Atomic Layer Deposition *ACS Appl. Mater. Interfaces* **12** 44225–37

[3] Comstock D J and Elam J W 2012 Atomic Layer Deposition of Ga2O3 Films Using Trimethylgallium and Ozone *Chem. Mater.* **24** 4011–8

[4] Allen T G and Cuevas A 2015 Plasma enhanced atomic layer deposition of gallium oxide on crystalline silicon: demonstration of surface passivation and negative interfacial charge *physica status solidi (RRL) – Rapid Research Letters* **9** 220–4

Atomic Layer Deposition of Hard Epitaxial $(Cr_{1-x}Al_x)_2O_3$ Thin Films on Sapphire.

M. Salari Mehr, Lauri Aarik, Taivo Jõgiaas, Aarne Kasikov, Hugo Mändar
University of Tartu, Institute of Physics, W.Ostwald Str.1, 50411, Tartu, Estonia
e-mail: mahtab.salari.mehr@ut.ee

Aluminum oxide (Al_2O_3) and chromium oxide (Cr_2O_3) are well-known ceramic materials due to their corrosion and wear resistance, high mechanical hardness, and good diffusion barrier properties. The polymorphs eskolaite (α-Cr_2O_3) and corundum (α-Al_2O_3) share an isostructural crystal structure with minor differences in the unit cell parameters. These thermodynamically stable materials could be valuable for fundamental research and technological applications. One approach to improve the properties (e.g. mechanical properties) of the oxide films is using a suitable dopant element for composition of composite or ternary coatings [1-4]. Thin films in epitaxial form are essential in advancing various applications across electronics, optoelectronics, and magneto-optics [5,6]. This study presents the results of characterization of ternary chromium-aluminium oxide films ($(Cr_{1-x}Al_x)_2O_3$) in thickness range from 33 to 80 nm that were deposited at 275 °C on c- and r-plane α-Al_2O_3 substrates by atomic layer deposition (ALD) using ALD cycle formula of [n (Cr(thd)$_3$-O_3) + (TMA-O_3), $n = 0$ to 75]. X-ray diffraction analysis (Fig. 1 a and b) confirmed the textured epitaxial structure of ternary films showing reflection peaks following atomic planes of eskolaite when the atomic ratio x (Al/(Al+Cr)) was in the range of 0.68 to 0.29. The films with $x \geq 0.74$ were amorphous. Epitaxial quality of ternary films was characterized by XRD omega scan analysis that showed full width at half maximum (FWHM) in the range of 0.8° to 0.2°for 006 reflection from films deposited on c-plane sapphire and of 2.0° to 0.2° for 024 reflection from films deposited on r-sapphire, when x was in the range from 0.29 to 0.68. The density of the films was measured using X-ray reflectivity (XRR) showing the increase from 3.20 g/cm^3 to 4.69 g/cm^3 when the structure of the films changed from amorphous to textured epitaxial on both types of substrates. The nanoindentation hardness values at indentation displacement of 5 nm for $(Cr_{1-x}Al_x)_2O_3$ films with textured epitaxial structure was in the range of 21.1 to 27.3 GPa, depending on the composition of the films. For those ternary films with $x \geq 0.98$, the hardness was 12.3 GPa. Refractive index, and band gap energy values corresponding to the direct transition model were also influenced by chemical composition and structural changes of the $(Cr_{1-x}Al_x)_2O_3$ films. The band gap values changed from 5.5 eV for films with $x \geq 0.74$ to 4.4 - 4.2 eV when x was in the range of 0.68 - 0.29. This research suggest that precise control over the composition and structure of $(Cr_{1-x}Al_x)_2O_3$ films enables to tailor their properties, making them suitable for advanced protective coatings and applications in harsh environments.

This work was supported by the European Union and Estonian Research Council (grants TEM-TA31, PSG448, PRG753) and the Centre of Excellence in Sustainable Green Hydrogen and Energy Technologies (grant TK210U5).

References

[1] Y. He, E. Guo, F. Zhong, B. Fu, G. Cai, D. Zhang, C. Jiang, and F. Ren, *Ceram. Int.,* **50,** 20367–20375 (2024).
[2] B. Nalcaci, and M. Polat Gonullu, *Appl. Phys.,* **127**, 460 (2021).
[3] M. Salari Mehr, L. Aarik, T. Jõgiaas, A. Tarre, A. Kasikov, K. Roosalu, and H. Mändar, *J. Alloys*

Compd., **968**, 172041 (2023).
[4] M. Salari Mehr, L. Aarik, T. Jõgiaas, A. Kasikov, J. Kozlova, L. Vidal, K. Mougin, and H. Mändar, *Ceram. Int.,* **50**, 50367-50376 (2024).
[5] W. Liu, and H. Wang, *J Materiomics,* **6**, 385-396 (2020).
[6] D. Sando, Y. Yang, C. Paillard, B. Dkhil, L. Bellaiche, and V. Nagarajan, *Appl. Phys. Rev.,* **5**, 041108 (2018).

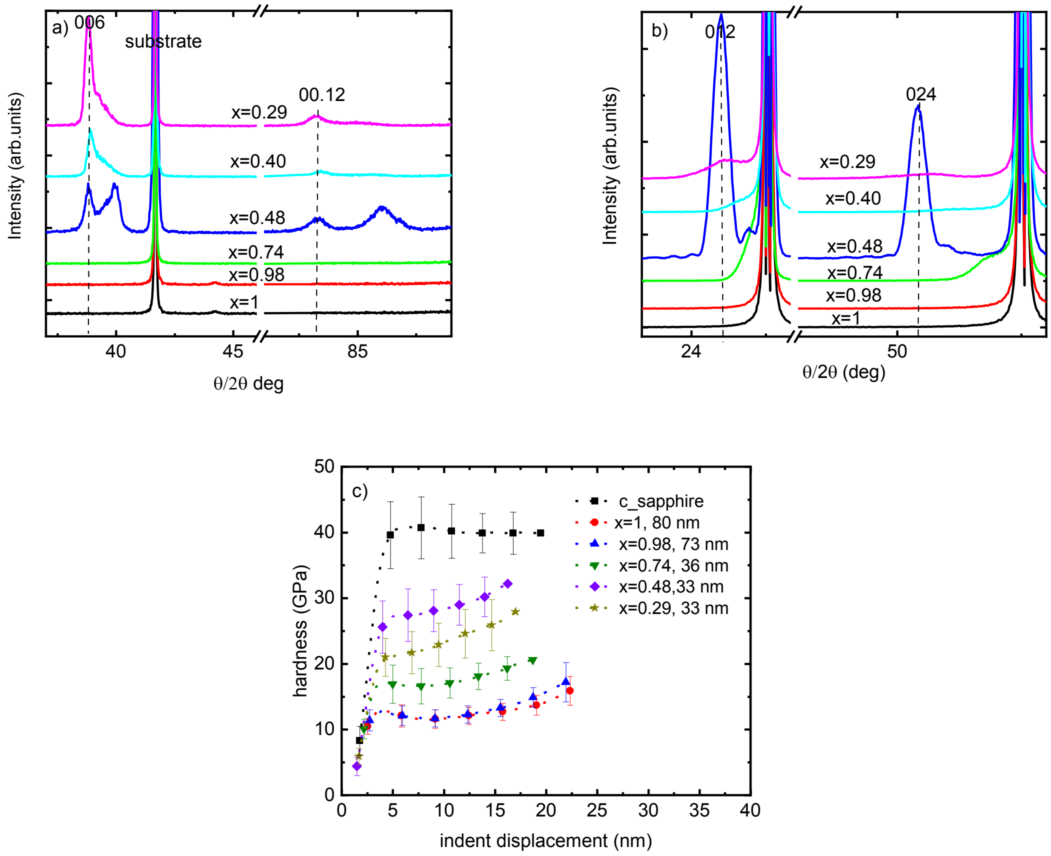

Fig. 1. High-resolution X-ray diffraction (HR-XRD) patterns of ternary $(Cr_{1-x}Alx)_2O_3$ films on a) c-plane sapphire and b) r-plane sapphire. The reflections are indexed by atomic planes of the eskolaite. c) mean values of hardness in the variation of indent displacement for films on c-plane sapphire substrate under the applied indentation load of 500 μN. The atomic ratio of Al/(Al+Cr) is denoted by *x*.

Session AM_4.1 C/N-BASED MATERIALS

Thursday 5th June 2025 | 8.30-10.30

Chair: **Ivo Utke** | Main Hall “Santo Mazzarino”

Conformal CVD of boron carbide onto carbon nanotubes

H. Pedersen*, A. H. Choolakkal, J. Birch
Linköping University, Department of Physics, Chemistry and Biology, Linköping, Sweden
e-mail: henrik.pedersen@liu.se

The discovery of graphene has significantly accelerated research into the synthesis of various 2D electronic materials such as WS_2, h-BN and MoS_2. The remarkable electronic and mechanical properties of graphene have had a profound impact on various fields since its discovery in 2004. The intrinsic zero-band gap nature of pristine graphene limits its application in semiconductor technologies. On the other hand, rolled graphene, which forms carbon nanotubes (CNTs) shows great promise as a channel material for next generation transistor technology.

Boron carbide (B_xC) can form compounds such as B_2C, B_4C_3, BC and BC_3, which form structures ranging from three-dimensional icosahedral structures connected by C–B–C chains, to two-dimensional (2D) allotropes. 2D boron carbides are predicted to exhibit a range of electronic behaviors from metallic to semiconducting, depending on the stoichiometry and bonding. B_xC could thus offer new possibilities to build conductor/semiconductor interphases with carbon nanotechnology. Given the potential application of rolled graphitic materials in the next generation field effect transistor (FET) technology, the synthesis of B_xC in a tubular fashion is particularly promising. The hexagonal lattice of graphitic boron carbide (g-BC_x) offers possible epitaxial growth over rolled graphene, which could facilitate the growth. This would allow for fabrication of either coaxial architecture with few walled carbon nanotubes (FWCNT) or the growth of a tubular g-BC_x structure using single walled carbon nanotubes (SWCNT) as a template.

This contribution will describe our explorations on conformal CVD of B_xC onto freestanding CNT membranes. We utilize a newly discovered CVD process where a heavy inert gas is used to enhance the step-coverage of the film.[1] We use tirethylboron ($B(C_2H_5)_3$) as a single source precursor for the boron carbide with a co-flow of xenon (Xe) to enhance the conformality of the process. We have discovered two process windows for the deposition; in the mass-transport-limited regime at 550 °C we can deposit B_4C, and in the thermodynamics-limited regime at 1000 °C we can deposit graphitic BC_3. For both processes, we see a fully conformal deposition, see Fig. 1 below for an example from the 550 °C process. The deposited B_xC coats the CNTs uniformly without clustering or clogging the pores between the CNTs. XPS, Raman spectroscopy and Electron diffraction measurement collectively show that the deposition of B_xC films does not cause any structural modification to the CNT lattice. Instead, the B_xC adds an additional layer around the CNTs in a coaxial fashion.

We believe that this conformal deposition process of B_xC on CNT membranes provides new possibilities to modify both the electrical- and mechanical properties of CNT membranes.

This work was supported by the Swedish research council (VR) under contract 2018-05499, and by the Swedish Government Strategic Research Area in Materials Science on Advanced Functional Materials at Linköping University (Faculty Grant SFO-Mat-LiU No. 2009-00971). Canatu Oy is gratefully acknowledged for providing the CNT membranes.

References

[1] A. H. Choolakkal, P. Niiranen, S. Dorri, J. Birch, and H. Pedersen, *Nat. Commun.* **15**, 10667 (2024).

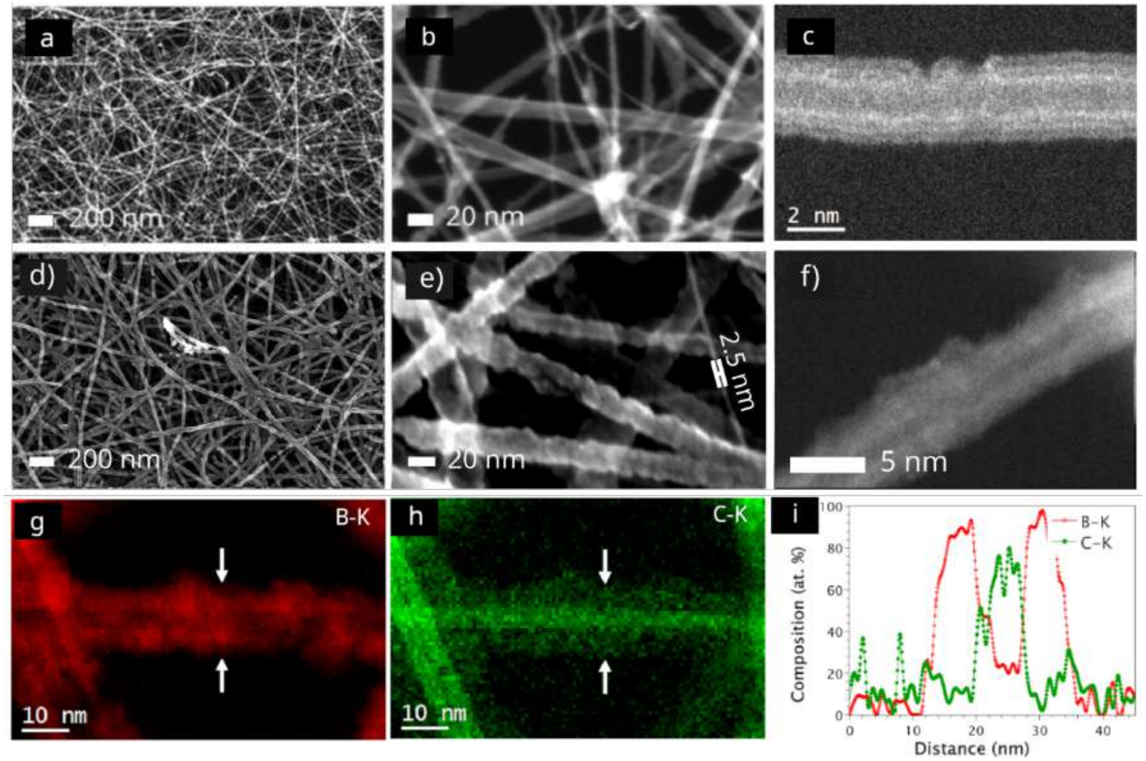
a
200 nm
b
20 nm
c
2 nm
d)
200 nm
e)
2.5 nm
20 nm
f)
5 nm
g
B-K
10 nm
h
C-K
10 nm
i
B-K
C-K
Composition (at. %)
0
20
40
60
80
100
0
10
20
30
40
Distance (nm)

Fig. 1. *a-b) SEM micrographs showing a pristine CNT membrane. c) ADF STEM image of a single CNT. d)-e) SEM images showing uniform deposition of a thin film on the CNT membrane. f) ADF STEM image showing a CNT after CVD. g) EELS B-K map. h) EELS C-K map. i) EELS line scans across the* B_4C *deposited CNT indicated by white arrows.*

Investigation of the Chemical Vapor Deposition of Boron Nitride using borazine

C. Marichy[1,*], **T. Souvignet**[1], **B. Toury**[1], **C. Journet**[1]
[1]Universite Claude Bernard Lyon 1, CNRS, LMI UMR 5615, Villeurbanne, F-69100, France.
e-mail: catherine.marichy@univ-lyon1.fr

Boron nitride (BN) has been identified as an excellent candidate for current and future electronic devices. During the last decade, sp^2-hybridized BN is proving to be a key material for future graphene-based optoelectronic devices due to its insulating properties and small lattice mismatch with graphene.[1,2] Recently, amorphous BN (aBN) has attracted much interest as it has been shown to exhibit an ultra-low dielectric constant of 1.16, whereas a value of 4.0 at 1MHz is observed for hexagonal BN.[3] Furthermore, the feasibility of an ultra-low k and ultra-thin aBN film (k=2 for a 3nm-thick layer) as a new capping layer for copper interconnects has been demonstrated.[4] However, to fully exploit BN's potential in electronics, optoelectronics, and spintronics, its structure and thus properties need to be tailored.[5]

Among the various deposition techniques, chemical vapor deposition (CVD) is widely used to deposit thin films from various precursors. Borazine ($B_3N_3H_6$), a volatile compound with a 1:1 boron-to-nitrogen ratio, has been extensively used for CVD of BN films, as it overcomes stoichiometric issues and enables efficient fabrication of sp^2-BN films. However, the mechanism involved and the effect of the CVD parameters (deposition parameters, substrates…) on the structure and quality of the BN films remain poorly understood.

In this study, borazine BN films were deposited on native oxide Si wafers by CVD under different conditions (temperature, flux, type of carrier gas...) in the range 400 °C - 1350 °C. The films were characterized by complementary means such as ellipsometry, XRD, SEM, EDS, TEM, XPS and Raman and infrared spectroscopy. The effect of the different growth parameters on the final material is discussed. In particular, the borazine flux and the deposition temperature strongly influence the properties of the films in terms of morphology, crystallinity and bonding. The results suggest the existence of two competing reactions that strongly influence the deposition mechanism: borazine polycondensation into oligomers and decomposition into reactive species such as BH_3 and NH_3. Depending on the CVD conditions, one of these reactions predominates, influencing the deposition mechanism and the resulting material. In this contribution a reaction mechanism is proposed.

This work was supported by the project MINERVA - ANR-21-GRF1-0002, FLAG-ERA JTC 2021 - 2021

References

[1] K. K. Kim et al., *ACS Nano*, **6**, 8583–8590 (2012).
[2] T. Niu et al., *Progress in Surface Science,* **90**, 21-45 (2015).
[3] S. Hong et al., *Nature*, **582**, 511–514 (2020).
[4] C.M. Lin et al. *Advanced Materials Technologies*, **7**, 2200022 (2022).
[5] A. Antidormi et al., *Nano Mater. Sci.*, **4**, 10-17 (2022).

Low-Temperature Atomic Layer Deposition of Boron Nitride using the In-Situ Decomposition of Ammonium Carbamate

A. Álvarez-Yenes[1,*], **V. O. Koroteev**[1], **M. Knez**[1,2]
[1]CIC nanoGUNE. 20018 San Sebastián, Spain
[2]IKERBASQUE, Basque Foundation for Science. 48011 Bilbao, Spain
e-mail: an.alvarez@nanogune.eu

Boron nitride (BN) is a binary compound of boron and nitrogen, alternatively linked, which can exist in multiple crystalline forms, all of them analogous to the carbon allotropes. These forms exhibit unique properties that make BN highly valuable for a wide range of applications, particularly in nanotechnology. ALD has been used to deposit BN thin films by using boron halogenides and ammonia (NH_3) as precursors at high temperatures (400 and 750°C) [1-3]. High growth temperatures allow for higher structural order but limit the range of usable substrates.

In this work, we introduce a new atomic layer deposition (ALD) process for low-temperature growth of amorphous boron nitride thin films at temperatures as low as 100-275°C. The process utilizes carbamic acid, a highly reactive intermediate species formed during the decomposition of ammonium carbamate, as the nitrogen source. Ammonium carbamate, a solid and easily handled material, eliminates the need for NH_3, a toxic, corrosive, and difficult-to-detect gas that poses safety risks in many laboratories. The use of ammonium carbamate introduces carbamic acid (H_2NCOOH) as a stable intermediate species during the decomposition process, which, combined with boron tribromide (BBr_3), enables BN growth at significantly reduced temperatures (100–275°C). This reduction in temperature expands the range of compatible substrates and applications.

X-ray reflectivity measurements demonstrate a constant growth per cycle and the self-limiting nature of the ALD reactions across the studied temperature range. The deposited thin films were characterized by means of X-Ray photoelectron spectroscopy (XPS) and electron energy loss spectroscopy (EELS), among other techniques, to confirm that the deposited material is amorphous boron nitride with a 1:1 stoichiometry. Calculations showed that the lowering of the deposition temperature is linked to the formation of carbamic acid as an intermediate species during the decomposition of ammonium carbamate.

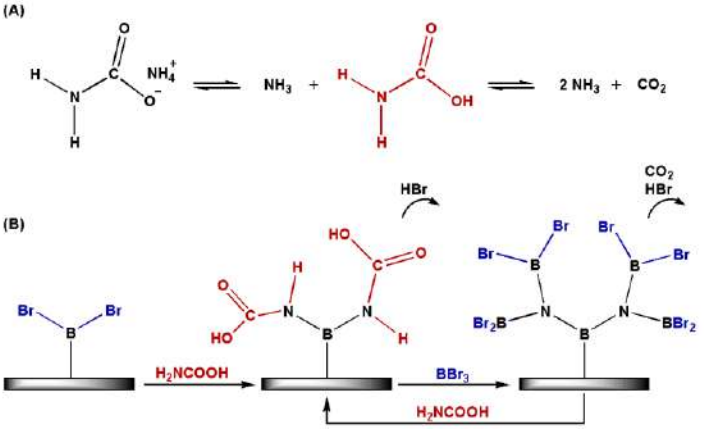

Fig, 1. Schematic of the reactions taking place during the deposition process. (A) Decomposition of ammonium carbamate. (B) ALD-growth of BN from BBr_3 and carbamic acid.

References

[1] J. D. Ferguson, A. W. Weimer, and S. M. George, *Thin Solid Films*, **413**, 16–25 (2002)

[2] B. Mårlid, M. Ottosson, U. Pettersson, K. Larsson, and J. O. Carlsson, *Thin Solid Films*, **402**, 167–171 (2002)

[3] M. Weber, B. Koonkaew, S. Balme, I. Utke, F. Picaud, I. Iatsunskyi, E. Coy, P. Miele and M. Bechelany, *ACS Appl Mater Interfaces*, **9**, 16669–16678 (2017)

Investigation of CVD-deposited $Ti_xW_{1-x}(C, N)$ hard coatings for cutting tool applications

L. Souqui[1], **S. Baserga**[1], **A. Hellgren**[1], **L. von Fieandt**[1,2], **P. Eklund**[1*]
[1]Uppsala University, SE-75120 Uppsala, Sweden
[2]AB Sandvik Coromant, SE-12679 Hägersten, Sweden
e-mail: laurent.souqui@kemi.uu.se

The lifetime of cutting tools for the machining of hard materials has been greatly improved with the development of protective hard coatings, therefore reducing manufacturing costs. Typically, transition metal carbides (e.g., WC, TiC), nitrides (e.g., TiN, WN) and carbonitrides (e.g., Ti(C, N))[1,2] are used as hard coatings due to their high mechanical strength (especially high hardness and elastic moduli) and these coating are commonly deposited at industrial scale by chemical vapor deposition. The focus of this work is on the development and improvement of W-based hard coatings on bulk cemented-carbide (WC-Co) tools. These coatings are of interest owing both to their high hardness as well as to the lattice match with the cemented-carbide substrate. In our previous work, we succeeded in depositing hexagonal tungsten carbonitride W(C, N), resulting in a combination of high hardness and high toughness.[3] However, the coatings exhibited a lower hardness than the commercially available TiN or Ti(C, N) coatings.

As such we propose to investigate the possibility of incorporating Ti into the W(C, N) lattice and its effect on the mechanical properties of the coatings. This presents a synthetic challenge since 1) an excess of Ti is expected to result in a cubic phase as often reported in $Ti_xW_{1-x}N$[4], 2) the ternary carbide $Ti_xW_{1-x}C$ is metastable, high-temperature phase[5] and 3) the process window for the synthesis W(C, N) by CVD is relatively narrow[3].

Here, our approach is to deposit $Ti_xW_{1-x}(C, N)$ coatings at 600-850 °C from the co-reaction of tungsten hexafluoride (WF_6) and titanium tetrachloride ($TiCl_4$) with acetonitrile ($N{\equiv}C{-}CH_3$) in a hot-wall CVD reactor on cemented-carbide tools. The thickness and morphology of the coating as well as the impact of the addition of $TiCl_4$ on the overall growth kinetics are evaluated by scanning electron microscopy. The compositional range of the hexagonal $Ti_xW_{1-x}(C, N)$ phase is obtained by a combination of X-ray diffraction and compositional analysis methods, namely X-ray photoelectron spectroscopy, Rutherford backscattering spectrometry and elastic recoil detection analysis. Finally, the influence of Ti on the mechanical behavior of the coating, especially hardness, Young modulus and toughness, are estimated by nano-indentation.

This work was supported by the Swedish foundation for strategic research (SSF) and the Knut and Alice Wallenberg Foundation.

References

1. Al-asadi, M. M. & Al-tameemi, H. A. A review of tribological properties and deposition methods for selected hard protective coatings. *Tribol. Int.* **176**, 107919 (2022).
2. Schalk, N., Tkadletz, M. & Mitterer, C. Hard coatings for cutting applications : Physical vs . chemical vapor deposition and future challenges for the coatings community. *Surf. Coat. Technol.* **429**, 127949 (2022).
3. Böőr, K., Lindahl, E., Fieandt, L. Von & Boman, M. On the growth kinetics, texture,

microstructure, and mechanical properties of tungsten carbonitride deposited by chemical vapor deposition. *J. Vac. Sci. Technol. A* **40**, 053101 (2022).

4. Ju, H. *et al.* Crystal structure and the improvement of the mechanical and tribological properties of tungsten nitride films by addition of titanium. *Surf. Coat. Technol.* **345**, 132–139 (2018).
5. Rudy, E. Constitution of Ternary Titanium-Tungsten-Carbon. *J. Less Common Met.* **33**, 245–273 (1973).

Boosting PEM electrolyser performance with niobium (oxy)nitride coating using Plasma-Enhanced ALD

A. Tzavara-Roussi[1], V. van Steijn[1], J. R. van Ommen[1]
[1]Delft University of Technology, Department of Chemical Engineering
e-mail: a.tzavararoussi@tudelft.nl

The increasing energy demands, due to population growth and rising living standards, coupled with the heavy reliance on fossil fuels, which are the predominant contributors of greenhouse gas emissions, intensify the urgency for energy transition. The aim of achieving carbon neutrality by 2050 has pushed forward a wider implementation of renewable sources. Green hydrogen has emerged as highly promising candidate to act as a buffer and store the excess energy generated by solar panels and wind turbines during their intermittent operation. [1,2,3]

Green hydrogen is produced via water electrolysis, represented by the reaction $2H_2O \rightarrow 2H_2 + O_2$, and utilizes renewable electricity to drive the non-spontaneous dissociation of water molecules (1.23V). Beside acting as a clean energy storage option with an energy density of 140MJ/kg, hydrogen functions as a versatile energy carrier and thus, can find application in multiple sectors; in fuel cells for transportation and in hard-to-abate industries, such as chemical production and steelmaking, as feedstock to produce synthetic fuels and decarbonise energy-intensive industrial processes. By integrating green hydrogen into the energy landscape, nations can minimise their carbon footprint while ensuring their energy security. [4,5]

The proton exchange membrane (PEM) water electrolyser is a key technology for green hydrogen production. The operating principle of the PEM cell begins with water introduction at the anode, where it permeates the porous transport layer (PTL) to reach the catalytic sites, where it undergoes oxidation producing oxygen gas and protons. Oxygen is directed to the outlet, while protons migrate through the -proton conductive- PEM, which is typically composed of a solid polymer electrolyte such as Nafion. These protons are subsequently reduced at the cathodic catalyst sites, forming hydrogen gas. PEM water electrolysers offer several advantages compared to the conventional alkaline electrolysers, including the high efficiency, the compact design and the rapid adaptability to an intermittent renewable electricity input. Furthermore, their ability to operate at higher current densities enables faster green hydrogen production rates. However, their competitiveness in large-scale applications depends on advancing their design by reducing and/or replacing scarce metals (e.g. platinum group metals) and extending its lifetime. Resolving these issues is essential to pave the way for the widespread commercialization of PEM water electrolysers. [4]

The PTL is an important component of the anodic side of a PEM electrolyser, that significantly influences its performance, durability and cost. Titanium, in form of powder, felt or mesh, is most commonly used due to its corrosion resistance, which is a crucial property for withstanding the harsh oxidative environment at the anode. This layer is responsible for the transport of water to the catalytic sites and the transport of oxygen gas to the flow plates for discharge, as well as providing an electrically conductive pathway for electron transfer. [6,7]

However, the PTL faces two critical challenges that impact their efficient operation and cost-effectiveness. The first challenge is the progressive growth of an oxide layer on the surface of titanium caused by the generated oxygen, which significantly reduces its electrical conductivity. To mitigate this challenge, a relatively thick coating of scarce metals, like platinum or gold, is commonly applied, but this increases further the manufacturing costs. The second challenge lies in the counter-current transport of two phases; liquid water and oxygen as dissolved gas and bubbles move in opposite directions through the porous network. This leads to the accumulation of oxygen gas within the pores of the PTL, obstructing water transport to the catalyst sites, which increases mass transport losses. This limitation becomes more pronounced at higher current densities due to the higher gas production, which is otherwise desirable for lowering the unit cost of hydrogen production. [6,7]

In this work, we demonstrate the deposition of niobium nitrides and oxynitrides by employing plasma-enhanced atomic layer deposition (PE-ALD) to fabricate an ultra-thin coating on the PTL surface to decrease the energy requirements of the cell. Niobium, as transition metal, is a valuable candidate to replace noble metals and as nitride it can promote the electron transfer to reduce ohmic losses by protecting the titanium substrate from oxidation and simultaneously being highly conductive itself. The niobium oxynitride coating provides the hydrophilicity to facilitate the water imbibition throughout the PTL, while accelerating the removal of oxygen bubbles to decrease mass transport losses. [8,9] We investigate how the elemental composition of the niobium oxynitride coating and its thickness influence the trade-off between its conductivity and hydrophilicity. In addition, we assess the impact of the PTL coating on the performance and stability of a 4cm^2 PEM cell.

This project receives a Dutch National Growth Fund contribution from the programme NXTGEN HIGHTECH.

References

[1] P.A. Owusu and S. Asumadu-Sarkodie, *Cogent Engineering*, **3(1)**, (2016)

[2] I. Perissi and A. Jones, *Sustainability*, **14(8)**, 4728 (2022)

[3] T, Capurso, M. Stefanizzi, M. Torresi and S.M. Camporeale, *Energy Conversion and Management*, **251**, 114898 (2022)

[4] S. Shiva Kumar and V. Himabindu, *Material Science for Energy Technologies*, **2(3)**, 442-454 (2019)

[5] B. S. Zainal, P. J. Ker, H. Mohamed, H. C. Ong, I. M. R. Fattah, S. M. Ashrafur Rahman, L. D. Nghiem and T. M. Indra Mahlia, *Renewable and Sustainable Energy Reviews*, **189(A)**, 113941(2024)

[6] E. Borgardt, O. Panchenko, F. J. Hackermueller, J. Giffin, M. Bram, M. Mueller, W. Lehnert and D. Stolten, *Journal of Power Sources*, **374**, 84-91 (2018)

[7] G. Stelmacovich and S. Pylypenko, *ChemElectroChem*, **11(20)**, e202400377 (2024)

[8] N.F. Daudt, A. D. Schneider, E. R. Arnemann, C. J. Scheuer, L.S. Dorneles and L. F. Schelp, *Journal of Materials Engineering and Performance*, **29**, 5174-5183(2020)

[9] X. Z. Wang, T. P. Muneshwar, H. Q. Fan, K. Cadien and J. L. Luo, *Journal of Power Sources*, **397**, 32-36 (2018)

Process Optimization of ALD TiN Thin Films for Superconducting Applications Using TFS-200 Reactor

Zahra Ahaliabadeh[1], Sanaz Zarabi[1], Ziying Wang[2], Peter Liljeroth[2], Otto Laitinen[1]
[1]Beneq Oy, Finland
[2]Aalto University, Department of Applied Physics, Finland
e-mail: sanaz.zarabi@beneq.com

Titanium nitride (TiN), a well-known transition metal nitride (TMN), is of high technological importance due to its superior electrical and mechanical properties, as well as its chemical and thermal stability. TiN has found applications in a variety of fields, including solar energy harvesting, energy storage and conversion devices, electrochemical devices, and barrier coatings. Its use at low temperatures in superconducting devices, such as microwave kinetic inductance detectors, microwave resonators, quantum bits, and tunnel junctions, has recently emerged, potentially opening up new possibilities in quantum technology (1,2).

In this work, we report the development of TiN thin films via thermal and plasma-enhanced atomic layer deposition (ALD) in a Beneq's TFS-200 reactor utilizing $TiCl_4$ and NH_3 as precursors. The effects of critical process parameters including deposition temperature, plasma power, and precursor pulse/purge durations on film quality were systematically investigated using spectroscopic ellipsometry. Particular attention was given to optimizing plasma-enhanced ALD conditions to achieve low impurity levels while maintaining uniform film thickness across large substrates.

The optimized TiN thin films were further evaluated for superconducting characteristics. Transmission electron microscopy (TEM) analysis was employed to examine the film thickness, while and four-point probe measurements were used to determine the film resistivity and superconducting transition temperature (Tc). Scanning tunneling microscopy (STM) was performed to analyze the superconducting gap and lattice morphology. These results provide insights into the interplay between ALD process parameters and the structural and electronic properties of TiN films, offering a scalable pathway for integrating high-quality TiN thin films into quantum devices.

References

[1] Mahajan, Ujjwal, Mahesh Dhonde, Kirti Sahu, Pintu Ghosh, and Parasharam M. Shirage. "Titanium nitride (TiN) as a promising alternative to plasmonic metals: a comprehensive review of synthesis and applications." *Materials Advances,* ***5,*** 846-895, (2024).

[2] Torgovkin, Andrii, Saumyadip Chaudhuri, Aki Ruhtinas, Manu Lahtinen, Timo Sajavaara, and I. J. Maasilta. "High quality superconducting titanium nitride thin film growth using infrared pulsed laser deposition." *Superconductor Science and Technology* **31**, no. 5 (2018)

Mitigating blistering in TaC_xN_{1-x} prepared by plasma-enhanced ALD for quantum technologies

S. A. Peeters[1], A. A. de Jong[1], G. F. K. Krieger[1], R. Bărbuceanu[1], W. M. M. Kessels[1], H. C. M. Knoops[1,2]
[1]Eindhoven University of Technology
[2]Oxford Instruments Plasma Technology
e-mail: s.a.peeters@tue.nl

Blistering is detrimental in the synthesis of superconducting metal nitrides by plasma-enhanced atomic layer deposition (PEALD) for quantum technologies. This work develops strategies to mitigate blistering while maintaining a high film quality. Blistering is typically ascribed to stress relief as a result of energetic ion bombardment and hydrogenation. In ALD this problem is generally not considered, with the exception of Al_2O_3 films involving a large amount of trapped hydrogen [1]. However, blistering becomes more prominent in the preparation of conductive nitrides by PEALD, which often requires H-containing plasmas. Moreover, ion bombardment during PEALD has the capability to drastically improve film quality, but also induces high compressive stress [2,3]. In quantum processor components, both the required film thickness of tens to hundreds of nanometers and removal of the lossy native oxide interface further promote blistering. Hence, mitigation strategies are key to establish PEALD of superconducting nitrides in the quantum field.

In this work, TaC_xN_{1-x} films were grown on HF-treated Si by PEALD with substrate biasing for ion energy control during Ar/H_2 plasma exposure. Energetic ion bombardment induces up to -2.5 GPa compressive stress for the most conductive film at which blisters are observed (Fig. 1). The first strategy to mitigate blistering is varying the $Ar/(Ar+H_2)$ gas flow ratio. An increase from 0.2 to 0.9 drastically reduces blistering and improves room-temperature resistivity (Figs. 2 and 3). Retarding field energy analyzer measurements show a decrease in the total ion flux from 3.1×10^{14} to 1.3×10^{14} cm^2 s^{-1}, which could play a role next to the reduction of the hydrogen concentration in the plasma. The second strategy is the use of a non-lossy interlayer. Especially 2 nm of PEALD AlN reduces blister size (Fig. 3). Combining these strategies allows for the growth of 23 nm, highly-stressed TaC_xN_{1-x} of high quality with virtually no blisters.

This contribution discusses the roles of ion bombardment and hydrogen in blister formation in TaC_xN_{1-x} films prepared by PEALD. The presented strategies enable the growth of metal nitrides on HF-dipped Si substrates that can be tailored through ion bombardment without inducing blistering. This strengthens the position of PEALD in the growth of superconducting films for quantum applications.

This work was supported by the Dutch Research Council NWO.

References

[1] G. Dingemans and W. M. M. Kessels, *J. Vac. Sci. Technol. A*, **30**, 040802 (2012).
[2] T. Faraz, H. C. M. Knoops, M. A. Verheijen, C. A. A. van Helvoirt, S. Karwal, A. Sharma, V. Beladiva, A. Szeghalmi, D. M. Hausmann, J. Henri, M. Creatore and W. M. M. Kessels, *ACS Appl. Mater. Interfaces.*, **10**, 13158 (2018).
[3] S. A. Peeters, C. T. Lennon, M. J. M. Merkx, R. H. Hadfield, W. M. M. Kessels, M. A. Verheijen and H. C. M. Knoops, *Appl. Phys. Lett.*, **123**, 132603 (2023).

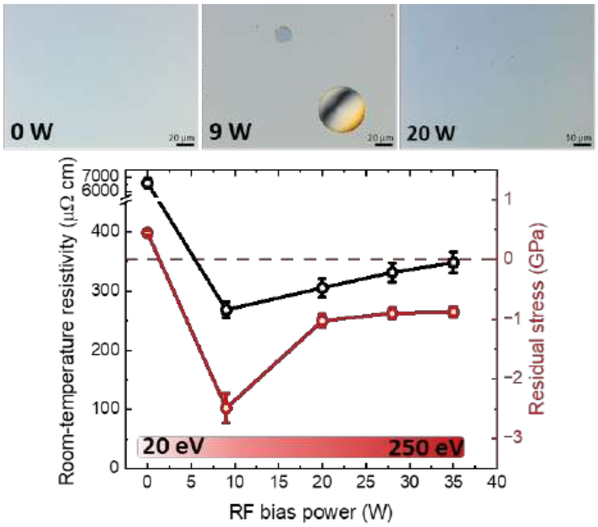

Fig. 1 Room-temperature resistivity and residual stress as a function of RF bias power for TaC_xN_{1-x} films of 20 nm thickness prepared with $Ar/(Ar+H_2) = 0.2$ gas flow ratio supplied to the plasma. The corresponding range of ion energies is indicated. Microscope images of the films show blistering and delamination for the film with the lowest 268 µΩ cm resistivity and highest -2.5 GPa stress. No blisters are observed for a grounded substrate and small blisters remain for bias powers of 20 W and beyond.

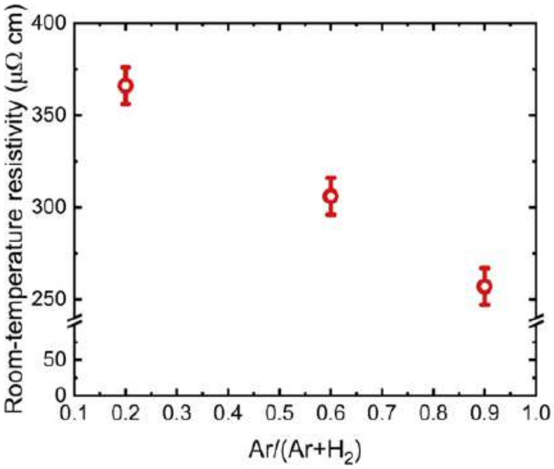

Fig. 2 Room-temperature resistivity of 5 nm TaC_xN_{1-x} films as a function of $Ar/(Ar+H_2)$ gas flow ratio supplied to the plasma. The total $Ar+H_2$ gas flow is kept constant at 50 sccm, resulting in a 6 mTorr pressure.

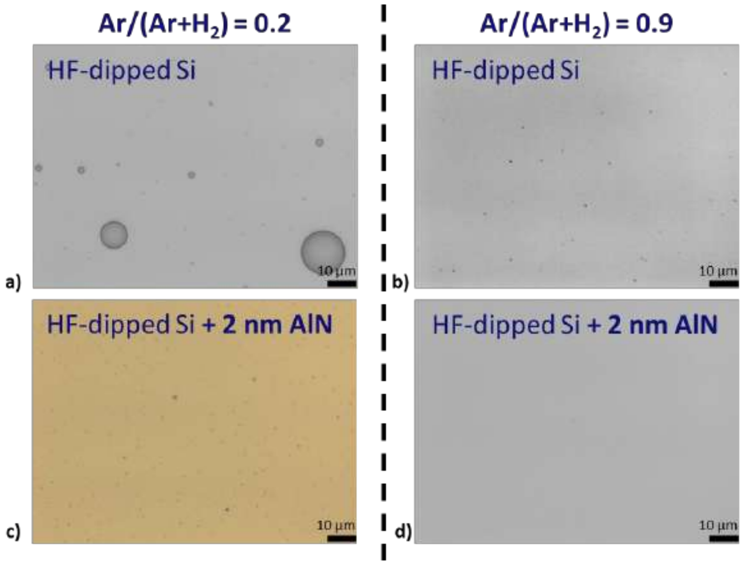
Ar/(Ar+H2) = 0.2
Ar/(Ar+H2) = 0.9
HF-dipped Si
10 µm
a)
HF-dipped Si
10 µm
b)
HF-dipped Si + 2 nm AlN
10 µm
c)
HF-dipped Si + 2 nm AlN
10 µm
d)

Fig. 3 Microscope images of **a,c)** 32 nm TaC_xN_{1-x} prepared with $Ar/(Ar+H_2) = 0.2$ and **b,d)** 23 nm TaC_xN_{1-x} prepared with $Ar/(Ar+H_2) = 0.9$. In **c,d)** a 2 nm AlN interlayer is included.

Session AM_4.2 MATERIALS FOR ENERGY: PHOTONICS

Thursday 5th June 2025 | 11.00-12.30

Chair: **Graziella Malandrino** | Main Hall “Santo Mazzarino”

Remote Plasma Assisted Vacuum Deposition (RPAVD) of Multifunctional coatings for Photonic and Energy Applications

Gloria P. Moreno, Triana Czermak, J. Obrero, F.J. Aparicio, J.R. Sánchez-Valencia, A. Borrás, Angel Barranco*

National Research Council of Spain (CSIC). Instituto de Ciencia de Materiales de Sevilla (CSIC-US) c/Américo Vespucio 49, 41092 Sevilla, SPAIN

*e-mail: angel.barranco@csic.es

The Remote Plasma Assisted Vacuum Deposition (RPAVD) process is a versatile methodology for fabricating functional nanocomposites from non-chemically polymerizable organic functional molecules and functional metal coordination compounds.[1-2] This approach combines the physicochemical reactions inherent to plasma polymerization processes with the vapor deposition of functional molecules tailored to the specific demands of target applications. The resultant cross-linked polymer thin films exhibit insolubility and exceptional thermal stability. These films can incorporate a precise concentration of virtually any thermally stable, photo-functional molecule.[1-3]

The method exhibits wafer scalability and compatibility with solvent-sensitive, delicate substrates and supported nanostructures. Initially, this process was applied to developing thin optical films and photonic devices, encompassing optical filters, photonic sensing chips, and lasing media. Nevertheless, the film properties can be fine-tuned for various other functional applications, such as creating controlled wetting and ice-retarding surfaces, antimicrobial coatings, and high-performance dielectric ultrathin films.[1-5]

In this presentation, we will also showcase very recent results about the encapsulation of nanostructures on surfaces and its role in encapsulating and modifying perovskite solar cells. Additionally, we will present recent results on developing aerogel-like conformal oxide nanostructures by combining RPAVD and plasma processing for photonic and energy applications as antireflective coatings, solar cells photoelectrodes, and thermochromic coatings for smart windows.[6]

References

[1] M. Alcaire et al. *ACS Applied Materials Interfaces*, **9**, 8948 (2017).
[2] M. Alcaire *Advanced Functional Materials,* **29**, 1903535 (2019).
[3] F. J. Aparicio et al. *Advanced Materials*, **23**, 761-765 (2011).
[4] J. Idígoras et al. *ACS Applied Mater. Interfaces*, **10**, 1801076 (2018).
[5] J. M. Obrero-Pérez, *Advanced Energy Materials*, **12**, 2200812 (2022).
[6] J. M. Obrero-Pérez *ACS Appl. Mater. Interfaces*, **16**, 39745 (2024).

Plasmonic Pd-TiO_2 Coatings via Aerosol Assisted Chemical Vapour Deposition for Enhanced Photocatalytic NO_x Remediation

K. Lambrecht[1], **B. Tam**[1], **Z. Lin**[1], **A. Kafizas**[1,2]
[1]Department of Chemistry, Molecular Sciences Research Hub, Imperial College London
[2]London Centre for Nanotechnology, Imperial College London, South Kensington, London
e-mail: kaat.lambrecht20@imperial.ac.uk

Abstract

Air pollution is a pressing modern-day challenge with significant impacts on public health and the environment. Among the key contributors to this crisis are nitrogen oxides (NO and NO_2 = NO_x). Photocatalytic coatings based on titanium dioxide (TiO_2) are a sustainable mitigation technology that utilise sunlight to convert NO_x into more benign products. However, TiO_2's reliance on ultraviolet (UV) light limits its effectiveness. [1] Incorporating plasmonic nanoparticles, such as palladium (Pd), onto TiO_2 is a promising approach for enhancing photocatalytic activity. Localised surface plasmon resonance (LSPR) can expand the range of light harvested and gives rise to hot-electron injection, plasmon-induced resonance energy transfer, and light scattering. [2]

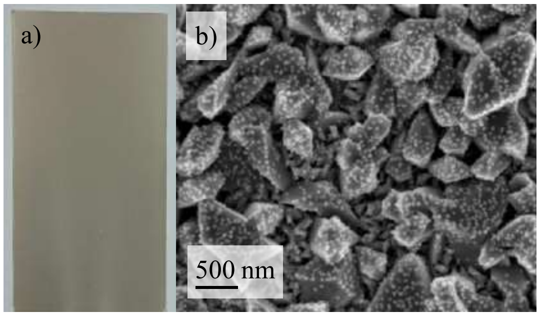

Fig.1. a) photo of a 5 x 10 cm Pd-TiO_2 coating; b) SEM image of Pd-TiO_2

Plasmonic Pd-TiO_2 coatings (Fig. 1a) are fabricated using aerosol-assisted chemical vapour deposition (AACVD), a scalable and industry-relevant method for large-area applications. Our custom-built reactor is operated under atmospheric pressure and substrates are loaded onto a base-heated graphite block. Precursors, dissolved in volatile solvents, are aerosolised using a nebuliser and transported over the substrates by gas flow. A typical synthesis involves sequential deposition of a TiO_2 coating on float glass, followed by deposition of Pd nanoparticles on the TiO_2 surface, both using AACVD. The amount of precursor used (2-10 mg of $Pd(acac)_2$), deposition temperature (250-500 °C) and carrier solvent (acetone, toluene, methanol, ethanol, ethyl acetate) for Pd nanoparticle synthesis were optimised to maximise photocatalytic performance. Characterisation techniques including X-ray diffraction (XRD), UV-vis spectroscopy, and scanning electron microscopy (SEM) were used to analyse structural, optical, and morphological properties (Fig. 1b). Photocatalytic NO_x remediation tests, conducted under an adapted ISO 22197-1 protocol, demonstrated significant enhancement in activity with the addition of Pd nanoparticles. The highest performing Pd-TiO_2 sample achieved 42.4% NO conversion under UV irradiation, an 8-fold increase compared to the base TiO_2 sample.

Building on the success of Pd-TiO_2 systems, we are now extending this research to examine the use of Cu nanoparticles to further enhance photocatalytic performance for NO_x removal. Using scalable CVD techniques, we have laid the groundwork to produce large-area, high-performance photocatalytic materials, offering an industrially relevant solution for critical environmental applications.

This work was supported by a Royal Society Equipment Grant (RSG\R1\180434) and an Imperial College London Dean's PhD Scholarship. K.L. further acknowledges the UK CPLAS: catalysis meets plasmonics programme for travel support.

References

[1] J. Ângelo, A. Mendes *et al.*, *J. Environ. Manage.*, **129**, 522– 539 (2013).

[2] E. Cortés, S. A. Maier *et al.*, *Chem. Rev.*, **122**, 15082-15176 (2022).

Lithium Sulfide (Li_2S_x) Deposition through Aerosol-Assisted Chemical Vapour Deposition for Battery Materials

D. M. Mason[1,2], **A. L. Johnson**[1]
[1]University of Bath, Department of Chemistry
[2]Advanced Automotive Propulsion Systems Centre for Doctoral Training
e-mail: dm864@bath.ac.uk and chsalj@bath.ac.uk

Conversion-type cathode materials are some of the prime candidates for future generations of secondary Li and Li-ion batteries. Compared to intercalation-type materials, they have the potential to be safer, more environmentally friendly and incorporate cheaper and more abundant materials [1]. One such cathode material is lithium sulfide (Li_2S). This boasts a theoretical specific capacity of 1166 mAh g^{-1}, approximately three times that of the current state-of-the-art intercalation-type materials, while facilitating the use of non-lithium-based anodes which can improve the safety aspects of a battery [2,3]. However, these systems require over-charging prior to use, due to the high activation voltage of 3.5 V required to overcome the high lattice enthalpy of Li_2S.

Since the film morphology, its ion transport ability and reactivity, can be altered with production method, Aerosol-Assisted Chemical Vapour Deposition (AA-CVD) offers a route to generate these materials which decreases the activation voltage, possibly eradicating it completely, as seen with other vapour deposition techniques [4]. In this instance single-source precursors for AA-CVD are used to alleviate any volatility requirements, expanding the pool of precursors to select from, such as the lithium polysulfide species seen in Fig. 1. [5], whilst reducing the potential energy requirements to produce the films [6].

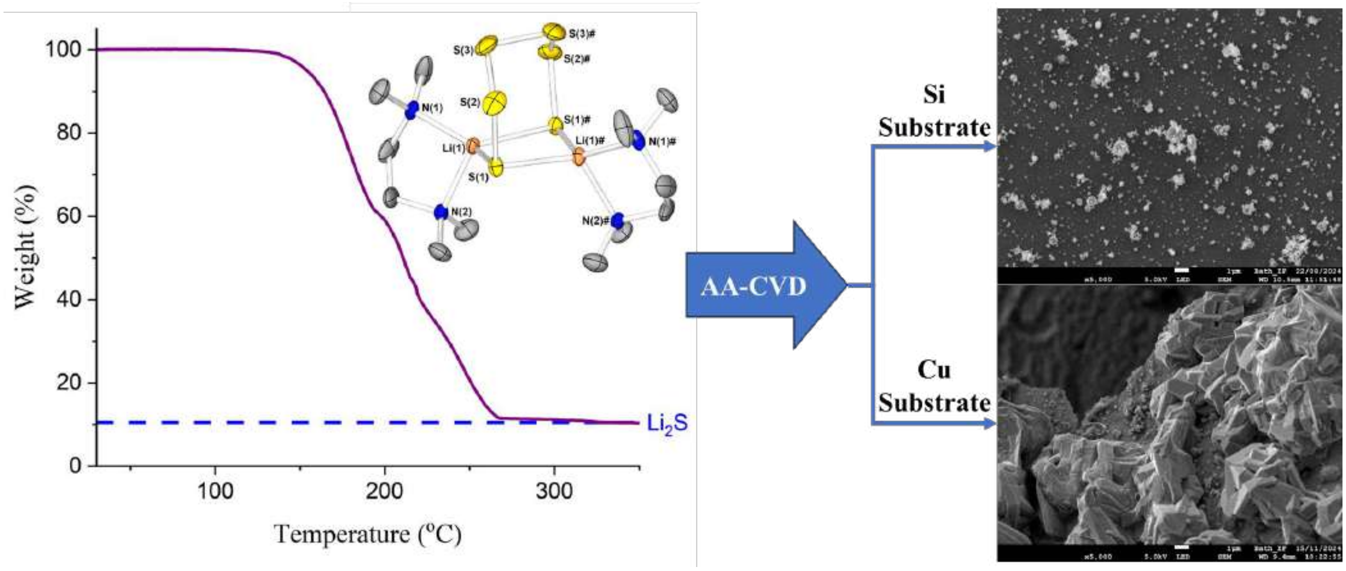

Fig. 1. TGA plot of lithium polysulfide precursor (Crystal structure inserted in plot. Thermal ellipsoids are shown at 50% probability. Hydrogens are omitted for clarity). Dotted lines highlight calculated weight % associated with Li_2S. This transitions to SEM images of resultant deposition using this precursor on both silicon and copper substrates.

The work entailed highlights the use of lithium polysulfide compounds as precursors to generate battery materials *via* AA-CVD. Deposition is being optimised with the aim of depositing on a suitable host material to produce coin cells to assess the resultant electrochemistry.

This work was supported by a scholarship from the EPSRC Centre for Doctoral Training in Advanced Automotive Propulsion Systems (AAPS), under the project EP/S023364/1.

References

[1] F. Wu and G. Yushin, *Energy Environ. Sci.,* **10**, 435-459 (2017).
[2] M. R. Kaiser, Z. Han, J. Liang, S.-X. Dou and J. Wang, *Energy Storage Mater.*, **19**, 1-15 (2019).
[3] S. Li, D. Leng, W. Li, L. Qie, Z. Dong, Z. Cheng and Z. Fan, *Energy Storage Mater.*, **27**, 279-296 (2020).
[4] X. Meng, D. J. Comstock, T. T. Fister and J. W. Elam, *ACS Nano*, **8**, 10963-10972 (2014).
[5] A. J. Banister, D. Barr, A. T. Brooker, W. Clegg, M. J. Cunnington, M. J. Doyle, S. R. Drake, W. R. Gill, K. Manning, P. R. Raithby, R. Snaith, K. Wade and D. S. Wright. *J. Chem. Soc., Chem. Commun.*, 105-107 (1990).
[6] M. A. Bhide, K. L. Mears, C. J. Carmalt and C. E. Knapp, *Nanomaterials via Single-Source Precursors*, Elsevier, (2022).

Analysing growth behaviour of low temperature ALD ZnO films on meso-porous Si/Gr battery anodes for improved performance

B. Hudec[1], **M. Pecz**[1], **A. Seifertová**[1], **P. P. Sahoo**[2], **M. Precnerová**[2], **and K. Fröhlich**[2]
[1]Institute of Electrical Engineering, Slovak Academy of Sciences, 841 04 Bratislava, Slovakia
[2]Centre for Advanced Materials Application, Slovak Academy of Sciences, 841 04 Bratislava, Slovakia
e-mail: boris.hudec@savba.sk

Application of ultra-thin ALD coatings has been shown to greatly improve the properties of various cathode and anode materials of Li-ion batteries [1]. ALD oxides SnO_2, Fe_2O_3 and ZnO have also been demonstrated as working anode materials [2, 3]. In our recent work [4], we have shown that the electrochemical performance of the silicon/graphite (Si/Gr) anodes can be improved by ultra-thin ALD ZnO coating grown at 100 °C. We have shown that the ZnO surface coating effectively modified the solid electrolyte interphase (SEI) layer, lowering the SEI, and charge-transfer resistances and thereby facilitating Li-ion transport to the anode volume. As a consequence, the rate capability became significantly improved for the ZnO-coated Si/Gr anodes. The ZnO-protected Si/Gr electrode minimized the amount of Li_2CO_3 formation during cell cycling (Fig. 1). In the study we have experimented with ALD ZnO films grown by 5-40 ALD cycles, coating Si/Gr anodes of ~20 μm of thickness with estimated porosity of ~70%. Batteries prepared with the ZnO films of 20 ALD cycles has shown the highest improvement in the rate capability (Fig. 2). As shown in Fig. 3, electrochemical cycling of the batteries can lead to significant volume expansion of the anode Si/Gr material.

Tackling the ALD growth on battery electrodes, which are essentially thick substrates of meso-porous nature, is inherently challenging due to extreme values of effective surface area and equivalent aspect ratio. Rather low thermal stability of the binder in the electrode puts a constraint on the deposition temperature, which was kept at 100 °C in this study. Beneq TFS-200 equipment has been used for all ALD experiments, with ZnO films grown using DEZn as a precursor and H_2O as a reactant.

In this study, we correlate the ALD experimental conditions with the film coverage on the Si/Gr anodes, with resulting electrochemical properties of the batteries in a half-cell configuration. We employ a combination of techniques, where first is a precise weighing of anodes before and after ALD, as shown in Fig.4 (left) for Si/Gr anodes with different Si content coated by 20 cycles of ALD ZnO using different DEZn pulse times. The Zn content as evaluated by depth profiling using FIB, SEM + EDS, which is shown in Fig. 4 (middle) correlates well with the weight measurements. The most important metric however, is the discharge specific capacity of batteries coated with such ALD ZnO (20 cycles), as shown in Fig. 4 (right). For simplicity, two extreme cases are shown here, an undersaturated process (pulse times 0.5/0.5 s) vs. a relatively saturated (according to weight and EDS data) process (pulse times 1.5/2.0 s). Surprisingly, better anode coverage does not result in a better battery performance, indicating there is an optimal coverage for improved battery performance, just like there is an optimal ALD ZnO thickness, which was shown to be 20 cycles (see Fig. 2), at least for process with pulse times of 0.5/0.5 s.

This work was supported by national grants VEGA 2/0162/22 and APVV-20-0111.

References

[1] Ma L., Nuwayhid R. B., Wu T., Lei Y., Amine K., Lu J., Adv. Mater. Interfaces, 3: 1600564 (2016). doi: 10.1002/admi.201600564
[2] Zhao et al., Front. Energy Res., 8 (2020), doi: 10.3389/fenrg.2020.609417
[3] Zhao et al., Electrochimica Acta 320, 134604 (2019). doi: 10.1016/j.electacta.2019.134604
[4] P. P. Sahoo et al., ACS Appl. Nano Mater. 2024, doi: 10.1021/acsanm.3c05066

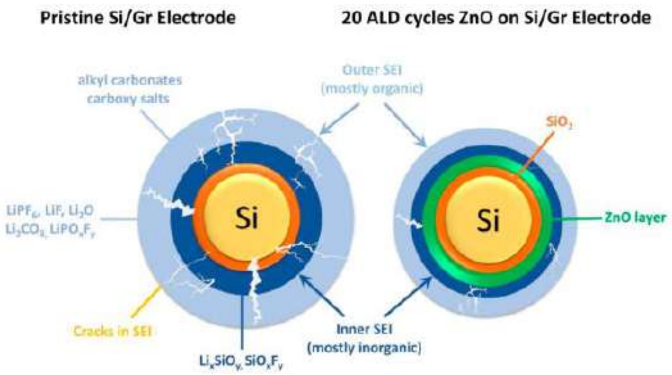
Pristine Si/Gr Electrode
20 ALD cycles ZnO on Si/Gr Electrode
alkyl carbonates
carboxy salts
Outer SEI
(mostly organic)
SiO$_2$
$LiPF_6$, LiF, Li_2O
Li_2CO_3, $LiPO_xF_y$
Si
Si
ZnO layer
Cracks in SEI
Inner SEI
(mostly inorganic)
Li_xSiO_y, SiO_xF_y

Fig. 1: Sketch of a natural (left) and artificial (right) ALD ZnO SEI formed on anodes [4].

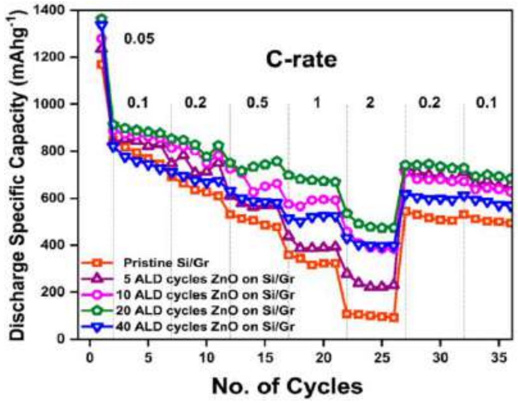

Fig. 2: Discharge specific capacity as a function of the charging/discharging cycles for uncoated and ALD ZnO coated Si/Gr anodes at different C-rates [4].

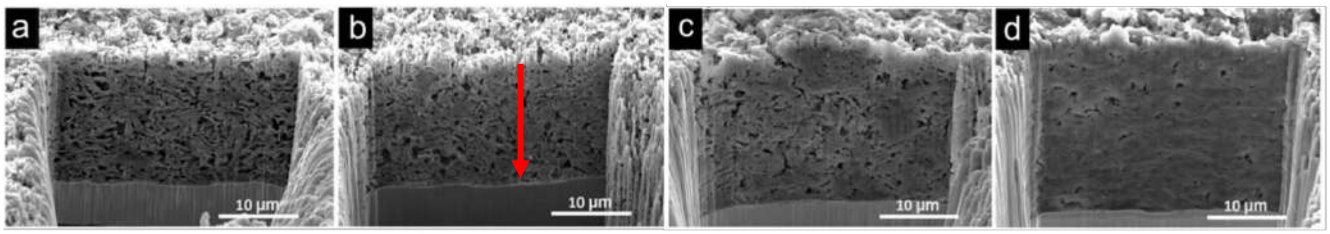
a
10 µm
b
10 µm
c
10 µm
d
10 µm

Si/Gr anode without ALD

Si/Gr anode with 20 cycles of ALD ZnO

Si/Gr anode without ALD after electrochemical measurements

Si/Gr anode with 20 cycles of ALD ZnO after electrochemical measurements

Fig. 3: FIB/SEM cross-sections of battery anodes of fully assembled batteries before (a,b) and after (c,d) electrochemical cycling, without (a,c) and with 20 ALD cycles of ZnO coating (b,d) [4].

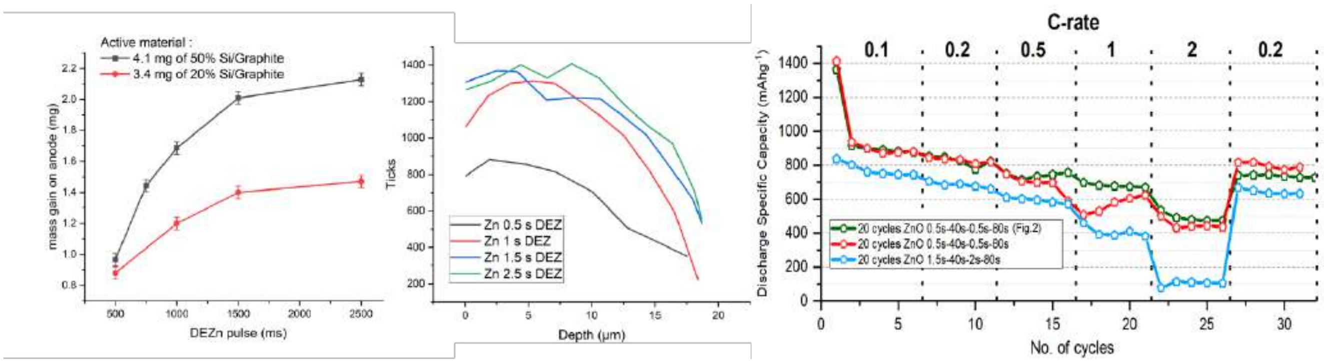

Fig. 4: Data for 20 ALD cycles of ZnO coated anodes. Left: Mass gain of Si/Gr anodes with different Si content after ALD ZnO using different DEZn pulse times. Middle: Corresponding EDS signal intensity of Zn along the depth profile shown in Fig. 3b (red arrow) for 20% Si/Gr anodes. Right: Discharge specific capacity of half-cell batteries coated with undersaturated (pulse times 0.5/0.5 s) vs. saturated (pulse times 1.5/2.0 s) ALD conditions. Better anode coverage does not result in a better battery performance, indicating there is an optimal coverage, just like in case of thickness (Fig. 2).

POSTER SESSION

Monday 2nd June 2025 | 18.00-20.00

Corridor of the Clock

Nanoengineering of tin-based coatings using nanostructured silicon matrix

Poting Liu[1, 2], Anna Makarova[3], Sergey Turishchev[5], and **Vladimir Sivakov**[1]

[1]Department Functional Interfaces, Leibniz Institute of Photonic Technology, Albert Einstein Str. 9, 07745 Jena, Germany

[2]Institute of Physical Chemistry, Friedrich Schiller University Jena, Helmholtzweg 4, 07743 Jena, Germany

[3]Institute of Chemistry and Biochemistry, Free University Berlin, Arnimallee 20, 14195 Berlin, Germany

[4]General Physics Department, Voronezh State University, Universitetskaya pl.1, 394018 Voronezh, Russian Federation

email: vladimir.sivakov@leibniz-ipht.de

Tin (Sn)-based nanostructures have gained enormous interest due to their outstanding physicochemical properties, such as high electron mobility and broad bandgap, which make them very promising for applications in energy conversion and storage devices as well as in biophotonics [1]. Our previous studies reported that phase-selective Sn/SnO/SnO_2 deposition can be realized using a matrix of silicon nanowires (SiNWs) in a metal-organic chemical vapor deposition (MOCVD) process [2-3]. As we noted earlier, the temperature gradient along SiNWs and the reduction reaction of precursor by-products, provide selective phase distribution. In this work, we investigate in details the influence of the geometrical features of the nanostructured silicon matrix on the ability to control the Sn/SnO/SnO_2 phase distribution in SiNWs matrix. Silicon nanostructures with different porosity and nanowire lengths were chosen as deposition matrices, in which different features of the tin phase distribution were observed. We found that matrices with lower porosity and longer nanowire length can provide more limited space for enhanced collisions between precursor by-products and the deposited SnO_2 thin film, leading to the highest amount of the most reduced features in the form of metallic Sn. Theoretical modeling, extensive surface and volume characterization techniques such as electron microscopy, X-ray diffraction, synchrotron radiation-based X-ray photoelectron (XPS) and X-ray absorption near edge structure (XANES) spectroscopies have been applied to study the structural and electronic properties of the deposited nanostructures. Our results reveal a new way to selectively deposit unique Sn-based functional materials and enable the tuning of their functional properties in various scenarios such as photocatalysts, Li(Na)-based batteries, biophotonics and thermal energy storage.

[1] P. Liu and V. Sivakov*, Nanomaterials* **13(17)**, 2391 (2023).
[2] P. Liu, A. Schleusener, G. Zieger, A. Bochmann, M. A. van Spronsen, and V. Sivakov*, Small* **19**, 2206318 (2023).
[3] S. Turishchev, A. Schleusener, O. Chuvenkova, E. Parinova, P. Liu, Maxim Manyakin, S. Kurganskii, and V. Sivakov, *Small* **19**, 2206322 (2023).

Volcano-like effect at the nanoscale: efficient oxygen exchange at the Si/SnO_2 interface

Poting Liu[1, 2], Anna Makarova[3], Stephanie Lippmann[4], Katharina Freiberg[5], David C. Grinter[6], Pilar Ferrer[5], Sergey Turishchev[7], and **Vladimir Sivakov**[1]
[1] Department Functional Interfaces, Leibniz Institute of Photonic Technology, Albert Einstein Str. 9, 07745 Jena, Germany.
2 Institute of Physical Chemistry, Friedrich Schiller University Jena, Helmholtzweg 4, 07743 Jena, Germany.
[3] Institute of Chemistry and Biochemistry, Free University Berlin, Arnimallee 20, 14195 Berlin, Germany
[4] Institute of Applied Physics, Friedrich-Schiller-University Jena, Albert-Einstein-Str. 15, 07745 Jena, Germany
[5] Otto Schott Institute of Materials Research, Friedrich-Schiller-University Jena, Löbdergraben 32, 07743 Jena, Germany
[6] Diamond Light Source Ltd., Didcot, OX11 0DE Oxfordshire, United Kingdom
[7] General Physics Department, Voronezh State University, Universitetskaya pl.1, 394018 Voronezh, Russian Federation
Email: vladimir.sivakov@leibniz-ipht.de

Tin (Sn)-based nanostructures have attracted significant attention due to their excellent physicochemical properties, such as high electron mobility and broad bandgap, which make them very promising for applications in energy conversion and storage devices as well as in biophotonics [1]. Our previous studies reported that phase-selective deposition of nanostructured tin-based thin films can be realized using a nanostructured silicon matrix [2-3]. In the present study, a metalorganic chemical vapor deposition (MOCVD) method on planar Si surfaces using a nature similar "volcanic eruption" effect is employed to grow unique Sn/SnO_{2-x} nanostructures. Theoretical calculations, wide-ranging surface and bulk characterization techniques such as electron microscopy, X-ray diffraction, and synchrotron radiation-based X-ray photoelectron (XPS) and X-ray absorption near edge structure (XANES) spectroscopies have been applied to study the formation mechanisms of unique tin-based nanostructures. An intense oxygen exchange reaction between the planar silicon surface and a thin layer of tin (IV) oxide during MOCVD was observed in a narrow temperature range of 725-735 °C, leading to the formation of a unique Sn:SiO_2 composite with nature similar shapes as "volcanoes" and "craters". The growth mechanism of "volcano-like" nanostructures is related to the effective oxygen attraction away between tin(IV) oxide and silicon surface, which leads to the formation of thermodynamically unstable Sn(II) oxide, which immediately disproportionates into metallic tin and SnO_2 phases localized in the SiO_2 matrix. The observed phenomenon of thin film growth at the nanoscale has similar principles to the formation of volcanoes in nature, reflecting the unique relationship between the laws of nature in the nanometer and macroscale world [4]. These discoveries open a new way to deposit unique Sn-based functional materials and enable the tuning of their functional properties in various scenarios such as photocatalysts, Li(Na)-based batteries, perovskite solar cells, and thermal energy storage.

[1] P. Liu and V. Sivakov, *Nanomaterials* **13**(17), 2391 (2023).
[2] P. Liu, A. Schleusener, G. Zieger, A. Bochmann, M. A. van Spronsen, and V. Sivakov, *Small* **19**, 2206318 (2023).
[3] S. Turishchev, A. Schleusener, O. Chuvenkova, E. Parinova, P. Liu, Maxim Manyakin, S. Kurganskii, and V. Sivakov, *Small* **19**, 2206322 (2023).
[4] P. Liu, A. Makarova, K. Freiberg, D. C. Grinter, D. Sharma, P. Ferrer, O. Chuvenkova, T. Deckert-Gaudig, S.Turishchev, St. Lippmann, V. Sivakov, *Small* **20**, 2404508 (2024).

Copper's Cozy Blanket – Even Metals Need Comfort

K. N. Ostermeijer[1], E. A. Pidko[1], J. R. van Ommen[1,*]
[1]Delft University of Technology, Department of Chemical Engineering
e-mail: K.N.Ostermeijer@tudelft.nl

In the past few decades, large scale interest has been made to valorise CO_2 as it offers a more carbon neutral pathway to chemicals and fuels. However, CO_2 reduction has proven to be problematic due to its high thermodynamic stability, making it difficult to break the carbon-oxygen bond [1]. Heterogeneous thermo-catalysts can break this bond more efficiently and selectively, therefore play an integral role in the push for the industrialization of sustainable chemicals and fuels. Methanol is considered a promising product thanks to being a key chemical building block. Currently, the commercial $Cu/ZnO/Al_2O_3$ (CZA) catalyst requires harsh conditions (50-100 bar H_2 and 200-300 ºC) [2]. Under these conditions, the Cu species are initially reduced to metallic Cu. After prolonged exposure to temperatures above 200 ºC, sintering of the dispersed active phase was observed [3]. This was shown to worsen in the presence of water vapour, which is produced in high amounts during the hydrogenation process. This accelerates hydrothermal aging, further increasing the sintering of the Cu active phase [4]. Therefore, protecting Cu nanoparticles from thermal and hydrothermal sintering is key to enhancing the operating productivity and efficiency of the methanol production process.

Atomic layer deposition (ALD) is a self-limiting technique that allows for the targeted deposition of various metals and metal oxides [5-6]. In this work we aim utilize this technique to protect Cu nanoparticles by forming overlayers on top of a Cu/SiO_2 catalyst, a more simplified version of the CZA variant. Changing the support from Al_2O_3 to SiO_2 allows for an easier downstream analysis while maintaining similar structural promotion effects (enhancing dispersion and distribution of Cu) [7]. Previous works have been studied to look at the effect of Al_2O_3 overcoats on various Cu hydrogenation catalysts [8-10]. In general, it was observed that the addition Al_2O_3 overcoats were able to stabilize the metal from sintering, even under harsh conditions. Our goal is to broaden this scope to include various other metal oxides, such as SiO_2 and TiO_2. This allows us to observe what effect the metal oxide composition and its thickness have on the stability and activity of the catalyst. We will connect these catalytic improvements to changes in acidity, wetting, different surface structure formations, and porosity. The results will be visualized through a combination of kinetic measurements, adsorption techniques, and electron microscopy, helping improve the rational design of catalysts using ALD.

This work is part of the Advanced Research Center for Chemical Building Blocks, ARC CBBC, which is co-founded and co-financed by the Dutch Research Council (NWO) and the Netherlands Ministry of Economic Affairs and Climate Policy

References

[1] A. Alvarez, A. Bansode, and A. Urakawa, *Chem. Rev*, **117**, 9804-9838 (2017).
[2] M. Behrens, F. Studt, and I. Kasatkin, *Science*, **336**, 893–897 (2012).

[3] J. B. Bulko, R. G. Herman, and K. Klier, *J. Phys. Chem.*, **83**, 3118–3123 (1979).
[4] M. B. Fichtl, D. Schlereth, and N. Jacobsen, *Applied Catalysis A: General*, **502**, 262-270 (2015).
[5] B. Zhang and Y. Qin, *ACS Catalysis*, **8**, 10064–10081 (2018).
[6] J.R. van Ommen, A. Goulas, and R. L. Puurunen, Atomic Layer Deposition, Kirk-Othmer Encyclopedia of Chemical Technology, 1-42 (2021)
[7] R. Becker and H. Parala, F. Hipler, *Angew. Chem. Int. Ed.*, **43**, 2839-2842 (2004).
[8] B. J. O'Neill, D. H. K. Jackson, and A. J. Crisci, *Angew. Chem. Int. Ed.*, **125**, 14053–14057 (2013).
[9] B. J. O'Neill, C. Sener, and D. H. K. Jackson, *ChemSusChem*, **7**, 3247–3251 (2014).
[10] H. Zhang, Y. Lei, and J. Kropf, *J. Catal.*, **317**, 284-292 (2014).

ALD of Zinc Phosphate films with Tuneable Structure and Stoichiometry

A. Chalishazar[1], A. Dhara[1], M. M. Minjauw[1], E. Solano[2], F. Munnik[3],
C. Detavernier[1], J. Dendooven[1, *]
[1]CoCooN Research Group, Department of Solid State Sciences, Ghent University, Belgium
[2]NCD-SWEET Beamline, ALBA Synchrotron Light Source, Spain
[3]Institute of Ion Beam Physics and Materials Research, HZDR, Dresden, Germany
e-mail: Aditya.Chalishazar@UGent.be, Jolien.Dendooven@UGent.be

Metal (M) phosphates are a versatile group of materials, that can be integrated in several applications, including battery technology, corrosion protection, electrocatalysis, and proton conduction. They exist in a variety of structures and stoichiometries, with the M/P ratio having a profound impact on functional properties [1]. Of the limited number of ALD chemistries available for metal phosphate growths, trimethylphosphate (TMP) is the most commonly used phosphorus precursor. However, P-doped metal oxides are often formed, instead of stoichiometric orthophosphates [1]. Previous work has demonstrated that the P-content can be increased by a plasma-enhanced ALD supercycle approach that combines alternating metal oxide (MO) and phosphorus oxide (PO) cycles to deposit near-stoichiometric metal phosphates [2-3].

In this work, we first investigate the ALD growth of PO using alternating exposures of TMP and O_2 plasma. *In situ* spectroscopic ellipsometry (iSE) data show non-linear ALD growth, with an initial "growth" region, followed by an "inhibition" region (Figure 1). *In situ* reflection Fourier transformed infrared (FTIR) spectroscopy was used to investigate the underlying surface chemistry, showing that in the "growth" region, phosphate species are incorporated in the growing film, but this incorporation saturates. The "inhibition" region is characterised by physisorption of phosphate precursor, which desorbs during the subsequent O_2 plasma pulse.

Secondly, we characterised a process in which a ZnO ALD cycle (DEZn/O_2 plasma) and a PO ALD cycle (TMP/O_2 plasma) are alternated to grow a $ZnPO_x$ film at 150 °C. Compared to previous work [4] that used water as an oxidant in a similar supercycle approach, the use of O_2 plasma as an oxidant results in improved, but still limited P incorporation of approximately 10% (Figure 2), indicative of the growth of P-doped ZnO films. The films are polycrystalline, with the PO interlayers impacting the long-range order of the ALD ZnO. This is evidenced by the decreased intensity of the (0 0 2) reflection (represented by the * in Figure 4b) in the diffraction pattern (labelled as '1-1' in Figure 4b), in comparison with the pattern of a pure wurtzite ZnO film (labelled as '1-0' in Figure 4b).

We further tuned the stoichiometry of the as-deposited films by using a supercycle approach of ZnO – *n*(PO) (*n:* 1–5). With an increase in the number of PO cycles, we observe the deposition of rough, polycrystalline films with varying morphologies (Figure 3). While each supercycle contains 1 ZnO cycle, the relative amount of Zn that is incorporated, dropped significantly when the supercycle contains more than 3 PO cycles (Figure 4a). Our results suggest that more PO cycles cause growth inhibition in the ZnO cycle, which must be considered when employing this approach for the deposition of Zn phosphates. Nevertheless, compositional analysis through XPS shows that the P/Zn ratio can be tuned with the number of PO cycles (Figure 4c), while the diffraction patterns show that a different crystalline phase is formed (Figure 4b).

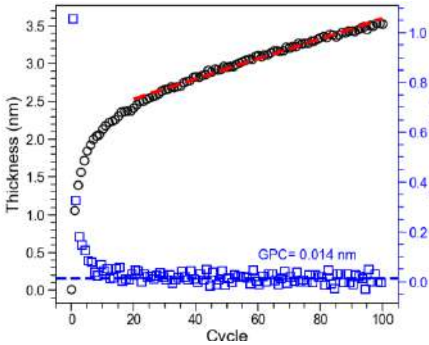

Figure 1. In-*situ ellipsometry data recorded during a TMP-O$_2$ plasma ALD process. The film growth is observed to saturate, with most growth observed during the first 10-20 cycles.*

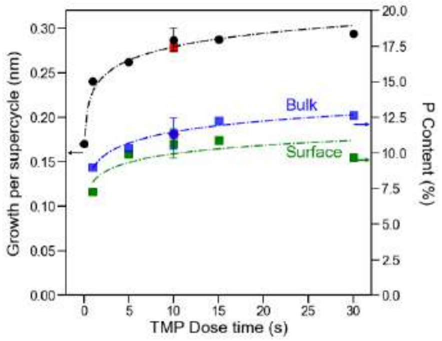

Figure 2. Growth per supercycle for a DEZn-O$_2$ plasma-TMP-O$_2$ plasma ALD process (left axis) and the P composition from XPS (right axis) against the TMP dose time. In saturated conditions, ca. 10-12% P is incorporated in the film, indicating the formation of a P-doped ZnO film.

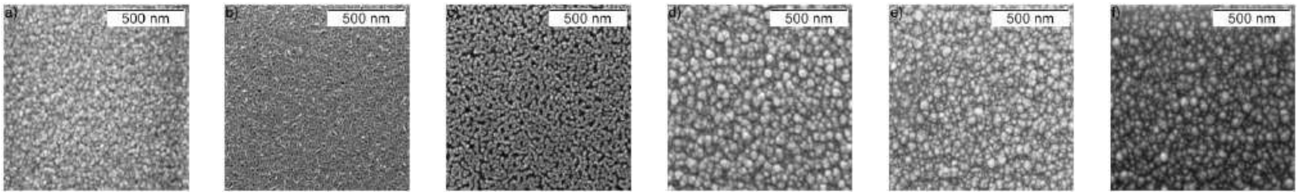

Figure 3. SEM images measured at an acceleration voltage of 20 kV, showing the variation in surface morphology for films grown using ZnO – nPO (n: 0-5) supercycles. From left to right, n increases from 0 to 5.

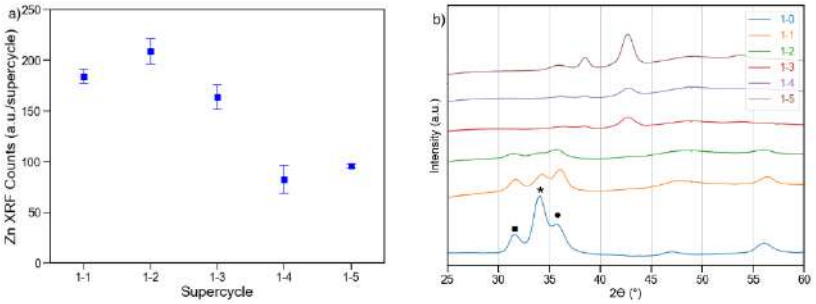

Film	%Zn	%P	%O	P/Zn
1-1	38	13	48	0.3
1-2	25	20	53	0.8
1-3	18	24	54	1.4
1-4	18	26	56	1.5
1-5	15	28	57	1.9

*Figure 4. (a) Variation in Zn XRF counts per supercycle with different compositions. As the number of PO cycles increases in the supercycle, Zn incorporation per DEZn pulse decreases. (b) XRD patterns for different supercycles extracted from GIWAXS data measured at an angle of incidence of 0.4°. The ■, *, ● represent the (1 0 0), (0 0 2) and (1 0 1) reflections for wurtzite ZnO, respectively. (c) Compositional analysis of different ZnPO$_x$ films from XPS after sputtering with a 500 V, 700 nA Ar$^+$ ion beam for 200 s, suggesting an increase in P/Zn ratio with increasing number of PO cycles.*

References

[1] Henderick et al., *Appl. Phys. Rev.*, **9**, 011310 (2022)

[2] Hornsveld et al., *J. Phys. Chem. C.*, **124(9)**, 5495 (2020)

[3] Di Palma et al., *J. Vac. Sci. Technol. A*, **38**, 022416 (2020)

[4] Tynell et al., *J. Mater. Sci.*, **48**, 2806 (2013)

Characterization of TiO_2 layer ALD deposited onto porous 4H-SiC fabricated by Electrochemical Etching

V. Spanò[1], M. Barcellona[2], G. Gautier[2], T. Defforge[2], B. Le Borgne[2], and M.E. Fragalà[1*]
[1]University of Catania, Department of Chemistry (Italy)
[2] GREMAN UMR-CNRS 7347, INSA Centre Val de Loire, Université de Tours (France)
e-mail: me.fragala@unict.it

Environmental pollution has been primarily driven by the growth of the global population and industrialization. In particular, industrial wastes, such as organic contaminants, are dangerous for human health, and various methods have been investigated for their efficient removal from water [1]. Advanced Oxidation Processes (AOPs) are defined as oxidative processes for removing pollutants from natural matrices, characterized by the *in situ* formation of reactive radical species, such as the hydroxyl radical and reactive oxygen species [2]. Among AOP techniques, photocatalysis has received attention thanks to its high efficiency, cost-efficiency, and environmentally friendly approach [3].

Titanium dioxide (TiO_2) is one of the most studied semiconductor oxides due to its characteristics, including wide band gap (3.2 eV) and low cost. In addition, TiO_2 nanoparticles are commonly employed in photocatalysis in the energy and environmental fields [4].

Silicon carbide (SiC) is considered as another important semiconductor thanks to its wide band gap, high thermostability, high mechanical strength, and high electrical conductivity [5]. SiC could be used as photocatalyst support material thanks to the aforementioned characteristics. However, the low surface area of commercial SiC particles limits their application [6].

The electrochemical etching process (ECE) of SiC wafers can reach the production of a porous substrate, increasing the surface area [7].

The aim of this work is focused on the deposition of a thin layer of TiO_2 through the atomic layer deposition (ALD) technique on a porous 4H-SiC substrate. Through the interaction of gaseous precursors with substrate surfaces, ALD is a powerful method that produces highly conformal thin films [8]. This approach reduces the process costs, minimizes the use of photocatalytic materials, prevents the removal of the photocatalyst powders from the treated water, and could enhance the photocatalytic activity.

In this work, the porous substrate is obtained by ECE of n-type highly doped (10 mΩ·cm) 4H-polytype SiC wafer in HF solution (30 wt. %). Once the porous 4H-SiC was prepared, TiO_2 deposition was carried out employing the ALD technique (BENEQ TFS 200 equipment).

The precursors used are $TiCl_4$ (STREAM Chemicals, Inc., U.S.A) and water in the liquid state at an initial temperature of 21°C.

The deposition is carried out in a stop-flow chamber, employing the extended exposure mode, commonly used to deposit on porous substrates to allow full pore coating. Every complete cycle is repeated a given number of times according to the thickness of the deposition to be reached. In this work, 210 cycles were necessary to obtain TiO_2 deposition with a thickness of 10 nm. The reactor temperature was set at 300°C with a deposition time of 6 hours due to long purging time (10 s) [9].

The TiO_2 ALD deposited onto a 4H-SiC porous substrate was characterized with Scanning Electron Microscopy (SEM), Raman Spectroscopy, X-Ray Diffraction (XRD), and X-Ray Photoelectron Spectroscopy (XPS).

Fig. 1 shows the surface morphology of the 4H-SiC porous substrate before (1) and after the deposition of 10 nm TiO_2 (2).

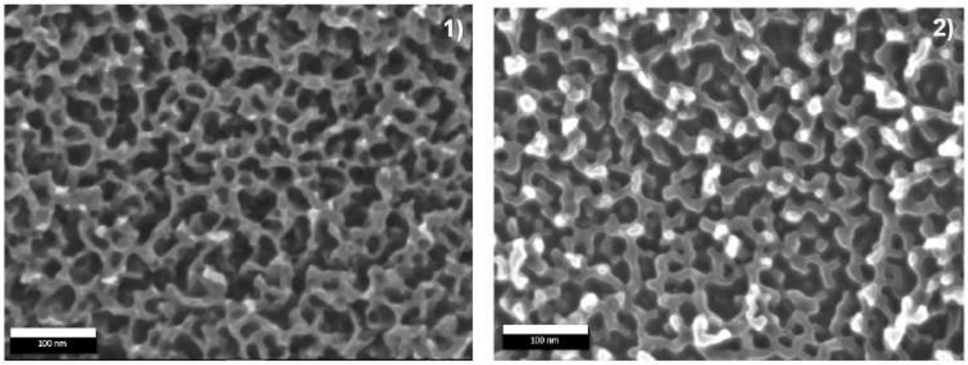

Fig. 1: SEM images of the 4H-SiC porous substrate sample (1), and the 10 nm thin layer of TiO_2 ALD deposited sample.

The results of the characterization validated the presence of a thin TiO_2 layer deposited on the porous 4H-SiC substrate. Raman and XRD analyses were able to identify the anatase crystalline phase of the thin layer of TiO_2 and demonstrate the structural integrity of the 4H-SiC substrate.

XPS analysis confirms the modification of the surface of the porous 4H-SiC substrate by the presence of the TiO_2 layer.

Finally, photocatalytic tests were performed to determine the 4H-SiC porous substrate and TiO_2 ALD deposited efficiency in removing methylene blue (MB) from water.

This work was supported by the technological platform CERTeM+. This work has been partially funded by the European Union (NextGeneration EU), through the MUR-PNRR project SAMOTHRACE.

References

[1] R.S. Pedanekar, S.K. Shaikh, and K.Y. Rajpure, *Current Applied Physics*, **20**, 931-952 (2020).
[2] M.N. Chong, B. Jin, C.W.K. Chow and C. Saint, *Water Research*, **40**, 2997-3027 (2010).
[3] R. Ma, S. Zhang, T. Wen, P. Gu, L. Li, G. Zhao, F. Niu, O. Huang, Z. Tang, and X. Wang, *Catalysis Today*, **335**, 20-30 (2019).
[4] D.C. Hurum, A.G. Agrios, K.A. Gray, T. Rajh and M.C. Thurnauer, *Journal of Physical Chemistry B*, **107**, 4545–4549 (2003).
[5] H. Yamashita, Y. Nishida, S. Yuan, K. Mori, M. Narisawa, Y. Matsumura, T. Ohmichi, and I. Katayama, *Catalysis Today*, **120**, 163-167 (2007).
[6] N. Keller, O. Reiff, V. Keller and M.J. Ledoux, *Diamond and Related Materials*, **14**, 1353-1360 (2005).
[7] G. Gautier, J. Biscarrat, D. Valente, T. Defforge, A. Gary and F. Cayrel, *Journal of The Electrochemical Society*, **160**, D372-D379 (2013).
[8] M. Ritala, M. Leskelä, J.P. Dekker, C. Mutsaers, P.J. Soininen, and J. Skarp, *Chemical Vapor Deposition*, **5**, 7-9 (1999).
[9] B. Al Chimali, I. Carrasco, T. Defforge, R. Dailleau, L. Monnier, K. Baishya, J.M. Macak, G. Gautier and B. Le Borgne, *Materials Advances*, **5**, 9270-9278 (2024).

Chemical Vapour Deposition of Silicon Films on Tungsten filaments

Y. Aviziotis[1,2], E. D. Koronaki[2], A. G. Boudouvis[2], Z. Georgiopoulou[1], M. Vasilopoulou[1], and D. Davazoglou[1]

[1]National Center of Scientific Research "Demokritos", POB 60228, 15310 Agia Paraskevi, Attiki, Greece.
[2]National Technical University of Athens, School of Chemical Engineering, Zographou, Athens, Grece
e-mail: d.davazoglou@inn.demokritos.gr

- *Introduction* The deposition of Silicon layers on metallic filaments may find applications in domains such as the large area and wearable electronics and optoelectronics. In this abstract we report on initial results of chemical vapor deposition on tungsten filaments at atmospheric pressure of undoped and Boron doped Silicon layers by decomposition of $SiCl_4$ vapors. Triphenylborane (TPB) was used as Boron precursor.
- *Experimental* A schematic of the reactor used is shown in Fig. 1(a). It was composed by a quartz bell jar in which the tungsten filament with diameter of 0.5 mm was placed between two current leads. The filament was heated by Joule effect and, dependent on the supplied power, its temperature was varying between 600 and 950 °C. For the calibration, the temperature was measured with a tiny thermocouple mechanically fixed on the filament. Samples were characterized by various methods including x-ray diffraction, scanning electron microscopy (SEM) and current-voltage (IV) electrical measurements.

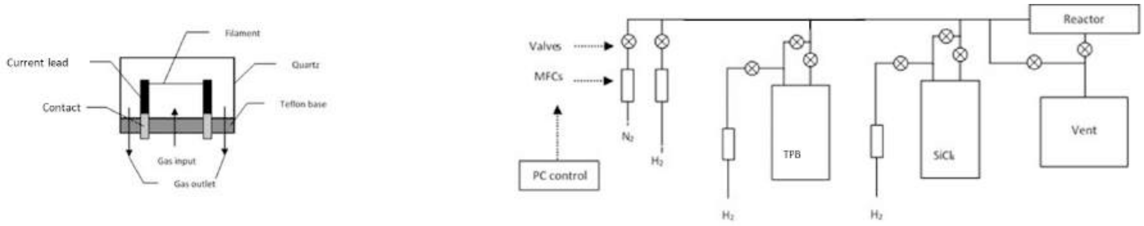

(a) (b)

Fig. 1. (a) Schematic drawing of the CVD reactor for deposition of Si on filaments from chlorinated precursors. (b) Schematic of the gas line for the CVD reactor.

- *Results* In Fig. 2 are shown SEM images of a W filament before (a) and after undoped Si deposition at 650 °C with a flow rate of $SiCl_4$ of 10 sccm (b). It can be observed that the deposition is uniform and that the initial roughness of the filament is still visible after deposition. It can also be observed the growth of low-dimensional features on the surface of the deposit. At lower deposition temperatures of 600 °C the growth of such features become even more visible as seen in Fig. 2(c) where wires with diameter of 300 nm and length of tens of microns can be observed. Elemental microanalysis has shown that they are composed by W, Si and Oxygen. At higher deposition temperatures (900 °C) large grained, Si deposits were obtained as seen in Fig. 3 where SEM images (a) and XRD patterns taken on samples deposited with various $SiCl_4$ flow rates (b) are shown. Boron doped deposits were shown to be photo-conductive as seen in Fig. 4(a) where I-V characteristics are shown taken at dark and under illumination of one sun, which caused an enhancement of current by one order of magnitude. In Fig. 4(b) an I-V characteristic is shown taken on a W/Si:B/SnO_2 sample for which the forward current is two orders of magnitude higher than the reverse, i.e., exhibits diode characteristics.

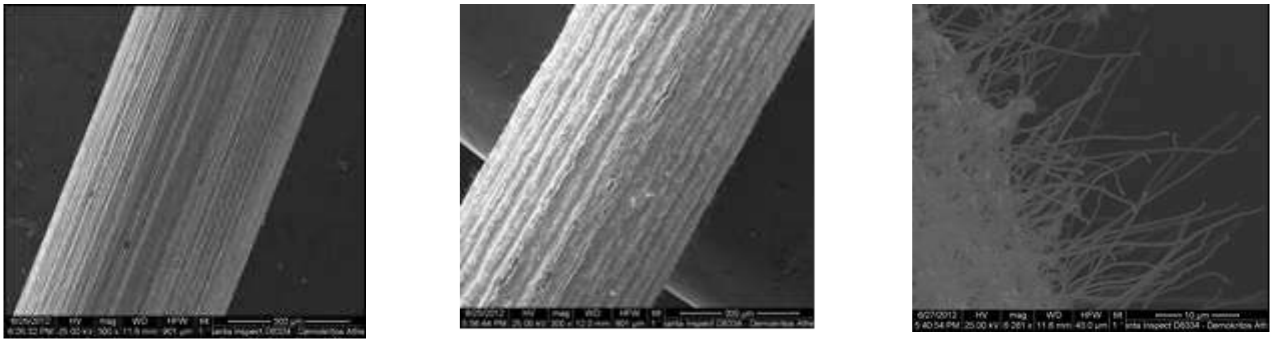

(a) (b) (c)

Fig. 2. SEM images of: (a) a bare W filament, (b) after undoped silicon deposition at 650°C at a flow rate of $SiCl_4$ of 10 sccm and (c) after deposition at 600 °C.

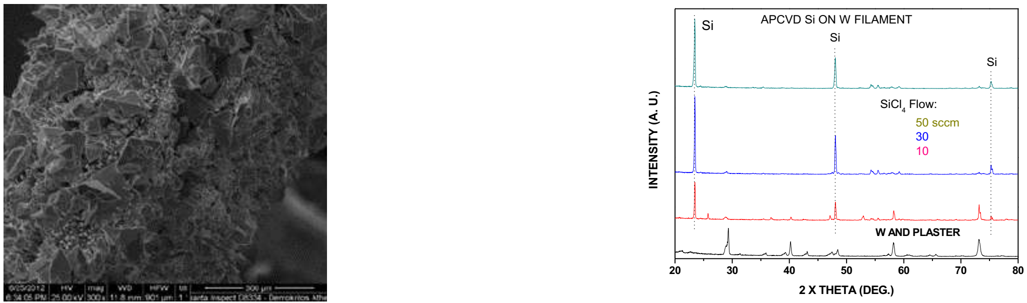

(a) (b)

Fig. 3. (a) An SEM image taken on a Si sample deposited at 900 °C. (b) XRD patterns taken on undoped samples deposited at 900 oC and various flow rates. The XRD pattern of a bare W filament is also shown.

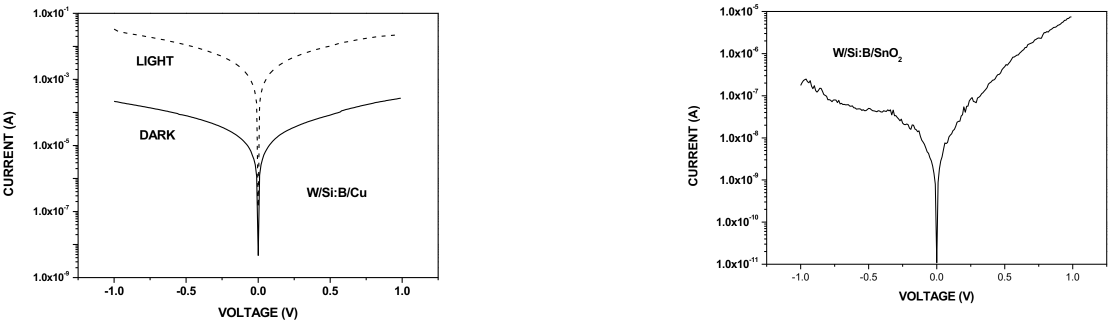

(a) (b)

Fig. 4. (a) I-V characteristics taken on a W/Si:B/Cu device at dark and under one-sun illumination. (b) I-V characteristic taken on a $W/Si:B/SnO_2$ device at dark.

This work was supported by ELIDEK: Data4Solar, contract number 016568. ...

Supported MOCVD TiO_2 Thin Films Grown on Modified Stainless-Steel Mesh for Sensing Applications

N. El Habra[1,*], F. Visentin[1], F. Russo[2], A. Galenda[1], A. Famengo[1], M. Rancan[3], M. Losurdo[1], L. Armelao[4]
[1]Institute of Condensed Matter Chemistry and Technologies for Energy (ICMATE), National Research Council (CNR), Corso Stati Uniti 4, 35127 Padova, Italy
[2]Department of Chemical Sciences, University of Padova, Via Marzolo 1, 35131 Padova, Italy
[3]Institute of Condensed Matter Chemistry and Technologies for Energy (ICMATE), National Research Council (CNR), c/o Department of Chemical Sciences, University of Padova, Via Marzolo 1, 35131 Padova, Italy
[4]Department of Chemical Sciences and Materials Technologies (DSCTM), National Research Council (CNR), Piazzale A. Moro 7, 00185 Roma, Italy
e-mail: naida.elhabra@cnr.it

The detection, quantification, and monitoring of chemical and biological compounds have become of huge interest in the last decades [1,2]. The recent drastic increase in human population and industrialization has made necessary better environmental management and, therefore, the development of more and more accurate and timely systems for the detection of water pollutants, as also stated by UN Agenda for Sustainable Development Goal 6. Chemical Oxygen Demand (COD) is an indicator for assessing the concentration of organic contaminants in water resources, directly affecting the health of aquatic systems [1,3–5]. Traditional COD techniques require expensive and toxic reagents to induce oxidative degradation, involving complex and long time-consuming analyses. Therefore, it is necessary to develop more advanced and faster alternatives.

Among semiconductor metal oxides, that are an important class of sensing materials, titanium dioxide (TiO_2), in thin films form, is a promising material for rapid, accurate, and real-time monitoring of water quality [1,2,5,6]. It is widely employed as a sensor thanks to its high chemical and mechanical stability in harsh environments, non-toxicity, and eco-compatible properties. Specifically, TiO_2-based COD sensors exploit the TiO_2 excellent oxidative capabilities under UV irradiation (to convert organic compounds to CO_2), and high photostability [2,5].

A metal-supported photocatalyst consists of the coating of a suitable substrate with a thin layer of photoactive material to be easily recovered and reused [7]. Nevertheless, the immobilization of the catalyst inevitably reduces the active surface leading to a loss of photocatalytic activity. The utilization of high surface area substrates could be a way to overcome this problem, allowing a higher number of active sites available for interaction with the organic pollutants, consequently leading to enhanced COD quantification sensitivity and accuracy.

In this work, to fully exploit the TiO_2 performance as COD sensor, nanostructured TiO_2 thin films have been grown via Low-Pressure Metal Organic Chemical Vapor Deposition (LP-MOCVD) on metallic stainless-steel AISI 316 meshes (SS) as supporting substrates. To further increase the surface area of the pristine mesh, while maintaining its supporting properties, different inorganic acid-based chemical etching protocols have been developed and tested at different temperatures and for different durations. The best etching results have been obtained by using a single-acid solution of HCl or a mixed-acid solution of HCl/H_2SO_4, operating at 55°C for 15 minutes. The final choice of the HCl/H_2SO_4 solution as the best-performing etching system was supported by economic aspects.

Chemically acid-treated meshes (SS-AT), as well as MOCVD-coated ones (SS-AT-TiO_2), have been studied by SEM, XRD, EDX, and XPS. The morphological, chemical, and structural characterizations of SS-AT-TiO_2 show that the TiO_2 supported films are made up of dense and homogenous poly-crystalline anatase, well-adherent, and highly conformal to the underlying SS-AT substrates (Fig. 1).

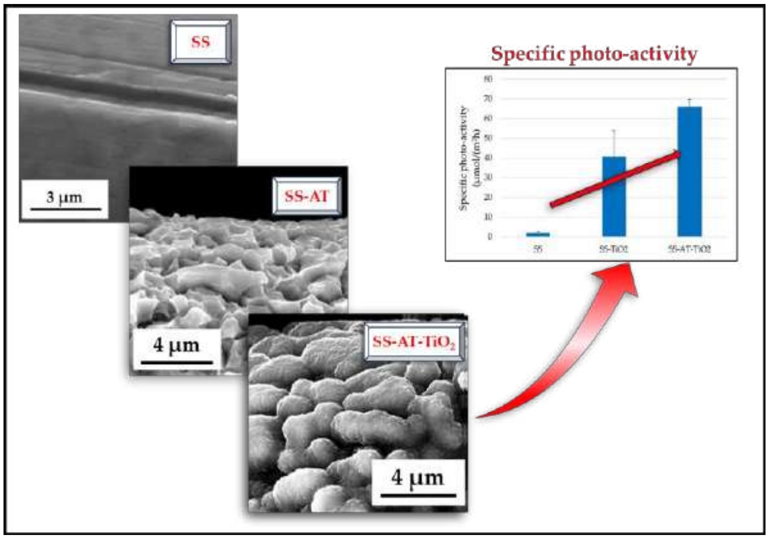

Fig. 1. SEM micrographs of the pristine (SS), the acid-treated (SS-AT), and the TiO_2 MOCVD deposited (SS-AT-TiO_2) meshes. The specific photo-activity for the SS, SS-TiO_2, and SS-AT-TiO_2 meshes is reported.

To preliminary investigate the detection properties of the developed high surface area supported TiO_2 thin films as COD sensors, photocatalytic degradation tests on functional model pollutants, based on ISO 10678:2010 protocol for methylene blue (MB) removal, have been carried out. Bare SS mesh shows insignificant photocatalytic activity, the SS-TiO_2 mesh is able to remove about 40 µmol of MB per square meter per hour, while the SS-AT-TiO_2 mesh degrades 66 µmol of MB per square meter per hour, with more than 60% of activity gained (Fig. 1). The etching treatment, therefore, can be employed as an efficient and relatively economical method to increase the surface area of the metallic supporting substrate, and consequently the photocatalytic activity of the coated systems.

These preliminary outcomes demonstrate that the development of high surface area TiO_2-supported thin film represents a potential COD sensor towards a more efficient, cost-effective, and environmentally sustainable method of water quality assessment. The findings of this study could provide valuable starting points for research and industry toward a sustainable future, ensuring water monitoring and preservation.

This work was supported by PON Energy for TARANTO (ARS01_00637).
ICMATE also acknowledges the support of the European Commission under the Grant Agreement 101079455 — NET4Air — HORIZON-WIDERA-2021.

References

[1] Mele, G.; Del Sole, R.; Lü, X. *Titanium Dioxide (TiO_2) and Its Applications*, Parrino, F., Palmisano, L., Eds. (2021)
[2] J. Bai , B. Zhou, *Chem. Rev.*, **114**, 10131–10176 (2014).
[3] D.M. El Mekkawi, H.R. Galal, R.M. et al., *Int. J. Environ. Sci. Technol.* **13**, 1077–1088 (2016).
[4] Y. Kim, K. Lee, S. Sasaki, K. Hashimoto, et al., *Anal. Chem.*, **72**, 3379–3382 (2000).
[5]. B. Bastug Azer,A. Gulsaran, J.R. Pennings, et al. *J. Electroanal. Chem.*, **918**, 116466 (2022).
[6] J. Chen, J. Zhang, Y. Xian, X. Ying, M. Liu, L. Jin, *Water Res.*, **39**, 1340–1346 (2005).
[7] S. Murgolo, V. Yargeau, R. Gerbasi, F. Visentin, N. El Habra, et al., *Chem. Eng. J.*, **318**, 103 (2017).

Film thickness non-uniformity and crucial role of water dosage for atomic layer deposition of yttrium oxide from cyclopentadienyl yttrium precursor

Weihua Wu, Robbert van de Kruijs, and Alexey Y. Kovalgin*
MESA+ Institute for Nanotechnology, University of Twente, P.O Box 217, 7522NB
Enschede, The Netherlands
*e-mail: a.y.kovalgin@utwente.nl

Yttrium oxide (Y_2O_3) is a promising dielectric material for various applications in micro- and optoelectronics due to its high permittivity (k = 10 ~ 15), wide band gap ($\Delta E \sim 5.5$eV), high refractive index (n ~ 1.9), and high thermal stability [1]. Among the existing techniques to grow Y_2O_3, atomic layer deposition (ALD) gained an increasing attention due to the ease to form layers of excellent conformality and desired stoichiometry with an accurate thickness control [1]. In the past, yttrium β-diketonates, such as $Y(thd)_3$, have been widely investigated as precursors for ALD of Y_2O_3, but they required highly reactive co-reactants such as ozone (O_3) or oxygen (O_2) plasma [2]. In contrast, the cyclopentadienyl-type yttrium precursors, namely $Y(RCp)_3$ (R = H, Me, Et, or ^{i}Pr), were found to be more reactive and they enabled thermal ALD with H_2O [3] as co-reactant even without applying plasma. Besides, ALD of Y_2O_3 from $Y(RCp)_3$ is more attractive because of the higher growth per cycle (GPC) rate, as compared to that of the β-diketonates, considerably improving the throughput. For example, ALD from $Y(MeCp)_3$ and H_2O shows a GPC of ~ 0.12 nm/cycle, being nearly 5 times higher than that for ALD from $Y(thd)_3$ and O_3 [3]. The $Y(MeCp)_3$-type precursors are also available from commercial suppliers, in opposite to the precursor family recently developed by introducing O or N-coordination into $Y(MeCp)_x$ (x = 1 or 2).

ALD of Y_2O_3 from $Y(MeCp)_3$ and H_2O was reported to occur between 200 and 400 °C with a near-constant GPC of approx. 0.12 nm/cycle [3]. The need for an accurate control of the water vapor was mentioned elsewhere [4]. These conclusions were obtained solely via ex-situ characterization of the film growth kinetics. Studying the kinetics of Y_2O_3 ALD from $Y(MeCp)_3$ and H_2O in real time, specifying the influence of water dosage, and finally demonstrating a high level of film thickness uniformity on a wafer scale, naturally expected for ALD, is still missing.

This work explores in detail the temperature window and the crucial role of introducing well-controlled dosage of H_2O for ALD of Y_2O_3 from $Y(MeCp)_3$, by utilizing real-time *in-situ* characterization of the process kinetics by means of spectroscopic ellipsometry (SE) (Fig. 1 (a)). We verify the reported ALD window by combining the *in-situ* SE measurements with ex-situ wafer-scale mapping of the film thickness. This work demonstrates that growing a Y_2O_3 film at conditions corresponding to standard saturation of GPC curves versus pulse- and purge-duration (Figs. 1 (b), (d) and (e)) does not necessarily guarantee a high level of the film thickness uniformity (Fig. 1 (c)), as it must be for an ALD process. Our results suggest a significant narrowing of the reported ALD window from 200 ~ 400 °C to just ~ 200 °C, in order to keep the film thickness non-uniformity within 5% over a 4" Si wafer and a decent GPC of ~ 0.08 nm/cycle (Fig. 1 (f)). Increasing the temperature from 200 to 225 °C already provides a GPC of 0.11 nm/cycle, i.e., close to the value reported in the literature. However, the corresponding thickness non-uniformity increases up to 16%. Further raise of the temperature to 250

°C provides a slightly higher GPC of 0.13 nm/cycle but increases the thickness non-uniformity to 22% (Fig. 1 (f)). This implies a significant non-self-limiting (CVD) component of the ALD process, being rapidly enhanced by the temperature. More details can be seen in caption to Fig. 1 and our presentation.

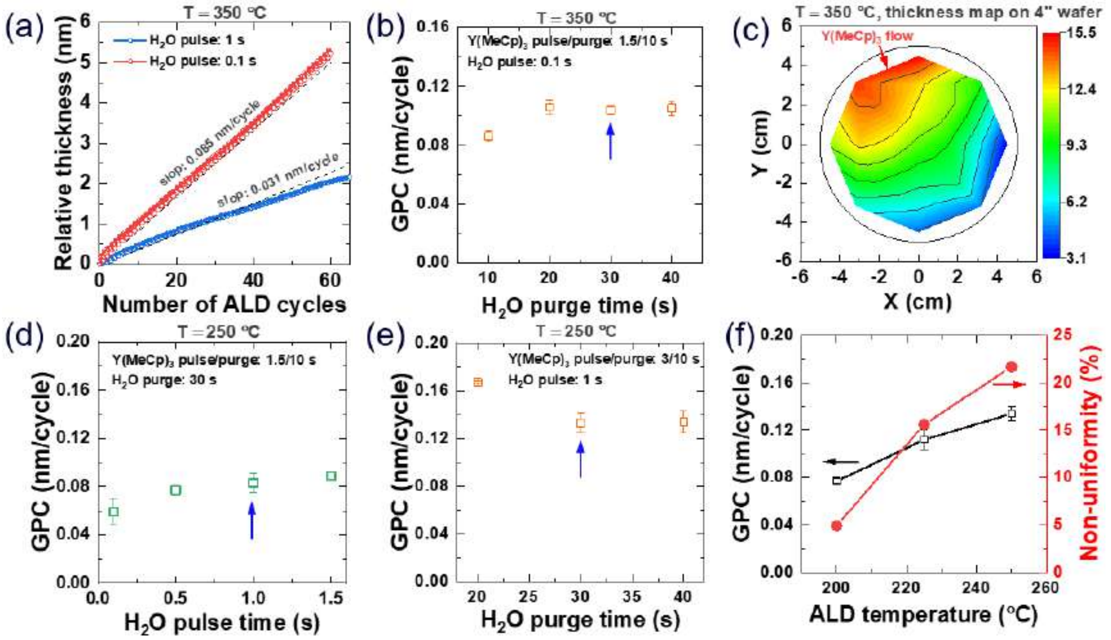

Fig. 1. (a) Real-time thickness change of ALD Y_2O_3 films from $Y(MeCp)_3$ and H_2O measured by in-situ SE. Film growth rate (the slope) decreases from 0.085 to 0.031 nm/cycle by an increase in H_2O pulse from 0.1 to 1.0 s, emphasizing the importance of accurate control of H_2O overdosage. (b) The GPC stabilizes with increasing the H_2O purge time above 20 s. A purge time of 30 s, indicated by the arrow, is further selected for (c) thickness wafer map showing a variation of approx. 63%; it's presumably due to thermal decomposition of the precursor (partial CVD), and implies reducing the temperature. (d) and (e) Graphs showing optimization of the H_2O pulse and purge duration at 250 °C, respectively. The graphs indicate the GPC saturation regions, but the optimized H_2O pulse and purge durations of 1 and 30 s (indicated by arrows) still lead to the film-thickness non-uniformity above 20%, suggesting a co-existing CVD component. (f) Further decrease of the temperature to 200 °C results in lowering both GPC (from 0.12 to 0.08 nm/cycle) and non-uniformity (from 22% to 5%). The severe increase of the non-uniformity with elevating the temperature, even within the range showing the saturation of GPC, strongly indicates a narrow window for ALD of Y_2O_3 from $Y(MeCp)_3$ and H_2O.

This work was supported by the “X-tools” program of the Dutch Research Council.

References

[1]. Y. Tang, Y. Liu, and Z, Wan, et al., *Journal of Alloys and Compounds*, **991**, 174532 (2024).
[2]. N. Boysen, D. Zanders, and T. Berning, et al., *RSC Advances*, **11**, 2565 (2021)
[3]. J. Niinisto, M. Putkonen, and L. Niinisto, *Chemistry of Materials*, **16**, 2953 (2004)
[4] P. Majumder, G. Jursich, and A. Kueltzo, et al., *Journal of The Electrochemical Society*, **155**, G152 (2008).

Functionalization of Metal Powders with Atomic Layer Deposition in Fluidized Bed Reactor for Nanocomposites Fabrication

H.-M. Piirsoo[1], P. Krížik[2], Š. Nagy[2], and B. Hudec[1]
[1]Institute of Electrical Engineering, Slovak Academy of Sciences, 841 04 Bratislava, Slovakia
[2]Institute of Materials and Machine Mechanics, Slovak Academy of Sciences, 841 04 Bratislava, Slovakia

e-mail: boris.hudec@savba.sk

The development of methodologies to coat various powders and nanoparticles at nanoscale thickness (Fig.1) is important as it can become useful for many applications from lithium-ion batteries to combustion engines. For example, Al_2O_3 coated Al powder could be used to fabricate nanocomposites with high specific strength even at elevated temperatures [1]. The super thin amorphous alumina layer between metal grains can help to restrict grain boundary sliding at higher temperatures [2]. Oxide layers could also improve the corrosion resistance of metal composites [3]. The physical properties of the composites fabricated from coated particles could be tuned with coating material and its thickness.

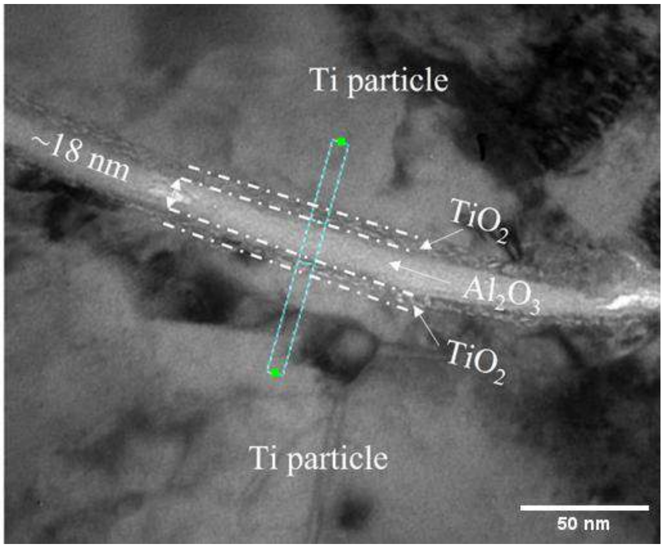

Fig. 1: TEM image of interface between two Al_2O_3-coated Ti powder particles (with their native oxide) in compacted bulk composite.

Atomic layer deposition is the preferred method for the fabrication of such nanocomposites because of the precise control of the film thickness. Therefore, one can control the nanostructure of the resulting composite which, for example, determines the deformation mechanisms. Scalable ALD on powders can be achieved with the help of a fluidized bed [4]. Mechanical vibration along with pressure gradient along the reaction chamber help to create a fluid-like state for powders. The benefits of this state are high mixing rate and uniform temperature distribution [4]. Mixing ensures uniform film thickness and shorter pulse times compared to ALD on powders in conventional reactors where diffusion is restricted and can occur preferentially.

Residual gas analysis (RGA) allows one to study the reaction mechanisms and determine the proper precursor doses and pulse times for self-terminating reactions [5]. RGA can be done with a reactor equipped with a quadrupole mass spectrometer (QMS). The time dependence of precursor and byproduct concentration can be determined to optimize the pulse times for uniform powder coating.

In this work Al, Ti and Mg powders are coated with metal oxides using Beneq TFS-200 tool equipped with a fluidized bed reactor for the fabrication of metal matrix composites stabilized and strengthened with continuous metal oxide network. ALD process parameters are tuned with the help of QMS-RGA system Vision 2000C from MKS.

Figure 2 exhibits the uniform coverage achieved with FBR-ALD. 100 g of Ti powder with particles in the microscale resulting in total surface area of 14 m^2 was coated with Al_2O_3 at 150 °C using TMA and H_2O. One deposition cycle consisted of multiple consecutive TMA and multiple consecutive H_2O pulses and lasted all together for 6 minutes. 50 cycles of deposition resulted in about 9 nm thick film as determined with TEM (Fig.1).

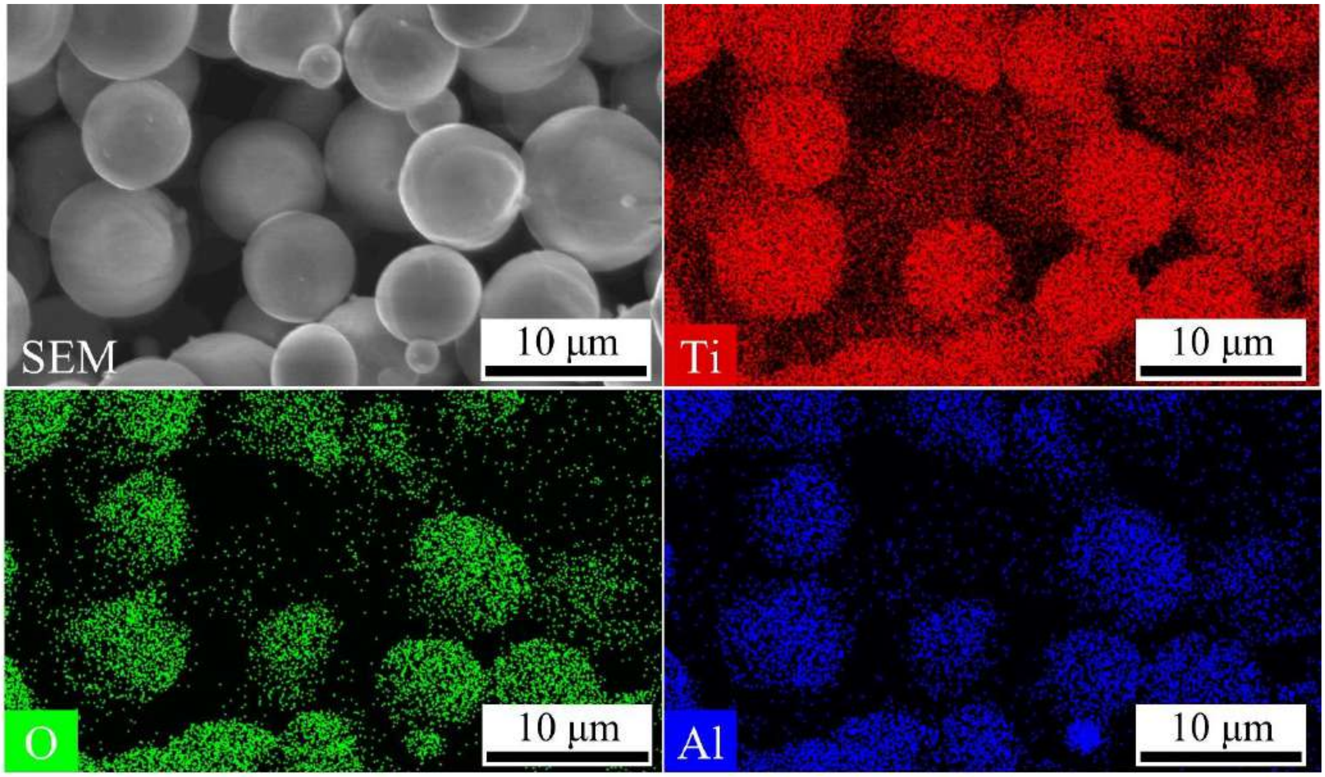

Fig. 2: Uniform distribution of Al and O on Ti powder particles after FBR ALD as determined using energy dispersive X-ray spectroscopy.

In this work we will first investigate the influence of the powder type, its total load and the carrier gas flow towards the fluidization state, and then the Al_2O_3 ALD process parameters towards the coating homogeneity on the powder. The eventual goal of this work is to establish the effect of the coating film thickness and structure on the mechanical properties of the final composites.

This work was supported by VEGA 2/0162/22 grant of Slovak Academy of Sciences. H.-M. Piirsoo acknowledges the support of National Scholarship Programme of the Slovak Republic.

References

[1] P. Krizik, M. Balog, B. Sadeghi, J. Dvorak, and A. Sikora*, J. Mater. Sci.* **59**, 16240 (2024).
[2] S. Zhang, *Nanostructured Thin Films and Coatings: Mechanical Props.*, CRC Press, Boca Raton (2010).
[3] M. Merisalu, L. Aarik, J. Kozlova, H. Mändar, A. Tarre, H.-M. Piirsoo, and V. Sammelselg, *Surf. Coat. Tech.* **435**, 128240 (2022).
[4] D. M. King, et al., *Surf. Coat. Tech.* **201**, 9163 (2007).
[5] A. Werbrouck, M. Shirazi, F. Mattelaer, S. D. Elliott, J. Dendooven, and C. Detavernier, *J. Phys. Chem. C* **124**, 26443 (2020).

Characterization of Submicron Ni-, Co-, and Fe-Doped ZnO Fibers Fabricated by Electrospinning and Atomic Layer Deposition

B.S. Blagoev[1], **B. Georgieva**[1,2], **K. Starbova**[1], **N. Starbov**[1], **I. Avramova**[3], **K. Buchkov**[1], **P. Tzvetkov**[3] **and V. Mehandzhiev**[1]
[1]Institute of Solid State Physics, Bulgarian Academy of Sciences, 72 Tsarigradsko Chaussee, 1784 Sofia, Bulgaria
[2]Institute of Electronics, Bulgarian Academy of Sciences, 72 Tsarigradsko Chaussee, 1784 Sofia, Bulgaria
[3]Institute of General and Inorganic Chemistry, Bulgarian Academy of Sciences, 1113 Sofia, Bulgaria

e-mail: blago_sb@yahoo.com; blago@issp.bas.bg

This work describes the preparation and characterization of transition metal oxide (TMO) nanofibers using a combined electrospinning and atomic layer deposition (ALD) approach. Electrospinning, a cost-effective method, produces submicron polymer fibers from a solution under an electric field. ALD enables the deposition of uniform, defect-free nanocoatings and nanolaminates on various substrates, including those with high aspect ratios.

The synthesis protocol involves the following steps: (1) electrospinning of polyvinyl alcohol (PVA); (2) low-temperature ALD of Al_2O_3 (AlO); (3) high-temperature annealing to remove the polymer; and (4) standard thermal ALD of the TMO. Because PVA softens around 70 °C, the AlO coating was deposited at 60 °C using ALD to create a scaffold for subsequent TMO deposition, which requires significantly higher temperatures. After polymer removal by annealing (24 h at 500 °C in air), ZnO doped with Co, Ni, or Fe was deposited via thermal ALD at 200 °C.

For the AlO films, trimethylaluminum (TMA) and deionized (DI) water were used as precursors with 150 cycles, 300 ms pulses, and 5 s purges. For the ZnO:TMO films (where TMO represents Co, Ni, and Fe oxides), diethylzinc (DEZ)/DI water and a metallocene (cobaltocene, nickelocene, or ferrocene)/ozone precursor system was employed. A sub-cycle consisting of 16 ZnO cycles and 5 TMO cycles was repeated eight times. Pulse and purge durations were the same as for the AlO deposition.

Scanning electron microscopy (SEM), X-ray photoelectron spectroscopy (XPS), and X-ray diffraction (XRD) were used to characterize the resulting ZnO:TMO nanofibers. Due to their high specific surface area, these structures have potential applications in catalysis and sensing.

Acknowledgment. This work has been financially supported by the Bulgarian National Scientific Fund, Project КР-06-Н88/7.

In situ AP-XPS study of Cu ALD from copper (II) hexafluoroacetylactonate

Aleksandra Figura-Jagoda[1], Mateusz Marzec[1], Sylwia Klejna[1], Camilla Minzoni[2-3], Krzysztof Mackosz[2], Caroline Hain[2], Aleksandra Szkudlarek[1], Ivo Utke[2], Esko Kokkonen[4], Marcin Sikora[5]

[1] AGH University of Krakow, al. A. Mickiewicza 30, Krakow, 30-059, Poland
[2] Empa, Feuerwerkerstrasse 39, CH-3602 Thun, Switzerland
[3] EPFL, Rte Cantonale, 1015, Lausanne, Switzerland
[4] MAX IV Laboratory, Lund University, Fotongatan 2, 224 84 Lund, Sweden
[5] SOLARIS Centre, Jagiellonian University, ul. Czerwone Maki 98, Krakow, 30-392, Poland

e-mail: marzecm@agh.edu.pl

This study investigates the atomic layer deposition (ALD) growth of copper (Cu) thin films using dehydrated Cu(hfac)$_2$ as the metal precursor and hydrogen (H$_2$) as the reducing agent. To explore the relationship between substrate surface chemistry and ALD reaction mechanisms, we simultaneously studied nucleation on two different surfaces – SiO$_2$ (native oxide) and Pt (150 nm, deposited via PVD). Ambient pressure X-ray photoelectron spectroscopy (AP-XPS) was employed for its surface and element sensitivity, providing cycle-by-cycle insight into the chemical states of deposited films during the nucleation stage.

The results revealed substrate-dependent behavior of precursors during early-stage growth. A higher copper signal was observed on SiO$_2$ compared to Pt under identical conditions (Fig. 1). Conversely, the Pt substrate required a larger number of ALD cycles to initiate observable surface reactions (Fig. 2). This suggests significant differences in precursor-surface interaction mechanisms between the two substrates. The study also demonstrated that using H$_2$ as a co-reactant simplified the ligand elimination mechanism, reducing the risk of film contamination and enhancing process reproducibility.

These findings provide valuable insight into the substrate-dependent nucleation mechanisms of Cu ALD and underline the challenges of achieving uniform and compact conductive films. By shedding light on the fundamental reaction mechanisms, this study contributes to the optimization of ALD processes for advanced electronic and catalytic applications.

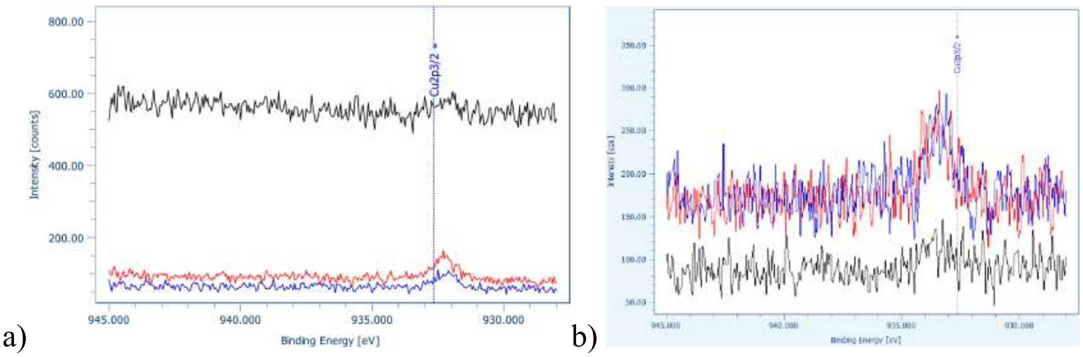

a) b)

Fig. 1. *In situ* high resolution XPS spectra of Cu 2p3/2 acquired on (a) Pt substrate and (b) SiO$_2$ substrate. Spectra collected from fresh substrates (black line), after first half-cycle (red lines) and second half-cycle (blue lines).

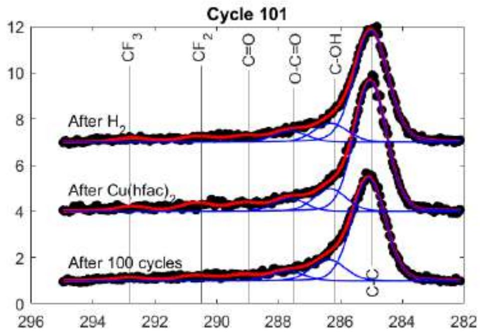

Fig. 2. Deconvoluted *in-situ* high resolution XPS spectra of C 1s region acquired on the Pt substrate after 100 cycles of Cu(hfac)$_2$ + H$_2$, and after half-cycle of Cu(hfac)$_2$ precursor pulse and half-cycle of H$_2$ co-reactant pulse.

This work was supported by Swiss National Science Foundation and National Science Centre, Poland, projects no. 202492 and 2020/39/I/ST5/03561, respectively. MAX IV Laboratory is acknowledged for granting experimental time at SPECIES beamline.

Transmission Electron Microscopy Analysis of Ga$_2$O$_3$ Thin Films Homoepitaxially Grown on (010), (-201) and (001) Substrates

V. Sallet[1,*], A. Perez[2], B. Mundet[2], B. Ballesteros[2], J. Santiso[2], C. Sartel[1], E. Chikoidze[1], Z. Chi[1], J.M. Chauveau[1], Y. Zheng[3]
[1]Groupe d'étude de la matière condensée (GEMAC), CNRS, Université de Versailles St Quentin en Yvelines, Université Paris-Saclay, Versailles France.
[2]Institut Català de Nanociència i Nanotecnologia (ICN2), Barcelone, Spain
[3]Institut des NanoSciences de Paris (INSP), CNRS, Sorbonne Université, Paris, France
e-mail: vincent.sallet@uvsq.fr

β -Ga$_2$O$_3$ epilayers were grown simultaneously on (010), (-201), and (001) oriented Ga$_2$O$_3$ substrates by Metal-Organic Chemical Vapor Deposition (MOCVD). The crystalline structure of these homoepitaxial films was characterized with atomic scale resolution by using high angle annular dark field (HAADF) scanning transmission electron microscopy (STEM, ThermoFisher Spectra microscope operating at 300 kV). The system includes energy dispersive X-ray spectroscopy (EDS) enabling chemical analysis and mapping. The images in the figure below reveal that homoepitaxial growth on (010) occurred without generation of extended defects or dislocations. For this (010) orientation, STEM was performed across [001] zone axis and we remark the occurrence of additional contrasts between two Ga$_1$ atomic columns, as indicated by the blue arrow in the insert of figure (c), which we attributed to columns of interstitial Ga, as suggested in reference [1]. Results are also given on homoepitaxies carried out on (-201) orientation, where V-shape defects have been characterized, and on (001) orientation which shows more pronounced heterogeneity.

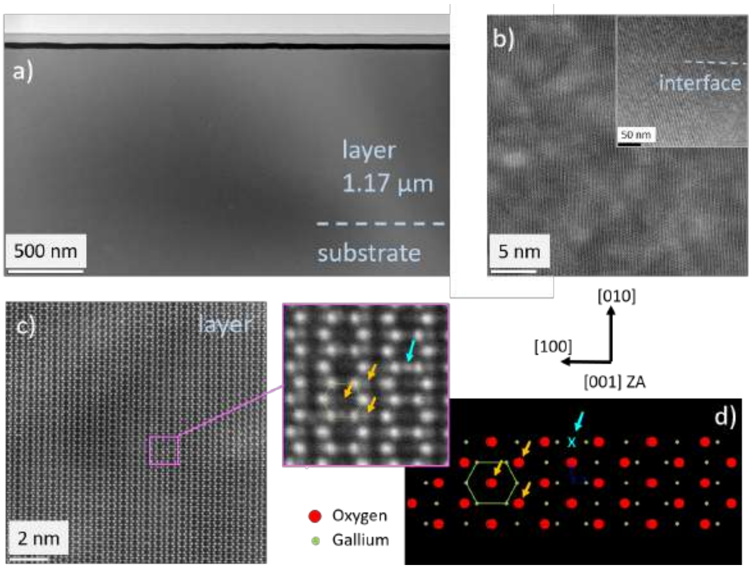

Figure : STEM analysis of a Ga$_2$O$_3$ epilayer grown on (010) Ga$_2$O$_3$ substrate, with [001] zone axis

This work was supported by Agence Nationale de la Recherche GOPOWER project ANR-21-CE50-0015

References

[1] A.F.M. Anhar Uddin Bhuiyan et al, *Appl. Phys. Lett.* **115**, 120602 (2019)

Combine SALD/MLD Synthesis and XPS Characterization of ZnO-Europium Complex Bilayers for Enhanced Photovoltaic Applications

Francesca Lo Presti[1], Anna Lucia Pellegrino[1], **Luca Pulvirenti**[1], Guglielmo Guido Condorelli[1], David Munoz-Rojas[2], and Graziella Malandrino[1]

1. Dipartimento di Scienze Chimiche, Università di Catania and INSTM UdR Catania V.le A. Doria 6, 95125 Catania, Italy.

2. Univ. Grenoble Alpes, CNRS, Grenoble INP, LMGP, 38000 Grenoble, France.

This research investigates the innovative development of bilayers comprising zinc oxide (ZnO) and europium-based metal-organic complexes to enhance the performance of photovoltaic devices. The primary objective is to harness the synergistic properties of these materials, combining ZnO's high electron mobility and excellent optical transparency with the unique luminescent characteristics of europium complexes. By integrating these complementary attributes, the bilayer configuration aims to maximize light absorption, improve charge carrier dynamics, and ultimately enhance the energy conversion efficiency of solar cells.

The combination of ZnO and europium complexes in a bilayer structure represents a promising strategy to enhance light absorption and charge carrier dynamics. ZnO contributes exceptional electronic properties, while europium complexes provide additional functionalities such as luminescence and energy downshifting, potentially broadening the absorption spectrum and improving the overall efficiency of solar cells.

ZnO thin films were deposited using spatial atomic layer deposition (SALD), a technique that offers precise control over film thickness and uniformity—crucial for optimizing device performance [1]. A customized SALD reactor was utilized to achieve high-quality films on glass substrates, with careful control of parameters such as precursor flow rates, nitrogen gas barriers, and substrate temperatures maintained at 200 °C. The resulting films exhibited excellent optical and electronic properties, forming an ideal foundation for subsequent functionalization.

To enhance the density of hydroxyl (-OH) active sites—critical for effective chemisorption of the europium precursor—surface activation of ZnO films was performed. This process involved exposing the ZnO films to oxygen flow saturated with water vapor under controlled conditions. The activated substrates were then prepared for molecular layer deposition (MLD) of $Eu(hfa)_3phen$ complexes at very low temperature (100 °C) under vacuum [2,3]. The process was carefully controlled to ensure the deposition of a uniform monolayer, halting the MLD after the initial chemisorption step.

Surface functionalization was step-by-step monitored using X-ray photoelectron spectroscopy (XPS). To track the activation process of the ZnO surface, the O 1s region of freshly deposited ZnO samples was compared with that of activated samples. The increase in the -OH peak at 531.9 eV confirmed successful activation of the ZnO surface, as OH termination facilitates chemisorption of the europium precursor.

After the functionalization with $Eu(hfa)_3phen$ and $Eu(hfa)_3diglyme$, the presence of Eu 3d signals in both cases confirmed successful attachment of the europium complexes to the ZnO surface. Additionally, the F 1s peak at 688.5 eV and the CF_3 group at 293.0 eV in the C 1s region validated the presence of fluorine atoms characteristic of the europium complexes [4]. The simultaneous detection of fluorine, CF_3 and europium peaks further corroborated the covalent anchoring of the europium-based precursors ($Eu(hfa)_3phen$ and $Eu(hfa)_3diglyme$) on the ZnO surface.

In summary, the integration of ZnO thin films with europium-based metal-organic complexes represents a novel and effective approach to enhancing photovoltaic device performance. The precise control of deposition processes, strategic design of bilayers, and detailed XPS analyses of activation and precursor attachment leverage the synergistic properties of these materials, paving the way for next-generation solar energy solutions.

This work has been partially funded by the European Union, through the MUR-PNRR project SAMOTHRACE (ECS00000022).

References

[1] R. W. Johnson, A. Hultqvist and S. F. Bent, *Materials Today*, ***17***, 236–246 (2014). https://doi.org/10.1016/j.mattod.2014.04.026.

[2] A. L. Pellegrino, C. Tudisco, F. Lo Presti, E. Milan, A. Speghini, G. G. Condorelli and G. Malandrino, *Nano Energy*, **116**, (2023): 108804. https://doi.org/10.1016/j.nanoen.2023.108804.

[3] H. Li, C. Chen, J. Jin, W. Bi, B. Zhang, X. Chen, L. Xu, D. Liu, Q. Dai and H. Song, *Nano Energy*, **50**, 699-709 (2018). https://doi.org/10.1016/j.nanoen.2018.06.024.

[4] J. Moulder, W. Stickle, W. Sobol and K. D. Bomben, Handbook of X-Ray Photoelectron Spectroscopy (1992).

A Novel Microwave ECR Plasma System for Damage-Free PEALD

Dominik Hartmann[1], Paul Dreher[1], Julian Pilz[2], Jörg Patscheider[1]
1 Evatec AG, Trübbach, Switzerland
2 Thin Film Technologies, Microsystems Division, Silicon Austria Labs, Villach, Austria

While most materials will not suffer radiation damage at ion energies below ~20 eV, some crucial compounds do show deterioration already at lower energies. Examples for ion irradiation-sensitive materials are many group III nitrides such as GaN, InN etc., but also sputter-sensitive oxides, e.g. ITO, MoO_3 and other transition metal oxides, as well as sulfides like MoS_2 and other 2D materials [1] [2]. Microwave-excited plasmas can reach these favorable conditions due to low sheath voltages. Such a microwave-excited electron cyclotron resonance (ECR) plasma has been successfully integrated into a novel plasma-enhanced atomic layer deposition (PEALD) system. In this study, we investigate the electronic and structural properties of the produced Al_2O_3 and AlN films *in-situ* as well as *ex-situ* with Ellipsometry, AFM, FIB-SEM, XRR and XPS.

In-situ diagnostics, including optical emission spectroscopy (OES), residual gas analysis (RGA) and retarding field energy analysis (RFEA) were employed to study the deposition processes of Al_2O_3 and AlN films. These studies provided central information on precursor decomposition and reaction kinetics during the different process steps, which can be used to optimize the materials properties. At 250°C a growth-per-cycle (GPC) of 1.3 Å/cycle was achieved for alumina films, with thickness uniformity below 0.5% on 200 mm silicon wafers (see Fig. 1). The 60 nm thick alumina films have a refractive index of 1.65 at 633 nm (see Fig. 2). XPS measurements showed carbon contents below 1 atomic percent.

In further investigations the influence of substrate biasing with RF power and its influence on the materials roughness and density, as measured with AFM and XRR, were studied. The ion energies and flux were monitored with an RFEA system during the process. As the ion energy in microwave discharges is typically small, the energy range can be modified from a few eV without RF power up to >200 eV ion energy using an RF bias.

The findings show that microwave ECR plasma is indeed a versatile type of plasma source, which can be beneficial for high quality PEALD processes to deposit for damage-free films. The possibility to combine this new PEALD module in an Evatec cluster system with separate modules for PECVD, sputter deposition and etching opens up new paths to investigate and develop innovative processes and devices.

Bibliography

[1] D. R. Boris, V. D. Wheeler, N. Nepal, S. B. Qadri, S. G. Walton and C. R. Eddy, “The role of plasma in plasma-enhanced atomic layer deposition of crystalline films,” *J. Vac. Sci. Technol. A 38, 040801,* 2020.

[2] T. Faraz, K. Arts, S. Karwal and H. C. M. K. a. W. M. M. Kessels, “Energetic ions during plasma-enhanced atomic layer deposition and their role in tailoring material properties,” *Plasma Sources Sci. Technol. 28 024002,* 2019.

Supplemental information

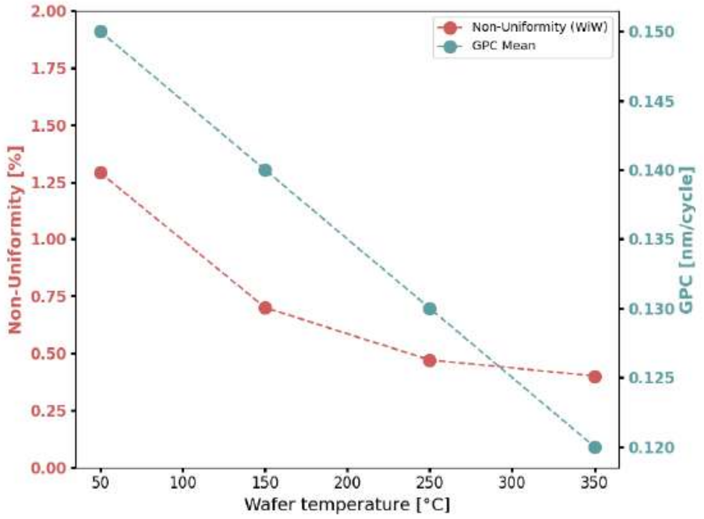

Figure 1 Al_2O_3 process: Uniformity and growth per cycle as function of substrate temperature.

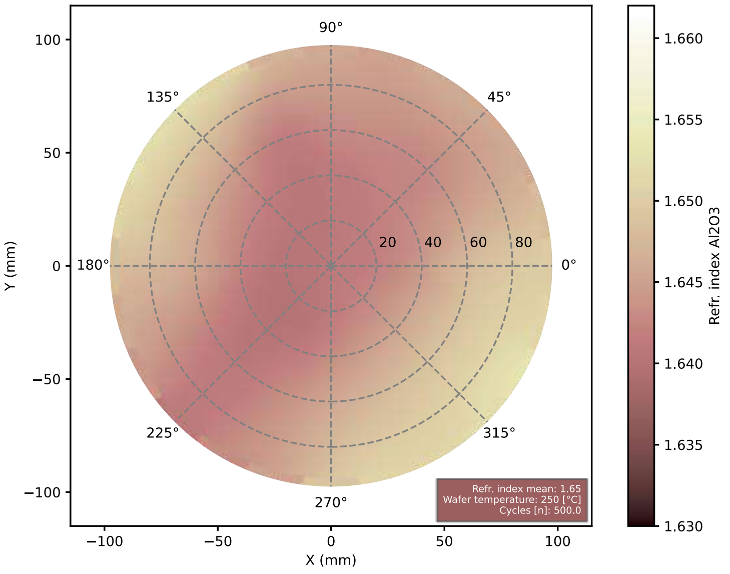

Figure 2 Refractive index of Al_2O_3 200mm wafer.

On the properties of tungsten carbonitride as a function of the composition

S. Baserga[1], **L. Von Fieandt**[1,2], **P. Eklund**[1]

[1]Department of Chemistry, Uppsala University, SE-75120 Uppsala, Sweden
[2]AB Sandvik Coromant, SE-12679 Hägersten, Sweden
e-mail: sara.baserga@kemi.uu.se

Transition metals carbonitrides are solid solutions of the respective carbides and nitrides and they show combined properties of both, resulting in hard, conductive and corrosion resistant materials. These properties have made them attractive as both bulk materials[1] and coatings[2] for applications including corrosion and wear- resistant coatings and cutting tools. In the latter, the main bulk components are based on titanium and tungsten compounds such as tungsten carbide in a cobalt matrix (cemented carbide). A work by Böőr K. *et al.*[3] has shown the possibility to deposit tungsten carbonitrides coating via chemical vapor deposition on cemented carbide substrates. In this work, we aim to continue the investigation of this material which shows highly desirable properties for wear resistant coatings. In this study, tungsten carbonitride [W(C,N)] was deposited by chemical vapor deposition on cemented carbide substrates in a hot-wall reactor with the aim to control the composition of W(C,N), focusing on varying the C/N ratio, and to establish a process window as a function of the precursor partial pressures and the deposition temperature. X-ray diffraction, scanning electron microscopy, nanoindentation and X-ray photoelectron spectroscopy were used to investigate the material properties such as the microstructure, hardness, texture and composition. The coatings are expected to have a high hardness and elastic modulus, values between 36.6 – 45.7 GPa and 564 – 761 GPa respectively were reported in the previous study[3]. Highly textured and crystalline columnar coatings were obtained.

This work was supported by the Swedish Energy Agency, The Swedish Agency for Innovation systems (VINNOVA) through the Excellence Center FunMat-II, Sandvik Coromant and Westinghouse. The Swedish foundation for strategic research (SSF) is acknowledged through the Adjunct Professor 2023 program grant APR23-0017.

References

[1] García, J., Collado Ciprés, V., Blomqvist, A. and Kaplan, B. Cemented carbide microstructures: a review. *International Journal of Refractory Metals and Hard Materials*, **80**, 40–68 (2019).

[2] Bobzin, K. High-performance coatings for cutting tools. *CIRP Journal of Manufacturing Science and Technology*, **18**, 1–9 (2017).

[3] Böőr, K., Lindahl, E., von Fieandt, L. and Boman, M. On the growth kinetics, texture, microstructure, and mechanical properties of tungsten carbonitride deposited by chemical vapor deposition. *Journal of Vacuum Science & Technology A*, **40**, (2022).

Metalorganic chemical vapor deposition of ferromagnetic metal sulfides

H. Parala[1,4], J.-L. Wree[4], S. Beer[4], A. Devi[1,2,3,4]
[1]Leibniz Institute for Solid State and Materials Research, IFW, Dresden, Germany
[2]Dresden University of Technology, TUD, Dresden, Germany
[3] Fraunhofer Institute for Microelectronic Circuits and Systems, IMS, Duisburg, Germany
[4]Ruhr University Bochum, Germany
h.parala@ifw-dresden.de

Thin films of magnetic materials are in great demand for microelectronics and spintronics. The recent attention in investigating the magnetic properties of metal sulfide thin films is driven by the scope of implementing them in future device technologies. Particularly, cobalt sulfide (CoS_x) and europium sulfide (EuS) are interesting material systems, and they are known for their versatile structures accompanied by promising magnetic properties.

CoS_x show paramagnetic as well as ferromagnetic properties and this depends on the phase and purity of the material. Among the different phases, CoS_2 can be potentially used as ferromagnetic electrodes in spintronics. EuS crystallizes in the rock salt structure, and it is a natural ferromagnetic semiconductor material. Owing to its promising optical and magnetic properties, it is appealing for luminescent and spintronic devices. For both metal sulfides, the fabrication of the materials in thin film form is challenging in terms of phase control. The deposition process plays a significant role. Metalorganic chemical vapor deposition (MOCVD) is a promising method as the process parameters employed can be tuned to control the phase of the material. In our research, we have developed new MOCVD processes for CoS_x and EuS by tuning the deposition conditions.

In this presentation, we demonstrate the tailored MOCVD processes for the deposition of high-quality ferromagnetic CoS_2 and EuS thin films. The influence of CVD process parameters on the growth and quality of the films was investigated using XRD, SEM, XPS, Raman Spectroscopy.

References

References

[1] J.-L. Wree, J.-P. Glauber, D. Zanders, D. Rogalla, M. Becher, M. B. E. Griffiths, A. Ostendorf, S.T. Barry, A. Ney, A. Devi, *ACS Appl. Electron. Mater*. **4**, 3772 (2022).

[2] S. M. J. Beer, A. Muriqi, P. Lindner, M. Winter, D. Rogalla, M. Nolan, A. Ney, J. Debus, A. Devi, *Chem. Mater*., **34**, 152 (2022).

Study of chemical-physical properties of HfO_2 thin layers from TEMAHf and H_2O in thermal ALD at low temperature down to 100 °C

A. Cataldo[1,2*], A. Li Bassi[1,3], A. Lamperti[1*]

[1]*CNR-IMM, Agrate Brianza Unit, via C. Olivetti 2, Agrate Brianza, I-20864, Italy;*
[2]*Dipartimento di Chimica, Materiali e Ingegneria Chimica, Politecnico di Milano, P.zza Leonardo da Vinci 32, edificio 6, I-20133 Milano, Italy;*
[3]*Dipartimento di Energia, Politecnico diMilano, Via Giuseppe Ponzio 34/3, Milano 20133, Italy.*
e-mail: alessandro.cataldo@mdm.imm.cnr.it, alessio.lamperti@cnr.it

In the last 30 years, the research on the growth by thermal atomic layer deposition (ALD) of high permittivity oxides, characterized by a dielectric constant k larger than SiO_2, has been driven by the need to overcome the SiO_2 limit as insulator in devices scaling in microelectronics. Among high-k binary oxides, hafnium dioxide (HfO_2) is one of the most promising candidates due to its dielectric constant equal to 20-25 and a bandgap of 5.3-5.7 eV [1]. While efforts have successfully demonstrated the integrability of HfO_2 layer in standard CMOS processes as a charge trap layer in non-volatile memories [2] or MEMS [3], when considering flexible and organic electronics, which are becoming more and more relevant nowadays, the challenge of finding a trade-off between the deposition temperature and the quality of the grown HfO_2 is one of the major issues that hinder the entrance of this high-k oxide in the current back-end-of-line processes.

Further, in the last decade, HfO_2 has been widely studied for its resistive switching properties, suitable to be integrated into different concept devices, such as RRAM and memristors, for its ferroelectric behavior, and in magnetic-based memories [4-5]. In particular, HfO_2 has been recently demonstrated to be of particular significance when considered in neuromorphic applications, from its established use in configurations exploiting its memristive characteristics, to new concepts such as magnetoionics. Magnetoionics is a new promising path to mimic the synaptic behavior in spintronic-based stacks at low power consumption and environmental impact, while avoiding catastrophic forgetting [6], thus overcoming limiting factors suffered by the present neuromorphic circuitry and architectures. This is achieved through the coupling of a magnetic substrate, typically an ultrathin ferromagnet, with a high-k oxide layer, such as HfO_2. The properties of the oxide layer, such as ion mobility, structure, stoichiometry, k value and voltage breakdown, are crucial in controlling the magnetic state of the adjacent ferromagnetic layer under an external voltage bias. As such, to fully exploit the magnetoionic effect, it is necessary to finely tune the properties of the high-k oxide by engineering its growth, especially the deposition temperature. The growth temperature must be limited to 150 °C, or better as low as 100 °C, to preserve the magnetic properties and avoid damage in the ferromagnetic layer.

This study investigates a method to grow HfO_2 in a thermal ALD reactor from tetrakis(ethylmethylamido)hafnium (TEMAHf) and H_2O precursors at low deposition temperature, from 200 °C down to 100 °C, assessing the impact of the reduced thermal budget through physical, structural, and chemical characterizations. The ALD recipe used for the process at 200 °C is shown in Figure 1 along with the strategies followed to reduce the deposition temperature without deviating from the ALD regime. Spectroscopic ellipsometry (SE) and X-ray reflectivity (XRR) reveal a 35% increase in the growth per cycle (GPC) from 0.82 Å/cy at 200°C to 1.10 Å/cy at 100°C, potentially due to enhanced precursor absorption, adsorbed impurities, or reduced film density. Further, from XRR analysis, no clear trend in HfO_2 (electron) density variability is seen with the deposition temperature reduction. X-ray photoelectron spectroscopy (XPS) shows consistent HfO_2 chemical states across the investigated temperature range but reveals that lower temperatures (i.e. 125°C and 100°C) promote the formation of under-stoichiometric oxide species. Time-of-flight secondary ion mass spectrometry (ToF-SIMS) demonstrates increased -OH and -CN groups content below 150°C probably due to inefficient ligand exchange reactions. Moreover, further analysis carried out on HfO_2 samples grown with an optimized ALD recipe shows a lower amount of contaminants, pointing towards a specific direction for the possibility of controlling the properties of HfO_2 layers grown at 100°C finely.

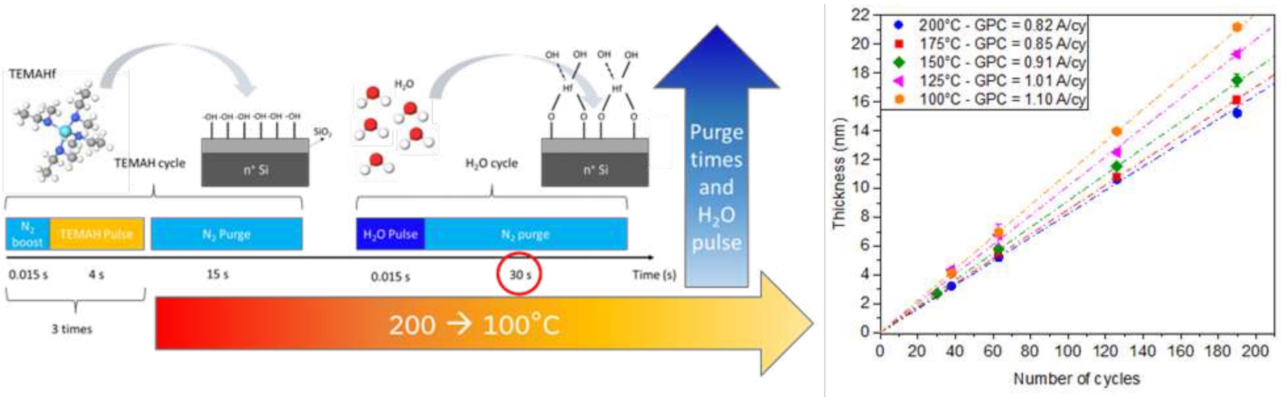

Fig. 1 – Left panel: ALD (super)cycle for HfO_2 deposition @200°C; Right panel: GPC of ALD HfO_2 from 200°C to 100°C.

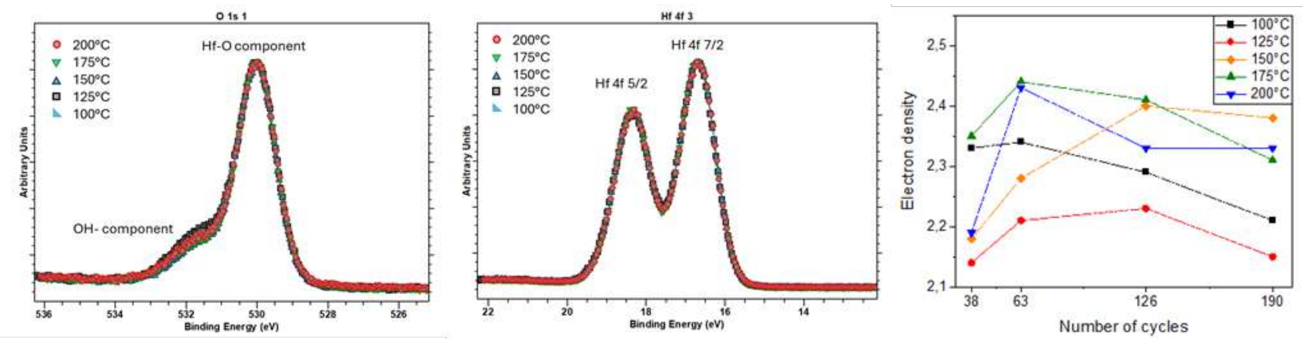

Fig. 2 – Left: Overlapping of XPS spectra of ALD HfO_2 synthetized at different temperatures; Right: HfO_2 electron density.

This work was supported by the European Union Horizon Europe programme, through the European Innovation Council (EIC) Pathfinder project METASPIN "Metaplastic Spintronics Synapses", grant n. 101098651.

References

[1] W. Banerjee, A. Kashir, and S. Kamba, *Small*, **18**, 2107575 (2022).
[2] S. Spiga, F. Driussi, G. Congedo, C. Wiemer, A. Lamperti, E. Cianci, *ACS Appl. Nano Mater.*, **1**, 4633–4641 (2018)
[3] M. Berdova, C. Wiemer, A. Lamperti, G. Tallarida, E. Cianci, L. Lamagna et al., *Appl. Surf. Sci.*, **368**, 470-476 (2016)
[4] G. Indiveri et al., *Front. Neurosci.,* **5**, 1-23 (2011).
[5] M. A. Zidan, J. P. Strachan, and W. D. Lu, *Nat. Electron.*, **1**, 22-29 (2018).
[6] J. Kirkpatrick et al., Proc. *Natl. Acad. Sci. U.S.A.*, **114**, 3521-3526 (2017).

Influence of different ALE process sequences on the electrical performance of gate recessed AlGaN/GaN HEMTs

C. Miersch[1], S. Seidel[1], J. Heitmann[1,2], F.C. Beyer[1]

[1] Fraunhofer Institute of Integrated Systems & Device Technology IISB
[2] Institute of Applied Physics, TU Bergakademie Freiberg
e-mail: christian.miersch@iisb.fraunhofer.de

In modern power electronics, miniaturization continues, particularly in III-V semiconductor technologies such as AlGaN/GaN high-electron-mobility transistors (HEMTs). These devices feature an AlGaN/GaN heterojunction that creates a two-dimensional electron gas (2DEG) [1, 2] with high electron mobility (~. 2000 $cm^2V^{-1}s^{-1}$ at 300 K [3]) and high carrier concentration ($> 10^{13}$ cm^{-2} [4]), making them ideal for high-frequency and high-voltage switching applications. AlGaN/GaN HEMTs operate in depletion mode (d-mode) [5] but more and more focus is set on enhancement mode (e-mode) [5] operation for integration into MOSFET-based circuits. Beside the normally used p-Gate architecture [6] one possibility for achieving a positive threshold voltage (V_{th}) is a gate recess of the AlGaN barrier via dry etching [7, 5, 8–11]. This recess necessitates etching techniques with exceptional precision and control. Atomic Layer Etching (ALE) enables a low etch per cycle (EPC) and minimizes structural damage[12]. The plasma ALE process consists of two independent steps forming a repeatable cycle. In the case of AlGaN etching, the first step involves chemical surface modification, achieved through halogenation using Cl_2 plasma. In the second step, the modified surface layer is removed by low energy Ar ion bombardment [13–19]. Due to this and additional purging and evacuation sequences after each step, an ALE process lasts longer than a conventional reactive ion etching (RIE) process [20]. Gradually reducing the need for purges and switching to continuous plasma operation effectively shortens the cycle time. The shortening of the process duration would raise sustainability and lower process costs, decrease energy consumption and environmental footprint in general. Previous works demonstrate decreasing cycle times by leaving out purges [20, 21] or combining chemistry [22]. In this work five specific ALE modifications were developed: full-purge (1), half-purge (2), purge-free (3), continuous plasma (4) and pulsed-bias (5). Their sequential structure over time is shown in Fig 1(a). All modes provide a low surface roughness of 0.3 nm. The first four modes exhibit a consistently low EPC of (0.2 ± 0.02) nm/cycle. It turned out that, under optimized process parameters, the continuous plasma mode is the most suitable method for reducing the processing time by up to 60% [23]. In a previous study, a purge-free ALE mode was successfully applied for gate recess of AlGaN/GaN HEMTs. A linear relationship between V_{th} and etch depth was shown, achieving an e-mode HEMT (normally-off) at 21 nm deep recess [21].In addition, the evaluation of the developed processes will be performed by morphological and electrical characterization, including atomic force measurements (AFM) and capacitance-voltage (CV) as well as transfer curves of processed devices, providing information about the V_{th} shift, leakage and saturation current. Hence, the impact of time-reduced ALE processes on the electrical properties of the processed HEMTs will be discussed.

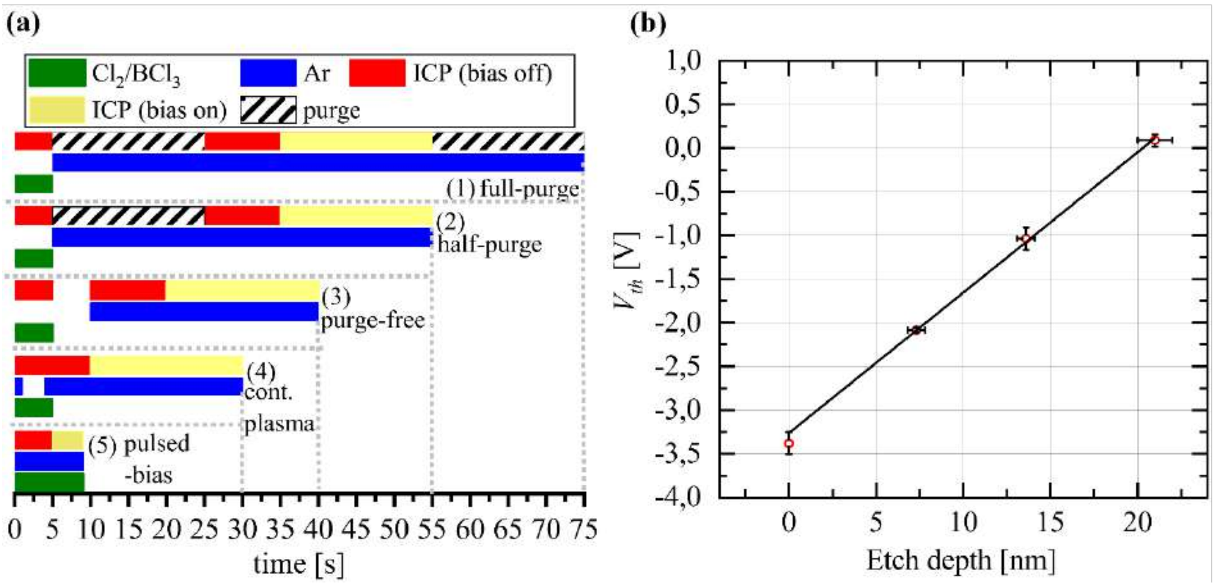

FIG. 1. (a) Cycle sequence over time for the five different ALE modes. (b) Threshold voltage Vth extracted from step in gate capacitance. V_{th} increases linearly with etch depth.

This work was financially supported by the Fraunhofer Internal Programs under Grant No. Attract 079-600865

References

[1] M. Asif Khan, J. N. Kuznia and D. T. Olson, *Appl. Phys. Lett.,* **65,** 1121–1123 (1994).
[2] V. Kumar, A. Kuliev and R. Schwindt, *Solid State Electron.,* **47,** 1577–1580 (2003).
[3] P. Javorka, *Fabrication and characterization of AlGaN/GaN high electron mobility transistors*, Aachen (2004).
[4] B. A. Klein, A. A. Allerman and A. G. Baca, *Journal of Microelectronics and Electronic Packaging,* **20,** 1–8 (2023).
[5] W. B. Lanford, T. Tanaka and Y. Otoki, *Electron. Lett.,* **41,** 449–450 (2005).
[6] L. Efthymiou, G. Longobardi and G. Camuso, *Appl. Phys. Lett.,* **110 (**2017).
[7] T. Oka and T. Nozawa, *IEEE Electr. Device L.,* **29,** 668–670 (2008).
[8] Q. Hu, S. Li and T. Li, *IEEE Electr. Device L.,* **39,** 1377–1380 (2018).
[9] W. Saito, Y. Takada and M. Kuraguchi, *IEEE T. Electron Dev.,* **53,** 356–362 (2006).
[10] N. M. Shrestha, Y. Li and T. Suemitsu, *IEEE T. Electron Dev.,* **66,** 1694–1698 (2019).
[11] Y.-K. Lin, S. Noda and H.-C. Lo, *IEEE Electr. Device L.,* **37,** 1395–1398 (2016).
[12] K. J. Kanarik, T. Lill and E. A. Hudson, *J. Vac. Sci. Technol. A,* **33,** 20802 (2015).
[13] C. Kauppinen, S. A. Khan and J. Sundqvist, *J. Vac. Sci. Technol. A,* **35 (**2017).
[14] C. Mannequin, C. Vallée and K. Akimoto, *J. Vac. Sci. Technol. A,* **38 (**2020).
[15] S. Aroulanda, O. Patard and P. Altuntas, *J. Vac. Sci. Technol. A,* **37,** 41001 (2019).
[16] H. Fukumizu, M. Sekine and M. Hori, *J. Vac. Sci. Technol. A,* **37,** 21002 (2019).
[17] L. Guan, X. Li and C. Guo, *J. Vac. Sci. Technol. A,* **41 (**2023).
[18] T. Ohba, W. Yang and S. Tan, *Jpn. J. Appl. Phys.,* **56 (**2017).
[19] S. Ruel, P. Pimenta-Barros and F. Le Roux, *J. Vac. Sci. Technol. A,* **39 (**2021).
[20] Y. S. Lee, S. J. Kim and J. J. Lee, *J. Phys. D: Appl. Phys.,* **55,** 365203 (2022).
[21] C. Miersch, S. Seidel and A. Schmid, *J. Vac. Sci. Technol. A,* **42 (**2024).
[22] J. A. Michaels, N. Delegan and Y. Tsaturyan, *J. Vac. Sci. Technol. A,* **41 (**2023).
[23] C. Miersch, *Comparison of different PEALE modes of Al0.25Ga0.75N/GaN heterostructures*, Helsinki (06.08.2024).

Advances in a PEALD TiN Deposition Process at Temperatures below 300°C for Ferroelectric Hafnium Zirconium Oxide Integration

G. Kökbudak Baldan[1], Suzanne Lancaster[1], Uwe Schroeder[1], Thomas Mikolajick[1,2], Ruben Alcala[1]

[1]NaMLab gGmbH, 01187 Dresden, Germany
[2] TU Dresden, Dresden, Germany
e-mail: Gamze.KoekbudakBaldan@namlab.com

Titanium nitride (TiN) is an essential electrode material in modern microelectronics, widely appreciated for its high electrical conductivity, thermal stability, and good diffusion barrier properties [1,2]. Its integration with temperature-sensitive ferroelectric materials, such as hafnium-zirconium oxide (HZO), presents a unique challenge, as deposition temperatures must be maintained within a specific range to preserve the ferroelectric properties of HZO [3]. Plasma-enhanced atomic layer deposition (PEALD) has shown promising results as a technique enabling high-quality TiN films within a thermal budget, facilitating its use for device fabrication requiring ferroelectric functionality and thermal sensitivity.

The deposition of TiN films has been achieved through various physical vapor deposition (PVD) and chemical vapor deposition (CVD) techniques, each with certain drawbacks. Traditional CVD methods deposit TiN films using Titanium Tetrachloride ($TiCl_4$), H_2, and N_2 at temperatures exceeding 750 °C, significantly surpassing the thermal budget established for manufacturing the back-end of line in advanced circuits [4]. Alternatively, employing NH_3 instead of H_2 and N_2 can lower the deposition temperature to around 550 °C and yield reasonably high-quality films, but this is still well beyond the desired limit of 400 °C [5-7]. Similarly, PVD TiN processes may encounter issues with increased residual stress and reduced conformality, especially for 3D structures, degrading overall performance and reliability [8].

This study investigates the deposition of TiN using PEALD in a temperature range below 300°C, focusing on analyzing the relationship between deposition temperature and fundamental film properties, including sheet resistance, uniformity, and growth-per-cycle (GPC). The aim is to provide a comprehensive understanding on how deposition conditions influence the electrical properties and structural characteristics of the resulting TiN films. Particularly, achieving an optimal resistivity value for electrode applications can directly impact the efficiency and reliability of fully-fabricated ferroelectric-based devices.

Initial PEALD experiments were conducted at a temperature of 300 °C using 200 mm silicon wafers. $TiCl_4$ served as the titanium precursor, while a reactive gas mixture of hydrogen and nitrogen (H_2/N_2) was employed, with a fixed flow ratio of 10:1 of H_2 to N_2. Additionally, the $TiCl_4$ precursor pulse time was fixed at 50 ms. The only variables adjusted in these experiments were the plasma power and the duration of the plasma exposure. Four-point probe (4pp) measurements were performed to determine the sheet resistance of the deposited TiN thin films. Spectroscopic ellipsometry and X-ray reflectometry (XRR) were used to evaluate thickness and uniformity across the 200 mm wafer and determine the GPC. Elers et al. showed a significant increase in sheet resistance for film thicknesses below 20 nm as the thickness approaches the mean free path of conducting electrons and the grain boundary distance [9]. Hence, we analyzed sheet resistance at a constant thickness of about 10 nm, noting that previous studies reported values over 300 Ω/□ for similar thicknesses using PEALD [9,10].

As illustrated in Fig. 1, both the 5 s and 7 s plasma pulse durations reveal that increased plasma power in the 150-250 W range decreases sheet resistance. Additionally, increasing the plasma pulse duration from 5 to 7 s at the same power level significantly reduces the sheet resistance. This is attributed to the fact that the chlorine concentration decreases with longer RF pulse length and higher RF power [9]. This indicates that lowering the RF power allows more chlorine to remain in the system, likely due to ionization or reaction dynamics changes. An average GPC of 0.46 Å was obtained at 150 W plasma power for 5 s, while a GPC of 0.50 Å was achieved at 250 W plasma power for 7 s. Other results fall within this range. Across all conditions, the thickness and sheet resistance uniformity remained under 5% across the 200 mm wafer. These findings highlight the critical role of plasma parameters in optimizing TiN film properties. These results already show that the TiN films exhibit satisfactory electrical characteristics and uniformity, suggesting that PEALD TiN deposition at this temperature meets the conductivity and material compatibility requirements for HZO integration in ferroelectric devices.

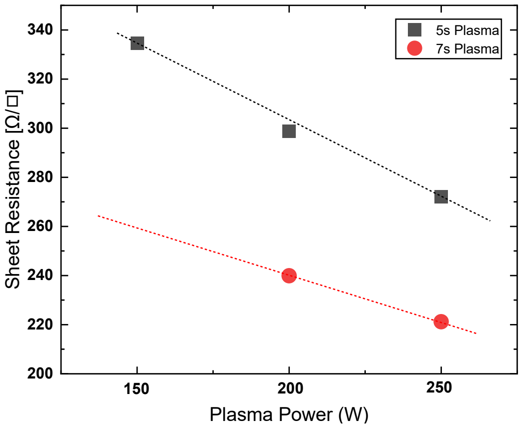

Fig. 1. Sheet resistance vs. plasma power for a PEALD TiN process with two different plasma durations

This study will further expand to identify a combination of parameters that can simultaneously reduce temperature and resistivity. These first findings already provide the foundation for further research; however, depositing at temperatures below 300°C will be further explored. The aim is to advance the understanding of low-temperature TiN PEALD processes, contributing to developing high-performance electrode solutions for next-generation microelectronics and ferroelectric devices, where thermal sensitivity and material robustness are critical. The results regarding the deposition of the TiN layer on 3D structures and capacitor configurations will be additionally addressed in this work.

References

[1] Hedge et al., *J. Vac. Sci. & Technol. B*, **11**, 1287 (1993).
[2] Fillot et al., *Microelec. Eng.*, **82**, 248 (2005).
[3] Silva et al., *APL Mater.*, **11**, 8 (2023).
[4] Chatterjee et al., *J. Mater. Sci.*, **27**, 3409 (1992).
[5] Sherman A., *Jpn. J. Appl. Phys.*, **30**, 3553 (1991).
[6] Kaizuka et al., *Jpn. J. Appl. Phys.*, **33**, 470 (1994).
[7] Hillman et al., *Microelectron. Eng.*, **19**, 375 (1992).
[8] L. Combadiere and J. Machet, *Surf. Coat. Technol.*, **88**, 17-27 (1996).
[9] Elers et al., *Journal of The Electrochemical Society*, **152**, 8 (2005).
[10] Junghans et al., *ALD 2017/ALE 2017*, Denver, Colorado (2017).

Exploring the Role of Process Parameters in oCVD-PEDOT: Toward Tailored Material and Functional Properties

Beatriz De Morais Batista[1], Diane Samélor[2], Jérôme Esvan[2], Cedric Charvillat[2], Hugues Vergnes[1],
Brigitte Caussat[1,*], Abderrahime Sekkat[1,*]
[1]LGC, Université de Toulouse, CNRS, Toulouse, France.
[2]CIRIMAT, Université de Toulouse, CNRS, Toulouse, France
e-mail: abderrahime.sekkat@toulouse-inp.fr and brigitte.caussat@toulouse-inp.fr

Conjugated polymer poly(3,4-ethylenedioxythiophene) (PEDOT) represents a promising, cost-effective alternative to conventional transparent conducting oxides (TCOs) due to its high optical transparency, excellent electrical conductivity, and mechanical flexibility [1,2]. Several studies have explored the fabrication of PEDOT thin films via the oxidative chemical vapor deposition (oCVD) process, in which 3,4-ethylenedioxythiophene (EDOT) serves as the monomer and (e.g., $FeCl_3$ and $SbCl_5$) as oxidants, which are sent in the gas phase to allow PEDOT polymerization [3–6]. This one-step, dry deposition process enables the formation of high-quality PEDOT films under mild conditions, with substrate temperatures ranging from 20 to 180 °C and a reduced pressure of 150–300 mTorr (Fig.1) [7,8]. The impact of increasing substrate temperature on the structure and properties of PEDOT films fabricated by oCVD, using one of the least expensive and less toxic oxidants ($SbCl_5$), has been previously demonstrated [9]. These films were successfully integrated into deep blue OLED devices, exhibiting slightly better performance compared to reference devices based on ITO [9].

In this study, we aim to build upon previous work to thoroughly investigate the role of all process parameters and understand how to tailor the final properties of PEDOT. This will open up further opportunities for exploring the integration of the developed thin films into different types of devices. Toward this goal, the influence of several key deposition conditions, such as, total pressure, partial pressure of the reactants, oxidant/monomer ratio, on the chemical composition, structure, electrical, and optical properties, as well as the deposition rate and spatial uniformity, will be discussed. In particular, it was observed that decreasing the reactor pressure from 300 to 160 mTorr reduced the deposition rate from 12 to 6 nm/min while enhancing the films' transmittance in the visible range from 50% to 75% and conductivity from 610 to 675 S/cm. Similarly, lowering the partial pressures of the monomer from 37 mTorr to 26 mTorr and the oxidant from 18 mTorr to 13 mTorr, achieved by increasing the carrier gas flow of nitrogen (from 20 to 30 sccm), led to comparable improvements in both optical and electrical properties, reaching transmittance and conductivity values of 75% and 680 S/cm, respectively. For these conditions, the film uniformity in terms of deposition rate and properties was excellent over 25 cm long.

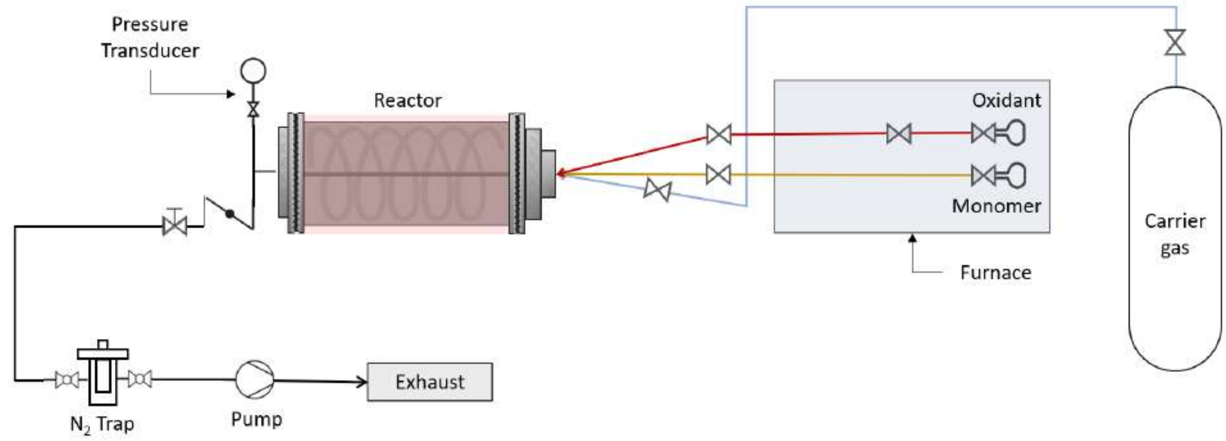
Pressure Transducer
Reactor
Oxidant
Monomer
Furnace
Carrier gas
N_2 Trap
Pump
Exhaust

Fig. 1. Schematic representation of the oCVD setup

References

[1] L. Krieg et al., *Nat Commun*, **11**, 5092, (2020).
[2] M. N. Gueye et al., *Progress in Materials Science*, **108**, 100616 (2020).
[3] M. Mirabedin et al., *Applied Surface Science*, **554**, 149501 (2021).
[4] S. Kaviani et al., *ACS Appl. Polym. Mater.*, **1**, 552–560 (2019).
[5] M. Heydari Gharahcheshmeh, *MRS Communications*, **14**, 785–804 (2024).
[6] M. Heydari Gharahcheshmeh et al., *Adv Funct Materials*, **31**, 2008712 (2021).
[7] M. Mirabedin et al., *Synthetic Metals*, **266**, 116419 (2020).
[8] M. Heydari Gharahcheshmeh and K. K. Gleason, *Adv Materials Inter*, **6**, 1801564 (2019).
[9] A. Sekkat et al., *ACS Appl. Polym. Mater.*, **5**, 10205–10216 (2023).

Enhancing Thermochromic Smart Windows via Low-Temperature ALD of Rutile Titanium Dioxide

J. Leithäuser[1], **M. Becker**[1], **P. Klement**[1] **and S. Chatterjee**[1]
[1] Institute of Experimental Physics I, Justus Liebig University Giessen, Germany
e-mail: jan.leithaeuser@physik.jlug.de

Thermochromic smart windows dynamically regulate indoor temperatures by transmitting infrared light in cold conditions and reflecting it in hot weather, reducing energy consumption for heating and cooling. Unlike alternative technologies, thermochromic smart windows operate autonomously without external driving forces, leveraging the phase transition temperature of the active material. This simplicity positions them as a highly promising energy-saving solution. Vanadium dioxide (VO_2) is a leading thermochromic material due to its reversible metal-to-insulator transition near room temperature, which is accompanied by a significant shift in infrared transmittance. However, due to competing phases in the vanadium-oxygen system, elevated growth temperatures are needed to ensure phase-pure material. Thus, to enable industrial process feasibility, a major challenge remains: lowering VO_2's growth temperature.[1]

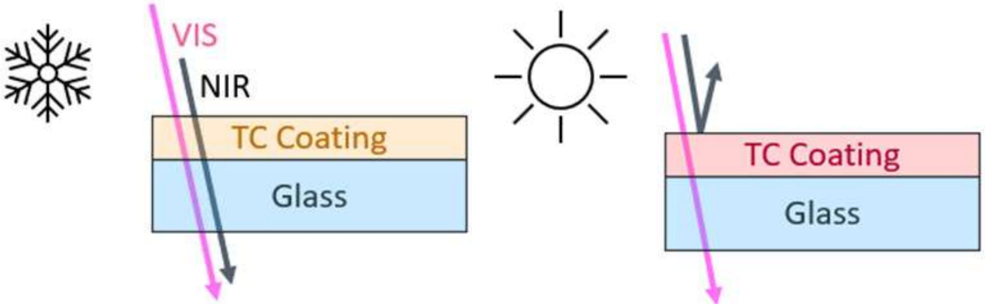

Fig. 1. Ideally, thermochromic windows transmit both near-infrared (NIR) and visible light (VIS) in their cold state, while selectively reflecting NIR in their hot state, maintaining high visible light transmittance.

In this study, we introduce a novel approach using an ALD-grown rutile TiO_2 seed layer to both reduce the growth temperature of VO_2 and prevent parasitic ion diffusion from the glass substrate into the thermochromic layer.[1] TiO_2 is deposited at a low temperature of 200 °C and directly crystallized into the rutile phase via mild in-situ post-deposition annealing at 250 °C. We control the crystallization by growing a sub-stoichiometric $TiO_{x<2}$ thin film, where oxygen vacancies promote rutile phase formation during annealing.[3,4] The combination of this low-temperature ALD process with its intrinsic low surface roughness and the subsequent low-temperature sputter deposition of VO_2 additionally results in a significantly enhanced transmittance modulation in the smart window device. This innovative integration of ALD and sputtering techniques demonstrates a viable pathway for next-generation energy-efficient smart windows, offering both improved performance and scalable fabrication potential.

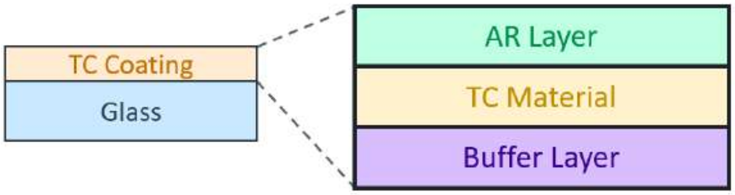

Fig. 2. Schematic of the thermochromic coating structure: an antireflective (AR) layer, a thermochromic (TC) VO_2 layer, and a rutile TiO_2 buffer layer.

References

[1] M. Becker, F. Kuhl, J. Hauptmann, J. Kessler, S. L. Benz, S. Chatterjee, A. Polity, P. J. Klar, *ACS Appl. Electron. Mater.* **2023**, *5*, 3560.

[2] J. Pointet, P. Gonon, L. Latu-Romain, A. Bsiesy, C. Vallée, *Journal of Vacuum Science & Technology A: Vacuum, Surfaces, and Films* **2014**, *32*, 01A120.

[3] J. Saari, H. Ali-Löytty, K. Lahtonen, M. Hannula, L. Palmolahti, A. Tukiainen, M. Valden, *J. Phys. Chem. C* **2022**, *126*, 15357.

[4] D. Rafieian, W. Ogieglo, T. Savenije, R. G. H. Lammertink, *AIP Advances* **2015**, *5*, 097168.

Atomic Layer Deposition of Metal Oxide Monolayers on Thermal Oxide for SiO_2-Modulation Acceptor Doping

D. Hiller[1,*], **S. Shams**[1], **S. Shah**[1], **S. Schneider**[1], **I. Ratschinski**[1] , **M. Venzke**[2], **P. Hönicke**[2,3]
[1]Institute of Applied Physics (IAP), Technical University Bergakademie Freiberg, Germany
[2]Physikalisch-Technische Bundesanstalt (PTB), Abbestraße. 2-12, 10587, Berlin, Germany
[3]Helmholtz-Zentrum Berlin, Hahn-Meitner Platz 1, 14109, Berlin, Germany
e-mail: daniel.hiller@physik.tu-freiberg.de

Modulation doping of silicon using specific metal impurities in SiO_2 is a novel doping concept that overcomes the limitations of conventional impurity doping, especially for nanostructures (diffusion, dielectric and quantum confinement, statistics of small numbers, etc.). An impurity doped SiO_2 layer within a direct tunneling distance to a silicon (nano-)volume interacts via a charge transfer process that ionizes unoccupied acceptor states induced by the impurities and leave holes behind in the silicon as free charge carriers [1]. Hence, by this method the free carriers are separated from their parent dopant atoms, which are embedded in the adjacent SiO_2. Based on this concept, extensive experimental evidence of the doping mechanism was gathered by studying capacitance-voltage characteristics of MOS-capacitors made of modulation acceptor doped SiO_2 [2-4] as well as by current-voltage characteristics and Hall-effect measurements Si nanowires and Hall-bars with such a doped SiO_2 shell [5-7]. Most importantly, the latter revealed a high hole density of $\sim 3\times10^{18}$ cm^{-3}, which enabled a low resistivity of less than ~30 mΩ·cm [7] and proves the general applicability of this doping method for Si nanowires.

In order to optimize this doping method, which is based on ALD surface functionalization of a thermally grown tunnel-SiO_2 by (sub-)monolayers of e.g., Al_2O_3 or Ga_2O_3 [8], we studied the initial growth by synchrotron-based reference-free grazing incidence X-ray fluorescence spectrometry (GIXRF) [9]. It is well established that a hydrophilic, Si-OH terminated Si-surface allows for steady-state ALD using metal alkyls (such trimethylaluminum or trimethylgallium) almost from the first ALD-cycle on, whereas the hydrophobic, Si-H terminated Si-surface delays the onset of steady-state ALD by a significant number of incubation cycles [10,11]. However, in our case the growth surface is a dry-thermal tunnel oxide fabricated by rapid thermal oxidation of Si and is therefore not comparable to either one of the above surface conditions. As a consequence, a slightly incubated deposition is observed, such that, for instance, the first complete Al_2O_3 ALD-monolayer requires about 4 ALD-cycles [12].

In this contribution, we present for the SiO_2-modulation acceptor elements Al and Ga, how the initial ALD-growth, as measured by GIXRF, correlates to electrical properties of the doped SiO_2 and to the resulting doping behavior.

This work was supported by the German Research Foundation (DFG) via project MADSiNano (456993281) and a Heisenberg grant (434030435).

References

[1] D. König et al., *Sci. Rep.* **7**, 46703 (2017)
[2] D. Hiller et al., *ACS Appl. Mater. Interfaces* **10**, 30495 (2018)
[3] D. Hiller et al., *J. Appl. Phys.* **125**, 015301 (2019)
[4] D. Hiller et al., *J. Phys. D Appl. Phys.* **54**, 275304 (2021)
[5] I. Ratschinski et al., *Phys. Status Solidi A* **220**, 2300068 (2023)

[6] S. Nagarajan et al., *Adv. Mater. Interfaces* **11**, 2300600 (2023)
[7] S. Nagarajan et al., *Adv. Funct. Mater.* 2415230 (2024)
[8] D. König et al., *Phys. Rev. Appl.* **10**, 054034 (2018)
[9] P. Hönicke et al., *J. Vac. Sci. Technol.* **37**, 041502 (2019)
[10] R. L. Puurunen, *Appl. Surf. Sci.* **245**, 6 (2005)
[11] A. Delabie et al., *J. Vac. Sci. Technol. A* **30**, 01A127 (2012)
[12] D. Hiller et al., *Sol. Energy Mater. Sol. Cells* **215**, 110654 (2020)

8Pulsed e-CVD of iron

P. Niiranen, Daniel Lundin, and Henrik Pedersen
Linköping University, Department of Physics, Chemistry and Biology
E-mail: pentti.niiranen@liu.se

CVD of metallic films has been widely studied for many metals. Since many metal precursors have a metal center with positive valency, the deposition scheme requires a reducing agent to transfer electrons to the metal for the reduction to occur. The more electropositive the metal is, the more powerful the reducing agent needs to be. Powerful reducing agents are scarce, although a few have been showcased in CVD. The nature of powerful reducing agents is that they should be highly reactive, suggesting that it might be problematic to scale up to an industrial scale.

As an alternative, we recently showcased a method which we now refer to as electron chemical vapor deposition (e-CVD) for deposition of metals.[1] The deposition process in e-CVD process relies on reactions between the metal precursor and free electrons from a plasma, which reduce the metal centers. In e-CVD, the substrate is positively biased to electrostatically draw the plasma electrons to the substrate. We have observed self-saturated growth using our developed biased quartz crystal microbalance (QCM) [2] when depositing Cu and it has also given insight into the different growth stages of the process.

In this contribution, we describe pulsed e-CVD of iron using ferrocene ($FeCp_2$). We have utilized various *in-situ* techniques, such as RF Sobolewski probe to study the plasma characteristics [3] and mass spectrometry (MS), optical emission spectroscopy (OES), coupled with density functional theory (DFT) to study the decomposition pattern of $FeCp_2$.[4] Studying the plasma characteristics, it revealed an electron temperature and electron density in the range of 1-5 eV and 10^{16} electrons/cm^3, respectively and when mapping the plasma potential, it showed that the electron flux to the substrate is energetically favorable. We utilized our knowledge of the electron temperature in a following study, when we explored the plasma decomposition of $FeCp_2$.[4] The decomposition study showed that $FeCp_2$ decomposes, forming various fragments, containing *e.g.*, iron and various hydrocarbons such as acetylene. Supported by the use of these techniques, we will suggest a deposition mechanism when using $FeCp_2$ and plasma electrons in e-CVD.

This work was supported by Swedish Research Council (VR). The Swedish Government Strategic Research Area in Material Science on Functional Materials and LAM research are gratefully acknowledged.

References

[1] H.Nadhom, D.Lundin, P.Rouf, and H.Pedersen, *J.Vac.Sci.Technol. A*, **38**, 033402, (2020).
[2] P.Niiranen, H.Nadhom, M.Zanáska, R.Boyd, M.Sortica, D.Primetzhofer, D.Lundin and H.Pedersen, *Rev.Sci.Instrum.*, **94**, 023902, (2023).
[3] P.Niiranen, A.Kapran, H.Nadhom, M.Čada, Z.Hubička, H.Pedersen and D.Lundin, *J.Vac.Sci.Technol.A*, **42**, 023006, (2024).
[4] P.Niiranen, F.Andersson, D.Lundin, L.Ojamäe, and H.Pedersen, *J.Chem.Phys*, **162**, 034703 (2024).

Pulsed heating atomic layer deposition of TiO_2 thin films on soft substrates

G. Arnould Dallet[1], L. Imhoff[1], G. Combe[1], P. Buirey[1], B. Huynh[1],
I. Pochard[2], M. C. Marco de Lucas[1]
[1]Laboratoire Interdisciplinaire Carnot de Bourgogne (ICB), UMR 6303 CNRS-Université Bourgogne Europe, 9 Av. Alain Savary, BP 47870, 21078 Dijon
[2]Laboratoire UTINAM, UMR 6213 CNRS-Université Marie et Louis Pasteur, Besançon, France
e-mail: Galaad.Arnould-Dallet@u-bourgogne.fr

One of the strengths of the atomic layer deposition (ALD) technique is its ability to produce very thin and uniform deposits conform to the morphology of the substrates even in the case of high roughness or porosity. The range of potential substrates to support ALD films continues to expand. Among them, porous, flexible, organic and natural substrates are attracting increasing interest. Even though the deposition temperature is low in thermal ALD (the ALD window is commonly in between 150 and 400 °C for most metal oxide deposits), the risk of degradation cannot be excluded for sensitive substrates. To reduce this risk, it would be interesting to limit heating to short periods of time in ALD cycles. Moreover, the energy cost of the production process would also be reduced.

To date, several approaches have been proposed to provide additional energy in short periods of time during an ALD process such as photo-assisted ALD using a pulse light source [1], atomic layer annealing (ALA) using in-situ plasma bombardment [2] and in-situ rapid thermal annealing introducing a heat pulse after a deposition cycle [3]. The goal was mainly to improve the quality of the ALD films by reducing the presence of defects and promoting the compound stoichiometry and the atomic arrangement in crystalline layers.

In previous works [4,5], we reported the ALD synthesis of inverse opal TiO_2 films using a template of polystyrene (PS) micro-beads deposited on a silicon substrate. A post-annealing treatment was used to remove the template to obtain inverse opal layers. The interest of these kind of films for photocatalysis and sensor applications was also shown. However, the possibility of reducing the size of PS beads, in order to increase the specific surface area, has run up against the problem of their softening, even at low ALD temperatures (90-100 °C).

The aim of this work is to explore the possibility of using pulsed heating to preserve the morphology of the template, and more broadly to use soft thermal-sensitive substrates. In particular, we herein report the ALD synthesis of TiO_2 films on flat substrates and PS micro-bead templates (Fig.1) using pulsed heating induced by short pulses of power supplied to infrared lamps. Several examples of TiO_2 films deposited on soft substrates (polymer foams and natural material fibers) will also be presented. SEM observations, together with XPS and micro-Raman analysis, were carried out to study the morphology, stoichiometry and structure of the deposits.

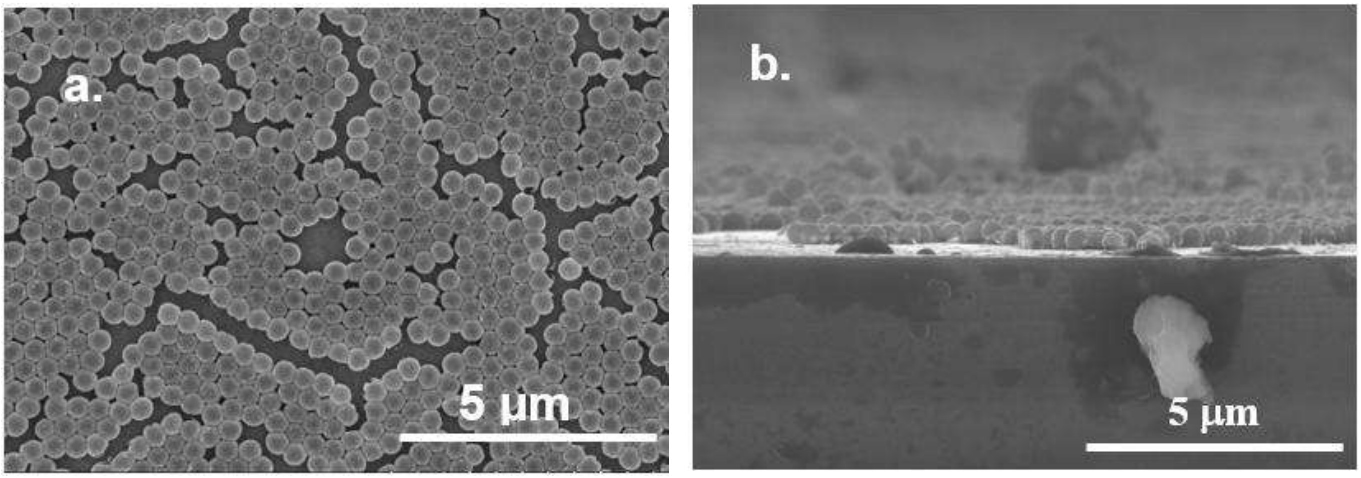

Fig. 1. SEM images of the surface (a) and cross-section (b) of TiO_2 inverse opal films produced by pulsed heating ALD.

This work was supported by EIPHI Graduate School (Contract ANR-17-EURE-0002).

References

[1] V. Miikkulainen, M. Vehkamäki, K. Mizohata, T. Hatanpää, M. Ritala, Highly Material Selective and Self-Aligned Photo-assisted Atomic Layer Deposition of Copper on Oxide Materials. Adv. Mater. Interfaces 2021, 8, 2100014.
[2] Wei-Hao Lee, Wei-Chung Kao, Yu-Tung Yin, Sheng-Han Yi, Kuei-Wen Huang, Hsin-Chih Lin, and Miin-Jang Chen, Applied Surface Science, **525**, 146615 (2020).
[3] B. D. Piercy, J. P. Wooding, S. A. Gregory, and M. D. Losego, Dalton Transactions, **51**, 303–311 (2022).
[4] P. Birnal, M. C. Marco de Lucas, I. Pochard, B. Domenichini, and L. Imhoff, Applied Surface Science, **512**, 145693 (2020).
[5] P. Birnal, M.C. Marco de Lucas, I. Pochard, F. Herbst, O. Heintz, L. Saviot, B. Domenichini, and L. Imhoff, Applied Surface Science, **609**, 155213 (2023).

Advanced Functional Coatings via Atomic Layer Deposition for High-Performance Proton Exchange Membrane Water Electrolysis

B. S. Chavan[1], R. Kortlever[2], J. R. van Ommen[1,*]
[1]Product and Process Engineering, Department of Chemical Engineering, Faculty of Applied Sciences, TU Delft
[2]Large-Scale Energy Storage, Process & Energy, Faculty of Mechanical Engineering, TU Delft
*e-mail: j.r.vanommen@tudelft.nl

Proton-exchange membrane (PEM) water electrolysis is a leading technology for sustainable hydrogen production, offering high efficiency and compact design. However, its widespread adoption is hindered by the reliance on expensive materials, such as platinum group metals and titanium-based components that can withstand the highly acidic and oxidizing conditions during electrolysis [1].

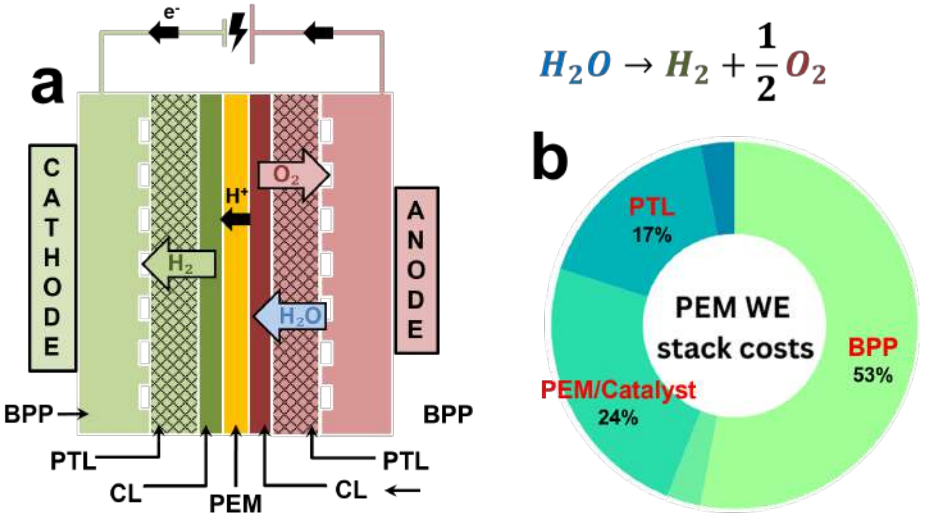

Figure 1. (a) Schematics of a PEM water electrolyzer showing inlets/outlets: H_2O, O_2 and H_2; and major components like the proton exchange membrane (PEM), catalyst layers (CL), porous transport layers (PTL) and bipolar plates (BPP). (b) Costs breakdown of major components in a PEM water electrolyzer cell, showing 17% and 53% of the costs coming from the PTL and BPP [2].

Titanium-based components, such as the porous transport layer (PTL) and bipolar plates (BPP), play critical roles in facilitating mass transport, ensuring uniform current and heat distribution, and providing mechanical stability to the system (see Figure 1 (a)). However, under operational conditions, these components form semiconducting oxide layers, which reduce electrical conductivity and compromise system efficiency. Additionally, they require high hydrophilicity to improve gas-liquid contact and mass transfer. To address these challenges, these components are often coated with thick layers of precious metals such as platinum or gold, increasing costs significantly (see Figure 1 (b)) [3]. Developing cost-effective alternatives to these materials is essential to advancing PEM water electrolysis as a scalable and economical solution for green hydrogen production.

Atomic layer deposition (ALD) – a gas-phase coating method – has emerged as a promising approach to address these challenges by providing exceptional control over material deposition, enabling the creation of ultra-thin, uniform films with atomic precision [4]. Its unparalleled conformality makes ALD particularly well-suited for coating complex 3D structures, such as PTL and BPP. In this research, functional coatings, such as titanium nitrides (TiN) and Magnéli phase oxides (Ti_4O_7), are explored as cost-effective alternatives to replace state-of-the-art Pt or Au coatings for titanium components, aiming to combine superior corrosion resistance, conductivity, and hydrophilicity (see Figure 2 for 3D structures and a comparison based on electrical conductivity, cost, and stability) [5,6]. TiN films are first grown on Si wafers and titanium flat sheets, followed by the more complex 3D PTLs. For the Magnéli phase oxide films, titanium dioxide are first grown by ALD, where afterwards the films are annealed at high temperature in a reducing atmosphere to achieve the phase transformation. Finally, the ALD-based titanium nitride and Magnéli phase oxides are further optimized and tested for conductivity, hydrophilicity, and stability under actual PEM water electrolysis conditions. These advances demonstrate the potential of ALD in PEM water electrolysis, paving the way for the production of green hydrogen.

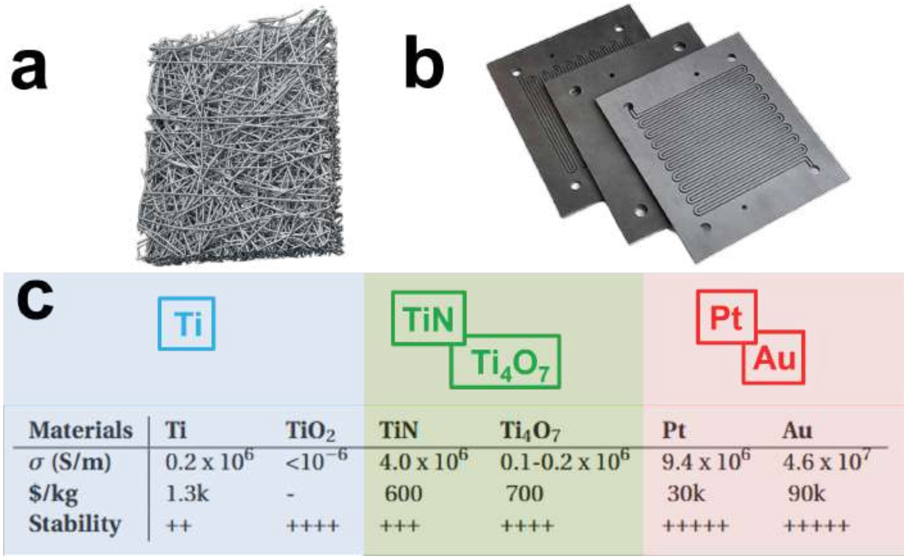

Materials	Ti	TiO_2	TiN	Ti_4O_7	Pt	Au
σ (S/m)	0.2 x 10^6	$<10^{-6}$	4.0 x 10^6	0.1-0.2 x 10^6	9.4 x 10^6	4.6 x 10^7
$/kg	1.3k	-	600	700	30k	90k
Stability	++	++++	+++	++++	+++++	+++++

Figure 2. (a) Titanium porous transport layer (PTL) and (b) titanium bipolar plates (BPP) showing 3D structure of the components. (c) Comparison of electrical conductivity, cost and stability of proposed coatings with the noble metal coatings [5,6].

This project receives a Dutch National Growth Fund contribution from the programme NXTGEN HIGHTECH.

References

[1] U. Babic, M. Suermann, F. Büchi, L. Gubler, and T. Schmidt, *Journal of Electrochemical Society*, **164**, F387 (2017).

[2] K. Zhang, X. Liang, L. Wang, K. Sun, Y. Wang, Z, Xie, Q. Wu, X. Bai, M. Hamdy, H. Chen, and X. Zou, *Nano Research Energy*, **1**, 9120032 (2022).

[3] T. Srour, K. Kumar, V. Martin, L. Dubau, F. Maillard, B. Gilles, J. Dillet, S. Didierjean, B. Armoury, T. Dung Le, and G. Maranzana, *International Journal of Hydrogen Energy,* **58**, 351-361 (2024).

[4] J.R. van Ommen, A. Goulas, and R. Puurunen, *Atomic layer deposition, Kirk-Othmer Encyclopaedia of Chemical Technology,* 1-42 (2021).

[5] H. Wakayama, and K. Yamazaki, *American Chemical Society Omega*, **6**, 4161-4166 (2021).

[6] G. Liu, D. Shan, B. Fang, and X. Wang, *International Journal of Hydrogen Energy*, **48**, 18996-19007 (2023).

MOCVD as a Versatile Tool for Luminescent Europium-Doped GdF_3 and GdOF Thin Films

F. Scardaci[1], F. Lo Presti[1], R. Valiente[2], G. Malandrino[1*]

[1]Dipartimento Scienze Chimiche, Università di Catania, and INSTM UdR Catania, Viale Andrea Doria 6, 95125 Catania, Italy
Applied Physics Department, Universidad de Cantabria-IDIVAL, Avenida de los Castros 48, 39005, Santander, Spain
Email: graziella.malandrino@unict.it

Europium-doped gadolinium-based thin films have garnered significant interest for advanced photonic applications due to their efficient luminescence, tunable optical properties, and structural versatility, which enable their integration into diverse technological platforms [1-2].

This study presents a comparative spectroscopic study of the luminescent properties of Eu^{3+}-doped GdF_3 and GdOF thin films. These materials combine the low phonon energy of fluorides, which minimizes non-radiative decay processes, with the enhanced mechanical and chemical stability provided by oxyfluorides, making them an ideal platform for rare-earth ion doping [3-4]. The films were deposited using low-pressure Metal-Organic Chemical Vapor Deposition (MOCVD) onto SiO_2/Si and quartz substrates. The deposition process, optimized in a horizontal hot-wall reactor with β-diketonate precursors, ensured uniform film growth on SiO_2/Si and quartz substrates, while achieving distinct crystal phases under controlled conditions [5].

MOCVD offers several advantages, including conformal coating on complex geometries, precise stoichiometric control, and scalability, positioning it as a superior technique for fabricating high-quality luminescent thin films tailored for specific applications [6].

Structural characterization confirmed the formation of orthorhombic GdF_3 and trigonal or monoclinic GdOF phases, depending on the deposition parameters. Optical analyses demonstrated the characteristic Eu^{3+} red emissions, with the emission intensities and transitions –such as $^5D_0 \rightarrow {}^7F_1$ and $^5D_0 \rightarrow {}^7F_2$– strongly influenced by local symmetry and site occupancy.

The incorporation of europium, a well-known photoluminescence activator , enhances the functionality of these materials in optoelectronic devices by enabling efficient energy transfer mechanisms and potential down-conversion processes. These mechanisms allow the conversion of high-energy photons into multiple lower-energy photons, improving the efficiency of photonic devices such as solar cells and LEDs [7].

Overall, the findings underscore the potential of MOCVD for fabricating high-performance luminescent materials, paving the way for innovative applications in optoelectronics, solid-state lighting, and anti-counterfeiting technologies.

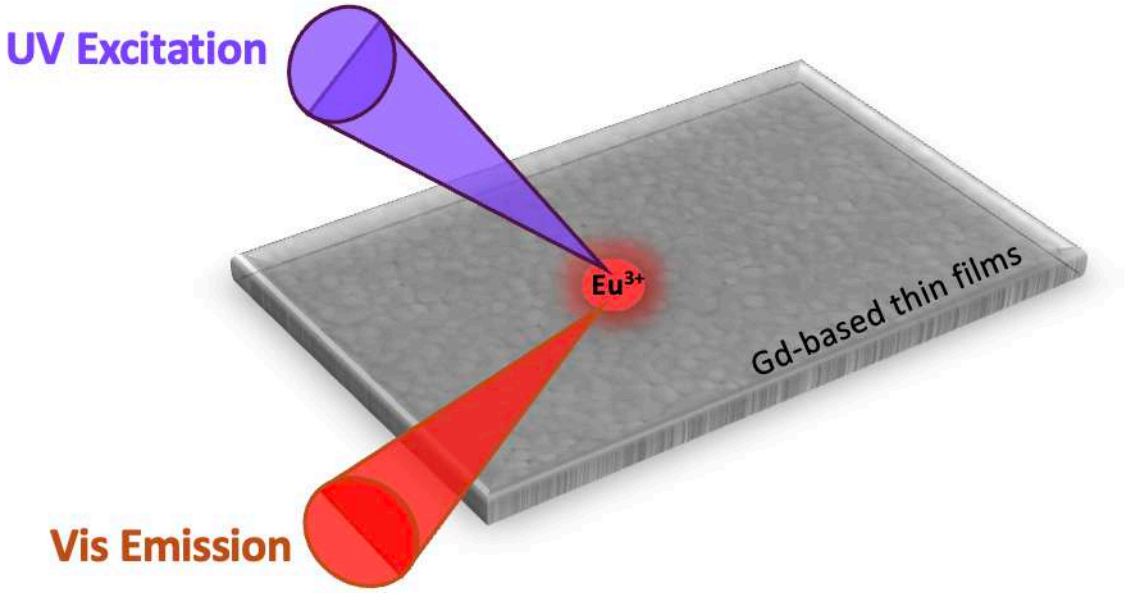

Fig. 1. Schematic representation of the UV excitation and Visible emission (Vis) of Gd-based thin films doped with Eu^{3+}, showing the europium-induced luminescence process.

References

[1] J. H. Zeng, Z. H. Li, J. Su, L. Wang, R. Yan, Y. and Li, Synthesis of complex rare earth fluoride nanocrystal phosphors *Nanotechnology* **17** 3549–55 (2006).

[2] X. Li, S. Zhou, X. Wei, F. Hu, Y. Qin, Y. Chen, M. Yin, and C. Duan, Two-wavelength two-photon process for optical selection of rare-earth ions *Journal of Alloys and Compounds* **660** 226–30 (2016).

[3] D. Chen, Y. Wang, Y. Yu, and P. Huang, Structure and Optical Spectroscopy of Eu-Doped Glass Ceramics Containing GdF_3 Nanocrystals *J. Phys. Chem. C* **112** 18943–7 (2008).

[4] T. Wen, X. Li, D. Ning, J. Yao, B. Yang, and Y. Wang, Selective synthesis, polymorphism, reversible phase transition and structure-dependent optical functionalities of gadolinium oxyfluorides *J. Mater. Chem. C* **6** 11007–14 (2018).

[5] G. Malandrino, M. Bettinelli, A. Speghini, I. L. and Fragalà, Europium "Second Generation" Precursors for Metal-Organic Chemical Vapor Deposition: Characterization and Optical Spectroscopy *Eur. J. Inorg. Chem.* 1039–44 (2001).

[6] Yan, Xiu-Tian, and Yongdong Xu. Chemical vapour deposition: an integrated engineering design for advanced materials. Springer Science & Business Media (2010).

[7] F. Baur, and T. Jüstel. "Eu^{3+} activated molybdates–Structure property relations." Optical Materials: X, Volume 1 (2019): 100015 (2019).

From engineering of heterobimetallic Na-Y precursor to MOCVD synthesis of $NaYF_4$ thin films

A. L.Pellegrino,* F. Lo Presti, G. Malandrino

Dipartimento Scienze Chimiche, Università degli Studi di Catania, and INSTM UdR Catania, Viale Andrea Doria 6, 95125 Catania, Italy.
e-mail: annalucia.pellegrino@unict.it

Alkaline earth fluoride materials have attracted great attention due to a wide variety of applications in optoelectronics field [1]. In particular, alkaline earth fluoride such as MF_2 (M: Ca, Sr) and $MREF_4$ (M: Na, K; RE: Y, Gd) has been regarded as the most efficient hosts for up-conversion (UC) or down-conversion emissions. Alkaline earth fluoride materials, properly doped, can act as UC and DC layers enhancing the efficiency of photovoltaic devices [2]. They, in fact, make possible to collect the solar radiation energy outside the absorption range of the photoactive material (usually silicon) and shifting its energy to a more suitable optical region. In addition, doped fluoride compounds are promising luminescent materials as phosphors and in technological applications as micro- and nanoscale thermometry for microelectronics and for biomedical assays [3].

Several studies are available on the deposition methods applied for their fabrication in form of thin films such as sputtering, ALD, MBE, and sol–gel routes. Nevertheless, the metal organic chemical vapor deposition (MOCVD) has the potential advantage of being a very reliable and reproducible method for the fast production of films with high uniformity degree in both thickness and composition over large areas.

In the present work, preliminary results on the MOCVD synthesis of $NaYF_4$ nanostructured thin films are reported using the novel fluorinated heterobimetallic β-diketonate compound, synthetized in a previous work [4], $NaY(hfa)_4$•tetraglyme (Hhfa = 1,1,1,5,5,5 – hexafluoro - 2,4 - pentanedione; tetraglyme = 2, 5, 8, 11, 14 – pentaoxapentadecane), which acts as a single precursor for the metal components and the fluorine. An accurate optimization of the operative parameters, such as the deposition temperature and the substrate positions inside the reactor, has been carried out to stabilize the fluoride hexagonal β-$NaYF_4$ phase that shows the best host behavior for the luminescence doping ions compared to the cubic α-$NaYF_4$ structure in the energy conversion applications. X-ray diffraction and field emission scanning electron microscopy, lead to the evaluation of the deposition temperature on the final phase of the film and point to the formation of good quality hexagonal $NaYF_4$ films with a uniform and nanostructured morphology (fig. 1).

This work was partially supported by the European Union (NextGeneration EU) through the MUR-PNRR project SAMOTHRACE (ECS00000022).

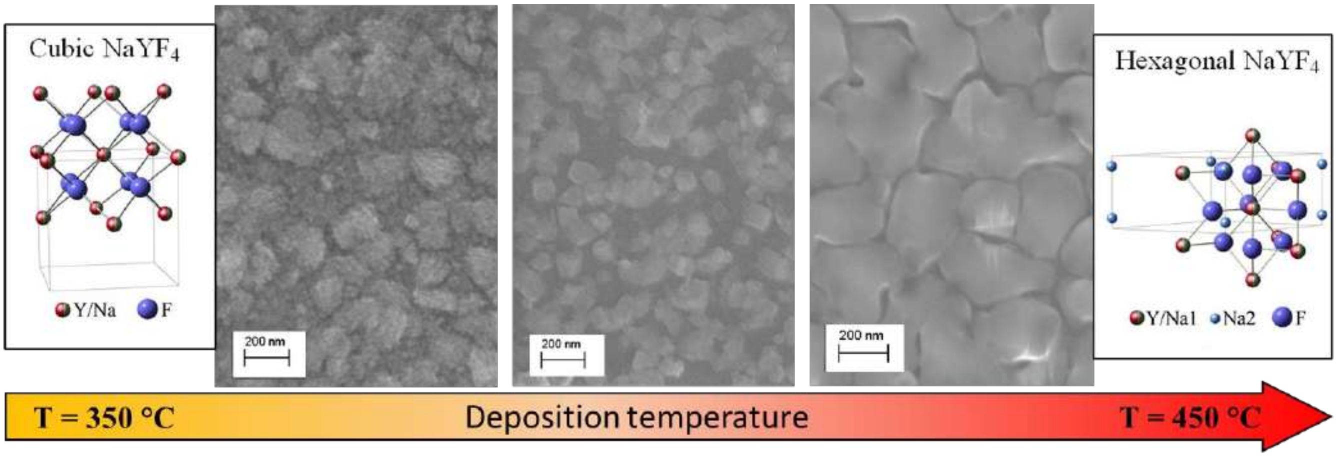
Cubic NaYF4
Y/Na
F
200 nm
200 nm
200 nm
Hexagonal NaYF4
Y/Na1
Na2
F
T = 350 °C
Deposition temperature
T = 450 °C

Fig. 1. FE-SEM images of the $NaYF_4$ deposited on Si(100) as function of deposition temperatures.

References

[1] H. Xu, M. Dai, Z. Fu, *Small* **20,** 2400218 (2024).

[2] C. Huang, P. Li, X. Li, J. Gu, N. Fu, W. Zhang, *Solar RRL* **7,** 2300518 (2023).

[3] R. A. Janjua1, W.Ji, N. A. Shah, J. Evans, R. Zhang, S. Zhang, S. He, *Progress In Electromagnetics Research M*. **122**, 117 (2023).

[4] S. Battiato, P. Rossi, P. Paoli and G. Malandrino, *Inorg. Chem.* **57, 24**, 15035–15039 (2018).

MOCVD of ferrite materials: a novel approach to promising photoelectrodes for water splitting

L. Salamone[1], M. Bombaci[1], F. Lo Presti[1], M. Urso[2], S. Mirabella[2], G. Malandrino[1]*

[1]Dipartimento Scienze Chimiche, Università degli Studi di Catania, and INSTM UdR Catania, Viale Andrea Doria 6, 95125 Catania, Italy.
[2]MATIS IMM-CNR and Dipartimento di Fisica e Astronomia, Università di Catania, via S. Sofia 64, 95123 Catania, Italy
e-mail: graziella.malandrino@unict.it

In the last decades, ferrites have attracted significant attention from the scientific community due to their magnetic properties, environmental compatibility, and photochemical stability. Moreover, the ease of synthesis and low cost have paved the way for the application of these materials in the fields of electronics and catalysis. In particular, various ferrites, such as $CoFe_2O_4$, $NiFe_2O_4$, $CuFe_2O_4$, and $ZnFe_2O_4$, have been studied for applications in hydrogen production and engineered to be used in photoelectrochemical cells.[1] The advantages associated with the use of ferrites as materials for the construction of photoelectrodes, such as excellent redox behavior, low toxicity, natural abundance, and ease of synthesis, make ferrites ideal materials for applications in eco-sustainable energy conversion processes.[2]

It is widely recognized that an efficient synthesis technique is crucial for producing high-performance electrodes, as it allows to tailor semiconducting properties, including defect states, electronic conductivity, and optical properties. In this context, vapor-phase chemical methods emerge as a promising approach, as they offer numerous advantages, including large-area deposition, easy process scalability, conformal film production, and the ability to produce chemically complex systems.[3] The use of this technique for the formation of active layers in photoelectrochemical or electrochemical cells would thus provide an economical industrial production protocol, which would, in turn, lower the cost of green hydrogen production, making it economically competitive with hydrogen produced from fossil sources and enabling its wider adoption.

In this study, nickel ferrite ($NiFe_2O_4$), cobalt ferrite ($CoFe_2O_4$), and zinc ferrite ($ZnFe_2O_4$) thin films have been synthesized via Metal Organic Chemical Vapor Deposition (MOCVD) technique using β-diketonate precursors. Special focus has been directed toward the development of nanostructured spinel ferrite thin films through a low-temperature chemical vapor deposition process, with the aim to significantly lower synthesis temperatures compared to the conventional 800 °C, commonly used for the fabrication of such electrodes. Moreover, particular attention is given to the use of nickel foam (Ni-foam) as a conductive and structurally suitable substrate for potential applications in electrochemical energy conversion and storage.

Comprehensive characterization of the resulting materials was carried out to assess their structural, morphological, and compositional features. Finally, electrochemical measurements were performed to gain insight into how the coexistence of different phases may impact the electrochemical behavior toward the HER and OER, while identifying the crystalline phase with superior catalytic efficiency.

This work opens up new possibilities for the use of MOCVD-grown spinel ferrites in various applications, including photoelectrochemical cells, where characteristics such as high crystallinity, phase-control and low-temperature deposition are strongly required.

References

[1] Kim J H, Kim H E, Kim J H and Lee J S, *J. Mater. Chem. A,* **8**, 9447–82 (2020)

[2] Taffa D H, Dillert R, Ulpe A C, Bauerfeind K C L, Bredow T, Bahnemann D W and Wark M, *J. Photon. Energy*, **7**, 012009 (2016)

[3] Miller L M and Coleman J J, *Critical Reviews in Solid State and Materials Sciences*,**15**, 1–26 (1988)

Cu_xO-gCN-TiO_2-Au (x=1,2) nanosystems as efficient platforms for photoactivated hydrogen evolution

C. Maccato[1,2]*, M. Benedet[1,2], D. Barreca[2], A. Gasparotto[1,2], G. A. Rizzi[1,2],
G. Pagot[3], V. Di Noto[3], L. Zeng[4], E. Olsson[4]
[1]Department of Chemical Sciences, Padova University and INSTM, 35131 Padova, Italy
[2]CNR-ICMATE and INSTM, 35127 Padova, Italy
[3]Section of Chemistry for the Technology (ChemTech), Department of Industrial
Engineering, Padova University and INSTM, 35131 Padova, Italy
[4]Department of Physics, Chalmers University of Technology, 41296 Gothenburg, Sweden.
* e-mail: chiara.maccato@unipd.it

Green hydrogen generation, promoted by photoassisted water splitting, represents an appealing strategy for sustainable energy production. Nevertheless, its large-scale diffusion is still hampered by the availability of suitable photoelectrocatalysts for the hydrogen evolution reaction (HER), featuring a good stability, economic viability, and low toxicity. Various materials have been used for this purpose, and, among them, CuO/Cu_2O-based systems are very appealing candidates. In fact, they are characterized by an extended sunlight absorption and a low electron-hole recombination if compared to bare Cu_2O. To gain a further enhancement of functional activity, an attractive approach is represented by the tailored development of nanocomposites that can valuably profit by the construction of effective heterojunctions. To this regard, we designed a hybrid synthetic strategy allowing to take advantage from the incorporation of: i) graphitic carbon nitride (gCN), a cheap and eco-friendly semiconductor with attractive photoactivity; ii) TiO_2, a well-known semiconductor that can act both as protective agent against Cu_xO photocorrosion, and as a fundamental component to enhance interfacial charge mobility and suppress detrimental electron-hole recombination; iii) homogeneously dispersed Au nanoparticles (NPs), as electric/catalytic mediators promoting the overall system photoactivity [1,2]. The target multi-step preparation procedure is sketched in Fig. 1a. The anodization of a copper foam slice and its subsequent annealing promoted the growth of nanowire array (mean aspect ratio ≈ 33), some of which featured the presence of spheres (≈100 nm diameter) on their tips (Fig. 1b,c). Subsequently, the introduction of gCN was performed by a liquid-phase process, whereas the functionalization with TiO_2 and Au was carried out by means of radio frequency (RF)-Sputtering under mild operational conditions. The high infiltration power of RF-sputtering power, coupled with the high surface area of Cu_xO nanowires, favors an intimate contact between each of the system components. Detailed multi-technique analyses revealed the formation of a layered structure, in which Cu_2O is confined in the material inner regions, whereas CuO is located in the outermost ones, and gold particles feature a homogeneous spatial distribution.

Functional HER tests (Fig. 1d,e) revealed a progressive photocurrent density enhancement upon the insertion of each functionalizing agent in the Cu_xO hosting matrix. The most active system turned out to be Cu_xO-gCN-TiO_2-Au, whose performances [photocurrent density of ≈ -5.7 mA/cm^2 at 0.0 V *vs*. the reversible hydrogen electrode (RHE) and a Tafel slope of ≈ -190 mV/dec] compare favorably with analogous materials reported in the literature up to date. These results can be mainly related to the obtainment of efficient nanoheterojunctions, providing two fundamental benefits: a) a protective action towards Cu_2O corrosion; b) an enhanced charge carrier separation, guaranteed by an improved electron injection into the electrolyte supported byTiO_2 and an optimized electrical contact implemented by Au NPs, which, in turn, act as electron sinks. Such characteristics, along with the very good operational stability, pave the way to further implementations of the developed materials in view of eventual practical end-uses.

References

[1] M. Benedet, G.A. Rizzi, A. Gasparotto, O.I. Lebedev, L. Girardi, C. Maccato, and D. Barreca, *Chem. Eng. J.*, **448**, 137645 (2022).

[2] M. Benedet, G. A. Rizzi, A. Gasparotto, L. Zeng, G. Pagot, E. Olsson, V. Di Noto, C. Maccato, and D. Barreca, *RSC Adv.,* **14**, 7221 (2024).

The present work was financially supported by CNR (Progetti di Ricerca @CNR—avviso 2020—ASSIST), Padova University (P-DiSC#02BIRD2023-UNIPD RIGENERA), INSTM Consortium (TRI.25/013-CIMENTO), and PRIN 2022474YE8 (SCI-TROPHY project).

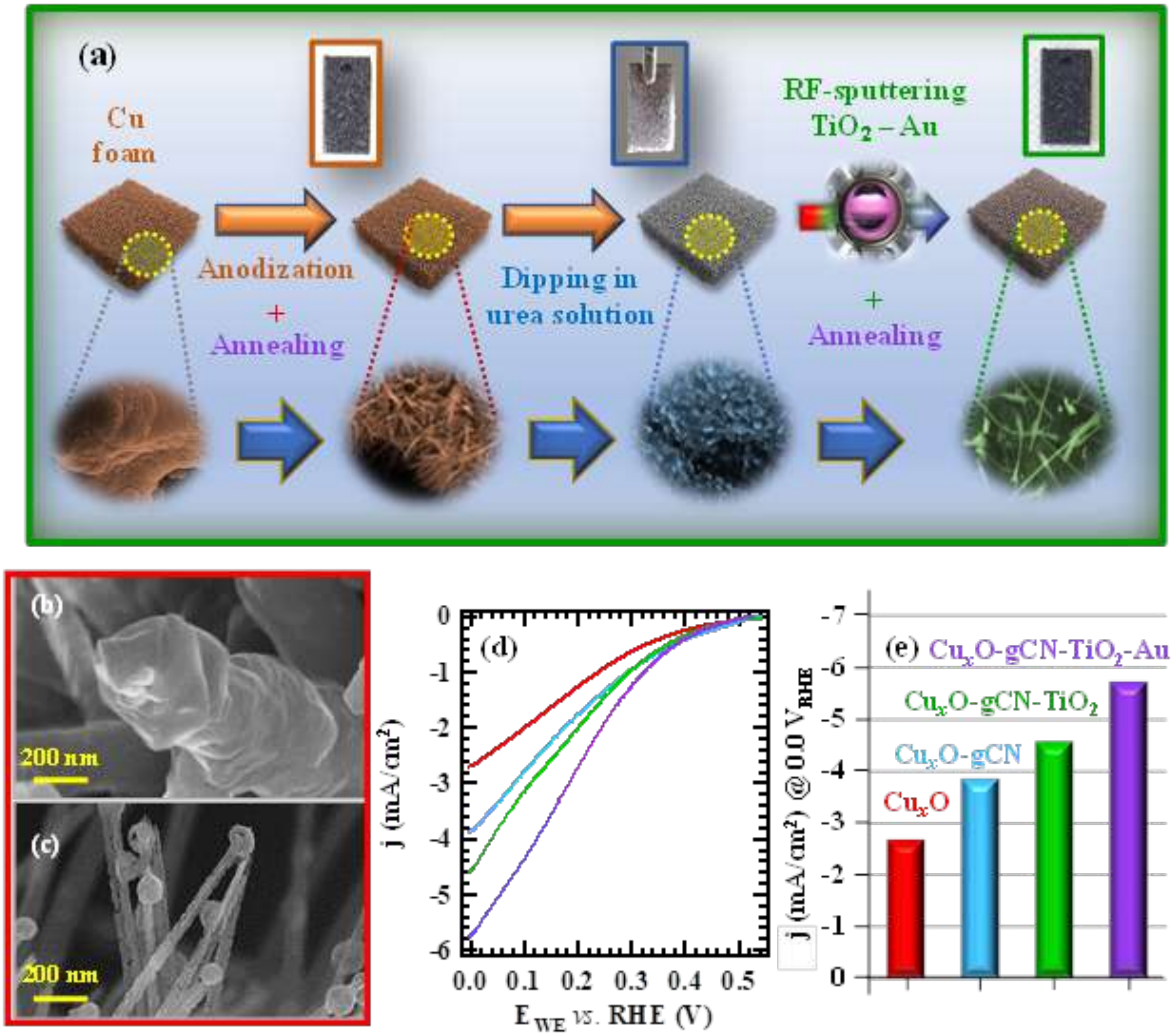

Figure 1. (a) Sketch of the fabrication route adopted in the present study. (b,c) Scanning electron microscopy (SEM) images of Cu_xO systems. (d) Linear-sweep voltammetry (LSV) curves of photocurrent *vs*. the applied bias, and (e) bar diagram reporting photocurrent densities at 0.0 V *vs*. RHE for composite systems.

LaPrNiO4+ δ films grown by MOCVD as oxygen electrode thin films

Silvère Panisset[1,2], Kosova Kreka[3], David Jauffres[2], Carmen Jiménez[1], Albert Tarancón[3], Mónica Burriel[1]

[1] . Univ. Grenoble Alpes, CNRS, Grenoble INP, LMGP, 38000 Grenoble, France
2. Univ. Grenoble Alpes, CNRS, Grenoble INP, SIMaP, 38000 Grenoble, France
3. Catalonia Institute for Energy Research (IREC), 08930, Barcelona, Spain

The study explores the potential of $LaPrNiO_{4+\delta}$ (LPNO) thin films as oxygen electrodes for low-temperature solid oxide cells (LT-SOCs), using Pulsed Injection Metal-Organic Chemical Vapor Deposition (PI-MOCVD). LPNO materials, offer promising mixed ionic and electronic conductivity, and high oxygen reduction reaction kinetics. This work investigates microstructural and electrochemical properties of LPNO thin films deposited at various temperatures (600–650 °C), revealing that a two-temperature process yields films with a dense bottom layer and a porous upper layers.

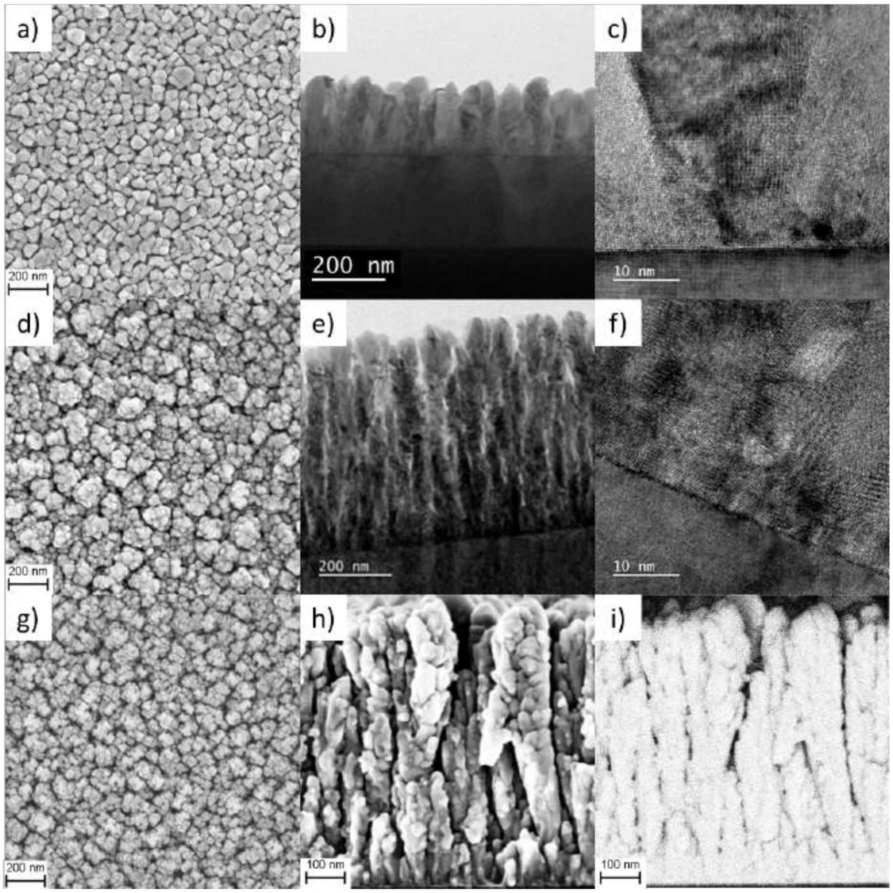

Figure: SEM and TEM images of a 200 nm dense (a-b-c), 560 nm porous (d-e-f), and 700 nm porous (g-h-i) LPNO thin films deposited at 650 °C, 600 °C and 600+650 °C, respectively. The cross-sectional SEM images in secondary electron (h) and back scattered electron (i) modes shows the dense first 80 nm (deposited at 650 °C) and the remaining porous film (depositied at 600 °C).

Electrochemical impedance spectroscopy (EIS) and electrical conductivity relaxation (ECR) experiments demonstrate high performance, with polarization resistances as low as 0.10 $\Omega\cdot\text{cm}^2$ at 600 °C. The films exhibit enhanced surface exchange coefficients compared to bulk LPNO and $La_2NiO_{4+\delta}$. Performance in solid oxide fuel cell (SOFC) and electrolysis cell (SOEC) modes was evaluated, achieving 0.34 W/cm^2 in SOFC mode at 600 °C. Aging studies highlight thermal stability concerns, including chemical decomposition and microstructural densification, emphasizing the need for further optimization. This work underscores the promise of LPNO thin films for efficient LT-SOCs while addressing challenges in durability and stability.

This work was funded by the European Union's Horizon 2020 research and innovation program under Grant Agreement No. 824072 (Harvestore project) and by the Centre of Excellence of Multifunctional Architectured Materials 'CEMAM' n° ANR-10-LABX-44-01 as part of the 'Investments for the Future' Program.

DFT Simulations on the Precursor Ligand Exchange Mechanism for Depositing $BaTiO_3$

Ji Liu[1], **Michael Nolan**[1], **Henrik Hovde Sønsteby** [2]

[1]Tyndall National Institute, University College Cork, Cork, Ireland
[2]University of Oslo, Department of Chemistry, Oslo, Norway
Presenting author: e-mail: ji.liu@tyndall.ie

Atomic layer deposition (ALD) is widely used in microelectronics and semiconductor industry to deposit metal and its oxide and nitride thin films as part of device fabrication in nano- or subnano-dimensions.[1] The key advantages of ALD are the conformality and precise thickness control at the atomic scale, which are difficult for physical or chemical vapor deposition methods. The atomic scale understanding of ALD is vital and essential to design and optimize the deposition process, and density functional theory (DFT) calculations play an important role in providing detailed reaction mechanism, theoretical screening of suitable precursors and estimated growth-per-cycle (GPC).

$BaTiO_3$, known as BTO, is one of the famous ferroelectric oxides with perovskite structure (ABO_3) which has attracted research attention in various electronic and optoelectronic applications. For example, BTO has shown great applicability as a robust UV absorber with an energy band gap of around 3.2 eV.[2] As chip manufacturers face significant challenges of very little room left for further downscaling of silicon transistors, there is a high demand to develop manufacture process enabling epitaxial growth at CMOS compatible conditions, for example allowing for integrating ferroelectric BTO on silicon.[3] To tackle this challenge, we need to develop ALD approach for epitaxial ferroelectric, where understanding the chemistry promoting the direct epitaxial is critical.

Here, this presentation will deliver the atomic understanding of precursor design and screen for depositing BTO by density functional theory (DFT) simulations. $Ba(acac)_2$ and $Ba(thd)_2$ are selected for Ba precursors and Titanium isopropoxide (TTIP) is selected for Ti precursor. The co-reactants are water and ozone. We first simulated the gas-phase reactions between selected Ba precursors and co-reactants. The results show that the usual liang exchange of protonated ligand is endothermic for both acac and thd ligands with H_2O, whereas O_3 can lead to exothermic ligand exchange by inserting into acac and thd ligands.

We then simulate the deposition ligand exchange mechanism on BTO substrates with both BaO termination and TiO termination. TTIP is placed on top of BaO terminated BTO substrates and $Ba(thd)_2$ is placed on top of TiO terminated BTO substrates. For TTIP, the results show that at most two ligands can be protonated via H transfer from surface hydroxyl OH groups, with a computed overall reaction energy at -1.30eV. However, if we continue to protonate the 3rd ligand, the overall reaction energy is positive at the value of 2eV. For $Ba(thd)_2$, the results show that the two THD ligands can be fully protonated and eliminated, with a computed overall reaction energy at -0.27eV. We introduce a 2nd Ba precursor and simulate the ligand exchange, only one THD ligand can be eliminated with a computed reaction energy at -1.73eV, whereas the overall reaction energy is positive for the 2nd THD ligand elimination (0.24eV). Lastly, we introduce O_3 on these precursor-treated BTO substrates and evaluate the plausible reaction mechanisms of how the remaining ligands are oxidized and removed and how the substrates recover into hydroxyl-terminated BTO substrates.

These works showcase how we can apply DFT calculations to elucidate the ligand exchange mechanism during metal or metal oxide thin film growth and give some insights on how the selection of precursors and reducing agent or co-reactant affects the growth behavior.

This work was supported by HEU project CONCEPT (Grant number: 101135946, https://conceptproject.eu/). We acknowledge the generous support from ICHEC and EuroHPC for the computing time.

References

[1] Johnson, Richard W., Adam Hultqvist, and Stacey F. Bent. "A brief review of atomic layer deposition: from fundamentals to applications." *Materials today* 17.5 (2014): 236-246.
[2] Elmahgary, Maryam G., et al. "Optical investigation and computational modelling of BaTiO3 for optoelectronic devices applications." *Scientific Reports* 13.1 (2023): 4761.
[3] Sønsteby, Henrik Hovde, Helmer Fjellvåg, and Ola Nilsen. "Functional perovskites by atomic layer deposition–An overview." *Advanced Materials Interfaces* 4.8 (2017): 1600903.

Modelling Surface -OH Defects on NiO (100) thin films fabricated via CVD Routes.

E. Fois[1*] , C. Maccato[2], D. Barreca[2,3], C. Invernizzi[1], G. Tabacchi[1]
[1]University of Insubria, Department of Science and High Technology, and INSTM.
[2]University of Padova, Department of Chemistry, and INSTM
[3]CNR-ICMATE, and INSTM
e-mail: ettore.fois@uninsubria.it

Nickel oxide-based thin films and nanomaterials are currently the focus of intense research efforts due to the broad range of end-uses in a variety of applications. Bulk NiO crystals have been extensively investigated and are characterized by a wide band gap (4.0–4.3 eV), antiferromagnetic (AF) ordering and p-type character [1,2].

On the other hand, the atomic-level relationships between the structure of surface defects on NiO films/nanomaterials and their electronic properties are still far from being completely elucidated.

Here we show that, by using density functional theory (DFT) with the Hubbard correction (DFT+U), –OH surface defects, almost ubiquitous on oxide surfaces, can deeply influence the electronic structure of NiO(100) surfaces. Actually, the (100) facet was found to be the dominant termination in thin films obtained via CVD routes [3-5]. This facet is the least polar one among NiO surface terminations, and it is characterized by an equal number of spin-up and spin-down Ni(II) cations. Interestingly, band gaps for NiO nanomaterials/thin films are generally lower than the homologous values measured for bulk NiO (see e.g. Ref. [3]) and are close to the Vis spectral region, thus fostering their possible use in sunlight-powered devices, such as solar cells and photocatalysts.

We have investigated two kinds of -OH surface defects [6], as sketched in Figure 1. In order to keep the AF ordering, typical of NiO materials, the defects have been introduced in pairs, with the aim of evenly perturb the two magnetic sub-lattices. Indeed, the introduction of a single -OH defect affects only one of the two magnetic sub-lattices, leading to half-metallic behavior [6].

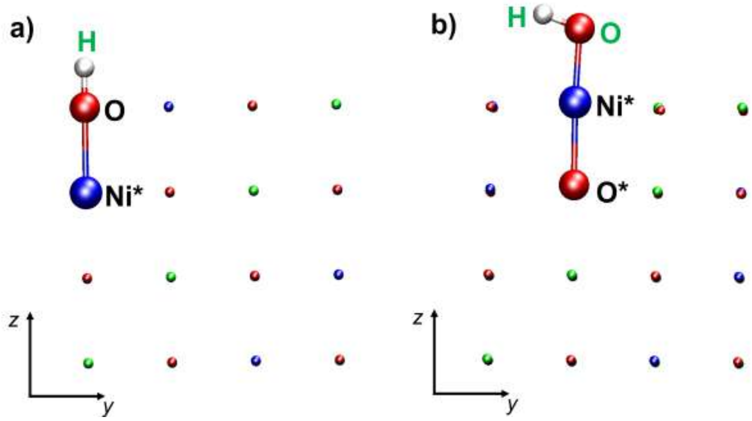

Fig 1. The two kinds of –OH defects considered in this work: (a) –OH defect built by adding a H atom on top of a (100) oxygen site; (b) –OH defect built by adding an OH group to a (100) Ni site. Color codes: oxygen, red; hydrogen, white; nickel (spin up), green; nickel (spin down), blue. Labels of defect atoms in green.

We have investigated the effect of the presence of increasing amounts of –OH defects on the NiO(100) topmost layer.

Overall, our results indicate that, depending on the defect chemical structure and surface density, the energy gap of the –OH bearing NiO(100) nanofilms can be engineered. In particular, the electronic behavior of these materials can be modulated from p-type to n-type. The insights provided herein may be of importance for the tailoring of NiO nanosystem properties as a function of specific applications, an important issue for their eventual real-world utilization.

An important result of this study is the description of two novel reconstructed NiO(100) surfaces, induced at high coverages by the two kinds of defects considered herein, namely H adsorbed on O sites (Figure 1a) and –OH adsorbed on Ni sites (Figure 1b). In spite of the different structures of the reconstructed surfaces, both systems are characterized by three-coordinated Ni sites on the top layer and, in one case, even by tetra-coordinated $Ni(OH)_4$ moieties, leading to a plane of under-coordinated Ni sites.

References

[1] G. A. Sawatzky and J. W. Allen, *Phys. Rev. Lett.*, **53**, 2339–2342, (1984)

[2] J. Zaanen, G. A. Sawatzky and J. W. Allen, *Phys. Rev. Lett.*, **55**, 418–421 (1985)

[3] M. Benedet, C. Maccato, G. Pagot, C. Invernizzi, C. Sada, V. Di Noto, G. A. Rizzi, E. Fois, G. Tabacchi and D. Barreca, *J. Phys. Chem. C*, **127**, 22304–22314 (2023)

[4] M. Benedet, D. Barreca, E. Fois, R. Seraglia, G. Tabacchi, M. Roverso, G. Pagot, C. Invernizzi, A. Gasparotto, A. A. Heidecker, A. Pöthig, E. Callone, S. Dirè, S. Bogialli, V. D. Noto and C. Maccato, *Dalton Trans.*, **52**, 10677– 10688 (2023)

[5] C. Invernizzi, G. Tabacchi, R. Seraglia, M. Benedet, M. Roverso, C. Maccato, S. Bogialli, D. Barreca and E. Fois, *Molecule*s, **29**, 642 (2024)

[6] E. Fois, C. Maccato, D. Barreca, C. Invernizzi, G. Tabacchi, *Dalton Trans.*, DOI: 10.1039/d4dt03340j (2025).

A HYBRID COMPUTATIONAL MODEL FOR THE DESIGN OF CVD PROCESSES. THE CASE OF SILICON DEPOSITION ON FILAMENTS

I.G. Aviziotis[1,2], **G.P. Gakis**[1], **E.D. Koronaki**[1,3], **D. Davazoglou**[2], **A.G. Boudouvis**[1]
[1] School of Chemical Engineering, National Technical University of Athens (NTUA), Heroon Polytechniou 9, 15780 Zografou, Greece
[2] NCSR "Demokritos", Institute of Nanoscience and Nanotechnology, POB 60228, 153 10 Agia Paraskevi Attiki, Greece.
[3] Interdisciplinary Center for Security, Reliability and Trust, University of Luxembourg, 29 John F. Kennedy Avenue, Luxembourg, L-1855, Luxembourg
e-mail: boudouvi@chemeng.ntua.gr

The deposition of silicon thin films has a broad range of applications including computer microchips, wearable electronics and optoelectronics. The most common method for depositing silicon is the chemical vapor deposition (CVD). This work focuses on the CVD of silicon on tungsten filaments at atmospheric pressure, using $SiCl_4$ as precursor [1]. However, CVD is a complex process owing to the interplay between transport phenomena and chemistry mechanisms occurring within the reactor. Thus, a computational framework is employed to assist the design of the process and its optimization. The modeling procedure consists of a computational fluid dynamics (CFD) model that takes into account the transport phenomena within the CVD reactor, namely fluid flow, species transport and heat transfer. The mechanistic analysis of the transport phenomena, facilitated with the use of CFD modelling, allows the optimization of the reactor and process design with regard to deposition thickness and uniformity. This model will serve as a basis for the development of a data-driven surrogate model using Polynomial Chaos Expansion (PCE) and data from CFD simulations for a CVD reactor [2] to achieve efficient and accurate predictions of physical variables. Surrogate models based on data-driven techniques have demonstrated outstanding performance in accurately emulating CVD processes [3, 4] while maintaining low computational requirements. This hybrid computational framework will not only provide invaluable information for the CVD of Si on filaments but more importantly, it will result in the efficient design and optimization of the process under investigation, enabling the fabrication of low-cost and environmentally-friendly connections for optoelectronic applications.

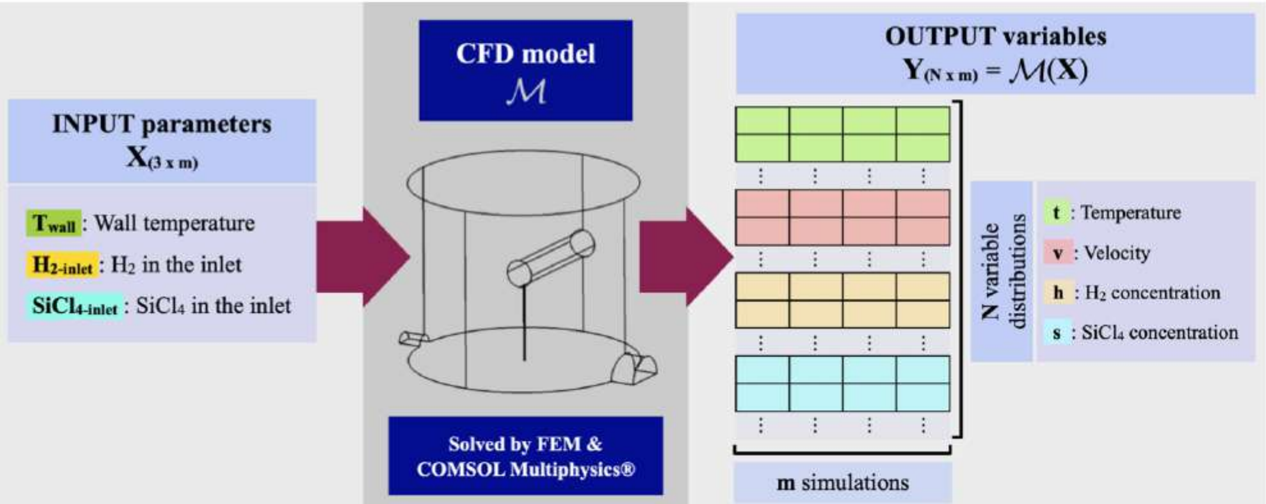
INPUT parameters
$X_{(3 \times m)}$
T_{wall} : Wall temperature
$H_{2\text{-inlet}}$: H_2 in the inlet
$SiCl_{4\text{-inlet}}$: $SiCl_4$ in the inlet
CFD model
$\mathcal{M}$
Solved by FEM & COMSOL Multiphysics®
OUTPUT variables
$Y_{(N \times m)} = \mathcal{M}(X)$
N variable distributions
t : Temperature
v : Velocity
h : H_2 concentration
s : $SiCl_4$ concentration
m simulations

Fig. 1. The hybrid computational framework developed for the computer-aided design of the CVD of Si on cylindrical wires.

This work has received funding from the Hellenic Foundation for Research and Innovation (HFRI) program Data4Solar, project ID No 16568. Prof. A.G. Boudouvis is the PI of Data4Solar.

References

[1] J. Bloem, W.A.P. Claassen, W.G.J.N. Valkenburg, *J. Cryst. Growth*, **57**, 177 (1982).
[2] G. Loachamín-Suntaxi, P. Papavasileiou, E.D. Koronaki, D.G. Giovanis, G. Gakis, I.G. Aviziotis, M. Kathrein, G. Pozzetti, C. Czettl, S.P.A. Bordas, A.G. Boudouvis, *Chemical Engineering Journal Advances*, **20,** 100667 (2024).
[3] P. Papavasileiou, E.D. Koronaki, G. Pozzetti, M. Kathrein, C. Czettl, A.G. Boudouvis, S.P.A. Bordas, *Comput. Ind.*, **149,** 103938 (2023).
[4] E.D. Koronaki, A.M. Nikas, A.G. Boudouvis, *J. Chem. Eng.,* **397**, 125475 (2020).

Automated modeling of reaction mechanisms for batch CVD processes based on multi-objective optimization algorithms

Takahiro Takahashi[1,*], **Akinari Morishita**[2], **Teppei Ozawa**[2]
[1]Department of Electrical and Electronic Engineering, Faculty of Engineering, Shizuoka University
[2]Graduate School of Integrated Science and Technology, Shizuoka University
e-mail: takahashi.takahiro@shizuoka.ac.jp

Identifying a suitable reaction mechanism model that describes the pathways from the source gases to the resulting films is one of the most important aspects in the development of chemical vapor deposition (CVD) processes [1,2]. By using a process simulator informed by the reaction model, we can predict the results of deposition experiments, leading to more efficient and strategic research and development. To accelerate progress in this area and reduce the associated workload, we have developed a system that automatically identifies the reaction models involved in the experimental results of CVD processes [3,4]. These reaction models are determined both quantitatively and qualitatively based on chemical kinetics.

In selecting the appropriate model, we focused on two key criteria: reproducibility of experimental data and simplicity of reaction model structure. However, these criteria may have a trade-off relationship, indicating that there may be several optimal reaction models rather than just one. To address this, we proposed a novel method for identifying reaction models using multiple evaluation functions through NSGA-III, a powerful algorithm for multi-objective optimization problems [5]. This approach generates multiple candidate reaction models as Pareto solutions during the optimization process. Ultimately, the best model that matches the actual deposition scenario can be selected from these candidates.

We have demonstrated the performance and validity of our system using the deposition profiles of thermal CVD silicon nitride films grown from dichlorosilane and ammonia in a batch furnace suitable for mass production with round substrates (silicon wafers) [6] (Fig. 1). The system successfully proposed several candidate reaction models, considering both reproducibility and model simplicity. Finally, we determined the optimal reaction model by screening among the proposed candidates (Fig. 2).

References

[1] H. Liao and T. S. Cale, *Thin Solid Films* **236**, 352 (1993).
[2] H. Komiyama, Y. Shimogaki and Y. Egashira, *Chem. Eng. Sci.* **54**, 1941 (1999).
[3] T. Takahashi, K. Funatsu and Y. Ema, *Meas. Sci. Technol.* **16**, 278 (2005).
[4] T. Takahashi, H. Nakai, H. Kinpara and Y. Ema, *J. Nanosci. Nanotechnol.* **11**, 8044 (2011).
[5] K. Deb and H. Jain, “An evolutionary many-objective optimization algorithm using reference-point based non-dominated sorting approach, part I: solving problems with box constraints,” IEEE Trans. on Evolutionary Computation (TEVC), vol.18, no.4, pp.577–601 (2014).
[6] T. Sorita, PhD Thesis, University of Tokyo (in Japanese) (1995).

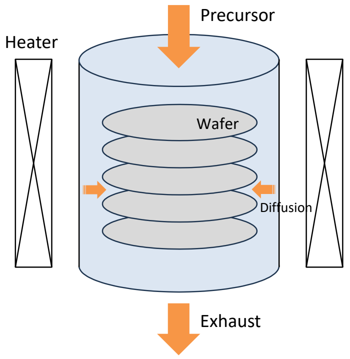
Precursor
Heater
Wafer
Diffusion
Exhaust

Figure 1. Schematic structure of the batch CVD furnace with round substrates (silicon wafers).

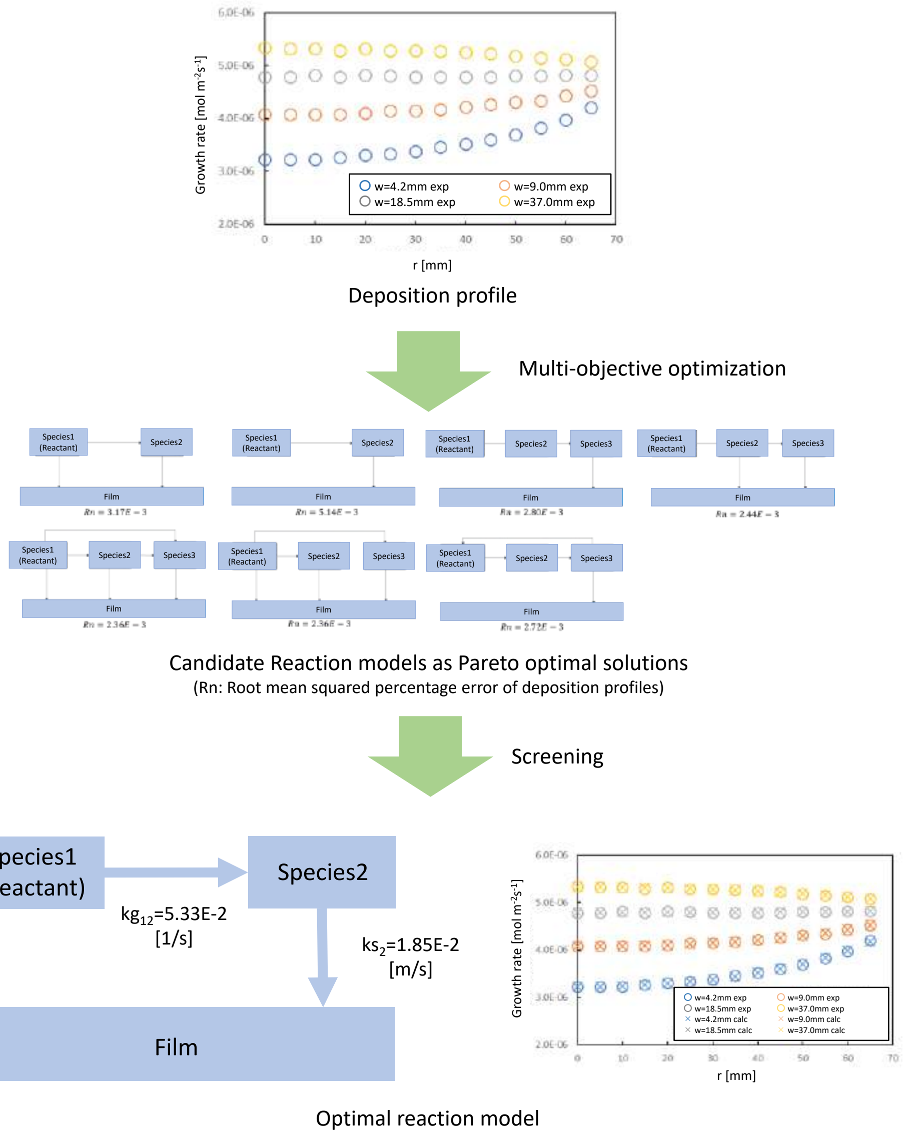
Growth rate [mol m-2s-1]
6.0E-06
5.0E-06
4.0E-06
3.0E-06
2.0E-06
0
10
20
30
40
50
60
70
r [mm]
w=4.2mm exp
w=9.0mm exp
w=18.5mm exp
w=37.0mm exp
Deposition profile
Multi-objective optimization
Species1 (Reactant)
Species2
Species3
Film
Rn = 3.17E−3
Rn = 5.14E−3
Rn = 2.80E−3
Rn = 2.44E−3
Rn = 2.36E−3
Rn = 2.36E−3
Rn = 2.72E−3
Candidate Reaction models as Pareto optimal solutions
(Rn: Root mean squared percentage error of deposition profiles)
Screening
Species1 (Reactant)
Species2
kg12=5.33E-2 [1/s]
ks2=1.85E-2 [m/s]
Film
Growth rate [mol m-2s-1]
w=4.2mm exp
w=9.0mm exp
w=18.5mm exp
w=37.0mm exp
w=4.2mm calc
w=9.0mm calc
w=18.5mm calc
w=37.0mm calc
r [mm]
Optimal reaction model

Figure 2. An example of the schematic process of modeling using thermal CVD silicon nitride films, which are grown from dichlorosilane and ammonia in the batch furnace.

MOCVD modelling for large scale deposition oh wide HTS tapes

H. Rouch, [1] **D. Longo**, [1]
[1]Renaissance Fusion
e-mail: herve.rouch@renfusion.eu

Renaissance Fusion develops high-temperature superconductor (HTS) tapes on wide substrates for high-magnetic field applications. Strong magnetic fields are necessary, among others, for the efficient confinement of nuclear fusion plasmas, and this requires large amounts of HTS tape. Stellarators are very promising fusion devices, typically requiring complicated 3D magnets. Renaissance Fusion conceived a way to generate complicated stellarator fields via simplified, effectively 2D magnets featuring wide, engraved HTS tapes. Other applications (from medical imaging to energy storage, to generators and accelerator magnets) share similar requirements of field strength and precision over large volumes and will benefit from this innovation. With this motivation, the company is developing a large-scale, roll-to-roll machine for Metal Organic Chemical Vapor Deposition (MOCVD) of Yttrium Barium Copper Oxide (YBCO).

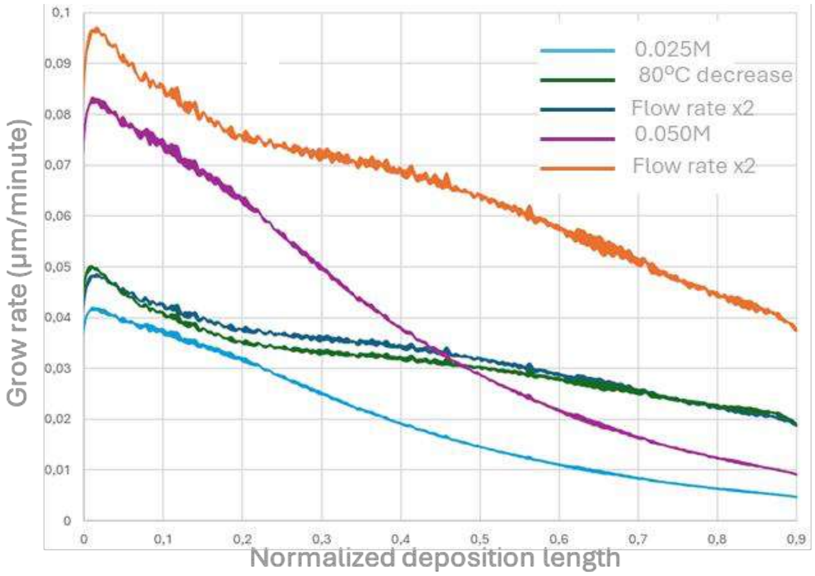

Figure 1: Growth rates vs the position in the reactor (injection side at 0, exhaust side at 1) for nominal flow rate and molarity of precursors of 0,025M (light blue), double molarity (pink), double flow rate (dark blue), double molarity and flow rate (orange), at nominal tape temperature. The effect of 80C temperature decrease is studied (green vs dark blue).

The MOCVD of YBCO has been investigated and optimized for over 25 years [1-9]. Commercially available tapes are typically up to 12 mm wide, and few hundred meters long. Here we consider similar lengths but a major increase in width, up to 1 m. To that end, MOCVD modeling is crucial for production and scale-up, and namely to: predict gas flow effects by Computational Fluid Dynamics (CFD), optimize the injection in the reactor [10], predict the deposition rates, homogeneity, and reactivity [11]. Well-known models of GaAs deposition were used to optimize the new YBCO reactor deposition [12].

The data for CVD depositions [13] (such as thermodynamic [14] or kinetic data [15], and transport data [16] using kinetic theory [17]) are available in the literature and were used to model the MOCVD of YBCO. The main assumption of this model, previously used in Refs. [15, 16], is that the main gaseous species transported to the surface, after decomposition of the precursors, are the oxides, Y2O3, BaO, CuO. The model was previously benchmarked against experimental results [12], and found to provide reliable estimates of growth rate. Some diffusion coefficients were calibrated to fit experimental composition of the deposited layer.

A large-scale reactor was simulated. The nominal tape temperature is 800°C. Figure 1 shows the growth rate and deposition rate of each oxide. The growth rate is presented as a function of the position in the reactor, in normalized units. The maximum growth rate amounts to around 0,1 µm/mn close to injection (that is, where the concentrations of oxides are the highest). Following the flow to the exhaust, the growth rate decreases due to the depletion in reactive species (the oxides in our model). The same figure also shows the effects of the flow rate and the molarity of precursors.

Soon, this model will be validated by comparison to experimental deposition data and will be used to optimize our reactor and deposition conditions.

References

[1] K. Salama, K. Ravi-Chandar, V. Selvamanickam, D. F. Lee, P. K. Reddy, and S. Rele *J. Metals* **40,** 6 (1988).

[2] F. Schmaderer and G. Wahl, J. de Physique, Coll C5,50 p119 (1989)

[3] F. Weiss, K. Frohlich, R. Haase, M. Labeau, D. Selbmann, J.P. Senateur and 0. Thomas ***J.*** de Physique ***IV*** **C3,3** p321 (1993)

[4] O Stadel, J Schmidt, G Wahl, F Weiss, D Selbmann, J Eickemeyer, O.Yu Gorbenko, A.R Kaul, C Jimenez, Physica C Vol. 372-376 part 2, p751 (2002)

[5] V. Selvamanickam, H.G. Lee, Y. Li, X. Xiong, Y. Qiao, J. Reeves, Y. Xie, A. Knoll, and K. Lenseth, *Physica C*. **392-396,** pp. 859-862 (2003)

[6] O. Stadel, in *IEEE Transactions on Applied Superconductivity*, vol. 19, no. 3, pp. 3160-3163 (2009)

[7] V. Selvamanickam, Y. Chen, J. Xie, Y. Zhang, A. Guevara, I. Kesgin, G. Majkic, and M. Martchevsky, *Physica C* **469,** 2037 (2009)

[8] N Dechoux, C Jiménez, P Chaudouët, L Rapenne, E Sarigiannidou, F Robaut, S Petit, S Garaudée, L Porcar, J L Soubeyroux, P Odier, C E Bruzek and M Decroux, *Supercond. Sci. Technol.* **25** n°12 (2012)

[9] N. D. Khatri, G. Majkic, T. Shi, Y. Chen, and V Selvamanickam, *Supercond. Sci. Technol.* **26,** 085022 (2013)

[10] Shudong Zhang , Ziming Fan, Ping Jiang, Shiwei Xu, Zhichen Han, Gang Yang, Yujie Liu, and Yimin Chen, *ieee transactions on applied supercond*. **29 n° 5** (2019)

[11] A. Michau, Y. Gazal, A. Yoan, F.Addo, F. Maury, T. Duguet, R. Boichot, M. Pons, E. Monsifrot, H. Maskrot, F. Schuster, *Surface and Coatings Technology*, **375**, 894 (2019)

[12] R. Pratap PhD thesis (2019)

[13] H. Rouch, M. Pons, C. Bernard, R. Madar, *Journal De Physique III,* **5 n°6**, 759 (1995)

[14] F. Weiss, A. Pisch, C. Bernard, U. Schmatz, *J. Phys. IV*, **5 n°C5**, 151 (1995)

[15] L. L. Raja, R. J. Kee, R. Serban, and L. R. Petzold, *J. Electrochem. Soc.* **147,** 7 p. 2718 (2000)

[16] F. Schmaderer and G. Wahl, *Journal de Physique C5* p. 119 (1989)

[17] R. B. Bird, W. E. Stewart, and E. N. Lightfoot, *Transport Phenomena,* Wiley, New York (1960)

Development of a New Class of Precursors for Atomic Layer Deposition of Tin(II) Oxide (SnO)

J. C. Goodall[1] and A. L. Johnson[1]*
[1]Department of Chemistry, University of Bath, BA2 7AY, UK
[2]School of Engineering, University of Liverpool, L69 3GH, UK
[3]Electrical Engineering Division, University of Cambridge, CB3 0FA, UK
e-mail: chsalj@bath.ac.uk, jcg69@bath.ac.uk

Tin(II) oxide (SnO) is a p-type semiconductor material which is of particular interest for the fabrication of thin film transistors (TFTs) and complementary metal oxide semiconductors, with a band gap of 2.7 – 3.4 eV. Atomic layer deposition (ALD) of tin(II) oxide has been reported for tin(II) (amino)alkoxide,[1,2] amide[3] and formamidinate[4] complexes, in conjunction with H_2O. However, many of the 'state-of-the-art' tin(II) oxide ALD processes suffer with chemical vapor deposition (CVD) pathways or contamination of SnO with tin(IV) oxide (SnO_2) and/or Sn metal, negatively impacting the electronic properties.

Here, previously unexplored tin(II) amido, alkyl and aryl complexes are investigated as potential precursors for ALD of SnO with H_2O. The synthesis, thermal stability and volatility, as well as computational insight of these species is discussed.

This work was supported by the EPRSC and Pragmatic Semiconductor.

References

[1] S. H. Kim, I. Baek, D. H. Kim, J. J. Pyeon, T. Chung, S. Baek, J. Kim, J. H. Han and S. K. Kim, *J. Mater. Chem. C.*, **5**, 3139-3145 (2017).
[2] D. E. Gomersall, K. M. Niang, J. D. Parish, Z. Sun, A. L. Johnson, J. L. MacManus-Driscoll and A. J. Flewitt, *J. Mater. Chem. C.*, **11**, 5740-5749 (2023).
[3] J. Heo, A. S. Hock and R. G. Gordon, *Chem. Mater.*, **22**, 4964-4973 (2010).
[4] N. Huster, R. Ghiyasi, D. Zanders, D. Rogalla, M. Karppinen and A. Devi, *Dalton Trans.*, **51**, 14970-14979 (2022).

Development of Novel Precursors for Atomic Layer Deposition of Tin(II) Oxide (SnO)

Oliver W. S. Clark and Andrew L. Johnson
University of Bath, Claverton Down, Bath, BA2 7AY, United Kingdom

Over the last few decades, the advent of microelectronic circuitry in which millions of electronic components may be incorporated into a very small space has revolutionized electronics, driven by advances in processing and fabrication techniques. Semiconducting metal oxide materials such as those found in transistors have facilitated high-density integrated circuits and more complex system architectures, increasing processing power [1]. At present, further technological advancement in areas such as MOSFET and TFT devices is hindered by the limited availability of suitable metal oxide semiconductor materials, with good p-type conductivity [2]. This issue is exacerbated by a lack of suitable precursors, compatible with modern industrial fabrication processes for depositing thin films of the metal oxide materials.

One of the most promising candidates for a p-type metal oxide is tin(II) oxide (SnO)[3,4]. To date, the deposition of SnO has been reported using a range of different methods, however, deposition of SnO by ALD is relatively unexplored, with only a handful of suitable precursor compounds known [5].

Here we describe the development of a series of novel precursors, such as that shown in Figure 1, with their intended application being the deposition of SnO thin films via ALD. The hetero- and homoleptic tin(II) amido complexes have been fully characterized multinuclear NMR spectroscopy and where applicable, single crystal X-ray diffraction. Thermal properties of the precursors were then assessed by thermogravimetric analysis and related thermal studies, to gauge the suitability of the compounds for future deposition trials.

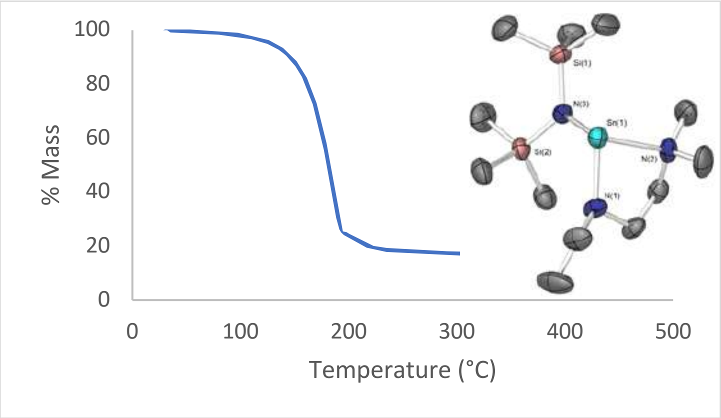

Fig. 1. TGA plot and corresponding crystal structure of a heteroleptic tin(II) prospective precursor. Thermal ellipsoids are shown at 50% probability and hydrogen atoms are omitted for clarity.

References

[1] N. C. A. van Fraassen, S. Han, K. Niang and A. J. J. Flewitt; 2022 *ECS Trans.* **109** 13

[2] E. Fortunato, P. Barquinha and R. Martins, *Advanced Materials*, 2012, 24, 2945 2986

[3] A. Mameli, J. D. Parish, T. Dogan, G. Gelinck, M. W. Snook, A. J. Straiton, A. L. Johnson and A. J. Kronemeijer, *Advanced Materials Interfaces*, 2022, **9**, 2101278.

[4] D. E. Gomersall, K. M. Niang, J. D. Parish, Z. Sun, A. L. Johnson, J. L. MacManus-Driscoll and A. J. Flewitt, *Journal of Materials Chemistry C*, 2023, **11**, 5740-5749.

[5] J. D. Parish, M. W. Snook and A. L. Johnson, *Dalton Transactions*, 2021, **50**, 13902-13914.

Bismuth precursors for the atomic layer deposition of p-type Bi_2O_3

Macsen Laming and A. L. Johnson
Department of Chemistry, University of Bath, BA2 7AY, UK
E-mail: ml2272@bath.ac.uk and chsalj@bath.ac.uk

Bismuth(III) oxide (Bi_2O_3) is a known p-type semiconducting material with a relatively wide band gap. As a result of its wide band gap, relatively good environmental stability (chemical and thermal) and high carrier mobility, Bi_2O_3 is a promising material for use in electronic and optoelectronic devices and therefore has potential applications in fields such as photocatalysis and gas sensing.[1, 2] Studies have identified seven different crystalline forms of bismuth oxide: α-Bi_2O_3, β-Bi_2O_3, γ-Bi_2O_3, δ-Bi_2O_3, ε-Bi_2O_3, ω-Bi_2O_3 and η-Bi_2O_3 and depending on the method of preparation, thin-films of Bi_2O_3 can be either n-type or p-type, making Bi_2O_3 amphoteric.[1, 3] The current lack of commercially viable p-type metal oxide materials available hinders technology dependent on p-type metal oxide thin-film transistors and Bi_2O_3 could be a promising p-type metal oxide material.

Therefore, developing potential bismuth(III) atomic layer deposition (ALD) precursors that could be used to deposit Bi_2O_3 thin-films is of interest. A number of bismuth(III) alkoxide and amide complexes have previously been investigated as ALD precursors for the production of Bi_2O_3 thin-films.[4, 5] Here we report the synthesis and development of several homoleptic bismuth(III) alkoxide and aminoalkoxide complexes, which were analysed using NMR spectroscopy, single-crystal X-ray diffraction and thermogravimetric analysis (TGA). Of these complexes, $[Bi(OC(Me)_2CH_2NMe_2)_3]$ has shown the most favorable TGA data and is currently the best candidate for further ALD studies.

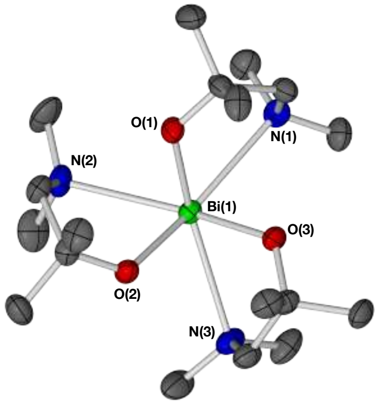

Figure. 1. Molecular structure of the prospective ALD precursor $[Bi(OC(Me)_2CH_2NMe_2)_3]$. The thermal ellipsoids are shown at a 50% probability level. The hydrogen atoms are excluded for clarity.

This work was supported by the EPRSC and Pragmatic Semiconductor.

References

[1] A. R. Khan, M. Ramzan, S. J. F. Alanazi, A. M. Al-Mohaimeed, S. Ali, M. Imran, Muhammad A. Majid, and M. H. Sarfraz, *ACS Omega*, 2024, **9**, 22650-22659

[2] A. Cabot, A. Marsal, J. Arbiol and J. R. Morante, *Sensors and actuators. B, Chemical*, 2004, **99**, 74-89

[3] H.-Y. Deng, W. C. Hao, H. Z. Xu, *Chinese Physics Letters*, 2011, **28**, 056101

[4] T. Hatanpää, M. Vehkamäki, M. Ritala and M. Leskeläa, *Dalton Trans.*, 2010, **39**, 3219-3226

[5] M Vehkamäki, T. Hatanpää, Mikko Ritala and M. Leskeläa *J. Mater. Chem.*, 2004,**14**, 3191-3197

Phosphorus Precursors for ALD of Metal Phosphides

J. Charvot,[1] **R. Zazpe,**[2] **J. Rodriguez Pereira,**[2] **J. Macák,**[2] **F. Bureš**[1]

[1]*Institute of Organic Chemistry and Technology, Faculty of Chemical Technology, University of Pardubice, Studentská 573, 532 10 Pardubice, Czech Republic*
[2]*Center of Materials and Nanotechnologies, Faculty of Chemical Technology, University of Pardubice, Nám. Čs. Legií 565, 53002 Pardubice, Czech Republic*

e-mail: jaroslav.charvot@upce.cz

Thin films of metal and other phosphides are gaining significant attention in material sciences; however, the development of ALD processes for these materials remains limited. One of the primary challenges hindering further research and application of metal phosphides is the lack of suitable phosphorus precursors for their deposition. The most commonly employed precursor is phosphine (PH_3), used for depositing CoP[1] and GaP[2]. However, PH_3 is difficult to handle, requires strict safety precautions, and is relatively unreactive, often necessitating activation by plasma. Other precursors, such as *tert*butylphosphine (*t*$BuPH_2$) and tris(dimethylamino)phosphine ($P(NMe_2)_3$), have been utilized for the deposition of InP[3] and GaP[4]. Nevertheless, these reactions typically require high temperatures exceeding 320 °C to promote the reaction. More recently, tris(trimethylsilyl)phosphide (TMS_3P) has shown promise as a precursor for depositing Co_2P thin films[5]. While TMS_3P has demonstrated value as an ALD precursor, its reactivity with other metal precursors remains unexplored.

Building on prior research, this work investigates the chemistry of phosphides and evaluates potential phosphorus precursors. TMS_3P and related compounds are synthesized, and their thermal behavior is analyzed using Differential Scanning Calorimetry (DSC) and Thermogravimetric (TG) analysis. The scalability of the preparation process is critically reviewed. Finally, selected candidates are employed in ALD processes with various counter-precursors to reveal their chemical behavior and evaluate their applicability as ALD precursors.

The authors acknowledge the financial support from the Czech Science Foundation (grant no. 2307071S) and the Ministry of Education, Youth and Sports of the Czech Republic for the support of large research infrastructures CEMNAT (project LM2023037).

References

[1] H. Zhang, D. J. Hagen, X. Li, A. Graff, F. Heyroth, B. Fuhrmann, I. Kostanovskiy, S. L. Schweizer, F. Caddeo, A. W. Maijenburg, S. Parkin, R. B. Wehrspohn, Angew. *Chem. Int. Ed.,* **59**, 17172–17176 (2020).
[2] A. V. Uvarov, A. S. Gudovskikh, V. N. Nevedomskiy, A. I. Baranov, D. A. Kudryashov, I. A. Morozov, J. P. Kleider, *J. Phys. D Appl. Phys.*, **53**, 345105 (2020).
[3] N. Otsuka, J. I. Nishizawa, H. Kikuchi, Y. Oyama, Jpn. *J. Appl. Phys.*, **38**, L20–L23 (1999).
[4] E. Graugnard, V. Chawla, D. Lorang, C. J. Summers, *Appl. Phys. Lett.*, **89**, 211102 (2006).
[5] E. Atosuo, P. Deminskyi, K. Mizohata, T. Hatanpää, M. Ritala, *ALD/ALE 2024*, AVS, Helsinki; ALD of Co_2P Thin Films, p. 47 (2024).

Design of new fluorinated aminoalkoxide ligands for MOCVD alkali niobate precursors: Synthesis, characterizations, and thermal validation

L. Matchim-Fondjo[1*], **A. Tacnet**[1], **S. Daniele**[1]
[1] CP2M CPE Lyon, University Claude Bernard Lyon 1, CNRS-UMR 5128
e-mail: laurianne-ornella.matchim-fondjo@univ-lyon1.fr

In recent years, significant attention has been directed toward developing new ligands that meet the stringent requirements for thin-film deposition via MOCVD. For $MNbO_3$ (M = Li or K) thin films, there is an urgent need for innovative precursors, particularly ligands capable of effectively complexing alkali metals **[1-2]**. These ligands must exhibit high volatility, exceptional purity, and thermal stability during evaporation. Among the candidates, aminoalkoxides have emerged as ideal due to their ability to meet these criteria. To further enhance their volatility, this study focuses on the development of fluorinated aminoalkoxides. Although alkoxides have been widely used in precursor development **[3]**, their application in complexing alkali metals, such as lithium (Li) and potassium (K), remains underexplored. This research addresses this gap by investigating fluorinated aminoalkoxides as promising ligands for alkali niobate deposition.

Numerous fluorinated aminoalkoxide ligands were synthesized, representing a novel contribution to the field. A variety of parameters were systematically varied to study their effects on the thermal properties of the ligands (Figure 1). Structural modifications, including the design of bidentate and tridentate ligands, were explored, as well as the incorporation of additives like Lewis bases to mitigate oligomerization with alkali metals, thereby enhancing volatility. This research spans the entire process of ligand development—from organic synthesis to the evaluation of their impact on the thermal properties of alkali metal precursors. The study demonstrates the critical relationship between ligand structure and precursor performance, with a specific focus on optimizing volatility and compatibility with CVD processes. By tailoring the molecular design, the findings highlight the importance of ligand chemistry in advancing the deposition of high-quality alkali niobate thin films. These insights contribute to the broader understanding of how precursor design can drive innovation in thin-film fabrication technologies.

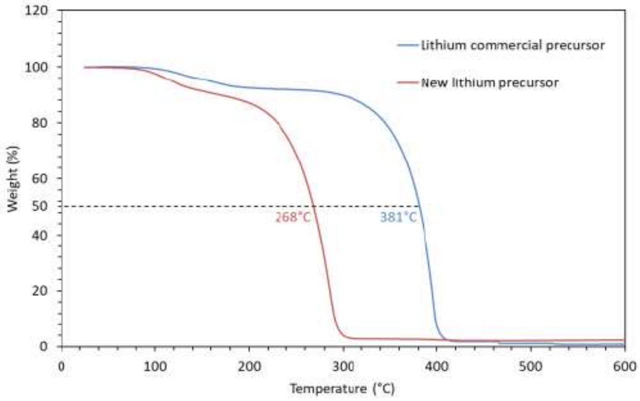

Fig. 1. Comparison of TGA curves between commercial lithium precursor ($[Li(thd)]_m$) and first-synthesized lithium precursor at CP2M laboratory.

References

[1] I. Labbaveettil Basheer, *Ph.D. thesis*, Universite Bourgogne Franche-Comte (2023).
[2] V. Astié, *Ph.D. thesis*, University of Franche-Comté (2020).
[3] A. Wolfgang, W. Hubert, O. Runte, *Angewandte chemie international*, **34**, 2187-2206 (1995).

Novel heterobimetallic precursors for fluoride-based functional materials

Claudia Barbagallo[1], Francesca Lo Presti[1], Anna L. Pellegrino[1] and Graziella Malandrino[1]

[1]Department of Chemistry, Università degli Studi di Catania and INSTM UdR Catania

e-mail: graziella.malandrino@unict.it

Multifunctional fluoride-based systems represent an emerging class of materials for several technological application, such as optics, sensors and photovoltaics.[1] In particular, the development of both binary and ternary rare earth-based fluoride films, doped with luminescence species, has been deeply investigated for energy conversion system in solar cell devices.[2] This technology allows the exploration of a wide range of solar energy portion, thus enhancing the efficiency of photovoltaic panels.[3] The engineering of energy conversion layers requires an inorganic fluoride host material, based on sodium, yttrium and/or gadolinium, and a luminescence center, such as europium.[4-5] Thus, the development of stable multimetallic complexes which contain in the structure all the elements forming the final inorganic layer represents a crucial aspect for their massive use. Recently, novel materials containing cesium as alkali metal have been reported, such as the inorganic perovskite $CsPbI_3$ for photovoltaic applications.[6] In this contest, the present work reports the design of novel cesium-based metalorganic compounds containing rare earth metals. The adducts shows high stability and promising thermal properties, such as high volatility and good mass transport properties, that make them excellent candidates for both vapor and solution deposition approaches of fluoride-based functional materials.

Particularly, this work reports an efficient one-pot synthesis of two novel bimetallic precursors based on cesium-yttrium or cesium-europium, using β-diketonate ligands to balance the charge of the cations, and polyethers to complete the coordination sphere of the central metals. The structures of Cs(I) metal-organic compounds is "$CsRE(hfa)_4 \cdot 2$tetraglyme", with RE = Y(III) or Eu(III), Hhfa = 1,1,1,5,5,5-hexafluoro-2,4-pentanedione and tetraglyme = 2,5,8,11,14-pentaoxa-pentadecane.

These compounds have been fully characterized in terms of structural, optical and thermal properties. Particularly, considering their high volatility and good thermal stability, they represent promising candidates as precursors for the fabrication of Cs-RE films using vapor deposition methods as MOCVD.

References:

[1] R. Rajeswari, N. Islavath, M. Raghavender and L. Giribabu, *Chem. Rec.*, **20**, 65–88 (2020).
[2] R.K. Sharma, A. Mudring and P.Ghosh, *Journal of Luminescence*, **189**, 44–63 (2017).
[3] A. Ghazy, M. Safdar, M. Lastusaari, H. Savin and M. Karppinen, *Solar Energy Materials and Solar Cells*, **230**, 111234 (2021).
[4] S. Battiato, P. Rossi, P. Paoli and G. Malandrino, *Inorg. Chem.*, **57**, 15035-15039 (2018).
[5] F. Lo Presti, A. L. Pellegrino, E. Milan, E.Radicchi, A.Speghini and G. Malandrino, *J. Mater. Chem. C*, **11**, 12195-12205 (2023).
[6] J. Chen, S. Wang, J. Lina and D. Chen, *Nanoscale*, **11**, 22359–22368 (2019).

Innovative β-diketonate Alkali Metal Precursors for Lead Free Piezoelectric Crystals

Stijn Engelaar[1], Francesca Lo Presti[1], Anna L. Pellegrino[1] and Graziella Malandrino[1]

[1]Dipartimento di Scienze Chimiche, Università degli Studi di Catania and INSTM UdR Catania

e-mail: graziella.malandrino@unict.it

Piezoelectric materials represent a growing class of functional systems with applications in microelectronics, integrated photonic circuits, surface acoustic wave devices, and catalysis [1]. A significant challenge in this field comes from the increasing regulations on the use of lead, restricting the use of the widely implemented material PZT ($Pb(Zr,Ti)O_3$). In response, perovskite-based crystals, such as niobates like $LiNbO_3$ (LN) and $(Na,K)NbO_3$ (KNN) have gained increasing attention due to their high Curie temperature, strong ferroelectric properties, and excellent thermal stability [2]. Various methods have been explored for the fabrication of niobate-based thin films, including magnetron sputtering, hydrothermal techniques, MOCVD, sol-gel processes, and solvothermal methods. However, for some of these processes, the development of suitable precursors with sufficient vapor pressure remains a significant challenge, particularly for deposition techniques such as metal-organic chemical vapor deposition (MOCVD) and solution-based sol-gel methods.

In this context, β-diketonate-coordinated alkali metals have emerged as promising candidates due to their stability, high volatility, and favorable mass transport properties. Previous research has demonstrated the versatility of fluorinated β-diketonate-stabilized Li, Na, and K precursors [3]. However, a limitation is the formation of the more thermally stable MF phase, which should be avoided.

In this work we present the synthesis of a fluorine-free K precursor using a simple one-pot method for the deposition of KNN thin films. The adduct is coordinated by a fluorine-free anionic ligand and is further stabilized with polyethers.

The adducts have been characterized in terms of structural, compositional, and thermal properties. The deposition of KNN using a sol-gel/spin coating method demonstrates significant potential for future solution-assisted MOCVD.

This work was partially supported by the European Community under the HORIZON-MSCA-2023-DN-01-01 HINA Project.

References

[1] Presti, F. L.; Pellegrino, A. L.; Micard, Q.; Guglielmo Guido Condorelli; Margueron, S.; Ausrine Bartasyte; Malandrino, G. LiNbO3 Thin Films through a Sol–Gel/Spin-Coating Approach Using a Novel Heterobimetallic Lithium–Niobium precursor. *Nanomaterials* **2024**, 14 (4), 345–345. DOI: 10.3390/nano14040345.

[2] Yao, L.; Zhu, K. Citrate Complexing Sol–Gel Process of Lead-Free (K,Na)NbO3 Ferroelectric Films. *Modern Physics Letters B* **2016**, 30 (13), 1650157–1650157. DOI: 10.1142/s0217984916501578.

[3] Nishant Peddagopu; Sanzaro, S.; Rossi, P.; Paoli, P.; Malandrino, G. A One-Pot Synthesis of "K(Hfa) Glyme" Adducts: Effect of the Polyether Length on the Ion Coordination Sphere. *European Journal of Inorganic Chemistry* **2021**, *2021* (36), 3776–3780. https://doi.org/10.1002/ejic.202100553.

Atomic layer deposition of subwavelength epsilon-near-zero indium tin oxide thin films for nonlinear photonics

M. Napari[1, *], **A. Y. Bykov**[1,2], **H. Cossey**[1], **A. V. Zayats**
[1]King's College London, Department of Physics
[2]University of Cambridge, Nanophotonics Centre, Cavendish laboratory, Department of Physics
e-mail: mari.napari@kcl.ac.uk

Epsilon-near-zero (ENZ) media have emerged as a foundation for strong nonlinear light-matter interaction and a building block of time-varying and four-dimensional metamaterials. Transparent conductive oxides (TCO) are considered as potential materials for ENZ nanophotonics due to their ability to withstand high pump powers and to provide strong modulations of refractive index on a sub-picosecond timescale [1,2]. There is a strong demand for versatile fabrication methods for high-quality thin films with controlled morphology, spectral tuneability and coupling to plasmonic or dielectric metasurfaces. Here we report the fabrication of high-quality nonlinear ENZ indium tin oxide (ITO) thin films by atomic layer deposition (ALD) using trimethyl indium, tetrakisdimethylamino tin and ozone using a supercycle approach and varying the binary In_2O_3:SnO_2 cycle rations between 12:1 and 19:1, which correspond to the SnO_2 content of 10 and 15 %, respectively, according to the rule of mixtures. The as-deposited 30nm thick films have sufficiently low resistivity (~10^{-4} Ωcm) which can be improved by an order of magnitude by post-deposition annealing in low-vacuum forming gas. By varying the Sn content, deposition temperature, and post-deposition annealing conditions, a broad tuneability of ENZ wavelength in the range of 1.1 – 2.5 µm can be achieved. By employing a spectroscopic Z-scan technique in reflection we measured an order of unity modulation of reflection coefficient in the vicinity of ENZ wavelength. Our results indicate that the ALD ITO is competitive to the state-of-the art commercial ITO films [2], while providing the benefit of precise thickness and composition control and ability to produce conformal coatings on nanostructured metamaterial surfaces.

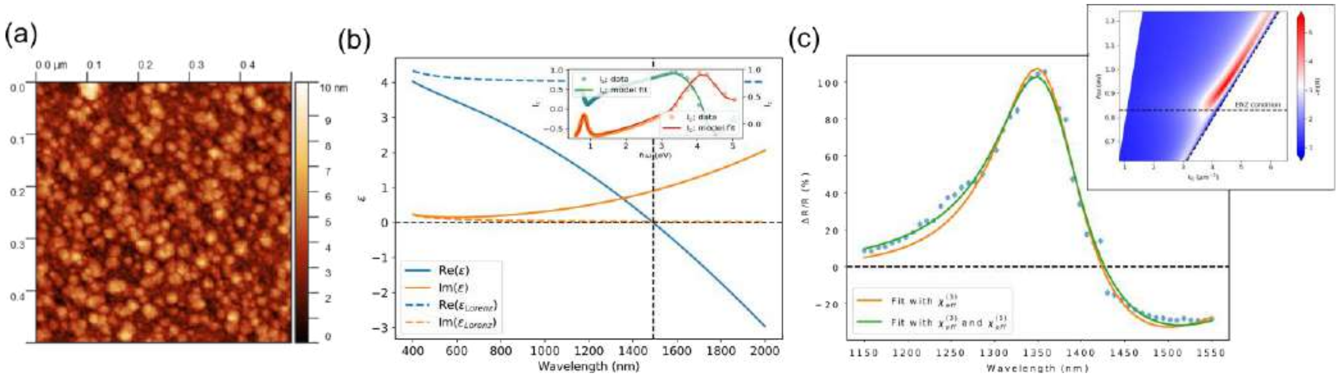

Fig. 1. a) An AFM image of a 30nm ALD ITO film on silicon. (b) Optical constants of an ALD ITO film, vertical dashed line indicates the ENZ wavelength; inset shows the fit of a Drude + single Lorentz oscillator model to the ellipsometry data. (c) Experimental spectrum of the reflection coefficient modulation at 25GW/cm2; inset shows the calculated reflection spectrum of ALD ITO calculated with transfer matrix method.

References

[1] Reshef, O. *et al.* Nonlinear optical effects in epsilon-near-zero media. *Nat Rev Mater* **4**, 535 (2019).
[2] M. Zahirul Alam *et al.* Large optical nonlinearity of indium tin oxide in its epsilon-near-zero region *Science* **352**,795 (2016)

Atomic Layer Deposited P-type Tin Monoxide Thin Film Transistors for low power CMOS Applications

K. M. Niang[1], **Xiao Chen**[1], **Ben Peek**[2], **O. Clark**[3], **J. Goodall**[3], **P. Chalker**[2], **A. Johnson**[3] **and A. Flewitt**[1]

[1]Dept. of Engineering, University of Cambridge, Cambridge, UK.
[2] School of Engineering, University of Liverpool, Liverpool, UK.
[3]Dept. of Chemistry, University of Bath, Bath, UK.
e-mail: kmn36@cam.ac.uk

Metal oxide semiconductors are technologically important materials due to their high mobility, transparency, scalability and possibility of deposition at room temperature. Amorphous indium gallium zinc oxide (a-IGZO) is arguably the most well-known n-type oxide semiconductor which has been used in various optical and electronic devices and display applications [1]. There is an urgent need for the p-type counterpart for the realization of low power complementary metal oxide semiconductor (CMOS) technology.

Tin monoxide (SnO) is a promising p-type material with a relatively high mobility (μ_{Hall} up to 19 $cm^2V^{-1}s^{-1}$) due to the less localised valence band maximum arising from hybridization between O 2*p* and Sn 5*s* orbitals [2] [3].Even though sputtering and pulsed laser deposition have been reported, such physical vapour deposition methods are generally challenging due to the narrow process window to obtain SnO with correct valency (Sn^{2+}) [3]. On the other hand, phase pure SnO can be reliably produced by atomic layer deposition (ALD) if Sn precursors with 2+ valency are used. Such precursors recently reported include bis(1-dimethylamino-2-methyl-2-propoxy)tin and Sn (II) bis(*tert*-butoxide); their corresponding thin film transistors (TFTs) exhibit a field effect mobility, μ_{FE}, ~ 1 $cm^2V^{-1}s^{-1}$ and I_{ON}/I_{OFF} ~ $10^4 - 10^6$ [4] [5] [6]. Indeed, ALD has been increasingly used for the development of p-type oxides.

Future development of p-type oxides requires concerted effort from the precursor chemistry development to optimization of the ALD process and device engineering. Here, we show that the surface morphology of SnO can be tuned from polycrystalline with different grain sizes to predominantly amorphous by varying the ALD parameters. Likewise, the electrical property of SnO can be varied either p-type or ambipolar by changing the post annealing temperature. Different TFT architectures and the use of high-k gate dielectric materials such as Al_2O_3 or Ta_2O_5, also deposited by ALD, are assessed to improve TFT performance and reduce the operation voltage range.

In summary, ALD technology enables the deposition of SnO thin films with characteristics that are attractive for low cost, low power CMOS applications.

This work was supported by the EPSRC Prosperity Partnership EP/X025195/1

References

[1] K. Nomura, H. Ohta, A. Takagi, T. Kamiya, M. Hirano, and H. Hosono, "Room-temperature fabrication of transparent flexible thin-film transistors using amorphous oxide semiconductors," (in eng), *Nature,* vol. 432, no. 7016, pp. 488-92, Nov 25 2004, doi: 10.1038/nature03090.

[2] Y. Ogo *et al.*, "Tin monoxide as an s-orbital-based p-type oxide semiconductor: Electronic

structures and TFT application," *physica status solidi (a),* vol. 206, no. 9, pp. 2187-2191, 2009, doi: 10.1002/pssa.200881792.

[3] J. A. Caraveo-Frescas, P. K. Nayak, H. A. Al-Jawhari, D. B. Granato, U. Schwingenschlogl, and H. N. Alshareef, "Record Mobility in Transparent p-Type Tin Monoxide Films and Devices by Phase Engineering," *ACS Nano,* vol. 7, no. 6, pp. 5160-5167, 2013, doi: 10.1021/nn400852r.

[4] S. H. Kim *et al.*, "Fabrication of high-performance p-type thin film transistors using atomic-layer-deposited SnO films," *Journal of Materials Chemistry C,* vol. 5, no. 12, pp. 3139-3145, 2017, doi: 10.1039/c6tc04750e.

[5] J. H. Han *et al.*, "Growth of p-Type Tin(II) Monoxide Thin Films by Atomic Layer Deposition from Bis(1-dimethylamino-2-methyl-2propoxy)tin and H2O," *Chemistry of Materials,* vol. 26, no. 21, pp. 6088-6091, 2014, doi: 10.1021/cm503112v.

[6] D. E. Gomersall *et al.*, "Multi-pulse atomic layer deposition of p-type SnO thin films: growth processes and the effect on TFT performance," *Journal of Materials Chemistry C,* vol. 11, no. 17, pp. 5740-5749, 2023, doi: 10.1039/d3tc00255a.

Bandgap Tunable $RuS_{2x}Se_{2-2x}$ Thin Films for Near-Infrared Photodetector by Chemical Vapor Deposition and Post-Sulfurization Process

Jaehyeok Kim[1], **Hwi Yoon**[1], **Inkyu Sohn**[1], **Tatsuya Nakazawa**[3], **Yusuke Ohshima**[4], **Hiroki Sato**[4], **Jisang Yoo**[1], **Sojeong Eom**[1], **Seungmin Chung**[2], **Hyungjun Kim**[1,*]

[1]School of Electrical and Electronic Engineering, Yonsei University, Seodaemun-Gu, Seoul 03722, Korea
[2]Division of Materials Science and Engineering, Hanyang University, 222 Wangsimni-Ro, Seongdong-Gu, Seoul 133-791, Republic of Korea
[3]Metallic Materials Development Department, TANAKA Kikinzoku Kogyo K.K., Isehara Technical Center, Isehara, Kanagawa, 259-1146, Japan
[4]Chemical Materials Development Department, TANAKA Kikinzoku Kogyo K.K, Tsukuba Technical Center, Ibaraki 300-4247, Japan
e-mail: hyungjun@yonsei.ac.kr

Near infrared (NIR) photodetectors (for wavelengths ranging from 800 to 2500 nm) have been studied for a wide range of applications such as telecommunications, night-vision, biomedical sensing, and autonomous vehicles. NIR photodetectors are typically composed of semiconductor materials with band gap from 0.4 eV to 1.6 eV. However, traditional NIR silicon-based photodetectors are limited to ~900 nm due to their relatively large bandgap (1.1 eV), whereas InGaAs photodetectors cover wider wavelengths but require complex synthesis methods such as molecular beam epitaxy (MBE) [1].

Ruthenium-based chalcogenides (RuS_2, $RuSe_2$) have been widely studied in the field of catalysts due to their high corrosion resistance and low hydrogen binding energy similar to Pt. Also, they are considered to have great potential for optoelectronic applications because they have appropriate bandgaps for the NIR region as well as excellent electrical conductivity and high absorption coefficient ($\sim 10^4$ cm^{-1}). Recently, Nakazawa et al. demonstrated a RuS_2 photodetector which operates at a wavelength of 940 nm using atomic layer deposition Ru film and post sulfurization process [2-5]. However, it exhibits low photoresponsivity due to its insufficient thickness for effective light absorption and a relatively large bandgap of 1.14 eV compared to other NIR photodetector materials. On the other hand, $RuSe_2$ has a smaller bandgap compared to RuS_2 and can operate over a broad range of NIR. Nevertheless, it has not yet been investigated for use in NIR photodetectors, nor has a simple synthesis method for the absorbing layers been developed.

Herein, we synthesized $RuSe_2$ thin films through a chemical vapor deposition (CVD) process. The properties of the material were confirmed through analysis such as Raman spectroscopy, XPS, XRD, SEM, TEM and UV-Vis-NIR spectrometer. We fabricated a $RuSe_2$ metal-semiconductor-metal (MSM) device and evaluated its electrical properties. It showed high dark current due to its narrow bandgap. To suppress dark current, we performed post-sulfurization after the CVD $RuSe_2$ process. The $RuS_{2x}Se_{2-2x}$ material can be synthesized from almost RuS_2 and $RuSe_2$, indicating that it has a bandgap from 0.52 eV to 1.39 eV. Finally, we investigated the ternary $RuS_{2x}Se_{2-2x}$ photodetector for the NIR region. It showed photoresponse at room temperature even at zero-bias due to the slight difference in the barrier height. The CVD and post sulfurization process offers a promising path for synthetic Ru-based chalcogenide and band gap engineering for future infrared detection.

.

This work was supported by TANAKA KIKINZOKU KOGYO K.K. Also, this work was supported by the National Research Foundation of Korea (NRF) grant funded by the Korea government (MSIT) (No. NRF-2022R1A2C2006764), the Materials and Components Technology Development Program of MOTIE/KEIT [20012460] and the Technology Innovation Program (or Industrial Strategic Technology Development Program) (RS-2023-00232222, High-temperature atomic layer deposition precursors and processes for dielectrics in 3D V-NAND devices) funded by the Ministry of Trade, Industry &amp; Energy (MOTIE, Korea) (1415187363).

References

[1] 1. Peng Wang, Hui Xia, Qing Li, Fang Wang, Lili Zhang, Tianxin Li, Piotr Martyniuk,, Antoni Rogalski, and Weida Hu, Sensing Infrared Photons at Room Temperature: From Bulk Materials to Atomic Layers, 15, 1904396 (2019)

[2] Yuanmeng Zhao, Hengjiang Cong, Peng Li, Dean Wu, Shengli Chen, and Wei Luo, Hexagonal RuSe2 Nanosheets for Highly Efficient Hydrogen Evolution Electrocatalysis, Angew. Chem. 133(13), 7089 (2021)

[3] H P Vaterlaus, R Bichsel, F Levy and H Berge, RuS2 and RuSe2 single crystals: a study of phonons, optical absorption and electronic properties, J. Phys. C: Solid State Phys. 18 6063 (1985)

[4] Dongze Li, Meng Zha, Ligang Feng, Guangzhi Hu, Chaoquan Hu, Xiang Wu and Xinzhong Wang, Increased crystallinity of RuSe2/carbon nanotubes for enhanced electrochemical hydrogen generation performance, Nanoscale, 14, 790 (2022)

[5] Tatsuya Nakazawa, Donghyun Kim, Jaehyeok Kim, Yohei Kotsugi, Taehoon Cheon, Seung-Min Chung, Soo-Hyun Kim, and Hyungjun Kim, Development of RuS2 for near-infrared photodetector by atomic layer deposition and post-sulfurization, Rare Metals 41, 3086 (2022)

Advancing Transparent Conductive Oxides: SrNbO₃ Thin Films by Pulsed Liquid Injection MOCVD

Johnny Azzi [1,2], **Hérvé Roussel**[2], **Sonia Ortega**[2], **Frédérique Ducroquet** [1], **Jean Luc Deschanvres** [2]

[1]Univ. Grenoble Alpes, CNRS, Grenoble INP, USMB, CROMA F-38000 Grenoble, France
[2]Univ. Grenoble Alpes, CNRS, Grenoble INP, LMGP, F-38000 Grenoble, France
e-mail: johnny.azzi@grenoble-inp.fr
frederique.ducroquet@grenoble-inp.fr
jean-luc.deschanvres@grenoble-inp.fr

The demand for advanced photovoltaic materials has driven research toward compounds with exceptional electronic and optical properties. Strontium niobate $SrNbO_3$ (SNO) is a highly promising candidate due to its perovskite structure, high electrical conductivity, bandgap tunability (Fig. 1) and exceptional transparency in the visible spectrum (Fig. 2), making it an attractive material for applications such as transparent electrodes in photovoltaic devices [1]. These properties position SNO as a potential game-changer, offering improved efficiency and compatibility with emerging solar cell designs. However, achieving precise control over film quality, including stoichiometry, morphology, and oxidation states, is critical to fully unlocking its potential.

This study focuses on the deposition of SNO thin films using pulsed liquid injection metal-organic chemical vapor deposition (PLI-MOCVD). While the literature reports SNO deposition typically requiring high temperatures between 800°C and 900°C [2][3] using physical vapor deposition techniques, PLI-MOCVD enables significantly lower deposition temperatures, achieving films at 600°C. This reduction in temperature decreases energy consumption and enhances substrate compatibility. Additionally, PLI-MOCVD offers precise control over precursor delivery and uniform dopant incorporation, making it ideal for multi-metallic systems. A combination of precursors—Bis(tri-isopropylcyclopentadienyl) strontium, Bis(2,2,6,6-tetramethyl-3,5-heptanedionato) strontium tetraglyme adduct, Niobium(V) ethoxide, and Tetrakis(2,2,6,6-tetramethyl-3,5-heptanedionato) niobium (IV)—was utilized to optimize deposition parameters, including temperature, precursor combination, gas flow and oxygen content and injection rates.

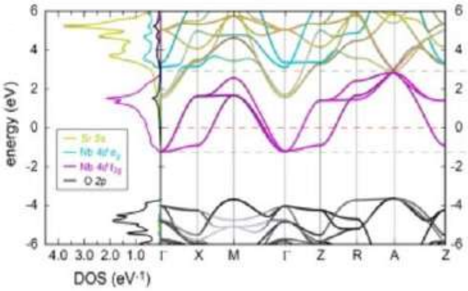

Fig. 1. Density of states and band structure of $SrNbO_3$ calculated by DFT [1]

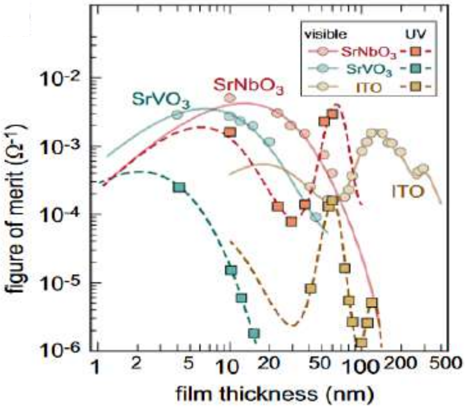

Fig. 2. Figure of merit of SNO, SVO (SrVO3) and ITO according to their thickness in the visible and UV [1].

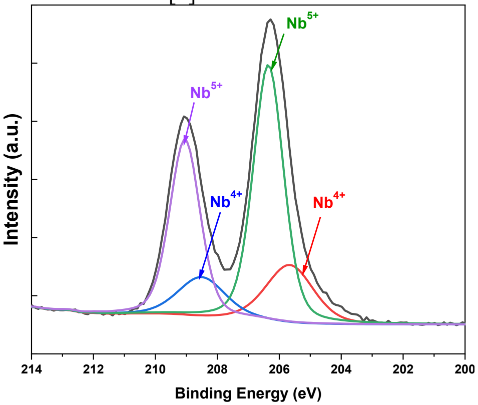

Fig. 3. XPS spectra showing the oxidation states of niobium (Nb^{5+} and Nb^{4+}) in the film.

Advanced characterization techniques such as scanning electron microscopy (SEM), atomic force microscopy (AFM), X-ray diffraction (XRD), Raman spectroscopy, and X-ray photoelectron spectroscopy (XPS) revealed the intricate relationships between deposition conditions and film properties. Key findings include strategies to minimize carbon contamination, achieve a stoichiometric Sr/Nb ratio, stabilize the Nb^{4+}/Nb^{5+} oxidation states (Fig. 3) which is consistent with the literature [4], and control oxygen content, all of which are essential for maintaining the material's functional properties. Optimized deposition conditions yielded films with superior crystallinity, improved transparency in the visible range, and enhanced surface morphology. These properties, which are crucial for effective light management and charge transport in photovoltaic devices, can be influenced by various factors, including subtle variations in the initial precursor ratio (Fig. 4).

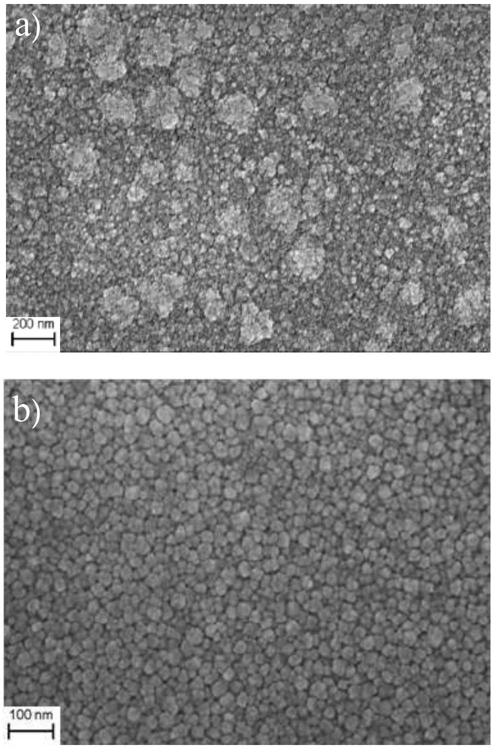

Fig. 4. SEM images highlighting the surface morphology variations between two samples deposited at 600°C differing only in the Sr/Nb ratio of the precursor solution:

a) Sr/Nb=3,5
b) Sr/Nb=3,6

PLI-MOCVD ensures reproducibility and adaptability across various substrates, including silicon, silicon oxide, and Corning glass, making it an ideal technique for scalable production. This work demonstrates the feasibility of producing high-quality SNO thin films at a relatively low temperature of 600°C, paving the way for integrating this material into next-generation energy conversion technologies. Furthermore, the multi-metallic compatibility of PLI-MOCVD facilitates the uniform incorporation of dopants, such as lanthanum (La), to further enhance SNO's properties. Future work will focus on reducing deposition temperatures to 400–450°C, broadening the range of potential applications for this transparent conductive oxide.

This research work was supported by state funding managed by the French National Research Agency under the France 2030 program, reference 22-PETA-0005, PEPR TASE IOTA project.

References

[1] Park, Y. *et al.* SrNbO3 as a transparent conductor in the visible and ultraviolet spectra. *Commun. Phys.* **3**, 102 (2020).

[2] Thapa, S. *et al.* Surface stability of SrNbO3+δ grown by hybrid molecular beam epitaxy. *APL Mater.* **10**, 091112 (2022).

[3] Jeong, J. *et al.* Transparent conducting oxides SrNbO3 thin film with record high figure of merit. *J. Eur. Ceram. Soc.* **44**, 6764–6770 (2024).

[4] Kumar, S. *et al.* Modulation of the optical and transport properties of epitaxial SrNbO3 thin films by defect engineering. *J. Appl. Phys.* **135**, 015303 (2024).

Atomic Layer Deposition of Aluminium-doped Zinc Oxide Thin-Films for Electrodes in Transparent TFTs

C. Matos[1], I. Santos[1], M. Cortinhal[1], J. Deuermeier[1], P. Barquinha[1]
[1] CENIMAT|i3N, Department of Materials Science, School of Science and Technology, NOVA University Lisbon and CEMOP/UNINOVA, Caparica, Portugal
e-mail: pmcb@fct.unl.pt

The growing demand for transparent conductive oxides (TCOs) in applications such as flexible displays, solar cells, and transparent transistors highlights the need for materials with excellent electrical conductivity, optical transparency, and compatibility with large-area, low-temperature processing. Aluminium-doped zinc oxide (AZO), grown by atomic layer deposition (ALD), has emerged as a promising TCO candidate due to its tuneable electronic and optical properties and compatibility with the previous requirements, standing out as a versatile and cost-effective alternative to conventional indium tin oxide. Leveraging ALD for AZO deposition enables precise control over film thickness and composition, a significant advantage over sputtering, chemical vapour deposition and solution methods [1], which is crucial for optimizing its performance in devices such as thin-film transistors (TFTs).

ALD of AZO thin films was performed at two distinct temperatures (150 ˚C and 180 ˚C) and using five (39:1, 29:1, 19:1, 15:1 and 9:1) Zn:Al precursor ratios (DEZ (Diethylzinc):TMA (trimethylaluminium)). Comprehensive characterization was conducted to analyse film thickness, structure, composition, electrical and optical properties. Increasing the aluminium content in the ZnO structure resulted in the following effects: (i) a decrease in film thickness due to Al_2O_3 having a lower growth per cycle and also due to the etching effect of the exchange reactions between TMA and surface Zn atoms, (ii) a shift in crystalline orientation from (002) to (100), (iii) a significant increase in electrical carrier concentration alongside a decrease in mobility due to ionized impurity scattering (Fig. 1), and (iv) an increase in transmittance in the visible range, and in the bandgap (E_g) via the Burstein-Moss effect. X-ray photoelectron spectroscopy and electron dispersive spectroscopy analyses indicated higher aluminium incorporation at 180 ˚C compared to 150 ˚C, which proportionally impacted the effects enumerated above. Notably, the results demonstrated a resistivity as low as 1.8×10^{-3} Ω.cm for a 64 nm thick AZO film using a 19:1 DEZ:TMA ratio at 180 ˚C (Fig. 1), which further decreased to 1.1×10^{-3} Ω.cm for a thicker film of 186 nm, due to improved crystallinity which led to higher carrier mobility.

To further reduce the AZO film resistivity another ALD pulse sequence was adopted while maintaining a 19:1 DEZ:TMA cycle ratio and 180 ˚C deposition temperature. While in the original sequence a DEZ/H_2O/TMA/H_2O traditional supercycle was used, in the new a DEZ/TMA/H_2O pulse in between the remaining DEZ/H_2O pulses was adopted. Results indicated an improvement of both the film mobility and carrier concentration, reducing the resistivity from 1.8×10^{-3} Ω.cm in the original recipe to 1.1×10^{-3} Ω.cm.

The optimized AZO film was introduced as the gate, source and drain electrodes in staggered bottom-gate Indium-Gallium-Zinc oxide TFTs, using RF sputtering for the IGZO channel and an Al_2O_3 ALD gate dielectric (Fig. 2). These TFTs were compared with ones using metal Molybdenum electrodes and results confirmed that AZO can effectively substitute Mo electrodes for TFTs without compromising the device mobility (19.9 $cm^2.V^{-1}.s^{-1}$) (Fig. 3) while achieving high transmittance in the visible range.

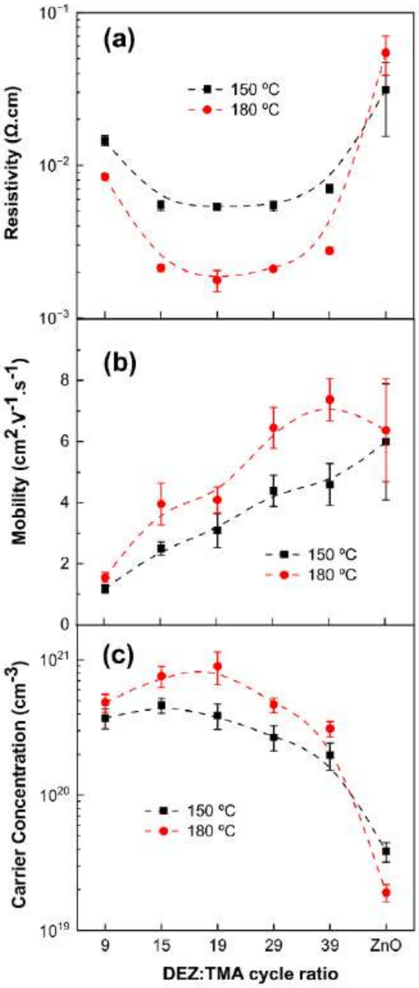

Fig. 1: a) Resistivity, b) mobility and c) carrier concentration of ZnO and AZO films deposited at 150 ºC and 180 ºC as a function of Al concentration (DEZ:TMA cycle ratio).

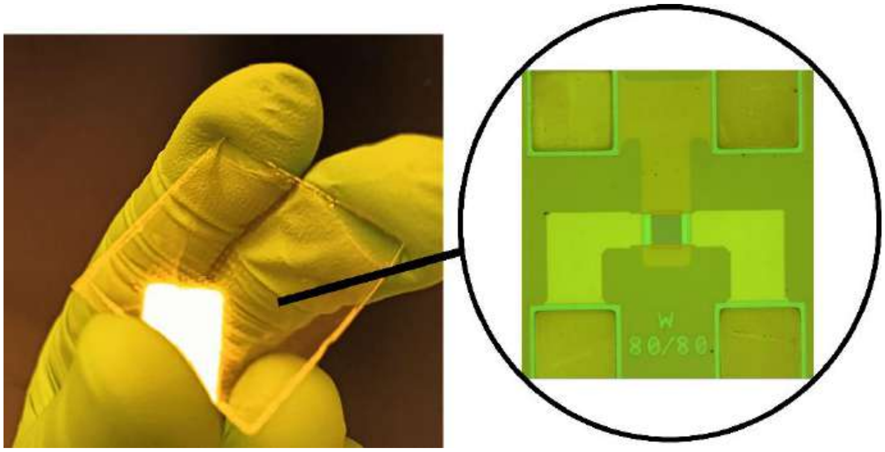

Fig. 2: Photograph of transparent TFTs using AZO electrodes with zoom in to an optical microscope image of one TFT.

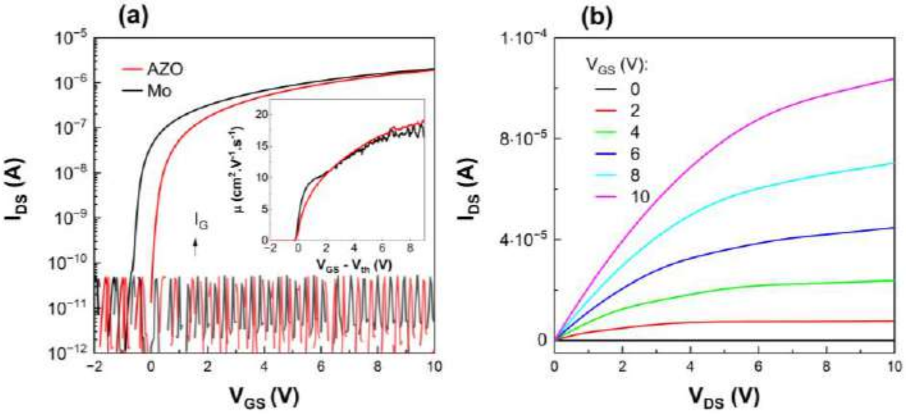

Fig. 3: a) Linear transfer curve (V_{DS}=0.1 V) of TFTs using AZO (red) and Mo (black) electrodes, with inset of the field-effect mobility, b) Output curves of an AZO TFT for V_{GS} = 0 to 10 V.

This work was financed by National Funds through FCT, references LA/P/0037/2020, UIDP/50025/2020 and UIDB/50025/2020 and DRI/India/0430/2020 (VOCMemsense). This work also received funding from the European Community's Horizon 2020 Research and Innovation Programme, under grant agreement 951774 (FOXES).

References

[1] H. C. M. Knoops, S. E. Potts, A. A. Bol, and W. M. M. Kessels, "Atomic Layer Deposition," in *Handbook of Crystal Growth*, T. Kuech, Ed., Elsevier, 2015, pp. 1101–1134. doi: 10.1016/B978-0-444-63304-0.00027-5.

Growth Optimisation of $KNbO_3$, $KTaO_3$ and $KTa_{1-x}Nb_xO_3$ thin Films by DLI-CVD

M. Mirushchenko[1], **I. Labbaveettil**[1], **L. Basyrova**[1], **S. Margueron**[1], **F. Lo Presti**[2], **G. Malandrino**[2], **V. Astié**[3], **J.M. Decams**[3], **A. Bartasyte**[1,4,5]
[1]FEMTO-ST Institute, Université Marie & Louis Pasteur, Besançon, France
[2]University of Catania, Catania, Italy
[3]Annealsys, Montpellier, France
[4]Centre de nanosciences et de nanotechnologies, Université Paris Saclay, CNRS, Palaiseau, France
[5]Institut Universitaire de France
mikhail.mirushchenk@femto-st.fr

Potassium niobate ($KNbO_3$, KN), potassium tantalate ($KTaO_3$, KT), and their solid solutions (KTN), presenting exceptionally high electro-optic properties (in certain compositions up to 300 times higher than that of conventional electro-optic material $LiNbO_3$ [1]), are considered as promising materials for nonlinear and electro-optical photonics, piezoelectric, acousto-optic, and surface acoustic wave (SAW) devices. The composition $KTa_{0.65}Nb_{0.35}O_3$ (KTN-35) is in particular interesting, as it demonstrates a high quadratic electro-optic effect in its paraelectric phase. Since KTN is a mixed crystal formed from the solid solution of KT and KN, the growth of bulk KTN crystals poses significant challenges due to the absence of congruent composition, thermodynamic instability of the composition, and a wide crystallization temperature range. In this context, thin film growth becomes a promising alternative. However, direct epitaxy of KTN films is also associated with several difficulties, such as high volatility of alkali oxides, formation of secondary phases, and challenges in controlling the growth orientation.

In this work, KN, K, and KTN films were deposited using direct liquid injection chemical vapor deposition (DLI-CVD) on lithium niobate substrates of various orientations. The following precursors were used: $[K_4(hfa)_4tetraglyme]_n$ for potassium, $Nb(tmhd)_4$ for niobium, and $Ta(EtO)_4acac$ for tantalum. X-ray diffraction (XRD) was employed to identify the phase composition, scanning electron microscopy (SEM) was used for surface morphology analysis, and energy-dispersive X-ray spectroscopy (EDX) was used to determine the element ratios in the grown films. A substrate temperature of 700 °C was chosen as optimal for high-quality epitaxial film growth. The influence of the K/Nb molar ratio in the solution was studied, and the optimal value was found to be 8.0-8.8 for obtaining single-phase $KNbO_3$ films. Tantalum was then introduced into the system, and the Ta/Nb ratio was optimized. It was found that achieving the target composition of 35% niobium and 65% tantalum is possible by adding the Nb and Ta precursors in equal molar amounts to the deposition solution. Due to the different growth rates of potassium niobate and potassium tantalate phases and K_2O volatility dependence on the Nb/Ta ratio, potassium composition in the film required reoptimisation. According to the XRD analysis, the KTN films deposited by using the same K precursor concentration as that for growth of pure KN films resulted in the films presenting KTN phase and parasitic phase structurally close to $K_4(Ta,Nb)_6O_{17}$. As a result, it was found that significantly more potassium precursor is required than Nb is replaced by Ta in the films.

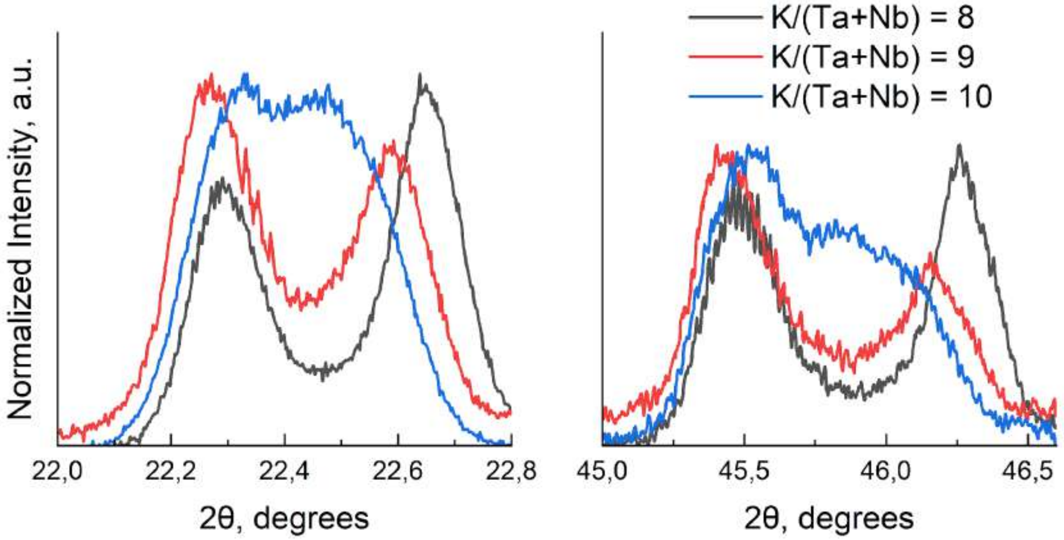

Fig. 1 ∪/2Θ XRD diffraction patterns of KTN-35 films grown by using different K precursor concentrations, indicating gradual change of parasitical phase (represented by a reflection at higher angles than that of KTN phase) with the increase of K concentration in the film.

This work was supported by the French RENATECH network and its FEMTO-ST technological facility and C2N micro nanotechnologies platform, the European HORIZON-MSCA-2023-DN-01 project HINA Grant Agreement No: 101169557, and the graduate school EUR EIPHI contract ANR-17-EURE-0002.

References

[1] J. Li at al., 2013, Opt. Mater. Express 3(12), 2063–2071, DOI:10.1364/OME.3.002063

Challenges and Advances in Ultra-Thin $LiNbO_3$ Film Deposition by DLI-CVD for Beyond-5G Acoustic Resonator Integration

Z. Viéron-Lepoutre[1,2], G. Larger[1,3], S. Margueron[1], V. Astié[4], J.M. Decams[4], N. Findling[5], L. Largeau[5], A. Bartasyte[1,5,6]
[1]FEMTO-ST Institute, Université Marie & Louis Pasteur, Besançon, France
[2]Laboratoire Nanotechnologies Nanosystèmes, Université de Sherbrooke, CNRS, Sherbrooke, Canada
[3]Exail, Besançon, France
[4]Annealsys, Montpellier, France
[5]Centre de nanosciences et de nanotechnologies, Université Paris Saclay, CNRS,Palaiseau, France
[6]Institut Universitaire de France
zoe.vl@femto-st.fr

The rapid evolution of communication technologies towards 5G and 6G requires a significant increase in operating frequencies, potentially enabling signals up to ten times faster than current standards. These performance levels can only be achieved by leveraging frequency bands above 7 GHz [1]. However, existing radio-frequency components—especially resonators based on aluminium nitride (AlN)—are inherently limited and cannot efficiently operate at such high frequencies.

AlN, despite being widely used for its piezoelectric properties, suffers from a low electromechanical coupling coefficient ($k^2 \approx 7.5\%$). While doping with scandium (AlScN) improves this coefficient [2,3], the k^2/quality factor ratio remains insufficient for applications beyond 7 GHz. To overcome this limitation, research has shifted toward single-crystal films such as lithium niobate ($LiNbO_3$), which exhibits highly coupled orientations and promising performance. Thin $LiNbO_3$ layers obtained via wafer bonding and polishing or ion slicing have demonstrated a coupling coefficient of 18.5% at 7.6 GHz for bulk acoustic wave (BAW) resonators [4]. However, these fabrication techniques are costly, face difficulties in precision control of film thickness required for BAW devices, and are constrained by a minimum achievable thickness of around 300 nm.

Since the resonance frequency, f_R, is inversely proportional to the thickness of the active layer, t, ($f_R = \frac{v_\varphi}{2t}$, where v_φ) [5], developing deposition methods that yield thinner films while maintaining high crystalline quality and piezoelectric response has become essential. In this context, our group has demonstrated the feasibility of depositing functional 200 nm-thick $LiNbO_3$ layers on bottom electrodes using Direct Liquid Injection Chemical Vapor Deposition (DLI-CVD) [6].

Current efforts focus on reducing the film thickness to 50 nm and understanding how thickness affects growth dynamics, chemical composition, and film orientation. The growth of ultrathin $LiNbO_3$ films by DLI-CVD proves highly sensitive to the deposition parameters, especially concerning the supply of Li precursor, requiring precise optimization for each target thickness. Additionally, the relationship between the 50 nm thick thin film phase composition and the Li/Nb ratio in the precursor solution is drastically different from that of 200 nm thick films.

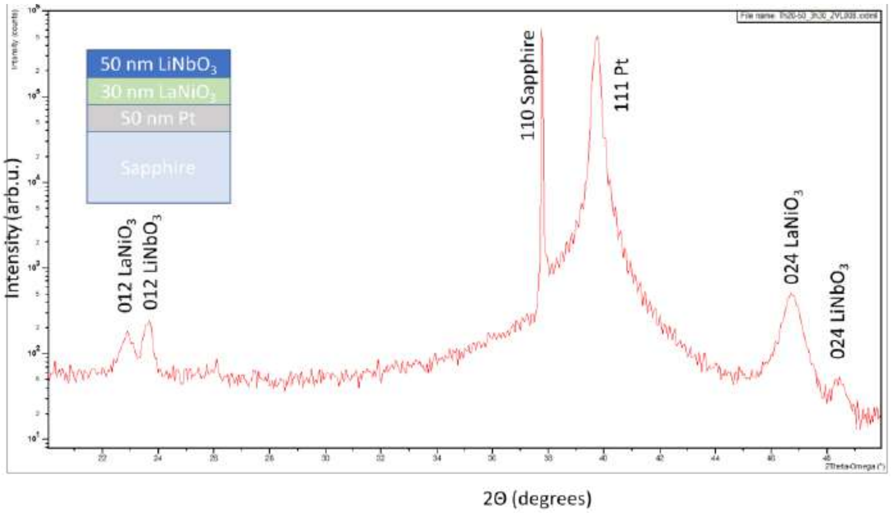

Fig. 1 Θ/2Θ XRD diffraction pattern of 50 nm thick $LiNbO_3$ film on Pt bottom electrode.

In parallel, we are exploring two integration strategies for transferring these films onto standard BAW structures: a direct growth by using a seed layer to promote film texture offering high-electromechanical coupling (Fig. 1), and a transfer of $LiNbO_3$ layers from sapphire by bonding and etching the sacrificial layer. These approaches may open the way for a new generation of high-frequency resonators, compatible with the requirements of future wireless communication systems.

This work was supported by the French RENATECH network and its FEMTO-ST technological facility and C2N micro nanotechnologies platform, the French national ANR project ANTARES ANR ANR-24-CE51-0541, and the graduate school EUR EIPHI contract ANR-17-EURE-0002.

References

[1] F. Qamar, T. Abbas, M. N. Hindia, K. Dimyati, K. A. Noordin and A. Irfan*, IEEE 13th Malaysia International Conference on Communications (MICC)*, November 28-30, Johor Bahru, Malaysia, pp. 265-270 (2017)

[2] M. Akiyama, T. Kamohara, K. Kano, A. Teshigahara, Y. Takeuchi and N. Kawahara, *Advanced materials*, **21**, pp. 593-596 (2009)

[3] R. Matloub, A. Artieda, C. Sandu, E. Milyutin and P. Muralt, *Applied Physics Letters*, **99** (2011)

[4] A. Reinhardt, M. Bousquet, A. Joulie, C-L. Hsu, F. Delaguillaumie, C. Maeder-Pachurka, G. Enyedi, P. Perreau, G. Castellan and J. Lugo, *Joint Conference of the European Frequency and Time Forum and IEEE International Frequency Control Symposium (EFTF/IFCS),* July 7-17*,* virtual (2021)

[5] Y. Liu, Y. Cai, Y. Zhan, A. Tovstopyat, S. Liu and C. Sun, *Micromachines*, **11**, p. 630 (2020).

[6] S. Boujnah, et al., EFTF/IFCS, Toyama, Japan: IEEE, pp. 1–2, (2023) & Proceedings IUS (2024).

Surface chemistry of copper (II) hexafluoroacetylactonate studied by DFT and APXPS for copper ALD

Sylwia Klejna[1], Aleksandra Figura-Jagoda[1], Camilla Minzoni[2-3], Krzysztof Mackosz[2], Caroline Hain[2], Mateusz Marzec[1], Aleksandra Szkudlarek[1], Marcin Sikora[4], Esko Kokkonen[5], Ivo Utke[2]

[1] AGH University of Krakow, al. A. Mickiewicza 30, Krakow, 30-059, Poland
[2] Empa, Feuerwerkerstrasse 39, CH-3602 Thun, Switzerland
[3] EPFL, Rte Cantonale, 1015, Lausanne, Switzerland
[4] SOLARIS Centre, Jagiellonian University, ul. Czerwone Maki 98, Krakow, 30-392, Poland
[5] MAX IV Laboratory, Lund University, Fotongatan 2, 224 84 Lund, Sweden

e-mail: sylwia.klejna@agh.edu.pl

The reactions of copper (II) hexafluoroacetylactonate, Cu(hfac)$_2$, on two different types of substrates: SiO$_2$ (native oxide) and Pt (150 nm deposited by the PVD process) were studied by density functional theory (DFT) calculations and ambient pressure X-ray photoelectron spectroscopy (APXPS). The adsorption of the Cu(hfac)$_2$ precursor was monitored in APXPS experiments over a temperature range: room temperature, 100°C, 190°C, and 220°C. The XPS spectra showed a reduction in the intensity of the C 1s peak and a peak shift at temperatures as low as 100°C for the Pt substrate, suggesting that the precursor undergoes decomposition. DFT studies provided further insight into the reactions taking place. The adsorption (Fig.1) and decomposition (Fig.2) pathways during the metal precursor pulse were calculated. Surface bound species and possible volatile products were identified. The influence of temperature on the stability of these species was investigated. Two competing pathways of ligand decomposition were identified: the first leading to trifluoromethane (CHF$_3$) desorption and the second to carbon monoxide (CO) desorption. This low temperature decomposition of the Cu precursor on the Pt substrate may be the reason for Cu growth inhibition on the metallic substrates and explains the observed differences in early stage copper ALD growth compared to oxide substrates.

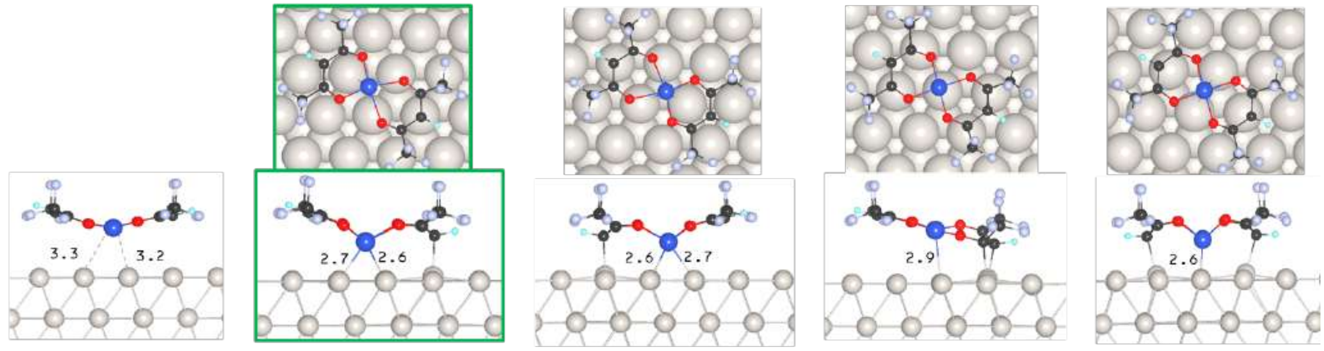

physisorption +0.16 eV **(A) fcc** -0.15 eV **(B) hcp** -0.05 eV **(C) top** -0.02 eV **(D) bridge** 0.25 eV

Fig. 1. DFT-PBE study of adsorption: physisorption and chemisorption of Cu(hfac)$_2$ on Pt (111) surface. Top and side views on the surface models. Colour code: grey – Pt, blue – Cu, red – O, black – C, violet – F, cyan – H.

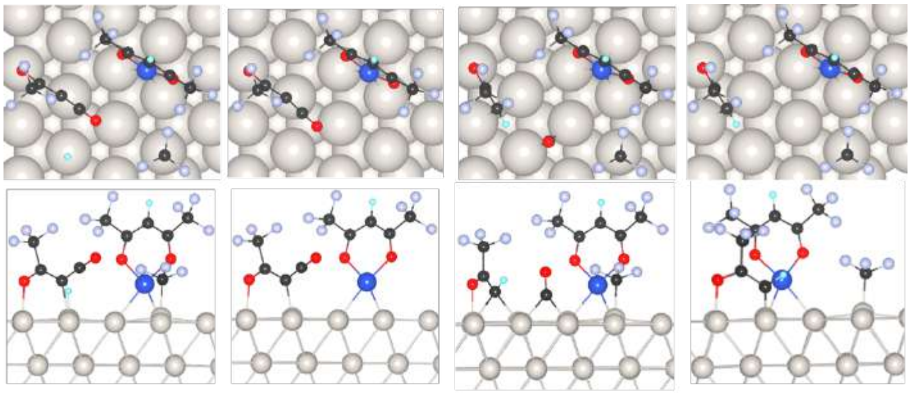

(A) -1.17 eV **(B)** CHF_3↑ -1.02 eV **(C)** -2.17 eV **(D)** CO↑ -0.55 eV

Fig. 2. DFT-PBE study of the decomposition of the hfac ligand on a Pt (111) surface leading to: desorption of CHF_3 (A)→(B) and CO (C)→(D). Side and top view of the models. Colour code: grey – Pt, blue – Cu, red – O, black – C, violet – F, cyan – H.

This work was supported by the Swiss National Science Foundation and National Science Centre, Poland, projects no. 202492 and 2020/39/I/ST5/03561, respectively. The MAX IV Laboratory is acknowledged for granting experimental time at the SPECIES beamline. We gratefully acknowledge the Polish High Performance Infrastructure PLGrid ACK Cyfronet AGH for providing computing facilities and support under the computational grant no. plgald.

It is a pleasure to welcome you to Catania. We have faith that you will depart with not just priceless memories but also the basis for lasting connections and inspiring scientific interactions.

Thank you!

Additionally, we would like to express our gratitude to our partners and sponsors, without whom this conference would not be possible:

Silver Sponsor

Veeco

Bronze Sponsor

ANNEALSYS

BROOKS® INSTRUMENT

SEMILAB

SEMPA® PART OF MEPTAGON GROUP

Dock

Kurt J. Lesker® Company

ECM Components FLOWLINK KEMSTREAM

Pegasus

Beneq

Exhibitor

ASM